FROM TRADITIONAL TO MODERN: PROGRESS OF MOLDS AND YEASTS IN FERMENTED-FOOD PRODUCTION, VOLUME II

EDITED BY: Wanping Chen, Xucong Lv, Jun Liu, Kap-Hoon Han and Van-Tuan Tran
COORDINATED BY: Chengcheng Zhang
PUBLISHED IN: Frontiers in Microbiology

frontiers Research Topics

ISSN 1664-8714
ISBN 978-2-83250-816-9
DOI 10.3389/978-2-83250-816-9

About Frontiers

Frontiers is more than just an open-access publisher of scholarly articles: it is a pioneering approach to the world of academia, radically improving the way scholarly research is managed. The grand vision of Frontiers is a world where all people have an equal opportunity to seek, share and generate knowledge. Frontiers provides immediate and permanent online open access to all its publications, but this alone is not enough to realize our grand goals.

Frontiers Journal Series

The Frontiers Journal Series is a multi-tier and interdisciplinary set of open-access, online journals, promising a paradigm shift from the current review, selection and dissemination processes in academic publishing. All Frontiers journals are driven by researchers for researchers; therefore, they constitute a service to the scholarly community. At the same time, the Frontiers Journal Series operates on a revolutionary invention, the tiered publishing system, initially addressing specific communities of scholars, and gradually climbing up to broader public understanding, thus serving the interests of the lay society, too.

Dedication to Quality

Each Frontiers article is a landmark of the highest quality, thanks to genuinely collaborative interactions between authors and review editors, who include some of the world's best academicians. Research must be certified by peers before entering a stream of knowledge that may eventually reach the public - and shape society; therefore, Frontiers only applies the most rigorous and unbiased reviews.
Frontiers revolutionizes research publishing by freely delivering the most outstanding research, evaluated with no bias from both the academic and social point of view. By applying the most advanced information technologies, Frontiers is catapulting scholarly publishing into a new generation.

What are Frontiers Research Topics?

Frontiers Research Topics are very popular trademarks of the Frontiers Journals Series: they are collections of at least ten articles, all centered on a particular subject. With their unique mix of varied contributions from Original Research to Review Articles, Frontiers Research Topics unify the most influential researchers, the latest key findings and historical advances in a hot research area! Find out more on how to host your own Frontiers Research Topic or contribute to one as an author by contacting the Frontiers Editorial Office: frontiersin.org/about/contact

FROM TRADITIONAL TO MODERN: PROGRESS OF MOLDS AND YEASTS IN FERMENTED-FOOD PRODUCTION, VOLUME II

Topic Editors:
Wanping Chen, University of Göttingen, Germany
Xucong Lv, Fuzhou University, China
Jun Liu, Central South University Forestry and Technology, China
Kap-Hoon Han, Woosuk University, South Korea
Van-Tuan Tran, Vietnam National University, Hanoi, Vietnam

Coordinator Editor:
Chengcheng Zhang, Zhejiang Academy of Agricultural Sciences, China

Citation: Chen, W., Lv, X., Liu, J., Han, K.-H., Tran, V.-T., Zhang, C., eds. (2022). From Traditional to Modern: Progress of Molds and Yeasts in Fermented-food Production, Volume II. Lausanne: Frontiers Media SA.
doi: 10.3389/978-2-83250-816-9

Table of Contents

frontiers | Frontiers in Microbiology

TYPE Editorial
PUBLISHED 04 November 2022
DOI 10.3389/fmicb.2022.1075162

OPEN ACCESS

EDITED AND REVIEWED BY
Aldo Corsetti,
University of Teramo, Italy

*CORRESPONDENCE
Wanping Chen
chenwanping1@foxmail.com

SPECIALTY SECTION
This article was submitted to Food Microbiology, a section of the journal Frontiers in Microbiology

RECEIVED 20 October 2022
ACCEPTED 25 October 2022
PUBLISHED 04 November 2022

CITATION
Lv X, Liu J, Zhang C, Tran V-T, Han K-H and Chen W (2022) Editorial: From traditional to modern: Progress of molds and yeasts in fermented-food production, Volume II. *Front. Microbiol.* 13:1075162. doi: 10.3389/fmicb.2022.1075162

Editorial: From traditional to modern: Progress of molds and yeasts in fermented-food production, Volume II

Xucong Lv[1], Jun Liu[2], Chengcheng Zhang[3], Van-Tuan Tran[4,5], Kap-Hoon Han[6] and Wanping Chen[7]*

[1]College of Biological Science and Technology, Fuzhou University, Fuzhou, China, [2]College of Food Science and Engineering, Central South University Forestry and Technology, Changsha, China, [3]Food Science Institute, Zhejiang Academy of Agricultural Sciences, Hangzhou, China, [4]Department of Microbiology, University of Science, Vietnam National University, Hanoi, Vietnam, [5]National Key Laboratory of Enzyme and Protein Technology, University of Science, Vietnam National University, Hanoi, Vietnam, [6]Department of Pharmaceutical Engineering, Woosuk University, Wanju, South Korea, [7]Department of Molecular Microbiology and Genetics, Georg-August-Universität Göttingen, Göttingen, Germany

KEYWORDS

fermented food, mold, yeast, *Monascus*, *Saccharomyces*

Editorial on the Research Topic
From traditional to modern: Progress of molds and yeasts in fermented-food production, Volume II

Molds (filamentous fungi) and yeasts are important fermentation microorganisms that have been used for the production of foods and beverages throughout the world since ancient times (Venturini Copetti, 2019). Generally, fermented foods together with their functioning microorganisms, have strong regional characteristics (Chen, 2022). Therefore, this Research Topic was launched as a sequel to our previous topic (Chen et al., 2022), which aims to offer a collection of articles associated with different types of fermentation products and processes from different regions and provide a comparable perspective for molds and yeasts in fermented food production. The articles in this collection are introduced in the following.

Monascus species are important fermentation molds and are well-known for their fermentation products, red mold rice, used as a food colorant, brewing starter, and monacolin K supplement (Chen et al., 2015). This topic collects five research articles related with *Monascus* genetics and secondary metabolite synthesis. Xu, Li et al. constructed a markerless genetic modification system in *Monascus ruber* M7, in which the endogenous gene *mrpyrG* instead of the resistance marker gene was used as the screening marker. Then, the authors applied the system to delete multiple genes from *M. ruber* M7 separately or continuously without any resistance marker gene and found that the average gene replacement frequency of Δ*mrpyrG*Δ*mrlig4* was about 18 times higher than that of the wild-type. The markerless and highly efficient genetic modification system constructed in the current study will not only be used

for multi-gene simultaneous modification in *Monascus* spp. and also lays a foundation for investigating the effects of multi-genes modification on *Monascus*. Ramzan et al. screened and characterized an ABC transporter involved in the transportation of phenylacetic acid in *Monascus ruber* M7. This study contributes to the clarification of the penicillin biosynthetic pathway in *Monascus*. Yin, Yang et al. investigated the effect of methionine and S-adenosylmethionine on *Monascus* pigments biosynthesis in *Monascus purpureus* RP2. The results found that the addition of methionine in fermentation significantly reduced *Monascus* pigments production by 60–70%, while the addition of S-adenosylmethionine in fermentation promoted *Monascus* pigments production by a maximum of 35%. This work also proposed a possible regulation mechanism of *Monascus* pigments biosynthesis by S-adenosylmethionine metabolism from methionine and provided a new perspective for a deep understanding of *Monascus* pigments biosynthesis regulation in *Monascus purpureus*. Yin, Zhu et al. added 20 free amino acids to the fermentation medium to evaluate their effects on *Monascus* pigments biosynthesis in *Monascus purpureus* RP2. Six amino acids, including histidine, lysine, tyrosine, phenylalanine, methionine, and cysteine, exerted significant effects on the production yield. The authors further investigated the dose-dependent and synergistic effects of these amino acids on *Monascus* pigments biosynthesis. This study would contribute to the industrial production of *Monascus* pigments. Bai et al. generated a mutant strain *Monascus purpureus* H14 with high production of water-soluble yellow *Monascus* pigments and optimized their production in submerged fermentation. The yellow pigments exhibited good tone stability when subjected to environmental factors, including pH, heat, light, and metal ions. However, their pigment values were unstable with pH, light, and high concentrations of Ca^{2+}, Zn^{2+}, Fe^{2+}, Cu^{2+}, and Mg^{2+}.

This topic collects three review articles. Chi et al. summarized the principles and advantages of space microorganism breeding. Tu et al. reviewed the typical flavor substances of different types of Chinese Baijiu, the types of microorganisms involved in the brewing process, and their functions, and introduced methods that use microbial technology to enhance the flavor of Baijiu and to detect flavor substances in Baijiu. This review systematically summarizes the role and application of Chinese Baijiu flavor components and microorganisms in Baijiu brewing and provides data support for understanding Chinese Baijiu and further improving its quality. Li et al. summarized the effective approaches to producing humanized products in yeasts, and focused on yeast species selection, glycosyltransferase deletion, expression of endoglycosidase, and expression of proteins with galactosylated and or sialylated glycans. The authors also pointed out the future challenges of producing humanized glycosylated proteins.

The remaining two articles focus on the mechanism of chemical changes during fermentation. Liang et al. sequenced a *Saccharomyces cerevisiae* strain isolated from Wuyi Hongqu starters with low urea production and inferred a key gene responsible for low urea production. The results will improve our understanding on the mechanism of low urea production by *Saccharomyces cerevisiae* during Hongqu Huangjiu fermentation and may provide a way to control the urea and ethyl carbamate contents in Hongqu Huangjiu production. Xu, Miao et al. investigated the microbial succession and volatile compound dynamics of spontaneous fermentation in Xinjiang flat peach wine. The results showed that *Kazachstania*, *Pichia*, *Aspergillus*, *Fructobacillus*, *Leuconostoc*, and *Lactobacillus* were the dominant genera during the spontaneous fermentation of flat peach wine. Meanwhile, ethyl hexanoate, 3-hexen-1-yl acetate, ethyl caprate, ethyl caprylate, phenethyl acetate, ethanol, γ-decalactone, decanal, 1-hexanoic acid, and octanoic acid endued flat peach wine with a strong fruity and fatty aroma. The authors also analyzed the relationship between microorganisms and volatile chemicals. This study provides insights into the microorganisms involved in flat peach wine fermentation and could guide the production of flat peach wine with desirable characteristics.

In general, compared to the collections of the previous topic (Chen et al., 2022), the collections of this Research Topic focused more on the changes of metabolites during fermentation and tried to find out the inner mechanism. Hopefully, this topic collection will provide a reference on how to control metabolite synthesis during fermentation.

Author contributions

All authors contributed to this work and approved it for publication.

Conflict of interest

The authors declare that the research was conducted in the absence of any commercial or financial relationships that could be construed as a potential conflict of interest.

Publisher's note

References

Chen, W. (2022). Demystification of fermented foods by omics technologies. *Curr. Opin. Food Sci.* 46, 100845. doi: 10.1016/j.cofs.2022.100845

Chen, W., He, Y., Zhou, Y., Shao, Y., Feng, Y., Li, M., et al. (2015). Edible filamentous fungi from the species *Monascus*: early traditional fermentations, modern molecular biology, and future genomics. *Compr. Rev. Food Sci. Food Saf.* 14, 555–567. doi: 10.1111/1541-4337.12145

Chen, W., Lv, X., Tran, V.-T., Maruyama, J.-I., Han, K.-H., and Yu, J.-H. (2022). Editorial: from traditional to modern: progress of molds and yeasts in fermented-food production. *Front. Microbiol.* 13, 876872. doi: 10.3389/fmicb.2022.876872

Venturini Copetti, M. (2019). Yeasts and molds in fermented food production: an ancient bioprocess. *Curr. Opin. Food Sci.* 25, 57–61. doi: 10.1016/j.cofs.2019.02.014

frontiers | Frontiers in Microbiology

ORIGINAL RESEARCH
published: 26 April 2022
doi: 10.3389/fmicb.2022.894661

Analysis of Key Genes Responsible for Low Urea Production in *Saccharomyces cerevisiae* JH301

Zhangcheng Liang[1,2], Hao Su[1,2], Xiangyun Ren[1,2], Xiaozi Lin[1,2], Zhigang He[1,2]*, Xiangyou Li[3] and Yan Zheng[1,2]*

[1] Institute of Agricultural Engineering Technology, Fujian Academy of Agricultural Sciences, Fuzhou, China, [2] Fujian Key Laboratory of Agricultural Products (Food) Processing, Fuzhou, China, [3] Fujian Pinghuhong Biological Technology Co., Ltd., Fuzhou, China

There is a potential safety risk with ethyl carbamate (EC) in Hongqu Huangjiu production; 90% of the EC in rice wine is produced by the reaction of the urea with the alcohol of *Saccharomyces cerevisiae*. In our previous experiments, we screened and obtained a *S. cerevisiae* strain JH301 that offered low urea production. However, the key genes responsible for low urea production of strain JH301 remain unclear. Here, the whole genome sequencing of *S. cerevisiae* strain JH301 was accomplished via a next-generation high-throughput sequencing and long-read sequencing technology. There are six main pathways related to the urea metabolism of strain JH301 based on KEGG pathway mapping. Three species-specific genes are related to the urea metabolism pathways and were found in comparative genome analysis between strains JH301 and S288c during Hongqu Huangjiu production for the first time. Finally, the *ARG80* gene was found to be likely a key gene responsible for low urea production of *S. cerevisiae* strain JH301, as determined by PCR and qRT-PCR check analyses from DNA and RNA levers. In conclusion, the results are useful for a scientific understanding of the mechanism of low urea production by *Saccharomyces cerevisiae* during Hongqu Huangjiu fermentation. It also is important to control the urea and EC contents in Hongqu Huangjiu production.

Keywords: key gene, whole genome sequencing, comparative genomic analysis, Hongqu Huangjiu, *Saccharomyces cerevisiae*, low urea production

OPEN ACCESS

Edited by:
Xucong Lv,
Fuzhou University, China

Reviewed by:
Shuangping Liu,
Jiangnan University, China
Zhilei Zhou,
Jiangnan University, China

***Correspondence:**
Xiaozi Lin
lyne00@163.com
Zhigang He
njgzx@163.com

Specialty section:
This article was submitted to Food Microbiology, a section of the journal Frontiers in Microbiology

Received: *12 March 2022*
Accepted: *31 March 2022*
Published: *26 April 2022*

Citation:
Liang Z, Su H, Ren X, Lin X, He Z, Li X and Zheng Y (2022) Analysis of Key Genes Responsible for Low Urea Production in Saccharomyces cerevisiae JH301. Front. Microbiol. 13:894661. doi: 10.3389/fmicb.2022.894661

INTRODUCTION

There are potential safety risks around ethyl carbamate (EC) in Hongqu Huangjiu production (Luo et al., 2017; Zhou et al., 2020). EC is produced in trace amounts during the fermentation or aging of many fermented foods and alcoholic beverages and is a likely carcinogen to humans (i.e., class 2A) (Xian et al., 2019). Indeed, 90% of EC in rice wine is produced by the reaction of the urea and the alcohol of *Saccharomyces cerevisiae* (Vázquez et al., 2017; Fang et al., 2018). Hongqu Huangjiu is a traditional rice wine in China (Huang et al., 2019); "Hong Qu" (a traditional Chinese fermentation

starter) has a unique flavor and rich functional nutrients (Lv et al., 2015; Huang et al., 2018; Liang et al., 2020a). However, it also has a high EC safety risk. Our previous studies found that Hongqu Huangjiu contained rich amino acids such as arginine, which are precursors of urea production (Liang et al., 2020b). If the urea production level is not targeted repression, then there could be higher EC content in Hongqu Huangjiu production. This has harmed the development of the Hongqu Huangjiu industry.

There are currently several common methods to control urea content. (1) Urease can degrade the urea content. Urease is often added to hydrolyze the urea during the production of grape wine and Japanese sake (Yang et al., 2019). The urea content in rice wine could be reduced by more than 90% using urease (Liu et al., 2019). However, urease quickly loses activity, and its use can dramatically increase production costs. (2) Rice wine yeast can be screened for low urea production. For example, *Saccharomyces cerevisiae* mutant strains with low urea production levels (14.91 mg/L and 17.89 mg/L) were screened with He-Ne laser radiation and nitroso arc combined with mutagenesis, UV, and γ-ray combined mutagenesis (Kuribayashi et al., 2017). (3) Low-yield urea *Saccharomyces cerevisiae* can be engineered. A non-urea-producing *Saccharomyces cerevisiae* strain was obtained by knocking out the arginase gene *CAR1* in sake yeast (Yoshiuchi et al., 2000). *Saccharomyces cerevisiae* strain with low urea production was constructed by over-expressing the intracellular urea amidase genes *DUR1* and *DUR2* (Wu et al., 2016). However, most of these strains are mutagenesis and engineering strains with potential problems in food safety.

In our previous experiments, we screened and obtained a *S. cerevisiae* strain JH301 that had lower urea production. However, the key genes responsible for low urea production of strain JH301 have not yet been researched; the molecular mechanism of low urea production of strain JH301 remains unclear. Here, we assessed the whole genome of strain JH301 using a high-throughput sequencing technology in MiSeq from Illumina and long-read sequencing technology in a PacBio Sequel platform. We focused on the key genes in strain JH301 using comparative genomics with *Saccharomyces cerevisiae* model strain S288c. Finally, we used PCR and Quantitative real-time PCR (qRT-PCR) analyses to verify the key genes from DNA and RNA levels. The results could guide the screening of similar yeasts and provide a basis for molecular breeding of yeasts with low urea production. This is also useful for a scientific understanding of the mechanism of low urea production by *Saccharomyces cerevisiae* during Hongqu Huangjiu fermentation and it is important to control the urea and EC contents in Hongqu Huangjiu production.

MATERIALS AND METHODS

Strain Material and Mediums

Saccharomyces cerevisiae strains JH301, JH303, JH401, JH405, and JH505 are usually used for Hongqu Huangjiu production; both were isolated from Wuyi Hongqu starters in the Fujian Province of China. *Saccharomyces cerevisiae* strain AQ was provided by a wine company (Fujian, China). *Saccharomyces cerevisiae* strain S288c was obtained from NITE Biological Resource Center.

Activation of *Saccharomyces Cerevisiae* Strains

The *Saccharomyces cerevisiae* strains were precultured on YPD plates at 25°C for 24 h. A single colony was activated in 50 mL YPD medium (25°C, 200 rpm). The growth was monitored by determining the optical density at 600 nm (OD 600).

Determination of the Content of Alcohol, Urea, and Ethyl Carbamate of *Saccharomyces cerevisiae* Strains

Here, 5% activation liquid of *Saccharomyces cerevisiae* strain was mixed with 200 mL rice liquid medium. The medium underwent fermentation at 25°C for 20 days. Solid-liquid separation was performed, and the fermented liquid was centrifuged to obtain the supernatant for future alcohol, urea, and EC content determination. Full evaporation headspace gas chromatography measurements were used to assess the content of alcohol as previously described (Liang et al., 2020c). The urea content was measured by high-performance liquid chromatography (Clark et al., 2007). The EC content in Hongqu Huangjiu was analyzed using solid-phase extraction and stable isotope dilution GC/MS (Lachenmeier et al., 2006). The urea and EC contents were determined in each sample after dilution to 15% alcohol. Each group of liquids was fermented using the same *Saccharomyces cerevisiae* strain in three independent experiments.

Whole Genome Sequencing Analysis of *Saccharomyces cerevisiae* Strains

A total of four PacBio 20-kb libraries were generated with a SMRTbell Template Prep Kit (PacBio), and the libraries were sequenced on the PacBio Sequel platform. A total of 72 Gb (∼124×) of PacBio sequence data were generated. A total of ∼113 Gb (∼194 × fold coverage) of 10X Chromium library data were sequenced on an Illumina MiSeq system with paired-end 150-bp reads. The RNA library preparation, sequencing, genome assembly, genome annotation, and quality assessment were performed by Shanghai Personal Biotechnology Co., Ltd. (Shanghai, China). Function annotation was completed by BLAST search against KEGG (Kyoto Encyclopedia of Gene and Genomes) database (Moriya et al., 2007).

Comparative Genome Analysis

Through collinearity analysis between the two genomes, we can observe the insertion and deletion of sequences between the target species genome and the reference genome. Such analysis confirms the local positional arrangement relationship and finds the regions of translocation, inversion, and translocation + inversion. The software Mummer (version 3.23) and Mauve (version 2.3.1) were used to conduct a rapid comparison between the two genomes, determine the relative direction of the sequence, and adjust the genome to align the starting point of the genome. Chainnet software was used to join the comparison results into longer comparisons. LastZ (Version

TABLE 1 | List of PCR primer pairs designed and used for this study.

Primers	Sequence	Amplification conditions
ARG80	5'-CGAATAGCGACGGTTCAAGT-3'; 5'-CGTCAGGAGTGTCTGAAGCA-3'	35 cycles 94°C 30 s/61°C 30 s/72°C 2 min
BIO3	5'-CATATACACCAGATGTCGCG-3'; 5'-CCTTCGTCAATTCCTCTGTC-3'	35 cycles 94°C 30 s/61°C 30 s/72°C 2 min
VTC4	5'-GGTGAGCACTTGAGCAAGTC-3'; 5'-AAACACAGAAACCATGCCGG-3'	35 cycles 94°C 30 s/61°C 30 s/72°C 2 min

TABLE 2 | List of QPCR primer pairs designed and used for this study.

Primers	Sequence	Product size (bp)
ARG80	5'-CAACTCCCACCCCAACCATA-3'; 5'-GGCGTTGTGAAAGTGTAGACCAG-3'	232
BIO3	5'-AGGATTTGGTAGAACAGGTG-3'; 5'-AGTAGGGCTATTTGGAGAAG-3'	208
VTC4	5'-AGTTTGGTGAGCACTTGAGC-3'; 5'-CGTCCACTGACCGTTATTCT-3'	119
QACT	5'-TATGGAAAAGATCTGGCATCA-3'; 5'-CGGTTTGCATTTCTTGTTCG-3'	205

Primer QACT is the primer of house-keeping gene.

1.03.54) software was used to detect the indels (Shalhub et al., 2014) with a length of less than 50 bp. A database based on the data set was constructed and used as a query to perform all-VS-all BLASTP analysis. The result of sequence alignment was processed with OrthoMCL (version 2.0.8) software (Fischer et al., 2011); the length of sequence alignment was set to 70%, and MCL was used to cluster gene families. Finally, Perl script was used to sort and count the results of the clustering. Unique or missing genes were identified.

DNA Extraction and PCR Conditions

Saccharomyces cerevisiae strain cells were pre-grown in YPD at 28°C for 48 h. The yeast DNA was extracted from the pure cultures using the method described by Duarte (Duarte et al., 2009). The 25-μL PCR mixture contained 12·5 μL de Mix GoTaq® Green Master 2X (omega), 2 μL of DNA diluted to 10 ng/μL and 0.5 μmol/L of each primer. The sequences of the primers (De Melo Pereira et al., 2010) utilized in this study and the amplification conditions are shown in **Table 1**. Amplification products were separated by electrophoresis on a 0.8% (w/v) agarose gel and stained with SYBR Green (Invitrogen, United States). DNA fragments were visualized by UV transillumination, and images were captured using a Polaroid camera. A ladder marker was used as a size reference.

Quantitative Real-Time PCR Analysis

RNA Extraction

The total RNA samples were isolated by TRIzol reagent (TIANGEN BIOTECH, Beijing). The RNA purity and concentration were then measured using a NanoPhotometer spectrophotometer (IMPLEN, CA, United States).

Quantitative Real-Time PCR Analysis

cDNA was synthesized using 2 μg RNA using a PrimeScript™ RT reagent Kit with gDNA Eraser (TaKaRa). Gene-specific primers for quantitative real-time PCR (qRT-PCR) analysis were designed using Primer 5.0 by Allwegene Technology (Allwegene Technology Co., Ltd., Beijing, China). The QACT gene was used as a house-keeping gene. qRT-PCR reaction was performed using SYBR® Premix Ex Taq™ II (Tli RNaseH Plus) on an ABI 7500 real-time Detection System (Thermo Fisher Scientific, United States). The PCR reaction was conducted with the following reaction conditions: 95°C for 30 s, followed by 45 cycles of 95°C for 5 s, and 60°C for 40 s. The sequences of the primers utilized in this study are shown in **Table 2**. Samples for qRT-PCR were run in three biological replicates, with three technical replicates, and the data were represented as the mean ± *SD* ($n = 3$) for Student's *t*-test analysis. The relative gene expression was calculated using the $2^{-\Delta\Delta CT}$ algorithm (Pfaffl, 2001).

Statistical Analysis

All experiments were performed in triplicate. Data are represented as means ± standard deviation (± s). Statistical analyses were performed using SPSS 15.0 software using one-way analysis of variance, and $P < 0.05$ indicates statistical significance.

RESULTS

Urea and Ethyl Carbamate Production Levers of Different *Saccharomyces cerevisiae* Strains

The urea and EC production levers of different *Saccharomyces cerevisiae* strains were measured by HPLC and SPE-GC/MS analysis, respectively, as shown in **Table 3**. There were significant differences in the levels of urea and EC production among strains.

TABLE 3 | Comparison of fermentation quality indexes of different *Saccharomyces cerevisiae* strains.

***Saccharomyces cerevisiae* strains**	**JH301**	**JH303**	**JH401**	**JH405**	**JH505**	**S288c**
Alcohol (%)	16.67 ± 0.47^{a}	14.77 ± 0.38^{c}	14.46 ± 0.15^{c}	16.44 ± 0.23^{a}	15.25 ± 0.18^{b}	15.53 ± 0.68^{b}
Urea content (mg/L)	16.33 ± 1.15^{c}	55.22 ± 3.19^{a}	33.54 ± 1.64^{b}	36.22 ± 2.82^{b}	35.47 ± 1.42^{b}	53.23 ± 3.19^{a}
EC content at baseline (μg/L)	53.25 ± 2.80^{c}	113.87 ± 7.23^{a}	89.49 ± 4.28^{b}	85.82 ± 3.47^{b}	85.82 ± 6.93^{b}	108.99 ± 10.42^{a}
EC content after 6 months (μg/L)	70.66 ± 3.69^{c}	135.38 ± 4.28^{a}	101.84 ± 5.31^{b}	104.48 ± 7.14^{b}	105.19 ± 6.22^{b}	132.88 ± 8.46^{a}

JH301 fermented using Saccharomyces cerevisiae strain JH301; S288c fermented using Saccharomyces cerevisiae strain S288c; JH303, JH401, JH405, and JH505 fermented using Saccharomyces cerevisiae strain JH303, JH401, JH405, and JH505, respectively. The urea and EC content were determined in each sample. Data points represent the means of three biological repeats, and error bars represent standard deviations. Significant difference shown as lowercase letters means the significance level was lower than 0.05 ($P < 0.05$).

TABLE 4 | Whole genome sequencing and annotation results.

Property	JH301	S288C
Total sequence length (Mb)	11.97	12.16
GC content (%)	38.02	38.15
Genes percentage of genome (%)	67.07	75.37
Predicted genes number	5,228	5,906
Average gene length (bp)	1536.5	1,369
The number of tRNA	297	299
The number of rRNA	66	10

JH301 fermented using Saccharomyces cerevisiae strain JH301; S288c fermented using Saccharomyces cerevisiae strain S288c.

The urea and EC production levers of *S. cerevisiae* strain JH301 was the lowest. Compared with strain S288c, the urea content of JH301 was decreased by 69.32%, the EC content at baseline was decreased by 51.14%, and the EC content after 6 months decreased by 46.82%, respectively. The results showed that strain JH301 had a lower urea and EC production levers than other strains in this study.

Whole Genome Sequencing Analysis of *Saccharomyces cerevisiae* Strain JH301

The whole genome sequencing of *S. cerevisiae* strain JH301 was accomplished using the PacBio Sequel and Illumina MiSeq platforms. The sequencing quality data included sequence base quality by next-generation high-throughput sequencing technology (**Supplementary Figure 1**), length of reads by the long-read sequencing technology (**Supplementary Figure 2** and **Supplementary Table 1**), and assembly integrity of the whole genome of strain JH301 (**Supplementary Table 2**). The results of *de novo* assembly showed that the total sequence length of 11.97 Mb was predicted to contain 5,228 predicted genes in *S. cerevisiae* strain JH301. The genome was predicted to comprise 16 chromosomes by pairwise comparison against the chromosomes of the public reference strain S288c from the National Center for Biotechnology Information (NCBI). The genome characteristics of strain JH301 had considerable differences with S288c for genome parameters that include total sequence length. In addition, the number of rRNA in strain JH301 was 6.6-fold higher than strain S288c. **Table 4** summarizes the whole genome sequencing and annotation results. This whole genome shotgun project has been deposited at GenBank under the accession JALDNA000000000.

Among the 5,228 predicted genes in the entire strain genome, 3,155 (63.85%) genes could be annotated according to the KEGG database. These genes could be classified into five gene functional annotations: genetic information processing (2,237 genes), metabolism (1,421 genes), cellular processes (710 genes), environmental information processing (521 genes), and organismal systems (495 genes). Based on KEGG pathway mapping, we annotated 346 pathways in the JH301 genome. Of these, there are six main pathways related to urea metabolism. The overall response pathways are shown in **Figure 1**. (1) map00220: arginine biosynthesis (most

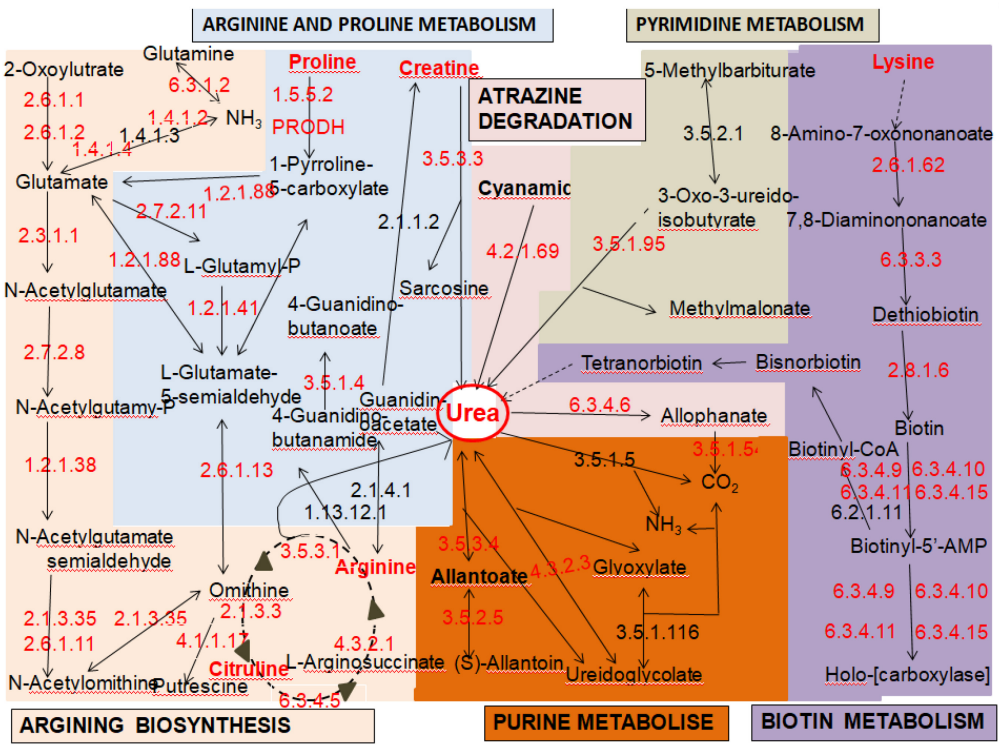

FIGURE 1 | Pathways related to the urea metabolism of *S. cerevisiae* strain JH301.

common pathway of urea metabolism), (2) map00230: purine metabolism, (3) map00240: pyrimidine metabolism, (4) map00330: arginine and proline metabolism, (5) map00780: biotin metabolism, and (6) map00791: atrazine degradation. The results showed that strain JH301 could convert amino acids such as arginine, citrulline, lysine, proline, and ornithine to produce urea. It also had urea carboxylase (EC6.3.4.6), urease (EC3.5.3.4), and ureidoglycolate lyase (EC4.3.2.3) to decompose urea.

Analysis of Key Genes Responsible for Low Urea Production of Strain JH301

A comparative genomic analysis between *S. cerevisiae* strain JH301 and the model *S. cerevisiae* strain S288c was performed

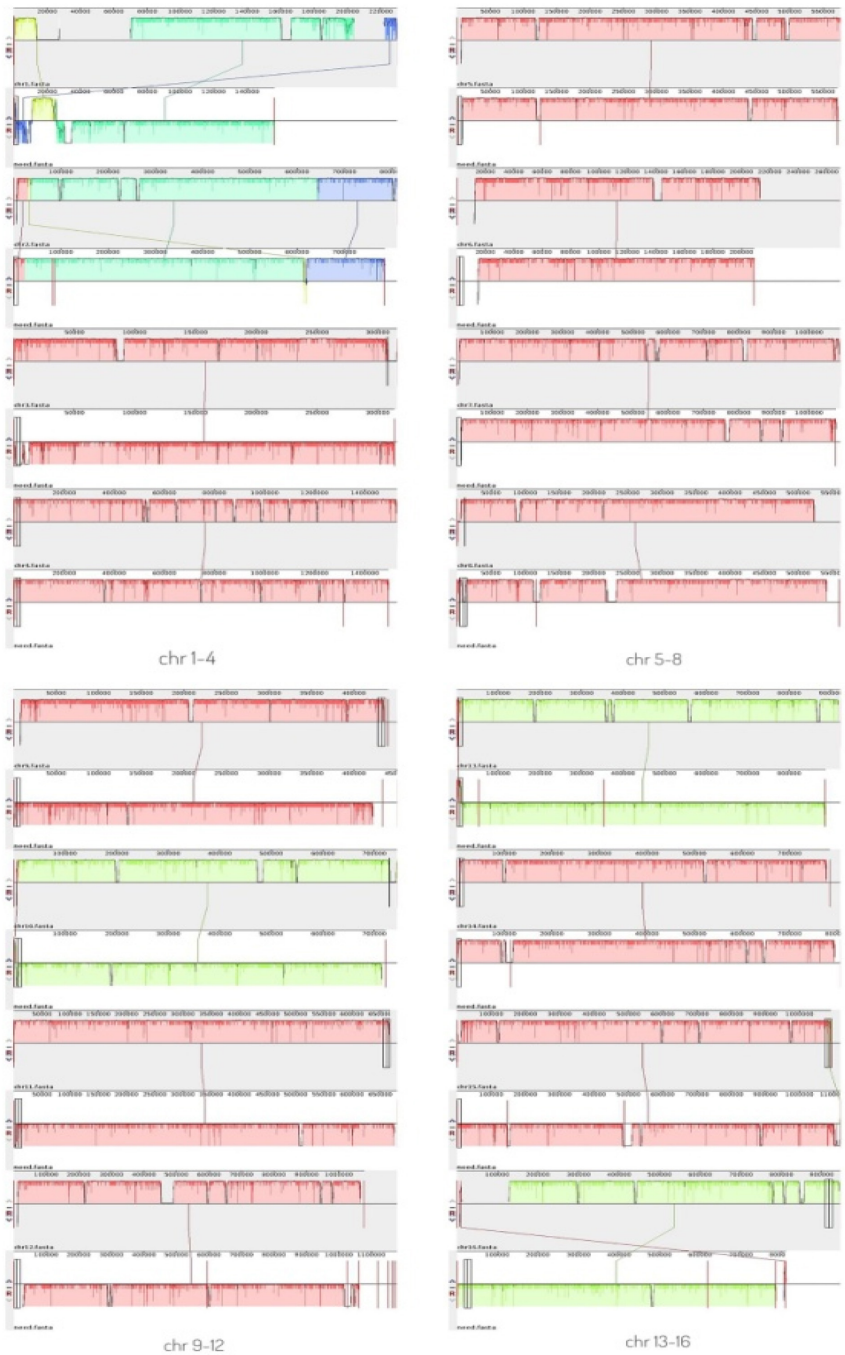

FIGURE 2 | Mauve analysis on 16 chromosomes between the genome of strains JH301 and S288c. The top bar shows the chromosome of strain JH301; the bottom bar shows the chromosome of strain S288c.

using MUMmer, Mauve, and OrthoMCL software. **Figure 2** compares the differential genes on 16 chromosomes between the genome of JH301 and S288c using the Mauve analysis. A detailed circular genome diagram between the genome of JH301 and S288c is shown in **Figure 3**. A total of 60,885 SNPs (53,933 homozygous SNPs, 6,952 heterozygous SNPs) and 5,412 InDels (<50 bp, 4,391 homozygous InDels, 1,021 heterozygous InDels) were detected. By annotating SNPs and InDels, we found 12,518 non-synonymous mutations and 25,551 synonym mutations in SNPs. There were 95 mutations leading to frameshift insertion (product extension) and 98 mutations leading to frameshift deletion (product shortening) in InDels. These results indicated that there were two types of chromosomal structural variations between the genome of JH301 and S288c. One type is a lack of fragments. The other is an increase in fragments. To identify species-specific genes, we performed pairwise comparisons using a series of All-VS-All BLASTP searches between the two strains in KEGG database and "PANTHER" Classification System.[1] **Figure 4** shows 4,770 genes identified based on sequence similarities: 234 genes and 1,246 genes were species-specific in *S. cerevisiae* strains JH301 and S288c, respectively.

We next performed KEGG pathway mapping of the species-specific genes. There were three species-specific genes referred to the urea production pathway that missed in strain JH301 but involved in S288c via comparative genomic analysis of the lack and increase of fragments. Three species-specific genes included the following: (1) The *ARG80* gene (NC_001145.3; in Chromosome: XIII) is for arginine metabolism regulation protein I (K19808). It is a key protein for pathway of arginine biosynthesis (map00220). (2) The *BIO3* gene (NC_001146.8; in Chromosome: XIV) is for adenosylmethionine-8-amino-7-oxononanoate aminotransferase protein (K00833), which is a key protein in the pathway of biotin metabolism (map00780). (3) The *VTC4* gene (NC_001142.9; in Chromosome: X) is for proline dehydrogenase protein (K00318) which is a key protein in the pathway of arginine and proline metabolism (map00330).

[1]http://www.pantherdb.org/

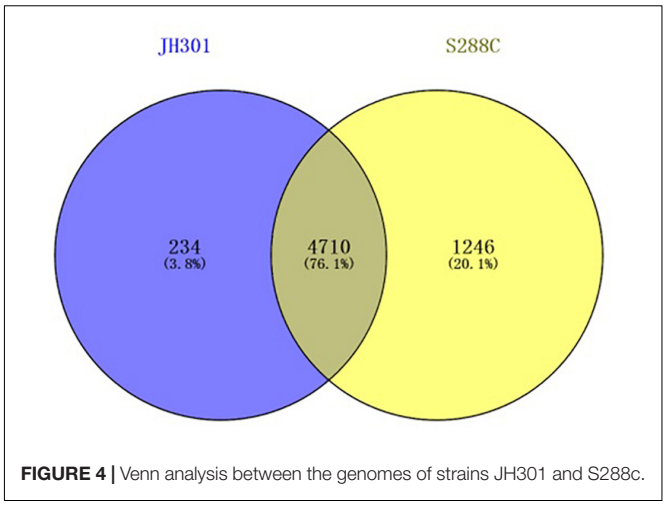

FIGURE 4 | Venn analysis between the genomes of strains JH301 and S288c.

Verification of Key Genes Responsible for Low Urea Production of Strain JH301

We further conducted PCR analysis of key genes to verify them at the DNA level. **Figure 5** shows that strain JH301 is not completely

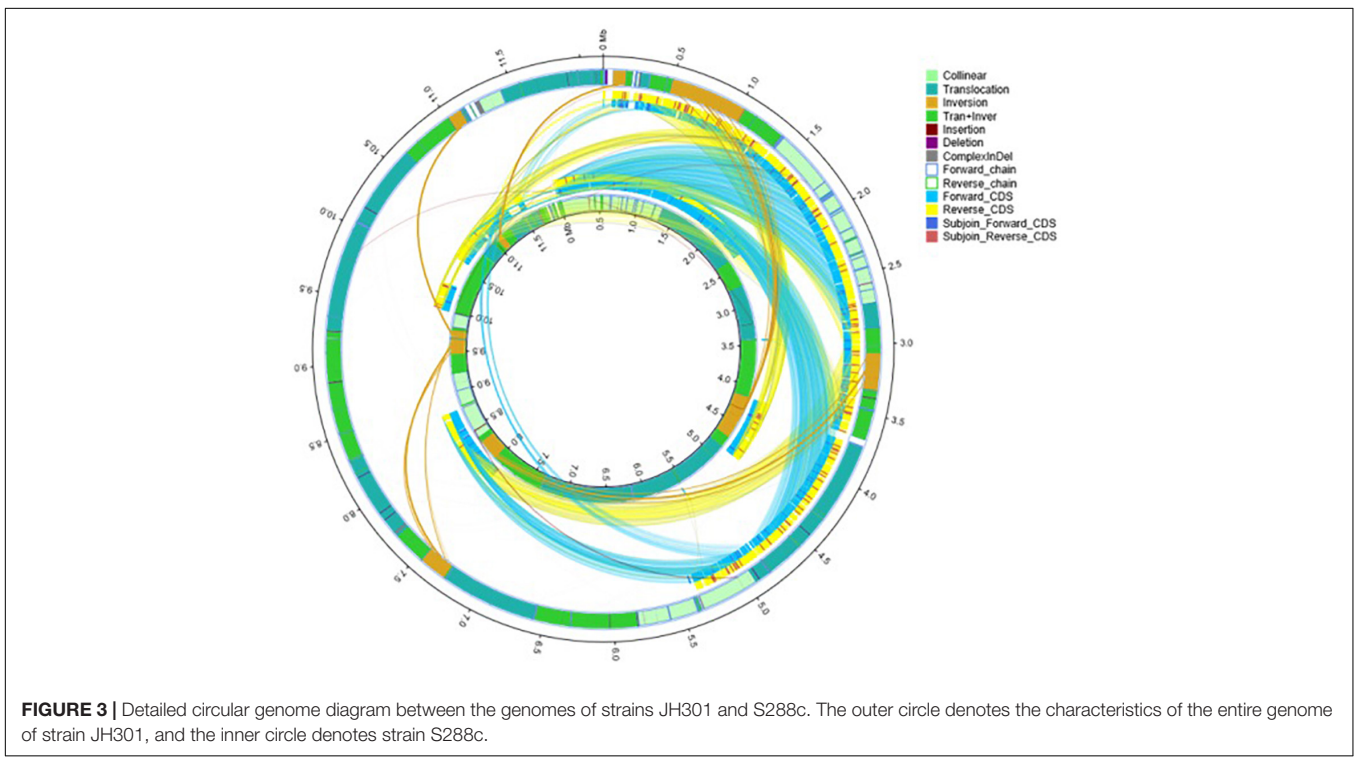

FIGURE 3 | Detailed circular genome diagram between the genomes of strains JH301 and S288c. The outer circle denotes the characteristics of the entire genome of strain JH301, and the inner circle denotes strain S288c.

missing from these three genes. This is probably because these three genes were also identified at other chromosomes along the whole genome of strain JH301. Therefore, the total expression levels of these three genes were further investigated by qRT-PCR to verify the key genes from the RNA level (Capece et al., 2016). **Table 5** show quantitative expression levels of these three genes investigated by quantitative real-time PCR vs. strain S288c, the expression levels of the *ARG80* gene in strain JH301 were significantly reduced 40.09 times ($P < 0.05$); and the expression levels of the other two genes were not significantly different ($P > 0.05$). The results showed that *ARG80* gene is likely to be the key gene responsible for low urea production. This gene had low expression and could restrict the expression of arginine metabolism regulation protein. Therefore, it should likely limit the pathways whereby arginine is converted to the urea in strain JH301.

TABLE 5 | Quantitative real-time PCR analysis results.

Gene name	Gene description	Sequence	Strain JH301	Strain S288c
ARG80	K19808	Chromosome: XIII; NC_001145.3	1.00 ± 0.05b	40.09 ± 0.32a
BIO3	K00833	Chromosome: XIV; NC_001146.8	1.06 ± 0.09a	1.11 ± 0.19a
VTC4	K00318	Chromosome: X; NC_001142.9	1.06 ± 0.32a	0.99 ± 0.39a

JH301 fermented using Saccharomyces cerevisiae strain JH301; S288c fermented using Saccharomyces cerevisiae strain S288c. Data represent the means of three biological replicates. Significant difference shown as lowercase letters means the significance level was lower than 0.05 ($P < 0.05$).

DISCUSSION

Next-generation high-throughput sequencing technology combined with long-read sequencing technology such as Pacific Biosciences (PacBio) can complete whole genome analysis of yeast (Goodwin et al., 2016). These data can mine key functional genes of *S. cerevisiae* vs. *S. cerevisiae* species model strain S288c (Baert et al., 2021). For example, some researchers have used this technique to study the whole genome of yeast Cen.PK113-7D and *Saccharomyces cerevisiae* S288c was used as the control to investigate functional genes related to the fermentation process in the strain Cen.PK113-7D (Jenjaroenpun et al., 2018). The key genes of low acetaldehyde production in brewer's yeast M14 were studied and compared to the S288c genome, and the molecular mechanism of low acetaldehyde production in this strain was described (Liu et al., 2018). The key genes of high ethanol tolerance in *Saccharomyces cerevisiae* YF17 were analyzed using *Saccharomyces cerevisiae* S288c and Japanese sake strain K7 as a control (Li et al., 2014). The differences between *Saccharomyces cerevisiae* N85 and sake yeast K7 in rice wine were also analyzed (Zhang et al., 2018). Therefore, we used the whole genome sequencing and comparative genomic analysis in this study and found that *ARG80* gene was the key gene responsible for low urea production of *S. cerevisiae* JH301 for the first time.

To the best of our knowledge, the urea metabolic pathway of *Saccharomyces cerevisiae* in rice wine mainly focuses on the arginine metabolic pathway (map00220 Arginine biosynthesis). Arginine is a conventional nitrogen source used by *Saccharomyces cerevisiae*. During the growth and reproduction of *Saccharomyces cerevisiae*, a large amount of urea is synthesized through argininase *car1* (Wu et al., 2014). It satisfies its own needs for growth, but the excess urea is secreted into the fermentation broth (Lee et al., 2017). When the utilization of ammonia is complete, *Saccharomyces cerevisiae* will start to use urea as a nitrogen source; urea is then decomposed into ammonia and carbon dioxide by the urea-amidase *DUR1* and *DUR2* (Gowd et al., 2018). Other studies found alternative key genes in the arginine biosynthesis pathway. For example, the expression of arginine transporter gene *VBA2* could be significantly up-regulated by adding bamboo leaf extract during fermentation (Zhou et al., 2020). The expression of arginine deiminase gene *adi* could be inhibited by added gallic acid and protocatechuic acid (Zhou et al., 2017). These both inhibited the transformation of arginine to produce urea. In this study, we found that the *ARG80* gene is also the key gene responsible for urea production of *S. cerevisiae* JH301. The *ARG80* gene is an important gene

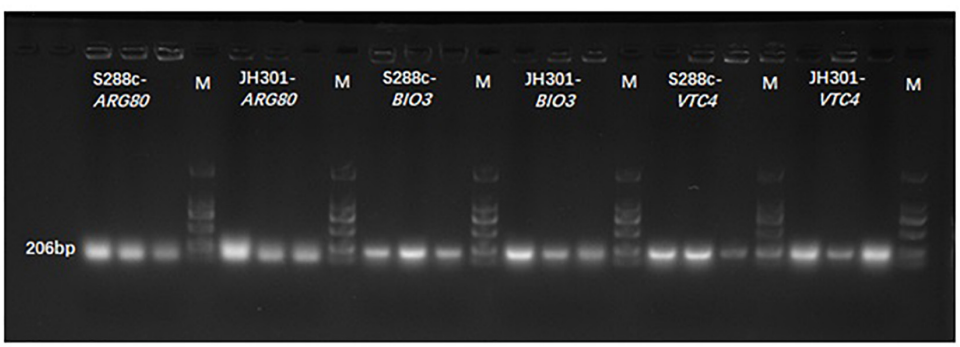

FIGURE 5 | Banding patterns of the PCR products. M means marker; S288c-*ARG80* means the PCR bands of *ARG80* gene of strain S288c; JH301-*ARG80* means the PCR bands of *ARG80* gene of strain JH301; S288c-*BIO3* means the PCR bands of *BIO3* gene of strain S288c; JH301-*BIO3* means the PCR bands of *BIO3* gene of strain JH301; S288c-*VTC4* means the PCR bands of *VTC4* gene of strain S288c; JH301-*VTC4* means the PCR bands of *VTC4* gene of strain JH301.

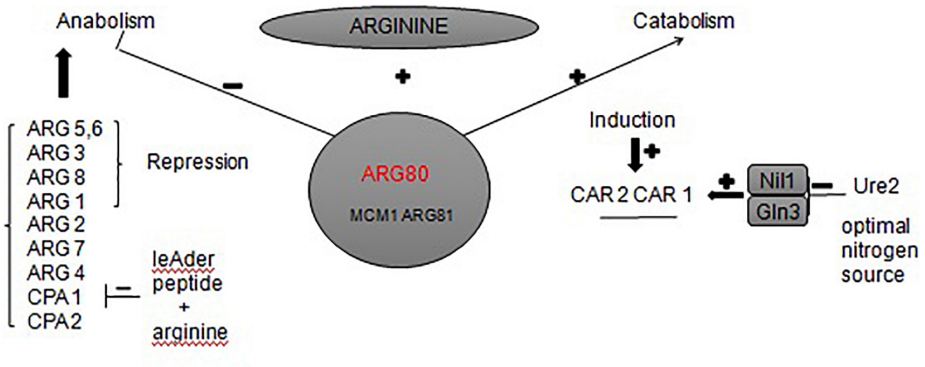

FIGURE 6 | Network of regulatory circuits controlling the arginine anabolic and catabolic genes in response to nitrogen signals.

for the transport of arginine to yeast cells and is one of the four regulatory genes in the regulation of arginine metabolism (Kloosterman and Kuipers, 2013). **Figure 6** summarizes different regulations involved in the control of the expression of arginine anabolic and catabolic genes. *ARG80*, *ARG81,* and *MCM1* could form a complex interacting with DNA sequences called »arginine boxes« present in the promoters of arginine co-regulated genes (Messenguy and Dubois, 1999). In the presence of arginine, they are required to repress the synthesis of five anabolic enzymes and to induce the synthesis of two catabolic enzymes (Jamai et al., 2002). If *ARG80* gene had low expression, it could restrict the activity of arginine metabolism regulation protein. Therefore, this gene is likely one of the main reasons for the low urea production of strain JH301 during Hongqu Huangjiu fermentation. Further studies can verify the function of this gene through construction of new engineering strains such as *ARG80* gene overexpression in strain JH301 and *ARG80* gene knockout in strain S288c.

Ethanol reacts with the urea produced during metabolism of arginine to give EC. Previous studies have reported that the formation of EC in wine was correlated to the concentration of urea, and the concentration increased substantially with increasing temperature (Weber and Sharypov, 2009). Increased EC content during fermentation increases the risk of cancer through consumption of alcoholic beverages (Jiao et al., 2014). Therefore, it is imperative to control urea content to control EC content. Further research will focus on regulating the expression of the key gene *ARG80* to decrease the urea content during Hongqu Huangjiu fermentation. This step is useful to control the quality and safety of Hongqu Huangjiu.

CONCLUSION

In conclusion, we assessed the whole genome of *S. cerevisiae* strain JH301 using next-generation high-throughput sequencing technology in MiSeq from Illumina and the long-read sequencing technology in PacBio Sequel platform. We also found that gene *ARG80* is likely to be responsible for the low urea production of strain JH301 for the first time using comparative genomics analysis vs. *Saccharomyces cerevisiae* model strain S288c. Finally, we used PCR and qRT-PCR analyses to verify the key genes from DNA and RNA levels. Further studies can verify the functions of this gene via gene overexpression and gene knockout techniques. The results are important to control the urea and EC contents in Hongqu Huangjiu production.

DATA AVAILABILITY STATEMENT

The datasets presented in this study can be found in online repositories. This whole genome shotgun project has been deposited at GenBank under the accession JALDNA000000000.

AUTHOR CONTRIBUTIONS

ZL and ZH: conceptualization. ZL, HS, XR, XZL, and XYL: methodology. ZL and HS: software. ZL, XZL, and ZH: validation. ZH: formal analysis, writing—review, and editing. XZL: investigation. ZL and YZ: data curation. ZL: writing—original draft preparation and visualization. All authors have read and agreed to the published version of the manuscript.

FUNDING

This study was financially supported by the Natural Science Foundation of Fujian Province, China (No. 2021J01501).

ACKNOWLEDGMENTS

We thank Shanghai Personal Biotechnology Co., Ltd. (Shanghai, China) for the whole genome analysis. We thank LetPub (www.letpub.com) for its linguistic assistance during the preparation of this manuscript.

SUPPLEMENTARY MATERIAL

The Supplementary Material for this article can be found online at: https://www.frontiersin.org/articles/10.3389/fmicb.2022.894661/full#supplementary-material

REFERENCES

Baert, L., McClure, P., Winkler, A., Karn, J., Bouwknegt, M., and Klijn, A. (2021). Guidance document on the use of whole genome sequencing (WGS) for source tracking from a food industry perspective. *Food Control* 130:108148. doi: 10.1016/j.foodcont.2021.108148

Capece, A., Votta, S., Guaragnella, N., Zambuto, M., Romaniello, R., and Romano, P. (2016). Comparative study of *Saccharomyces cerevisiae* wine strains to identify potential marker genes correlated to desiccation stress tolerance. *FEMS Yeast Res.* 16:fow015. doi: 10.1093/femsyr/fow015

Clark, S., Francis, P. S., Conlan, X. A., and Barnett, N. W. (2007). Determination of urea using high-performance liquid chromatography with fluorescence detection after automated derivatisation with xanthydrol. *J. Chromatogr. A* 1161, 207–213. doi: 10.1016/j.chroma.2007.05.085

De Melo Pereira, G. V., Ramos, C. L., Galvão, C., Souza Dias, E., and Schwan, R. F. (2010). Use of specific PCR primers to identify three important industrial species of *Saccharomyces* genus: *Saccharomyces cerevisiae*, *Saccharomyces bayanus* and *Saccharomyces pastorianus*. *Lett. Appl. Microbiol.* 51, 131–137. doi: 10.1111/j.1472-765X.2010.02868.x

Duarte, W. F., Dias, D. R., de Melo Pereira, G. V., Gervásio, I. M., and Schwan, R. F. (2009). Indigenous and inoculated yeast fermentation of gabiroba (*Campomanesia pubescens*) pulp for fruit wine production. *J. Ind. Microbiol. Biotechnol.* 36, 557–569. doi: 10.1007/s10295-009-0526-y

Fang, F., Qiu, Y., Du, G., and Chen, J. (2018). Evaluation of ethyl carbamate formation in Luzhou-flavor spirit during distillation and storage processes. *Food Biosci.* 23, 137–141. doi: 10.1016/j.fbio.2018.02.007

Fischer, S., Olsen, K. W., Nam, K., and Karplus, M. (2011). Unsuspected pathway of the allosteric transition in hemoglobin. *Proc. Natl. Acad. Sci.* 108:5608. doi: 10.1073/pnas.1011995108

Goodwin, S., McPherson, J., and McCombie, W. (2016). Coming of age: ten years of next-generation sequencing technologies. *Nat. Rev. Genet.* 17, 333–351. doi: 10.1038/nrg.2016.49

Gowd, V., Su, H., Karlovsky, P., and Chen, W. (2018). Ethyl carbamate: an emerging food and environmental toxicant. *Food Chem.* 248, 312–321. doi: 10.1016/j.foodchem.2017.12.072

Huang, Z., Guo, W., Zhou, W., Li, L., Xu, J., Hong, J., et al. (2019). Microbial communities and volatile metabolites in different traditional fermentation starters used for Hong Qu glutinous rice wine. *Food Res. Int.* 121, 593–603. doi: 10.1016/j.foodres.2018.12.024

Huang, Z., Hong, J., Xu, J., Li, L., Guo, W., Pan, Y., et al. (2018). Exploring core functional microbiota responsible for the production of volatile flavour during the traditional brewing of Wuyi Hong Qu glutinous rice wine. *Food Microbiol.* 76, 487–496. doi: 10.1016/j.fm.2018.07.014

Jamai, A., Dubois, E., Vershon Andrew, K., and Messenguy, F. (2002). Swapping functional specificity of a MADS box protein: residues required for arg80 regulation of arginine metabolism. *Mol. Cell. Biol.* 22, 5741–5752. doi: 10.1128/MCB.22.16.5741-5752.2002

Jenjaroenpun, P., Wongsurawat, T., Pereira, R., Patumcharoenpol, P., Ussery, D. W., Nielsen, J., et al. (2018). Complete genomic and transcriptional landscape analysis using third-generation sequencing: a case study of *Saccharomyces cerevisiae* CEN.PK113-7D. *Nucleic Acids Res.* 46, 32–38. doi: 10.1093/nar/gky014

Jiao, Z., Dong, Y., and Chen, Q. (2014). Ethyl carbamate in fermented beverages: presence, analytical chemistry, formation mechanism, and mitigation proposals. *Compr. Rev. Food Sci. Food Saf.* 13, 611–626. doi: 10.1111/1541-4337.12084

Kloosterman, T. G., and Kuipers, O. P. (2013). Regulation of arginine acquisition and virulence gene expression in the human pathogen *Streptococcus pneumoniae* by transcription regulators ArgR1 and AhrC. *J. Biol. Chem.* 288:10950. doi: 10.1074/jbc.A111.295832

Kuribayashi, T., Sato, K., Joh, T., and Kaneoke, M. (2017). Breeding of a non-urea-producing sake yeast carrying a FAS2 mutation. *Mycoscience* 58, 302–306. doi: 10.1016/j.myc.2017.02.005

Lachenmeier, D. W., Nerlich, U., and Kuballa, T. (2006). Automated determination of ethyl carbamate in stone-fruit spirits using headspace solid-phase microextraction and gas chromatography–tandem mass spectrometry. *J. Chromatogr. A* 1108, 116–120. doi: 10.1016/j.chroma.2005.12.086

Lee, G., Bang, D., Lim, J., Yoon, S., Yea, M., and Chi, Y. (2017). Simultaneous determination of ethyl carbamate and urea in Korean rice wine by ultra-performance liquid chromatography coupled with mass spectrometric detection. *J. Chromatogr. B* 1065-1066, 44–49. doi: 10.1016/j.jchromb.2017.09.011

Li, Y., Zhang, W., Zheng, D., Zhou, Z., Yu, W., Zhang, L., et al. (2014). Genomic evolution of *Saccharomyces cerevisiae* under Chinese rice wine fermentation. *Genome Biol. Evol.* 6, 2516–2526. doi: 10.1093/gbe/evu201

Liang, Z., Lin, X., He, Z., Su, H., Li, W., and Guo, Q. (2020a). Comparison of microbial communities and amino acid metabolites in different traditional fermentation starters used during the fermentation of Hong Qu glutinous rice wine. *Food Res. Int.* 136:109329. doi: 10.1016/j.foodres.2020.109329

Liang, Z., Lin, X., He, Z., Su, H., Li, W., and Ren, X. (2020b). Amino acid and microbial community dynamics during the fermentation of Hong Qu glutinous rice wine. *Food Microbiol.* 90:103467. doi: 10.1016/j.fm.2020.103467

Liang, Z., Lin, X., He, Z., Li, W., Ren, X., and Lin, X. (2020c). Dynamic changes of total acid and bacterial communities during the traditional fermentation of Hong Qu glutinous rice wine. *Electron. J. Biotechnol.* 43, 23–31. doi: 10.1016/j.ejbt.2019.12.002

Liu, C., Niu, C., Zhao, Y., Tian, Y., Wang, J., and Li, Q. (2018). Genome analysis of the Yeast M14, an industrial brewing yeast strain widely used in China. *J. Am. Soc. Brew. Chem.* 76, 223–235. doi: 10.1080/03610470.2018.1496633

Liu, Q., Jin, X., Fang, F., Li, J., Du, G., and Kang, Z. (2019). Food-grade expression of an iron-containing acid urease in *Bacillus subtilis*. *J. Biotechnol.* 293, 66–71. doi: 10.1016/j.jbiotec.2019.01.012

Luo, L., Lei, H., Yang, J., Liu, G., Sun, Y., Bai, W., et al. (2017). Development of an indirect ELISA for the determination of ethyl carbamate in Chinese rice wine. *Anal. Chim. Acta* 950, 162–169. doi: 10.1016/j.aca.2016.11.008

Lv, X., Cai, Q., Ke, X., Chen, F., Rao, P., and Ni, L. (2015). Characterization of fungal community and dynamics during the traditional brewing of Wuyi Hong Qu glutinous rice wine by means of multiple culture-independent methods. *Food Control* 54, 231–239. doi: 10.1016/j.foodcont.2015.01.046

Messenguy, F., and Dubois, E. (1999). Regulation of arginine metabolism in *Saccharomyces cerevisiae*: a network of specific and pleiotropic proteins in response to multiple environmental signals. *Food Technol. Biotechnol.* 38, 277–285. doi: 10.1016/0378-1119(87)90287-3

Moriya, T., Hiraishi, K., Horie, N., Mitome, M., and Shinohara, K. (2007). Correlative association between circadian expression of mouse Per2 gene and the proliferation of the neural stem cells. *Neuroscience* 146, 494–498. doi: 10.1016/j.neuroscience.2007.02.018

Pfaffl, M. W. (2001). A new mathematical model for relative quantification in real-time RT–PCR. *Nucleic Acids Res.* 29, 40–45. doi: 10.1093/nar/29.9.e45

Shalhub, S., Black, J. H., Cecchi, A. C., Xu, Z., Griswold, B. F., Safi, H. J., et al. (2014). Molecular diagnosis in vascular ehlers-danlos syndrome predicts pattern of arterial involvement and outcomes. *J. Vasc. Surg.* 60, 160–169. doi: 10.1016/j.jvs.2014.01.070

Vázquez, L., Prados, I. M., Reglero, G., and Torres, C. F. (2017). Identification and quantification of ethyl carbamate occurring in urea complexation processes commonly utilized for polyunsaturated fatty acid concentration. *Food Chem.* 229, 28–34. doi: 10.1016/j.foodchem.2017.01.123

Weber, J. V., and Sharypov, V. I. (2009). "Ethyl carbamate in foods and beverages – a review," in *Climate Change, Intercropping, Pest Control and Beneficial Microorganisms: Climate change, intercropping, Pest Control and Beneficial Microorganisms*, ed. E. Lichtfouse (Dordrecht: Springer). doi: 10.1007/978-90-481-2716-0_15

Wu, D., Li, X., Lu, J., Chen, J., Xie, G., and Zhang, L. (2016). The overexpression of DUR1,2 and deletion of CAR1 in an industrial *Saccharomyces cerevisiae* strain and effects on nitrogen catabolite repression in Chinese rice wine production. *J. Inst. Brew.* 122, 480–485. doi: 10.1002/jib.347

Wu, D., Li, X., Shen, C., Lu, J., Chen, J., and Xie, G. (2014). Decreased ethyl carbamate generation during Chinese rice wine fermentation by disruption of CAR1 in an industrial yeast strain. *Int. J. Food Microbiol.* 180, 19–23. doi: 10.1016/j.ijfoodmicro.2014.04.007

Xian, Y., Wu, Y., Dong, H., Liang, M., Wang, B., Wang, L., et al. (2019). Ice-bath assisted sodium hydroxide purification coupled with GC–MS/MS analysis for simultaneous quantification of ethyl carbamate and 12 N-nitrosoamines in

yellow rice wine and beer. *Food Chem.* 300:125200. doi: 10.1016/j.foodchem.2019.125200

Yang, L., Liu, X., Zhou, N., and Tian, Y. (2019). Characteristics of refold acid urease immobilized covalently by graphene oxide-chitosan composite beads. *J. Biosci. Bioeng.* 127, 16–22. doi: 10.1016/j.jbiosc.2018.06.012

Yoshiuchi, K., Watanabe, M., and Nishimura, A. (2000). Breeding of a non-urea producing sake yeast with killer character using a kar1-1 mutant as a killer donor. *J. Ind. Microbiol. Biotechnol.* 24, 203–209. doi: 10.1038/sj.jim.2900797

Zhang, W., Li, Y., Chen, Y., Xu, S., Du, G., Shi, H., et al. (2018). Complete genome sequence and analysis of the industrial *Saccharomyces cerevisiae* strain N85 used in Chinese rice wine production. *DNA Res.* 25, 297–306. doi: 10.1093/dnares/dsy002

Zhou, W., Fang, R., and Chen, Q. (2017). Effect of gallic and protocatechuic acids on the metabolism of ethyl carbamate in Chinese yellow rice wine brewing. *Food Chem.* 233, 174–181. doi: 10.1016/j.foodchem.2017.04.113

Zhou, W., Hu, J., Zhang, X., and Chen, Q. (2020). Application of bamboo leaves extract to Chinese yellow rice wine brewing for ethyl carbamate regulation and its mitigation mechanism. *Food Chem.* 319:126554. doi: 10.1016/j.foodchem.2020.126554

Conflict of Interest: XYL was employed by Fujian Pinghuhong Biological Technology Co., Ltd.

The remaining authors declare that the research was conducted in the absence of any commercial or financial relationships that could be construed as a potential conflict of interest.

frontiers | Frontiers in Microbiology

MINI-REVIEW
published: 29 April 2022
doi: 10.3389/fmicb.2022.896556

Aerospace Technology Improves Fermentation Potential of Microorganisms

Yan Chi[1], Xuejiang Wang[1], Feng Li[1], Zhikai Zhang[1] and Peiwen Tan[2]*

[1] Wuzhoufeng Agricultural Science and Technology Co., Ltd., Yantai, China, [2] Department of Computer Science, University of California, Irvine, Irvine, CA, United States

It is highly possible to obtain high-quality microbial products in appreciable amounts, as aerospace technology is advancing continuously. Genome-wide genetic variations in microorganisms can be triggered by space microgravity and radiation. Mutation rate is high, mutant range is wide, and final mutant character is stable. Therefore, space microorganism breeding is growing to be a new and promising area in microbial science and has greatly propelled the development of fermentation technology. Numerous studies have discovered the following improvements of fermentation potential in microorganisms after exposure to space: (1) reduction in fermentation cycle and increase in growth rate; (2) improvement of mixed fermentation species; (3) increase in bacterial conjugation efficiency and motility; (4) improvement of the bioactivity of various key enzymes and product quality; (5) enhancement of multiple adverse stress resistance; (6) improvement of fermentation metabolites, flavor, appearance, and stability. Aerospace fermentation technology predominantly contributes to bioprocessing in a microgravity environment. Unlike terrestrial fermentation, aerospace fermentation keeps cells suspended in the fluid medium without significant shear forces. Space radiation and microgravity have physical, chemical, and biological effects on mutant microorganisms by causing alternation in fluid dynamics and genome, transcriptome, proteome, and metabolome levels.

Keywords: extreme environment, microorganism, production improvement, fermentation improvement, genetic mutant, aerospace technology

OPEN ACCESS

Edited by:
Xucong Lv,
Fuzhou University, China

Reviewed by:
Xia Wan,
Oil Crops Research Institute (CAAS), China
Junfeng Wang,
People's Liberation Army General Hospital, China

****Correspondence:***
Yan Chi
1115625548@qq.com

Specialty section:
This article was submitted to Food Microbiology, a section of the journal Frontiers in Microbiology

Received: *15 March 2022*
Accepted: *29 March 2022*
Published: *29 April 2022*

Citation:
Chi Y, Wang X, Li F, Zhang Z and Tan P (2022) Aerospace Technology Improves Fermentation Potential of Microorganisms. Front. Microbiol. 13:896556. doi: 10.3389/fmicb.2022.896556

INTRODUCTION

Microorganism fermentation is the most prominent and rapidly growing segment of biological sciences, and fermentation of microbes and their products are closely associated with agriculture and the food and pharmaceutical industries (Kalsoom et al., 2020). However, there are some challenges for industrial fermentation, including limited biomass, time-consuming to reach steady-state and low cell densities (Yang and Sha, 2019), and low yields and nutri. Electrical energy is mainly used for industrial fermentation. However, electrical fields may affect the fermentation bioprocess by altering its micronutrients (Gavahian and Tiwari, 2020). Semi-solid and submerged fermentations have been widely conducted in industries but with low-level yields and time spent because of terrestrial gravity. The space's extreme environment, with high-level radiation and microgravity, may address these important issues *via* wide-range mutants.

The space's extreme environment, with a temperature above absolute zero degrees, mainly includes microgravity, space radiation (in the form of rays, electromagnetic waves, and/or high energic particles), the ionosphere ionized by solar and cosmic radiations, ultra-vacuum, etc. (**Figure 1**). Space microgravity is defined as gravity less than 10^{-4} G (1 G is defined as 9.8 m/s^2) in the space's environment. Under the space environment, mutant DNA occurs at a global chromosomal level because of the deletion, replacement, or insertion of bases, which is higher than on the earth (Mulkey, 2010) and improves the fermentation potentials of microorganisms, such as *Lactobacillus acidophilus* (Shao et al., 2017), *Saccharomyces cerevisiae* (Liu et al., 2008), and *Bacillus subtilis* (Nicholson and Ricco, 2019).

Since September 21, 1992, China Manned Space Engineering has been burgeoning. In the past 30 years, it has attained significant success in aerospace technology, including the launch of a series of Shenzhou spacecraft. China started space microorganism experiments in the Shenzhou I spacecraft on November 20, 1999 (Fang et al., 2005), and has accumulated a visual experience in effects of the space's extreme environment on microorganisms (**Figure 1** and **Supplementary Table 1**). In September 2010, China officially launched its space station program, and space microorganism sciences have been steadily developing ever since (Long, 2016). On November 1, 2011, the Shenzhou VIII spacecraft began a large-scale space microbiology experiment equipped with 15 microorganisms (Su et al., 2013). The study revealed changes in bacterial invasion, antibiotic resistance, and environmental adaptation. The mechanisms may be caused by various factors, including genome, transcriptome, proteome, and metabolome. On the same date, engineered bacterial strains with recombinant human interferon a1b were launched into the space station. Five mutant engineered bacterial strains showed significantly higher production of recombinant human interferon a1b and one strain with twofold increase in antibiotic activities (Wang et al., 2014). The mutant tetrodotoxin strains *via* spatial mutagenesis can be used for industrial production of toxins. After purification of toxins, they are mainly used for detoxification and effectively reduce the relapse rate of addicts (China patent no. CN103160454B) (Mulkey, 2010). On June 11, 2013, *Lysobacter enzymogenes* was trained in the space environment *via* the Shenzhou X spacecraft (Liu, 2017). The mutants showed increase in the production of endoproteinase Lys-C by up to 40.2% with perfect stability. On October 17, 2016, *Acinetobacter baumannii* was trained in the space environment *via* the Shenzhou XI spacecraft. The ability for biofilm formation of the mutant strain was reduced (Zhao et al., 2019).

The effect of the space environment on production of antibiotic actinomycin D by *Streptomyces plicatus* was tested in US Space Shuttle STS-80. The space flight reduced the number of cells in CFU/ml of *S. plicatus* and increased the productivity of actinomycin D (Lam et al., 2002). Deletion of the ribosomal protein gene in the yeast *Saccharomyces cerevisiae* was detected after flight in the Russian space station, suggesting that space radiation containing high-linear energy transfer causes deletion-type mutants (Fukuda et al., 2000). In another study, three fungal species, *Aspergillus sydowii*, *Penicillium palitans*, and *Rhodotorula mucilaginosa,* grew in the Japanese Space Station KIBO for 7 years and the fungi are still increasing and expanding over time (Satoh et al., 2021).

Whole-genome sequencing and bioinformatics indicated changes at the genome, transcriptome, proteome, and metabolome levels, which contribute to phenotypic changes of mutant strains (Kimura et al., 2006; Sakai et al., 2018). Most mutants may be induced with improvement of fermentation potentials *via* the space's extreme environment. Mutants can be screened *via* high-throughput techniques in a laboratory on Earth and can be found with improvement in fermented microorganisms, including (1) shortened fermentation cycle and increased growth rate because of decreasing lag phase and prolonging exponential phase *via* upregulation of DNA replicon gene (*srmB*) and repression of nucleoside metabolism genes (dfp, pyrD, and spoT) (Arunasri et al., 2013; Senatore et al., 2018); (2) optimization of fermented mixed species (Zongzhou and Yaping, 2009); (3) increase in bacterial conjugation efficiency and motility by stimulation of plasmid transfer (Beuls et al., 2009) and gene regulation of flagellar synthesis and function and/or taxis (Acres et al., 2021); motility induces three-dimensional transitions of bacterial monolayers (Takatori and Mandadapu, 2020); (4) improvement of key enzyme bioactivity and product quality (Zhang et al., 2015); and (5) improvement of metabolite production, flavor, appearance, and stability (**Figure 1** and **Supplementary Table 1**; Bin et al., 2015; Senatore et al., 2020). Therefore, aerospace technology provides an unprecedented platform for exploring microorganism's utilization systems.

MECHANISMS FOR THE PHYSICAL, CHEMICAL, AND BIOLOGICAL EFFECTS OF SPACE MICROGRAVITY AND RADIATION ON THE FERMENTATION POTENTIAL OF MICROORGANISMS

Space microgravity induces mutant microorganisms. Microgravity can affect physical and chemical environmental parameters and induce mutant strains. Kanglemycin C is an immunosuppressant produced by *Nocardia mediterranei var. kanglensis* but with limited yields. Space flight can induce Kanglemycin C-producing mutant strains with high-level products (Zhou et al., 2006). The marine bacterium *Vibrio fischeri* was tested during long-duration spaceflight. The results showed that rodA was depleted, but that impacts on symbiont genes were minimal under microgravity (Burgos et al., 2020). On the other hand, microgravity may increase bacterial conjugation efficiency by stimulating plasmid transfer (De Boever et al., 2007). Some phenotype changes of space microorganisms may be caused by alternation in the metabolic pathway and fluid dynamics.

Although the space's microgravity can induce microbe mutants at the genome, transcriptome, proteome, and metabolome levels, the exact mechanism for microgravity-inducing mutants remains unclear. Molecular weight affects steric forces, interfacial tension, and surface viscosity, which all have an influence on molecule distribution

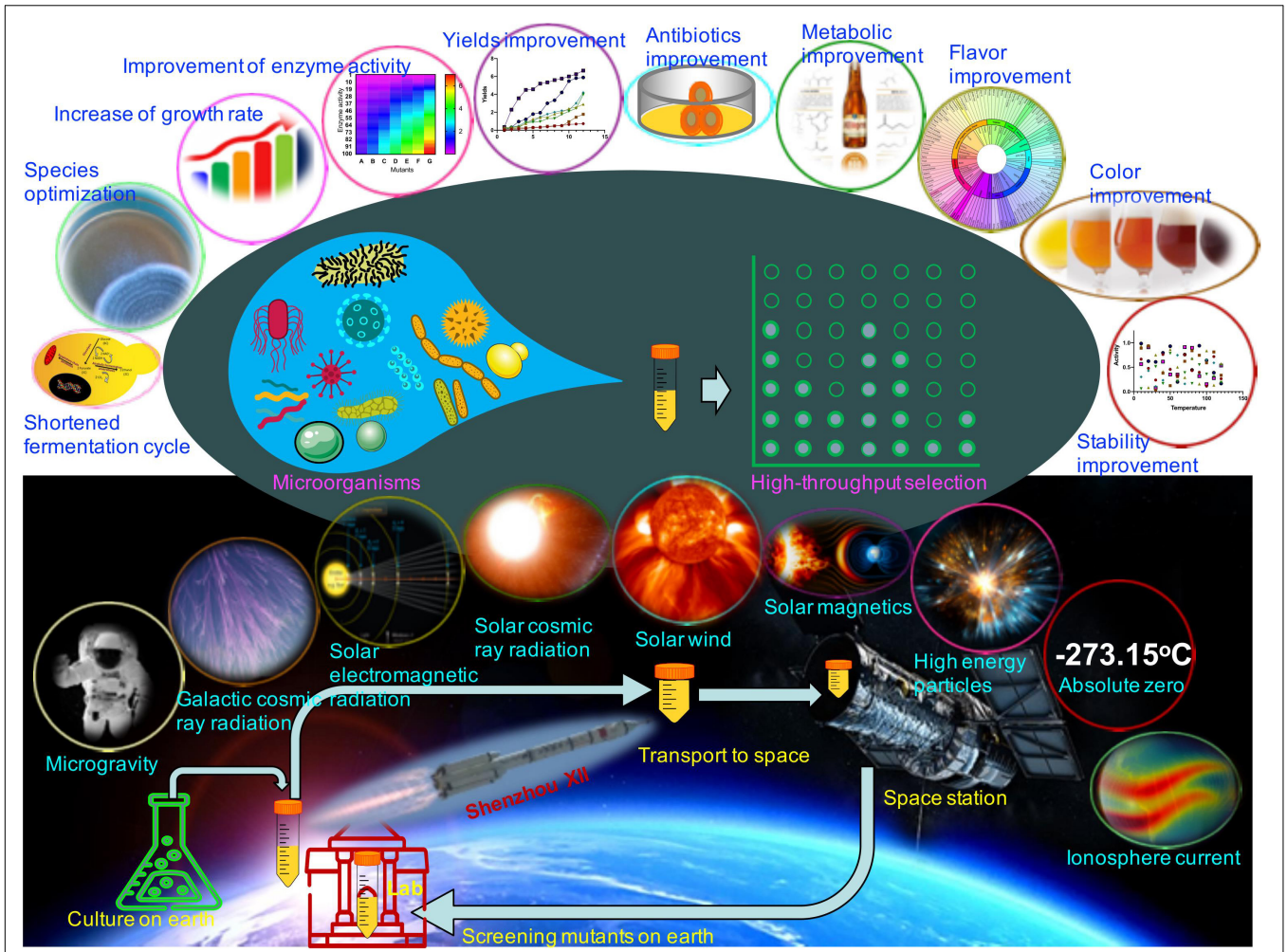

FIGURE 1 | Possible effects of the space's extreme environment on the fermentation potential of microorganisms. The space's environment mainly includes microgravity, space radiation (galactic cosmic ray, electromagnetic waves, solar cosmic ray, solar wind, and solar magnetic and/or high energetic particles), ionosphere current, and a degree above absolute zero. Most microorganism mutants may be induced with the improvement of fermentation potentials *via* the space's extreme environment, including species, growth rate, enzyme activities, product yields, antibiotic activities, metabolite composition, fermentation flavor and color, and strain stability (**Supplementary Table 1**).

(Bąk and Podgórska, 2016). Thus, microgravity will change these parameters, which possibly affect protein crystallization (Durbin and Feher, 1996). Protein crystallization is found to be easily formed in the space's microgravity environment (Scott and Vonortas, 2021). Therefore, we propose that microgravity will affect the physical environment of biological molecules and their interaction. Changes in macromolecules interaction will lead to changes in genome structure, transcriptome, proteome, metabolome, and glycomics (**Figure 2A**).

SPACE RADIATION INDUCES MUTANT MICROORGANISMS

Space is filled with high-energy particles (including alpha, protons, electrons, and neutrons) and electromagnetic waves (gamma rays and X-rays), which can cause high-level mutation of DNAs and proteins. Space radiation causes changes in spore survival and rifampicin resistance in Bacillus species by inducing amino acid mutants at sites Q469L, A478V, and H482P/Y (Moeller et al., 2010). An interplay between microgravity and space radiation can induce DNA strand breaks, chromosome abnormalities, micronucleus formation, or various mutants (Moreno-Villanueva et al., 2017). Some forms of radiation affect the ability for microbial biofilm formation by surface barrier discharge (Salgado et al., 2021). *S. cerevisiae* irradiated with gamma rays had genome-wide variants because of DNA strand break (Chan et al., 2007).

Space radiation has physical, chemical, and biological effects on mutant microorganisms with various rays and particles. X-ray and alpha-particles induce DNA double-strand break (Newman et al., 1997) and UV- and gamma-irradiation-induced DNA single-strand breaks in microorganisms (**Figure 2B**; Lankinen et al., 1996). An electron particle or X-ray triggers H_2O molecules

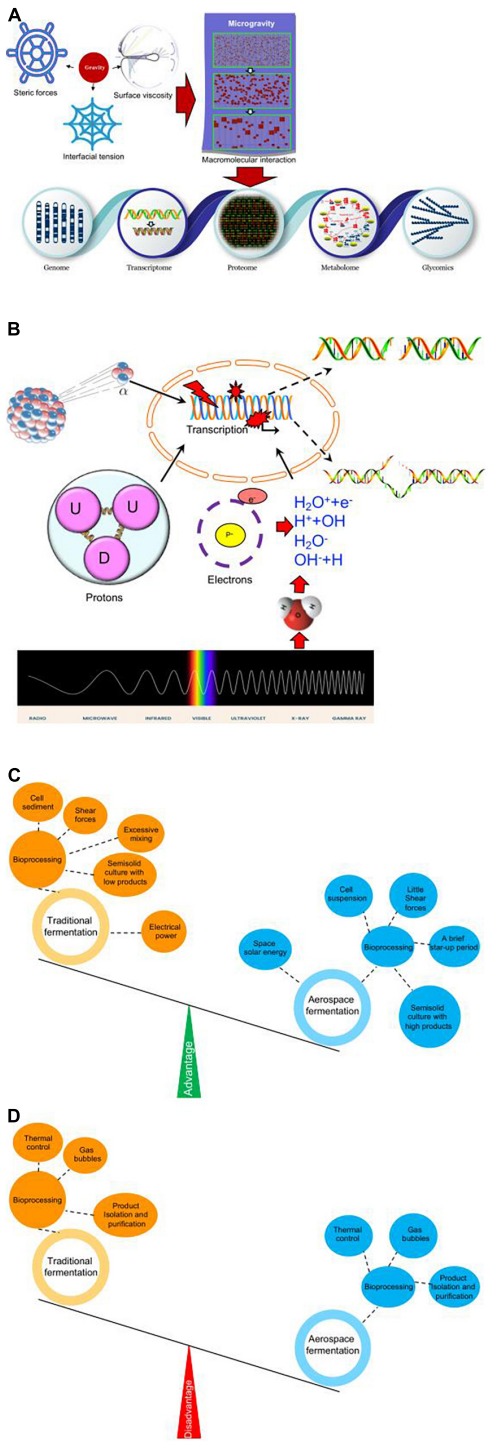

FIGURE 2 | Possible functional mechanisms for space microbiology technology. **(A)** Possible physical and molecular mechanisms for space microgravity-inducing mutant microorganisms. **(B)** Physical, chemical, and biological effects of space radiation. X-ray and alpha-particles induce DNA double-strand break and UV irradiation and gamma irradiation induce DNA single-strand breaks. **(C)** Advantages of space fermentation technology when compared with terrestrial fermentation technology. **(D)** Disadvantages of space fermentation technology when compared with terrestrial fermentation technology.

to ionize and disrupt, and produce low-energy electrons and OH-radicals, which contribute to DNA strand break (**Figure 2B**).

COMPARISON OF TERRESTRIAL FERMENTATION AND SPACE FERMENTATION TECHNOLOGY

Aerospace fermentation technology predominantly contributes to bioprocessing with its unique space microgravity environment. Unlike terrestrial fermentation, aerospace fermentation keeps cells suspended in the fluid medium without significant shear forces, which are often caused by stirred terrestrial systems (**Figure 2C**). A space fermentation device, clinostat, provides a method of keeping cell movement in liquid without introducing excessive mixing *via* the rotational velocity of vessel's inner walls (Topolski, 2021). Meanwhile, cell sedimentation can be prevented *via* microgravity (**Figure 2C**). On the other hand, semi-solid culture is often limited to low-level target products in a terrestrial lab because of gravity, which can be overcome *via* space fermentation technology (**Figure 2C**). Finally, energy can be saved during space fermentation *via* space solar energy, while electrical power is a predominant way to supply energy during terrestrial fermentation (**Figure 2C**). Certainly, there are some disadvantages for space fermentation technology when compared with terrestrial fermentation; there are some difficulties in dealing with thermal control, gas bubbles, and product isolation and purification because of the lack of gravity (**Figure 2D**).

DISCUSSION

Space is a special environment consisting of microgravity and strong radiation, and plays an important role in producing various mutant microorganisms with health-promoting properties or improved fermentation potentials. Important research results and practical applications of microorganisms with the help of aerospace technology have been achieved in microbial pharmaceuticals, microbial fertilizers, and wine-making fields. Mutant microorganisms caused by aerospace technology have broad research prospects and research value.

To improve the quality of fermentation products, the quality of yeast is very crucial. In the brewing process, yeast plays an important role during the conversion of sugar into ethanol, and this process will affect the quality and yield of wine. To get better-performing brewing functional flora, creation of mutant strains at a genome-wide level is available *via* aerospace technology. The wine and beer industries have been dominated by *Saccharomyces cerevisiae* in the world (Peris et al., 2018). *S. cerevisiae* is "indispensable" as a contributor to the flavor-active metabolite profile and aroma-active compounds of beers (Kutyna and Borneman, 2018). Beer yeast mutants (*S. cerevisiae* HT-1, HT-2, and HT-3) were obtained from the Shenzhou VIII spacecraft and produced more active metabolites that are beneficial to human health and further improve product quality, flavor, and appearance (Bin et al., 2015). The fermentation beer was separated from the yeast sediment by centrifugation.

Aerospace biotechnology opens a way for effectively cultivating new varieties and special germplasm resources and has a bright future ahead. With the improvement of fermentation products, there is a boom in modern industry and agriculture. With the continuous development of world spacecraft, space methods will be applied to various areas, pushing for more reliable studies on space microorganisms. However, there are still some challenges for space microorganism research. Apparently, there is still a lack of effective methods to avoid the generation of harmful mutant microbes, and some of them may be deadly. Post-spaceflight lab screening lacks methods for controlling the direction of mutagenesis, and more mutagenesis pathways need to be further explored and investigated. Most human pathogenic isolates from space stations have been found to be multidrug-resistant, such as sulfamethoxazole, erythromycin, and ampicillin, which will cause adilemma in the antibiotic industry.

AUTHOR CONTRIBUTIONS

YC and XW involved in the initial conceptualization of the manuscript. PT led the review of the literature, wrote the first draft, and involved in the visualization of concepts. FL and ZZ collected important background information and provided assistance for data acquisition. YC, XW, PT, FL, and ZZ provided revisions and additional conceptual input to the manuscript. All authors contributed to the article and approved the submitted version.

SUPPLEMENTARY MATERIAL

The Supplementary Material for this article can be found online at: https://www.frontiersin.org/articles/10.3389/fmicb.2022.896556/full#supplementary-material

REFERENCES

Acres, J. M., Youngapelian, M. J., and Nadeau, J. (2021). The influence of spaceflight and simulated microgravity on bacterial motility and chemotaxis. *Npj. Microgravity*. 7, 1–11. doi: 10.1038/s41526-021-00135-x

Arunasri, K., Adil, M., Venu Charan, K., Suvro, C., Himabindu Reddy, S., and Shivaji, S. (2013). Effect of simulated microgravity on *E. coli* K12 MG1655 growth and gene expression. *PLoS One* 8:e57860. doi: 10.1371/journal.pone.0057860

Bąk, A., and Podgórska, W. (2016). Influence of poly (vinyl alcohol) molecular weight on drop coalescence and breakage rate. *Chem. Eng. Res. Design*. 108, 88–100. doi: 10.1016/j.cherd.2015.10.027

Beuls, E., Houdt, R. V., Leys, N., Dijkstra, C., Larkin, O., and Mahillon, J. (2009). *Bacillus thuringiensis* conjugation in simulated microgravity. *Astrobiology* 9, 797–805. doi: 10.1089/ast.2009.0383

Bin, Z., Mingyang, Z., Jinhua, W., and Tao, Y. (2015). Research on Space Breeding of Brewing Microorganisms and Its Application in Production (III) Application of Space Bacteria in Sesame Flavor Liquor in Production. *Winemaking* 2, 21–27.

Burgos, E., Vroom, M. M., Rotman, E., Murphy-Belcaster, M., Foster, J. S., and Mandel, M. J. (2020). Bacterial gene essentiality under modeled microgravity. *BioRxiv* [Preprint] doi: 10.1101/2020.08.13.250431

Chan, C. Y., Kiechle, M., Manivasakam, P., and Schiestl, R. H. (2007). Ionizing radiation and restriction enzymes induce microhomology-mediated illegitimate recombination in Saccharomyces cerevisiae. *Nucleic. Acids Res*. 35, 5051–5059. doi: 10.1093/nar/gkm442

De Boever, P., Mergeay, M., Ilyin, V., Forget-Hanus, D., Van der Auwera, G., and Mahillon, J. (2007). Conjugation-mediated plasmid exchange between bacteria grown under space flight conditions. *Microgravity. Sci. Technol*. 19, 138–144. doi: 10.1007/bf02919469

Durbin, S., and Feher, G. (1996). Protein crystallization. *Annual. Rev. Phys. Chem*. 47, 171–204.

Fang, X.-M., Zhao, Z.-J., and Gu, H.-K. (2005). A study on space mutation of Streptomyces fradiae. *Space Med. Med. Eng*. 18, 121–125.

Fukuda, T., Fukuda, K., Takahashi, A., Ohnishi, T., Nakano, T., Sato, M., et al. (2000). Analysis of deletion mutations of the rpsL gene in the yeast *Saccharomyces cerevisiae* detected after long-term flight on the Russian space station Mir. *Mutat. Res. Genet. Toxicol. Environ. Mutagen*. 470, 125–132. doi: 10.1016/s1383-5742(00)00054-5

Gavahian, M., and Tiwari, B. K. (2020). Moderate electric fields and ohmic heating as promising fermentation tools. *Innov. Food. Sci. Emerg. Technol*. 64:102422. doi: 10.1016/j.ifset.2020.102422

Kalsoom, M., Rehman, F., Shafique, T., Junaid, S., Khalid, N., Muhammad, Adnan, et al. (2020). Biological importance of microbes in agriculture, food and pharmaceutical industry: A review. *Innov. J. Life. Sci*. 8, 1–4. doi: 10.22159/ijls.2020.v8i6.39845

Kimura, S., Ishidou, E., Kurita, S., Suzuki, Y., Shibato, J., Rakwal, R., et al. (2006). DNA microarray analyses reveal a post-irradiation differential time-dependent gene expression profile in yeast cells exposed to X-rays and gamma-rays. *Biochem. Biophys. Res. Commun*.346, 51–60. doi: 10.1016/j.bbrc.2006.05.126

Kutyna, D. R., and Borneman, A. R. (2018). Heterologous production of flavour and aroma compounds in *Saccharomyces cerevisiae*. *Genes* 9:326. doi: 10.3390/genes9070326

Lam, K. S., Gustavson, D. R., Pirnik, D. L., Pack, E., Bulanhagui, C., Mamber, S. W., et al. (2002). The effect of space flight on the production of actinomycin D by *Streptomyces plicatus*. *J. Industrial. Microbiol. Biotechnol*. 29, 299–302. doi: 10.1038/sj.jim.7000312

Lankinen, M. H., Vilpo, L. M., and Vilpo, J. A. (1996). UV-and γ-irradiation-induced DNA single-strand breaks and their repair in human blood granulocytes and lymphocytes. *Mutat. Res. Fundam. Mol. Mech. Mutagen*. 352, 31–38. doi: 10.1016/0027-5107(95)00172-7

Liu, C. (2017). The theory and application of space microbiology: China's experiences in space experiments and beyond. *Environ. Microbiol*. 19, 426–433. doi: 10.1111/1462-2920.13472

Liu, H.-Z., Wang, Q., Liu, X.-Y., and Tan, S.-S. (2008). Effects of spaceflight on polysaccharides of *Saccharomyces cerevisiae* cell wall. *Appl. Microbiol. Biotechnol*. 81, 543–550. doi: 10.1007/s00253-008-1692-y

Long, J. (2016). China's space station project and international cooperation: potential models of jurisdiction and selected legal issues. *Space Policy* 36, 28–37. doi: 10.1016/j.spacepol.2016.05.002

Moeller, R., Reitz, G., Berger, T., Okayasu, R., Nicholson, W. L., and Horneck, G. (2010). Astrobiological aspects of the mutagenesis of cosmic radiation on bacterial spores. *Astrobiology* 10, 509–521. doi: 10.1089/ast.2009.0429

Moreno-Villanueva, M., Wong, M., Lu, T., Zhang, Y., and Wu, H. (2017). Interplay of space radiation and microgravity in DNA damage and DNA damage response. *Microgravity* 3:14. doi: 10.1038/s41526-017-0019-7

Mulkey, T. J. (2010). 2010 Annual Meeting Abstracts. *Gravit. Space Res*. 24:4299

Newman, C., Prise, K. M., Folkard, M., and Michael, B. D. (1997). DNA double-strand break distributions in X-ray and alpha-particle irradiated V79 cells: evidence for non-random breakage. *Int. J. Radiat. Biol*. 71, 347–363. doi: 10.1080/095530097143978

Nicholson, W. L., and Ricco, A. J. (2019). Nanosatellites for biology in space: in situ measurement of *Bacillus subtilis* spore germination and growth after 6 months in Low Earth Orbit on the O/OREOS mission. *Life* 10:1. doi: 10.3390/life10010001

Peris, D., Pérez-Torrado, R., Hittinger, C. T., Barrio, E., and Querol, A. (2018). On the origins and industrial applications of *Saccharomyces cerevisiae*× *Saccharomyces kudriavzevii* hybrids. *Yeast* 35, 51–69. doi: 10.1002/yea.3283

Sakai, T., Moteki, Y., Takahashi, T., Shida, K., Kiwaki, M., Shimakawa, Y., et al. (2018). Probiotics into outer space: feasibility assessments of encapsulated

freeze-dried probiotics during 1 month's storage on the International Space Station. *Scientific. Rep*. 8:10687. doi: 10.1038/s41598-018-29094-2

Salgado, B. A., Fabbri, S., Dickenson, A., Hasan, M. I., and Walsh, J. L. (2021). Surface barrier discharges for *Escherichia coli* biofilm inactivation: modes of action and the importance of UV radiation. *PLoS One* 16:e0247589. doi: 10.1371/journal.pone.0247589

Satoh, K., Alshahni, M. M., Umeda, Y., Komori, A., Tamura, T., Nishiyama, Y., et al. (2021). Seven years of progress in determining fungal diversity and characterization of fungi isolated from the Japanese Experiment Module KIBO. *Microbiol. Immunol*. 65, 463–471. doi: 10.1111/1348-0421.12931

Scott, T. J., and Vonortas, N. S. (2021). Microgravity protein crystallization for drug development: a bold example of public sector entrepreneurship. *J. Technol. Transf*. 46, 1442–1461. doi: 10.1007/s10961-019-09743-y

Senatore, G., Mastroleo, F., Leys, N., and Mauriello, G. (2018). Effect of microgravity & space radiation on microbes. *Fut. Microbiol*. 13, 831–847.

Senatore, G., Mastroleo, F., Leys, N., and Mauriello, G. (2020). Growth of lactobacillus reuteri DSM17938 Under two simulated microgravity systems: changes in Reuterin production, gastrointestinal passage resistance, and stress genes expression response. *Astrobiology* 20, 1–4. doi: 10.1089/ast.2019.2082

Shao, D., Yao, L., Riaz, M. S., Zhu, J., Shi, J., Jin, M., et al. (2017). Simulated microgravity affects some biological characteristics of *Lactobacillus acidophilus*. *Appl. Microbiol. Biotechnol*. 101, 3439–3449. doi: 10.1007/s00253-016-8059-6

Su, L., Chang, D., and Liu, C. (2013). The development of space microbiology in the future: the value and significance of space microbiology research. *Fut. Microbiol*. 8, 5–8. doi: 10.2217/fmb.12.127

Takatori, S. C., and Mandadapu, K. K. (2020). Motility-induced buckling and glassy dynamics regulate three-dimensional transitions of bacterial monolayers. *arXiv* [preprint] doi: 10.13140/RG.2.2.31609.62568

Topolski, C. R. (2021). *Validation of a Two-Dimensional Clinostat Design to Provide Functional Weightlessness to Custom Gas Exchange Vessels*. Ph D thesis, Florida: Embry–Riddle Aeronautical University.

Wang, J., Liu, C., Liu, J., Fang, X., Xu, C., Guo, Y., et al. (2014). Space mutagenesis of genetically engineered bacteria expressing recombinant human interferon α1b and screening of higher yielding strains. *World. J. Microbiol. Biotechnol*. 30, 943–949. doi: 10.1007/s11274-013-1512-0

Yang, Y., and Sha, M. (2019). *A Beginner's Guide to Bioprocess Modes–Batch, Fed-Batch, and Continuous Fermentation*. Enfield, CT: Eppendorf Inc.

Zhang, X., Yan, L., Li, L., Lin, S., Guo, J., Li, J., et al. (2015). Beneficial Effect of Spaceflight Experience on Producing of Endoproteinase Lys-C by *Lysobacter enzymogenes*. *J. Pure. Appl. Microbiol*. 9, 231–237.

Zhao, X., Yu, Y., Zhang, X., Huang, B., Bai, P., Xu, C., et al. (2019). Decreased biofilm formation ability of *Acinetobacter baumannii* after spaceflight on China's Shenzhou 11 spacecraft. *MicrobiologyOpen* 8:e00763. doi: 10.1002/mbo3.763

Zhou, J., Sun, C., Wang, N., Gao, R., Bai, S., Zheng, H., et al. (2006). Preliminary report on the biological effects of space flight on the producing strain of a new immunosuppressant. *J. Industrial. Microbiol. Biotechnol*. 33, 707–712. doi: 10.1007/s10295-006-0118-z

Zongzhou, Z., and Yaping, X. (2009). The impact of spaceborne on the microflora of Daqu. *Food. Sci*. 3, 214–216.

Conflict of Interest: YC, XW, FL, and ZZ were employed by the Wuzhoufeng Agricultural Science and Technology Co., Ltd.

The remaining author declares that the research was conducted in the absence of any commercial or financial relationships that could be construed as a potential conflict of interest.

frontiers | Frontiers in Microbiology

ORIGINAL RESEARCH
published: 09 June 2022
doi: 10.3389/fmicb.2022.914828

Increased Water-Soluble Yellow *Monascus* Pigment Productivity *via* Dual Mutagenesis and Submerged Repeated-Batch Fermentation of *Monascus purpureus*

*Jie Bai[1†], Zihan Gong[1†], Meng Shu[1], Hui Zhao[1], Fanyu Ye[1], Chenglun Tang[2,3], Song Zhang[1], Bo Zhou[1], Dong Lu[4], Xiang Zhou[4], Qinlu Lin[1] and Jun Liu[1,5]**

[1]National Engineering Research Center of Rice and Byproduct Deep Processing, Central South University of Forestry and Technology, Changsha, China, [2]Nanjing Sheng Ming Yuan Health Technology Co. Ltd., Nanjing, China, [3]Jiangsu Institute of Industrial Biotechnology JITRI Co. Ltd., Nanjing, China, [4]Biophysics Research Laboratory, Institute of Modern Physics, Chinese Academy of Sciences, Lanzhou, China, [5]Hunan Provincial Key Laboratory of Food Safety Monitoring and Early Waring, Changsha, China

OPEN ACCESS

Edited by:
Hui Ni,
Jimei University, China

Reviewed by:
Bo-Bo Zhang,
Shantou University, China
Po-Ting Chen,
Southern Taiwan University of Science and Technology, Taiwan
Li Ni,
Fuzhou University, China

***Correspondence:**
Jun Liu
liujundandy@csuft.edu.cn

[†]These authors have contributed equally to this work and share first authorship

Specialty section:
This article was submitted to Food Microbiology, a section of the journal Frontiers in Microbiology

Received: 07 April 2022
Accepted: 16 May 2022
Published: 09 June 2022

Citation:
Bai J, Gong Z, Shu M, Zhao H, Ye F, Tang C, Zhang S, Zhou B, Lu D, Zhou X, Lin Q and Liu J (2022) Increased Water-Soluble Yellow Monascus Pigment Productivity via Dual Mutagenesis and Submerged Repeated-Batch Fermentation of Monascus purpureus. Front. Microbiol. 13:914828. doi: 10.3389/fmicb.2022.914828

Monascus pigments (MPs) have been used in the food industry for more than 2,000 years and are known for their safety, bold coloring, and physiological activity. MPs are mainly yellow (YMPs), orange (OMPs), and red (RMPs). In this study, a mutant strain *Monascus purpureus* H14 with high production of water-soluble YMPs (WSYMPs, λ_{max} at 370 nm) was generated instead of primary YMPs (λ_{max} at 420 nm), OMPs (λ_{max} at 470 nm), and RMPs (λ_{max} at 510 nm) produced by the parent strain *M. purpureus* LQ-6 through dual mutagenesis of atmospheric and room-temperature plasma and heavy ion beam irradiation (HIBI), producing 22.68 U/ml extracellular YMPs and 10.67 U/ml intracellular YMPs. WSYMP production was increased by 289.51% in optimal conditions after response surface methodology was applied in submerged fermentation. Application of combined immobilized fermentation and extractive fermentation improved productivity to 16.89 U/ml/day, 6.70 times greater than with conservative submerged fermentation. The produced WSYMPs exhibited good tone stability to environmental factors, but their pigment values were unstable to pH, light, and high concentrations of Ca^{2+}, Zn^{2+}, Fe^{2+}, Cu^{2+}, and Mg^{2+}. Furtherly, the produced exYMPs were identified as two yellow monascus pigment components (monascusone B and $C_{21}H_{27}NO_7S$) by UHPLC-ESI-MS. This strategy may be extended to industrial production of premium WSYMPs using *Monascus*.

Keywords: yellow *Monascus* pigments, stability, mutation, response surface methodology, immobilized fermentation

INTRODUCTION

Monascus pigments (MPs) are polyketide secondary metabolites produced by the genus *Monascus* and have been used as natural edible colorants in Asian food for thousands of years (Feng et al., 2012). Generally, MPs are red (RMPs, such as monascorubramine and rubropunctamine), orange (OMPs, such as rubropunctatin and monascorubrin), and yellow (YMPs, such as monascin

and ankaflavin; Kim and Ku, 2018; Liu et al., 2019a). It has been reported that YMPs are an excellent colorants and are safe, with anti-inflammatory, anti-fatty, antitumor, and antioxidant functions (Wu et al., 2021; Huang et al., 2021b), improving alcoholic liver injury and preventing lipid accumulation (Zhou et al., 2019; Lai et al., 2021), with great prospects for use in food and pharmaceutical industries. However, YMPs are normally hydrophobic or alcohol-soluble intracellular pigments in submerged fermentation, increasing the cost of separation and purification, and limiting their application (Gong and Wu, 2016; Yang et al., 2020). Water-soluble yellow *Monascus* pigments (WSYMPs) and extracellular YMPs (exYMPs) have been studied extensively by researchers.

It has been reported that WSYMPs and exYMPs are not produced on a large scale as a result of their low yield and productivity (Qian et al., 2021; Huang et al., 2021b). Current research efforts often focus on increasing WSYMP/exYMP production through optimization of fermentation broth components, fermentation biotechnology, and chemical modification. Recently, extractive fermentation (EF) with the addition of nonionic surfactants in submerged fermentation of the *Monascus* genus has been widely used. The addition of Triton X-100 can change the mycelium morphology without harming cell growth in the EF of *M. anka* GIM 3.592, and increases exYMP production (Chen et al., 2017a,b). Xiong et al. (2015) intensified the transfer of intracellular YMPs into an extracellular nonionic surfactant micelle aqueous solution using EF and enhanced exYMP production. Huang et al. (2021b) increased WSYMP production by 69.68% compared to conventional fermentation by adding sodium starch octenyl succinate. In addition, high glucose stress can promote YMP biosynthesis and significantly increase extracellular YMP production (Huang et al., 2017c). Changing the extracellular oxidoreduction potential can also enhance WSYMP production in submerged fermentation of *Monascus ruber* CGMCC 10910 (Huang et al., 2017b). Chemical modification was performed by introducing H_2SO_3 into the double bond at the MP sidechain to produce WSYMPs with high stability over a wide pH range (Liu et al., 2020a). However, the application of these strategies, especially EF, to enhance exMPs has been problematic, increasing the cost of YMP purification.

Breeding of wild strains is most critical in microbial fermentation production of metabolites. Zhou et al. (2009) obtained a mutant strain with high YMP production through physical and chemical mutagenesis. Traditional methods of mutation breeding use chemical agents such as LiCl and nitrosoguanidine (Kodym and Afza, 2003; Sun et al., 2011). However, chemical mutagens can remain in the food industry and are harmful to human health; development of new and powerful mutagenesis methods is required. With the development of breeding biotechnology, atmospheric and room-temperature plasma (ARTP) mutagenesis systems have emerged as a novel methodology for strain breeding (Zhang et al., 2014). In our previous studies, mutant strains including *M. purpureus* M183 with high MP production, *M. purpureus* M630 with high exMP production, and *M. purpureus* M523 with high rice husk hydrolysate tolerance were generated using the ARTP screening system (Liu et al., 2019b, 2020b). In addition, heavy ion beam irradiation (HIBI), a novel and more efficient irradiation method for strain mutagenesis, has unique physical and biological advantages due to its high linear energy transfer and relative biological effectiveness, wide mutation spectrum, and high mutation rate (Gao et al., 2020; Guo et al., 2020; Zhang et al., 2022). Previous studies have demonstrated that HIBI produces a high mutation rate, mainly attributed to deletions, nucleotide exchange, and insertions (Chen et al., 2018). However, the combined application of ARTP and HIBI mutagenesis to enhance MP production has not been reported.

Generation of a mutant strain is difficult in industrial WSYMP production using *Monascus*. In this study, we obtained a mutant strain in WSYMP production through dual mutagenesis of HIBI ($^{12}C^{6+}$) and ARTP. Response surface methodology (RSM), EF, and immobilized fermentation (IF) were used to increase WSYMP yield and productivity.

MATERIALS AND METHODS

Microorganisms and Chemical Materials

Monascus purpureus LQ-6 [CCTCC M 2018600, China Central for Type Culture Collection (CCTCC), Wuhan, China] was isolated from red mold rice obtained from a local market (Changsha, China) as the parent strain. The mutant strain *M. purpureus* H14 was obtained through dual mutagenesis of ARTP and HIBI. Analytical-grade chemicals were obtained from Sangon Biotech Co., Ltd. (Shanghai, China). Chemical reagents of vitamins were purchased from Coolaber (Beijing, China). Potatoes used to produce potato dextrose agar (PDA) medium were purchased from a local market (Changsha, China).

Mutagenesis and Screening

Monascus purpureus strains were cultured on PDA medium (200 g/L potato, 20 g/L glucose, and 20 g/L agar) for 7 days at 30°C in darkness. The mycelium on a PDA Petri dish containing a fully grown culture of *M. purpureus* strain was aseptically scraped and inoculated in a 100-ml conical flask containing 20 ml of sterile water and glass beads, and agitated for 3 min to prepare the spore suspension; the concentration was adjusted to approximately 10^7 spores/ml.

Heavy ion beam irradiation was performed using carbon ion beams ($^{12}C^{6+}$, 80 MeV/u, and 20 keV/μm) at the Heavy Ion Research Facility in Lanzhou (HIRFL), Institute of Modern Physics, Chinese Academy of Sciences. The spore suspension (1.5 ml) was transferred into a 35-mm irradiation dish. The detailed steps were reported by Gao et al. The irradiation dose was set as 0, 50, 100, 150, 200, 250, and 300 Gy (Gao et al., 2020). The ARTP mutagenesis process was presented in our previous study (Liu et al., 2019b). The conditions were the same as in our previous study, except the variable parameter treatment time T was set to 0, 40, 80, 120, 160, 200, 240, and 280 s. After mutagenesis, 100 μl of the spore suspension was spread onto PDA plates and incubated at 30°C in darkness to generate the mutant strains. The fatality and survival rates

were analyzed by normalizing the colony counts of irradiated spores on PDA plates with those of untreated spores.

The spore suspension (5 ml, 10^7 spores/ml) was inoculated in a 250-ml conical flask containing 45 ml of screening fermentation broth (80 g/L rice flour, 2.5 g/L yeast extract, 2.5 g/L peptone, 5 g/L KH_2PO_4, and 0.01 g/L $FeSO_4•7H_2O$), incubated for 10 days at 30°C, and agitated at 150 rpm in the dark.

Fermentation Biotechnologies

Conventional submerged batch fermentation (SBF) was conducted as follows: 5 ml of the spore suspension (10^7 spores/ml) was inoculated in a 250-ml conical flask containing 45 ml of fermentation broth (50 g/L glucose, 2 g/L malt extract, 10 g/L peptone, 2.5 g/L KH_2PO_4, 5 g/L $NaNO_3$, 1 g/L $MgSO_4•7H_2O$, 2 g/L $ZnSO_4•7H_2O$, and pH 3.8), incubated for 10 days at 30°C, and agitated at 150 rpm in the dark.

Recent studies (Hu et al., 2012; Chen et al., 2017a; Lu et al., 2021) have revealed that the concentration of 40 g/L of Triton X-100 is the preferred effective strategy for improving MP production in extractive SBF by parent strain. Thus, Triton X-100 (40 g/L) was added to the optimized conventional submerged batch-fermentation broth (20 g/L glucose, 12.29 g/L malt extract, 15 g/L peptone, 2.5 g/L KH_2PO_4, 5 g/L $NaNO_3$, 0.2 g/L $MgSO_4•7H_2O$, 0.32 g/L $ZnSO_4•7H_2O$, 0.1 g/L $MnSO_4•H_2O$, 0.15 g/L $CaCl_2$, 0.15 g/L $FeSO_4•7H_2O$, 0.4 g/L vitamin B5, and pH 4.8) using RSM to construct the extractive SBF.

Immobilized fermentation was performed according to the method in our previous study, with several modifications (Liu et al., 2019b; Zhang et al., 2022). The spores of mutant strain *M. purpureus* H14 were immobilized in different ratios of sodium alginate (SA) and polyvinyl alcohol (PVA) solution [3% (wt/wt):0% (wt/wt), 2.5% (wt/wt):0.5% (wt/wt), 2% (wt/wt):1% (wt/wt), and 1.5% (wt/wt):1.5% (wt/wt)] instead of in 3% (wt/wt) sodium alginate solution.

The kinetics of SBF and repeated-batch fermentation (RBF) of *M. purpureus* H14 were determined in a 1,000-ml conical flask containing 300 ml of optimized fermentation broth. During fermentation, 10-ml samples were collected to measure metabolite concentrations.

Experimental Design and Statistical Analysis

Response surface methodology was used to optimize four conventional SBF broth components ($ZnSO_4•7H_2O$, $MnSO_4•H_2O$, malt extract, and vitamin B5) to enhance WSYMP production after fermentation of *M. purpureus* H14. The Box–Behnken design (BBD) was used to optimize the components. The four independent variables used in the experimental design were $ZnSO_4•7H_2O$ (0.1–0.5 g/L), $MnSO_4•H_2O$ (0.05–0.2 g/L), malt extract (5–15 g/L), and vitamin B5 (0.3–0.5 g/L); three levels were used to optimize the fermentation process.

Physicochemical Property Assays

To determine the polarity of YMPs produced by the mutant strain *M. purpureus* H14, 1 ml of fermentation medium was collected and centrifuged at 10,000 rpm for 5 min, followed by the addition of 1 ml of pure water or ethyl acetate to the fermentation medium and ankaflavin-methanol solution, respectively.

As in our previous study, the YMP alcohol solution was generated using the adsorption–separation system with the macroporous adsorption resin LX300C (Liu et al., 2019b). Resin LX300C (2 g) was added to a 100-ml conical flask containing 50 ml of the centrifuged fermentation medium to adsorb the YMPs at 30°C for 24 h and agitated at 150 rpm in the dark. The YMPs were desorbed using 70% (v/v) alcohol eluent in the same conditions. The same volume of pure water was added to the YMPs prepared by freeze-drying to generate the WSYMP solution.

The pH of the WSYMP solution and ankaflavin-methanol solution (the concentration was adjusted to 1 g/L, equal to 30.08 U/ml) was regulated from 1 to 14 with 1 mol/L HCl or NaOH. A full-band scan was performed to determine the maximum absorption wavelength and measure the WSYMPs with different concentrations (1–100 mmol/L) of metal ions added to the WSYMP solution, including Na^+, Mg^{2+}, K^+, Ca^{2+}, Zn^{2+}, Cu^{2+}, and Fe^{2+}. Five milliliters of WSYMP solution and ankaflavin-methanol solution was poured into a 60 mm × 20 mm culture dish before irradiation (3,000 lx of light intensity, 30 cm of irradiation distance) in a constant-temperature incubator (adjusted to 30°C) with incandescent LED lamps; the group left in darkness (0 lx) was used as the control. WSYMP solution (5 ml) was treated in an electro-thermostatic water bath at different temperatures (25°C–90°C) to evaluate the pH, metal ions, temperature, and visible light stability.

Composition of YMPs

Yellow *Monascus* pigments were detected by ultra-high-performance liquid chromatography (Dionex Ultimate 3000 UHPLC). The mobile phase was 0.1% formic acid (20%) and methanol (80%) at a flow rate of 0.5 ml/min, with separation carried out using an Eclipse Plus C18 column (100 mm × 4.6 mm, 3.5 μm) at 30°C, run time for 15 min and 5 μl of injection volume. Mass spectrometry was carried out by Ultimate 3000 UHPLC-Q Exactive (Thermo Scientific, United States) equipped with an HESI source. The parameters were set as follows: 10 ml/min of aux gas flow rate, 40 ml/min of sheath gas flow rate, capillary temperature at 300°C, 3.8 kv of capillary voltage, and 50% S-Lens. Each sample was analyzed in positive modes with a mass scan range of 100–800 m/z, and resolution was set at 70,000.

Determination of Metabolites and Calculations

The concentrations of glucose, biomass, and YMPs were measured according to our previously described methods (Liu et al., 2019a,b). The residual glucose concentration was determined using the standard 3, 5-dinitrosalicylic acid method. The YMP concentration was analyzed by measuring the absorbance of the supernatant at 370 nm, which included intracellular YMP content (inYMPs) and exMP content.

For the data analysis, F test was applied to evaluate the effect of independent variables on the RSM; the significant results were identified by a value of $p < 0.05$; the fitness of second-order model was evaluated by multiple correlation coefficient (R^2) and adjusted R^2(R^2adj.). Each experiment was repeated at least three times; the numerical data are presented as the mean ± SD.

RESULTS AND DISCUSSION

Obtaining Mutant Strain

From **Figure 1A**, the fatality rate of parent strain *M. purpureus* LQ-6 was 89.64% (approximately 90%) at an irradiation dose of 200 Gy. Over 250 Gy, the fatality rate exceeded 95.47%; at 300 Gy, the active *M. purpureus* LQ-6 spores were almost completely killed. According to modern theory of breeding and positive / negative mutation rate, a 90% fatality rate was set as the target (Dong et al., 2017). Thus, an irradiation dose of 200 Gy was chosen for further evaluation. The morphology and color of the mutant strains were observed for 7 days during growth on PDA plates. We found three distinct mutant strains among hundreds of potential mutant colonies; mutant strain No. 2 exhibited a smooth surface (almost no hypha), and the color was light in comparison with others. From the reversed colony on the PDA plate, mutant strain No. 23 exhibited the reddest color, and the hypha was abundant. Mutant strain No. 20 exhibited niveous hypha, but the PDA agar broth was yellow (**Figure 1B**). It remained yellow after inoculation with multiple passages of mutant strain No. 20; thus, this mutant strain (denoted as H1) was selected for further YMP production by ARTP.

From the survival rate curve for mutant strain H1 by ARTP, the mortality rate reached 90.28% at $T = 160$ s (**Figure 1C**), which was different from reported ($T = 180$ s) in our previous study (Liu et al., 2019b), illustrating that the sensitivity of different strains to ARTP mutagenesis is distinct. Subsequently, 68 mutant strains were selected for the determination of the target mutant strain *via* SBF after preliminary investigation of the morphology and color of mutant strains generated by ARTP mutagenesis with T = 160 s. **Figure 1D** indicates that the mutant strain *M. purpureus* H14 produced the highest concentration of YMPs (λ_{max} at 370 nm, 21.41 U/ml) by SBF in the screening fermentation broth, which was approximately 3.47 times greater than the concentration produced by the mutant strain *M. purpureus* H1. However, the primary YMPs (λ_{max} at 420 nm),

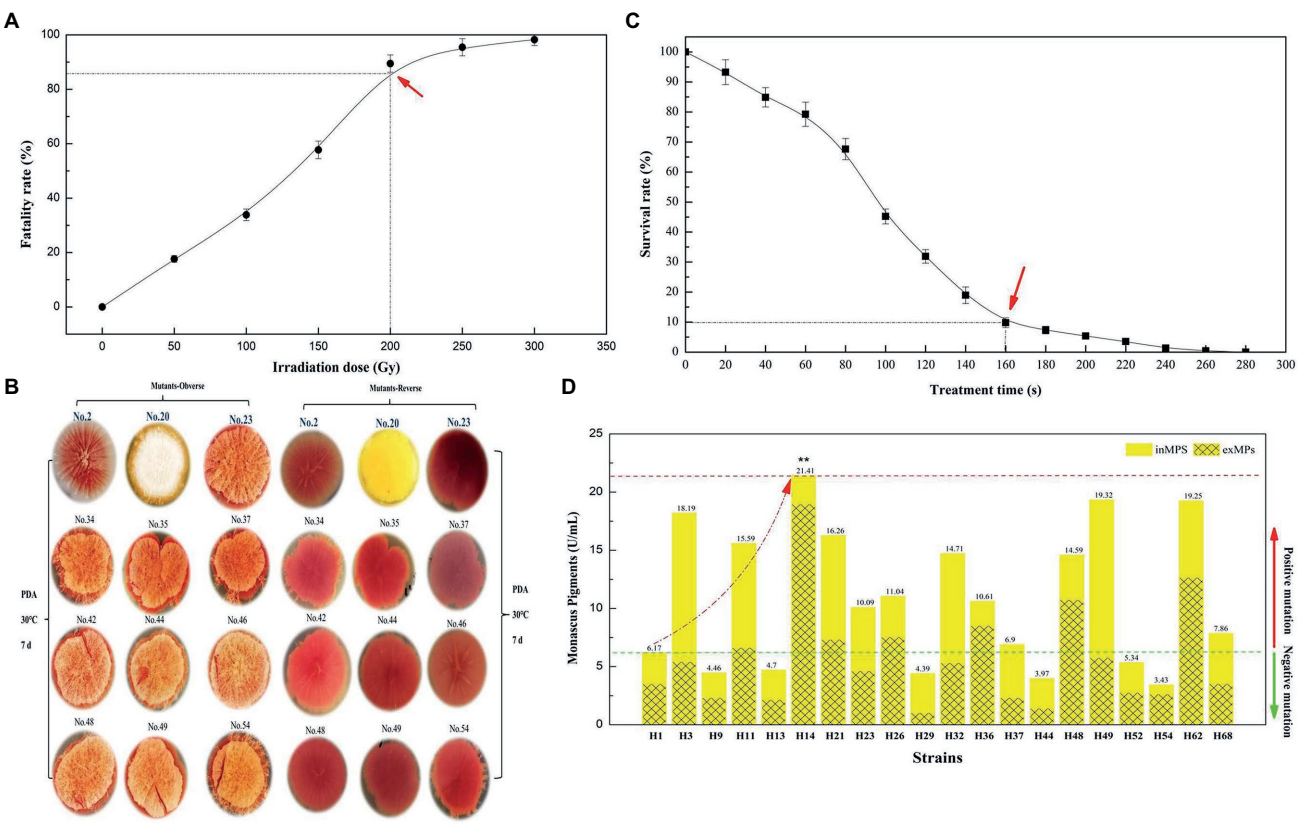

FIGURE 1 | Fatality rate **(A)** and survival rate **(C)** of parent strain *Monascus purpureus* LQ-6 subjected to heavy ion beam irradiation (HIBI) and atmospheric and room-temperature plasma (ARTP) mutation breeding system for various irradiation dose and treatment times, respectively; the morphology and color of mutant strains on potato dextrose agar (PDA) plates **(B)**; the production of total yellow *monascus* pigments by the mutant strains obtained *via* using ARTP by submerged batch fermentation (SBF) for 10 days at 30°C and agitated at 150 rpm in the dark **(D)**.

OMPs (λ_{max} at 470 nm), and RMPs (λ_{max} at 510 nm) were produced by the parent strain *M. purpureus* LQ-6 in these conditions. The ratio of exYMPs to inYMPs was 7.81, indicating that mutant strain *M. purpureus* H14 with high production of exYMPs was obtained through dual mutagenesis of HIBI and ARTP.

Effect of Glucose Concentration and pH on YMP Production

It is known that fermentation parameters, including substrate concentration and pH, play a vital role in targeted product biosynthesis. Pigment production by the genus *Monascus* has been reported to be significantly affected by glucose concentration (Chen and Johns, 1994; Wang et al., 2017a). The composition and color characteristics of *Monascus* pigments can be controlled by pH and nitrogen sources in SBF (Shi et al., 2015). Based on these findings, we determined the optimal original glucose concentration and pH of the fermentation broth for *M. purpureus* H14 in SBF; the initial glucose concentration was increased from 10 to 70 g/L (the raw concentration was 50 g/L), and the pH of the conventional SBF broth was adjusted from 2.8 to 6.8 (the raw pH was 3.8).

Figure 2 shows the effect of initial glucose concentration and pH on YMP production *via* SBF. The total YMP production and the ratio of exYMPs to inYMPs (exYMPs/inYMPs) in SBF for *M. purpureus* H14 were significantly affected by regulating the original glucose concentration and pH. YMP production and the exYMPs/inYMPs ratio were increased by 35.17 and 109.86% (to 45.08 U/ml and 4.47), respectively, when the initial glucose concentration was 20 g/L, compared to a raw concentration of 50 g/L (33.35 U/ml and 2.13). **Figure 2A** also shows that YMP production decreased as the glucose concentration increased beyond 30 g/L. When the glucose concentration was 70 g/L, total YMP production decreased to 15.25 U/ml, but a high exYMPs/inYMPs ratio was maintained. **Figure 2B** shows that YMP production and the exYMPs/inYMPs ratio increased by 50.22 and 14.55% (to 50.10 U/ml and 2.44), respectively, when the initial pH was adjusted to 4.8, compared with a raw pH of 3.8 (33.35 U/ml and 2.13). The exYMPs/inYMPs ratio decreased when the initial pH was greater than 5.8; the change was insignificant when the pH was less than 4.8. It has been reported that glucose (and pH) can control the oxidoreduction potential (ORP) level, which can further regulate the ratio of NADH/NAD^+ and intracellular enzyme activity (Wang et al., 2017b). High glucose stress can promote YMP biosynthesis by changing ORP levels (Wang et al., 2017b). High exYMP production was generated by adding 30 g/L glucose in fed-batch fermentation (Hu et al., 2012). Chen and Johns reported that the growth of *M. purpureus* and the biosynthesis of ankaflavin (a type of YMP) were favored at low pH (4.0); the growth and biosynthesis of other pigments were independent of pH (Chen and Johns, 1993).

The optimal initial glucose concentration and pH in SBF broth were determined to be 20 g/L and 4.8, respectively, for maximum exYMP yield and cost-efficiency for industrialized application.

Optimization of Fermentation Medium by RSM

It is known that RSM can effectively increase the yield of a target product using liquid-state fermentation (or submerged fermentation). YMP production in this study using *M. purpureus* H14 with different concentrations of vitamins, nitrogen, and metal ions is shown in **Table 1**. According to the experimental data, vitamin B5 (0.4 g/L), malt extract (10 g/L), $ZnSO_4 \cdot 7H_2O$ (0.2 g/L), and $MnSO_4 \cdot H_2O$ (0.1 g/L) significantly upregulated YMP production (increased by 90.64, 185.31, 153.61, and 123.42%, respectively). In order of importance to YMP production, these can be ranked as malt extract (a representative nitrogen source), $ZnSO_4 \cdot 7H_2O$, $MnSO_4 \cdot H_2O$ (representative of metal ions), and vitamin B5 (representative of growth cofactors). In addition, we found that the ratio of exYMPs

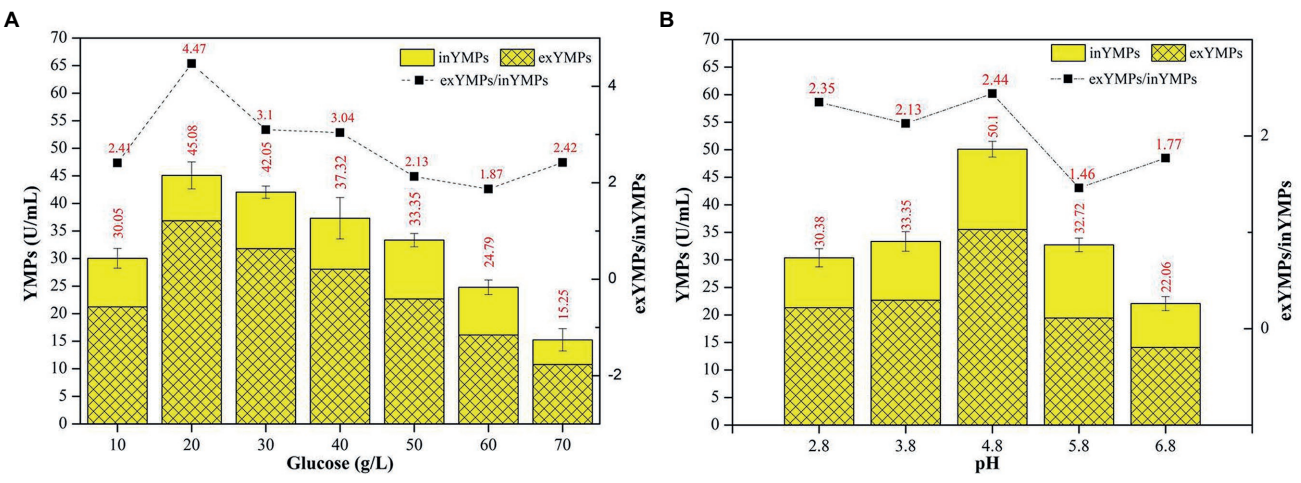

FIGURE 2 | The effect of initial glucose concentration **(A)** and pH **(B)** in the fermentation broth on the production of yellow *monascus* pigments (YMPs) and the ratio of extracellular YMPs to intracellular YMPs.

TABLE 1 | The effect of different fermentation medium compounds on the production of yellow *Monascus* pigments in submerged fermentation for 10 days at 30°C and agitated at 150 rpm in the dark.

Composition	Compound	Concentration (g/L)	inMPs (U/ml)	exMPs (U/ml)	T-MPs (U/ml)	exMPs/T-MPs (%)	Increased by (%)
CK	–	–	10.67	22.68	33.35	68.01	–
Growth factor	B1	0.2	17.79	29.82	47.61	62.63	42.76
	B3	0.2	15.06	27.86	42.52	65.52	27.50
	B5	0.2	15.10	36.53	51.63	70.75	54.81
	B6	0.2	12.04	28.22	40.26	70.09	20.72
	VC	0.2	14.57	32.28	46.85	68.90	40.48
	B5	0.1	10.76	24.84	35.60	69.78	6.75
		0.2	15.10	36.53	51.63	70.75	54.81
		0.3	15.28	40.17	55.45	72.45	66.27
		0.4	19.09	44.49	63.58	69.98	90.64
		0.5	15.38	33.24	48.62	68.37	45.79
Nitrogen source	Peptone	5	23.66	36.70	60.36	60.80	80.99
		10	26.80	46.50	73.30	63.44	119.79
		15	36.76	52.80	89.56	58.95	168.55
		20	21.48	46.35	67.83	68.33	103.39
	Malt extract	5	27.64	54.65	82.29	66.41	146.75
		10	35.80	59.35	95.15	62.37	185.31
		15	26.46	48.45	74.91	64.68	124.62
		20	23.84	44.55	68.39	65.14	105.07
	NaNO3	1	14.45	28.20	42.65	51.24	27.89
		3	19.90	45.65	65.55	69.64	96.55
		5	28.40	51.50	79.90	64.46	139.58
		7	18.59	39.46	58.05	67.96	74.06
		9	11.85	32.80	44.65	73.46	33.88
Metal ion	Mg^{2+}	0.05	15.62	29.30	44.92	65.23	34.69
		0.1	15.58	36.73	52.31	70.22	56.85
		0.2	17.65	43.27	60.92	71.03	82.67
		0.5	19.59	36.81	56.40	65.26	69.12
	Mn^{2+}	0.01	13.65	39.12	52.77	74.13	58.23
		0.05	15.17	48.16	63.33	76.05	89.90
		0.1	19.63	54.88	74.51	73.65	123.42
		0.2	17.46	34.08	51.54	66.12	54.54
	Fe^{2+}	0.5	12.35	29.57	41.92	70.55	25.70
		1	13.20	34.15	47.35	72.13	41.98
		1.5	13.08	39.76	52.84	75.25	58.44
		2	16.32	28.04	44.36	63.22	33.01
	Ca^{2+}	0.5	9.73	24.23	33.96	71.35	1.83
		1	13.01	30.91	43.92	70.38	31.69
		1.5	17.16	36.92	54.08	68.26	62.16
		2	11.60	25.30	36.90	68.56	10.64
	Zn^{2+}	0.05	17.99	47.03	65.02	72.33	94.96
		0.1	22.41	52.65	75.06	70.15	125.07
		0.2	26.75	57.83	84.58	68.37	153.61
		0.5	18.78	42.22	61.00	69.22	82.91

The data were expressed as the mean from three experiments.

to total YMPs was generally approximately 70%, which was equal to the ratio of exYMPs/inYMPs at 2.33 (similar to that with different initial pH). From the glucose and pH regulation findings, we confirmed that *M. purpureus* H14 was a high-production exYMP mutant strain, possibly due to the high cell permeability or the hydrophilia of the YMPs (WSYMPs). Thus, an increase in YMP production by RSM was imminent.

Recently, the use of RSM to increase MP production using *Monascus* spp. has increased. Our previous study showed that the total MPs and exMPs were increased by 33.38 and 150.32%, respectively, *via* SBF of *M. purpureus* (Liu et al., 2019b). Srivastav et al. (2015) used RSM to optimize a sweet potato-based medium to increase red MP production using *M. purpureus*. The four medium compounds, vitamin B5, malt extract, $ZnSO_4 \cdot 7H_2O$, and $MnSO_4 \cdot H_2O$, were selected for RSM.

According to the BBD for these four compounds with a three-level optimization (−1, 0, and 1), 29 experimental runs were conducted in this study (**Table 2**), and the experimental YMPs production were marked with arrows in **Figure 3**. State-ease Design Expert 8.0.6 software was used to analyze the relationship between YMP production (Y) and parameters (X_i) in each experimental run; the following multiple nonlinear regression model (Equation 1) was generated to express the relationship.

TABLE 2 | Box–Behnken design for process parameters of yellow *monascus* pigments production by *M. purpureus* H14 in submerged fermentation for 10 days.

Compounds	Symbol	Coded levels				
		−1		0	1	
$ZnSO_4•7H_2O$	A	0.1		0.3	0.5	
$MnSO_4•H_2O$	B	0.05		0.13	0.2	
Malt extract	C	5		10	15	
Vitamin B5	D	0.3		0.4	0.5	
Run order	A	B	C	D	YMPs (U/ml)	
					Experimental	Predicted
1	0	1	0	1	82.06	81.34
2	−1	0	1	0	98.56	98.76
3	−1	0	0	1	77.92	76.20
4	0	0	0	0	103.28	104.69
5	0	0	−1	1	77.52	76.76
6	−1	0	−1	0	75.26	77.41
7	1	0	1	0	91.66	90.82
8	0	0	0	0	105.88	104.69
9	0	−1	1	0	97.18	96.90
10	1	−1	0	0	93.67	91.89
11	0	1	−1	0	74.38	73.24
12	0	0	1	−1	91.48	92.65
13	0	1	1	0	95.71	94.23
14	0	−1	0	−1	75.37	74.30
15	0	−1	0	1	79.38	81.77
16	−1	−1	0	−1	82.94	81.13
17	1	0	0	−1	73.98	73.98
`18	0	0	0	0	104.56	104.69
19	1	1	0	0	68.94	71.17
20	−1	0	0	−1	89.16	88.15
21	0	−1	0	−1	87.04	89.07
22	0	0	−1	−1	80.24	79.12
23	1	0	−1	0	79.54	80.65
24	0	0	0	0	104.37	104.69
25	−1	1	0	0	84.45	86.64
26	1	0	0	1	86.38	85.66
27	0	−1	−1	0	86.32	86.07
28	0	0	0	0	105.36	104.69
29	0	0	1	1	93.21	94.75

The data were expressed as the mean from three experiments.

$$\begin{aligned} Y = {} & 104.69 - 1.18X_1 - 3.80X_2 \\ & + 7.88X_3 - 0.067X_4 - 6.56X_1X_2 - 2.80X_1X_3 \\ & + 5.91X_1X_4 + 2.62X_2X_3 + 3.59X_2X_4 \\ & + 1.11X_3X_4 - 11.30{X_1}^2 - 10.68{X_2}^2 \\ & - 6.48{X_3}^2 - 12.39{X_4}^2 \end{aligned} \quad (1)$$

where Y represents the response values of YMP production, and X_1, X_2, X_3, and X_4 represent $ZnSO_4•7H_2O$, $MnSO_4•H_2O$, malt extract, and vitamin B5, respectively.

The statistical significance of the regression model equation was evaluated by the F test analysis of variance; the associated p-values were lower than 0.001 for YMPs production, indicating that the developed model and the terms were statistically significant; besides, the value of lack of fit was 0.0704, higher than 0.05, demonstrated the precision and the accuracy of the constructed models; what is more, the data show that $MnSO_4•H_2O$ and malt extract were the principal factors on YMPs production (**Table 3**). Based on the experimental data, there were six response surface graphs in multiple nonlinear quadratic regression models. The adequacy and accuracy of the generated model were evaluated using coefficient of determination (R^2), adjusted R^2 (R^2_{adj}), predicted R^2 (R^2_{pred}), and coefficient of variation (CV%). In this study, the results of ANOVA for RSM quadratic model showed that the value of R^2 was 0.9842 for YMPs production and R^2_{adj} was 0.9683, which was high and significantly close to the R^2 value. These results indicated that the predicted model was appropriate. In addition, the value of R^2_{pred} (0.9138 for YMPs production) was in reasonable agreement with that of R^2_{adj}, which also demonstrated that the predicted values of YMP productions were accurate. Furthermore, adequate precision (Adeq. Pre.) of 24.113 indicated an adequate signal (greater than 4 is desirable); this model can be used to navigate the design space. Thus, from **Figure 3**, the YMPs production point prediction was used in the Design Expert software to determine the four medium parameters with optimized values. The optimal values of $ZnSO_4•7H_2O$, $MnSO_4•H_2O$, malt extract, and vitamin B5 were determined as 0.32, 0.1, 12.29, and 0.4 g/L, respectively. In optimized fermentation conditions

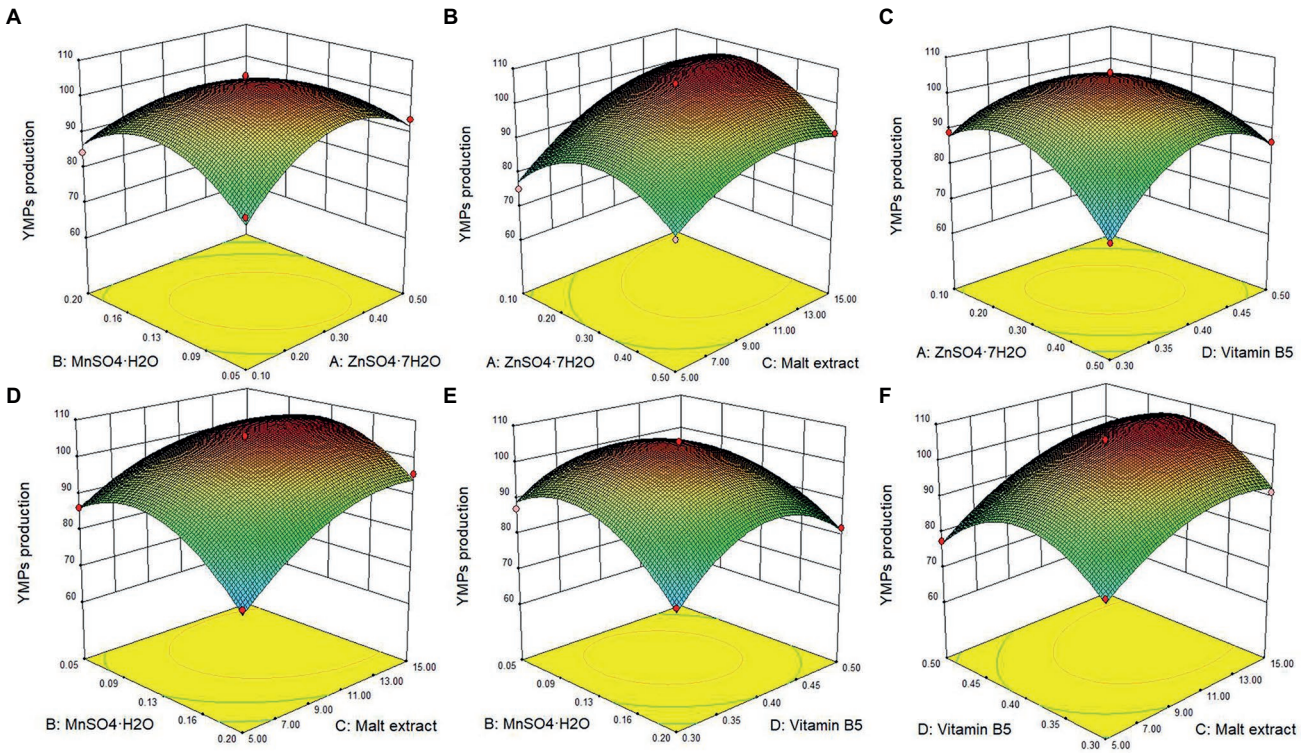

FIGURE 3 | Response surface plot of the effect of the interaction of ZnSO4•7H2O, MnSO4•H2O, malt extract, and vitamin B5 on the YMPs production in submerged fermentation by mutant strain *M. purpureus* H14. Effect of ZnSO4•7H2O and MnSO4•H2O **(A)**, effect of ZnSO4•7H2O and malt extract **(B)**, effect of ZnSO4•7H2O and vitamin B5 **(C)**, effect of MnSO4•H2O and malt extract **(D)**, effect of MnSO4•H2O and vitamin B5 **(E)**, and effect of malt extract and vitamin B5 **(F)**.

for 10 days, triplicate experiments resulted in a mean YMP production of 104.67 U/ml, which was 98.26% of the predicted value. YMP production and exYMP production increased by 213.85 and 289.51%, respectively, using RSM, and the ratio of exYMPs/inYMPs increased from 2.13 to 5.41. These results indicate that RSM dramatically increased exYMP production; the yield and productivity of exYMPs were 4,417 U/g (glucose) and 8.83 U/ml/day. Subsequently, IF and EF were performed together to increase exYMP productivity.

Improvement of exYMP Productivity *via* RBF

Extractive fermentation has been proven to efficiently increase the production of *Monascus* pigments in submerged fermentation of *Monascus* spp.; the exMPs increased by 127.48% with the addition of 3 g/L Triton X-100 in submerged fermentation of *M. purpureus* DK (Lu et al., 2021). Our previous study prevented further improvement of the yield and productivity of exMPs by IF (Liu et al., 2019b). In this study, a novel RBF biotechnology was developed by combining EF and IF to significantly increase exYMP production.

It has been reported that the use of Ca-alginate to embed the mycelium of *M. purpureus* C322 resulted in high pigment production in RBF (Fenice et al., 2000). Our previous study investigated the effect of SA concentration on exMP production and immobilization efficiency and found that the optimal concentration of SA was 3% (wt/wt; Liu et al., 2019b). In this study, we further evaluated the effect of different SA and PVA ratios with a total concentration of 3% on exMP production and immobilization efficiency by immobilizing the spores of *M. purpureus* H14. As in our previous study, with a maximum of seven cycles, a large amount of batch fermentation could not be achieved in RBF (**Figure 4A**). In addition, although their immobilization efficiencies were good, exYMP production was different with different SA and PVA ratios in RBF with each cycle for 10 days. In descending order of exYMP production, they can be ranked as 2.5% SA and 0.5% PVA, 2% SA and 1% PVA, 1.5% SA and 1.5% PVA, and 3% SA, with mean values of 140.90, 124.90, 107.72, and 106.06 U/ml, respectively. The immobilization efficiency of *M. purpureus* H14 was desirable when the concentration of SA in the immobilized solution was less than 1.5%; it was flocculent and irregular, but not regularly spherical. Concentrations of 2.5% SA and 0.5% PVA in the immobilized solution were selected for immobilization of *M. purpureus* H14 spores in IF.

As shown in **Figure 4B**, the glucose consumption rate and exYMP biosynthesis rate were increased in IF compared to those in conventional SBF. The residual glucose was consumed at approximately 96 and 108 h, with glucose consumption rates of 0.21 g/L/h (5.04 g/L/day, increased by 16.67%) and 0.18 g/L/h (4.32 g/L/day) in IF and SBF, respectively. The biosynthesis rate

TABLE 3 | ANOVA for the effect of $ZnSO_4•7H_2O$, $MnSO_4•H_2O$, vitamin B5, and malt extract on yellow *monascus* pigment production and regression coefficients.

Source	Sum of squares-type III	df	Mean square	*F* value	*p* value Prob > *F*	Significance
Model	3249.06	14	232.08	62.12	<0.0001	**
A ($ZnSO_4•7H_2O$)	16.61	1	16.61	4.45	0.0535	–
B($MnSO_4•H_2O$)	173.43	1	173.43	46.42	<0.0001	**
C (malt extract)	744.82	1	744.82	199.36	<0.0001	**
D (vitamin B5)	0.053	1	0.053	0.014	0.9066	–
AB	172.13	1	172.13	46.07	<0.0001	**
AC	31.25	1	31.25	8.36	0.0118	*
AD	139.71	1	139.71	37.40	<0.0001	**
BC	27.41	1	27.41	7.34	0.0170	*
BD	51.48	1	51.48	13.78	0.0023	*
CD	4.95	1	4.95	1.33	0.2690	–
A^2	828.56	1	828.56	221.77	<0.0001	**
B^2	739.81	1	739.81	198.02	<0.0001	**
C^2	272.13	1	272.13	72.84	<0.0001	**
D^2	996.09	1	996.09	266.61	<0.0001	**
Residual	52.31	14	3.74			
Lack of fit	48.33	10	4.83	4.87	0.0704	–
Pure error	3.97	4	0.99			
Corrected total	3301.36	28				
SD	1.93					
Mean	87.79					
CV%	2.20					
R^2	0.9842					
R^2_{adj}	0.9683					
R^2_{pred}	0.9138					
Adep. pre	24.113					

*CV, coefficient of variation; R^2, coefficient of determination; R^2_{adj}, adjusted R^2; R^2_{pred}, predicted R^2; and Adep. Pre, adequate precision. **p < 0.01 highly significant. *p < 0.05, significant; –, not significant.*

of exYMPs using *M. purpureus* H14 was evenly matched in the mid-early period of fermentation (before 144 h) in SBF and IF; subsequently, the biosynthesis rate significantly increased in IF compared to that in SBF, with a maximum exYMP production of 139.75 U/ml at 288 h (a productivity of 11.64 U/ml/day) and 104.13 U/ml at 300 h (a productivity of 8.33 U/ml/day), respectively. In RBF without the addition of Triton X-100 for five cycles, the mean glucose consumption rate and exYMP productivity were 8.23 and 10.28 U/ml/day, respectively, not including the first batch (**Figure 4C**). However, these values were increased to 8.54 g/L/day and 15.21 U/ml/day, respectively, in RBF with Triton X-100 (**Figure 4D**). Similarly, Evans and Wang (1984) further increased the maximum *Monascus* pigment yield and production rate through immobilized cell fermentation with the addition of resin, illustrating that a novel RBF with some modifications could increase the yield and productivity of a target product. To evaluate the maximum exYMP production using this novel RBF, we extended the fermentation time to 10 days (the same as conventional SBF) in the last cycle. An exYMP production of 152.08 U/ml was obtained, and the exYMP productivity was almost constant (16.89 U/ml/day). The exYMP yield and productivity increased by 570.55 and 570.04%, respectively, compared with SBF after RSM and RBF (22.68 U/ml and 2.27 U/ml/day).

In addition, we compared the yield and productivity of YMPs produced by *Monascus* strains *via* SBF. As shown in **Table 4**, various biotechnologies were carried out to increase the YMPs production, including addition of exogenous compounds [such as ethanol, sodium starch octenyl succinate (OSA-SNa), and microparticle], pH and sharking speed regulation, temperature control, and response surface methodology, changing oxidation–reduction potential (high glucose stress, addition of H_2O_2 and dithiothreitol). The highest exYMPs production was 209 U/ml in submerged fermentation by *M. ruber* CGMCC 10910 after optimizing the amount of H_2O_2 added and the timing of the addition, with 17.42 U/ml/day of productivity (Huang et al., 2021b), which was similar to the value of that obtained in this study. Besides, it showed that high production of YMPs (328.36 U/ml) was obtained by *M. ruber* CGMCC 10910 under condition of high glucose stress, but the productivity of exYMPs was low (5.22 U/ml/day; Wang et al., 2017b). Although most YMPs productions were much higher than that in this present study, the productivity of exYMPs generated *via* RBF was advantageous and predominant.

Physicochemical Property of Produced Yellow *Monascus* Pigments

Feng et al. (2012) reviewed the categories, structures, and properties (including solubility, stability, and safety) of MPs in the journal of Applied Microbiology Biotechnology. YMPs (absorption at 420 ± 10 nm), OMPs (absorption at 470 ± 10 nm), and RMPs (absorption at 510 ± 10 nm) are traditionally accumulated in the mycelium during SBF (Kim and Ku, 2018). The four identified MPs, N-glutarylmonascorubramine, N-glutarylrubropunctamine, N-glucoslmonascorubramine, and

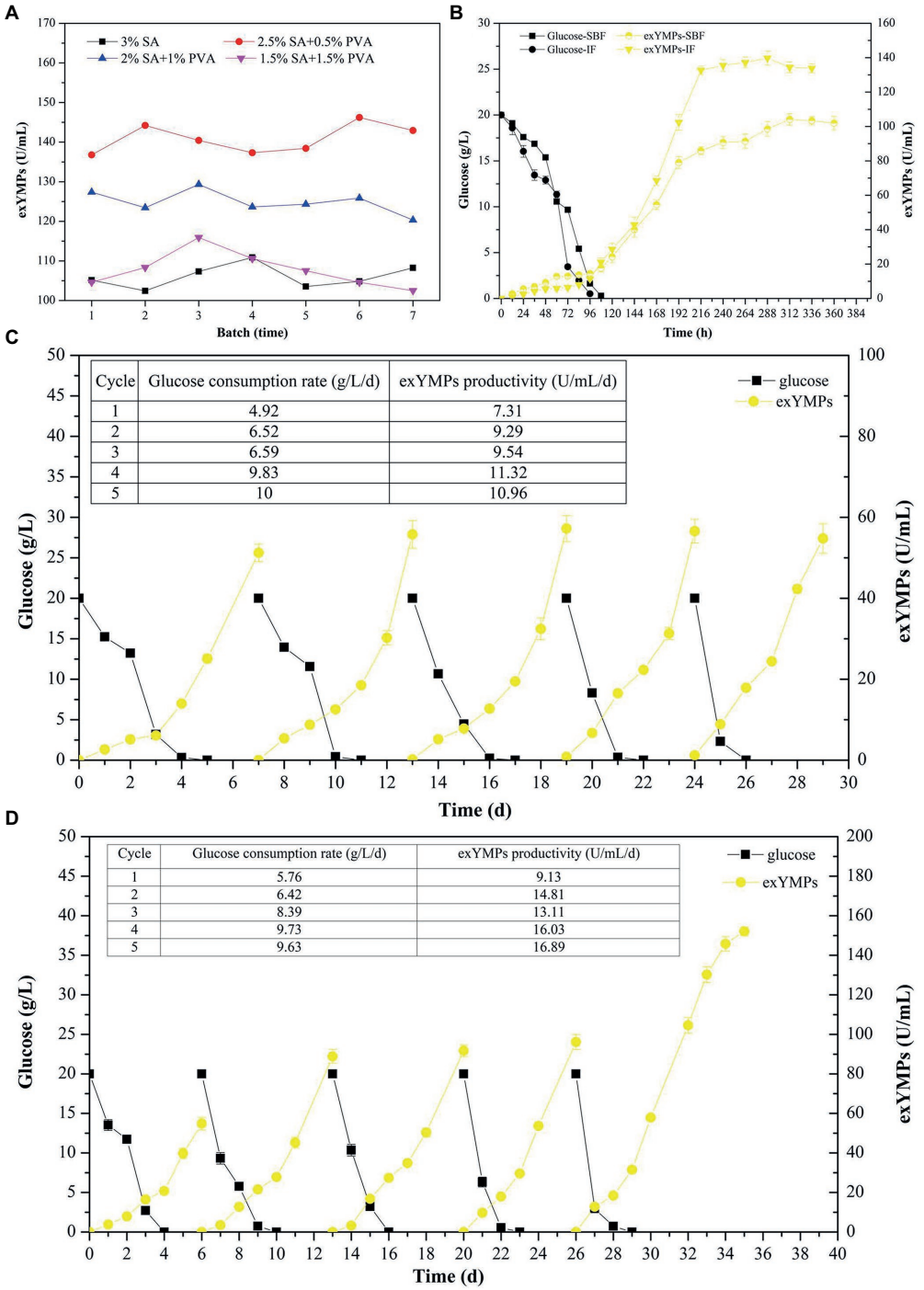

FIGURE 4 | The effect of different ratios of sodium alginate and polyvinyl alcohol solution on the production of extracellular yellow *monascus* pigments *via* repeated batch fermentation of *M. purpureus* H14 **(A)**; glucose consumption and the biosynthesis of extracellular yellow *monascus* pigments of *M. purpureus* H14 during conventional SBF and immobilized fermentation **(B)**; glucose consumption and the biosynthesis of extracellular yellow *monascus* pigments of *M. purpureus* H14 during repeated-batch fermentation without **(C)** and with **(D)** Triton X-100 addition.

N-glucosylrubropunctamine are hydrophilic MPs (exMPs) with a red tone (Chen et al., 2015). In this study, a large number of YMPs produced by the mutant strain *M. purpureus* H14 in SBF were secreted out of the cell; we speculated that the exYMPs were hydrophilic or water-soluble. From the polarity test (**Figure 5A**), we found that the exYMPs were soluble in pure water, but were not dissolved in the hydrophobic phase of ethyl acetate. However, ankaflavin, an alcohol-soluble standard

TABLE 4 | Comparison of the production and productivity of yellow *monascus* pigments by *Monascus* strains in submerged fermentation.

Strain	Biotechnology	exYMPs (U/ml)	T-YMPs (U/ml)	Productivity (U/ml/day)	Reference
M. ruber CGMCC 10910	Temperature control	190	–	23.75 (exMPs)	Huang et al., 2017a
M. ruber CGMCC 10910	Controlling oxidoreduction potential	209	–	17.42 (exMPs)	Huang et al., 2017b
M. ruber CGMCC 10910	High glucose stress	114.80	328.36	5.22 (exMPs)	Wang et al., 2017b
M. ruber CGMCC 10910	Addition of OSA-SNa	131.50	220	16.44 (exMPs)	Huang et al., 2021b
M. anka mutant MYM	Response surface methodology	–	87.24	12.46 (T-YMPs)	Zhou et al., 2009
M. purpureus sjs-6	Adjusting pH and shaking speed	–	401	57.28 (T-YMPs)	Lv et al., 2017
M. purpureus ZH106-E	Addition of ethanol	–	394	56.29 (T-YMPs)	Qian et al., 2021
M. purpureus CH01	Potato pomace as carbon source	–	19.70	2.81 (T-YMPs)	Chen et al., 2021
M. purpureus ZH106-M	Addition of microparticles		554.20	79.17 (T-YMPs)	Huang et al., 2021a
M. purpureus H14	Immobilized fermentation	152.08	–	16.89 (exMPs)	In this study

compound, is easily dissolved in the hydrophobic phase. These observations verify that the WSYMP hypothesis was correct. **Figure 5B** shows that the yellow tone of the produced WSYMPs is stable in a pH range of 1–14. However, the maximum absorption peaks are different: 360 nm for pH 1–5, 370 nm for pH 6–12, and 390 nm for pH 13–14. The maximum absorption peaks for WSYMPs were different from those of YMPs. However, the WSYMP values changed with the addition of 1 M HCl or NaOH, decreasing to 13.98 U/ml (65.84%) and 22.52 U/ml (44.97%) from 40.92 U/ml at pH 1 and pH 14, respectively (**Figure 5C**). The produced WSYMPs have high stability in neutral solution environments, decreasing in alkaline and acidic environments. Similarly, the color value degraded at different pH values; degradation was more significant from pH 4–8 (Carvalho et al., 2005). Although the color tone was changeless, **Figure 6A** shows that ankaflavin has relatively high stability in a pH range of 3–8, the value dramatically decreased when pH lower than 2 (decreased by more than 79.15%) and more than 9 (decreased by more than 43.35%). The results stated that the generated WSYMPs by mutant strain *M. purpureus* H14 have higher stability in response to pH than ankaflavin. Besides, in **Figure 5D**, the WSYMPs are almost stable with heat treatment (25–90°C) for 8 h, exhibiting a slight reduction in yellow tone. It has been reported that MPs are generally stable with heat and a wide range of pH values, but are less stable with light (Wang et al., 2017a). However, traditionally the focus is tone stability, without considering the value. Water-soluble RMPs were generated by chemical modification using aminoacetic acid and glutamic acid and exhibited heat discoloration when dissolved in a buffer at pH 3, 7 and 9.2 (Wong and Koeler, 1983). A type of RMP produced by *M. purpureus* using corn bran in SBF produced thermal (sterilization and 40°C–80°C) and pH (4–7) stability for tone and value (Almeida et al., 2021). In this study, the WSYMP value was almost constant in the dark for 10 h, exhibiting a downward trend over time (0–10 h) in light, but remaining nearly constant with an initial value of 17.16 U/ml until 2 h (**Figure 5E**). Similarly, the color value of ankaflavin sharply decreased to 16.84 U/ml for ten hours from 30.08 U/ml in light, but almost constant in the dark (**Figure 6B**). However, the stability of WSYMPs is relatively higher than that of ankaflavin when they are irradiated within 2 h. **Figure 5F** shows that the WSYMPs were stable in Na^+ and K^+ solutions, with low concentrations (<5 mM) of Ca^{2+}, Zn^{2+}, Fe^{2+}, Cu^{2+}, and Mg^{2+}. However, when the concentration reached 10 mM, the pigment value decreased by 32.60, 32.16, 36.35, 35.03, and 25.30%, and 52.62, 50.63, 50.90, 55.97, and 43.43%, respectively, at a concentration of 100 mM. The pigment tone changed to green when the Cu^{2+} concentration exceeded 50 mM; the YMPs solution with the addition of other metal ions maintained a yellow tone (**Figure 5G**). Traditionally, MPs are stable with a small quantity of Na^+, K^+, Mg^{2+}, Ca^{2+}, Zn^{2+}, Al^{3+}, and Cu^{2+}, but less stable in the presence of Fe^{2+} and Fe^{3+} (Feng et al., 2012; Wang et al., 2017a). These findings illustrated that the WSYMPs showed good stability of tone to environmental factors, including pH, heat, light, and metal ions, in this present study. However, the pigment value was unstable to pH, light, and high concentrations of Ca^{2+}, Zn^{2+}, Fe^{2+}, Cu^{2+}, and Mg^{2+}.

Characterization of Produced Yellow *Monascus* Pigments

In the past decade, 12 YMP compounds have been investigated (Feng et al., 2012). In this study, we found that the HPLC peak time of produced WSYMPs different to that of ankaflavin and monascin in our laboratory. Thus, we further determined the compound structures of the YMPs through HPLC–MS. From **Figure 7**, a total of five peaks were appeared in the raw fermentation broth (the first tested sample, T1), and the retention time (t_R) was 1.58, 1.95, 2.16, 2.55, 7.16, and 7.59 min, respectively. However, the peaks with t_R of 2.55, 7.16, and 7.59 disappeared in the WSYMPs solution (the second tested sample, T2), and the t_R of residual three peaks occurred rearward shift within the range of recognition, which changed to 1.71, 2.01, and 2.19 min, respectively. Besides, the compounds with t_R of 7.16 and 7.59 min both showed pseudo-molecular $[M+H]^+$ ions at m/z 301.14 and 301.14, with the fragment ions in UPLC-ESI-MS^2 at m/z 149.02343 and 163.03858. The fragment ions of the compound with t_R of 2.55 min in UHPLC-ESI-MS^2 at m/z 362.32822, 300.28851, and 265.26337. This phenomenon illustrated that some compounds or impurities (not WSYMPs) were cleared away *via* the adsorption–separation system with the macroporous adsorption resin LX300C. Furtherly, we analyzed the peaks with t_R of 2.01 min (or 1.95 min) and 2.19 min (or 2.16 min) by UHPLC-ESI-MS. The peaks of T1-2.16 and T2-2.19 min both showed

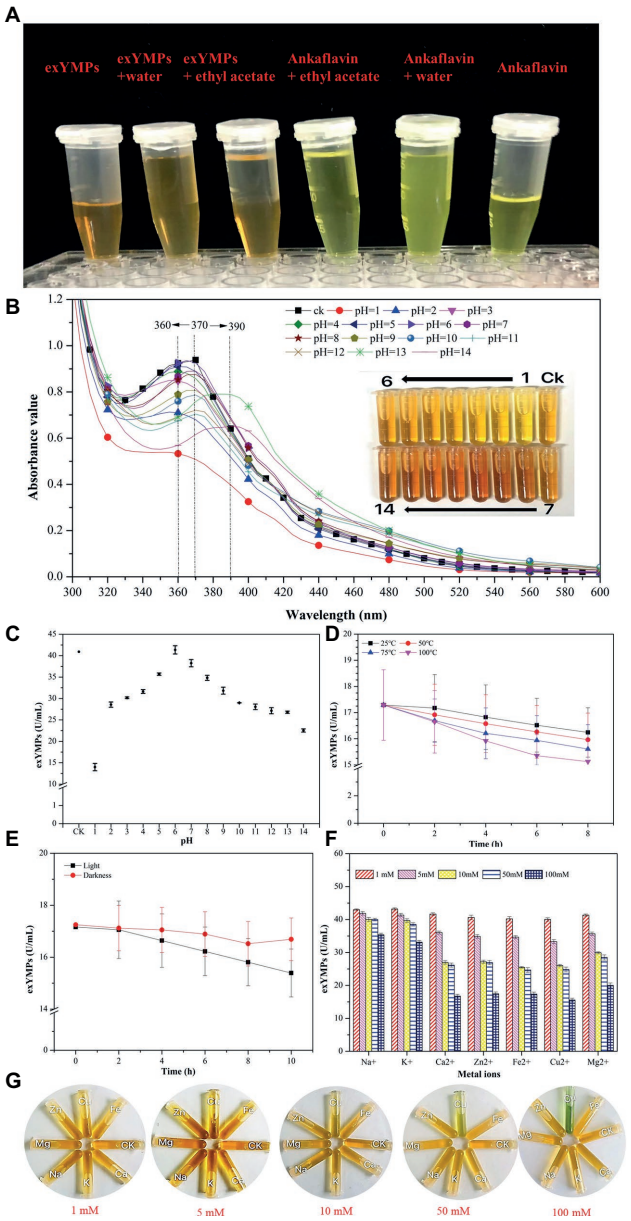

FIGURE 5 | The polar analysis of extracellular yellow *monascus* pigments produced by the mutant strain *M. purpureus* H14 **(A)**; spectral scan results **(B)** and the value **(C)** of extracellular yellow *monascus* pigments in a pH range of 1–14; the value stability of extracellular yellow *monascus* pigments produced by the mutant strain *M. purpureus* H14 subject to heat **(D)**, light **(E)**, metal ions **(F)**; the tone of extracellular yellow *monascus* pigments in response to various metal ions with different concentrations **(G)**.

pseudo-molecular $[M+H]^+$ ions at m/z 114.09134 (**Figure 8**). Although a pseudo-molecular $[M+H]^+$ ion with m/z 155.383183 in T1 – 1.95 min, it disappeared after purification treatment (in T2 2.01 min). In addition, the peak of T1-1.95 min mainly showed pseudo-molecular $[M+H]^+$ ions at m/z 303.723239, 435.33057, and that of T2-2.01 min at m/z 303.723239 and 435.2188. Furtherly, the components of exYMPs solution were separated *via* dynamic desorption of fully saturated absorbent with glass absorbent columns of 200 mm length and 10 mm diameter. The sample with the darkest yellow color tone was analyzed by Nanjing Sheng Ming Yuan Health Technology Co. Ltd., and the result showed that the molecular weight of component was m/z at 440.1150 of $[M+H]^+$ (**Supplementary Figure S1**—HPLC and **Supplementary Figure S2**—MS). Compared with the information in studies, we found that the molecular, monascusone B ($C_{17}H_{18}O_5$), has a weight of m/z 302 [observed m/z at 303.1235 of $(M+H)^+$] and UV λ_{max} value at 375 nm (Jongrungruangchok et al., 2004); compound **7** ($C_{21}H_{27}NO_7S$, a kind of WSYMPs) observed m/z at 435.7 of $[M+H]^+$ (Yang et al., 2018). The results indicated that most possibly only two yellow *Monascus* pigment components were produced by mutant strain *M. purpureus* H14 in submerged fermentation, and the exYMP was identified as monascusone B and $C_{21}H_{27}NO_7S$ (WSYMP; the structures are shown in **Figure 9**).

Besides, Jongrungruangchok et al. (2004) have reported that monascusone A (a precursor substance of monascusone B) produced by *M. kaoliang* KB20M10.2 showed no cytotoxicity against breast cancer and human epidermoid carcinoma of cavity cell lines. Monascusone B possesses the same stereochemistry as that of monascin, which exhibited no cytotoxicity against Hep G2 (human cancer cell lines) cells (Su et al., 2005). In addition, the IC50 of ankaflavin on human cancer cell lines is 15 μg/ml, but ankaflavin has no significant cytotoxicity against on normal diploid fibroblast cell lines (Su et al., 2005). These results indicated that the constructed fermentation system (including dual mutagenesis, immobilized fermentation, and extractive fermentation) is beneficial for the production of exYMP in submerged fermentation by *M. purpureus*.

CONCLUSION

Yellow *Monascus* pigments are excellent colorants, are safe, and have several physiological functions. In this study, a mutant strain, *M. purpureus* H14, was generated using dual mutagenesis of atmospheric and room-temperature plasma and HIBI. The physicochemical property of the produced YMP was water-soluble, and two yellow monascus pigment components were identified by UHPLC-ESI-MS. It exhibited good tone stability when subjected to environmental factors including pH, heat, light, and metal ions, but the pigment value was unstable with pH, light, and high concentrations of Ca^{2+}, Zn^{2+}, Fe^{2+}, Cu^{2+}, and Mg^{2+}. Application of IF and EF significantly improved the exYMP yield and productivity.

DATA AVAILABILITY STATEMENT

The data analyzed in this study is subject to the following licenses/restrictions. The data presented in this study are available on request from the corresponding author. Requests to access these datasets should be directed to JL, liujundandy@csuft.edu.cn.

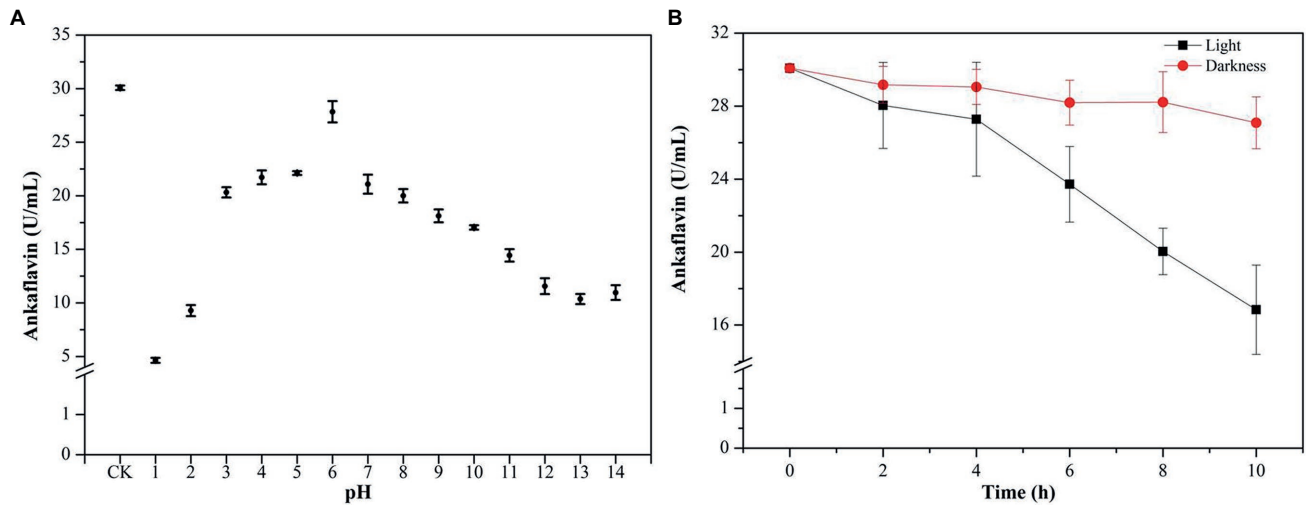

FIGURE 6 | The value stability of ankaflavin subject to pH **(A)** and light **(B)**.

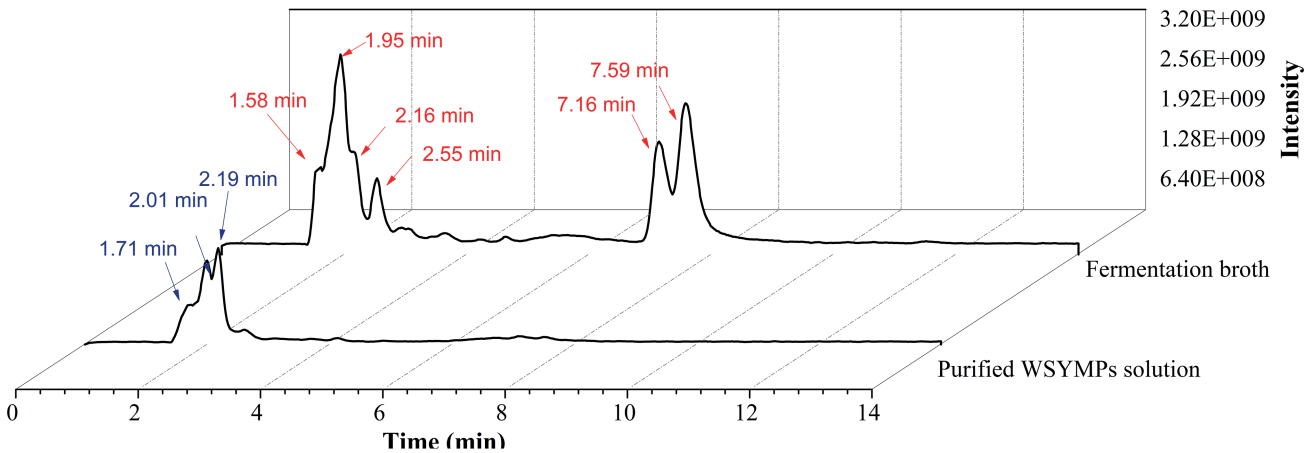

FIGURE 7 | Ultra-high-performance liquid chromatography analysis of fermentation broth and WSYMP solution.

AUTHOR CONTRIBUTIONS

JL and QL designed experiments. JB, ZG, and HZ performed experiments. JB wrote the manuscript. JL revised the manuscript. MS collected important background information. FY analyzed the RSM results. JL and BZ analyzed the data. DL and XZ performed heavy ion-beam irradiation. CT analyzed the HPLC-MS data. All authors contributed to the article and approved the submitted version.

FUNDING

This work was supported by the National Natural Science Foundation of China (no. 32101906), Hunan Provincial Natural Science Foundation (no. 2021JJ31146), Open Project Program of the Hunan Provincial Key Laboratory of Food Safety Monitoring and Early Waring (no. 2021KFJJ02), and Education Department of Scientific Research Project of Hunan Province (no. 20B619), and Education Department of Postgraduate Research and Innovation Project of Hunan Province (no. CX20210863).

ACKNOWLEDGMENTS

The authors would like to thank Editage for English language editing, DL and XZ from Chinese Academy of Science, for kindly performing the heavy ion-beam irradiation.

SUPPLEMENTARY MATERIAL

The Supplementary Material for this article can be found online at: https://www.frontiersin.org/articles/10.3389/fmicb.2022.914828/full#supplementary-material

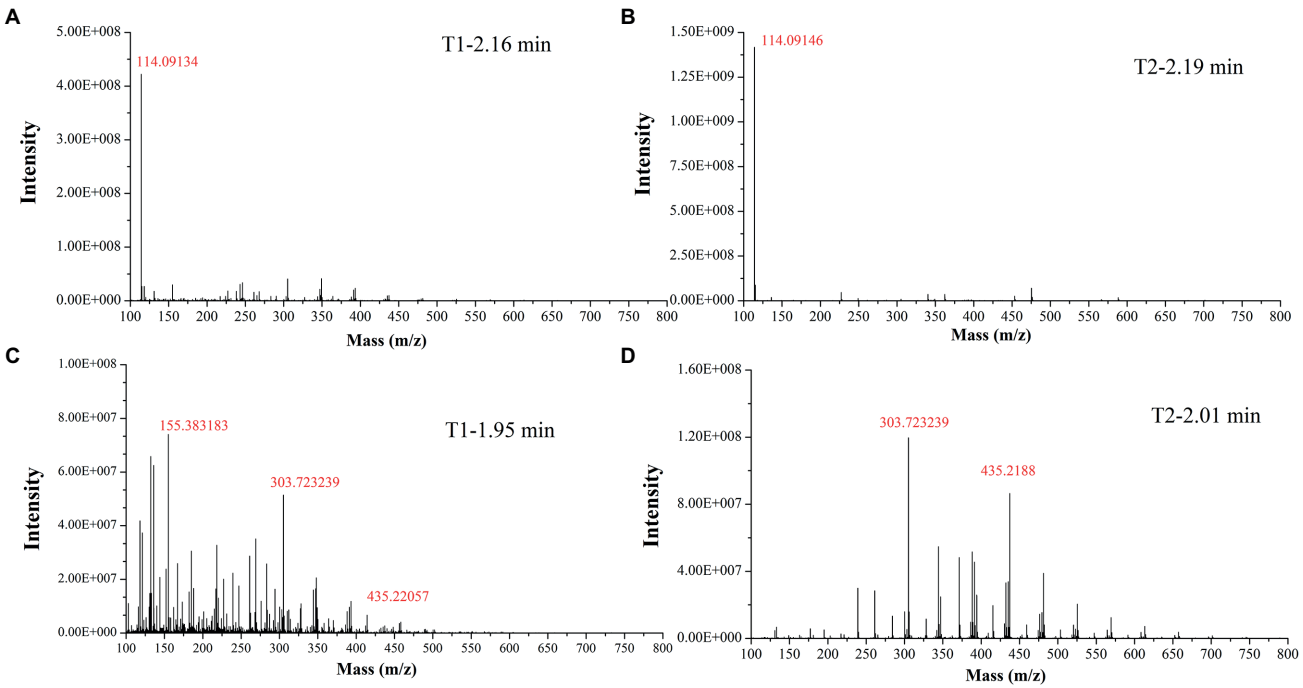

FIGURE 8 | Identification of yellow *monascus* pigment from WSYMP solution and fermentation broth by UHPLC-ESI-MS.

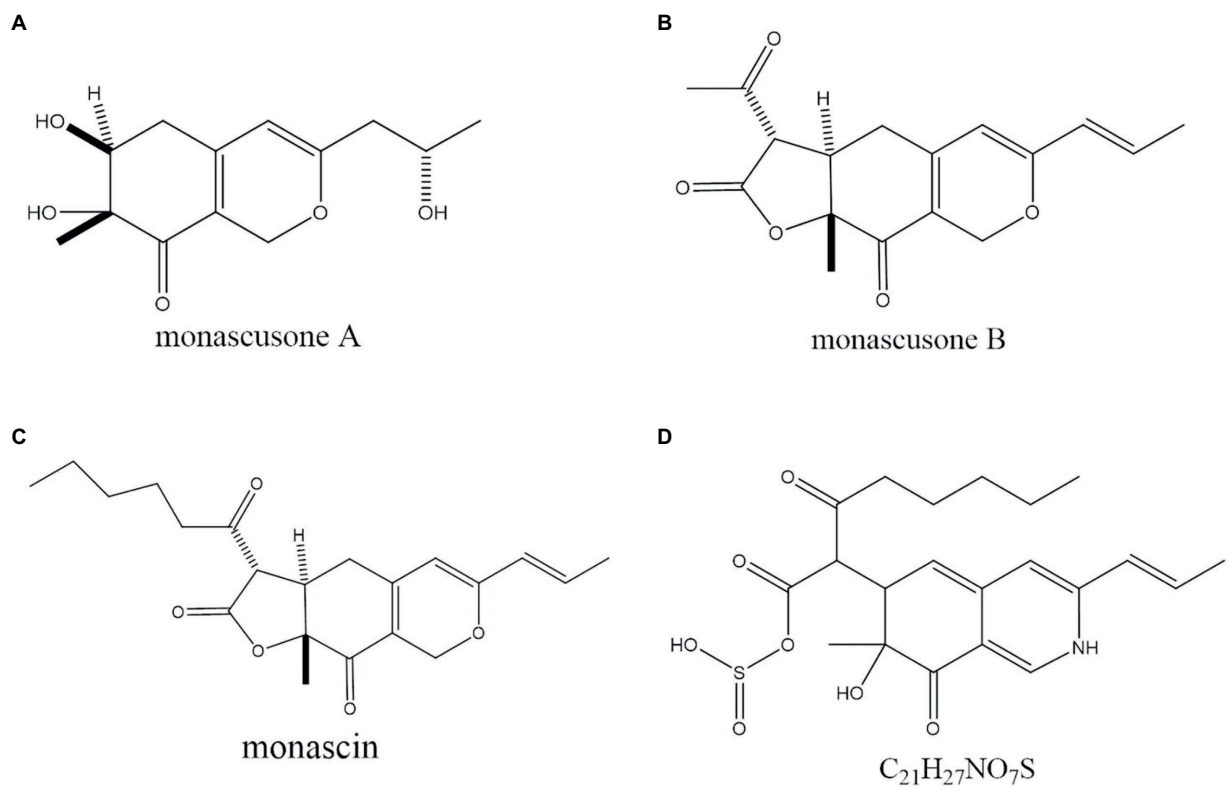

FIGURE 9 | The chemical structure of monascusone A **(A)**, monascusone B **(B)**, and monascin **(C)**, and $C_{21}H_{27}NO_7S$ **(D)**.

REFERENCES

Almeida, A. B. D., Santos, N. H., Lima, T. M. D., Santana, R. V., de Oliveira Filho, J. G., Peres, D. S., et al. (2021). Pigment bioproduction by *Monascus purpureus* using corn bran, a byproduct of the corn industry. *Biocatal. Agric. Biotechnol.* 32:101931. doi: 10.1016/j.bcab.2021.101931

Carvalho, J. C. D., Oishi, B. O., Pandey, A., and Soccol, C. R. (2005). Biopigments from *Monascus*: strains selection, citrinin production and color stability. *Braz. Arch. Biol. Technol.* 48, 885–894. doi: 10.1590/S1516-89132005000800004

Chen, G., Bei, Q., Huang, T., and Wu, Z. (2017a). Tracking of pigment accumulation and secretion in extractive fermentation of *Monascus anka* GIM 3.592. *Microb. Cell Factories* 16:172. doi: 10.1186/s12934-017-0786-6

Chen, X. J., Chen, M. M., Wu, X. F., and Li, X. J. (2021). Cost-effective process for the production of *Monascus* pigments using potato pomace as carbon source by fed-batch submerged fermentation. *Food Sci. Nutr.* 9, 5415–5427. doi: 10.1002/fsn3.2496

Chen, W., He, Y., Zhou, Y., Shao, Y., Feng, Y., Li, M., et al. (2015). Edible filamentous Fungi from the species Monascus: early traditional fermentations, modern molecular biology, and future genomics. *Compr. Rev. Food Sci. Food Saf.* 14, 555–567. doi: 10.1111/1541-4337.12145

Chen, G., Huang, T., Bei, Q., Tian, X., and Wu, Z. (2017b). Correlation of pigment production with mycelium morphology in extractive fermentation of *Monascus anka* GIM 3.592. *Process Biochem.* 58, 42–50. doi: 10.1016/j.procbio.2017.04.012

Chen, M. H., and Johns, M. R. (1993). Effect of pH and nitrogen source on pigment production by *Monascus purpureus*. *Appl. Microbiol. Biotechnol.* 40, 132–138. doi: 10.1007/BF00170441

Chen, M. H., and Johns, M. R. (1994). Effect of carbon source on ethanol and pigment production by *Monascus purpureus*. *Enzym. Microb. Technol.* 16, 584–590. doi: 10.1016/0141-0229(94)90123-6

Chen, L., Tang, H., Du, Y., Dai, Z., Wang, T., Wu, L., et al. (2018). Induction of reproductive cell death in *Caenorhabditis elegans* across entire linear-energy-transfer range of carbon-ion irradiation. *DNA Repair* 63, 39–46. doi: 10.1016/j.dnarep.2018.01.009

Dong, T. T., Gong, J. S., Gu, B. C., Zhang, Q., Li, H., Lu, Z. M., et al. (2017). Significantly enhanced substrate tolerance of *Pseudomonas putida* nitrilase via atmospheric and room temperature plasma and cell immobilization. *Bioresour. Technol.* 244, 1104–1110. doi: 10.1016/j.biortech.2017.08.039

Evans, P. J., and Wang, H. Y. (1984). Pigment production from immobilized *Monascus* sp. utilizing polymeric resin adsorption. *Appl. Environ. Microbiol.* 47, 1323–1326. doi: 10.1128/aem.47.6.1323-1326.1984

Feng, Y., Shao, Y., and Chen, F. (2012). Monascus pigments. *Appl. Microbiol. Biotechnol.* 96, 1421–1440. doi: 10.1007/s00253-012-4504-3

Fenice, M., Federici, F., Selbmann, L., and Petruccioli, M. (2000). Repeated-batch production of pigments by immobilised *Monascus purpureus*. *J. Biotechnol.* 80, 271–276. doi: 10.1016/S0168-1656(00)00271-6

Gao, Y., Zhang, M., Zhou, X., Guo, X., and Lu, D. (2020). Effects of carbon ion beam irradiation on Butanol tolerance and production of *Clostridium acetobutylicum*. *Front. Microbiol.* 11:602774. doi: 10.3389/fmicb.2020.602774

Gong, C., and Wu, Z. (2016). Production and biological activities of yellow pigments from *Monascus* fungi. *World J. Microbiol. Biotechnol.* 32:136. doi: 10.1007/s11274-016-2082-8

Guo, X., Zhang, M., Gao, Y., Lu, D., and Zhou, L. (2020). Repair characteristics and time-dependent effects in response to heavy-ion beam irradiation in *Saccharomyces cerevisiae*: a comparison with X-ray irradiation. *Appl. Microbiol. Biotechnol.* 104, 4043–4057. doi: 10.1007/s00253-020-10464-8

Hu, Z., Zhang, X., Wu, Z., Qi, H., and Wang, Z. (2012). Export of intracellular *Monascus* pigments by two-stage microbial fermentation in nonionic surfactant micelle aqueous solution. *J. Biotechnol.* 162, 202–209. doi: 10.1016/j.jbiotec.2012.10.004

Huang, J., Guan, H. W., Huang, Y. Y., Lai, K. S., Chen, H. Y., Xue, H., et al. (2021a). Evaluating the effects of microparticle addition on mycelial morphology, natural yellow pigments productivity, and key genes regulation in submerged fermentation of *Monascus purpureus*. *Biotechnol. Bioeng.* 118, 2503–2513. doi: 10.1002/bit.27762

Huang, T., Tan, H., Chen, G., Wang, L., and Wu, Z. (2017a). Rising temperature stimulates the biosynthesis of water-soluble fluorescent yellow pigments and gene expression in *Monascus ruber* CGMCC10910. *AMB Express* 7:134. doi: 10.1186/s13568-017-0441-y

Huang, T., Tan, H., Lu, F., Chen, G., and Wu, Z. (2017b). Changing oxidoreduction potential to improve water-soluble yellow pigment production with *Monascus ruber* CGMCC 10910. *Microb. Cell Factories* 16:208. doi: 10.1186/s12934-017-0828-0

Huang, T., Wang, M., Shi, K., Chen, G., Tian, X., and Wu, Z. (2017c). Metabolism and secretion of yellow pigment under high glucose stress with *Monascus ruber*. *AMB Express* 7:79. doi: 10.1186/s13568-017-0382-5

Huang, Z. F., Yang, S. Z., Liu, H. Q., Tian, X. F., and Wu, Z. Q. (2021b). Sodium starch octenyl succinate facilitated the production of water-soluble yellow pigments in *Monascus ruber* fermentation. *Appl. Microbiol. Biotechnol.* 105, 6691–6706. doi: 10.1007/s00253-021-11512-7

Jongrungruangchok, S., Kittakoop, P., Yongsmith, B., Bavovada, R., Tanasupawat, S., Lartpornmatulee, N., et al. (2004). Azaphilone pigments from a yellow mutant of the fungus *Monascus* kaoliang. *Phytochemistry* 65, 2569–2575. doi: 10.1016/j.phytochem.2004.08.032

Kim, D., and Ku, S. (2018). Beneficial effects of *Monascus* sp. KCCM 10093 pigments and derivatives: a mini review. *Molecules* 23:98. doi: 10.3390/molecules23010098

Kodym, A., and Afza, R. (2003). Physical and Chemical Mutagenesis. *Methods in Molecular Biology* 236, 189–204.

Lai, J. R., Hsu, Y. W., Pan, T. M., and Lee, C. L. (2021). Monascin and Ankaflavin of *Monascus purpureus* prevent alcoholic liver disease through regulating AMPK-mediated lipid metabolism and enhancing Both anti-inflammatory and anti-oxidative systems. *Molecules* 26:6301. doi: 10.3390/molecules26206301

Liu, J., Chai, X., Guo, T., Wu, J., Yang, P., Luo, Y., et al. (2019a). Disruption of the Ergosterol biosynthetic pathway results in increased membrane permeability, causing overproduction and secretion of extracellular *Monascus* pigments in submerged fermentation. *J. Agric. Food Chem.* 67, 13673–13683. doi: 10.1021/acs.jafc.9b05872

Liu, J., Guo, T., Luo, Y., Chai, X., Wu, J., Zhao, W., et al. (2019b). Enhancement of *Monascus* pigment productivity via a simultaneous fermentation process and separation system using immobilized-cell fermentation. *Bioresour. Technol.* 272, 552–560. doi: 10.1016/j.biortech.2018.10.072

Liu, J., Luo, Y., Guo, T., Tang, C., Chai, X., Zhao, W., et al. (2020b). Cost-effective pigment production by *Monascus purpureus* using rice straw hydrolysate as substrate in submerged fermentation. *J. Biosci. Bioeng.* 129, 229–236. doi: 10.1016/j.jbiosc.2019.08.007

Liu, L., Wu, S., Wang, W., Zhang, X., and Wang, Z. (2020a). Sulfonation of *Monascus* pigments to produce water-soluble yellow pigments. *Dyes Pigments* 173:107965. doi: 10.1016/j.dyepig.2019.107965

Lu, P., Wu, A., Zhang, S., Bai, J., Guo, T., Lin, Q., et al. (2021). Triton X−100 supplementation regulates growth and secondary metabolite biosynthesis during in-depth extractive fermentation of *Monascus purpureus*. *J. Biotechnol.* 341, 137–145. doi: 10.1016/j.jbiotec.2021.09.018

Lv, J., Zhang, B. B., Liu, X. D., Zhang, C., Chen, L., Xu, G. R., et al. (2017). Enhanced production of natural yellow pigments from Monascus purpureus by liquid culture: the relationship between fermentation conditions and mycelial morphology. *J. Biosic. Bioeng.* 124, 452–458. doi: 10.1016/j.jbiosc.2017.05.010

Qian, G. F., Huang, J., Farhadi, A., and Zhang, B. B. (2021). Ethanol addition elevates cell respiratory activity and causes overproduction of natural yellow pigments in submerged fermentation of *Monascus purpureus*. *LWT Food Sci. Technol.* 139:110534. doi: 10.1016/j.lwt.2020.110534

Shi, K., Song, D., Chen, G., Pistolozzi, M., Wu, Z., and Quan, L. (2015). Controlling composition and color characteristics of *Monascus* pigments by pH and nitrogen sources in submerged fermentation. *J. Biosci. Bioeng.* 120, 145–154. doi: 10.1016/j.jbiosc.2015.01.001

Srivastav, P., Yadav, V. K., Govindasamy, S., and Chandrasekaran, M. (2015). Red pigment production by *Monascus purpureus* using sweet potato-based medium in submerged fermentation. *Forum Nutr.* 14, 159–167. doi: 10.1007/s13749-015-0032-y

Su, N. W., Lin, Y. L., Lee, M. H., and Ho, C. Y. (2005). Ankaflavin from Monascusfermented red rice exhibits selective cytotoxic effect and induces cell death on Hep G2 cells. *J. Agric. Food Chem.* 53, 1949–1954. doi: 10.1021/jf048310e

Sun, J. L., Zou, X., Liu, A. Y., and Xiao, T. F. (2011). Elevated yield of Monacolin K in *Monascus purpureus* by fungal elicitor and mutagenesis of UV and LiCl. *Biol. Res.* 44, 377–382. doi: 10.4067/S0716-97602011000400010

Wang, C., Chen, D., and Qi, J. (2017a). "Biochemistry and molecular mechanisms of Monascus pigments" in *Bio-pigmentation and Biotechnological Implementations*, 173–191.

Wang, M., Huang, T., Chen, G., and Wu, Z. (2017b). Production of water-soluble yellow pigments via high glucose stress fermentation of *Monascus ruber* CGMCC 10910. *Appl. Microbiol. Biotechnol.* 101, 3121–3130. doi: 10.1007/s00253-017-8106-y

Wong, H. C., and Koeler, P. E. (1983). Production of red water-soluble *Monascus* pigments. *J. Food Sci.* 48, 1200–1203. doi: 10.1111/j.1365-2621.1983.tb09191.x

Wu, L., Zhou, K., Chen, F., Chen, G., Yu, Y., Lv, X., et al. (2021). Comparative study on the antioxidant activity of *Monascus* yellow pigments From two different types of Hongqu—functional Qu and coloring Qu. *Front. Microbiol.* 12:715295. doi: 10.3389/fmicb.2021.715295

Xiong, X., Zhang, X., Wu, Z., and Wang, Z. (2015). Accumulation of yellow *Monascus* pigments by extractive fermentation in nonionic surfactant micelle aqueous solution. *Appl. Microbiol. Biotechnol.* 99, 1173–1180. doi: 10.1007/s00253-014-6227-0

Yang, X., Dong, Y., Liu, G., Zhang, C., and Wang, C. (2020). Effects of nonionic surfactants on pigment excretion and cell morphology in extractive fermentation of *Monascus* sp. NJ1. *J. Sci. Food Agric.* 100:1832. doi: 10.1002/jsfa.10171

Yang, H. H., Li, J., Wang, Y., and Gan, C. J. (2018). Identification of water-soluble *Monascus* yellow pigments using HPLC-PAD-ELSD, high-resolution ESI-MS, and MS-MS. *Food Chem.* 245, 536–541. doi: 10.1016/j.foodchem.2017.10.121

Zhang, X., Zhang, X. F., Li, H. P., Wang, L. Y., Zhang, C., Xing, X. H., et al. (2014). Atmospheric and room temperature plasma (ARTP) as a new powerful mutagenesis tool. *Appl. Microbiol. Biotechnol.* 98, 5387–5396. doi: 10.1007/s00253-014-5755-y

Zhang, S., Zhao, W., Nkechi, O., Lu, P., Bai, J., Lin, Q., et al. (2022). Utilization of low-cost agricultural by-product rice husk for *Monascus* pigments production via submerged batch-fermentation. *J. Sci. Food Agric.* 102, 2454–2463. doi: 10.1002/jsfa.11585

Zhou, W., Rui, G., Guo, W., Hong, J., Lu, L., Li, N., et al. (2019). *Monascus* yellow, red and orange pigments from red yeast rice ameliorate lipid metabolic disorders and gut microbiota dysbiosis in Wistar rats fed on a high-fat diet. *Food Funct.* 10, 1073–1084. doi: 10.1039/C8FO02192A

Zhou, B., Wang, J., Pu, Y., Zhu, M., Liu, S., and Liang, S. (2009). Optimization of culture medium for yellow pigments production with *Monascus* anka mutant using response surface methodology. *Eur. Food Res. Technol.* 228, 895–901. doi: 10.1007/s00217-008-1002-z

Conflict of Interest: CT was employed by Nanjing Sheng Ming Yuan Health Technology Co. Ltd. and Jiangsu Institute of Industrial Biotechnology JITRI Co. Ltd.

The remaining authors declare that the research was conducted in the absence of any commercial or financial relationships that could be construed as a potential conflict of interest.

Publisher's Note: All claims expressed in this article are solely those of the authors and do not necessarily represent those of their affiliated organizations, or those of the publisher, the editors and the reviewers. Any product that may be evaluated in this article, or claim that may be made by its manufacturer, is not guaranteed or endorsed by the publisher.

frontiers | Frontiers in Microbiology

ORIGINAL RESEARCH
published: 14 June 2022
doi: 10.3389/fmicb.2022.921540

Methionine and S-Adenosylmethionine Regulate *Monascus* Pigments Biosynthesis in *Monascus purpureus*

Sheng Yin[1,2,3]*, *Dongmei Yang*[3], *Yiying Zhu*[3] and *Baozhu Huang*[3]

[1] Beijing Advanced Innovation Center for Food Nutrition and Human Health, Beijing Technology and Business University, Beijing, China, [2] Beijing Engineering and Technology Research Center of Food Additives, Beijing Technology and Business University, Beijing, China, [3] School of Food and Health, Beijing Technology and Business University, Beijing, China

Amino acid metabolism could exert regulatory effects on *Monascus* pigments (MPs) biosynthesis. In this work, MPs biosynthesis regulated by methionine and S-adenosylmethionine (SAM) was investigated in *Monascus purpureus* RP2. The results indicated that the addition of methionine in fermentation significantly reduced MPs production by 60–70%, and it induced a higher expression of SAM synthetase Mon2A2272 and consequently led to SAM accumulation. However, the addition of SAM in fermentation promoted MPs production by a maximum of 35%, while over-expression of the gene *Mon2A2272* led to a decrease in MPs yield, suggesting that SAM synthetase and SAM were likely to play different regulatory roles in MPs biosynthesis. Furthermore, the gene transcription profile indicated that SAM synthetase expression led to a higher expression of the transcriptional regulatory protein of the MPs biosynthesis gene cluster, while the addition of SAM gave rise to a higher expression of MPs biosynthesis activator and the global regulator LaeA, which probably accounted for changes in MPs production and the mycelium colony morphology of *M. purpureus* RP2 triggered by methionine and SAM. This work proposed a possible regulation mechanism of MPs biosynthesis by SAM metabolism from methionine. The findings provided a new perspective for a deep understanding of MPs biosynthesis regulation in *M. purpureus.*

Keywords: methionine, S-adenosylmethionine, SAM synthetase, *Monascus* pigments, *Monascus purpureus*

OPEN ACCESS

Edited by:
Jun Liu,
Central South University Forestry and Technology, China

Reviewed by:
Fusheng Chen,
Huazhong Agricultural University, China
Chuannan Long,
Jiangxi Science and Technology Normal University, China

***Correspondence:**
Sheng Yin
yinsheng@btbu.edu.cn

Specialty section:
This article was submitted to Food Microbiology, a section of the journal Frontiers in Microbiology

Received: *16 April 2022*
Accepted: *17 May 2022*
Published: *14 June 2022*

Citation:
Yin S, Yang D, Zhu Y and Huang B (2022) Methionine and S-Adenosylmethionine Regulate Monascus Pigments Biosynthesis in Monascus purpureus. Front. Microbiol. 13:921540. doi: 10.3389/fmicb.2022.921540

INTRODUCTION

Monascus pigments (MPs) are Chinese traditional natural colorants with an application history of thousands of years. Nowadays, they are still widely used in the fields of food, pharmaceutical, cosmetic manufacture, and printing, dyeing, and textile industries (Lin et al., 2008; Mapari et al., 2010; Feng et al., 2012; Patakova, 2013; Dufosse et al., 2014; Mostafa and Abbady, 2014; Srianta et al., 2014; Chen et al., 2015). MPs are a large class of structurally related secondary polyketide metabolites shared with a common azaphilone skeleton produced by *Monascus* spp. and are traditionally classified as red, orange, and yellow pigments (Chen et al., 2015, Chen W. et al., 2017). It is generally recognized that MPs are biosynthesized *via* the polyketide synthase (PKS) pathway, and the

conserved PKS gene cluster in *Monascus* is identified to be composed of a dozen gene elements encoding the polyketide synthase, transcription factors, and other functional enzymes (Yang et al., 2014; Chen et al., 2015, Chen W. et al., 2017).

The PKS pathway responsible for MPs biosynthesis is quite complicated and still ambiguous. Continuous studies (Yang et al., 2014; Chen et al., 2015, Chen W. et al., 2017) revealed that MPs biosynthesis started with the esterification of a β-ketoacid from the fatty acid synthase pathway to the chromophore from the PKS pathway, generating the yellow intermediates. The yellow intermediates are then reduced and oxidized into the classical yellow MPs (Monascin and Ankaflavin) and orange MPs (Rubropunctatin and Monascorubrin), respectively. Finally, the classical red MPs (Rubropunctamine and Monascorubramine) are formed by direct integration of the amido group (amines or amino acids) into the orange MPs.

Based on current understanding of the MPs biosynthesis pathway, the amino donors are believed to be directly involved in the red MPs molecule formation (Chen et al., 2015, Chen W. et al., 2017). However, *in vitro* chemical reactions demonstrated that only 4 of 18 amino donors (arginine, lysine, γ-aminobutyric acid, and ammonia) directly reacted with the orange MPs to form the red MPs (Chen W. et al., 2017), indicating that not all the amino compounds could act as the precursor substrates of MPs. Even though, it is indispensable to take into account the roles of nitrogen sources in MPs biosynthesis. Several previous studies reported that different nitrogen sources supplemented in fermentation medium made a significant impact on the yield and component composition of MPs (Chen and Johns, 1993; Jung et al., 2003, 2005, 2011; Dhale et al., 2011; Hajjaj et al., 2012; Arai et al., 2013; Zhang et al., 2013; Said et al., 2014; Shi et al., 2015; Xiong et al., 2015). Therefore, it is reasonable to conclude that various nitrogen sources could exert regulatory effects on MPs biosynthesis in different ways.

Methionine is an important sulfur-containing amino acid that plays essential roles in multiple biological processes, such as DNA methylation, protein structure, and polyamine synthesis (Brosnan et al., 2007; Cavuoto and Fenech, 2012). Methionine could be transformed into S-adenosylmethionine (SAM) by the catalysis of SAM synthetase (EC 2.5.1.6) (Lieber and Lester, 2002). SAM is the major cellular methyl group donor in living organisms and it is involved in the methylation processes of DNA, RNA, proteins, metabolites, and phospholipids (Lieber and Lester, 2002; Brosnan et al., 2007; Gerke et al., 2012). In microorganisms, SAM is involved in a variety of processes, such as protection of DNA and mRNA integrity, the function of restriction enzymes, regulation of gene expression, efficient translation, cellular differentiation, stress response, and secondary metabolites biosynthesis (Lieber and Lester, 2002; Brosnan et al., 2007; Gerke et al., 2012). It is evident that the metabolism of SAM from methionine serves not only as the nitrogen source supply but also as the regulator of multiple biological processes. In this study, the bidirectional regulatory effects of methionine and SAM on MPs biosynthesis were observed in *Monascus purpureus* RP2. SAM and SAM synthetase were proved to be the key effector molecules for MPs biosynthesis regulation, which probably interacted with the global regulator LaeA and the PKS gene cluster. These findings provided new insights into the regulation mechanism of MPs biosynthesis in *M. purpureus.*

MATERIALS AND METHODS

Strains, Plasmids, and Culture Conditions

The strains and plasmids used in this work are listed in **Table 1**. *Escherichia coli* strains were grown at 37°C in Luria-Bertani (LB) medium with vigorous shaking at 220 rpm in a shaking incubator with a rotational radius of 10 cm. *M. purpureus* strains were cultured in Potato Dextrose Agar (PDA) medium at 30°C. When needed, 200 μg/ml ampicillin for *E. coli* or 20 μg/ml hygromycin B for *M. purpureus* was added to the medium for recombinant screening.

For MPs production by liquid-state fermentation, *M. purpureus* was cultured at 30°C in PDA medium for 10 days and the spore suspension was prepared by washing the mycelium with sterile water and collected by filtration with sterile gauze. The spore suspension (10%) was inoculated into seed medium (40 g/L rice flour, 8 g/L peptones, 5 g/L soybean meal, 1 g/L $MgSO_4{\cdot}7H_2O$, 2 g/L KH_2PO_4, and 2 g/L $NaNO_3$) and cultured at 33°C with vigorous shaking at 200 rpm in a shaking incubator with a rotational radius of 10 cm for 48 h. The seed culture (10%) was then inoculated into a fermentation medium (20 g/L glucose, 5 g/L Yeast Nitrogen Base W/O Amino acids, 5 g/L $K_2HPO_4{\cdot}3H_2O$, 0.5 g/L $MgSO_4{\cdot}7H_2O$, 5 g/L KH_2PO_4, 0.1 g/L $CaCl_2$, 0.03 g/L $MnSO_4{\cdot}H_2O$, 0.01 g/L $FeSO_4{\cdot}7H_2O$, and 0.01 g/L $ZnSO_4{\cdot}7H_2O$) and cultured at 33°C with vigorous shaking at 200 rpm in a shaking incubator with a rotational radius of 10 cm for 12 days. When needed, 3 g/L methionine or 1 g/L SAM was added to the fermentation medium. For colony

TABLE 1 | Strains and plasmids used in this work.

Strains or plasmids	Relevant features	Reference or source
Plasmids		
pBARGPE1-Hygro	Shuttle vector for gene expression in *E. coli* and *M. purpureus*, Amp^R, $Hygro^R$	Laboratory collection
pBARGPE1-2272	SAM synthetase gene *Mon2A2272* cloned in pBARGPE1-Hygro, Amp^R, $Hygro^R$	This work
Strains		
E. coli DH5α	Host for cloning	TIANGEN, Beijing, China
E. coli 2272	*E. coli* DH5α harboring pBARGPE1-2272, Amp^R	This work
M. purpureus RP2	Wild strain; Donor of SAM synthetase gene *Mon2A2272*	Laboratory collection
M. purpureus 2272	*M. purpureus* RP2 harboring pBARGPE1-2272, $Hygro^R$	This work

morphology observation, *M. purpureus* was cultured at 30°C in the fermentation medium containing agar (20 g/L) for 6–9 days.

Measurement of *Monascus* Pigments Production

For measurement of MPs production, the fermentation culture was centrifuged at 8,000 × *g* for 10 min to collect mycelia and medium supernatant, respectively. Samples of the mycelia or medium supernatant were soaked in 50 ml of 70% (v/v) ethanol and incubated in a water bath (60°C) for 1 h to extract MPs. The extraction mixture was centrifuged at 8,000 × *g* for 10 min to collect the supernatant, which was used to measure MPs concentration by spectrophotometer (OD 410 nm for yellow MPs, OD 468 nm for orange MPs, and OD 505 nm for red MPs).

DNA Manipulation Techniques

Standard DNA manipulation techniques were performed as described by Green and Sambrook (2012). Total RNA from *M. purpureus* was prepared using the RNAprep Pure Plant Kit (TIANGEN, Beijing, China) following the manufacturer's instructions. RNA was subjected to reverse transcription to generate cDNA using the Quantscript RT Kit (TIANGEN, Beijing, China) following the manufacturer's protocol. Quantitative Real-Time PCR (q RT-PCR) was performed using the SuperReal PreMix Plus (SYBR Green) Kit (TIANGEN, Beijing, China) in the CFX96 Touch Real-Time PCR System (Bio-Rad, United States) with the following cycling conditions: 95°C for 2 min, followed by 40 cycles of 94°C for 20 s, 63°C for 45 s, and 60°C for 5 min. The *GAPDH* gene was used for transcript normalization. All reactions were performed in triplicate. The $2^{-\Delta\Delta Ct}$ method was used to analyze the data, which was corrected for primer efficiencies using the untreated group means as the reference condition (Schmittgen and Livak, 2008; Putt et al., 2017).

DNA amplification and recombinant DNA construction were performed using the Ex Taq DNA Polymerase and DNA Ligation Kit (Takara, Beijing, China) following the manufacturer's protocol. Plasmid DNA from *E. coli* was isolated using the High-purity Plasmid Miniprep Kit (TIANGEN, Beijing, China) according to the manufacturer's instructions. A standard heat shock transformation method was used to introduce plasmid DNA to *E. coli* (Green and Sambrook, 2012). Primers used for gene transcription level assay by q RT-PCR and gene cloning by PCR are listed in **Supplementary Table 1**.

Vector Construction for Over-Expression of the S-Adenosylmethionine Synthetase Gene *Mon2A2272*

The SAM synthetase gene *Mon2A2272* was amplified by PCR from the cDNA derived from the total RNA of *M. purpureus* RP2 using the specific primers SAMS-F/R designed according to the genomic sequence of *M. purpureus* RP2. The amplicon was inserted into the shuttle vector pBARGPE1-Hygro for gene expression in *E. coli* and *M. purpureus* to construct the recombinant vector pBARGPE1-2272. The DNA ligation mixture was transformed into *E. coli* DH5α and transformants were screened on LB agar plates containing ampicillin. The recombinant vector was verified by sequencing and alignment analysis using the DNAMAN software package and BLAST Program at NCBI against the GenBank database.

Electroporation of *Monascus purpureus*

The recombinant vector pBARGPE1-2272 was introduced into *M. purpureus* RP2 by electroporation as previously described with modifications (Kim et al., 2003; Lakrod et al., 2003). For the preparation of the electrocompetent protoplast of *M. purpureus* RP2, a fresh spore suspension was prepared as described previously and was spread on a PDA plate and cultured at 30°C for 30–40 h. Mycelia (300 mg) were collected and washed with 1 M $MgSO_4$ and incubated at 30°C for 3 h in 50 ml of enzymolysis buffer (1% snailase, 0.1% cellulase, and 0.3% lysozyme). The enzymolysis solution was filtered with sterile gauze and the spheroplast suspension was collected and centrifuged at 8,000 × *g* at 4°C for 5 min. The spheroplasts were harvested and washed with cooled sorbitol buffer (1 M) and resuspended in 200 μl of the cooled protoplast buffer (25 mM Tris-HCl, pH 7.5; 25 mM $CaCl_2$, 1.2 M sorbitol).

For electroporation of *M. purpureus* RP2, the purified recombinant plasmid pBARGPE1-2272 (1 μg) and the cooled protoplast suspension (100 μl, 10^9 protoplasts/ml) were mixed well and transferred to a cooled electroporation cuvette (Bio-Rad, United States) with a 0.2-cm electrode gap. The electroporation cuvette was incubated in an ice bath for 15 min and electroporated in Gene Pulser (Bio-Rad, United States) using the following settings: voltage, 3 kV/cm; capacitance, 25 μF; and resistance, 400 Ω. Following the electric pulse, 1 ml of regeneration broth (Potato Dextrose Broth plus 1.2 M sorbitol) was immediately added to the cuvette and the electroporation mixture was transferred to a sterile 1.5 ml tube and incubated with agitation at 1,000 × *g* at 30°C for 2 h. The mixture was plated onto PDA plates containing hygromycin B and cultured at 30°C in the dark for 3–6 days. The recombinant strain *M. purpureus* 2272 was screened and validated by colony PCR of the hygromycin resistance gene using the specific primers Hyg-F/R. Additionally, q RT-PCR was carried out for analysis of the transcriptional level of *Mon2A2272* in *M. purpureus* 2272.

Measurement of S-Adenosylmethionine

For measurement of SAM produced by *M. purpureus*, the fermentation culture was centrifuged at 8,000 × *g* for 10 min to collect mycelia and medium supernatant, respectively. The medium supernatant was filtered with a 0.22 μm pore membrane and used for SAM determination. The wet mycelia were dried at −80°C by vacuum freezing and incubated in the solution containing 4 ml of 1.5 M perchloric acid and 4 ml of 1.5 M ammonia water at 4°C for overnight. The mixture was centrifuged at 10,000 × *g* for 15 min to collect the supernatant for SAM determination. SAM was determined by high-performance liquid chromatography (HPLC) (SHIMADZU, Shanghai, China) as previously described with modifications (Wang et al., 2012).

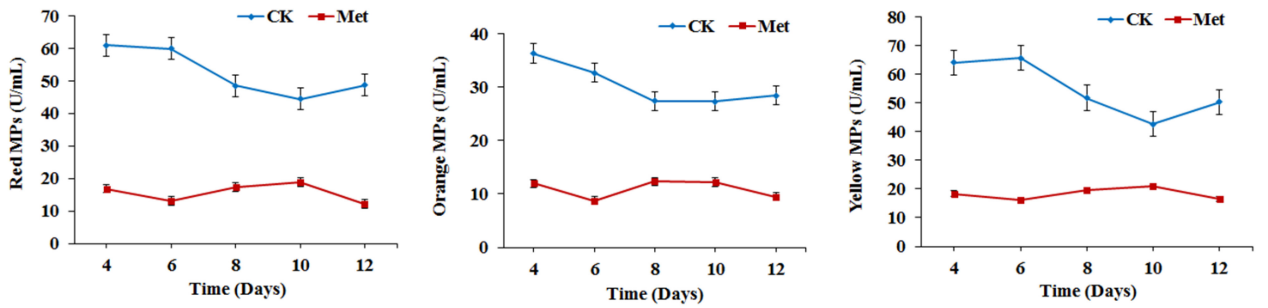

FIGURE 1 | *Monascus* pigments (MPs) production in *Monascus purpureus* RP2. CK, fermentation without addition of methionine; Met, fermentation with addition of 3 g/L methionine.

The HPLC analysis conditions were as follows: Inertsil ODS-3 column (4.6 mm × 250 mm, 5 μm, SHIMADZU, Shanghai, China); injection volume 20 μl; oven temperature 30°C; flow rate 1 ml/min; the eluate was monitored at 260 nm. Mobile phase A (10 mM ammonium formate buffer, pH 3.5) and phase B (methanol) were run on an isocratic elution program (95% phase A buffer and 5% phase B buffer). The standard chemicals SAM was purchased from Macklin Biochemical Co., Ltd (Shanghai, China).

RESULTS AND DISCUSSION

Addition of Methionine Reduced *Monascus* Pigments Production and Enhanced S-Adenosylmethionine Synthetase Expression and S-Adenosylmethionine Generation

The fermentation medium containing YNB without amino acids as the nitrogen source was used to evaluate the effect of methionine addition on MPs biosynthesis in *M. purpureus* RP2. Evaluation of serial gradient concentrations (1–9 g/L) of methionine indicated that 3 g/L was the optimal volume of addition that exerted a significant effect on MPs production (data not shown). Fermentation results showed that the yields of red, orange, and yellow MPs were all significantly reduced by 60–70% during 12 days of liquid fermentation with the addition of 3 g/L methionine (**Figure 1**). Meanwhile, the bright red, orange, and yellow colors of MPs became much more intense within and around the mycelium colony cultivated without methionine than with methionine in the fermentation agar plates (**Figure 2**). MPs production was remarkably inhibited in the presence of methionine in both liquid fermentation and plate culture. In addition, it is noteworthy that the morphologies were quite different between the mycelium colonies grown in plates with and without methionine as shown in **Figure 2**, indicating that the addition of methionine also changed the mycelial development of *M. purpureus* RP2.

To figure out the reason that methionine inhibited MPs production, the metabolism of methionine was investigated in *M. purpureus* RP2. Generally, methionine could be transformed

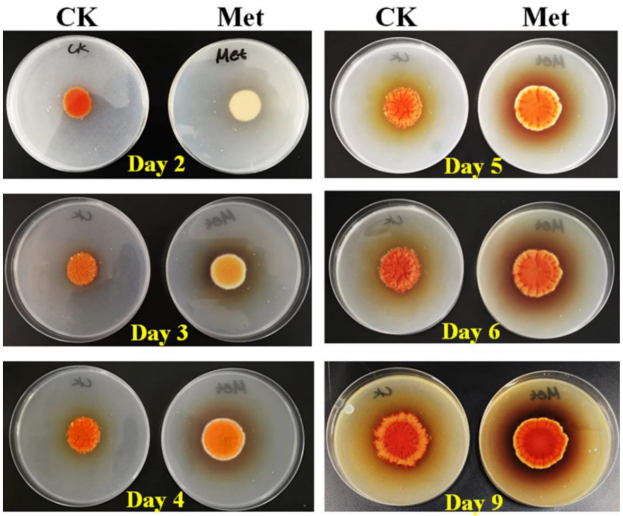

FIGURE 2 | Cultivation of *M. purpureus* RP2 in fermentation agar plates. CK, fermentation without addition of methionine; Met, fermentation with addition of 3 g/L methionine.

to SAM by the catalysis of SAM synthetase and the derivative would act as the major cellular methyl donor and precursor to organic radicals involved in a variety of important biological processes (Lieber and Lester, 2002; Brosnan et al., 2007). Unsurprisingly, it was detected that the concentration of intracellular SAM in *M. purpureus* RP2 increased by 100–200 μg/ml in fermentation with methionine compared with that without methionine. In addition, q RT-PCR analysis also showed that the transcriptional level of the SAM synthetase gene *Mon2A2272* in *M. purpureus* RP2 at the beginning of fermentation was about 12-fold higher with methionine than without methionine, which could account for SAM generation. Therefore, it is reasonable to conclude that the addition of methionine in the fermentation medium induced SAM synthetase Mon2A2272 expression and consequently enhanced SAM generation, directly or indirectly leading to a significant reduction in MPs production in *M. purpureus* RP2. However, it is still questionable whether SAM synthetase Mon2A2272

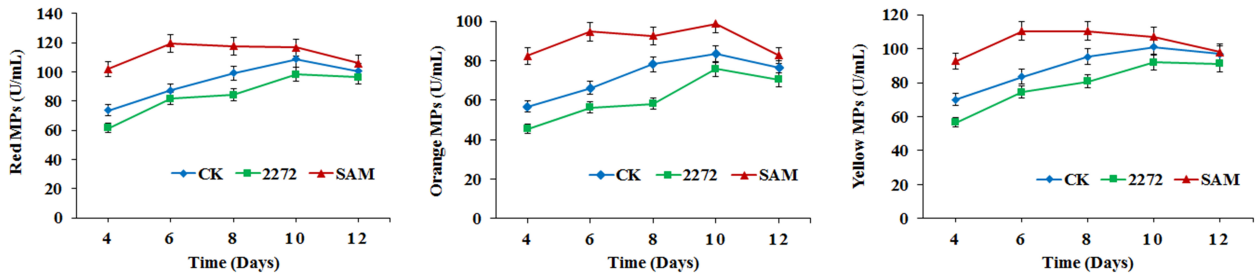

FIGURE 3 | *Monascus* pigments production in *M. purpureus* RP2 and *M. purpureus* 2272. CK, *M. purpureus* RP2 fermentation without addition of amino acid; 2272, *M. purpureus* 2272 fermentation without addition of amino acid; (SAM), *M. purpureus* RP2 fermentation with addition of 1 g/L SAM.

expressed at a higher level or SAM accumulation acted as the effector that affected MP production.

Addition of S-Adenosylmethionine Enhanced *Monascus* Pigments Production

As the addition of methionine led to SAM generation and MP production reduction in *M. purpureus* RP2, it is essential to reveal the causal connection between SAM accumulation and MP production. The fermentation with the addition of 1 g/L SAM was conducted to investigate the effect of high-level SAM on MP production in *M. purpureus* RP2. Unexpectedly, a maximum 35% increase in MPs production was detected in fermentation with SAM in comparison with that without SAM (**Figure 3**). The fermentation agar plate cultivation also showed that a brighter yellow or orange halo was observed around the mycelium colony with SAM (**Figure 4**), which was in accordance with MPs yield determination. Moreover, the addition of SAM also altered the morphology of the mycelium colony (**Figure 4**), but it is a different pattern from that derived from the addition of methionine (**Figure 2**). In addition, though the addition of SAM resulted in a higher accumulation of SAM in *M. purpureus* RP2 after 3 days of fermentation as shown in **Figure 5**, q RT-PCR assay indicated that extra SAM did not affect the expression of the SAM synthetase gene *Mon2A2272* (**Figure 6**). It suggested that SAM individually played the regulatory role in MP production and mycelium development in *M. purpureus* RP2.

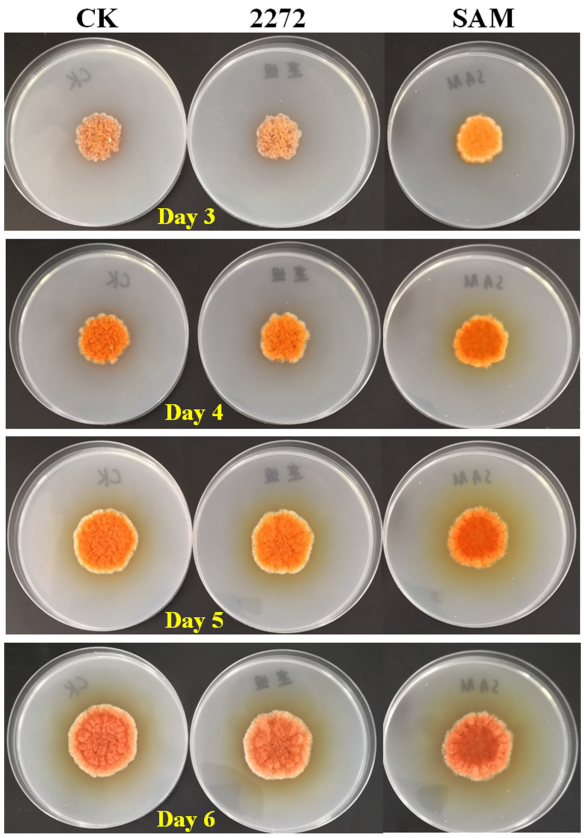

FIGURE 4 | Cultivation of *M. purpureus* RP2 and *M. purpureus* 2272 in fermentation agar plates. CK, *M. purpureus* RP2 fermentation without addition of amino acid; 2272, *M. purpureus* 2272 fermentation without addition of amino acid; SAM, *M. purpureus* RP2 fermentation with addition of 1 g/L SAM.

S-Adenosylmethionine Synthetase Mon2A2272 Over-Expression Enhanced S-Adenosylmethionine Generation and Reduced *Monascus* Pigments Production

As previously reported, the addition of methionine induced SAM synthetase Mon2A2272 expression, enhanced SAM generation, and inhibited MPs production. SAM synthetase or SAM was suspected to be the effector of the reduction in MP production. However, when a high concentration of SAM was added in fermentation, MP production increased as shown in **Figures 3**, **4**. Hence, the causal connection between the high expression level of SAM synthetase and MPs production was further investigated by the construction of the recombinant strain *M. purpureus* 2272 with over-expression of the SAM synthetase gene *Mon2A2272*. The SAM synthetase gene *Mon2A2272* cloned from *M. purpureus* RP2 was 1,161 bp in size and encoded a protein containing 386 amino acid residues, which shared a 100% homology with the SAM synthase from *M. purpureus* (GenBank Accession No. TQB68059.1). The q RT-PCR analysis showed that the transcriptional level of the SAM synthetase gene *Mon2A2272* in *M. purpureus* 2272 was about 4.5-fold higher than that in

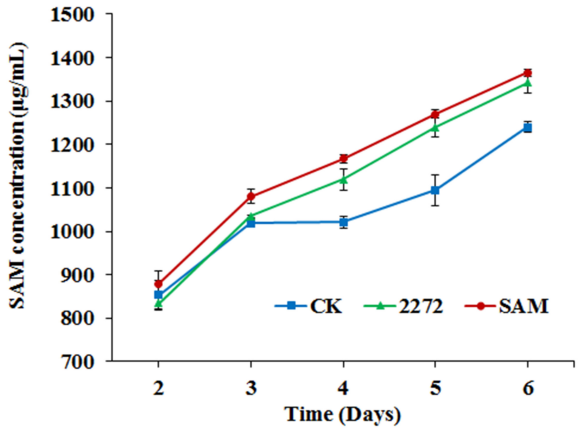

FIGURE 5 | S-adenosylmethionine accumulation in the fermentation broth of *M. purpureus* RP2 and *M. purpureus* 2272. CK, *M. purpureus* RP2 fermentation without addition of amino acid; 2272, *M. purpureus* 2272 fermentation without addition of amino acid; SAM, *M. purpureus* RP2 fermentation with the addition of 1 g/L SAM.

the wild strain *M. purpureus* RP2 on day 2 of fermentation (**Figure 6**). Consequently, much more SAM was generated and accumulated in the fermentation broth in *M. purpureus* 2272 than that in *M. purpureus* RP2 after 3 days of fermentation (**Figure 5**). In addition, the yields of red, orange, and yellow MPs all decreased in *M. purpureus* 2272 in comparison with *M. purpureus* RP2 during 12 days of fermentation (**Figure 3**). Morphology observation showed no obvious difference between the mycelium colonies of *M. purpureus* 2272 and *M. purpureus* RP2 (**Figure 4**), indicating that expression of the SAM synthetase gene *Mon2A2272* did not affect the mycelial development. The results gave a probable explanation for MPs reduction by the addition of methionine in fermentation. SAM synthetase expression likely exerted the negative regulation on MPs production in *M. purpureus* RP2.

S-Adenosylmethionine and S-Adenosylmethionine Synthetase Mon2A2272 Both Regulated *Monascus* Pigments Biosynthesis Gene Cluster Expression

The conserved PKS gene cluster was responsible for MPs biosynthesis in *Monascus* (Yang et al., 2014; Chen et al., 2015, Chen W. et al., 2017). A classical PKS gene cluster was detected in *M. purpureus* RP2 and it consisted of 15 structural genes encoding functional enzymes and two regulatory elements *Mon2A4595* and *Mon2A4602* (**Supplementary Figure 2**). *Mon2A4595* encoded the transcriptional regulatory protein and shared a 99% homology with the transcription factor MpigI

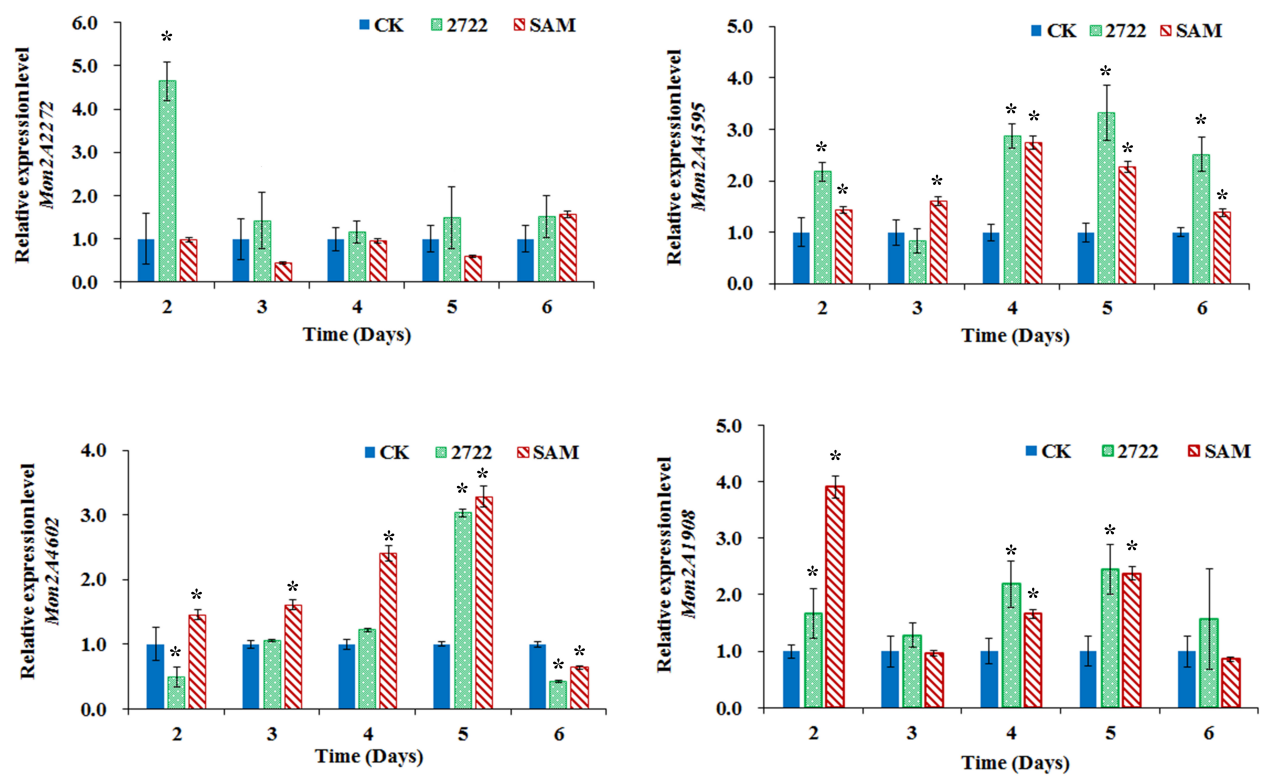

FIGURE 6 | Gene transcriptional level assay in *M. purpureus* RP2 and *M. purpureus* 2272. CK, *M. purpureus* RP2 fermentation without addition of amino acid; 2272, *M. purpureus* 2272 fermentation without addition of amino acid; SAM, *M. purpureus* RP2 fermentation with the addition of 1 g/L SAM; Bars with an asterisk are significantly different ($p < 0.05$).

(GenBank Accession No. APZ73944.1) from *Monascus ruber* M7; and *Mon2A4602* encoded the pigment biosynthesis activator and shared a 97% homology with the pigment biosynthesis activator PigR (GenBank Accession No. AGL44390.1) from *M. ruber* M7. Yang et al. (2014) reported that most genes in the PKS cluster including the two regulatory elements were expressed at higher levels under high pigment production conditions in *M. purpureus* YY-1 and Chen D. et al. (2017) reported that expression of the transcriptional regulatory protein in the PKS cluster was upregulated when pigment biosynthesis was induced by blue light in *M. purpureus* M9. Hence, the MPs biosynthesis regulatory elements *Mon2A4595* and *Mon2A4602* were selected for gene transcriptional level analysis by qRT-PCR during fermentation. As shown in **Figure 6**, the transcriptional levels of *Mon2A4595* and *Mon2A4602* both increased in *M. purpureus* RP2 with addition of SAM and in *M. purpureus* 2272 with an expression of SAM synthetase Mon2A2272 during the early 6 days of fermentation when MPs was synthesized in large amounts. Generally, SAM synthetase Mon2A2272 expression led to a higher expression of the transcriptional regulatory protein Mon2A4595, while the addition of SAM gave rise to a higher expression of the pigment biosynthesis activator Mon2A4602. Furthermore, the addition of SAM in fermentation resulted in higher expressions of most functional enzymes encoding genes in the PKS cluster in comparison with that without SAM addition and with Mon2A2272 expression (**Supplementary Figure 3**). This could probably explain the difference in MP production yield between *M. purpureus* RP2 with and without the addition of SAM and *M. purpureus* 2272 with the expression of SAM synthetase Mon2A2272. It suggested that SAM and SAM synthetase both could affect the expression of the PKS gene cluster by the regulatory elements to regulate MPs biosynthesis.

Furthermore, the global regulator, Mon2A1908 that shared a 100% homology with the global regulator of sporulation and secondary metabolism LaeA (GenBank Accession No. AIY63188.1) from *M. ruber* M7 was subjected to transcription analysis in response to the addition of SAM and expression of SAM synthetase Mon2A2272. It is observed that the transcriptional level of *Mon2A1908* was about 4-fold higher in *M. purpureus* RP2 with the addition of SAM than that in *M. purpureus* RP2 without SAM and *M. purpureus* 2272 at the beginning of fermentation (**Figure 6**). The biosynthesis of many secondary metabolites in filamentous fungi is regulated by global transcriptional regulators, such as LaeA (Lind et al., 2018). In *Aspergillus* species, the global regulatory proteins VeA and LaeA have been shown to control both development and secondary metabolism (Calvo and Cary, 2015). Liu et al. (2016) reported that inactivation of LaeA in *M. ruber* drastically reduced the production of multiple secondary metabolites, such as *Monascus* pigments and citrinin and also resulted in the formation of an abnormal colony phenotype with abundant aerial hyphae. As previously reported, the addition of SAM enhanced MPs production and altered the morphology of the mycelium colony of *M. purpureus* RP2, it is reasonable to conclude that SAM probably regulates MPs biosynthesis and the mycelial development by interaction with the global regulator Mon2A1908.

Secondary metabolites biosynthesis coupled with asexual and sexual development in *Aspergillus* fungi is regulated by various environmental signals, such as temperature, pH, light, and carbon or nitrogen sources (Calvo et al., 2002; Calvo and Cary, 2015; Liu et al., 2016; Lind et al., 2018). In addition, it is controlled by a complex global network involved multiple regulators at the cellular level (Calvo et al., 2002; Calvo and Cary, 2015; Lind et al., 2018). This work proposed a possible bi-directional control mechanism of MPs biosynthesis by SAM metabolism from methionine in *M. purpureus* RP2. It is interesting to note that methionine could induce expression of SAM synthetase and SAM generation and exhibit the inhibited effect on MPs production, while high-level SAM inversely enhanced MPs biosynthesis. It is possible that the dynamic change in SAM synthetase expression level and the pool of SAM would be important signals of the regulatory network for MPs biosynthesis. Nevertheless, it is indispensable to dig out more details on the molecule components and their interactions involved in the regulatory network triggered by methionine and SAM. The findings in this work would provide a new perspective for a deep understanding of MPs biosynthesis regulation in *M. purpureus*.

DATA AVAILABILITY STATEMENT

The datasets presented in this study can be found in online repositories. The names of the repository/repositories and accession number(s) can be found in the article/ **Supplementary Material**.

AUTHOR CONTRIBUTIONS

SY conceived and designed the experiments, wrote the manuscript, contributed to the manuscript revision, financial support, and supervision. DY, YZ, and BH performed the experimental work and data analysis. All authors contributed to the article and approved the submitted version.

FUNDING

This work was supported by National Natural Science Foundation of China (31401669), Joint Program of Beijing Natural Science Foundation and Beijing Municipal Education Commission (KZ201910011014), Support Project of High-level Teachers in Beijing Municipal Universities (IDHT20180506), and the Talent Training Quality Construction-First Class Professional Construction (PXM2019-014213-000010).

SUPPLEMENTARY MATERIAL

The Supplementary Material for this article can be found online at: https://www.frontiersin.org/articles/10.3389/fmicb.2022.921540/full#supplementary-material

REFERENCES

Arai, T., Koganei, K., Umemura, S., Kojima, R., Kato, J., Kasumi, T., et al. (2013). Importance of the ammonia assimilation by *Penicillium purpurogenum* in amino derivative *Monascus* pigment. PP-V, production. *AMB Exp.* 3:19. doi: 10.1186/2191-0855-3-19

Brosnan, J. T., Brosnan, M. E., Bertolo, R., and Brunton, J. A. (2007). Methionine: A metabolically unique amino acid. *Livest. Sci.* 112, 2–7. doi: 10.1016/j.livsci.2007.07.005

Calvo, A. M., and Cary, J. W. (2015). Association of fungal secondary metabolism and sclerotial biology. *Front. Microbiol.* 6:62. doi: 10.3389/fmicb.2015.00062

Calvo, A. M., Wilson, R. A., Bok, J. W., and Keller, N. P. (2002). Relationship between secondary metabolism and fungal development. *Microbiol. Mol. Biol. Rev.* 66, 447–459. doi: 10.1128/MMBR.66.3.447-459.2002

Cavuoto, P., and Fenech, M. F. (2012). A review of methionine dependency and the role of methionine restriction in cancer growth control and life-span extension. *Cancer Treat Rev.* 38, 726–736. doi: 10.1016/j.ctrv.2012.01.004

Chen, D., Chen, M., Wu, S., Li, Z., Yang, H., and Wang, C. (2017). The molecular mechanisms of *Monascus purpureus* M9 responses to blue light based on the transcriptome analysis. *Sci. Rep.* 7:5537. doi: 10.1038/s41598-017-05990-x

Chen, M. H., and Johns, M. R. (1993). Effect of pH and nitrogen source on pigment production by *Monascus purpureus*. *Appl. Microbiol. Biot.* 40, 132–138. doi: 10.1007/BF00170441

Chen, W., Chen, R., Liu, Q., He, Y., He, K., Ding, X., et al. (2017). Orange, red, yellow: biosynthesis of azaphilone pigments in *Monascus* fungi. *Chem. Sci.* 8, 4917–4925. doi: 10.1039/c7sc00475c

Chen, W., He, Y., Zhou, Y., Shao, Y., and Chen, F. (2015). Edible filamentous fungi from the species *Monascus*: early traditional fermentations, modern molecular biology, and future genomics. *Compr. Rev. Food Sci. F.* 14, 555–567. doi: 10.1111/1541-4337.12145

Dhale, M. A., Puttananjaiah, M. K. H., Sukumaran, U. K., and Govindaswamy, V. (2011). Production of *Monascus purpureus* pigments; influenced by amidase and acid protease activity. *J. Food Biochem.* 35, 1231–1241. doi: 10.1111/j.1745-4514.2010.00447.x

Dufosse, L., Fouillaud, M., Caro, Y., Mapari, S. A., and Sutthiwong, N. (2014). Filamentous fungi are large-scale producers of pigments and colorants for the food industry. *Curr. Opin. Biotech.* 26, 56–61. doi: 10.1016/j.copbio.2013.09.007

Feng, Y., Shao, Y., and Chen, F. (2012). *Monascus* pigments. *Appl. Microbiol. Biot.* 96, 1421–1440. doi: 10.1007/s00253-012-4504-3

Gerke, J., Bayram, Ö, and Braus, G. H. (2012). Fungal S-adenosylmethionine synthetase and the control of development and secondary metabolism in *Aspergillus nidulans*. *Fungal Genet. Biol.* 49, 443–454. doi: 10.1016/j.fgb.2012.04.003

Green, M., and Sambrook, J. (2012). *Molecular Cloning: A Laboratory Manual, edition no.4*. New York, NY: Cold Spring Harbor Laboratory Press.

Hajjaj, H., François, J. M., Goma, G., and Blanc, P. J. (2012). Effect of amino acids on red pigments and citrinin production in *Monascus ruber*. *J. Food Sci.* 77, M156–M159. doi: 10.1111/j.1750-3841.2011.02579.x

Jung, H., Choe, D., Nam, K. Y., Cho, K. H., and Shin, C. S. (2011). Degradation patterns and stability predictions of the original reds and amino acid derivatives of *Monascus* pigments. *Eur. Food Res. Technol.* 232, 621–629. doi: 10.1007/s00217-011-1427-7

Jung, H., Kim, C., Kim, K., and Shin, C. S. (2003). Color characteristics of *Monascus* pigments derived by fermentation with various amino acids. *J. Agric. Food Chem.* 51, 1302–1306. doi: 10.1021/jf0209387

Jung, H., Kim, C., and Shin, C. S. (2005). Enhanced photostability of *Monascus* pigments derived with various amino acids via fermentation. *J. Agric. Food Chem.* 53, 7108–7114. doi: 10.1021/jf0510283

Kim, J. G., Choi, Y. D., Chang, Y. J., and Kim, S. U. (2003). Genetic transformation of *Monascus purpureus* DSM1379. *Biotechnol. Lett.* 25, 1509–1514. doi: 10.1023/a:1025438701383

Lakrod, K., Chaisrisook, C., and Skinner, D. Z. (2003). Expression of pigmentation genes following electroporation of albino *Monascus purpureus*. *J. Ind. Microbiol. Biotechnol.* 30, 369–374. doi: 10.1007/s10295-003-0058-9

Lieber, C. S., and Lester, P. (2002). S-adenosylmethionine: molecular, biological, and clinical aspects – an introduction. *Am. J. Clin. Nutr.* 76, 1148S–1150S. doi: 10.1093/ajcn/76/5.1148S

Lin, Y. L., Wang, T. H., Lee, M. H., and Su, N. W. (2008). Biologically active components and nutraceuticals in the *Monascus*-fermented rice: a review. *Appl. Microbiol. Biot.* 77, 965–973. doi: 10.1007/s00253-007-1256-6

Lind, A. L., Lim, F. Y., Soukup, A. A., Keller, N. P., and Rokas, A. (2018). An LaeA- and BrlA-dependent cellular network governs tissue-specific secondary metabolism in the human pathogen *Aspergillus fumigatus*. *mSphere* 3, e00050–18. doi: 10.1128/mSphere.00050-18

Liu, Q., Cai, L., Shao, Y., Zhou, Y., Li, M., Wang, X., et al. (2016). Inactivation of the global regulator LaeA in *Monascus ruber* results in a species-dependent response in sporulation and secondary metabolism. *Fungal Biol.* 120, 297–305. doi: 10.1016/j.funbio.2015.10.008

Mapari, S. A., Thrane, U., and Meyer, A. S. (2010). Fungal polyketide azaphilone pigments as future natural food colorants? *Trends Biotechnol.* 28, 300–307. doi: 10.1016/j.tibtech.2010.03.004

Mostafa, M. E., and Abbady, M. S. (2014). Secondary metabolites and bioactivity of the *Monascus* pigments review article. *Global J. Biotech. Biochem.* 9, 1–13. doi: 10.5829/idosi.gjbb.2014.9.1.8268

Patakova, P. (2013). *Monascus* secondary metabolites: production and biological activity. *J. Ind. Microbiol. Biot.* 40, 169–181. doi: 10.1007/s10295-012-1216-8

Putt, K. K., Pei, R. S., White, H. M., and Bolling, B. W. (2017). Yogurt inhibits intestinal barrier dysfunction in Caco-2 cells by increasing tight junctions. *Food Funct.* 8, 406–414. doi: 10.1039/c6fo01592a

Said, F. M., Brooks, J., and Chisti, Y. (2014). Optimal C:N ratio for the production of red pigments by *Monascus ruber*. *World J. Microbiol. Biotechnol.* 30, 2471–2479. doi: 10.1007/s11274-014-1672-6

Schmittgen, T. D., and Livak, K. J. (2008). Analyzing real-time PCR data by the comparative C_T method. *Nat. Protoc.* 3, 1101–1108. doi: 10.1038/nprot.2008.73

Shi, K., Song, D., Chen, G., Pistolozzi, M., Wu, Z., and Quan, L. (2015). Controlling composition and color characteristics of *Monascus* pigments by pH and nitrogen sources in submerged fermentation. *J. Biosci. Bioeng.* 120, 145–154. doi: 10.1016/j.jbiosc.2015.01.001

Srianta, I., Ristiarini, S., Nugerahani, I., Sen, S. K., Zhang, B. B., Xu, G. R., et al. (2014). Recent research and development of *Monascus* fermentation products. *Int. Food Res. J.* 21, 1–12.

Wang, Y., Wang, D., Wei, G., and Shao, N. (2012). Enhanced co-production of S-adenosylmethionine and glutathione by an ATP-oriented amino acid addition strategy. *Bioresour. Technol.* 107, 19–24. doi: 10.1016/j.biortech.2011.12.030

Xiong, X., Zhang, X., Wu, Z., and Wang, Z. (2015). Coupled aminophilic reaction and directed metabolic channeling to red *Monascus* pigments by extractive fermentation in nonionic surfactant micelle aqueous solution. *Proc. Biochem.* 50, 180–187. doi: 10.1016/j.procbio.2014.12.002

Yang, Y., Liu, B., Du, X., Li, P., Liang, B., Cheng, X., et al. (2014). Complete genome sequence and transcriptomics analyses reveal pigment biosynthesis and regulatory mechanisms in an industrial strain *Monascus purpureus* YY-1. *Sci. Rep.* 5, 8331–8331. doi: 10.1038/srep08331

Zhang, X., Wang, J., Chen, M., and Wang, C. (2013). Effect of nitrogen sources on production and photostability of *Monascus* pigments in liquid fermentation. *IERI Proc.* 5, 344–350. doi: 10.1016/j.ieri.2013.11.114

Conflict of Interest: The authors declare that the research was conducted in the absence of any commercial or financial relationships that could be construed as a potential conflict of interest.

frontiers | Frontiers in Microbiology

REVIEW
published: 16 June 2022
doi: 10.3389/fmicb.2022.919044

Chinese Baijiu: The Perfect Works of Microorganisms

Wenying Tu[1], Xiaonian Cao[2,3], Jie Cheng[1], Lijiao Li[1], Ting Zhang[1], Qian Wu[1], Peng Xiang[1], Caihong Shen[2,3] and Qiang Li[1,4]**

[1] Key Laboratory of Coarse Cereal Processing, Ministry of Agriculture and Rural Affairs, Sichuan Engineering and Technology Research Center of Coarse Cereal Industrialization, School of Food and Biological Engineering, Chengdu University, Chengdu, China, [2] Luzhou Laojiao Co. Ltd., Luzhou, China, [3] National Engineering Research Center of Solid-State Brewing, Luzhou, China, [4] Postdoctoral Research Station of Luzhou Laojiao Company, Luzhou, China*

Chinese Baijiu is one of the famous distilled liquor series with unique flavors in the world. Under the open environment, Chinese Baijiu was produced by two solid-state fermentation processes: jiuqu making and baijiu making. Chinese Baijiu can be divided into different types according to the production area, production process, starter type, and product flavor. Chinese Baijiu contains rich flavor components, such as esters and organic acids. The formation of these flavor substances is inseparable from the metabolism and interaction of different microorganisms, and thus, microorganisms play a leading role in the fermentation process of Chinese Baijiu. Bacteria, yeasts, and molds are the microorganisms involved in the brewing process of Chinese Baijiu, and they originate from various sources, such as the production environment, production workers, and jiuqu. This article reviews the typical flavor substances of different types of Chinese Baijiu, the types of microorganisms involved in the brewing process, and their functions. Methods that use microbial technology to enhance the flavor of baijiu, and for detecting flavor substances in baijiu were also introduced. This review systematically summarizes the role and application of Chinese Baijiu flavor components and microorganisms in baijiu brewing and provides data support for understanding Chinese Baijiu and further improving its quality.

Keywords: Chinese Baijiu, flavor substances, microorganisms, jiuqu, fermentation

OPEN ACCESS

Edited by:
Wanping Chen,
University of Göttingen, Germany

Reviewed by:
Zhihua Li,
Sichuan Academy of Agricultural Sciences, China
Yuanliang Hu,
Hubei Normal University, China

****Correspondence:***
Caihong Shen
shench@lzlj.com
Qiang Li
leeq110@126.com

Specialty section:
This article was submitted to Food Microbiology, a section of the journal Frontiers in Microbiology

Received: *13 April 2022*
Accepted: *23 May 2022*
Published: *16 June 2022*

Citation:
Tu W, Cao X, Cheng J, Li L, Zhang T, Wu Q, Xiang P, Shen C and Li Q (2022) Chinese Baijiu: The Perfect Works of Microorganisms. Front. Microbiol. 13:919044. doi: 10.3389/fmicb.2022.919044

INTRODUCTION

Chinese Baijiu is an alcoholic beverage with a long history and is one of the great inventions of ancient China, which is also one of the six most popular distilled spirits in the world, including brandy, whiskey, vodka, rum, and gin (Xu et al., 2017b). Chinese Baijiu is usually brewed by solid-state fermentation with different grains as starter materials. Chinese Baijiu can be divided into different types according to different classification methods. Different types of baijiu contain many complex trace components. Jiuqu is a type of starter for baijiu fermentation, which is composed of raw materials, microflora, enzymes, and aromatic precursor substances. There are three types of microbial starter-jiuqu, including Daqu, Xiaoqu, and Fuqu. Their preparation and alcoholic fermentation are conducted under semi-controlled conditions. The flavor in Chinese Baijiu results from the presence of volatile and non-volatile substances, which are mainly produced by microbial metabolism during fermentation. Volatile substances include compounds such as

esters, alcohols, acids, aldehydes, nitrogen-containing, and sulfur-containing compounds, and terpenes. These compounds exert important effects on the aromatic characteristics and quality of baijiu. Non-volatile substances are generally used as precursors of volatile substances, and their amount will affect the number of volatile substances in baijiu, thereby affecting its flavor and quality. Today, more than 2,400 chemicals have been identified in baijiu that contributes to flavor, some of which are beneficial to human health, such as short-chain fatty acids, peptides, and phenols (Sun et al., 2015; Fang et al., 2019; Xu et al., 2020; Jiang et al., 2021). Flavoring substances in Chinese Baijiu are detected using conventional detection technology, chromatographic technology, spectral technology, and other analysis and detection technologies, among which chromatographic technology is the most commonly used and effective (Jia et al., 2020a).

In the process of brewing Chinese Baijiu, fermentation is a complex microbial process. Many studies have shown that the raw materials and production process has a certain impact on baijiu flavor, and microorganisms from which play a key role (Zheng and Han, 2016; Jin et al., 2017; Wang et al., 2018b; Xu et al., 2017a). Microbial diversity is one of the important factors affecting baijiu flavor and microbial community in different jiuqu determines Chinese Baijiu flavor to a certain extent (Gou et al., 2015; Zheng and Han, 2016). Jiuqu provides microorganisms and enzymes to baijiu fermentation and significantly contributes to ethanol and flavor compound generation. Many studies revealed the structure and composition of microbial communities in jiuqu (Zheng et al., 2011). Furthermore, analysis indicates that jiuqu provides approximately 10 to 20% of the bacterial communities and 60 to 80% of the fungal communities to the baijiu fermentation (Wang et al., 2017c). The analysis of the Daqu microbial community showed that the formation of azines, esters, and aromatic compounds was affected by *Bacillus*, *Lactobacillus*, and *Aspergillus* (Jin et al., 2019). Jiuqu also provides abundant enzymes. Through the source-tracking analysis, Wang et al. (2020a) found that about 80% of carbohydrate hydrolases in baijiu fermentation were provided by jiuqu, and those enzymes were produced by *Aspergillus*, *Rhizomucor*, and *Rhizopus*. This can well indicate that the formation of baijiu flavor substances is inseparable from the interaction of jiuqu microbes. Recently, the role of microorganisms in regulating the formation of flavor compounds has been investigated. The contents of sulfur compounds, pyrazines, and acids in Chinese Baijiu were significantly increased when *Bacillus* was added to the fermentation microbiome. The initial fungal diversity also had a positive effect on fungal succession in fermentation, indicating the importance of the initial fungal diversity in promoting the formation of flavor compounds in Chinese Baijiu (Shen et al., 2020; Ji et al., 2022). Due to the open inoculation environment and complex fermentation environment, the quality of baijiu produced in different environments is different (Li et al., 2015). Many studies have found that microorganisms the from unique ecological environment are involved in the fermentation process of Chinese Baijiu, which promoted the formation of different flavor components in baijiu brewing (You et al., 2012; Calasso et al., 2016). Therefore, the baijiu fermentation process constructs the interaction among environment, microorganism, and baijiu flavor, in which microorganism is the key medium connecting environment and baijiu flavor (Wang, 2022). Many researchers have devoted themselves to examining the fermentation process, flavor components, microbial species and functions, and flavor detection methods for different flavors of baijiu. However, the main flavors of some baijiu and their aroma-generating mechanisms remain unclear, and there are relatively few comprehensive analyses of the characteristic flavors and microbial flora of the different flavors of baijiu. This review focuses on the introduction of different types of flavor components in Chinese Baijiu, and the types and functions of microorganisms involved in the process of brewing different flavors. In addition, methods of applying microbial technology to promote the synthesis of flavor substances and methods to detect flavor substances are also introduced. This paper provides a new and comprehensive perspective for the study of baijiu making, and provides data support for baijiu quality improvement.

FLAVOR TYPES AND FERMENTATION MICROORGANISMS OF CHINESE BAIJIU

Baijiu is an important part of the Chinese diet. Moderate drinking of baijiu plays an important role in people's health and life quality. Previous studies found that regular consumption of mild to moderate baijiu could significantly enhance lipid metabolism and liver function (Zhi et al., 2022). Chinese Baijiu brewing uses different grains as fermentation raw materials. Jiuqu is used as a saccharification starter, and its main production steps are completed by solid-state fermentation, solid-state distillation, storage, and deployment. The main components of Chinese Baijiu are alcohol and water, accounting for 98% of the total weight, and there is usually less than 2% of other trace components, which included esters, aldehydes, ketones, acids, acetals, furans, terpenes, nitrogen compounds and sulfides (Hong et al., 2020). Esters are the main flavoring substances in Chinese Baijiu, accounting for more than 60% of the total flavor substances, of which ethyl acetate, ethyl butyrate, ethyl hexanoate, and ethyl lactate are the four main esters, accounting for approximately 75% of the total esters (Qian et al., 2019). Different types of baijiu have their unique microbiota and flavor due to their unique production techniques. Microbial activity plays a key role in baijiu brewing. Microorganisms not only directly determine the fermentation rate, but also convert nutrients into a variety of volatile flavor compounds. The microbial and flavor characteristics of various baijiu types are shown in **Table 1**.

Brief Introduction to Chinese Baijiu

Chinese Baijiu, also known as Laobaigan or Shaojiu, is a clear distilled baijiu obtained through a complex fermentation process. The literal translation of its name is 'white alcohol,' and it is an alcoholic beverage. As Chinese national baijiu, baijiu has a long history and unique brewing methods and occupies a very important position in the economy of China's food industry. In 2020, Chinese Baijiu sales reached US$90.33 billion, with annual sales exceeding 10.7 billion liters. According to the ancient

TABLE 1 | Microbial and flavor characteristics of various baijiu types.

Classification	Microbial characteristics	Flavor characteristics	References
Maotai-flavored baijiu	Filamentous fungi (*Aspergillus*), Yeast (*Pichia*), and Bacteria (*Bacillus*); Bacteria are most numerous; mold species are the most abundant.	Phenolic compounds: tetramethylpyrazine and syringic acid; high content of organic acids, aldehydes, ketones, alcohols, amino compounds, pyrazine, furans, and nitrogen compounds.	Xiong, 2005; Bokulich et al., 2012; Cai et al., 2019
Strong-flavored baijiu	Aroma-producing yeasts, bacteria, and molds; Bacteria mainly include *Bacillus*, *Streptomyces*, *Lysinobacter*, *Staphylococcus*, *Lactobacillus*, *Brevibacterium*, and *Brevibacterium*	mainly ethyl caproate, followed by ethyl acetate, ethyl lactate, ethyl butyrate and ethyl caproate	Wang et al., 2011; Bokulich et al., 2012
Light-flavored baijiu	Bacteria: *Bacillus* and *Lactobacillus*; Yeast: *Pichia thermophilus*, *Saccharomyces cerevisiae*, and *Isacchinia orientalis*	Aromatic compounds: ethyl acetate; esters, acids, alcohols, phenolic compounds; the main flavor substances are ethyl acetate, followed by ethyl lactate.	Sun et al., 2021; Tang et al., 2022
Rice-flavored baijiu	Bacteria: *Lactobacillus*, *Welchiella*, *Lactococcus*, *Acetobacter*, mainly *Lactobacillus*; Fungi: *Rhizopus*. Yeast: *Pichia anomala*, *Saccharomyces cerevisiae*, and *Issatchenkia orientalis*	Phenyl ethanol in equilibrium with ethyl acetate and ethyl lactate	Wu et al., 2019; Huang et al., 2020; Hu Y.L. et al., 2021
Miscellaneous-flavored baijiu	Bacteria: *Bacillus* and *Lactobacillus*; Fungi: *Paecilomyces*, *Saccharomyces,* and *Zygomycetes*	High concentrations of ethyl lactate, 2,3-butanediol, and ethyl hexanoate, followed by heptanoic acid, ethyl heptanoate, isoamyl acetate, octane, isobutyric acid, and butyric acid	Huang et al., 2021
Feng-flavored baijiu	*Naumovozyma*, *Rhizopus, Thermoascus*, *Aspergillus*, *Candida*, *Pseudeurotium*, *Saccharomycopsis*, *Pichia*, *Saccharomyces*, *Lactobacillus*, *Bacillus*, *Pediococcus*, and *Streptomyces*, among which *Naumovozyma* and *Lactobacillus* are dominant	Ethyl acetate, ethyl hexanoate, and isoamyl alcohol	Wang, 2008; Chen et al., 2020; Huang et al., 2021
Te-flavored baijiu	The dominant strains are *Saccharomyces*, *Pichia*, and *Galactomyces*	High concentrations of ethyl acetate and ethyl hexanoate, followed by ethyl propionate, ethyl valerate, ethyl heptanoate, and ethyl nominate	Li et al., 2017; Fu et al., 2021
Sesame-flavored baijiu	Mold, yeast, and bacteria	Sulfur compounds: dimethyl disulfide, trithiodimethyl, 3-(methylthio) propanal, furfural mercaptan, and furfural disulfide	Tamura et al., 2010, 2011
Laobaigan-flavored baijiu	Mold, yeast, and bacteria	Esters: ethyl acetate, ethyl lactate; low content of ethyl acetate, ethyl butyrate, palmitate, and linoleic acid	Fan Q. et al., 2019; Cui et al., 2020
Chi-flavored baijiu	*B. licheniformis*, *B. subtilis*, etc.	Acetic, lactic or butyric acid, etc.	Li et al., 2016; Cui et al., 2020
Fuyu-flavored baijiu	Bacteria: *Lactobacillus*, *Welbachia*, and *Bacillus*; Fungi: *Rhizopus*, *Candida*, *Pichia*, and *Aspergillus*.	Aromatic compounds: ethyl caproate, ethyl lactate and ethyl acetate	Kang et al., 2021

Chinese book '*Huangdi Neijing*,' baijiu is the best medicine, and it emphasizes the importance of baijiu in medical care and disease treatment. In addition, the Compendium of Materia Medica noted that moderate consumption of alcohol can eliminate the feeling of cold, fatigue, and phlegm-dampness. This is by the results of some current clinical data analyses that indicated that moderate consumption of baijiu can accelerate blood circulation, improve the function of cardiovascular and circulatory systems, and decrease serum uric acid concentration and the risk of Alzheimer's disease. Moderate alcohol consumption can also improve the health level of young people, and prevent cardiovascular disease by reducing blood lipid levels, platelet aggregation, and endothelial cell adhesion molecules. The researchers found that pyrazines, mainly tetramethylpyrazines, have antioxidant activity, boost immunity, and lower triglycerides (Yan et al., 2021). Other studies have found that baijiu intake has a potential cancer suppressor effect in animals. In mouse models, the spread and progression of breast cancer can be inhibited (Wang et al., 2022b). Ji et al. (2021) analyzed the effects of different baijiu on gut microbiota and host metabolism, and the results showed that volatile compounds have the potential to mitigate alcoholic liver disease by regulating gut microbiota and host metabolism. Therefore, moderate drinking is healthy and safe, but it is also important to limit high intake.

The production of Chinese Baijiu involves a complex fermentation system with multiple strains of microorganisms and many different types of raw grains, such as sorghum, rice, wheat, or millet, which are processed using unique fermentation technology. Chinese Baijiu is usually produced by natural solid-state fermentation that utilizes different microbial species (yeasts, bacteria, and molds), and saccharification and fermentation are conducted at the same time. Therefore, in such a production environment, a unique microbial community is used to create Chinese Baijiu, which results in its different flavor types and complex flavor characteristics (Jin et al., 2017; Liu and Sun, 2018). Hundreds of different types of baijiu in China are produced

through different processes in different regions of China, as regional varieties. Chinese Baijiu can be classified according to the manufacturing technology, starter type, and product flavor. According to production technology, Chinese Baijiu can be divided into solid baijiu and semi-solid baijiu; according to the type of jiuqu, it can be divided into Daqu baijiu and Xiaoqu baijiu; and according to the flavor of the product, it can be divided into Maotai-flavored, light-flavored, Luzhou-flavored, rice-flavored, miscellaneous-flavored, te-flavored, feng-flavored, sesame-flavored, medicinal-flavored, chi-flavored, laobaigan, or fuyu-flavored baijiu. In recent years, there has been intense interest in studying the characteristic flavors of Chinese Baijiu, to excavate their main flavor and key flavor substances. The aroma and flavor of Chinese Baijiu are important factors that determine its type and quality. The formation of baijiu style characteristics is mainly related to approximately 2% of trace components in the baijiu body. Owing to the different flavors of Chinese Baijiu, its brewing process is complicated. It is produced mainly by solid-state microbial fermentation and brewing, solid-state saccharification fermentation, and solid-state retort distillation and brewing. It is also a key link shared by all flavored baijiu, and its unique brewing process distinguishes Chinese Baijiu from the other five major distilled spirits in the world.

Since ancient times, baijiu has been closely related to the life of the Chinese people. For the Chinese, baijiu is not only food but also a cultural heritage. At present, the characteristics of different types of Baijiu are still not clear. With the development of science and technology and the improvement of different brewing processes, baijiu with different flavors can be produced. However, Chinese Baijiu will require stricter and more accurate standards in the future to distinguish the myriad of flavor compounds in it.

Flavor Types and Fermentation Microorganisms

Chinese Baijiu can be divided into 12 types according to their flavors. Among them, Maotai flavor, Luzhou flavor, light flavor, and rice flavor are the basic four flavor types, and other baijiu is the extension of these four flavors (Zheng and Han, 2016; Xu et al., 2017b; Hu Y. et al., 2021). The relationship between the 12 flavored baijiu types is shown in **Figure 1**. The flavor characteristics of Maotai-flavored baijiu, Luzhou-flavored baijiu, and light-flavored baijiu are typical and representative, accounting for 60–70% of Chinese Baijiu. The production processes of the three baijiu are relatively standardized (Zheng and Han, 2016). Rice-flavor baijiu is produced from millet, which is inoculated Xiaoqu during fermentation, forming a unique flavor (Yin et al., 2020b). Chi-flavored baijiu was established based on rice-flavored baijiu and is different from rice-flavored baijiu due to different additives. Chi-flavored and rice-flavored baijiu are the only two types of baijiu produced by semi-solid fermentation. Sesame-flavored baijiu absorbed the flavor characteristics of three kinds of baijiu (Maotai flavor, Luzhou flavor, and light flavor) in the process of making jiuqu, and innovated the production of traditional baijiu by adding Fuqu (Jin et al., 2017). In addition, jiuqu brewed from barley and pea at low temperature was used in light-flavored baijiu, while laobaigan-flavored baijiu is made from pure wheat under medium temperature. A variety of jiuqu mixtures are usually used in the brewing of other baijiu flavors (Feng-flavor, Medicine-flavor, Te-flavor, etc.). For example, Xiaoqu made by adding some herbs is used to make baijiu with medicinal flavor.

Maotai-Flavored Baijiu

The four main steps in the production of Maotai-flavored baijiu are jiuqu making, alcoholic fermentation, solid-state distillation, and aging. In Maotai-flavored baijiu, sorghum (as a raw starch) and a unique Daqu (high-temperature Daqu) are mixed and fermented naturally in an open environment. Two-stage alcohol fermentation (including heap fermentation and cellar fermentation) occurs without directly or indirectly adding edible alcohol or non-self-fermented color, aroma, or taste substances (Jin et al., 2017; Liu and Miao, 2020). Maotai and Langjiu, are the most representative baijiu of Maotai-flavored baijiu, which provide a soy sauce-like aroma, full taste, and long-lasting aroma. To date, 528 compounds have been identified from Maotai-flavored baijiu (Zhu et al., 2007; Liang et al., 2019). Although over 30 major flavor substances have been identified in Maotai-flavored baijiu, the main aroma components remain inconclusive. Studies have shown that aromatic compounds (phenolic compounds) are its representative flavor, mainly tetramethylpyrazine and syringic acid, and a small number of amino acids, organic acids, and esters (Xiong, 2005). The contents of organic acids (acetic acid and lactic acid), aldehydes, ketones, alcohols, amino compounds, and nitrogen compounds in Maotai-flavor baijiu are high, while the total ester content is low. It is worth noting that the content of pyrazine and furan is also much higher than other baijiu (Wang et al., 2019).

Maotai-flavored baijiu has a unique fermentation process. It mainly uses high-temperature Daqu and combines the enrichment of various microorganisms in the natural fermentation environment to produce a variety of enzymes (mainly saccharifying enzymes) and microbial metabolites. Filamentous fungi, yeast, and bacteria work closely together in Maotai-flavored baijiu fermentation, and the enzymes produced by filamentous fungi degrade raw materials into fermentable sugars, which become substrates for yeast and bacteria to produce ethanol and other volatile compounds (Chen B. et al., 2014; Zheng and Han, 2016). When monitoring the microbial community in the solid fermentation substrate of Maotai-flavored baijiu, the researchers have found that the abundance of lactic acid bacteria was relatively high, so the quality and flavor of Maotai-flavored baijiu may be closely related to a variety of lactic acid bacteria (Wu et al., 2020a). In addition, reducing sugar is the key driving factor of microbial succession in heap fermentation, while acidity, alcohol, and temperature are the main driving factors of pit fermentation (Hao et al., 2021). Researchers also found that Daqu provided 95.6% of bacteria and 28.10% of fungi in Maotai-flavored baijiu fermentation, respectively. The environment (air, indoor floor, and tools) provided 71.9% of fungi (mainly *Pichia*) in Maotai-flavored baijiu fermentation, indicating that *Pichia* from the environment was also the

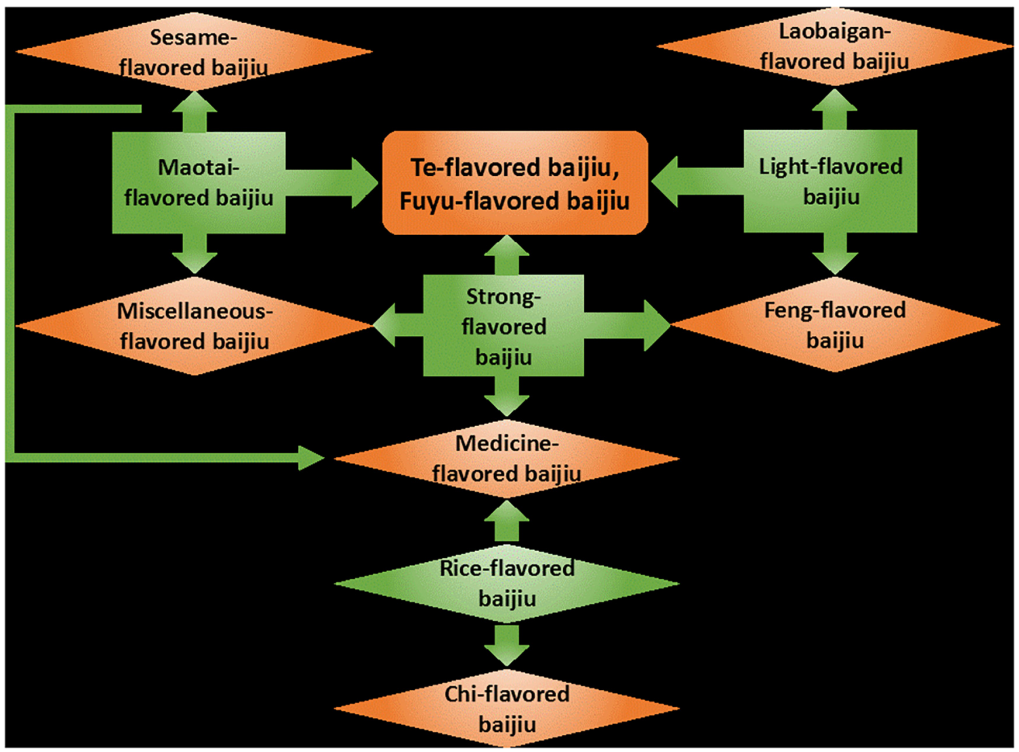

FIGURE 1 | Relationships of 12 flavored baijiu types in China.

dominant fungal genus involved in the fermentation process (Zhang et al., 2021). Environmental microbes play an important role in controlling and promoting the formation of microbial communities in baijiu fermentation. When high-temperature Daqu was used as a fermentation agent, the main microorganisms were bacteria, mold, and yeast, of which bacteria had the largest number, followed by mold and yeast. The most diverse species were fungi, followed by bacteria (Zuo et al., 2020). Wang et al. (2008) used phenotypic and conventional biochemical taxonomy to isolate and identify the microbial community structure of Maotai Daqu, and found that the bacterial genera included *Bacillus*, *Acetobacter*, *Lactobacillus*, and *Clostridium*, of which *Bacillus* has the largest number, *Bacillus* is the most important functional bacteria in the fermentation of Maotai-flavor baijiu (Zuo et al., 2020); the mold was present as mainly *Aspergillus*, and also with *Mucor*, *Rhizopus*, *Monascus*, and *Trichoderma*. Yeast included *Saccharomyces* spp., *Candida* spp., *Pichia* spp., and *Torula* spp. The most commonly isolated yeasts were from the genus *Saccharomyces*. The distribution of microbial species varies with the maturity stage of the Daqu. In high-temperature Maotai Daqu, the composition of microorganisms at different temperatures is different. At lower temperatures, yeasts, molds, and certain bacteria will accumulate in large quantities and will produce high levels of enzymes and other metabolites. Enzymes can hydrolyze proteins into various amino acids, and can also participate in the Maillard reaction and other chemical reactions with amino acids to produce the unique Maotai flavor. The microbiota plays an important role in the formation of flavor substances in the fermentation process. However, the flavor components and their proportion in Maotai-flavored baijiu are still uncertain. The mechanism of microbial diversity regulating the formation of flavor substances is complex. Thus on the research of Maotai-flavored baijiu is very challenging (Liu and Miao, 2020).

Strong-Flavored Baijiu

Strong-flavored baijiu is well known for its strong fragrance and sweetness, and it is the most popular type of Chinese Baijiu, also called Luzhou-flavored baijiu. The raw materials used in the fermentation of Luzhou-flavored baijiu are mixed with a variety of grains, mainly sorghum. Its production mostly adopts the process of steaming and slag, and fermentation occurs in old cellars, although there are also artificially cultivated cellars (Liu et al., 2017). Luzhou laojiao baijiu and Wuliangye baijiu are the most representative of the Strong-flavored baijiu, which possesses the characteristics of rich aroma, soft taste, and endless aftertaste. The most representative aromatic compounds in Luzhou-flavored baijiu are ethyl hexanoate, which is harmoniously balanced with ethyl lactate, ethyl acetate, and ethyl butyrate (Wang et al., 2020d). In addition, the acid content in Luzhou-flavored baijiu changed with the fermentation stage of base baijiu. The acetic acid, lactic acid, butyric acid, and hexanoic acid in the last mature Luzhou-flavored baijiu were stable, accounting for about 90% of the total acid content. Ethyl hexanoate is an ethyl ester that can produce an apple flavor and is one of the most important esters in Luzhou-flavored baijiu. The content of ethyl

hexanoate, the main aromatic substance of strong-aroma baijiu, exceeds 200 mg/L in high-quality Luzhou-flavored baijiu.

Luzhou-flavored baijiu is usually produced by a typical natural solid fermentation method using Daqu as the main saccharifying agent. The fermentation process is generally anaerobic and conducted in pit mud. The composition of the flavor compounds in Luzhou-flavored baijiu, like other types of baijiu, is determined by the diversity of microorganisms. In the traditional fermentation process, ethyl hexanoate in Luzhou-flavored baijiu is mainly produced by aroma-producing yeasts, bacteria, and molds with high esterification ability in the mud pit in the late fermentation stage. In Luzhou-flavor Baijiu, it is important because bacteria can produce caproic acid and then regenerate it into ethyl caproic acid. Wang et al. (2020f) studied the fermentation pit mud and found that *Syntrophomonas*, *Methanobacterium*, and *Methanocorpusculurn* were conducive to the production of caproic acid. Although they are not directly involved, they provide possible environmental factors for caproic acid production. Zou et al. (2018) reviewed the species diversity and metabolism of *Clostridium* spp. Therefore, the presence of *Clostridium* can promote the solid-state fermentation process of baijiu (Bokulich et al., 2012). The research on microorganisms in Luzhou-flavored baijiu originally began in the 1960s. Today, many microbial strains have been identified and determined. As far as bacteria are concerned, there are roughly 34 bacterial genera, among which *Bacillus*, *Streptomyces*, *Lysinobacteria*, *Staphylococcus*, *Lactobacillus*, and *Brevibacterium* were the most important, and other new bacteria have also been detected (Wang et al., 2011). According to previous research (Endo and Okada, 2005; Chen et al., 2011), it is known that the microorganisms that can metabolize ethyl hexanoate esterase in nature mainly include bacteria, filamentous fungi, and yeast, many of which secrete extracellular esterase that catalyzes the synthesis of ethyl hexanoate. Some researchers have found through sensory-guided fractionation and component analysis that there are 43 volatile compounds (mainly esters) in Luzhou-flavored baijiu that seem to contribute to its sweetness, among which ethyl hexanoate and hexyl hexanoate have been identified. Esters and ethyl 3-methyl butyrate are the main contributors to the sweetness of baijiu (Tang, 2021). These studies not only broaden our understanding of baijiu sweetness but also highlight the main contribution of volatile compounds to the perception of baijiu sweetness. There is no doubt that the Ethyl caproate is one of the most important factors in determining the quality of Strong-flavored baijiu. In recent years, increasing the number of esters has been the main goal to improve the flavor of some aromatic baijiu. Zhao et al., Yin et al., and Yan et al. improved the characteristic flavor of Luzhou-flavored baijiu by enrichment of specific microorganisms and overexpression of related microbial metabolic genes (Zhao et al., 2017; Yan and Dong, 2018; Yin et al., 2019).

Light-Flavored Baijiu

The alcoholic fermentation of light-flavored baijiu, also known as light-flavored baijiu, is conducted in clay tanks, unlike Maotai-flavored baijiu and Luzhou-flavored baijiu, which are carried out in mud cellars. Light- flavored baijiu utilizes sorghum and wheat as the raw material and is brewed by steaming twice with slag cleaning technology. The production process of light-flavored baijiu involves a solid, open, natural fermentation, and therefore, the fermentation microorganisms of the light-flavored baijiu not only are derived from jiuqu but also derived from the surrounding environment. The most representative product of light-flavored baijiu is Fenjiu, and there is also Erguotou baijiu, with its mellow sweetness and fresh aftertaste. In many studies, it was determined that most flavor substances in light-flavored baijiu were synthesized at the late fermentation stage, and its metabolites were esters, alcohols, alkenes, sulfides, and ketones, furans, aldehydes, nitrogen compounds, alkanes and so on. The aromatic compound ethyl acetate is one of the main characteristic aromatic substances, which is balanced with a considerable amount of ethyl lactate. The proportion of n-propanol and isobutanol in alcohols was higher, which had a great influence on the flavor characteristics of baijiu (Liu and Miao, 2020). In addition, acetic acid and lactic acid are the main acids, with concentrations of 1 and 0.28 g/L, respectively, accounting for about 98% of the total acid content (Fan et al., 2018; Wei et al., 2020). Moreover, the ester acid ratio of light-flavored baijiu was higher than that of Luzhou-flavored baijiu (Yu et al., 2014).

The jiuqu brewed in light-flavored baijiu is produced using traditional fermentation techniques. The ingredients in the jiuqu (barley, peas, millet, and so on) and their production environment (tools, soil, air, and machinery) contain naturally occurring microorganisms. The functions of the primary microbial groups participating in the process of brewing light-flavored baijiu have been widely reported, and it has been said that the main bacterial genera in light-flavored baijiu are *Bacillus* and *Lactobacillus*. The role of *Lactobacillus* is to produce a large number of organic acids, while *Bacillus* can promote the production of unique flavor components. Fan G. et al. (2019) detected 72 volatile compounds, mainly alcohols, esters, aldehydes, alkenes, and alkanes, from Daqu by solid-phase microextraction coupled with gas chromatography-mass spectrometry. In addition, through high-throughput sequencing, it was found that the bacteria mainly came from *Pantoea*, but decreased with the increase of age. The bacteria of *Lactobacillus* and *Weissella* increased, while *Pichia* remained unchanged. The fermentation time of light-flavored baijiu is closely related to the change in the microbial community, with its higher bacterial diversity and different non-yeast bacteria as compared to the microbiota involved in the fermentation of other styles of baijiu, resulting in the diversity of metabolites. It is concluded that the balance of interactions between microbial communities in jiuqu is of great significance to improve microbial quality, ensure its stability and ensure the quality of light-flavored baijiu.

Rice-Flavored Baijiu

Rice-flavored baijiu is a rare and one of the four basic flavor types of baijiu in China. The most representative is Guilin sanhua baijiu. Rice-flavored baijiu is a Xiaoqu baijiu made from rice. Its production consists of raw material pretreatment, inoculation, saccharification, fermentation, distillation, aging, and other processes. It tastes like honey, light and soft. The aromatic composition of this baijiu is mainly composed of phenyl ethanol, balanced with ethyl acetate and ethyl lactate. Among the

four basic flavor types, rice-flavored baijiu contains the highest content of phenylethanol. The total alcohol content of rice-flavored baijiu was higher than that of ester compounds, and the ratio of total acid, total ester, and total alcohol was 1:1.2:1.5. In addition, lactic and acetic acids account for more than 90% of the total acids. Among the ester compounds, ethyl lactate has the highest content, followed by ethyl acetate (Yin et al., 2020b).

Rice-flavored baijiu is made of Xiaoqu, which acts as a microbial starter. Various functional microorganisms provide hydrolytic enzymes, volatile substances, and other components for baijiu brewing, which thus form the unique flavor of the baijiu (Wu et al., 2019; Sakandar et al., 2020). In the process of brewing rice-flavored baijiu, bacteria and fungi are involved. The primary microorganisms originate from the environment and the raw rice materials, which mainly included yeast and *Rhizopus* (Hu Y.L. et al., 2021). Compared with Maotai-flavored and Luzhou-flavored baijiu, relatively few types of microorganisms participate in the brewing process for rice-flavored baijiu, but a few microbial species dominate this brewing process, and they contribute flavor substances to rice-flavored baijiu.

Miscellaneous-Flavored Baijiu

Combined-flavored baijiu, also known as compound-flavored baijiu and mixed baijiu, refers to baijiu with more than two main aromas, and one baijiu with multiple aromas is its style feature. The production process of miscellaneous-flavored baijiu is unique, with a brewing process that includes starter fermentation, stacking fermentation, cellar alcohol fermentation, and grain distillation (Li et al., 2016). The most representative product of miscellaneous-flavored baijiu is Baiyunbian baijiu, which is the most popular mixed-flavored baijiu in China. Its sensory characteristics are between the sauce flavor and strong-flavored baijiu. The representative aromatic compounds are heptanoic acid, ethyl heptanoate, isoamyl acetate, octane, isobutyric acid, and butyric acid.

Some studies have continuously tested fermented baiyunbian baijiu, and the results show that the bacterial community is dominated by *Bacillus*, and *Lactobacillus*; the most common fungi are *Paecilomyces* spp., yeast, and *Zygomycetes cerevisiae*. A large number of fungi were from the genera *Thermomyces*, *Aspergillus*, *Monascus*, and the subgenus *Isachenki*, as well as some prokaryotes belonging to the genera *Acetobacter*, *Lactobacillus*, and *Thermoactinomycetes*. Analysis by GC-MS showed that the distiller's grains contained high concentrations of ethyl lactate, 2,3-butanediol, and ethyl caproate, which were mainly produced by the co-fermentation of *Lactobacillus* and yeast (Liu and Miao, 2020). Dong et al. (2022) found that the dominant bacteria (*Weissella* and *Leuconostoc*) were replaced by *Acetobacter* and *Gluconobacter*, and the dominant fungus (*Rhizopus*) was partially replaced by *Thermomyces* in the saccharification stage of Baijiu brewing. While, in the fermentation stage, the dominant bacteria were replaced by lactic acid bacteria, and the dominant fungus was completely replaced by *Thermoascus* and other three yeasts, including *Saccharomyces, Kazachstania,* and *Apiotrichum*. The formation of flavor substances (acetic acid, lactic acid, hexanoic acid, ethyl lactate, and ethyl lactate) was found to be closely related to *Kazachstania* and *Apiotrichum*.

Feng-Flavored Baijiu

In the production of feng-flavored baijiu, sorghum is used as the raw material, and medium-temperature Daqu or Fuqu and yeast made of barley and peas are used as the starter. Continuous glutinous rice can also be used, and fermentation occurs in a cellar that is not more than 1-year-old. The most representative product of feng-flavored baijiu is Xifeng baijiu, which is the originator and typical representative of this type of baijiu that is widely known in China. The aroma of honey is a typical sensory characteristic of feng-flavored baijiu, which originates from a unique production process, and its formation mechanisms are still unclear. The main aromatic components of feng-flavored baijiu are ethyl acetate, ethyl hexanoate, and isoamyl alcohol, and its ethyl acetate and ethyl hexanoate are in balance. Known throughout the world as the 'Three Wonders' and 'Phoenix in baijiu,' it has a wide range of representations and a profound mass base in the country. It has been reported that the aroma of pineapple in feng-flavored baijiu is closely related to the amount of four esters, five alcohols, and two acids. Appropriate proportions of ethyl lactate, ethyl hexanoate, and ethyl acetate are essential for the formation of typical feng-flavored baijiu flavors. Crucially, if the amount of ethyl lactate is too high, it will weaken the aroma of the baijiu and increase its astringency (Jia et al., 2022b).

Medicine-Flavored Baijiu

To produce medicine-flavored baijiu, it is necessary to adopt the method of making incense sticks, making fermented grains from Xiaoqu and Daqu fragrant grains, and adopting a double glutinous rice method or re-steaming method (that is, a stringing incense method) or the double-steaming method. This baijiu has a medicinal-like aroma, moderate sweetness and sourness, and a lasting aftertaste. Dongjiu is a typical representative of medicinal baijiu. Additionally, 95 types of Chinese herbal medicines are added to Xiaoqu preparations, and 40 types of Chinese herbal medicines are added to Daqu preparations.

Previous studies on winter baijiu mainly focused on the production process, microorganisms, organic acids, and the separation and identification of a small number of terpenes. In previous studies, it was shown that the characteristic aromatic components of medicinal-flavored baijiu can be summarized as having high amounts of total acid, alcohol, and ethyl butyrate, and a low amount of ethyl lactate. In addition, the total amount of acid and alcohol in this type of baijiu is higher than that of ester baijiu, which contains different aromatic components as compared to other types of baijiu. However, thus far, the characteristic aromatic components contained in medicinal-flavored dongjiu baijiu are not clear.

Te-Flavored Baijiu

This special-flavored baijiu is made of whole grain rice as the main raw material, medium- and high-temperature Daqu as the saccharification starter, and it is fermented, distilled, aged, and blended by the traditional solid-state method. Te-flavored baijiu has the characteristics of multi-type, multi-layered fragrance, full-bodied, harmonious, sweet, and mellow in the entrance, refreshing aftertaste, and no discordant or miscellaneous flavors. The most representative Te-flavored baijiu is Si'te baijiu from Jiangxi, China. Si'te baijiu contains a high concentration of ethyl

acetate and ethyl caproate as the main aromatic compounds, which are balanced with heptanoate. This type of baijiu has a harmonious and rich flavor and light taste. The concentrations of ethyl propionate, ethyl valerate, ethyl heptanoate, and ethyl pelargonate in Si'te baijiu are higher than that in any other type of baijiu. The aromatic components of te-flavored baijiu have the following characteristics: rich in odd-carbon fatty acid ethyl ester, with the greatest quantity among all types of aromatic baijiu. The esters in special-flavored baijiu are mainly ethyl propionate, and also ethyl valerate, ethyl heptanoate, and ethyl pelargonate; volatile compounds are ethyl acetate and ethyl hexanoate, in equilibrium with heptyl ester (Fu et al., 2021).

Sesame-Flavored Baijiu

Sesame-flavored baijiu is an important baijiu style, and its representative is Jingzhi baijiu. Its production process includes steaming and slag continuation, use of a mud-bottomed brick cellar, large bran combination, and multi-microorganisms' co-fermentation. The fermentation technology of sesame-flavored baijiu is characterized by high nitrogen ingredients, high-temperature accumulation, high-temperature fermentation, and long-term storage. Modern biotechnology and traditional Daqu are combined with the use of bacteria, yeast, and mold for the fermentation production of sesame-flavored baijiu, which is an innovative improvement to the production of traditional baijiu. Sesame-flavored baijiu exhibits the 'purity' and 'elegance' of light-flavored baijiu, the 'softness' and 'fullness' of strong-flavored baijiu, and the 'refinement' and 'nuances' of Maotai-flavored baijiu. The comprehensive sensory evaluation indicates that the typical aroma of sesame-flavored baijiu is that of roasted sesame seeds (Yuan, 2009; Su et al., 2015; Sun et al., 2018a). Although there has been a great deal of research on sesame-flavored baijiu, their characteristic flavor compounds and their associated microbial metabolic mechanisms remain unclear. However, in recent years, research on sesame-flavored baijiu has been increasing, and it has been reported that some sulfur compounds in roasted sesame seeds have been identified as the source of the sesame-like aroma. Eleven sulfur-containing compounds have been identified in sesame-flavored baijiu, including dimethyl disulfide, trisulfide dimethyl ester, 3- (methyl sulfur) propionaldehyde, furfural mercaptan, and furfural disulfide. Therefore, sulfur compounds play a key role in sesame-flavored baijiu because they confer its roasted sesame-like aroma (Tamura et al., 2010, 2011; Yang et al., 2014).

Chi-Flavored Baijiu

Chi-flavored baijiu originates from the Pearl River Delta region, and it is named for its prominent soy flavor. Pure rice is used as the raw material, and large baijiu cakes act as saccharification starters in the fermentation process. The most representative soy flavor is Yubingshao baijiu, which is also called Xiaoqu baijiu. Its flavor is similar to that of fermented soybeans, with a very clean aftertaste. The main aromatic components of this baijiu are phenyl ethyl alcohol and ethyl ester. Testing of the microorganisms in the baijiu balls, baijiu cakes, and fermentation broth of soy-flavored baijiu revealed that there were 29 species of bacteria, of which *Lactobacillus* and *Halomonas* were the dominant flora. Additionally, there were 21 species of fungi, of which *Saccharomyces* and *Mucor* were the dominant bacteria.

Laobaigan-Flavored Baijiu

To produce Laobaigan-flavored baijiu, medium-temperature Daqu composed of pure wheat is necessary as the saccharification starter, with selected sorghum as the main material. The fermentation process involves ground tank fermentation, mixed steaming, segmented baijiu picking, graded storage, and careful blending. It has the characteristics of a short fermentation period, high production rate, and short storage period. Continued (Micha) mixed burning increases the utilization rate of starch, increases the yield, and steams the grains and baijiu at the same time, which increases its grain aroma. Its most representative product is Hengshui Laobaigan, which has a soft, mellow, and rich taste. The representative ester compounds in Laobaigan-flavored baijiu are ethyl acetate, ethyl lactate, and a small amount of ethyl butyrate, palmitate, and linoleic acid. The concentration of hexyl acetate is higher than that in light-flavored baijiu and Feng-flavored baijiu. The amount of fusel oil, especially isoamyl alcohol (7.17 mg/100 mL) in laobaigan-flavored baijiu is higher than that in light-flavored baijiu (flavored baijiu, 28.89 mg/mL), which enhances its sweetness and soft taste (Zhu et al., 2015; Wang et al., 2021).

Fuyu-Flavored Baijiu

The brewing process for fragrant-flavored baijiu is the inheritance and development of traditional baijiu production technology in China and has important practical significance for promoting the progress of traditional baijiu technology in China. Shen Yifang, the master of Chinese Baijiu, once highly evaluated the craftsmanship of jiugui baijiu and rich-flavored baijiu: 'Although there are many flavor types, in the final analysis, the main ones are strong, clear, and sauce-like. Jiugui baijiu combines these three, and the combination creates a rich fragrance, which is an innovation.' The representative product of fuyu-flavored baijiu is Jiugui baijiu, which has the sensory characteristics of clear fragrance, strong fragrance, and beige baijiu. The main aromatic compound is ethyl caproate, which contains equal amounts of ethyl lactate and ethyl acetate. By high-throughput sequencing, 11 bacterial genera were isolated, including *Bacillus*, *Lactobacillus*, *Leuconostoc*, *Weisseria*, *Lactococcus,* and *Acetobacter*; 8 yeast genera were isolated, including *Candida*, *Pichia*, and *Saccharomyces*, with *Lactobacillus*, *Welmanella*, and *Bacillus* in the bacterial community and *Rhizopus*, *Candida*, and *Pichia* in the fungal community, with *Aspergillus* predominating (Kang et al., 2021).

FORMATION OF FLAVOR SUBSTANCES IN BAIJIU

The brewing process for baijiu is conducted in an open environment, with grain as the fermentation substrate and jiuqu as the saccharification starter. In the process of jiuqu production, the factors affecting the diversity and richness of the jiuqu microbial community include raw materials, production

temperature, water, and so on. These bacteria, molds, and yeasts from their natural habitat all play a key role in jiuqu (Xiu et al., 2012). There were significant differences in microbial diversity among the three starter cultures, and the microbial community structure in starter cultures was the key factor determining the flavor diversity. It is reported that the bacterial species in Daqu and Fuqu are mainly thermophilic or heat-resistant. Fuqu and Xiaoqu both contain mold and *Rhizopus oryzae*. *Saccharomyces cerevisiae* and *Saccharomycopsis fibuligera* are also used in Fuqu and Xiaoqu, respectively. During the brewing process, the interaction of various microorganisms will produce the corresponding lipidosis, which plays a catalytic role and hastens the brewing process.

Microbial Starter-Jiuqu

Chinese Baijiu is produced through a solid-state fermentation process using a saccharified grain starter. Jiuqu provides raw materials, microorganisms, enzymes, and aromatic precursors for the brewing process. The production of Chinese Baijiu is the interaction of jiuqu and specific microflora in the environment, plus different materials and processing processes, creating different types of baijiu, which are also inseparable from the formation of flavor substances (Jin et al., 2017). According to the different production processes, jiuqu can be divided into three categories: Daqu, Xiaoqu, and Fuqu (Zheng and Han, 2016). The production process of the three kinds of jiuqu is shown in **Figure 2**.

Daqu is a grain distiller's jiuqu, made from wheat (the sauce-flavored type is pure wheat), barley, and/or peas, providing mainly a sauce-like roasted aroma and pleasantly fruity, floral aromas. Daqu is further categorized into high-temperature Daqu (Maotai-flavored baijiu), medium-temperature Daqu (strong-flavored baijiu), and low-temperature Daqu (light-flavored baijiu) (Guan et al., 2020). High-temperature Daqu is divided into three kinds according to different positions in the workshop (white-Qu, yellow-Qu, and black-Qu). White-Qu had the highest liquefaction and saccharification enzyme activity, while black-Qu had the highest neutral protease and cellulase activity among the three kinds of high-temperature Daqu. The total volatile content of yellow-Qu and black-Qu is about twice that of white-Qu. Studies have shown that there are significant differences in microbial communities and metabolites among the three Daqu (Shi et al., 2022). The production process of Daqu is relatively complicated, whereby 70% of Chinese Baijiu are brewed with Daqu starter, including the most well-known baijiu in China, such as Maotai, Luzhou laojiao, and fenjiu, which are Maotai-flavored baijiu, Luzhou- flavored baijiu, and light-flavored baijiu, respectively (Wang et al., 2020b). Many intrinsic and extrinsic factors in Daqu production affect the microbial community richness and structure, including feedstock species, moisture content, temperature control, geographic location, climate, and moisture (Song et al., 2017). Daqu mainly consists of three functional microbial communities, namely Filamentous fungi (*Rhizopus, Rhizomucor, Aspergillus,* and other genera), Yeasts (*Saccharomyces, Candida, Hansenula,* and other genera), Bacteria (acetic acid bacteria, lactic acid bacteria, and *Bacillus* spp.) (Zheng et al., 2011). They provide different enzymes and flavor precursors for baijiu production. A previous study found that fungi, lactic acid bacteria, and *Bacillus* are the main flora in Daqu production. As the relative abundance of lactic acid bacteria increases, the acidity of Daqu also increases. In addition, Bacillus and thermophilic fungi become the dominant flora.

Xiaoqu is suitable for the climatic conditions of southern China owing to its small size and less heat generation. The production process of Xiaoqu is relatively simple. It is made from rice, sorghum, or barley and several traditional Chinese

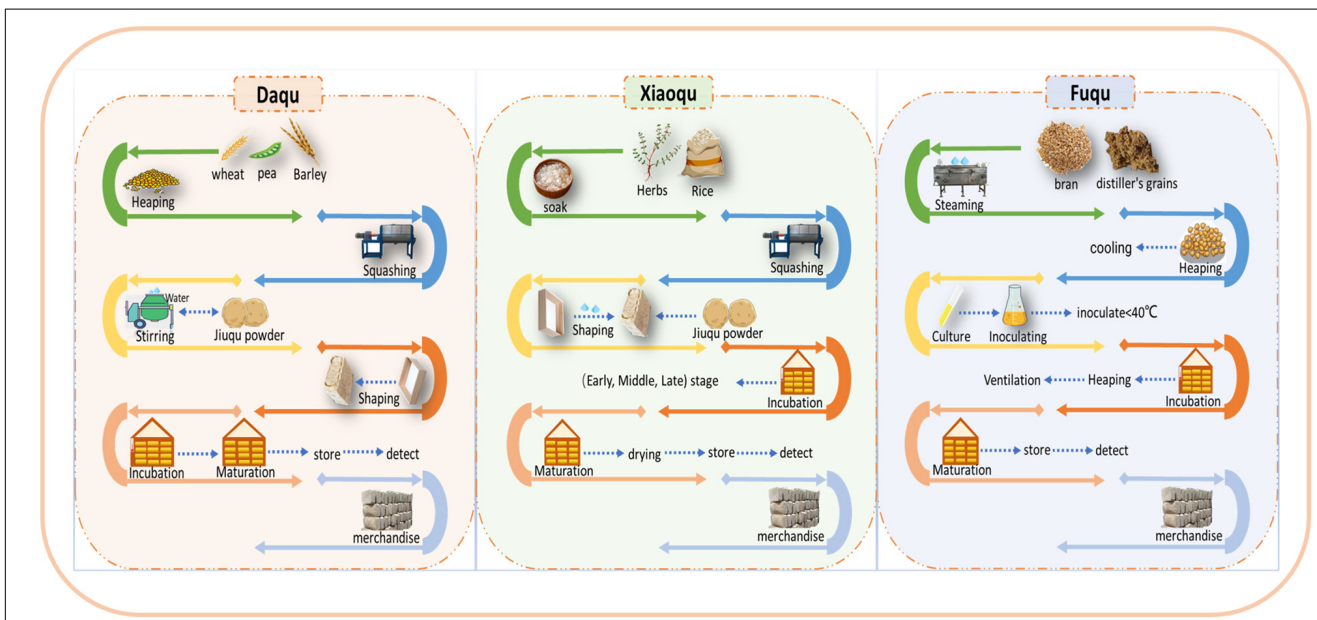

FIGURE 2 | The production process of the three kinds of jiuqu.

medicines. In the process of brewing baijiu, saccharification and fermentation occur at the same time in Xiaoqu, and the brewed baijiu is called Xiaoqu, which is different from Daqu. There are only a few types of microorganisms in Xiaoqu, including *Rhizopus*, *Mucor*, *Lactobacillus*, and yeast. These microorganisms are the executors of fermentation because only a small amount of starter and a shorter period are required to produce this type of baijiu. During the fermentation cycle, the baijiu contains less alcohol. Owing to the simple production process of Xiaoqu, the diversity of microorganisms is reduced, mainly *Saccharomyces cerevisiae* and *Saccharomycopsis fibuligera* (Zhou, 2011; Jin et al., 2017).

In Fuqu, bran is used as the raw material, and it is inoculated with jiuqu enzymes (*Aspergillus flavus*, *Aspergillus niger*, and *Aspergillus albus*), which mainly plays the role of saccharification, and then is cultivated by artificial control of temperature and humidity (Dai et al., 2020). When brewing, Fuqu also needs to be mixed with yeast (heat-resistant yeast, lipogenic yeast) for alcoholic fermentation. Fuqu has been successfully used to produce Maotai-flavored (Dai et al., 2020), light-flavored (Zhang et al., 2013), and sesame-flavored Chinese Baijiu (Wang et al., 2017a). Sesame-flavored baijiu is a new flavor produced with Fuqu as the main leavening agent and with Daqu. There is a saying in the baijiu industry that 'Jiuqu is the bone of baijiu,' which means that the type and quantity of microorganisms in baijiu determine the structure of the flavor substances in it, which verifies the importance of microbes in the process of brewing baijiu. **Table 2** lists the basic characteristics of each jiuqu.

Lipase Produced by Microorganisms

Esterase is a general term for a lipolytic enzyme, and they are very important in the brewing process of baijiu and mainly plays a catalytic role. Esterase in baijiu production mainly refers to lipase, ester synthase, and phosphatase as an extracellular enzyme that can catalyze ester synthesis and ester decomposition, which is mainly produced by microorganisms in the fermentation system. Most of the esterase-producing microorganisms are molds, such as *Aspergillus*, *Rhizopus*, and *Mucor*. Esters are important aromatic substances in baijiu. A large number of studies have found that various strains such as *Aspergillus niger* and *Rhizopus* have a strong ability to catalyze the production of fatty acid ethyl ester (Xu et al., 2021a). It was also found that Daqu is a saccharification agent and starter for brewing different types of baijiu. Because there is an increase during the brewing process in a large number of microorganisms that produce a variety of enzymes under the long-term open operating environment, Daqu not only contains abundant brewing microorganisms, but also contains enzymes including esterase, and therefore, Daqu is a very important flavoring agent (Nicholson, 2008). According to research data, the correlation between various enzymes and the production of total esters in baijiu is very small, while the correlation between various enzymes and the production of ethyl acetate, ethyl butyrate, ethyl hexanoate, and ethyl lactate is very different because the effect of the enzyme on total ester production reflects the combined effect of the enzyme on the production of various esters.

During the fermentation process of Chinese Baijiu, enzymes produced by microorganisms in the fermented grains decompose high molecular weight substances such as proteins, carbohydrates, and fats into low molecular weight substances such as amino acids, oligosaccharides, and fatty acids. Microorganisms utilize small molecules as nutrients and provide abundant precursors for flavor substances. The activity of enzymes not only affects the transformation of various substances in fermented grains but also directly affects the type and quantity of flavor substances, which has a profound impact on baijiu. For example, during fermentation, esterases directly catalyze the esterification of acetic and propionic acids with ethanol to synthesize ethyl acetate and ethyl propionate (Yu et al., 2012). According to Guo et al. (2018), increasing the lipase activity in fermented grains can increase the total ester content in baijiu, and adding cellulase to fermented grains can increase the ester content, especially ethyl acetate. The main application of esterase in baijiu production is to alter the production of various synthesized lipids, which in turn has an important impact on the formation of baijiu quality and its aroma. Therefore, the catalytic conditions under which different esterases perform have great guiding significance for their application in the brewing of baijiu.

Microbiological Compositions

An enzyme is a biological catalyst that is mainly derived from microorganisms in the process of brewing baijiu. Most baijiu is fermented by a variety of microorganisms that can produce carboxylate hydrolase. Enzymes originate from ethanol and sour substrates in the baijiu production process (Zheng et al., 2011, 2014). The study of enzymatic synthesis of lipids began as early as the 1990s when a Dutch company launched a series of lipid products. United States federal regulations and some non-Chinese literature also recognize that biosynthetic lipids can be used as natural flavors. In a simple enzymatic reaction, enzymes catalyze the synthesis of ethyl ester from anhydrous ethanol and acid in different organic media. Compared with the ester chemical synthesis method, this method produces less environmental pollution with simpler post-processing of the product. Enzymatic synthesis has the advantages of mild reaction conditions, high conversion rate, reusable enzymes, mild product flavor, and natural aroma. It has important research significance and application value.

The reaction environment of enzymatic synthesis can be divided into lipidation reactions in a reverse micelle system and a single environment. A reverse micelle is a microemulsion, which is a surfactant dispersed in a continuous organic phase. The film formed by the surfactant can separate oily and aqueous substances, simulating the natural environment of enzymes, and thus assisting in maintaining the activity of enzymes and stability. The researchers discovered a novel catalyst by combining genome sequencing, and transcriptome sequencing techniques. This enzyme may promote the synthesis of ethyl valerate, ethyl caproate, ethyl capryate, or ethyl decanoate (Xu et al., 2021b). The discovery of new biocatalysts is of great significance in increasing enzyme sources for the synthesis of short chain fatty acid esters in the aqueous phase. In recent years, there has been great interest in the catalysis of biological enzymes in the organic

TABLE 2 | Basic characteristics of each jiuqu.

Jiuqu	Types	Baijiu	Raw material	Microorganism species	References
High-temperature Daqu	Maotai-flavored baijiu	Moutai, Langjiu	Mostly made from wheat, barley, and/or peas; Maotai-flavored Daqu is only made from wheat	Some fungi, lactic acid bacteria; *Bacillus* are the main flora in Daqu production. *Ascomycota* and *Basidiomycota* were the dominant phyla	Jin et al., 2017; Song et al., 2017; Guan et al., 2020; Wang et al., 2020b; Cai et al., 2021
	Te-flavored baijiu	Si'te-jiu			
Medium/high-temperature Daqu	Strong-flavored baijiu	Luzhou laojiao, Wuliangye			
	Feng-flavored baijiu	Xifengjiu			
Medium-temperature Daqu	Laobaigan-flavored baijiu	Laobaigan			
Xiaoqu	Rice-flavored baijiu	Sanhua jiu	Rice, sorghum, and barley are used as main raw materials, and several traditional Chinese medicines are added.	*Rhizopus*, *Mucor*, *Lactobacillus*, and some Yeast, e.g., *Saccharomyces cerevisiae*, and *Saccharomycopsis fibuligera*	Zhou, 2011; Xiong et al., 2014; Jin et al., 2017
	Chi-flavored baijiu	Yubingshao jiu			
Daqu Xiaoqu mixture	Medicine-flavored baijiu	Dong jiu			
	Fuyu-flavored baijiu	Jiugui jiu			
Daqu and Fuqu mixture	Sesame-flavored baijiu	Jingzhijiu	Fuqu: bran as raw material	*Aspergillus flavus*, *Aspergillus niger*, some thermotolerant yeast, and lipogenic yeast	Jin et al., 2017; Wang et al., 2017a; Dai et al., 2020
Daqu (high-temperature Daqu/medium-temperature Daqu)	Miscellaneous-flavored baijiu	Baiyunbian	–	*Salmonella, Penicillium, Aspergillus, Streptococcus, Saccharomyces cerevisiae, Ssaccharomycopsisibuligera, Pichia pastoris* and *Debaryomycesansenii*	Xiong et al., 2014; Dong et al., 2022; Shi et al., 2022
Daqu, Xiaoqu, and Fuqu mixture	Light-flavored baijiu	Fenjiu		*Bacillus, Lactobacillius*, *Acetobacter* and *Lactococcus*	Dong et al., 2020; Su et al., 2020; Hu Y.A. et al., 2021; Tang et al., 2022

phase. In organic solvents containing trace amounts of water, an enzyme will not lose its activity, and it also increases the protein's catalysis due to the strengthening of intramolecular hydrogen bonds. Rigidity significantly increases the thermal stability of the enzyme and increases the solubility of non-polar substrates, which can reduce reaction byproducts and increase the reaction rate of synthesis.

Microbial Synthesis

The Chinese Baijiu brewing system contains a complex microbial flora, consisting of a variety of bacteria, yeasts, and molds. Daqu is the source of the main microbial bacteria, molds, and yeasts, with the number of bacteria being the largest and relatively stable; the abundance of molds is relatively high, followed by yeasts (Guo and Jia, 2014). The essence of baijiu brewing is the process of microbial growth and metabolite accumulation, and therefore, the synergy between different microbial populations is closely related to the flavor and quality of baijiu (Yu et al., 2014).

The primary compounds in light-flavored baijiu that provide flavor are ethyl acetate and ethyl lactate. Lactic acid bacteria are the dominant microbial group in fragrant baijiu-fermented grains, and they are relatively stable in number during the fermentation process. They metabolize lactic acid and acetic acid, which are the precursors of ethyl acetate and ethyl lactate, to maintain an acidic brewing environment and provide other fermenting microorganisms that are precursors of nutrients and flavor compounds. During the process of brewing Xiaoqu baijiu, the starch in sorghum, which is an important substrate for microbial metabolism, is decomposed by microorganisms and converted into reducing sugars. *Saccharomyces cerevisiae*, which is an ester-producing yeast, and lactic acid bacteria utilize reducing sugars for proliferation and fermentation to produce metabolites, which result in the production of ethanol, ethyl acetate, and other important aromatic substances in jiuqu (Kerjean et al., 2000; Zha et al., 2018). Pang et al. (2020) found that *Lactobacillus* and *Pichia* were the main bacterial and fungal genera in the pretreatment process of the materials used for making light flavored baijiu. And with the dynamic change of microbiota in fermentation, the types and concentrations of alcohols, esters, acids, phenols, ketones, aldehydes, and other volatile flavor substances also varied. Environmental conditions and microorganisms have always been important factors driving the production of flavor substances in baijiu (Chen et al., 2021). A study found that the amount of esters and the acidity of light-flavored baijiu were significantly reduced when production was resumed after the summer break

TABLE 3 | Chromatographic methods used to detect Chinese Baijiu flavor substances.

No.	Instrument	Type of baijiu	Flavor substances	Number of flavors	References
1	GC	Maotai-flavored baijiu, Strong-flavored baijiu, Light-flavored baijiu, Miscellaneous-flavored baijiu, Medicine-flavored baijiu	Organic acids, alcohols, esters, ketones, and aldehydes	62	He X. et al., 2020
2	GC-MS	Sesame-flavored baijiu, Light-flavored baijiu	Sulfur compounds: dimethyl disulfide, dimethyl trisulfide; propyl lactate; acetic acid; butyric acid; valeric acid, caproic acid	125	Ma and Zhang, 2014; Sun et al., 2017, 2018b
3	HPLC HPLC-Q-TOF-MS	Sesame-flavored baijiu	Esters and alcohols	1	Huang et al., 2019
4	SBSE and GC-MS	Maotai-flavored baijiu	Esters, alcohols, aldehydes, and ketones	76	Fan et al., 2011
5	GC-O	Strong-flavored baijiu	Ethyl esters, alcohols, aldehydes, acetals, alkyl pyrazines, furan derivatives, lactones, sulfur-containing compounds	126	Fan and Qian, 2006
6	GC-O and GC-MS	Strong-flavored baijiu, Light-flavored baijiu	Aromatic compounds: ethyl acetate, ethyl acrylate, ethyl isovalerate, ethyl butyrate, isoamyl acetate, ethyl caprylate, ethyl valerate	60/59	Zhao et al., 2018; Wang et al., 2022b
7	GC ×GC mil TOF/MS	Laobaigan-flavored baijiu	volatile chemicals	414	Fan Q. et al., 2019
8	MASTER GC/TOF MS	Strong-flavored baijiu	Organic acids, alcohols, esters, ketones, aldehydes, acetals, lactones, and nitrogen- and sulfur-containing compounds	528/262/606	Zhu et al., 2007; He Y.X. et al., 2020; Wang et al., 2020c
9	^{1}H (NMR)	Light-flavored baijiu, Strong-flavored baijiu, Maotai-flavored baijiu	Mannitol, trimethylamine, lactic acid, etc.	–	Wu et al., 2009
10	GC and ^{1} H NMR	Fuyue- flavored baijiu Light-flavored baijiu, Strong-flavored baijiu	acetaldehyde, butyrate, valeric acid, n-butanol, 2-butanol, hexanol, ethyl butyrate, ethyl valerate, ethyl heptanoate and ethyl caproate	10	Li Y. et al., 2021
11	GC-MS and MIR	Strong-flavored baijiu	Propionic acid, pentanoic acid, hexyl hexanoate, ethyl decanoate, etc.	–	Hu and Wang, 2021
12	GC-O and GC-MS	Maotai-flavored baijiu	Ethyl acetate, ethyl lactate, acetic acid	79	Niu et al., 2016
13	GC-O and GC-FPD	Light-flavored baijiu	ethyl acetate, diethyl succinate, phenylethyl alcohol, isoamyl alcohol, and n-propanol, A tetrapeptide (Asp-Arg-Ala-Arg)	80	Niu et al., 2017
14	HS-SPME and GCxGC-SCD	Laobaigan-flavored baijiu	Benzenemethanethiol, Dimethyl trisulfide, 2-methyl-3-Furanthiol and 2-furfurylthiol exhibited, etc.	65	Song et al., 2019
15	HS-SPME and GC × GC-TOFMS	Strong-flavored baijiu, Light-flavored baijiu, Maotai-flavored baijiu	Esters, alcohols, fatty acids, aldehydes, furans, pyrazines, sulfides, phenols, etc.	119/19	Tang et al., 2022
16	HS-SPME-GC-MS/O	Daqu	aromatic compounds:guaiacol, 4-ethyl-2-methoxy phenol, 2-ethyl-3,5-dimethylpyrazine, etc.	43	Wang et al., 2022a
17	UHPLC-Q-Orbitrap HRMS/UHPLC-Q-Orbitrap	Feng-flavored baijiu	non-volatile molecule, 15 organic acids, 8 esters, Ethyl carbamate	153/29	Jia et al., 2020b, 2021, 2022a
18	HS-SPME-AEDA	Sesame-flavored baijiu	Ethyl hexanoate, 2-furfuryl mercaptan, dimethyl trisulfide, 3-methyl butyraldehyde, ethyl butyrate, ethyl 2-methyl butyrate, ethyl valerate, and 4-methyl valeric acid ethyl ester	63	Sha et al., 2016
19	UPLC-MS/MS	Maotai-flavored baijiu, Strong-flavored baijiu, Light-flavored baijiu, Sesame-flavored baijiu	Pyrazines aroma compounds: 2,3-dimethylpyrazine, 2,3-diethylpyrazine, 2,3-diethyl-5-methylpyrazine and 2-acetyl-3-methylpyrazine	16	Yan et al., 2020, 2021
20	(Vis/NIR)	Various flavored baijius	–	–	Li et al., 2014

(Pang et al., 2018). Lack of acetyl resistant Lactobacillus may lead to delayed fermentation and lower the ester content. Environmental conditions (moisture, reducing sugar, and starch) and yeast are important factors in the brewing of light-flavored baijiu that affect the flavor substances in the fermented grains of Xiaoqu baijiu and promote changes in the composition and amount of flavor substances during different fermentation periods. During this process, with the change in the microbial community brewing structure, the flavor substances produced by its metabolism also changed.

Ethyl caproate is a strongly aromatic substance in Luzhou-flavored baijiu, and it is mainly produced by the high esterification of microorganisms such as aroma-producing yeast, bacteria, and mold in the mud pit in the later stage of fermentation. In the early stage of brewing, Luzhou-flavored baijiu mainly produces various acids and alcohols. In the middle and late stages, the acids and alcohols undergo biochemical reactions under the conditions of enzymes and appropriate temperatures to gradually generate various esters, which can form a unique style of baijiu (Liu et al., 2017). It has been reported that the quality of the Luzhou-flavored baijiu is closely related to the pit mud and the *Clostridium* spp. inhabiting the pit mud can produce caproic acid and ethyl caproate. At present, hexanoic acid and ethyl hexanoate have been identified as the key flavor substances in Luzhou-flavored baijiu (Guo and Jia, 2014; Li et al., 2014). Chen et al. constructed a recombinant strain EY15 by studying overexpression of EHT1 (encoding ethanol caproyltransferase) in which FAA1 (encoding acyl-CoA synthase) was deleted, followed by liquid fermentation of corn hydrolyzate and solid fermentation of sorghum. The yield of ethyl caproate was significantly increased to 2.23 and 2.83 mg/L, which were 2.97 times and 2.80 times that of the parental strain AY15, respectively. In addition, there was increased production of ethyl caprylate (52 and 43%) and ethyl caprate (61 and 40%) (Chen Y.F. et al., 2014).

During the saccharification process of brewing rice-flavored baijiu, the microorganisms and enzymes in Xiaoqu can degrade the starch in the rice into sugar (Devi and Radhika, 2018; Yin et al., 2020a). The main aromatic substances of rice-flavored baijiu are ethyl lactate and ethyl acetate, and the precursors of these two compounds are lactic acid and acetic acid. Relevant research analysis shows that in the brewing process of rice-flavored baijiu, bacteria and yeast genera have a great impact on flavor (Wang et al., 2017b; Gha et al., 2019; Xu et al., 2021b). Lactic acid bacteria (LAB) dominate the late fermentation stage and influence the sensory properties of baijiu by synthesizing flavor compounds that result from modulating the composition of other bacteria and yeasts. When there are acetic acid-tolerant lactobacilli participating in fermentation, the production of ethyl acetate, ethyl lactate, ethanol, acetic acid, and 2,4-di-tert-butyl-phenol can be significantly increased, and the lactic acid bacteria and the esters, acids, and flavor substances such as alcohol showed a strong positive correlation. However, in general, the microbial community diversity in rice-flavored baijiu is relatively higher than that of other types of baijiu during fermentation, because the different non-yeast composition leads to a diversity of metabolites.

Chinese Baijiu is rich in aromatic substances. Except for the characteristic aromatic substances in Luzhou-flavored, light-flavored, and rice-flavored baijiu, the characteristic flavor substances of other types of baijiu are still under consideration. Researchers are searching for new methods to increase the quality of baijiu and benefit human health by studying certain flavor substances. 2,3,5,6-Ligustrazine (TMP) is an important component in baijiu, and it has the effect of promoting cardiovascular and cerebrovascular health. During the process of brewing baijiu, the microorganisms in the jiuqu will produce acetone and then synthesize tetramethylpyrazine (TTMP), but the yield is low. Using the 2,3-butanediol dehydrogenase (BDH)-encoding gene BDH1 and another BDH2 gene deleted or overexpressed, Cui et al. (2020) showed that by disrupting BDH1 and overexpressing BDH2, acetoin synthesis in strain α5-D1B2 was significantly enhanced, resulting in a 2.6-fold increase in TTMP production.

ACTION MECHANISMS OF MICROORGANISMS IN BAIJIU FERMENTATION

Saccharomycetes

Saccharomycetes is a single-celled fungus, classified as a facultative anaerobic microorganism, and it can ferment sugars to produce alcohol. Most of them survive in an environment with high sugar concentration and acidity, and they play the role of alcoholization and esterification in the process of brewing baijiu (Liu and Miao, 2020). Saccharomycetes has a variety of enzyme systems, which is also rich in protein, amino acids, fats, carbohydrates, and other nutrients. Generally, under anaerobic conditions, yeasts convert sugars into pyruvate through a series of enzymatic reactions through the sugar metabolism pathway, and finally into ethanol under the action of aldehyde dehydrogenase and alcohol dehydrogenase.

Studies have shown that yeast can produce aldehyde esters, β-phenethyl alcohol, and other higher alcohols during the fermentation process, and it also uses ethyl acetate as the main ester to form flavor substances (Li H.S. et al., 2021). There are two yeasts primarily used in baijiu brewing. One is *S. cerevisiae* (Wang et al., 2018b), which mainly has the functions of fermenting sugar, fermenting, and producing alcohol, and it has a relatively high alcohol-producing capacity. The other is lipogenic yeast, whose alcohol-producing capacity is smaller than that of *S. cerevisiae*. However, during the fermentation of baijiu, lipogenic yeast can convert some metabolites into aldehydes, esters, higher alcohols, and other compounds. Song et al. (2017) found that yeast is the core fungal microorganism in the fermentation process that produces Maotai-flavored baijiu. The origin of yeast can be traced back to the production stage of Daqu. During the process of fermentation, yeast and other microorganisms can promote and inhibit each other. Yeast not only directly determines the fermentation rate, but also converts nutrients into a variety of volatile flavor compounds. Therefore, yeast is one of the key factors affecting the flavor type and product quality of Chinese Baijiu. However, it is unclear whether other microbes possess similar interaction mechanisms. Therefore, while studying the diversity of microorganisms, the types and mechanisms of interactions between microorganisms are important because they can increase the quality of baijiu.

Bacteria

Bacteria are prokaryotic organisms with a simple structure that undergo multiplication by binary division. Bacteria mostly survive in environments with suitable temperatures, high humidity, and saturated organic matter (Hu et al., 2015). In the

process of brewing baijiu, bacteria are mainly used to produce flavor components and precursors of flavor components, which are important sources of the unique flavor of Chinese Baijiu (Tao et al., 2017). Bacteria in baijiu brewing are acid-producing microorganisms, and their metabolites can be used as precursors for lipid substances, and can also promote the growth and reproduction of other brewing microorganisms.

Aerobic and anaerobic bacteria, e.g., *Lactobacillus*, *Bacillus*, and *Clostridium*, participate in the process of brewing baijiu. The fermentation products of *Bacillus* mainly include 4 compounds, pyrazine compounds, volatile acids, aromatic compounds, and phenolic compounds, which are very important for Chinese Baijiu and significantly contribute to its aroma (Zheng et al., 2013). Some studies have found that the introduction of bacteria into Daqu and pit mud will affect the relative abundance of microorganisms, and thus, synthetic flavor compounds have been used to affect the sensory properties of different baijiu. Wang et al. (2017a) added the strain *Bacillus licheniformis* to the fermentation mix, and the microbial community subsequently changed after inoculation. It was noted that the number of *Bacilli*, *Corynebacterium*, and *Aspergillus* increased, and the number of *Pichia*, *Saccharomyces* and other genera decreased, which in turn altered the metabolic activity during the fermentation process. In the process of baijiu brewing, in addition to providing corresponding acid substrates, bacterial metabolism can also ferment glucose into ethanol through the Entner-Doudoroff (ED) pathway, but the efficiency is relatively lower than that of yeast. Bacteria can also metabolize components from complex and diverse enzyme systems, such as proteases, amylases, and cellulases. Bacteria decompose raw and auxiliary materials such as potatoes, rice, and sorghum during the baijiu-making process, and these are then formed into various amino acids, sugars, and other substances that continue to ferment and undergo biochemical changes to produce a unique flavor. In addition, Bacillus also promotes a variety of free amino acids to participate in the Maillard reaction, which endows baijiu with a unique flavor (Wang et al., 2018a).

Mold

Mold was first recognized and utilized and is closely related to human life and material production. Mold is widespread, and its mycelium is composed of branched or unbranched hyphae and is relatively lush. Mold spores possess strong stress resistance and produce colonies that are loose and dry, in the form of spider webs, or fluffy, felt-like material (Hu et al., 2015). According to reports (Wang et al., 2008; Pang et al., 2018; Wang and Xu, 2019; Xnp et al., 2021), many fungal species such as *Aspergillus*, *Rhizopus*, *Mucor*, and *Penicillium* participate in the fermentation of cheese, baijiu, soy sauce, and other foods. *Rhizopus* produces glucoamylase and protease and some important flavor substances such as lactic acid, other organic acids, and aromatic compounds.

Studies have shown that starch in raw materials for brewing cannot be directly utilized by most yeasts and bacteria, and it must be hydrolyzed into fermentable sugars by α-amylasecuicui and saccharification enzymes produced by filamentous fungi during the process of saccharification and fermentation. The role of filamentous fungi is to secrete various enzymes to hydrolyze starch and protein to increase the digestibility and amount of probiotics in food and beverages (Wei et al., 2021). In the process of brewing baijiu, the brewing environment, various raw materials, and the mold in Daqu may all participate in the fermentation process, but the mold in Daqu plays the primary role. The saccharification power of mold can decompose the starch contained in the raw materials of brewing into reducing sugar that can be used by microorganisms. Mold possesses liquefaction power and esterification power, and it can also promote the decomposition and transformation of starch, protein, and other substances in the fermentation broth. This increases the concentration of sugars and amino acids throughout the fermentation process. Mold supplies nutrients for the metabolism of microorganisms in the fermentation system, and it also provides a unique flavor for the baijiu.

USING MICROBIAL TECHNOLOGY TO IMPROVE BAIJIU FLAVOR

The isolation, research, reproduction, and reuse of microorganisms in baijiu brewing can greatly improve the performance of jiuqu, improve the quality and yield of baijiu, shorten the production cycle, and reduce costs. In addition, microorganisms can also be applied in some related fields.

Jiuqu Strengthening

Based on microbial diversity research, isolated functional strains have been used to improve the quality of Daqu. *Lactobacillus*, *Aspergillus*, *Candida*, *Xanthomyces*, *Deba* spp., *Oosporium*, *Penicillium*, *Pichia*, *Saccharomyces*, and other strains have been added to improve the quality of Daqu during its production. Liu and Sun (2018) used red yeast rice or a mixture of fungi, yeast, and bacteria to fortify Daqu, and the results showed that the use of fortified Daqu increased the quality and yield of the produced baijiu, while decreasing the necessary amount of Daqu, which resulted in lower costs. Daqu fortification has the advantages of convenient operation, easy preparation, time-saving, and satisfactory batch-to-batch stability. In addition, the flavor and texture of the baijiu brewed with this new type of Daqu are comparable to those brewed with the traditional Daqu. These studies reveal the importance of microbial community investigation and the applicability of microbial resources in baijiu brewing to improve process control.

Controlled Fermentation

Traditional solid-state fermentation tends to lead to batch-to-batch instability of the product, which is a bottleneck that needs to be addressed. Given the importance of microorganisms in the fermentation process, there has been great interest in the use of functional microorganisms to manually regulate the fermentation process. Wang et al. (2020e) simulated solid fermentation by adding *Wickerhamomyces anomalus* and showed that *W. anomalus* altered ethyl acetate content and caused changes in levels of other flavor substances. The results showed that the flavor changes caused by the addition of *W. anomalus* were due to the change in fermentation

microbial community structure. Researchers have improved the flavor of baijiu using exogenous microorganisms to modulate the composition of the microbial community. The effect of exogenous microorganisms alters the growth and flavor metabolism of endogenous microorganisms, which suggests the possibility of using exogenous microorganisms to modulate the microbiota of the fermentation process. Further improvement and refinement will assist in maintaining product stability between batches and improve the quality of Chinese Baijiu (Fan and Qian, 2006).

Cellar Mud Maintenance

The pit mud produced by Chinese Baijiu is currently aging and degraded, and this is caused by the consumption of nutrients by microorganisms and the accumulation of secondary metabolites, the inhibition of the growth of functional microorganisms, and the degradation of bacterial strains. All of these will lead to the degradation of pit mud and reduce the quality of baijiu. Laojiao assists in producing high-quality baijiu, and therefore, the maintenance of Laojiao mud is very important. There have been attempts to grow microorganisms such as *Clostridium* and add them to the pit mud. The results showed that the amount of ethyl caproate was increased, and the quality of Luzhou-flavored baijiu was improved (He X. et al., 2020).

Researchers have isolated many functional strains of microorganisms from pit mud, lees, and Daqu. In addition to the above-mentioned applications, strains such as *Monascus* and *Rhizopus* are also used in other fields. The red pigment produced by *Monascus* can be used as a food additive, and this species can also produce lovastatin, which is an effective drug for the treatment of cardiovascular and cerebrovascular diseases (Sun et al., 2018b). *Rhizopus* can synthesize oligosaccharides with various physiological functions, which can be used to produce healthy food. Other species produce a range of enzymes such as lipases, proteases, and amylases that can be used in related fields (Ma and Zhang, 2014). Through continuous research, additional strains with new characteristics will be discovered, and they will promote the study of baijiu-brewing mechanisms and also provide valuable resources for applications in many fields.

METHOD FOR THE DETECTION OF FLAVOR SUBSTANCES IN BAIJIU

The trace components in Chinese Baijiu only account for 1 to 2% of the total but have an important impact on baijiu aroma and taste. After years of research, it has been proven that the flavor composition of Chinese Baijiu is extremely complex, with many types and a wide range of content. Flavor component analysis of baijiu is performed mainly to detect trace components. Nearly 2,400 flavor compounds have been detected in baijiu thus far, including alcohols, esters, aldehydes, ketones, acids, acetals, aromatic compounds, lactones, furans, terpenes, hydrocarbons, nitrogen-containing compounds, and sulfur-containing compounds. This includes 216 types of alcohols, 431 types of esters, 95 types of aldehydes, 126 types of ketones, 109 types of acids, 54 types of acetals, 167 types of aromatic compounds, 19 types of lactones, and 76 types of furans and terpenes. Additionally, there are 68 alkenes, 81 hydrocarbons, 115 nitrogen compounds, 55 sulfur compounds, and 125 others (Sun et al., 2015). A variety of substances has been detected in baijiu, but the contribution and influencing mechanism of most flavor components are still unclear. At present, researchers can use conventional detection techniques, chromatographic techniques, spectroscopic techniques, and other analysis and detection techniques. Chromatography techniques are relatively common and accurate research methods, and a system has been built with these techniques for the detection and analysis of Chinese Baijiu (Jia et al., 2020a; Wu et al., 2020b). The chromatographic methods used to detect some flavor substances in Chinese Baijiu are summarized as follows, in **Table 3**.

With the continuous development of science and technology, some novel detection methods have gradually emerged. For example, using simple organic reactions such as the hydroxylamine color reaction, 2,4-dinitrophenylhydrazine (DNPH) nucleophilic addition reaction, and localized surface plasmon resonance (LSPR) exhibited by noble metal nanoparticles, an eight-channel array sensor was constructed for the direct and qualitative detection of compounds such as aldehydes, ketones, esters, and acids in baijiu (Zhao et al., 2018).

In addition, some unscrupulous merchants have been illegally adulterating baijiu, such as adding sildenafil. It is difficult to detect sildenafil using ordinary methods, and its presence in baijiu can result in severe health effects. Xiao and He (2019) used Opto Trace Raman 202 (OTR 202) as a surface-enhanced Raman spectroscopy (SERS) active colloid to detect sildenafil, and the results showed that the Raman enhancement factor (EF) of the OTR 202 colloid reached 1.84×10^7. Thus, the limit of detection (LOD) for sildenafil in health baijiu and baijiu was found to be as low as 0.1 mg/L. In recent years, there has been increased quality monitoring of Chinese Baijiu, and its analysis and testing have been developed for more than 50 years. There was an initial stage of development that progressed to a stable and mature stage, and now, analysis and testing have entered a new and modern stage of development with remarkable results. The progress of analytical technology, especially the application of chromatographic analysis technology, has greatly promoted the use of technology in the baijiu industry and made outstanding contributions to the inheritance and development of the traditional Chinese Baijiu industry.

SUMMARY

Chinese Baijiu has been exported all over the world, and it is increasingly recognized and appreciated in the international market. The production process of baijiu, including the production of jiuqu, has been modernized. However, owing to the wide variety of baijiu, the production technology for the different types must be updated based on retaining the original flavor. Therefore, understanding the ecology and function of each type of baijiu-related microorganism is the primary condition for realizing the standardization of baijiu production, and research on microorganisms plays a positive role in promoting the development of China's baijiu industry. In the process of brewing

baijiu, almost all strains promote the production of flavors such as esters, alcohols, and acids, and especially the formation of esters. Therefore, the species and even the strains of microorganisms in the brewing process of baijiu determine the flavor substances of baijiu. The balance and interaction of various flavors in baijiu depend on the balance and interaction of the microbiota during fermentation. With the development of microbiology, molecular biology, and bioinformatics technology, it is possible to further study the microbial community, functional strains, and their properties to reveal the mechanism of baijiu brewing and to discover the relationship between microorganisms and baijiu quality and yield. On this basis, we can also enrich the resource pool of functional strains, develop application technologies for concurrent functional strains, improve jiuqu production and grain fermentation processes, and adjust the fermentation process to produce quality products that meet consumer requirements. This will satisfy the development of the baijiu industry and promote the standardization and modernization of Chinese Baijiu.

AUTHOR CONTRIBUTIONS

WT, LL, and XC contributed to literature retrieval and information collection. TZ, QW, JC, PX, and WT analyzed the data. WT, QL, and CS wrote and reviewed the manuscript. All authors contributed to the article and approved the submitted version.

FUNDING

This work was financially supported by Luzhou Laojiao Company Limited (Grant no. PCGS-2021000068) and the Open Project Program of the Key Laboratory of Brewing Molecular Engineering of China Light Industry (BME-202101). The authors declare that this study received funding from Luzhou Laojiao Company Limited. The funder was not involved in the study design, collection, analysis, interpretation of data, the writing of this article or the decision to submit it for publication.

REFERENCES

Bokulich, N. A., Bamforth, C. W., and Mills, D. A. (2012). A review of molecular methods for microbial community profiling of beer and wine. *J. Am. Soc. Brew. Chem.* 70, 150–162.

Cai, W. C., Xue, Y. A., Wang, Y. R., Wang, W. P., Shu, N., Zhao, H. J., et al. (2021). The fungal communities and flavor profiles in different types of high-temperature Daqu as revealed by high-throughput sequencing and electronic senses. *Front. Microbiol.* 12:784651. doi: 10.3389/fmicb.2021.784651

Cai, X. M., Shen, Y., Chen, M. Y., Zhong, M. G., and Luo, A. (2019). Characterisation of volatile compounds in Maotai flavour liquor during fermentation and distillation. *J. Inst. Brew.* 125, 453–463.

Calasso, M., Ercolini, D., Mancini, L., Stellato, G., Minervini, F., Cagno, R. D., et al. (2016). Relationships among house, rind and core microbiotas during manufacture of traditional Italian cheeses at the same dairy plant. *Food Microbiol.* 54, 115–126.

Chen, B., Wu, Q., and Xu, Y. (2014). Filamentous fungal diversity and community structure associated with the solid state fermentation of Chinese Maotai-flavor liquor. *Int. J. Food Microbiol.* 179, 80–84. doi: 10.1016/j.ijfoodmicro.2014.03.011

Chen, Y. F., Li, F., Guo, J., Liu, G. X., Guo, X. W., and Xiao, D. G. (2014). Enhanced ethyl caproate production of Chinese liquor yeast by overexpressing EHT1 with deleted FAA1. *J. Ind. Microbiol. Biotechnol.* 41, 563–572. doi: 10.1007/s10295-013-1390-3

Chen, M., Liu, H., Zhen, D., and Fang, S. (2011). Research on the esterification property of esterase produced by *Monascus* sp. *Afr. J. Biotechnol.* 10, 5166–5172.

Chen, X., Zhang, Y. L., Yan, Z. K., Meng, Q. Y., and Qi, H. L. H. (2020). Microbial community succession of Fengxiang-type fermented grains and its correlation with physical and chemical indicators. *Food Sci.* 41, 200–205.

Chen, Y. R., Li, K. M., Liu, T., Li, R. Y., Fu, G. M., Wan, Y., et al. (2021). Analysis of difference in microbial community and physicochemical indices between surface and central parts of chinese special-Flavor Baijiu Daqu. *Front. Microbiol.* 11:592421. doi: 10.3389/fmicb.2020.592421

Cui, D. Y., Wei, Y. N., Lin, L. C., Chen, S. J., Feng, P. P., Xiao, D. G., et al. (2020). Increasing Yield of 2,3,5,6-tetramethylpyrazine in Baijiu through *Saccharomyces cerevisiae* metabolic engineering. *Front. Microbiol.* 11:596306. doi: 10.3389/fmicb.2020.596306

Dai, Y., Tian, Z., Meng, W., and Li, Z. J. J. O. N. (2020). Microbial diversity and physicochemical characteristics of the Maotai-flavored liquor fermentation process. *J. Nanosci. Nanotechnol.* 20, 4097–4109. doi: 10.1166/jnn.2020.17522

Devi, N. A., and Radhika, G. B. (2018). Kinetic study of ethyl hexanoate synthesis using surface coated lipase from Candida Rugosa. *Iran. J. Chem. Chem. Eng.* 37, 81–92.

Dong, W., Zeng, Y., Cui, Y., Chen, P., Cai, K., Guo, T., et al. (2022). Unraveling the composition and succession of microbial community and its relationship to flavor substances during Xin-flavor baijiu brewing. *Int. J. Food Microbiol.* 372, 109679. doi: 10.1016/j.ijfoodmicro.2022.109679

Dong, W. W., Yang, Q., Liao, Y. X., Liu, Y. C., Hu, Y. L., Peng, N., et al. (2020). Characterisation and comparison of the microflora of traditional and pure culture xiaoqu during the baijiu liquor brewing process. *J. Inst. Brew.* 126, 213–220.

Endo, A., and Okada, S. (2005). Monitoring the lactic acid bacterial diversity during shochu fermentation by PCR-denaturing gradient gel electrophoresis. *J. Biosci. Bioeng.* 99, 216–221. doi: 10.1263/jbb.99.216

Fan, G., Fu, Z., Sun, B., Zhang, Y., Wang, X., Xia, Y., et al. (2019). Roles of aging in the production of light-flavored Daqu. *J. Biosci. Bioeng.* 127, 309–317. doi: 10.1016/j.jbiosc.2018.08.005

Fan, Q., Wang, X. L., Zhao, Y. F., Zheng, F. P., Li, H. H., Zhang, F. Y., et al. (2019). Characterization of key aroma compounds in Laobaigan Chinese Baijiu by GCxGC-TOF/MS and means of molecular sensory science. *Flavour Fragr. J.* 34, 514–525.

Fan, G. S., Sun, B. G., Fu, Z. L., Xia, Y. Q., Huang, M. Q., Xu, C. Y., et al. (2018). Analysis of Physicochemical Indices, Volatile Flavor Components, and Microbial Community of a Light-Flavor Daqu. *J. Am. Soc. Brew. Chem.* 76, 209–218.

Fan, W., and Qian, M. C. (2006). Characterization of aroma compounds of chinese "Wuliangye" and "Jiannanchun" liquors by aroma extract dilution analysis. *J. Agric. Food Chem.* 54, 2695–2704. doi: 10.1021/jf052635t

Fan, W., Shen, H., and Xu, Y. (2011). Quantification of volatile compounds in Chinese soy sauce aroma type liquor by stir bar sorptive extraction and gas chromatography-mass spectrometry. *J. Sci. Food Agric.* 91, 1187–1198. doi: 10.1002/jsfa.4294

Fang, C., Du, H., Zheng, X., Zhao, A., Jia, W., and Xu, Y. (2019). Solid-state fermented Chinese alcoholic beverage (baijiu) and ethanol resulted in distinct metabolic and microbiome responses. *FASEB J* 33, 7274–7288. doi: 10.1096/fj.201802306R

Fu, G. M., Deng, M. F., Chen, Y., Chen, Y. R., Wu, S. W., Lin, P., et al. (2021). Analysis of microbial community, physiochemical indices, and volatile compounds of Chinese te-flavor baijiu daqu produced in different seasons. *J. Sci. Food Agric.* 101, 6525–6532. doi: 10.1002/jsfa.11324

Gha, B., Yi, D. C., Jha, B., Xw, C., Sz, C., Cwa, B., et al. (2019). Alteration of microbial community for improving flavor character of Daqu by inoculation with *Bacillus velezensis* and *Bacillus subtilis*. *LWT* 111, 1–8.

Gou, M., Wang, H. Z., Yuan, H. W., Zhang, W. X., Tang, Y. Q., and Kida, K. (2015). Characterization of the microbial community in three types of fermentation starters used for Chinese liquor production. *J. Inst. Brew.* 121, 620–627.

Guan, T., Lin, Y., Chen, K., Ou, M., and Zhang, J. (2020). Physicochemical factors affecting Microbiota dynamics during traditional solid-state fermentation of Chinese Strong-Flavor Baijiu. *Front. Microbiol.* 11:2090. doi: 10.3389/fmicb.2020.02090

Guo, J., and Jia, S. (2014). Effects of enzymes on ester production during the course of a Chinese liquor fermentation as discussed by correlation analysis and path analysis. *J. Inst. Brew.* 120, 565–570.

Guo, J., Sun, L., Guo, H., Zou, D., Liu, X., Wang, Y., et al. (2018). Effect of cellulase-producing bacteria on fungi community structure and ester generation in Chinese Liquor Fermenting Grains. *J. Am. Soc. Brew. Chem.* 76, 130–140.

Hao, F., Tan, Y. W., Lv, X. B., Chen, L. Q., Yang, F., Wang, H. Y., et al. (2021). Microbial community succession and its environment driving factors during initial fermentation of Maotai-Flavor Baijiu. *Front. Microbiol.* 12:669201. doi: 10.3389/fmicb.2021.669201

He, X., Gaca, A., and Jeleń, H. (2020). Determination of volatile compounds in Baijiu using simultaneous chromatographic analysis on two columns. *J. Inst. Brew.* 126, 206–212.

He, Y. X., Liu, Z. P., Qian, M., Yu, X. W., Xu, Y., and Chen, S. (2020). Unraveling the chemosensory characteristics of strong-aroma type Baijiu from different regions using comprehensive two-dimensional gas chromatography-time-of-flight mass spectrometry and descriptive sensory analysis. *Food Chem.* 331:127335. doi: 10.1016/j.foodchem.2020.127335

Hong, J., Tian, W., and Zhao, D. (2020). Research progress of trace components in sesame-aroma type of baijiu. *Food Res. Int.* 137:109695.

Hu, S., and Wang, L. (2021). Age Discrimination Of Chinese Baijiu Based On Midinfrared Spectroscopy And Chemometrics. *J. Food Qual.* 2021:5527826.

Hu, X. L., Du, H., and Xu, Y. (2015). Identification and quantification of the caproic acid-producing bacterium Clostridium kluyveri in the fermentation of pit mud used for Chinese strong-aroma type liquor production. *Int. J. Food Microbiol.* 214, 116–122. doi: 10.1016/j.ijfoodmicro.2015.07.032

Hu, Y., Wang, L., Zhang, Z., Yang, Q., and Zhao, S. (2021). Microbial community changes during the mechanized production of light aroma Xiaoqu baijiu. *Biotechnol. Biotechnol. Equip.* 35, 487–495.

Hu, Y. L., Lei, X. Y., Zhang, X. M., Guan, T. W., Wang, L. Y., Zhang, Z. J., et al. (2021). Characteristics of the Microbial Community in the Production of Chinese Rice-Flavor Baijiu and Comparisons With the Microflora of Other Flavors of Baijiu. *Front. Microbiol.* 12:673670. doi: 10.3389/fmicb.2021.673670

Hu, Y. A., Huang, X. N., Yang, B., Zhang, X., Han, Y., Chen, X. X., et al. (2021). Contrasting the microbial community and metabolic profile of three types of light-flavor Daqu. *Food Biosci.* 44:101395.

Huang, M., Huo, J., Wu, J., Zhao, M., Sun, J., Zheng, F., et al. (2019). Structural characterization of a tetrapeptide from Sesame flavor-type Baijiu and its interactions with aroma compounds. *Food Res. Int.* 119, 733–740.

Huang, T., Yang, H., Zhang, S. H., Zai, Q. H., Guo, L., Ma, Y. F., et al. (2021). Changes of Main Chemical Components in Fengxiang Baijiu During Storage in Jiuhai. *Liquor Mak. Sci. Technol.* 4, 29–36.

Huang, X., Fan, Y., Lu, T., Kang, J., and Chen, J. (2020). Composition and metabolic functions of the microbiome in fermented grain during light-flavor Baijiu Fermentation. *Microorganisms* 8:1281. doi: 10.3390/microorganisms8091281

Ji, M., Fang, C., Jia, W., Du, H., and Xu, Y. (2021). Regulatory effect of volatile compounds in fermented alcoholic beverages on gut microbiota and serum metabolism in a mouse model. *Food Funct.* 12, 5576–5590. doi: 10.1039/d0fo03028g

Ji, X., Yu, X., Wu, Q., and Xu, Y. (2022). Initial fungal diversity impacts flavor compounds formation in the spontaneous fermentation of Chinese liquor. *Food Res. Int.* 155:110995. doi: 10.1016/j.foodres.2022.110995

Jia, W., Fan, Z., Du, A., Li, Y., and Chu, X. J. F. C. (2020a). Recent advances in Baijiu analysis by chromatography based technology–A review. *Food Chem.* 324:126899. doi: 10.1016/j.foodchem.2020.126899

Jia, W., Li, Y., Du, A., Fan, Z., and Chu, X. (2020b). Foodomics analysis of natural aging and gamma irradiation maturation in Chinese Distilled Baijiu by UPLC-Orbitrap-MS/MS. *Food Chem.* 315:126308. doi: 10.1016/j.foodchem.2020.126308

Jia, W., Fan, Z., Du, A., Shi, L., and Ren, J. (2022b). Characterisation of key odorants causing honey aroma in Feng-flavour Baijiu during the 17-year ageing process by multivariate analysis combined with foodomics. *Food Chem.* 374:131764. doi: 10.1016/j.foodchem.2021.131764

Jia, W., Fan, Z., Du, A., and Shi, L. (2022a). Molecular mechanism of Mare Nectaris and magnetic field on the formation of ethyl carbamate during 19 years aging of Feng-flavor Baijiu. *Food Chem.* 382:132357. doi: 10.1016/j.foodchem.2022.132357

Jia, W., Fan, Z. B., Du, A., and Shi, L. (2021). Untargeted foodomics reveals molecular mechanism of magnetic field effect on Feng-flavor Baijiu ageing. *Food Res. Int.* 149:110681.

Jiang, Y., Wang, R., Yin, Z., Sun, J., and Sun, B. (2021). Optimization of Jiuzao protein hydrolysis conditions and antioxidant activity *in vivo* of Jiuzao tetrapeptide Asp-Arg-Glu-Leu by elevating Nrf2/Keap1-p38/PI3K-MafK signaling pathway. *Food Funct.* 12, 4808–4824. doi: 10.1039/d0fo02852e

Jin, G., Yang, Z., and Yan, X. (2017). Mystery behind Chinese liquor fermentation. *Trends Food Sci. Technol.* 63, 18–28. doi: 10.3389/fmicb.2019.00696

Jin, Y., Li, D., Ai, M., Tang, Q., Huang, J., Ding, X., et al. (2019). Correlation between volatile profiles and microbial communities: A metabonomic approach to study Jiang-flavor liquor Daqu. *Food Res. Int.* 121, 422–432. doi: 10.1016/j.foodres.2019.03.021

Kang, J. M., Hu, Y. A., Ding, Z. Y., Ye, L., Li, H. R., Cheng, J., et al. (2021). Deciphering the Shifts in Microbial Community Diversity From Material Pretreatment to Saccharification Process of Fuyu-Flavor Baijiu. *Front. Microbiol.* 12:705967. doi: 10.3389/fmicb.2021.705967

Kerjean, J. R., Condon, S., and Lodi, R. (2000). Improving the quality of European hard-cheeses by controlling of interactions between lactic acid bacteria and propionibacteria. *Food Res. Int.* 33, 281–287.

Li, H., He, R., Xiong, X., Zhang, M., Yang, T., Jiang, Z., et al. (2016). Dynamic diversification of bacterial functional groups in the Baiyunbian liquor stacking fermentation process. *Ann. Microbiol.* 66, 1229–1237.

Li, H. S., Han, X. L., Liu, H. R., Hao, J. Q., Jiang, W., and Li, S. Z. (2021). Silage Fermentation on Sweet Sorghum Whole Plant for Fen-Flavor Baijiu. *Foods* 10:1477. doi: 10.3390/foods10071477

Li, Y., Fan, S., Li, A., Liu, G., Lu, W., Yang, B., et al. (2021). Vintage analysis of Chinese Baijiu by GC and 1H NMR combined with multivariable analysis. *Food Chem.* 360:129937. doi: 10.1016/j.foodchem.2021.129937

Li, K. M., Fu, G. M., Wu, C. F., Liu, C. M., Wang, Y., Pan, F., et al. (2017). Succession of eukaryotic microbial flora during special-flavor liquor brewing. *Food Sci.* 38, 131–136.

Li, W., Ya, Y. W., Di, Q. W., Jin, X., and Tao, J. (2015). Dynamic changes in the bacterial community in Moutai liquor fermentation process characterized by deep sequencing. *J. Inst. Brew.* 121, 603–608.

Li, Z., Wang, P. P., Huang, C. C., Shang, H., and Li, X. J. (2014). Application of Vis/NIR Spectroscopy for Chinese Liquor Discrimination. *Food Anal. Methods* 7, 1337–1344.

Liang, Y., Junjun, H. E., Chuxiang, L., and Chunlin, Z. (2019). Analysis of volatile flavor compounds from defective product of sauce-flavor Baijiu by GC×GC-TOF-MS. *China Brew.* 38, 67–72.

Liu, H. L., and Sun, B. G. (2018). Effect of Fermentation Processing on the Flavor of Baijiu. *J. Agric. Food Chem.* 66, 5425–5432. doi: 10.1021/acs.jafc.8b00692

Liu, M. K., Tang, Y. M., Guo, X. J., Zhao, K., Tian, X. H., Liu, Y., et al. (2017). Deep sequencing reveals high bacterial diversity and phylogenetic novelty in pit mud from Luzhou Laojiao cellars for Chinese strong-flavor Baijiu. *Food Res. Int.* 102, 68–76. doi: 10.1016/j.foodres.2017.09.075

Liu, P. L., and Miao, L. H. (2020). Multiple batches of fermentation promote the formation of functional Microbiota in Chinese Miscellaneous-Flavor Baijiu Fermentation. *Front. Microbiol.* 11:75. doi: 10.3389/fmicb.2020.00075

Ma, Y. H., and Zhang, S. W. (2014). Simultaneous Determination of Organic Acids in Chinese Liquor by GC-MS Method. *Asian J. Chem.* 26, 4707–4710. doi: 10.3390/molecules26226910

Nicholson, W. L. (2008). The *Bacillus subtilis* ydjL (bdhA) gene encodes acetoin reductase/2,3-butanediol dehydrogenase. *Appl. Environ. Microbiol.* 74, 6832–6838. doi: 10.1128/AEM.00881-08

Niu, Y., Chen, X., Xiao, Z., Ma, N., and Zhu, J. (2016). Characterization of aroma-active compounds in three Chinese Moutai liquors by gas chromatography-olfactometry, gas chromatography-mass spectrometry and sensory evaluation. *Nat. Prod. Res.* 31, 938–944. doi: 10.1080/14786419.2016.1255892

Niu, Y. W., Yao, Z. M., Xiao, Q., Xiao, Z. B., Ma, N., and Zhu, J. C. (2017). Characterization of the key aroma compounds in different light aroma type Chinese liquors by GC-olfactometry, GC-FPD, quantitative measurements, and

aroma recombination. *Food Chem.* 233, 204–215. doi: 10.1016/j.foodchem.2017.04.103

Pang, X. N., Han, B. Z., Huang, X. N., Zhang, X., Hou, L. F., Cao, M., et al. (2018). Effect of the environment microbiota on the flavour of light-flavour Baijiu during spontaneous fermentation. *Sci. Rep.* 8:3396. doi: 10.1038/s41598-018-21814-y

Pang, X. N., Huang, X. N., Chen, J. Y., Yu, H. X., Wang, X. Y., and Han, B. Z. (2020). Exploring the diversity and role of microbiota during material pretreatment of light-flavor Baijiu. *Food Microbiol.* 91:103514. doi: 10.1016/j.fm.2020.103514

Qian, Y. L., An, Y., Chen, S., and Qian, M. C. (2019). Characterization of Qingke Liquor Aroma from Tibet. *J. Agric. Food Chem.* 67, 13870–13881. doi: 10.1021/acs.jafc.9b05849

Sakandar, H. A., Hussain, R., Khan, Q. F., and Zhang, H. (2020). Functional Microbiota in Chinese Traditional Baijiu and Mijiu Qu (Starters): a review. *Food Res. Int.* 138:109830. doi: 10.1016/j.foodres.2020.109830

Sha, S., Chen, S., Qian, M., Wang, C., and Xu, Y. (2016). Characterization of the typical potent odorants in Chinese roasted sesame-like flavor type liquor by headspace solid phase microextraction–aroma extract dilution analysis, with special emphasis on sulfur-containing odorants. *Agric. Food Chem.* 65, 123–131. doi: 10.1021/acs.jafc.6b04242

Shen, T., Liu, J., Wu, Q., and Xu, Y. (2020). Increasing 2-furfurylthiol content in Chinese sesame-flavored Baijiu via inoculating the producer of precursor l-cysteine in Baijiu fermentation. *Food Res. Int.* 138:109757. doi: 10.1016/j.foodres.2020.109757

Shi, W., Chai, L.-J., Fang, G.-Y., Mei, J.-L., Lu, Z.-M., Zhang, X.-J., et al. (2022). Spatial heterogeneity of the microbiome and metabolome profiles of high-temperature Daqu in the same workshop. *Food Res. Int.* 156:111298.

Song, X. B., Zhu, L., Wang, X. L., Zheng, F. P., Zhao, M. M., Liu, Y. P., et al. (2019). Characterization of key aroma-active sulfur-containing compounds in Chinese Laobaigan Baijiu by gas chromatography-olfactometry and comprehensive two-dimensional gas chromatography coupled with sulfur chemiluminescence detection. *Food Chem.* 297:124959. doi: 10.1016/j.foodchem.2019.124959

Song, Z., Du, H., Zhang, Y., and Xu, Y. (2017). Unraveling core functional microbiota in traditional solid-state fermentation by high-throughput amplicons and metatranscriptomics sequencing. *Front. Microbiol.* 8:1294. doi: 10.3389/fmicb.2017.01294

Su, C., Zhang, K. Z., Cao, X. Z., and Yang, J. G. (2020). Effects of Saccharomycopsis fibuligera and *Saccharomyces cerevisiae* inoculation on small fermentation starters in Sichuan-style Xiaoqu liquor. *Food Res. Int.* 137:109425. doi: 10.1016/j.foodres.2020.109425

Su, Y., Yang, L., Hui, L., Yuan, Y. G., Ming, J. Z., Chun, H. X., et al. (2015). Bacterial communities during the process of high-temperature Daqu production of roasted sesame-like flavour liquor. *J. Inst. Brew.* 121, 440–448.

Sun, B., Wu, J. H., Huang, M. Q., Sun, J. Y., and Zheng, F. P. (2015). Recent advances of flavor chemistry in Chinese liquor spirits (Baijiu). *J. Chin. Inst. Food Sci. Technol.* 15, 1–8.

Sun, J., Li, Q., Luo, S., Zhang, J., Huang, M., Feng, C., et al. (2018a). Characterization of key aroma compounds in Meilanchun sesame flavor style baijiu by application of aroma extract dilution analysis, quantitative measurements, aroma recombination, and omission/addition experiments. *RSC Adv.* 8, 23757–23767. doi: 10.1039/c8ra02727g

Sun, J., Yin, Z. T., Zhao, D. R., Sun, B. G., and Zheng, F. P. (2018b). Qualitative and quantitative research of propyl lactate in brewed alcoholic beverages. *Int. J. Food Prop.* 21, 1351–1361.

Sun, J., Zhao, D., Zhang, F., Sun, B., Zheng, F., Huang, M., et al. (2017). Joint direct injection and GC–MS chemometric approach for chemical profile and sulfur compounds of sesame-flavor Chinese Baijiu (Chinese liquor). *Eur. Food Res. Technol.* 244, 145–160.

Sun, Y. L., Ma, Y., Chen, S., Xu, Y., and Tang, K. (2021). Exploring the mystery of the sweetness of Baijiu by sensory evaluation, compositional analysis and multivariate data analysis. *Food* 10:2843. doi: 10.3390/foods10112843

Tamura, H., Fujita, A., Steinhaus, M., Takahisa, E., Watanabe, H., and Schieberle, P. (2011). Assessment of the aroma impact of major odor-active thiols in pan-roasted white sesame seeds by calculation of odor activity values. *Agric. Food Chem.* 59, 10211–10218. doi: 10.1021/jf202183y

Tang, J., Liu, Y. C., Lin, B., Zhu, H., Jiang, W., Yang, Q., et al. (2022). Effects of ultra-long fermentation time on the microbial community and flavor components of light-flavor Xiaoqu Baijiu based on fermentation tanks. *World J. Microbiol. Biotechnol.* 38:3. doi: 10.1007/s11274-021-03183-3

Tang, K. (2021). Exploring the mystery of the sweetness of baijiu by sensory evaluation, compositional analysis and multivariate data analysis. *Foods* 10:2843.

Tao, Y., Wang, X., Li, X., Wei, N., Jin, H., Xu, Z., et al. (2017). The functional potential and active populations of the pit mud microbiome for the production of Chinese strong-flavour liquor. *Microb. Biotechnol.* 10, 1603–1615. doi: 10.1111/1751-7915.12729

Tamura, H., Fujitam, A., Steinhaus, M., Takahisa, E., Watanabe, H., and Schieberle, P. (2010). Identification of novel aroma-active thiols in pan-roasted white sesame seeds. *J. Agric. Food Chem.* 58, 7368–7375. doi: 10.1021/jf100623a

Wang, B., Wu, Q., Xu, Y., and Sun, B. (2020a). Synergistic effect of multiple saccharifying enzymes on alcoholic fermentation for Chinese Baijiu Production. *Appl. Environ. Microbiol.* 86:e000130-20. doi: 10.1128/AEM.00013-20

Wang, M. Y., Zhang, Q., Yang, J. G., Zhao, J. S., Su, C., Zhao, Q. S., et al. (2020b). Volatile compounds of Chinese Luzhou flavoured liquor distilled from grains fermented in 100 to 300 year-old cellars. *J. Inst. Brew.* 126, 116–130.

Wang, X. J., Zhu, H. M., Ren, Z. Q., Huang, Z. G., Wei, C. H., and Deng, J. (2020c). Characterization of microbial diversity and community structure in fermentation pit mud of different ages for production of strong-aroma Baijiu. *Pol. J. Microbiol.* 69, 151–164. doi: 10.33073/pjm-2020-018

Wang, C., Tang, J., and Qiu, S. (2020d). Profiling of fungal diversity and fermentative yeasts in traditional Chinese Xiaoqu. *Front. Microbiol.* 11:2103. doi: 10.3389/fmicb.2020.02103

Wang, W. H., Fan, G. S., Li, X. T., Fu, Z. L., Liang, X., and Sun, B. G. (2020e). Application of Wickerhamomyces anomalus in Simulated Solid-State Fermentation for Baijiu Production: Changes of Microbial Community Structure and Flavor Metabolism. *Front. Microbiol.* 11:598758. doi: 10.3389/fmicb.2020.598758

Wang, L. L., Gao, M. X., Liu, Z. P., Chen, S., and Xu, Y. (2020f). Three extraction methods in combination with GCxGC-TOFMS for the detailed investigation of volatiles in Chinese Herbaceous Aroma-Type Baijiu. *Molecules* 25:4429.

Wang, C. L., Shi, D. J., and Gong, G. L. (2008). Microorganisms in Daqu: a starter culture of Chinese Maotai-flavor liquor. *World J. Microbiol. Biotechnol.* 24, 2183–2190.

Wang, C. R. (2008). Research on Liquor Flavor Types & Their Flavoring Characteristics. *Liquor Mak. Sci.* 171, 49–52.

Wang, G., Jing, S., Song, X., Zhu, L., Zheng, F., and Sun, B. (2021). Reconstitution of the Flavor Signature of Laobaigan-Type Baijiu Based on the Natural Concentrations of Its Odor-Active Compounds and Nonvolatile Organic Acids. *J. Agric. Food Chem.* 70, 837–846. doi: 10.1021/acs.jafc.1c06791

Wang, H., and Xu, Y. (2019). Microbial succession and metabolite changes during the fermentation of Chinese light aroma-style liquor. *J. Inst. Brew.* 125, 162–170.

Wang, H. Y., Gao, Y. B., Fan, Q. W., and Xu, Y. (2011). Characterization and comparison of microbial community of different typical Chinese liquor Daqus by PCR–DGGE. *Lett. Appl. Microbiol.* 53, 134–140. doi: 10.1111/j.1472-765X.2011.03076.x

Wang, J., Zhong, Q., Yang, Y., Li, H., Wang, L., Tong, Y., et al. (2018a). Comparison of Bacterial Diversity Between Two Traditional Starters and the Round-Koji-Maker Starter for Traditional Cantonese Chi-Flavor Liquor Brewing. *Front. Microbiol.* 9:1053. doi: 10.3389/fmicb.2018.01053

Wang, L. (2022). Research trends in Jiang-flavor baijiu fermentation: From fermentation microecology to environmental ecology. *J. Food Sci.* 87, 1362–1374.

Wang, M. Y., Yang, J. G., Zhao, Q. S., Zhang, K. Z., and Su, C. (2019). Research Progress on Flavor Compounds and Microorganisms of Maotai Flavor Baijiu. *J. Food Sci.* 84, 6–18. doi: 10.1111/1750-3841.14409

Wang, X., Hai, D., Yan, Z., and Yan, X. (2018b). Environmental Microbiota Drives Microbial Succession and Metabolic Profiles during Chinese Liquor Fermentation. *Appl. Environ. Microbiol.* 84: e02369-17. doi: 10.1128/AEM.02369-17

Wang, P., Wu, Q., Jiang, X. J., Wang, Z. Q., Tang, J. L., and Xu, Y. (2017a). Bacillus licheniformis affects the microbial community and metabolic profile in the spontaneous fermentation of Daqu starter for Chinese liquor making. *Int. J. Food Microbiol.* 250, 59–67. doi: 10.1016/j.ijfoodmicro.2017.03.010

Wang, X., Du, H., and Xu, Y. (2017c). Source tracking of prokaryotic communities in fermented grain of Chinese strong-flavor liquor. *Int. J. Food Microbiol.* 244, 27–35. doi: 10.1016/j.ijfoodmicro.2016.12.018

Wang, X., Ban, S., Hu, B., Qiu, S., and Zhou, H. (2017b). Bacterial diversity of Moutai-flavour Daqu based on high-throughput sequencing method. *J. Inst. Brew.* 123, 138–143.

Wang, Z., Wang, Y., Zhu, T. T., Wang, J., Huang, M. Q., Wei, J. W., et al. (2022b). Characterization of the key odorants and their content variation in Niulanshan Baijiu with different storage years using flavor sensory omics analysis. *Food Chem.* 376:131851.

Wang, Z., Wang, S., Liao, P. F., Chen, L., Sun, J. Y., Sun, B. G., et al. (2022a). HS-SPME Combined with GC-MS/O to Analyze the Flavor of Strong Aroma Baijiu Daqu. *Foods* 11:116. doi: 10.3390/foods11010116

Wei, J. L., Du, H., Zhang, H. X., Nie, Y., and Xu, Y. (2021). Mannitol and erythritol reduce the ethanol yield during Chinese Baijiu production. *Int. J. Food Microbiol.* 337:108933.

Wei, Y., Zou, W., Shen, C., and Yang, J. (2020). Basic flavor types and component characteristics of Chinese traditional liquors: a review. *J. Food Sci.* 85, 4096–4107. doi: 10.1111/1750-3841.15536

Wu, Q., Wang, S., Yao, N., and Xu, Y. (2019). Construction of synthetic microbiota for reproducible flavor metabolism in Chinese light aroma type liquor produced by solid-state fermentation. *Appl. Environ. Microbiol.* 85:e03090-18. doi: 10.1128/AEM.03090-18

Wu, X. H., Zheng, X. W., Han, B. Z., Vervoort, J., and Nout, M. J. R. (2009). Characterization of Chinese Liquor Starter, "Daqu", by Flavor Type with 1H NMR-based nontargeted analysis. *J. Agric. Food Chem.* 57, 11354–11359. doi: 10.1021/jf902881p

Wu, Y. L., Hao, F., Lv, X. B., Chen, B., Yang, Y. B., Zeng, X. L., et al. (2020a). Diversity of lactic acid bacteria in Moutai-flavor liquor fermentation process. *Food Biotechnol.* 34, 212–227.

Wu, Z. Y., He, F., Li, H. H., Sun, J. Y., Sun, X. T., and Sun, B. G. (2020b). Determination of phenolic active compounds in light-aroma baijiu by solid phase extraction-high performance liquid chromatography. *Chin. J. Anal. Chem.* 48, 1400–1408.

Xiao, S., and He, Y. (2019). Analysis of sildenafil in liquor and health wine using surface enhanced Raman spectroscopy. *Int. J. Mol. Sci.* 20:2722. doi: 10.3390/ijms20112722

Xiong, X., Hu, Y., Yan, N., Huang, Y., Peng, N., Liang, Y., et al. (2014). PCR-DGGE analysis of the microbial communities in three different Chinese "Baiyunbian" Liquor Fermentation Starters. *J. Microbiol. Biotechnol.* 24, 1088–1095. doi: 10.4014/jmb.1401.01043

Xiong, Z. (2005). Research on three flavour type liquors in China (2) Introduction to Maotai-flavour liquor. *Liquor Mak. Sci. Technol.* 4, 25–30.

Xiu, L., Guo, K., and Zhang, H. (2012). Determination of microbial diversity in Daqu, a fermentation starter culture of Maotai liquor, using nested PCR-denaturing gradient gel electrophoresis. *World J. Microbiol. Biotechnol.* 28, 2375–2381. doi: 10.1007/s11274-012-1045-y

Xnp, A., Chang, C. A., Xnh, B., Yzy, C., Jyc, B., and Bzh, B. (2021). Influence of indigenous lactic acid bacteria on the volatile flavor profile of light-flavor Baijiu - ScienceDirect. *LWT* 147:111540.

Xu, Y., Sun, B., Fan, G., Teng, C., Xiong, K., and Zhu, Y. (2017a). The brewing process and microbial diversity of strong flavour Chinese spirits: a review. *J. Inst. Brew.* 123, 5–12. doi: 10.1111/1750-3841.16092

Xu, M. L., Yu, Y., Ramaswamy, H. S., and Zhu, S. M. (2017b). Characterization of Chinese liquor aroma components during aging process and liquor age discrimination using gas chromatography combined with multivariable statistics. *Sci. Rep.* 7:39671. doi: 10.1038/srep39671

Xu, Y., Huang, H., Lu, H., Wu, M., Lin, M., Zhang, C., et al. (2021a). Characterization of an *Aspergillus niger* for Efficient Fatty Acid Ethyl Ester Synthesis in Aqueous Phase and the Molecular Mechanism. *Front. Microbiol.* 12:820380. doi: 10.3389/fmicb.2021.820380

Xu, Y., Wang, X., Liu, X., Li, X., Zhang, C., Li, W., et al. (2021b). Discovery and development of a novel short-chain fatty acid ester synthetic biocatalyst under aqueous phase from *Monascus purpureus* isolated from Baijiu. *Food Chem.* 338:128025. doi: 10.1016/j.foodchem.2020.128025

Xu, Y., Zhu, Y., Li, X., and Sun, B. (2020). Dynamic balancing of intestinal short-chain fatty acids: The crucial role of bacterial metabolism. *Trends Food Sci. Technol.* 100, 118–130.

Yan, S. B., and Dong, D. (2018). Improvement of caproic acid production in a Clostridium kluyveri H068 and Methanogen 166 co-culture fermentation system. *AMB Express* 8:175. doi: 10.1186/s13568-018-0705-1

Yan, Y., Chen, S., He, Y. X., Nie, Y., and Xu, Y. (2020). Quantitation of pyrazines in Baijiu and during production process by a rapid and sensitive direct injection UPLC-MS/MS approach. *LWT* 128:109371.

Yan, Y., Chen, S., Nie, Y., and Xu, Y. (2021). Quantitative analysis of pyrazines and their perceptual interactions in soy sauce aroma type Baijiu. *Foods* 10:441. doi: 10.3390/foods10020441

Yang, Z., Zhao, J. W., Zhang, F. G., Huang, M. Q., Sun, B. G., Zheng, F. P., et al. (2014). Analysis of Volatile Compounds of Bandaojing Sesame-Flavor Liquor. *Food Sci.* 35, 60–65.

Yin, H., Liu, L. P., Yang, M., Ding, X. T., Jia, S. R., Dong, J. J., et al. (2019). Enhancing Medium-Chain Fatty Acid Ethyl Ester Production During Beer Fermentation Through EEB1 and ETR1 Overexpression in Saccharomyces pastorianus. *J. Agric. Food Chem.* 67, 5607–5613. doi: 10.1021/acs.jafc.9b00128

Yin, X., Yoshizaki, Y., Kurazono, S., Sugimachi, M., Takeuchi, H., Han, X. L., et al. (2020b). Characterization of Flavor Compounds in Rice-flavor baijiu, a Traditional Chinese Distilled Liquor, Compared with Japanese Distilled Liquors, awamori and kome-shochu. *Food Sci. Technol. Res.* 26, 411–422.

Yin, X., Yoshizaki, Y., Ikenaga, M., Han, X. L., Okutsu, K., Futagami, T., et al. (2020a). Manufactural impact of the solid-state saccharification process in rice-flavor baijiu production. *J. Biosci. Bioeng.* 129, 315–321. doi: 10.1016/j.jbiosc.2019.09.017

You, L., Wang, S., Feng, R. Z., Chen, Y. Z., Zhou, R. P., Feng, X. Y., et al. (2012). Correlations among Culturable Bacteria from Air,Mud on Pit Wall and Fermented Grains in Luzhou-Flavor Liquor-Brewing Workshop in Yibin. *Food Sci.* 33, 188–192.

Yu, K., Wu, Q., Zhang, Y., and Yan, X. (2014). *In situ* analysis of metabolic characteristics reveals the key yeast in the spontaneous and solid-state fermentation process of Chinese Light-Style Liquor. *Appl. Environ. Microbiol.* 80, 3667–3676. doi: 10.1128/AEM.04219-13

Yu, K. W., Lee, S. E., Choi, H. S., Suh, H. J., Ra, K. S., and Hwang, C. (2012). Optimization for rice koji preparation using aspergillus oryzae CJCM-4 isolated from a korean traditional meju. *Food Sci. Biotechnol.* 21, 129–135.

Yuan, M. Q. (2009). Cognition and investigation on the manufacturing of sesame-flavor liquor. *Mod. Appl. Sci.* 3, 92–95.

Zha, M., Sun, B., Wu, Y., Yin, S., and Wang, C. (2018). Improving flavor metabolism of *Saccharomyces cerevisiae* by mixed culture with Wickerhamomyces anomalus for Chinese Baijiu making. *J. Biosci. Bioeng.* 126, 189–195. doi: 10.1016/j.jbiosc.2018.02.010

Zhang, H., Wang, L., Tan, Y., Wang, H., Yang, F., Chen, L., et al. (2021). Effect of Pichia on shaping the fermentation microbial community of sauce-flavor Baijiu. *Int. J. Food Microbiol.* 336:108898. doi: 10.1016/j.ijfoodmicro.2020.108898

Zhang, R., Wu, Q., and Xu, Y. (2013). Aroma characteristics of Moutai-flavour liquor produced with Bacillus licheniformis by solid-state fermentation. *Lett. Appl. Microbiol.* 57, 11–18. doi: 10.1111/lam.12087

Zhao, C. Q., Yan, X. L., Yang, S. T., and Chen, F. F. (2017). Screening of Bacillus strains from Luzhou-flavor liquor making for high-yield ethyl hexanoate and low-yield propanol. *LWT* 77, 60–66.

Zhao, D. R., Sun, D. M., Sun, J. Y., Li, A. J., Bao, G., and Mou, M. (2018). Characterization of key aroma compounds in Gujinggong Chinese Baijiu by gas chromatography-olfactometry, quantitative measurements, and sensory evaluation. *Food Res. Int.* 105, 616–627. doi: 10.1016/j.foodres.2017.11.074

Zheng, J., Liang, R., Zhang, L., Wu, C., Zhou, R., and Liao, X. (2013). Characterization of microbial communities in strong aromatic liquor fermentation pit muds of different ages assessed by combined DGGE and PLFA analyses. *Food Res. Int.* 54, 660–666.

Zheng, X. W., and Han, B. Z. (2016). Baijiu, Chinese liquor: History, classification and manufacture. *J. Ethn. Foods* 3, 19–25.

Zheng, X. W., Tabrizi, M. R., Nout, M., and Han, B. Z. (2011). Daqu— A Traditional Chinese Liquor Fermentation Starter. *J. Inst. Brew.* 117, 82–90. doi: 10.1007/s10886-016-0809-5

Zheng, X. W., Yan, Z., Nout, M. J. R., Smid, E. J., Zwietering, M. H., Boekhout, T., et al. (2014). Microbiota dynamics related to environmental conditions during

the fermentative production of Fen-Daqu, a Chinese industrial fermentation starter. *Int. J. Food Microbiol.* 182, 57–62. doi: 10.1016/j.ijfoodmicro.2014.05.008

Zhi, N. N., Liu, G. Y., Wu, C. F., Xu, R. J., Lu, W., Zhang, S. L., et al. (2022). Effects of Light-To-Moderate Chinese Baijiu Consumption on Serum Lipid Metabolism and Liver Function of Sprague-Dawley Rats. *Curr. Top. Nutraceutical Res.* 20, 185–191.

Zhou, D. Q. (2011). *Microbiology Tutorial*, 3rd Edn. Beijing: Higher Education Press.

Zhu, H., Zhang, Y., Cheng, Z., Guo, Y., Huiling, A. N., Wang, W., et al. (2015). The Change Rules of the Main Flavoring Components during the Fermentation of Hengshui Laobaigan Liquor. *Liquor Mak. Sci. Technol.* 2, 36–39.

Zhu, S., Lu, X., Ji, K., Guo, K., Li, Y., Wu, C., et al. (2007). Characterization of flavor compounds in Chinese liquor Moutai by comprehensive two-dimensional gas chromatography/time-of-flight mass spectrometry. *Anal. Chim. Acta* 597, 340–348. doi: 10.1016/j.aca.2007.07.007

Zou, W., Ye, G. B., and Zhang, K. Z. (2018). Diversity, function, and application of Clostridium in Chinese strong flavor baijiu ecosystem: a review. *J. Food Sci.* 83, 1193–1199. doi: 10.1111/1750-3841.14134

Zuo, Q. C., Huang, Y. G., and MinGuo. (2020). Evaluation of bacterial diversity during fermentation process: a comparison between handmade and machine-made high-temperature Daqu of Maotai-flavor liquor. *Ann. Microbiol.* 70:57.

Conflict of Interest: XC, CS, and QL were employed by Luzhou Laojiao Co., Ltd.

The remaining authors declare that the research was conducted in the absence of any commercial or financial relationships that could be construed as a potential conflict of interest.

Publisher's Note: All claims expressed in this article are solely those of the authors and do not necessarily represent those of their affiliated organizations, or those of the publisher, the editors and the reviewers. Any product that may be evaluated in this article, or claim that may be made by its manufacturer, is not guaranteed or endorsed by the publisher.

frontiers | Frontiers in Microbiology

ORIGINAL RESEARCH
published: 22 June 2022
doi: 10.3389/fmicb.2022.923522

Exopolysaccharide Produced by *Pediococcus pentosaceus* E8: Structure, Bio-Activities, and Its Potential Application

*Guangyang Jiang[1,2], Juan He[3], Longzhan Gan[1,2], Xiaoguang Li[1,2], Zhe Xu[1,2], Li Yang[1,2], Ran Li[4] and Yongqiang Tian[1,2]**

[1] College of Biomass Science and Engineering, Sichuan University, Chengdu, China, [2] Key Laboratory of Leather Chemistry and Engineering, Ministry of Education, Sichuan University, Chengdu, China, [3] Key Laboratory of Bio-Resources and Eco-Environment of Ministry of Education, College of Life Sciences, Sichuan University, Chengdu, China, [4] Department of Microbiology, Faculty of Agriculture and Forestry, University of Helsinki, Helsinki, Finland

The novel exopolysaccharide EPS-E8, secreted by *Pediococcus pentosaceus* E8, was obtained by anion-exchange and gel filtration chromatography. Structural analyses identified EPS-E8 as a heteropolysaccharide containing mannose, glucose, and galactose. Its major backbone consists of →2)-α-D-Man*p*-(1→2,6)-α-D-Glc*p*-(1→6)-α-D-Man*p*-(1→, and its molecular weight is 5.02 × 10^4 g/mol. Using atomic force microscopy and scanning electron microscopy, many spherical and irregular reticular-like shapes were observed in the microstructure of EPS-E8. EPS-E8 has outstanding thermal stability (305.7°C). Both the zeta potential absolute value and average particle diameter increased gradually with increasing concentration. Moreover, at a concentration of 10 mg/ml, the antioxidant capacities of, 1-Diphenyl-2-picrylhydrazyl (DPPH), ABTS and hydroxyl radical were 50.62 ± 0.5%, 52.17 ± 1.4%, and 58.91 ± 0.7%, respectively. EPS-E8 possesses excellent emulsifying properties against several food-grade oils, and its activity is retained under various conditions (temperature, pH, and ionic strength). Finally, we found that EPS-E8 as a polysaccharide-based coating could reduce the weight loss and malondialdehyde (MDA) content of strawberry, as well as preserving the vitamin C and soluble solid content during storage at 20°C. Together, the results support the potential application of EPS-E8 as an emulsifier, and a polysaccharide-based coating in fruit preservation.

Keywords: exopolysaccharide, structural analysis, emulsifying activity, strawberry preservation, *Pediococcus pentosaceus*

OPEN ACCESS

Edited by:
Xucong Lv,
Fuzhou University, China

Reviewed by:
Reza Tahergorabi,
North Carolina Agricultural and Technical State University, United States
Clarita Olvera,
Universidad Nacional Autónoma de México, Mexico

****Correspondence:***
Yongqiang Tian
yqtian@scu.edu.cn

Specialty section:
This article was submitted to Food Microbiology, a section of the journal Frontiers in Microbiology

Received: *19 April 2022*
Accepted: *16 May 2022*
Published: *22 June 2022*

Citation:
Jiang G, He J, Gan L, Li X, Xu Z, Yang L, Li R and Tian Y (2022) Exopolysaccharide Produced by Pediococcus pentosaceus E8: Structure, Bio-Activities, and Its Potential Application. Front. Microbiol. 13:923522. doi: 10.3389/fmicb.2022.923522

HIGHLIGHTS

- An exopolysaccharide (EPS), purified from *Pediococcus pentosaceus* E8, showed noteworthy thermal stability under high temperature.
- EPS-E8 had unique backbone structure of →2)-α-D-Man*p*-(1→2,6)-α-D-Glc*p*-(1→6)-α-D-Man*p*-(1→.
- EPS-E8 exhibited excellent emulsifying activity and potent antioxidant activities.
- EPS-E8 as a coating could effectively delay the senescence of strawberries.
- EPS-E8 may be exploitable to improve the shelf-life of strawberries.

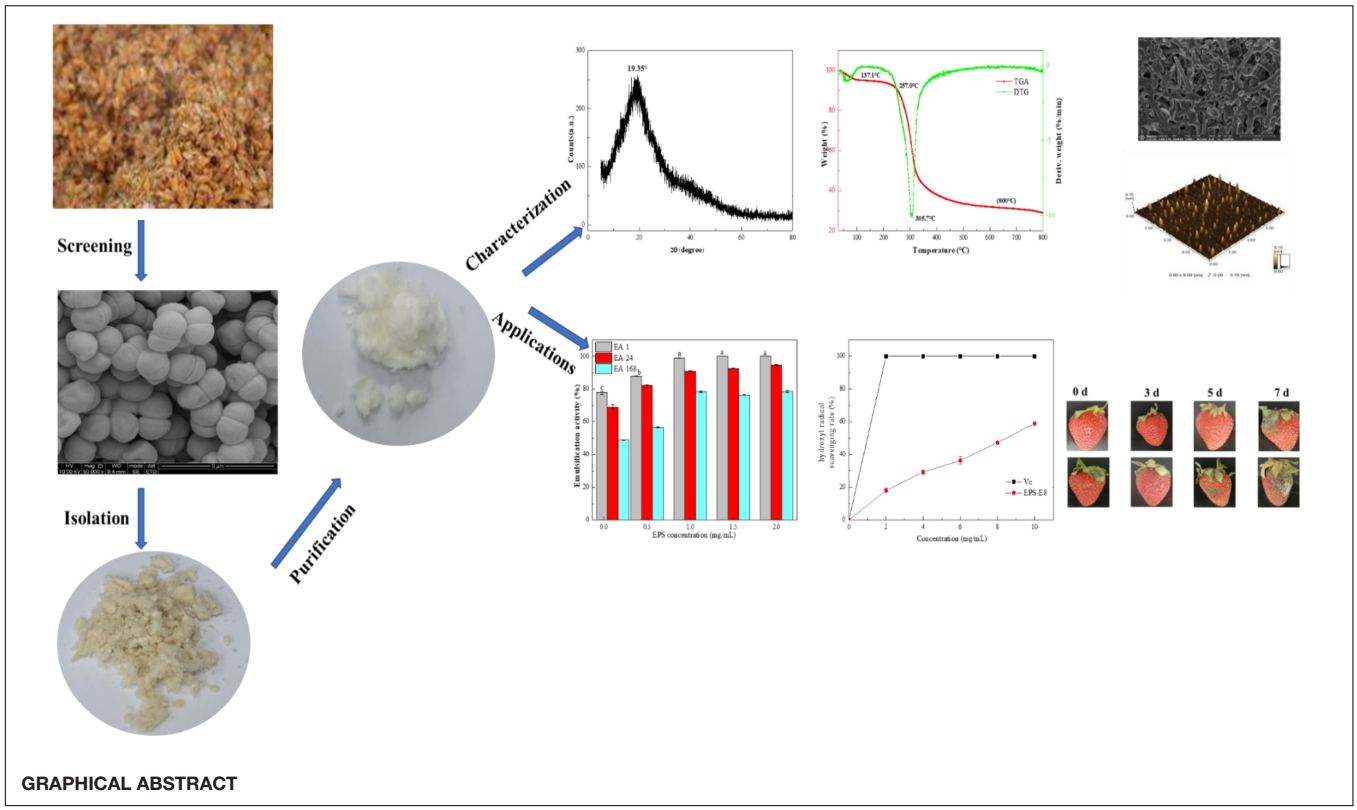

GRAPHICAL ABSTRACT

INTRODUCTION

As biologically synthesized macromolecules, exopolysaccharides (EPSs) are loosely attached to the bacterial cell wall or dispersed into their surroundings during the growth phase of microorganisms (Bai et al., 2021; Buksa et al., 2021). Depending on the diversity of monosaccharide subunits and their biosynthesis pathways, EPSs are classified into two types: homopolysaccharides, which contain repeats of one type of monosaccharide, and heteropolysaccharides, which contain two or more monosaccharides. As representatives of multifunctional natural polymers, EPSs possess an evident advantage over polysaccharides produced by animal and plant cells because they do not rely on external environmental conditions (e.g., season or geography). Among EPS-producing bacteria, lactic acid bacteria (LAB) stand out because of their status as generally recognized as safe (GRAS), and EPSs produced by LAB (LAB-EPSs) are considered as safe agents (Rajoka et al., 2020). In previous literature, a substantial number of EPS-producing LAB have been isolated from traditional Chinese fermented foods. Prominent examples are *Enterococcus* sp. F2, which has been isolated from fermented soy beans (Jiang et al., 2021), *Lactobacillus plantarum* HY, which has been isolated from pickle (Liu et al., 2019), and *Lactobacillus plantarum* YW11, which has been isolated from kefir (Wang et al., 2015). In addition to the isolation of EPS-producing LAB, studies have also clarified the potential bioactivities of LAB-EPSs, such as antioxidant, anti-cancer, immunomodulatory, and cholesterol-lowering activities (Saadat et al., 2019). Because of the unique health benefits and physicochemical properties, LAB-EPSs have been widely used in several fields, e.g., in the food additive and active edible packaging industry, and for adsorption treatment of heavy metal from wastewater. Recently, finding and characterizing novel EPSs with bioactivities and improved functional properties has drawn increasing interest, and EPSs from LAB are a particular focus. Structural characterizations, physiological activities, and functional properties of EPS secreted by *Pediococcus pentosaceus* have been rarely reported. Ayyash et al. (2020a) found that EPS isolated from *P. pentosaceus* M41 exhibited noteworthy antitumor, antioxidant, antidiabetic, and antibacterial activities. Bai et al. (2021) reported that EPS secreted by *P. acidilactici* MT41-11 could be a potential antioxidant agent, and a prebiotic substance added to food. *P. pentosaceus* is a Gram-positive, facultatively anaerobic, non-motile, and non-spore-forming species, that is crucial in the fermentation of Chinese cereal vinegar (Gong et al., 2021). To date, *P. pentosaceus* has not been isolated from Chinese cereal vinegar and its EPS-producing properties has not been characterized.

Due to the film-forming ability, EPSs can be applied as protective coatings in some foods. Moreover, EPSs own some healthy benefits and thus are distributed as bio-functional agents in the food and pharmaceutical industry. In addition, it has been found that these polysaccharide-based coatings can effectively preserve fruits due to their antioxidant activity (Guerreiro et al., 2015). For instance, Gol et al. (2015) found that polysaccharide-based coatings positively influenced soluble solid content and pH of Jamun fruit, and significant delayed the weight loss. Yuan et al. (2020) reported that EPSs from *Pythium arrhenomanes* as

a polysaccharide-based coating could be helpful prolonging the shelf-life of strawberries. Strawberry is one of the most fragile and perishable fruits, vulnerable to mechanical damage, physiological degradation, water loss and fungal decay, which makes the preservation of strawberries problematic (Matar et al., 2018).

In the present work, a new type of EPS-producing strain, *P. pentosaceus* E8, was screened from cereal vinegar. The chemical structure of the EPS produced by *P. pentosaceus* E8 was characterized by a series of analytical methods: ultraviolet-visible spectroscopy (UV-vis), high-performance liquid chromatography (HPLC), Fourier transform-infrared spectroscopy (FT-IR), nuclear magnetic resonance spectroscopy (NMR), thermogram analysis (TGA), differential scanning calorimeter (DSC), and scanning electron microscopy (SEM). Furthermore, the bioactive and emulsifying properties of the novel EPS from *P. pentosaceus* E8 have been assessed. Additionally, we explored the potential of this EPS to be utilized as a coating in the strawberry preservation.

MATERIALS AND METHODS

Screening of Strains and 16S rDNA Sequencing

Cereal vinegar samples (provided by Qianhe Food Co., Ltd., Meishan, China) were uniformly dispersed and then continuously diluted in sterile deionized water. Treated samples were cultured on de Man, Rogosa, and Sharpe (MRS) medium and incubated at 30°C to obtain a single colony. Colonies were picked and bacterial species were identified based on morphology and physiological characteristics coupled with 16S rDNA sequencing. Universal primers pairs 27F (5'-AGAGTTTGATCCTGGCTCAG-3') and 1492R (5'-GGTTACCTTGTTACGACTT-3') were obtained from Tsingke Biological Technology (Sichuan, China) and were used for PCR and sequencing. The phylogenetic tree was established using the neighbor-joining method by MEGA 7.0. The *P. pentosaceus* strain with the highest EPS yield of 1.37 ± 0.81 g/L was named E8 and used for the further production and characterization of EPSs.

Isolation and Purification of Exopolysaccharides

Pediococcus pentosaceus E8 was inoculated into MRS containing 4% sucrose and incubated for 48 h; then, crude EPS was isolated according to a previously reported method (Ayyash et al., 2020a). In short, the cell-free supernatant was first collected by centrifugation (10,000 × *g*, 15 min, 4 °C) after fermentation. Then, three volumes of pre-chilled 95% (v/v) ethanol were added, and the mixture was incubated overnight at 4°C to precipitate crude EPSs. After that, the precipitate was dissolved in ultrapure water as crude EPS. To remove proteins, crude EPSs were treated with papain (800 U/mL, pH 6.0) combined with Sevage reagent (chloroform/*n*-butanol at 4:1, v/v) (Gan et al., 2020a). Before chromatographic analysis, a dialysis bag (cut-off 14 kDa, Yibo Biological Technology Co., Ltd., Hunan, China) was used to dialyze the treated crude EPSs against distilled-deionized water for 3 days and the dialyzed sample was then lyophilized. The lyophilized EPSs sample was redissolved and sequentially separated by a DEAE-52 anion-exchange chromatographic column (2.6 × 20 cm; GE Healthcare, Gothenburg, Sweden) with different concentrations NaCl solution (0, 0.1, 0.3, and 0.5 M) at a flow rate of 2 mL/min. Then, the mixture was eluted with ultrapure water (1 mL/min) via Sephadex S-300 HR chromatography (1.6 × 100 cm; GE Healthcare, Gothenburg, Sweden). Finally, the major fraction of crude EPSs obtained from *P. pentosaceus* E8, designated EPS-E8, was combined and lyophilized for further analysis of structure and bio-functional activities.

Chemical Composition Assays

The total sugar and protein contents were measured by using the phenol-sulfuric acid colorimetric (Bradford, 1976) and Bradford methods (DuBois et al., 2002), respectively. The UV spectrum of the EPS-E8 solution (1 mg/mL) was measured via a U-3900H spectrophotometer (Hitachi, Japan) by scanning from 200 to 800 nm to test for the presence of protein or nucleic acids.

Molecular Weight and Monosaccharide Composition Analysis

To determine the homogeneity and average molecular weight of EPS-E8, high-performance size-exclusion chromatography (HPSEC) and multi-angle laser light scattering (MALLS) spectrometry (DAWN HELEOS II, Wyatt Technology, CA, United States) were used, respectively. Ten milligrams of EPS-E8 sample were dissolved in 0.1 mol/L $NaNO_3$ solution (1 mL) and filtered through a 0.22-μm filter (Xinya Purification Equipment Co., Ltd., Shanghai, China). After that, the EPS-E8 solution (10 mg/mL, 100 μL) was loaded onto separation system with different columns (Shodex Ohpak SB-805, 804, and 803, Shodex, Tokyo, Japan). Separation conditions were: 0.1 mol/L $NaNO_3$ solution as mobile phase, 0.4 mL/min, 60 °C. The data were acquired by ASTRA6.1 software (Wyatt Technology, CA, United States). Monosaccharide analysis of EPS-E8 was conducted by high-performance anion-exchange chromatography with pulsed amperometric detection (HPAEC-PAD). Before measurement, 5 mg of EPS-E8 were mixed with 1 mL of trifluoroacetic acid (TFA, 2.0 M) in a sealed glass ampoule and heated at 121 °C for 2 h, then dried by nitrogen blowing. The residue after drying was redissolved in deionized water and filtered through a 0.22-μm film. The EPS-E8 hydrolysate and standards (including fucose, rhamnose, arabinose, galactose, glucose, xylose, mannose, fructose, ribose, galacturonic acid, glucuronic acid, mannuronic acid, and guluronic acid) were further analyzed using a Dionex ICS-5000 ion chromatography system (Thermo Scientific, MA, United States) equipped with a Dionex CarboPac PA-20 analytical column and a Dionex ED50A electrochemical detector.

Methylation Analysis of EPS-E8

Methylation analysis was performed according to a previously described method (Gan et al., 2020a). Briefly, 5 mL DMSO

and 10 mg NaOH were used to dissolve the freeze-dried EPS-E8 (10 mg); then, 0.5 mL methyl iodide was added for the reaction. The obtained product was separated with CH_2Cl_2, washed 3–5 times, and dried by nitrogen blowing. The complete methylation product was further hydrolyzed by 2.0 M TFA at 121°C for 2 h, and then reduced with sodium borodeuteride and acetylated with acetic anhydride (1:1, v/v) at 100°C for 2.5 h. The obtained partially methylated alditol acetates were analyzed using a gas chromatography-mass spectrometer (GC-MS; 6890A-5975C, Agilent Technologies, Palo Alto, United States) equipped with an HP-5MS capillary column.

Spectroscopic Analysis by Fourier Transform-Infrared Spectroscopy and Nuclear Magnetic Resonance Spectroscopy

The main functional groups of EPS-E8 were analyzed on a Nicolet iS1S0 infrared spectrometer (Thermo Nicolet Inc., WI, United States) at a frequency range of 500–4000 cm^{-1} (Jiang et al., 2020). A total of 40 mg of dry EPS-E8 sample was exchanged with deuterium by lyophilizing against deuterium oxide (D_2O) twice and dissolved in D_2O (99.9% D) before NMR analysis. 1D NMR (1H- and 13C NMR) and 2D NMR (COSY, TOCSY, NOESY, HSQC, and HMBC) were recorded on a Bruker 600 MHZ spectrometer (Bruker, Karlsruhe, Switzerland).

Thermal Properties and X-ray Diffraction

The thermal properties were assessed by TGA, differential thermal analysis (DTG), and DSC (NETZSCH, Free State of Bavaria, Germany). TGA and DTG were recorded from a temperature of 35 to 800 °C. X-ray diffraction (XRD) data of EPS was obtained on a D8 advance X-ray diffractometer (Bruker, Karlsruhe, Switzerland), under running conditions of 40 mA, 40 kV, an angular range of 5° and 80°, and a steep of 0.02°/min.

Zeta Potential, Particle Size, Scanning Electron Microscopy, and Atomic Force Microscopy Examination

A ZEN5600 Zetasizer NanoPlus (Malvern Instruments, Malvern, United Kingdom) was used to examine the corresponding properties of EPS-E8 (1–5% w/v) at 25°C. The microscopic morphology of EPS-E8 was characterized via SEM (Apreo 2C, Thermo Scientific, MA, United States) at an accelerating voltage of 15 kV. The molecular morphology of EPS-E8 was identified using atomic force microscopy (AFM; SPM-9600, Shimadzu, Japan).

Emulsifying Properties of EPS-E8

The emulsifying property of the EPS-E8 sample was assessed according to a previously reported method (Maalej et al., 2016). A total of 6 mL of various edible oils (olive oil, coconut oil, peanut oil, sunflower oil, soybean oil, palm oil, rap oil, and soybean oil) and hydrocarbons (*n*-hexane and *n*-octane) were mixed with the EPS-E8 sample solution (1 mg/mL, 4 mL) and stirred for 5 min. Various emulsifying activities (EA, %), namely EA 1, EA 24, and EA 168, were recorded after 1, 24, and 168 h, respectively. Then, olive oil was utilized as testing oil to assess the influence of the EPS-E8 concentration on its emulsifying activity. The emulsions obtained with olive oil were investigated with different EPS-E8 concentrations (0–2%) for evaluating EA 1, EA 24, and EA 168. Moreover, the effects of temperature (25–100°C), pH (4.0–12.0), and ionic strength (0–2.0 M NaCl) on emulsion stability were also evaluated. EA was calculated as follows:

EA (%) = (emulsion layer height / mixture overall height) × 100

Analysis of Antioxidant Property

1,1-Diphenyl-2-picrylhydrazyl Radical Scavenging Ability

The 1,1-Diphenyl-2-picrylhydrazyl (DPPH) radical scavenging ability of EPS-E8 was assessed according to a previously published method (Teng et al., 2021). Vitamin C (VC) was used as positive control. The DPPH radical scavenging activity was calculated according to the following formula:

$$\text{Scavenging activity (\%)} = 1 - [(\text{absorbance of sample mixed with DPPH solution} - \text{absorbance of sample})/\text{absorbance of DPPH solution}] \times 100$$

$ABTS^+$ Free Radical Scavenging Ability

The ABTS radical scavenging activity of EPS-E8 was determined using a previously reported method (Gu et al., 2020). The absorbance of sample and control at 734 nm were recorded and then calculated using the formula:

$$\text{Scavenging capacity (\%)} = 1 - (\text{absorbance of sample}/\text{absorbance of control}) \times 100$$

Hydroxyl Free Radical Scavenging Ability

The hydroxyl radical scavenging activity of EPS was determined based on a previously reported method (Gu et al., 2020). The absorbance of the resulting mixture was measured at 510 nm. The scavenging capacity was calculated as follows:

Scavenging capacity (%) = 1 – [(absorbance of sample – absorbance of reagent blank)/absorbance of control] × 100

Application of Exopolysaccharide (EPS) From *Pediococcus pentosaceus* E8 in Strawberry Preservation

Treatment of Fruit

Fresh strawberries exhibiting analogous size, shape, and ripeness and without visual defects were purchased from the local market (Chengdu, Sichuan, China). All strawberries were divided into two groups: group A was dipped in 8% EPS-E8 solution for 5 min, air-dried, and then incubated at 20 ± 1°C for 7 days; group B was used as control, strawberries were dipped in ultrapure water and manipulated in the same way as group A. The preservation indexes were analyzed every 24 h for each group.

Determination of Weight Loss Ratio and Soluble Solids Content

The weight of strawberries was weighed every day via the method described by Yan et al. (2020). The weight loss of strawberries was monitored using an analytical balance by weight determination on each day to calculate the weight loss ratio by the following:

$$\text{weight loss rate (\%)} = [(\text{the initial weight} - \text{the sample weight after storage time})/\text{the initial weight}] \times 100$$

A PAL-1 digital refractometer (ATAGO Co. Ltd., Tokyo, Japan) was used to determine the soluble solid contents of strawberries.

Determination of Malondialdehyde Content

To determine the Malondialdehyde (MDA) content, a slightly modified method from Yuan et al. (2020) was applied. Briefly, strawberry sample (1 g) was thoroughly ground in 5 mL of 5% trichloroacetic acid (TCA) and centrifuged at 10,000 × *g* for 10 min at 4°C. Subsequently, the supernatant was mixed with 0.67% thiobarbituric acid (2 mL), and sequentially transferred to a water bath (100°C, 20 min) and an ice bath (0°C, 5 min). The treated mixture was finally centrifuged (10,000 × *g*, 4°C, 15 min), and supernatant was collected to measure its absorbance value at 450 nm (*A*450), 532 nm (*A*532), and 600 nm (*A*600). The MDA content was calculated according to following formula:

$$\text{MDA content} = 6.45 \times (A532 - A600) - 0.56 \times A450$$

Determination of Vitamin C Content

Vitamin C (VC) content was measured based on the method of Wu et al. (2015) with minor modifications. Briefly, 1 g of strawberry sample was ground with 5% TCA (5 mL) and then centrifuged at 10,000 × *g* (10 min, 4 °C). Afterwards, 1 mL of 5% TCA, absolute alcohol, 0.4% phosphoric acid, 0.5% 1,10-phenanthroline, and 0.03% ferric chloride were added to the supernatant. The mixture was maintained at 30 °C for 30 min, and then the absorbance value of the mixture was recorded at 510 nm. The VC content was calculated with the established standard curve:

$$Y = 0.0186X + 0.0084 (R^2 = 0.9994)$$

where X is VC content, Y is absorbance value at 510 nm.

Statistical Analyses

All measurements were carried out in triplicates, and the data are expressed as means ± standard deviations and analyzed for variance by SPSS 22.0 (IBM, Armonk, NY, United States), using ANOVA followed by Duncan's multiple-range test.

RESULTS AND DISCUSSION

Identification of Selected Strain

The EPS-producing strain, named E8, was isolated from cereal vinegar. Under the SEM, strain E8 was either found in pairs or short chains, which is the typical morphology of *Pediococcus* (**Supplementary Figure 1**). According to the 16S rDNA sequence of strain E8, a phylogenetic tree was constructed by the neighbor-joining method. The phylogenetic tree (**Figure 1A**) showed that strain E8 clustered with *P. pentosaceus* DSM 20336T (GenBank accession number: JQBF01000022). Thus, the identified strain was named *Pediococcus pentosaceus* E8. The 16S rDNA sequence of *P. pentosaceus* E8 was uploaded to the GenBank database under the accession number OK483363.

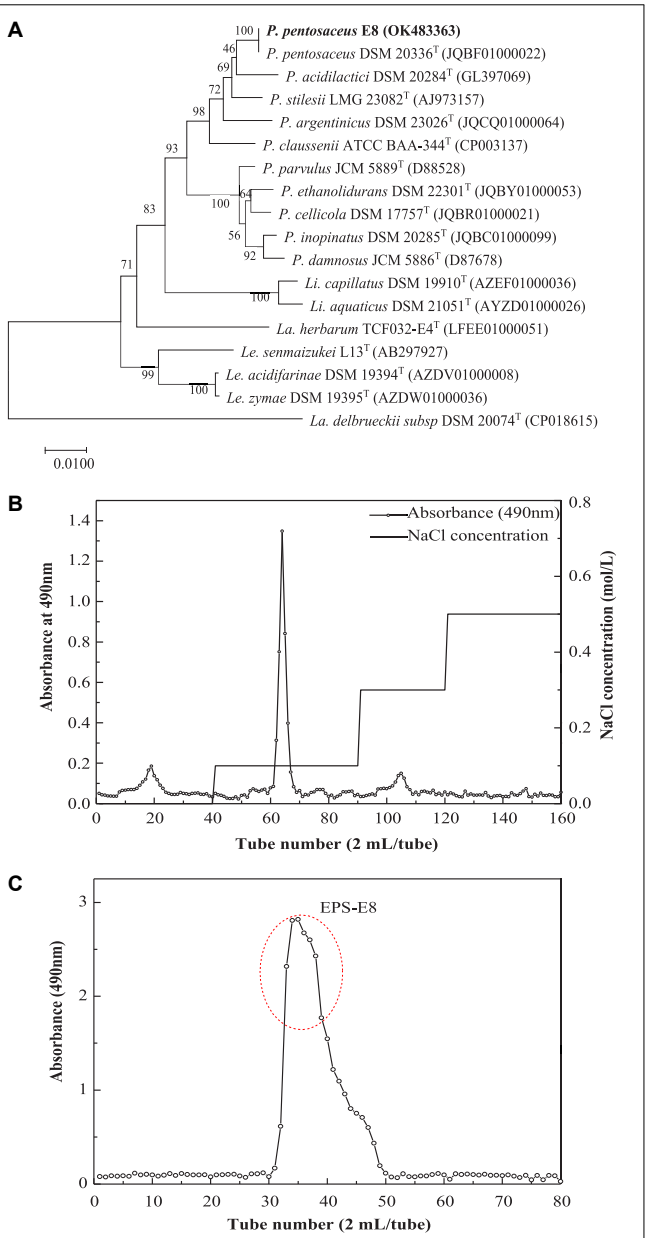

FIGURE 1 | (A) Neighbor-joining tree based on 16S rDNA sequences showing genetic relatedness between *Pediococcus pentosaceus* E8 and related species; **(B)** DEAE-52 anion-exchange chromatogram; **(C)** Sephacryl S-300 HR chromatographic profile.

TABLE 1 | The physicochemical properties of the purified EPS-E8.

Physicochemical properties	
Total carbohydrate	97.9 ± 1.8%
Protein	Nd*
Sulfates	Nd*
Relevant molecular parameters of the purified EPS-E8	
Mw (Da)	5.02×10^4
Monosaccharide composition/relative content (%)	
Mannose	80.39
Glucose	18.12
Galactose	1.49

**Nd, not detected.*

Exopolysaccharide Production and Purification

The crude EPSs of *P. pentosaceus* E8 were harvested via fermentation, ethanol precipitation, deproteinization, and dialysis. Crude EPSs were first purified by a DEAE-52 anion exchange chromatography column, and one major peak and two minor peaks were observed (**Figure 1B**). Next, the fractions from the major peak were collected and further separated using a Sephadex S-300 HR gel-filtration column. As shown in **Figure 1C**, a single peak was obtained, named EPS-E8. Finally, the fractions of EPS-E8 were collected and lyophilized to represent the purified polysaccharide. As tabulated in **Table 1**, the total sugar concentration of EPS-E8 was 97.9 ± 1.8%, whereas proteins and sulfates were not found in EPS-E8. The total sugar concentration of EPS-E8 was significantly higher than that of EPS obtained from *L. helveticus* LZ-R-5 (94.35 ± 1.03%) (You et al., 2020) and *L. plantarum* RS20D (84.21%) (Zhu et al., 2019). Moreover, the UV-vis spectrum of EPS-E8 showed no apparent peaks at 280 or 260 nm, further confirming that proteins and nucleic acids had been fully removed (**Figure 2A**).

Molecular Weight and Monosaccharide Composition

Multi-angle laser light scattering and refractive index detection were conducted to determine the molecular weight of EPS-E8 using HPSEC-MALLS-RI (**Table 1**). The molecular weight (Mw) of EPS-E8 is 5.02×10^4 g/mol, which is in line with the molecular weight range of LAB exopolysaccharides (10^4–10^6 g/mol) (Lynch et al., 2018). However, the Mw of EPS-E8 is lower than the Mw of EPS produced by *P. pentosaceus* M41 (6.82×10^5 g/mol) (Ayyash et al., 2020a) and *L. plantarum* C70 (3.8×10^5 g/mol) (Ayyash et al., 2020b), and higher than the Mw of EPS from *Bacillus* sp. S-1 (1.76×10^4 g/mol) (Hu et al., 2019). These differences in Mw may be the result of inter-species and inter-strain variations. Generally, better water solubility and expanded chain conformation are observed in polysaccharides with low molecular weight, resulting in better bioactivities. The monosaccharide composition of EPS-E8 was authenticated using HPAEC-PAD technique. As illustrated in **Figure 2B** and **Table 1**, EPS-E8 mainly consists of mannose, glucose, and galactose at a molar ratio of 80.39: 18.12: 1.49. Interestingly, uronic acid was not detected in EPS-E8. In addition, mannose and glucose were predominant sugar ingredients in EPS-E8, accounting for 98.5% of all monosaccharides. According to the monosaccharide

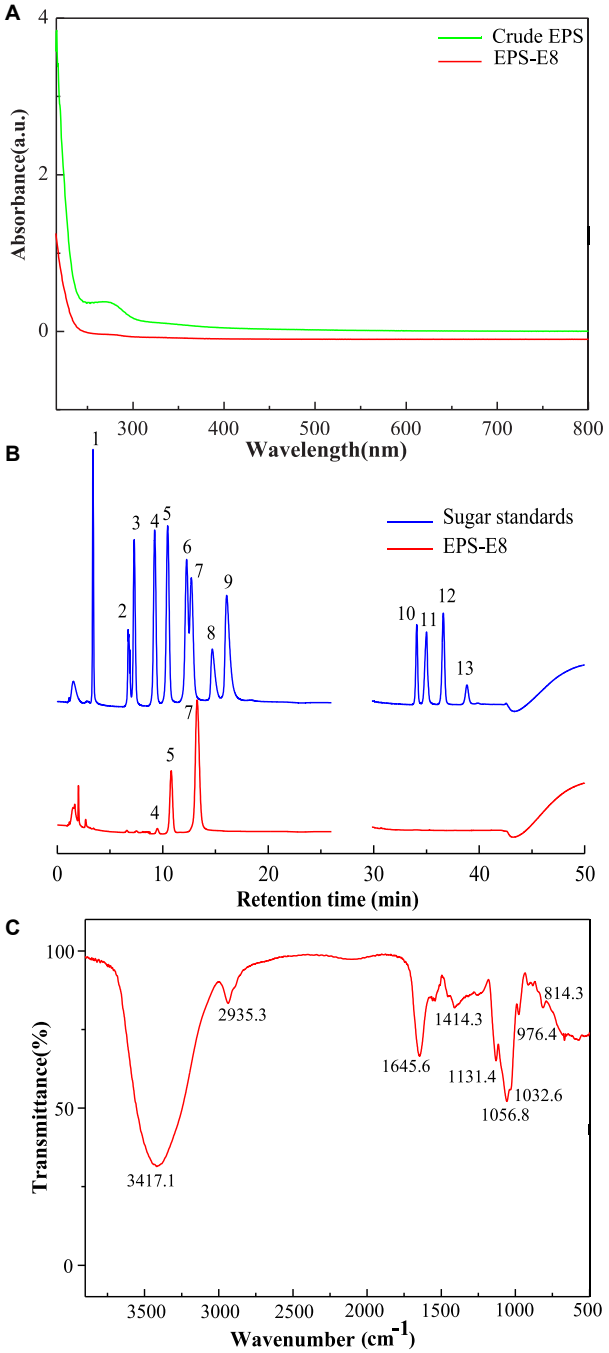

FIGURE 2 | (A) UV–vis absorption spectrum of the purified EPS-E8 sample; **(B)** HPAEC-PAD profiles of monosaccharide standards (blue curve, peak identities:1, fucose; 2, rhamnose; 3, arabinose; 4, galactose; 5, glucose; 6, xylose; 7, mannose; 8, fructose; 9, ribose; 10, galacturonic acid; 11, guluronic acid; 12, glucuronic acid; 13, mannuronic acid) and EPS-E8 (red curve); **(C)** FTIR spectrum of EPS-E8 sample.

composition of EPS-E8, it can be concluded that it was a neutral heteropolysaccharide. The monosaccharide composition of EPS-E8 differed from *P. pentosaceus* M41 (arabinose, mannose, glucose, and galactose) (Ayyash et al., 2020a) and *P. pentosaceus* DPS (glucose, mannose, and fructose) (Abid et al., 2018). These differences may be ascribed to the influence of strains, media ingredients, and environmental conditions.

Functional Groups and Glycosidic Linkages

FT-IR spectroscopy was used to analyze the main functional groups and chemical bonds of EPS-E8, the results of which are shown in **Figure 2C**. The strong and broad peak at 3417.1 cm^{-1} corresponds to the hydroxyl (OH) stretching vibration. The absorption band that appeared at 2935.3 cm^{-1} was assigned to the C–H stretching vibration of alkane, while the peak at 1645.6 cm^{-1} was probably caused by polymer-bound water. Peaks were found at 1131.4, 1056.8, and 1032.6 cm^{-1}, which could be attributed to C–O–C glycosidic bond vibrations and ring vibrations overlapping stretching vibrations of the group C–O–H, indicating a pyranose form of polysaccharides (Ding et al., 2012). Additionally, the α-glycosidic peak was reflected by the characteristic signal at 976.4 cm^{-1}, and the α-type configuration of the mannose units was reflected by the peak near 814.3 cm^{-1}.

To better capture the linkage patterns of EPS-E8, it was methylated and subjected to GC-MS. EPS-E8 contained at least 10 discernible methylated glycosidic residues (**Table 2**), namely 2,3,4,6-Me_4-Man*p*, 2,4,6-Me_3-Man*p*, 3,4,6-Me_3-Man*p*, 2,3,4-Me_3-Man*p*, 2,3,4-Me_3-Glc*p*, 2,3,6-Me_3-Glc*p*, 2,6-Me_2-Man*p*, 2,4-Me_2-Man*p*, 3,4-Me_2-Man*p*, and 3,4-Me_2-Man*p* at molar percentages of 35.53, 12.55, 20.83, 1.92, 0.96, 8.13, 0.31, 1.03, 7.49, and 11.25%, respectively. The total contents of mannose and glucose derivatives were about 79.66 and 20.34%, respectively, which is in accordance with the results of monosaccharide composition. Moreover, negative signals on linkages related to other monosaccharides (fucose, xylose, and arabinose) were obtained in this sample because of trace amounts of these monomers. Therefore, these available data confirmed that four types of corresponding glycosidic linkages, i.e., T-Man*p*-(1→ (35.53%), →3)-Man*p*-(1→ (12.55%), →2)-Man*p*-(1→ (20.83%), and →2,6)-Glc*p*-(1→ (11.24%)) were included in EPS-E8.

TABLE 2 | Glycosidic linkage composition of methylated EPS-E8 by GC–MS analysis.

Time (min)	Methylated sugars	Deduced linkages	Molar ratios
8.85	2,3,4,6-Me_4-Man*p*	T-Man*p*-(1→	35.53
12.33	2,4,6-Me_3-Man*p*	→3)-Man*p*-(1→	12.55
12.41	3,4,6-Me_3-Man*p*	→2)-Man*p*-(1→	20.83
13.63	2,3,4-Me_3-Man*p*	→6)-Man*p*-(1→	1.92
13.72	2,3,4-Me_3-Glc*p*	→6)-Glc*p*-(1→	0.96
14.07	2,3,6-Me_3-Glc*p*	→4)-Glc*p*-(1→	8.13
15.24	2,6-Me_2-Man*p*	→3,4)-Man*p*-(1→	0.31
17.93	2,4-Me_2-Man*p*	→3,6)-Man*p*-(1→	1.03
18.25	3,4-Me_2-Man*p*	→2,6)-Man*p*-(1→	7.50
18.25	3,4-Me_2-Glc*p*	→2,6)-Glc*p*-(1→	11.24

Nuclear Magnetic Resonance Spectroscopy Analysis

1D and 2D NMR spectra were used to elucidate the structural characteristics of EPS-E8. The aim was to provide information about the linkages between various monosaccharide types. In ^{1}H NMR (**Figure 3A**) and ^{13}C NMR spectra (**Figure 3B**), clusters of proton (H-1) and carbon (C-1) resonances was found around the region between δ 4.55–5.48 ppm and δ 99.46–104.46 ppm, respectively. The chemical shifts within δ 3.35–4.30 ppm and δ 61.04–81.25 ppm were assigned to H-2 to H-6 and C-2 to C-6 protons, respectively. EPS-E8 had 10 obvious anomeric proton signals at δ 5.42, 5.32, 5.19, 5.17, 5.15, 5.12, 5.07, 5.05, 4.93, and 4.56 ppm, labeled A–J, respectively. The remaining proton signals were corroborated by COSY and TOCSY (**Supplementary Figures 2A,D**), and the HSQC spectrum supported the carbon signals related to specific hydrogen signals (**Supplementary Figure 2B**).

In the HSQC spectrum, the chemical shift signal of anomeric residue B at δ 5.32 ppm and its correlating signal at δ 102.13 ppm were found, showing the α-configuration nature of residue B. Combined with the TOCSY spectral data, connected signals at δ 5.32/4.15, 4.15/4.01, 4.01/3.80, 3.80/3.94, and 3.94/3.79 (3.65) ppm of residue B were captured from the COSY spectrum. According to these signals, signals at δ 4.15, 4.01, 3.80, 3.94, and 3.79 (3.65) ppm were attributed to H-2 to H-6 of residue B, respectively. In combination with the HSQC spectrum, the corresponding carbon chemical shifts of C-2 to C-6 were δ 102.13, 79.37, 71.49, 67.98, 74.70, and 62.32 ppm, respectively. Notably, in comparison to previous data on mannose units, the C-2 carbon signal of 79.37 ppm shifted downward, indicating a substitution of residue B at the C-2 position. Based on these analyses, residue B was identified as →2)-α-D-Man*p*-(1→ (Wold et al., 2018; Bai et al., 2021).

Regarding the E residue, the anomeric proton chemical signal was observed at δ 5.15 ppm and its anomeric carbon at δ 99.77 ppm by HSQC spectrum. This demonstrates that residue E is an α-configuration. According to TOCSY and COSY spectra, associated signals were observed at δ 5.15/4.09, 4.09/3.79, 3.79/3.69, 3.69/3.82, and 3.82/3.92 (3.70) ppm, which was observed in the HSQC spectrum. The relative downward shifts of C-2 (δ 80.29 ppm) and C-6 carbon signals (δ 68.26 ppm) compared with published research implied that residue E was replaced at the C-2 and C-6 positions (Wang et al., 2021; Zhang et al., 2022). Therefore, residue E represented →2,6)-α-D-Man*p*-(1→. Moreover, linkages for other residues were verified using a similar approach, and the main chemical shifts of proton and carbon are listed in **Table 3**.

HMBC and NOESY spectra (**Supplementary Figures 2C,E**) were further employed to evaluate the correlations of these residuals and reflect the linkage positions among sugar residues. Cross-signals at δ 79.37/5.17 ppm (B C-2/D H-1), δ 71.84/5.32 ppm (E C-3/B H-1), δ 74.90/5.17 ppm (E C-5/D H-1), and δ 74.78/5.32 ppm (F C-5/B H-1) were observed in the

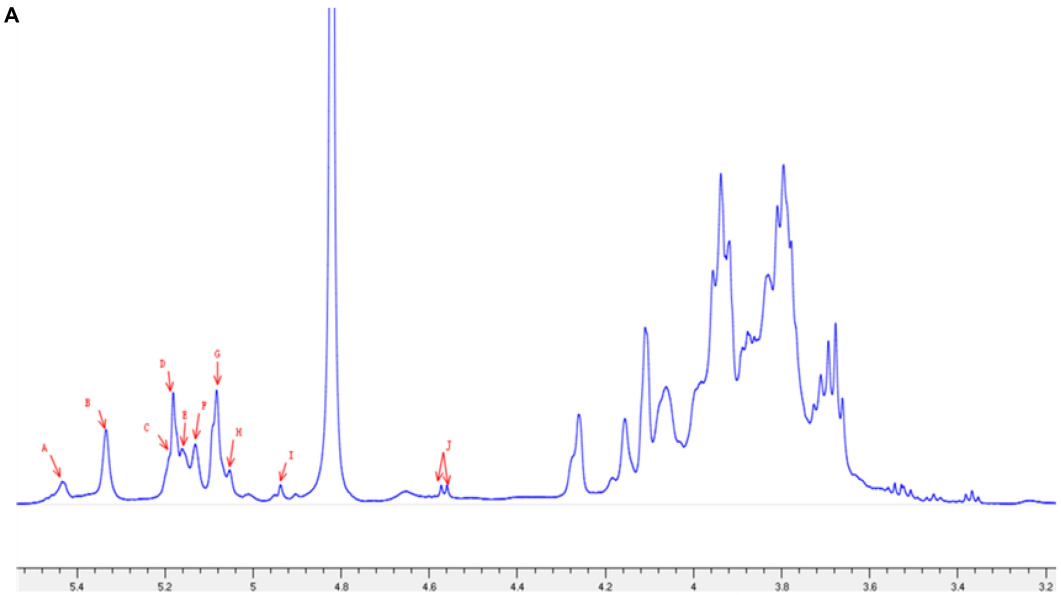

C

α-D-Man*p*-1 →[2)-α-D-Man*p*-(1→2)-α-D-Man*p*-(1→6)-α-D-Glc*p*-(1]$_n$→2)-α-D-Man*p*-(1→6)-α-D-Man*p*-(1→ 2)-α-D-Man*p*-(1→

α-D-Man*p*-(1→6)-

→2)-α-D-Man*p*-(1→2)-

→6)-β-D-Glc*p*-(1→6)-

α-D-Man*p*-(1→3)-

α-D-Man*p*-(1→6)-

FIGURE 3 | NMR spectra of EPS-E8 recorded in D_2O at 298 K: **(A)** 1D-1H spectrum; **(B)** 1D-13C spectrum. Different signals (A–J) were defined in **Table 3**, respectively. **(C)** One putative structure of EPS-E8.

TABLE 3 | ^{1}H and ^{13}C NMR chemical shift data for EPS-E8.

Sugar residue	Chemical shifts δ (ppm)						
	H-1/C-1	H-2/C-2	H-3/C-3	H-4/C-4	H-5/C-5	H-6/C-6	H-6′/C-6
A: →4)-α-D-Glc*p*-(1→	5.42/101.27	3.66/71.63	4.06/71.84	3.60/78.22	3.79/73.99	3.84/61.96	3.69
B: →2)-α-D-Man*p*-(1→	5.32/102.13	4.15/79.37	4.01/71.49	3.80/67.98	3.94/74.70	3.79/62.32	3.65
C: α-D-Man*p*-(1→	5.19/103.71	4.11/71.41	3.93/71.56	3.70/68.48	3.80/74.64	3.95/62.61	3.69
D: α-D-Man*p*-(1→	5.17/103.78	4.12/71.63	3.87/71.70	3.68/68.26	3.85/74.92	3.94/62.53	3.71
E: →2,6)-α-D-Man*p*-(1→	5.15/99.77	4.09/80.29	3.79/71.84	3.69/68.33	3.82/74.90	3.92/68.26	3.70
F: →2,6)-α-D-Glc*p*-(1→	5.12/99.63	4.06/80.15	3.82/71.79	3.68/68.05	3.84/74.78	3.92/68.19	3.69
G: →3,6)-α-D-Man*p*-(1→	5.07/103.42	4.25/71.56	4.00/79.92	3.69/68.19	3.83/74.64	3.97/67.37	3.67
H: →6)-α-D-Man*p*-(1→	5.05/103.56	4.28/71.20	3.88/71.91	3.79/68.05	3.94/74.85	3.82/68.05	3.78
I: →2,6)-β-D-Man*p*-(1→	4.93/100.99	4.04/80.07	3.82/71.84	3.72/68.08	3.81/74.89	3.82/68.49	3.68
J: →6)-β-D-Glc*p*-(1→	4.56/104.42	3.37/74.64	3.52/77.07	3.69/68.48	3.80/74.64	3.98/67.48	3.61

HMBC spectrum. These crossing phenomena indicated that C-1 of residue B was correlated with H-6 and H-2 of residue F [B (1→2) F, →2)-α-D-Man*p*-(1→2,6)-α-D-Glc*p*-(1→], C-1 of residue D was linked to H-6 of residue F [D (1→2) E, α-D-Man*p*-(1→2,6)-α-D-Man*p*-(1→], and C-1 of residue D was linked to H-2 of residue B [D (1→2) B, α-D-Man*p*-(1→2)-α-D-Man*p*-(1→]. Furthermore, the correlation signals between H-1 of residue E (δ 5.12 ppm), H-3 of residue G (δ 4.00 ppm), H-1 of residue D (δ 5.17 ppm), H-2 of residue B (δ 4.15 ppm), H-1 of residue H (δ 5.05 ppm), H-2 of residue B (δ 4.15 ppm), H-1 of residue J (δ 4.56 ppm), and H-6 of residue E (δ 3.92) were obtained from the NOESY spectrum. These indicated the existence of →2,6)-α-D-Man*p*-(1→3,6)-α-D-Man*p*-(1→, α-D-Man*p*-(1→2)-α-D-Man*p*-(1→, →6)-α-D-Man*p*-(1→2)-α-D-Man*p*-(1→, and →6)-β-D-Glc*p*-(1→2,6)-α-D-Man*p*-(1→. Based on the data above, a putative structure of EPS-E8 is illustrated in **Figure 3C**, classifying the structure of EPS-E8 as an undocumented novel type.

X-ray Diffraction and Thermal Stability Analysis

X-ray diffraction is used to determine the crystalline degree of polysaccharides. As presented in **Figure 4A**, the strong peak at 19.25° indicated that the interiors of EPS-E8 have an amorphous or semi-crystalline structure. A similar profile was observed in other studies for different types of EPSs (Krishnamurthy et al., 2020; Zhao et al., 2021). This crystalline structural arrangement is known to directly affect physical properties (including solubility, emulsification, swelling power, or viscosity) of polysaccharide (Gan et al., 2020b).

The thermal properties of EPS-E8 were analyzed by TGA, and variations of thermal stability are presented in **Figure 4B**. The TGA curve shows two distinct mass loss stages. In the first stage, there was a mass loss of nearly 5% at 35–137.1 °C, possibly caused by the loss of polysaccharide surface-bound water molecules. The mass remained constant from 137.1 to 257 °C, suggesting that EPS-E8 is relatively stable below 257°C. The second stage of mass loss included two continuous processes within a temperature range of 257–525°C with a total mass loss of 66.1%. The first process occurred rapidly until 319°C with a mass loss of 45%, and then, the second process began at 319°C and was gradually implemented at a slow rate. The initial loss may be caused by the breakage of carbon chains and hydrogen bonds, and the slow thermal degradation may be ascribed to the production of thermally stable polysaccharides in the process. As shown in the DTG curve, the degradation temperature (Td) of EPS-E8 was 305.7°C. These results highlight the outstanding thermal stability of EPS-E8, which suggests its application potential in fields where an excessive level of thermal processing is needed.

Endothermic and exothermic processes could affect the thermal behaviors of polysaccharides associated with phase changes or deformation of the crystalline structure. As shown in **Figure 4C**, DSC was used to analyze the melting point and energy changes of EPS-E8 from 25 to 260°C. The melting point is an endothermic peak at about 82.6°C, and the enthalpy change (ΔH) needed to melt 1 g of EPS-E8 is 284.3 J. This result differs from previous reports on EPSs isolated from different LAB strains. The melting point of EPS-E8 is lower than that of EPS obtained from *P. pentosaceus* M41 (158.82°C) (Ayyash et al., 2020a) and *P. pentosaceus* DPS (232°C) (Abid et al., 2018). Ahmed et al. (2013) and Lobo et al. (2019) reported that the melting point and ΔH of EPS produced by *Streptococcus thermophilus* CRL1190 and *L. kefiranofaciens* ZW3 were about 74.08°C/284.46 J and 93.38°C/249.7 J, respectively. These findings strongly support the idea that the thermodynamics properties of EPS from various strains may be different.

Particle Size and Zeta Potential

The particle size distribution and zeta potential trend of the aqueous solution of EPS-E8 are depicted in **Figure 4D**. As the concentration of EPS-E8 increased from 1 to 5 mg/mL, the absolute value of zeta potential increased from 22.3 to 33.85 mV. This trend indicates that the initial interfacial electric charge value and stability of the EPS-E8 aqueous solution improved with increasing concentration. Moreover, the average particle diameter of EPS-E8 in aqueous dispersion increased gradually from 44.1 to 164.1 nm with increasing concentration. The particle size of EPS-E8 is smaller than that of EPS produced by *P. pentosaceus* M41 (446.8 nm) (Ayyash et al., 2020a). The particle size may be attributed to molecular weights, types of

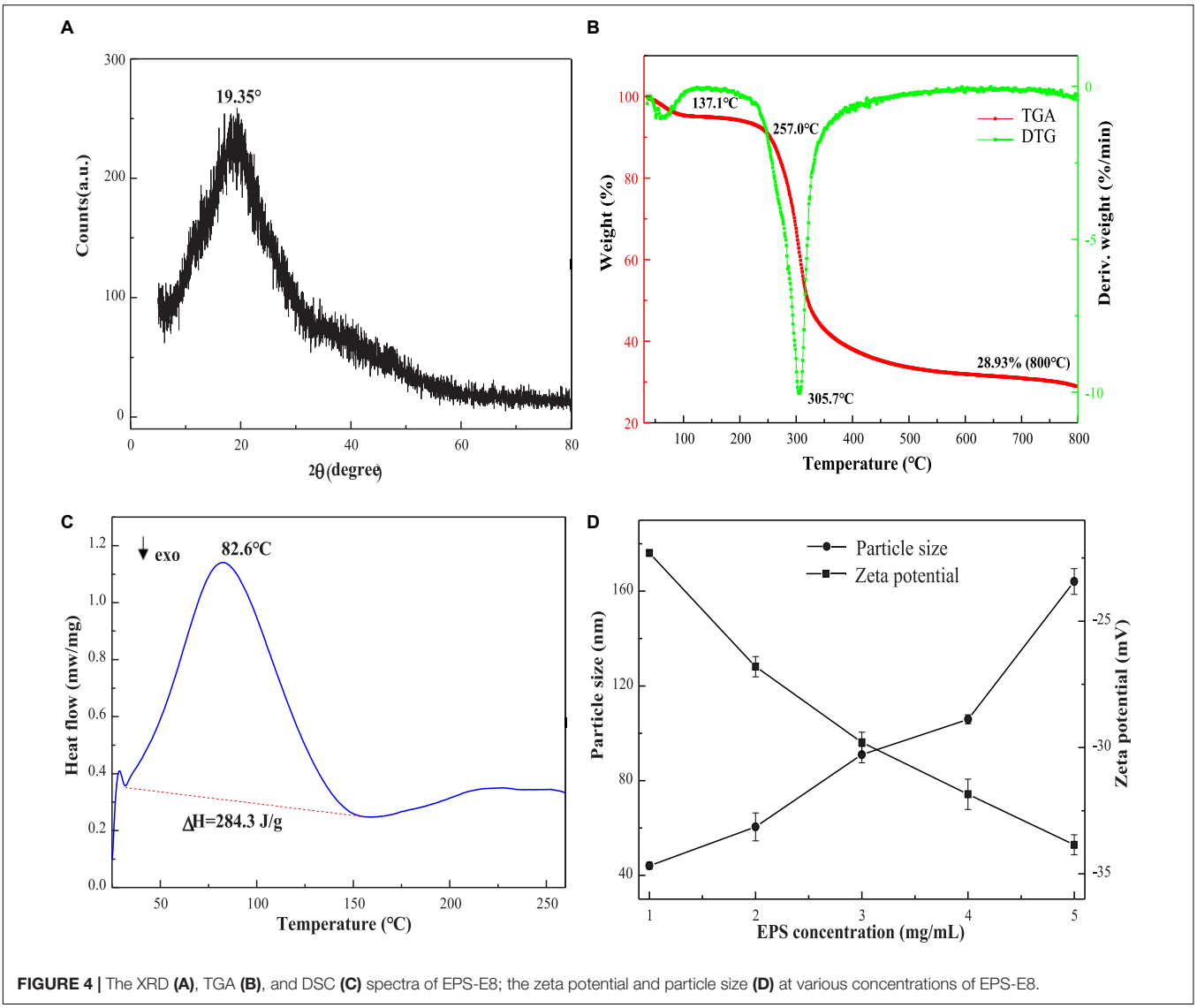

FIGURE 4 | The XRD **(A)**, TGA **(B)**, and DSC **(C)** spectra of EPS-E8; the zeta potential and particle size **(D)** at various concentrations of EPS-E8.

glycosyl linkages, and monosaccharide composition. Generally, maintaining system stability demands that negatively charged surface particles strongly interact, leading to an increase in particle diameter [30]. The regular change of zeta potential and particle size confirmed the potential application of EPS-E8 in products with high sugar contents.

Morphological Characteristics

To explore the morphological characteristics of EPS-E8, SEM and AFM were applied in this study. SEM images with different magnifications (1,000× and 5,000×) are displayed in **Figures 5A,B**, respectively. EPS-E8 has an irregular reticular-like shape and spherical-like structure with a relatively rough surface. Interestingly, the spherical structure of EPS-E8 clearly differed from that of previously reported LAB-EPSs. For instance, EPS-C47 has a stiff-like, smooth and flake-like, and layered structure (Ayyash et al., 2020c), EPS-M41 has a compact, stiff, and layer-like structure (Ayyash et al., 2020a), while the surface of EPS-1 obtained from *Pediococcus acidilactici* MT41-11 is rough, and EPS-1 is attached to irregular shapes of differently sized blocks, and shows flaky appearance (Bai et al., 2021).

Topographical AFM images of EPS-E8 are presented in **Figures 5C,D**. Large amounts of spherical clusters can clearly be observed, implying molecular aggregation of polysaccharide chains. Based on these morphological characteristics, it can be predicted that side-chain hydrogen bonds play a critical role in the aggregation of polysaccharides and considerably affect the molecule conformation, functional properties, and biological activities of EPS-E8 (Hu et al., 2020).

Emulsifying Behavior of EPS-E8

Emulsifying Activities With Different Oils and Hydrocarbons

LAB-EPSs emulsifiers have attracted great interest owing to their excellent biocompatibility and safety. In this study, the emulsifying activities of EPS-E8 (1 mg/mL) against several edible

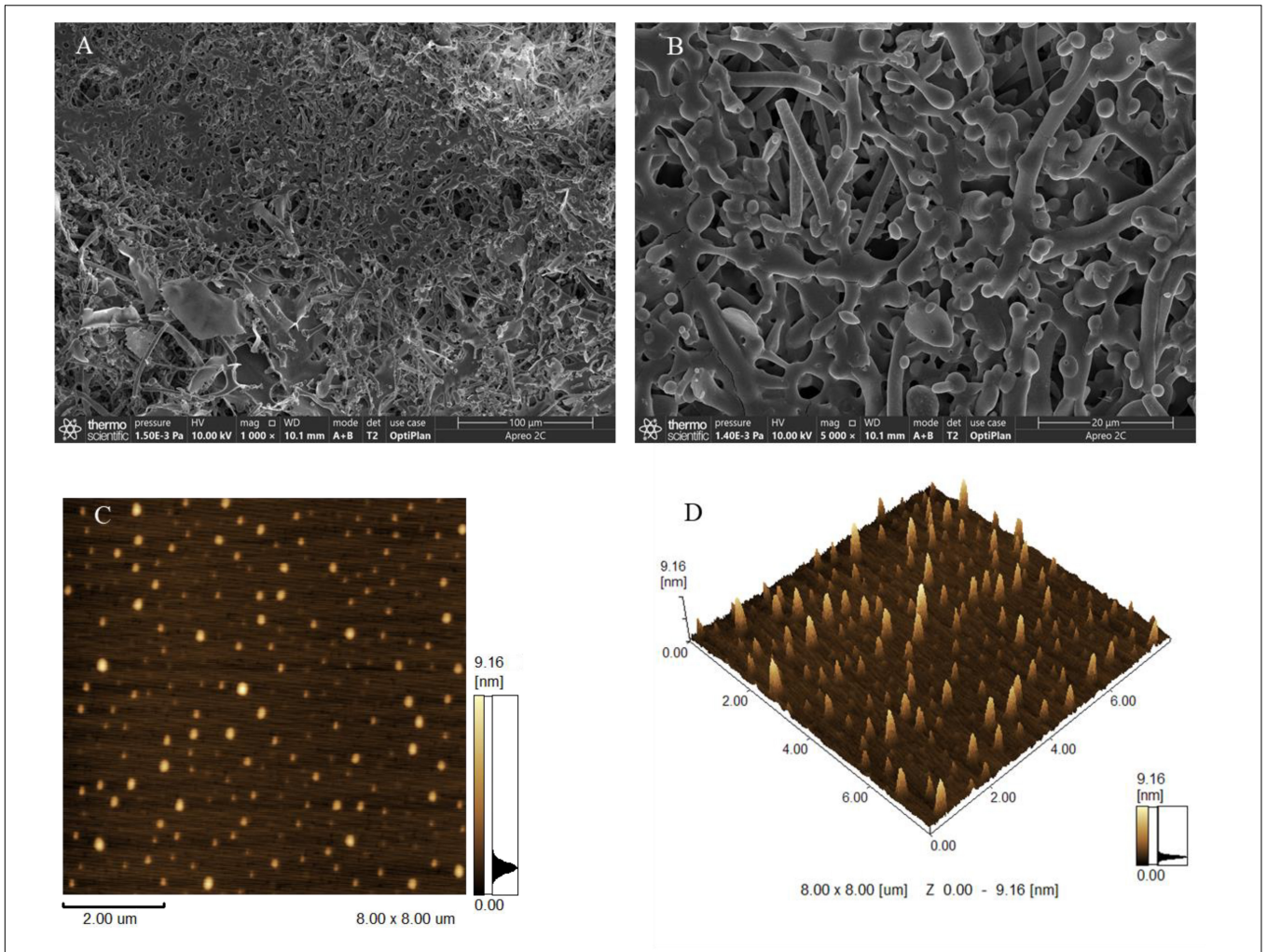

FIGURE 5 | Scanning electron microscopy images of EPS-E8 under 1,000 × **(A)** and 5,000× **(B)** magnification; AFM showing the topographic features of EPS-E8, planar view **(C)** and cubic view **(D)**.

oils and hydrocarbons were compared, and the results are shown in **Figure 6A**. EPS-E8 exhibited an excellent EA (100 ± 0.0%) against olive oil after 1 h. In addition, the EA values of EPS-E8 against palm oil (99.3 ± 1.5%), peanut oil (97.3 ± 1.1%), and soybean oil (81.3 ± 1.1%) were also high. Unlike the activities against tested edible oils, the EA of EPS-E8 against *n*-hexane and *n*-octane were lower, with values of 41.3 ± 0.7% and 28.7 ± 1.2%, respectively. An effective emulsifier should maintain at least 50% of the original emulsion volume 24 h after formation. According to this criterion, EPS-E8 displayed promising emulsion-stabilizing ability against all tested oils, as implied by the EA_{24} values, all of which remained much higher than 50%. However, the EA_{24} values of EPS-E8 against two hydrocarbons were lower than 50%. Notably, the EA values of EPS-E8 against all tested oils remained high even after 168 h with the lowest value of 50.7 ± 0.4% in rap oil. These results suggest that EPS-E8 has an excellent emulsifying ability against all tested oils, especially olive oil. Until now, the emulsification ability of the EPSs produced by *Pediococcus* species has not been reported. Compared to previously reported bacterial biopolymers, the emulsifying activity of EPS-E8 produced by *P. pentosaceus* E8 is promising. For instance, the EPS from *Virgibacillus salarius* BM02 showed the highest EA_{24} values of 58.82, 58.82, and 47.06% against sunflower oil, corn oil, and olive oil, respectively (Gomaa and Yousef, 2020). In research by Freitas et al. (2009), an EPS obtained from *Pseudomonas oleovorans* showed an EA_{24} value of 75% against olive oil, but EPS-E8 has a higher EA_{24} value of 86.7 ± 2.2% against olive oil at a similar concentration. These differences may be interpreted by the emulsion formation and stabilizing capacity of EPSs which is specific for certain hydrophobic compounds (Gomaa and Yousef, 2020).

Effect of EPS-E8 Concentration on Emulsifying Activity

To identify the probable influence of the EPS concentration on its emulsion stability against olive oil, EA values were assessed using emulsions prepared by EPS-E8 at different concentrations. Significant differences ($p < 0.05$) in the EA values were observed

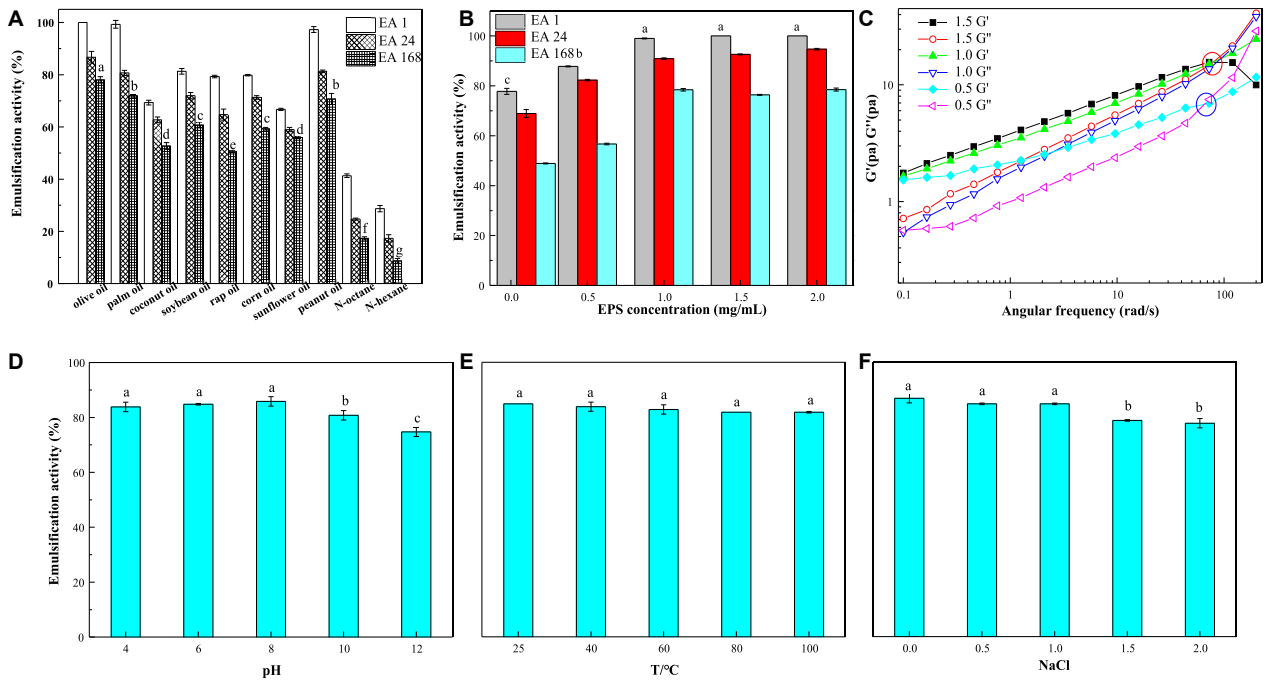

FIGURE 6 | Emulsification activity of emulsions prepared with different oils (olive oil, coconut oil, peanut oil, sunflower oil, soybean oil, palm oil, rap oil, and soybean oil) and hydrocarbons (*n*-hexane and *n*-octane) **(A)** and different EPS-E8 concentrations **(B)**; oscillatory shear tests of different emulsions **(C)**; influence of pH (4.0–12.0) **(D)**, temperature (25–100°C) **(E)**, and NaCl concentration (0–2.0 M) **(F)** on the emulsification activity of the emulsions prepared with olive oil. The statistic differences were indicated with different lowercase letters ($P < 0.05$).

for EPS-E8 when the emulsion was prepared with concentrations ranging from 0 to 1 mg/mL (**Figure 6B**). However, no significant differences ($p > 0.05$) in EA values were observed when the EPS concentration ranged from 1 to 2 mg/mL. Therefore, 1 mg/mL is the optimal concentration for EPS-E8 when it is used as emulsifier as there is no significant improvement in its emulsifying ability at higher concentrations. Similar findings were reported with EPS derived from other bacterial species. Han et al. (2015) reported that 1 mg/mL was the optimal concentration of EPS produced by *Bacillus amyloliquefaciens* LPL061 in emulsifying sunflower seed oil. In another study, 1 mg/mL of EPSs from *Bifidobacterium longum* subsp. *infantis* CCUG 52486 and *Bifidobacterium infantis* NCIMB 702205 effectively produced an emulsion with sunflower seed oil (Prasanna et al., 2012).

The stability of emulsions can be determined using small amplitude oscillatory shear tests. The results of olive oil-in-water emulsions stabilized with EPS at concentrations of 0.5, 1, and 1.5% (w/v) are shown in **Figure 6C**. The storage modulus values (G′) and loss modulus values (G″) of emulsions increased with increasing angular frequency, and G′ values exceeded G″ values at low frequencies. Thus, the emulsions showed a solid-like viscoelastic behavior. The curves of G′ and G″ had crossover points as the angular frequency increased. This phenomenon showed that emulsions are typical entangled polymer solutions. In addition, the crossover points of G′ and G″ moved rearward with increasing EPS-E8 concentration because of the polysaccharide network that formed around the dispersed phase droplet (Lopez-Ortega et al., 2020). Hence, a higher concentration of EPS in the emulsion can enhance the formation of a network structure and therefore, improve the physical stability of emulsions.

Effects of pH, Temperature, and Ionic Strength on Emulsion Stability

A challenge for most industries is to retain emulsifier activity when subjected to extreme physicochemical conditions, namely pH, temperature, and ionic strength. Therefore, the emulsion forming and stabilizing capacities of EPS-E8 were assessed for different EPS-E8 concentrations (0–2 mg/mL), temperatures (25–100 °C), pH (4–12), and NaCl concentrations (0–2 M). The results are shown in **Figure 6D**. The emulsions of EPS-E8 with olive oil were only stable in acidic and neutral conditions; however, a significant decrease in the EA was observed in alkaline conditions (pH 10 and 12). Similar stabilities have been reported for EPS produced by *Pseudomonas stutzeri* AS22 (Maalej et al., 2016). However, EPS-E8 was thermally stable and retained its emulsifying activity at temperatures of up to 100°C (**Figure 6E**). This contrasted with previously reported studies, wherein the emulsifying activity of certain natural polymers decreased at high temperatures, such as the emulsion prepared using EPS from *Virgibacillus salarius* BM02 with sunflower oil, which decreased to 47.06% at 100°C (Gomaa and Yousef, 2020). The EPS produced by haloarchaeon *Haloferax mucosum* was shown to hold good emulsifying stability with n-hexane, within a temperature range of 25–100°C (Lopez-Ortega et al., 2020). These results indicate that the emulsion

stability, at high temperatures, can be attributed to the utilized emulsifier, rather than to the employed hydrophobic compound, which may be explained by the thermal stability of EPS-E8 of up to 305.7°C (Maalej et al., 2016). Additionally, the emulsion stability was assessed under different salinities (0–2 M NaCl). EPS-E8 stabilized emulsions in combination with NaCl, showing less than 15% reduction in the initial EA_{24} values when the NaCl concentration reached up to 2 M (**Figure 6F**). According to these results, EPS-E8 might find potential applications in food, cosmetic, and detergent fields as an emulsifier.

Antioxidant Activities of Exopolysaccharide

Exopolysaccharide have been widely explored for their antioxidant capacities, and their antioxidant activity can be assessed based on various mechanisms and reactions (Jeddou et al., 2016). In this study, the *in vitro* antioxidant activity of EPS-E8 was explored by measuring its DPPH (**Figure 7A**), ABTS (**Figure 7B**), and hydroxyl radical (**Figure 7C**) scavenging activities. Within the tested EPS-E8 concentrations (0–10 mg/ml), the antioxidant capacities of EPS-E8 showed a positive correlation with its concentrations, but the antioxidant capacities of EPS-E8 were significantly lower than those of the control VC ($P < 0.05$). When the EPS concentration increased to 10 mg/mL, the scavenging activities of EPS-E8 towards DPPH, ABTS, and hydroxyl radical increased to 50.62 ± 0.5%, 52.17 ± 1.4%, and 58.91 ± 0.7%, respectively. The DPPH radical scavenging value exceeds those of EPSs produced by *L. plantarum* YW32 (30%) (Ji et al., 2015) and *L. plantarum* KX041 (37.48%) (Xu et al., 2019). These results demonstrate the good antioxidant activity of EPS-E8 and its further exploration as an antioxidant is warranted.

Effect of Exopolysaccharide on the Preservation of Strawberry

Weight Loss Ratio

The weight loss ratio of strawberry is an important parameter to reflect the respiration rate and moisture evaporation during preservation. As illustrated in **Figure 8A**, both control and EPS-E8-treated samples revealed an increased weight loss ratio along with the storage. However, the increase in the weight loss ratio of EPS-E8-treated samples was slower than that of the control samples. On the third day, the weight loss ratio of EPS-E8-treated samples reached 3.85 ± 0.3%, yet was still significantly lower than that of the control (4.80 ± 0.03%) ($p < 0.05$). The control reached the highest weight loss ratio value of 14.11 ± 0.89% on the seventh day, while samples treated with EPS-E8 showed a value of 9.56 ± 0.24% ($p < 0.05$). Xu and Wu (2021) reported that in mango fruits treated with fucoidan coating, the weight loss rates were lower than that of the control group. Therefore, our results suggest that the exploited exopolysaccharide-based coating forms a protective film to decrease respiration and transpiration rates, and thus delaying senescence while preserving quality of fruits (Guerreiro et al., 2015).

Vitamin C Content

A decline trend of VC content happens in fruit senescence, and it shows a weakened antioxidant activity of fruit. According to **Figure 8B**, the VC content of the control and EPS-E8-treated samples decreased gradually with the extension of storage period. However, the VC content of EPS-E8-treated strawberries was much higher than that of the control during storage ($p < 0.05$). The VC content of EPS-E8-treated strawberries reached its minimum value (35.37 ± 0.44 mg/100 g) on the seventh day but was still higher than that of the control group (29.71 ± 1.03 mg/100 g) ($p < 0.05$). This result suggested that EPS-E8 could effectively delay the senescence of strawberries. In a similar study, Hong et al. (2012) found that a polysaccharide-based coating effectively retarded the VC loss of guava. This could be attributed to EPS coating preventing the exchange of gasses between the inside and outside of the fruit and decelerating the oxidation of VC into dehydrogenated ascorbic acid (Mditshwa et al., 2017).

Malondialdehyde Content

Malondialdehyde is an end-product of lipid peroxidation of membranes and is considered an important indicator of the integrity and freshness of strawberry cell membranes (Saleem et al., 2021). As indicated in **Figure 8C**, the MDA content continuously increased during the storage period. However, the MDA content was significantly lower ($P < 0.05$) in EPS-E8-treated strawberries in comparison with the control group. This result was in agreement with the study conducted by Yuan et al. (2020), who reported that treatment with polysaccharides from *Pythium arrhenomanes* resulted in a lower MDA content than the control group during the storage of strawberry. The influence of EPS-E8 treatment on the MDA content of strawberries was probably caused by the deceleration of respiration and metabolism, thereby decelerating the maturation process. Thus, EPS-E8 can reduce the lipid peroxidation of cell membranes and alleviate tissue damage in fruits to some extent.

Soluble Solids

The soluble solids can mirror the maturity of fruits and represent the taste since they are mostly constituted of sugar and organic acids. The change of soluble solid content in all samples during storage is shown in **Figure 8D**. The soluble solids in the control and EPS-E8-treated strawberries reached the highest values (10.20 ± 0.10 and 9.93 ± 0.15, respectively) at the third day. This phenomenon might be caused by the original metabolic process that converts carbohydrates into sugars and other soluble compounds (Lan et al., 2019). After this period of increase, the soluble solids content decreased rapidly in the following four days, probably due to the quick consumption of soluble solids during respiration. However, the decrease in soluble solids contents of EPS-E8-treated samples was slower than that of the control samples. Thus, the utilization of EPS-E8 reduced the degradation of soluble solids and was beneficial to maintaining a better level of soluble solids. Our results are in line with Tahir et al. (2018), who determined that the lower respiration rates of fruit coated with polysaccharide-based may be ascribed to the preservation of higher carbohydrates in

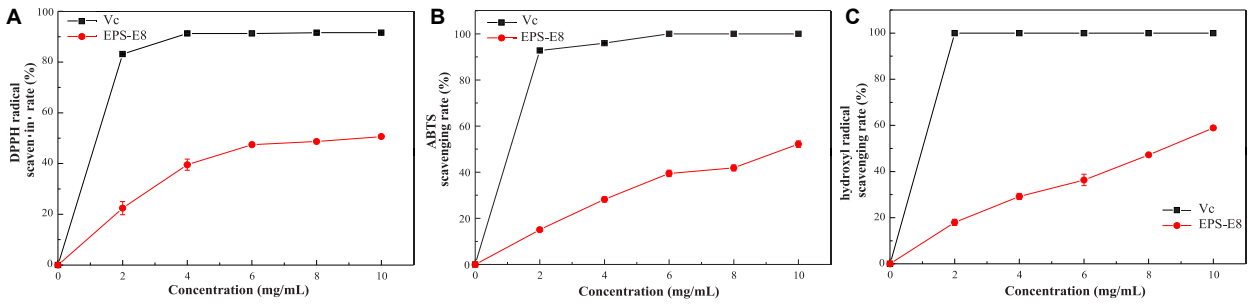

FIGURE 7 | The antioxidant activities of EPS-E8 at different concentrations using VC as a control: Scavenging activity toward DPPH **(A)**; ABTS radical **(B)**; Hydroxyl radical **(C)** of EPS-E8.

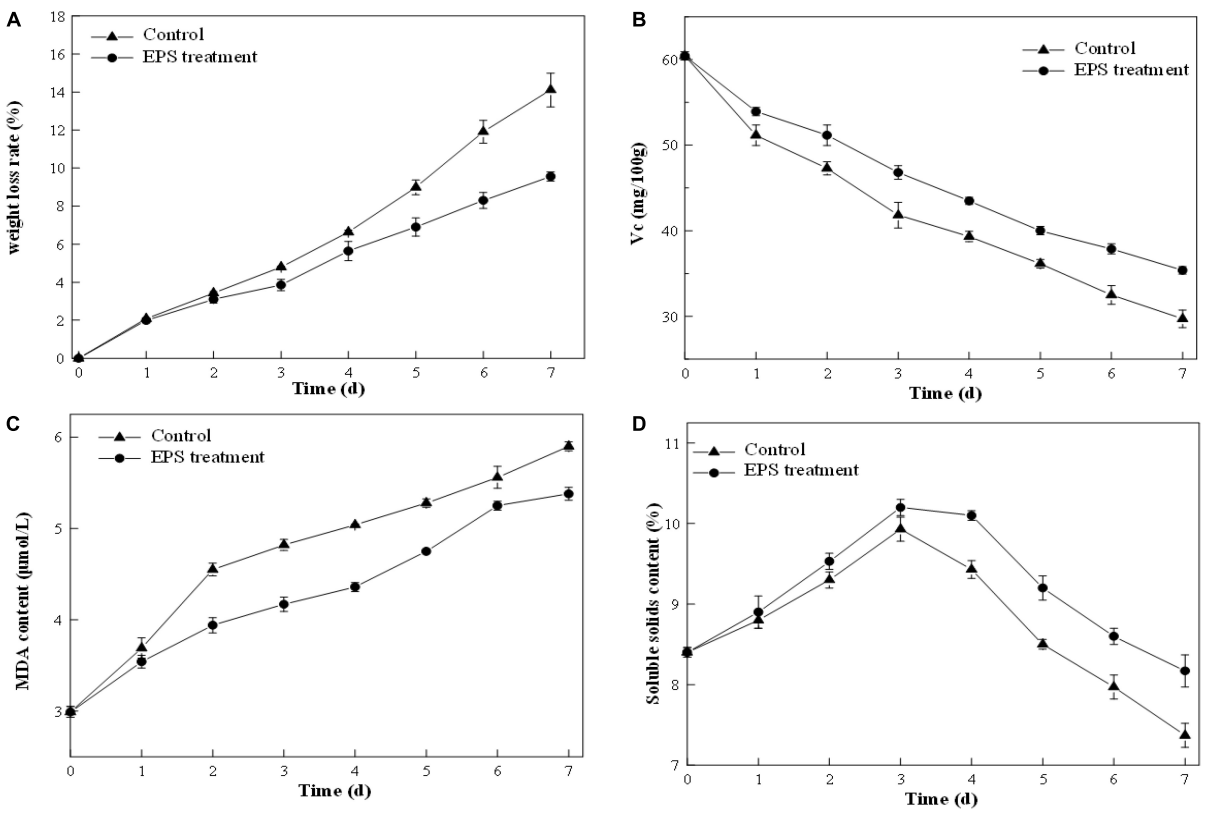

FIGURE 8 | Postharvest qualities of strawberry fruit: Weight loss ratio **(A)**, vitamin C content **(B)**, malondialdehyde content **(C)**, soluble solids content **(D)** of strawberry fruit coated with EPS-E8 and uncoated control fruit.

the fruits. Thus, it can be speculated that EPS-E8 might find application as a polysaccharide-based coating to improve the shelf-life of strawberries.

CONCLUSION

In this study, a novel EPS (EPS-E8), produced by *P. pentosaceus* E8, was isolated and characterized. EPS-E8 is a heteropolysaccharide with a molecular weight of 5.02×10^4 g/mol, possesses a main chain of →2)-α-D-Man*p*-(1→2,6)-α-D-Glc*p*-(1→6)-α-D-Man*p*-(1→, and branches with α-D-Man*p*-(1→2)-α-D-Man*p*-(1→ and α-D-Man*p*-(1→. EPS-E8 is a semicrystalline biopolymer with favorable thermal stability that has an irregular reticular-like shape when observed at magnification. The initial interfacial electric charge value and average particle diameter of EPS-E8 aqueous solution improved with increasing concentration. EPS-E8 exhibits significant antioxidant potential. In addition, EPS-E8 exhibits good emulsifying properties against various tested substrates, except for *n*-hexane and *n*-octane. The excellent stability of the emulsifying activity of the EPS-E8 at extreme physicochemical

conditions, suggests it as a promising emulsifier candidate in the food, pharmaceutical, and cosmetic industries, as well as for the biotreatment of hydrocarbon-polluted environments. In addition, when EPS-E8 was tested for its effects in strawberry preservation, the results obtained collectively revealed that EPS-E8 may be developed as a polysaccharide-based coating to extend the shelf-life of strawberry in the near future.

DATA AVAILABILITY STATEMENT

The Data presented in this study are deposition in the NCBI repository, accession number: ok483363.

AUTHOR CONTRIBUTIONS

GJ: conceptualization, investigation, and writing – original draft preparation. JH: software. LG: methodology. XL: validation and data curation. ZX and LY: formal analysis and software. RL: revision. YT: conceptualization, funding acquisition, supervision, writing – reviewing and editing, and project administration. All authors contributed to the article and approved the submitted version.

FUNDING

This work was supported by grants from the National Key Research and Development Program of China (2018YFC1802201) and the Sichuan Key Research and Development Program (2020YFS0287).

SUPPLEMENTARY MATERIAL

The Supplementary Material for this article can be found online at: https://www.frontiersin.org/articles/10.3389/fmicb.2022.923522/full#supplementary-material

REFERENCES

Abid, Y., Casillo, A., Gharsallah, H., Joulak, I., Lanzetta, R., and Corsaro, M. M. (2018). Production and structural characterization of exopolysaccharides from newly isolated probiotic lactic acid bacteria. *Int. J. Biol. Macromol.* 108, 719–728. doi: 10.1016/j.ijbiomac.2017.10.155

Ahmed, Z., Wang, Y., Anjum, N., Ahmad, A., and Khan, S. T. (2013). Characterization of exopolysaccharide produced by *Lactobacillus kefiranofaciens* ZW3 isolated from Tibet kefir – Part II. *Food Hydrocoll.* 30, 343–350. doi: 10.1016/j.foodhyd.2012.06.009

Ayyash, M., Abu-Jdayil, B., Olaimat, A., Esposito, G., Itsaranuwat, P., Osaili, T., et al. (2020a). Physicochemical, bioactive and rheological properties of an exopolysaccharide produced by a probiotic *Pediococcus pentosaceus* M41. *Carbohydr. Polym.* 229:115462. doi: 10.1016/j.carbpol.2019.115462

Ayyash, M., Abu-Jdayil, B., Itsaranuwat, P., Galiwango, E., Tamiello-Rosa, C., Abdullah, H., et al. (2020b). Characterization, bioactivities, and rheological properties of exopolysaccharide produced by novel probiotic Lactobacillus plantarum C70 isolated from camel milk. *Int. J. Biol. Macromol.* 144, 938–946. doi: 10.1016/j.ijbiomac.2019.09.171

Ayyash, M., Abu-Jdayil, B., Itsaranuwat, P., Almazrouei, N., Galiwango, E., Esposito, G., et al. (2020c). Exopolysaccharide produced by the potential probiotic *Lactococcus garvieae* C47: Structural characteristics, rheological properties, bioactivities and impact on fermented camel milk. *Food Chem.* 333:127418. doi: 10.1016/j.foodchem.2020.127418

Bai, Y., Luo, B., Zhang, Y., Li, X., Wang, Z., Shan, Y., et al. (2021). Exopolysaccharides produced by Pediococcus acidilactici MT41-11 isolated from camel milk: structural characteristics and bioactive properties. *Int. J. Biol. Macromol.* 185, 1036–1049. doi: 10.1016/j.ijbiomac.2021.06.152

Bradford, M. M. (1976). A rapid and sensitive method for the quantitation of microgramquantities of protein utilizing the principle of protein-dye binding. *Anal. Chem.* 72, 248–254. doi: 10.1006/abio.1976.9999

Buksa, K., Kowalczyk, M., and Boreczek, J. (2021). Extraction, purification and characterisation of exopolysaccharides produced by newly isolated lactic acid bacteria strains and the examination of their influence on resistant starch formation. *Food Chem.* 36:130221. doi: 10.1016/j.foodchem.2021.130221

Ding, X., Hou, Y., and Hou, W. (2012). Structure feature and antitumor activity of a novel polysaccharide isolated from *Lactarius deliciosus* gray. *Carbohydr. Polym.* 89, 397–402. doi: 10.1016/j.carbpol.2012.03.020

DuBois, M., Gilles, K. A., Hamilton, J. K., Rebers, P. A., and Smith, F. (2002). Colorimetric method for determination of sugars and related substances. *Anal. Chem.* 28, 350–356. doi: 10.1021/ac60111a017

Freitas, F., Alves, V. D., Carvalheira, M., Costa, N., Oliveira, R., and Reis, M. A. M. (2009). Emulsifying behaviour and rheological properties of the extracellular polysaccharide produced by *Pseudomonas oleovorans* grown on glycerol byproduct. *Carbohydr. Polym.* 78, 549–556. doi: 10.1016/j.carbpol.200

Gan, L., Li, X., Wang, H., Peng, B., and Tian, Y. (2020a). Structural characterization and functional evaluation of a novel exopolysaccharide from the moderate halophile *Gracilibacillus* sp. SCU50. *Int. J. Biol. Macromol.* 154, 1140–1148. doi: 10.1016/j.ijbiomac.2019.11.143

Gan, L., Li, X., Zhang, H., Zhang, R., Wang, H., Xu, Z., et al. (2020b). Preparation, characterization and functional properties of a novel exopolysaccharide produced by the halophilic strain *Halomonas saliphila* LCB169(T). *Int. J. Biol. Macromol.* 156, 372–380. doi: 10.1016/j.ijbiomac.2020.04.062

Gol, N. B., Vyas, P. B., and Rao, T. V. R. (2015). Evaluation of polysaccharide-based edible coatings for their ability to preserve the postharvest quality of indian blackberry (*Syzygium cuminiL.*). *Int. J. Fruit Sci.* 15, 198–222. doi: 10.1080/15538362.2015.1017425

Gomaa, M., and Yousef, N. (2020). Optimization of production and intrinsic viscosity of an exopolysaccharide from a high yielding *Virgibacillus salarius* BM02: study of its potential antioxidant, emulsifying properties and application in the mixotrophic cultivation of *Spirulina platensis*. *Int. J. Biol. Macromol.* 149, 552–561. doi: 10.1016/j.ijbiomac.2020.01.289

Gong, M., Zhou, Z., Liu, S., Zhu, S., Li, G., Zhong, F., et al. (2021). Formation pathways and precursors of furfural during *Zhenjiang aromatic* vinegar production. *Food Chem.* 354:129503. doi: 10.1016/j.foodchem.2021.129503

Gu, Y., Qiu, Y., Wei, X., Li, Z., Hu, Z., Gu, Y., et al. (2020). Characterization of selenium-containing polysaccharides isolated from selenium-enriched tea and its bioactivities. *Food Chem.* 316:126371. doi: 10.1016/j.foodchem.2020.126371

Guerreiro, A. C., Gago, C. M. L., Faleiro, M. L., Miguel, M. G. C., and Antunes, M. D. C. (2015). The effect of alginate-based edible coatings enriched with essential oils constituents on *Arbutus unedo* L. fresh fruit storage. *Postharvest Biol. Tec.* 100, 226–233. doi: 10.1016/j.postharvbio.2014.09.002

Han, Y., Liu, E., Liu, L., Zhang, B., Wang, Y., Gui, M., et al. (2015). Rheological, emulsifying and thermostability properties of two exopolysaccharides produced by *Bacillus amyloliquefaciens* LPL061. *Carbohydr. Polym.* 115, 230–237. doi: 10.1016/j.carbpol.2014.08.044

Hong, K., Xie, J., Zhang, L., Sun, D., and Gong, D. (2012). Effects of chitosan coating on postharvest life and quality of guava (*Psidium guajava* L.) fruit during cold storage. *Sci. Horticult.* 144, 172–178. doi: 10.1016/j.scienta

Hu, L., Liu, R., Wu, T., Sui, W., and Zhang, M. (2020). Structural properties of homogeneous polysaccharide fraction released from wheat germ by hydrothermal treatment. *Carbohydr. Polym.* 240:116238. doi: 10.1016/j.carbpol.2020.116238

Hu, X., Pang, X., Wang, P. G., and Chen, M. (2019). Isolation and characterization of an antioxidant exopolysaccharide produced by *Bacillus* sp. S-1 from Sichuan Pickles. *Carbohydr. Polym.* 204, 9–16. doi: 10.1016/j.carbpol.2018.09.069

Jeddou, K. B., Chaari, F., Maktouf, S., Nouri-Ellouz, O., Helbert, C. B., and Ghorbel, R. E. (2016). Structural, functional, and antioxidant properties of water-soluble polysaccharides from potatoes peels. *Food Chem.* 205, 97–105. doi: 10.1016/j.foodchem.2016.02.108

Ji, W., Xiao, Z., Yang, Y., Zhao, A., and Yang, Z. (2015). Characterization and bioactivities of an exopolysaccharide produced by lactobacillus plantarum YW32. *Int. J. Biol. Macromol.* 74, 119–126. doi: 10.1016/j.ijbiomac.2014.12.00

Jiang, G., Gan, L., Li, X., He, J., Zhang, S., Chen, J., et al. (2021). Characterization of structural and physicochemical properties of an exopolysaccharide produced by *Enterococcus* sp. F2 from fermented soya beans. *Front. Microbiol.* 12:744007. doi: 10.3389/fmicb.2021.744007

Jiang, G., Hou, X., Zeng, X., Zhang, C., Wu, H., Shen, G., et al. (2020). Preparation and characterization of indicator films from carboxymethyl-cellulose/starch and purple sweet potato (*Ipomoea batatas* (L.) lam) anthocyanins for monitoring fish freshness. *Int. J. Biol. Macromol.* 143, 359–372. doi: 10.1016/j.ijbiomac.2019.12.024

Krishnamurthy, M., Uthaya, C. J., Thangavel, M., Annadurai, V., Rajendran, R., and Gurusamy, A. (2020). Optimization, compositional analysis, and characterization of exopolysaccharides produced by multi-metal resistant *Bacillus cereus* KMS3-1. *Carbohydr. Polym.* 227:115369. doi: 10.1016/j.carbpol.2019.115369

Lan, W., Zhang, R., Ahmed, S., Qin, W., and Liu, Y. (2019). Effects of various antimicrobial polyvinyl alcohol/tea polyphenol composite films on the shelf life of packaged strawberries. *LWT-Food Sci. Technol.* 113, 108297. doi: 10.1016/j.lwt.2019.108297

Liu, T., Zhou, K., Yin, S., Liu, S., Zhu, Y., Yang, Y., et al. (2019). Purification and characterization of an exopolysaccharide produced by *Lactobacillus plantarum* HY isolated from home-made Sichuan Pickle. *Int. J. Biol. Macromol.* 134, 516–526. doi: 10.1016/j.ijbiomac.2019.05.010

Lobo, R. E., Gómez, M. I., Valdez, G. F. D., and Torino, M. I. (2019). Physicochemical and antioxidant properties of a gastroprotective exopolysaccharide produced by *Streptococcus thermophilus* CRL1190. *Food Hydrocoll.* 96, 625–633. doi: 10.1016/j.foodhyd.2019.05.036

Lopez-Ortega, M. A., Rodriguez-Hernandez, A. I., Camacho-Ruiz, R. M., Cordova, J., Lopez-Cuellar, M. D. R., Chavarria-Hernandez, N., et al. (2020). Physicochemical characterization and emulsifying properties of a novel exopolysaccharide produced by haloarchaeon *Haloferax mucosum*. *Int. J. Biol. Macromol.* 142, 152–162. doi: 10.1016/j.ijbiomac.2019.09.087

Lynch, K. M., Zannini, E., Coffey, A., and Arendt, E. K. (2018). Lactic acid bacteria exopolysaccharides in foods and beverages: isolation, properties, characterization, and health benefits. *Annu. Rev. Food Sci. Technol.* 9, 155–176. doi: 10.1146/annurev-food-030117-012537

Maalej, H., Hmidet, N., Boisset, C., Bayma, E., Heyraud, A., and Nasri, M. (2016). Rheological and emulsifying properties of a gel-like exopolysaccharide produced by *Pseudomonas stutzeri* AS22. *Food Hydrocoll.* 52, 634–647. doi: 10.1016/j.foodhyd.2015.07.010

Matar, C., Gaucel, S., Gontard, N., Guilbert, S., and Guillard, V. (2018). Predicting shelf life gain of fresh strawberries 'charlotte, cv' in modified atmosphere packaging. *Postharvest Biol. Tec.* 142, 28–38. doi: 10.1016/j.postharvbio.2018.03.002

Mditshwa, A., Magwaza, L. S., Tesfay, S. Z., and Opara, U. L. (2017). Postharvest factors affecting vitamin C content of citrus fruits: a review. *Sci. Horticult.* 218, 95–104. doi: 10.1016/j.scienta.2017.02.024

Prasanna, P. H., Bell, A., Grandison, A. S., and Charalampopoulos, D. (2012). Emulsifying, rheological and physicochemical properties of exopolysaccharide produced by *Bifidobacterium longum* subsp. infantis CCUG 52486 and *Bifidobacterium infantis* NCIMB 702205. *Carbohydr. Polym.* 90, 533–540. doi: 10.1016/j.carbpol.2012.05.075

Rajoka, R. M. S., Wu, Y., Mehwish, H. M., Bansal, M., and Zhao, L. (2020). *Lactobacillus exopolysaccharides*: new perspectives on engineering strategies, physiochemical functions, and immunomodulatory effects on host health. *Trends Food Sc. Tech.* 103, 36–48. doi: 10.1016/j.tifs.2020.06.003

Saadat, R. Y., Khosroushahi, A. Y., and Gargari, B. P. (2019). A comprehensive review of anticancer, immunomodulatory and health beneficial effects of the lactic acid bacteria exopolysaccharides. *Carbohydr. Polym.* 217, 79–89. doi: 10.1016/j.carbpol.2019.04.025

Saleem, M. S., Anjum, M. A., Naz, S., Ali, S., Hussain, S., Azam, M., et al. (2021). Incorporation of ascorbic acid in chitosan-based edible coating improves postharvest quality and storability of strawberry fruits. *Int. J. Biol. Macromol.* 189, 160–169. doi: 10.1016/j.ijbiomac.2021.08.051

Tahir, H. E., Xiaobo, Z., Jiyong, S., Mahunu, G. K., Zhai, X., and Mariod, A. A. (2018). Quality and postharvest-shelf life of cold-stored strawberry fruit as affected by gum arabic (*Acacia senegal*) edible coating. *J. Food Biochem.* 42:e12527. doi: 10.1111/jfbc.12527

Teng, C., Qin, P., Shi, Z., Zhang, W., Yang, X., Yao, Y., et al. (2021). Structural characterization and antioxidant activity of alkali-extracted polysaccharides from quinoa. *Food Hydrocoll.* 113:106392. doi: 10.1016/j.foodhyd.2020.106392

Wang, J., Zhao, X., Tian, Z., Yang, Y., and Yang, Z. (2015). Characterization of an exopolysaccharide produced by *Lactobacillus plantarum* YW11 isolated from Tibet Kefir. *Carbohydr. Polym.* 125, 16–25. doi: 10.1016/j.carbpol.2015.03.003

Wang, Q., Wei, M., Zhang, J., Yue, Y., Wu, N., Geng, L., et al. (2021). Structural characteristics and immune-enhancing activity of an extracellular polysaccharide produced by marine *Halomonas* sp. 2E1. *Int. J. Biol. Macromol.* 183, 1660–1668. doi: 10.1016/j.ijbiomac.2021.05.143

Wold, C. W., Kjeldsen, C., Corthay, A., Rise, F., Christensen, B. E., Duus, J. O., et al. (2018). Structural characterization of bioactive heteropolysaccharides from the medicinal fungus *Inonotus obliquus* (Chaga). *Carbohydr. Polym.* 185, 27–40. doi: 10.1016/j.carbpol.2017.12.041

Wu, B., Guo, Q., Wang, G. X., Peng, X. Y., Wang, J. D., and Che, F. B. (2015). Effects of different postharvest treatments on the physiology and quality of 'Xiaobai' apricots at room temperature. *J. Food Sci. Technol.* 52, 2247–2255. doi: 10.1007/s13197-014-1288-8

Xu, B., and Wu, S. (2021). Preservation of mango fruit quality using fucoidan coatings. *LWT Food Sci. Technol.* 143, 111150. doi: 10.1016/j.lwt.2021.111150

Xu, Y., Cui, Y., Wang, X., Yue, F., Shan, Y., and Liu, B. (2019). Purification, characterization and bioactivity of exopolysaccharides produced by lactobacillus plantarum kx041. *Int. J. Biol. Macromol.* 128, 480–492. doi: 10.1016/j.ijbiomac.2019.01.117

Yan, Y., Duan, S., Zhang, H., Liu, Y., Li, C., Hu, B., et al. (2020). Preparation and characterization of Konjac glucomannan and pullulan composite films for strawberry preservation. *Carbohydr. Polym.* 243:116446. doi: 10.1016/j.carbpol.2020.116446

You, X., Li, Z., Ma, K., Zhang, C. L., Chen, X. B., Wang, G. X., et al. (2020). Structural characterization and immunomodulatory activity of an exopolysaccharide produced by *Lactobacillus helveticus* LZ-R-5. *Carbohydr. Polym.* 235:115977. doi: 10.1016/j.carbpol.2020.115977

Yuan, Z., Shi, Y., Cai, F., Zhao, J., Xiong, Q., Wang, Y., et al. (2020). Isolation and identification of polysaccharides from *Pythium arrhenomanes* and application to strawberry fruit (*Fragaria ananassa* Duch.) preservation. *Food Chem.* 309:125604. doi: 10.1016/j.foodchem.2019.125604

Zhang, W. Y., Hu, B., Han, M., Guo, Y. H., Chen, Y. L., and Qian, H. (2022). Purification, structural characterization and neuroprotective effect of a neutral polysaccharide from *Sparassis crispa*. *Int. J. Biol. Macromol.* 201, 389–399. doi: 10.1016/j.ijbiomac.2021.12.165

Zhao, D., Jiang, J., Liu, L., Wang, S., Ping, W., and Ge, J. (2021). Characterization of exopolysaccharides produced by *Weissella confusa* XG-3 and their potential biotechnological applications. *Int. J. Biol. Macromol.* 178, 306–315. doi: 10.1016/j.ijbiomac.2021.02.182

Zhu, Y. T., Wang, X. J., Pan, W. S., Shen, X. F., Chen, S. J., and Liu, S. L. (2019). Exopolysaccharides produced by yogurt-texture improving *Lactobacillus plantarum* RS20D and the immunoregulatory activity. *Int. J. Biol. Macromol.* 121, 342–349. doi: 10.1016/j.ijbiomac.2018.09.201

Conflict of Interest: The authors declare that the research was conducted in the absence of any commercial or financial relationships that could be construed as a potential conflict of interest.

Publisher's Note: All claims expressed in this article are solely those of the authors and do not necessarily represent those of their affiliated organizations, or those of the publisher, the editors and the reviewers. Any product that may be evaluated in this article, or claim that may be made by its manufacturer, is not guaranteed or endorsed by the publisher.

frontiers | Frontiers in Microbiology

ORIGINAL RESEARCH
published: 29 June 2022
doi: 10.3389/fmicb.2022.919047

A Snapshot of Microbial Succession and Volatile Compound Dynamics in Flat Peach Wine During Spontaneous Fermentation

Xiaoyu Xu, Yuanyuan Miao, Huan Wang, Piping Ye, Tian Li, Chunyan Li, Ruirui Zhao, Bin Wang and Xuewei Shi**

Food College, Shihezi University, Shihezi, China

OPEN ACCESS

Edited by:
Van-Tuan Tran,
Vietnam National University, Hanoi, Vietnam

Reviewed by:
Lisa Granchi,
University of Florence, Italy
Dimitrios Tsaltas,
Cyprus University of Technology, Cyprus

***Correspondence:**
Bin Wang
binwang0228@shzu.edu.cn
Xuewei Shi
shixuewei@shzu.edu.cn

Specialty section:
This article was submitted to Food Microbiology, a section of the journal Frontiers in Microbiology

Received: *13 April 2022*
Accepted: *16 May 2022*
Published: *29 June 2022*

Citation:
Xu X, Miao Y, Wang H, Ye P, Li T, Li C, Zhao R, Wang B and Shi X (2022) A Snapshot of Microbial Succession and Volatile Compound Dynamics in Flat Peach Wine During Spontaneous Fermentation. Front. Microbiol. 13:919047. doi: 10.3389/fmicb.2022.919047

Flat peaches possess characteristic flavors and are rich in nutrients. The fermentation of flat peaches to produce wine through complex biochemical reactions is an effective method to overcome their seasonal defects. Spontaneously fermented flat peach wine has plentiful and strong flavors, but the microbiota of fermentation are still unknown. In this study, the microbial succession and volatile compound dynamics of spontaneous fermentation in Xinjiang flat peach wine were investigated using high-throughput sequencing (HTS) and headspace solid phase microextraction (HS-SPME) coupled with gas chromatography-mass spectrometry (GC-MS) technology, respectively, to better understand the microbiota involved. Multivariate data analysis was used to predict the relationship between microorganisms and volatile chemicals. The results showed that *Kazachstania*, *Pichia*, *Aspergillus*, *Fructobacillus*, *Leuconostoc*, and *Lactobacillus* were the dominant genera during the spontaneous fermentation of flat peach wine. Furthermore, ethyl hexanoate, 3-hexen-1-yl acetate, ethyl caprate, ethyl caprylate, phenethyl acetate, ethanol, γ-decalactone, decanal, 1-hexanoic acid, and octanoic acid endued flat peach wine with a strong fruity and fatty aroma. The core functional microbiota (primarily consisting of 11 bacterial and 14 fungal taxa) was strongly associated with the production of 27 volatile compounds in the spontaneously fermented flat peach wine, according to multivariate data analysis. Some alcohols and esters were positively linked with the presence of *Kazachstania* and *Pichia*. Meanwhile, the presence of *Fructobacillus*, *Leuconostoc*, *Lactobacillus*, and *Weissella* was significantly correlated with 2-non-anol, ethanol, 3-methyl-1-butanol, octyl formate, isoamyl lactate, and ethyl lactate. This snapshot of microbial succession and volatile compound dynamics provides insights into the microorganisms involved in flat peach wine fermentation and could guide the production of flat peach wine with desirable characteristics.

Keywords: flat peach, spontaneous fermentation, microbial communities, volatile composition, correlation analysis

INTRODUCTION

Peaches [*Prunus persica* (L.) Batsch] originated in western China and have been widely cultivated in China for more than 3,000 years. Today, peaches are also cultivated in over 80 countries and regions worldwide (Li and Wang, 2020). Flat peaches [*Prunus persica* (L.) Batsch. *var. compressa* Bean], a special variety of peaches, are popular among customers due to their rich smell, delicious taste, and nutritious nature. Owing to its typical continental climate and ample light and heat availability, the large temperature difference between day and night, and long daylight hours, Xinjiang—located in the Eurasian continental bridge's hinterland—offers considerable resource advantages for flat peach cultivation (Ma et al., 2002).

Flat peaches have become an important fruit from a consumer perspective. However, the flat peach is typical climacteric fruits, and its thin skin makes it extremely susceptible to mechanical damage and microbial infection during post-harvest transportation (Amoros et al., 1989). Therefore, it is necessary to develop different flat peach products to meet consumer and market needs. To this end, approaches such as physical preservation (e.g., irradiation treatment, pressure reduction treatment, air conditioning storage) (Fernández-Trujilio et al., 1998), chemical preservation (e.g., bioregulator treatment and calcium treatment) (Perkins-Veazie et al., 1999), and biological preservation (e.g., microbial preservation and preservation of natural extracted substances) (Fan et al., 2000) have been developed for peach preservation. However, these methods cannot fundamentally solve the problem of the post-harvest preservation of flat peaches. Therefore, other peach products such as peach juice (Wang et al., 2020), peach vinegar (Budak et al., 2021), and fruit wine have been prepared. Among these, fruit wine production is a suitable method for the deep processing of many fruits while still retaining the fruit's flavor and some of its beneficial compounds.

Aroma is responsible for a fruit's distinct flavor and has been extensively researched for its impact on consumer acceptability. Aroma is influenced by natural factors (e.g., fruit varieties and climatic conditions) (Sivilotti et al., 2017), winemaking techniques (Hu et al., 2018), and the presence of indigenous microorganisms (e.g., bacteria, yeasts, and filamentous fungi) (Liu et al., 2017). Several recent studies have focused on the changes in peach aroma throughout the ripening and storage stages (Bianchi et al., 2017), and the volatiles present in flat peach juice have also been explored (Zhang et al., 2010; Wang et al., 2019). More than 100 volatile compounds have been discovered across different peach cultivars, with esters, lactones, aldehydes, alcohols, and ketones being the most commonly found (Wang et al., 2009). Of these, lactones have the greatest effect on flat peach aroma (Sánchez et al., 2013). The aromatic active components in flat peach juice and their contribution have also been verified (Tan et al., 2022). The variability of esters is believed to underly the large differences in flavor quality between fresh flat peach juice and flat peach juice products (Wang et al., 2020).

In recent years, high-throughput sequencing (HTS) combined with multivariate data analysis has been widely used to identify microorganisms in many environments, such as the gut (Ross et al., 2019), as well as in food (Wang et al., 2018). This approach serves as a potent tool for studying the microbial diversity of fermented foods and the quality of fruit wines. The fermentation process of fruit wines is generally referred to as the fermentation process of wine. Usually, the microorganisms present in the skin of the fruit participate in the fermentation process of fruit wines together with the large variety of microorganisms present in the environment (picking, transporting, and crushing, etc.) (Chanprasartsuk et al., 2010). During the fermentation process, these bacteria generate a variety of metabolic substances that impact the flavor, safety, and product quality and stability of fruit wines (Xu X. et al., 2021). Flat peach wine fermentation can be classified into two types based on whether fermenters are used: inoculated fermentation and spontaneous fermentation. Spontaneous fermentation, caused by complex indigenous microorganisms, can provide more complex and richer wine flavors than inoculated fermentation (Lu et al., 2021). The native microorganisms present on the fruit skin serve as important microbial resources and contribute greatly to spontaneous fermentation (Raybaudi-Massilia et al., 2009). *Hanseniaspora uvarum*, *Issatchenkia terricola*, *Wickerhamomyces umomyces*, *Pichia kudriavzevii*, and *Lachancea thermotolerans* are among the microorganisms that have been discovered to contribute to the flavor of fruit wines (Belda et al., 2016; Shi et al., 2019). However, the succession pattern of microorganism populations during the spontaneous fermentation of flat peach wine and their corresponding metabolic characteristics have not been reported yet.

Spontaneously fermented flat peach wine is rich in flavor and aromatic compounds, but the microbiota involved in its fermentation remains unclear. In this study, HTS and headspace solid phase microextraction (HS-SPME) coupled with gas chromatography-mass spectrometry (HS-SPME-GC-MS) was used to examine microbial succession and flavor changes during the spontaneous fermentation of flat peach wine. Subsequently, multivariate data analysis was used to explore the characteristics of the spontaneous fermentation process of flat peach wine to provide a theoretical basis for the development of high-quality flat peach wine.

MATERIALS AND METHODS

Spontaneous Fermentation and Sample Collection

Flat peaches [*Prunus persica* (L.) Batsch cv. "Yingger"] were picked in August 2021 from a flat peach orchard in Shihezi, Xinjiang Uygur Autonomous Region, China. The picked flat peaches were crushed into a homogenized pulp using a pulper. The biochemical composition of these flat peaches was then determined: the residual sugar content was 134 g/L; total acidity, 5.5 g/L; pH, 4.3; and soluble solids 14.6°Bx. Then, pectinase 30 mg/L was added, and the total sugar level was adjusted to 220 g/L. Fermentation was carried out in a 5 L fermenter at 16 ± 0.5℃ under static fermentation conditions. Then, 150 mL of the fermentation liquid was collected on days 0, 3, 6, 9, 13, and 16 of fermentation (A, B, C, D, E, and F, respectively). All samples

were centrifuged for 10 min at 4°C and 8,000 × *g*. The precipitate was collected for HTS, while the supernatant was used to analyze the volatile compounds (Jia et al., 2020).

Determination of Physicochemical Properties

During fermentation, the pH, residual sugars, total acidity, and alcohol content were measured at points A–F. The residual sugar content was assessed using the dinitro salicylic acid method, and the pH was measured using a calibrated pH meter (Miller, 1959). The national standard GB/T 15038-2006 "General analytical procedure for wine and fruit wine" was used to detect total acid and alcohol content. The organic acids were examined using high-performance liquid chromatography (HPLC) using a modified version of a previously reported method (Ryan et al., 2020). Each sample was centrifuged and filtered into an injection vial using a 0.45μm filter. A Dikma C18 chromatographic column (5 m, 4.6 mm, 250 mm; Diamonsil Plus Technology, China) was then used. The mobile phase was a mixture of 0.1% phosphoric acid and methanol, the flow rate was 0.7 mL/min, and the column temperature was 40°C. UV detection was performed at 210 nm. Each indicator was assessed three times.

Determination of Volatile Compounds

The volatile compounds in flat peach wine were detected using the method described by Tufariello et al. (2019), with some modifications. Each sample (10 mL) was placed in a 25-mL SPME glass vial along with 0.1 g/mL NaCl and 2 μL of the internal standard, 3-octanol (30 mg/mL). Subsequently, SPME fibers (DVB/CAR/PDMS 50/30 μm; Supelco, Bellefonte, PA, United States) were inserted into the glass vials and exposed to the headspace for 40 min at 40°C. Then, they were removed and inserted into the inlet of the GC column (HP INNOWAX column, 30 m × 0.25 mm; Agilent) for desorption for 7 min at 210°C. The inlet temperature was 230°C, the carrier gas was helium with a flow rate of 1 mL/min, and the electron energy was 70 eV.

The GC procedure was performed under the following conditions: 5 min at 40°C, temperature increase of 4°C/min until 86°C, 86°C for 5 min, temperature increase of 1.5°C/min until 90°C, temperature increase of 5°C/min until 180°C, 180°C for 3 min, temperature increase of 10°C/min until 230°C, and 230°C for 5 min. A computer search was used to match compounds to the NIST 14 Library. The assay's accuracy was validated through comparisons with recognized compounds described in the literature, and the concentration of each constituent was measured using the internal standard 3-octanol.

Microbial Diversity Analysis

The OMEGA Soil DNA Kit (M5635-02) was used to extract total genomic DNA samples (Omega Bio-Tek, Norcross, GA, United States). Spectrophotometry and agarose gel electrophoresis were used to determine the amount and quality of isolated DNA samples. The forward primer ITS5F (5′-GGAAGTAAAAGTCGTAACAAGG-3′) and the reverse primer ITS1R (5′-GCTGCGTTCTTCATCGATGC-3′) were used to amplify the fungal *ITS1* region using PCR. Moreover, the forward primer 338F (5′ACTCCTACGGGAGGCAGCA-3′) and reverse primer 806R (5′-GGACTACHVGGGTWTCTAAT-3′) were used for the PCR amplification of the V3–V4 region of the bacterial 16S rRNA gene. The cycle included initial denaturation at 98°C for 5 min; followed by 25 cycles of denaturation at 98°C for 30 s, annealing at 53°C for 30 s, and extension at 72°C for 45 s; and a final extension for 5 min at 72°C (Hao et al., 2016). QIIME2 2019.4 was used for microbiome bioinformatics, with minor modifications made according to protocols provided in the official tutorials[1] (Bolyen et al., 2019).

Statistical Analysis

In this study, three parallel tests were performed for each stage of the flat peach wine samples. Statistical analysis was performed using SPSS (version 20; IBM, Chicago, United States) software. Origin 2021 was used to generate histograms, and heat maps of volatile compounds were created using R (version 3.3.1). Multifactorial analysis was performed using Simca 14.1 software to analyze differences between microorganisms and volatile compounds, and the data were visualized using the Cytoscape (version 3.6.1) software.

RESULTS AND DISCUSSION

Changes in Physicochemical Characteristics

General Physical and Chemical Indicators

The dynamic changes in the total sugars, pH, ethanol, and total acid content were detected at six time-points during the spontaneous fermentation of flat peach (**Figure 1**). During the fermentation process, the pH decreased from 4.3 to 3.7 and then remained relatively stable. The total acid concentration increased significantly from 4.4 g/L to 7.7 g/L ($p < 0.05$). The yeasts in the fermentation broth reproduced and grew by utilizing the fermentable sugars during the spontaneous fermentation of flat peach wine, causing the total sugar content to decline dramatically after the 3rd day. However, the total sugar content remained steady from the 16th day onward. Meanwhile, the yeast-mediated conversion of sugars to alcohol resulted in a significant increase in the ethanol concentration, which reached 9.4 ± 0.2% (v/v) on the 16th day and did not change thereafter. The gradual accumulation of ethanol inhibited the ability of the yeasts to metabolize and produce ethanol, consistent with prior findings (Chen et al., 2020).

Organic Acid Composition

The flavor and taste of flat peach wine are strongly influenced by its organic acid concentration. In this study, eight organic acids (succinic, lactic, acetic, citric, oxalic, malic, tartaric, and quinic acid) were identified in the fermentation broth using HPLC (**Figure 2A**). The proportion of these organic acids varied with fermentation time. At the beginning of spontaneous fermentation, tartaric, malic, and citric acids were predominantly

[1]https://docs.qiime2.org/2019.4/tutorials/

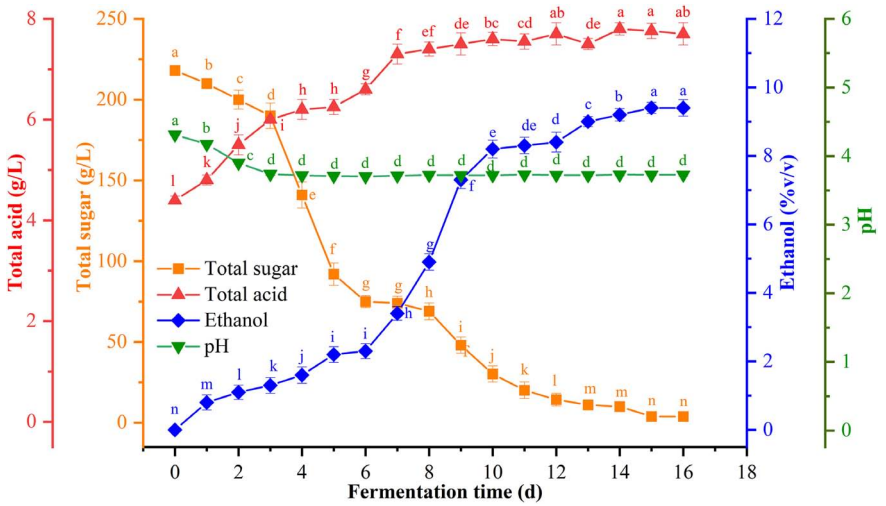

FIGURE 1 | Changes in physicochemical indexes [total sugar (orange), ethanol (blue), total acid (red), and pH (green)] at different stages of fermentation.

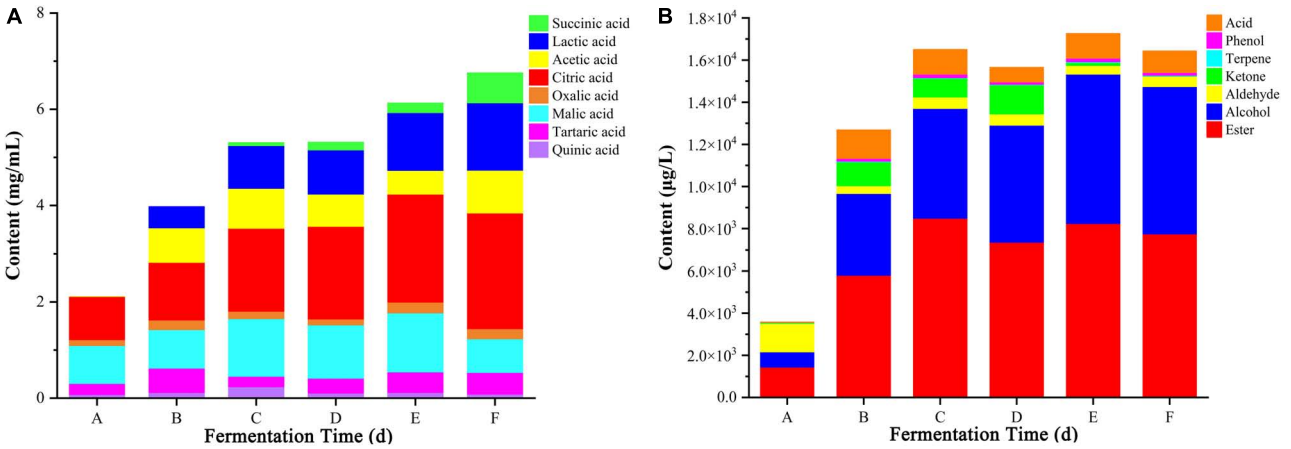

FIGURE 2 | Changes in the levels of 8 organic acids **(A)** and 7 types of volatile substances **(B)** across different fermentation stages. A, B, C, D, E, and F Represent samples collected on fermentation days 0, 3, 6, 9, 12, and 16, respectively.

observed. However, with prolongation of the fermentation time, there was a continuous increase in the proportion of lactic acid, which was produced by bacteria such as *Leuconostoc* and *Lactobacillus*. There was also an overall trend for increasing levels of citric acid. In contrast, the levels of oxalic, tartaric, and malic acid remained relatively stable during the fermentation process. At the final stage, the organic acid composition of the flat peach wine was as follows: succinic acid (9.32%), lactic acid (20.71%), acetic acid (13.16%), citric acid (35.5%), oxalic acid (3.1%), malic acid (10.36%), tartaric acid (6.66%), and quinic acid (1.19%). Spontaneous fermented flat peach wine has a sour taste. This harmonious acidity is determined by the substrate's composition ratio as well as the detectable concentration levels (Joshi et al., 2017). Considering the differences in acidity, in general, tartaric acid has a citrus-like flavor, malic acid has a metallic and green apple-like flavor, lactic acid has a tart and spicy taste, citric acid is fresh and pleasantly citrusy, and succinic acid has a sour, salty, and bitter taste. Each organic acid comparts different sensory characteristics to fruit wines (Mato et al., 2005; Izquierdo-Llopart et al., 2020).

Microbial Succession and Interactions

Sequencing Quality Assessment

HTS was used to assess the microbiological diversity and communities present at six different time-points during the spontaneous fermentation of flat peach wine. For the bacterial communities, after removing low-quality sequences and chimeras, valid sequences were obtained for each sample. Accordingly, 688,716 high-quality sequences were obtained from all samples. For the fungal communities, 474,803 high-quality sequences were obtained. The number of bacterial sequences and operational taxonomic unites (OTUs) significantly outnumbered the number of fungal sequences and OTUs. For all samples,

the coefficient curve sections were flat, and the coverage of high-quality sequences was greater than 99%, indicating that the sequencing results were adequate to indicate the microbiological variety of the samples (**Supplementary Figures 1**, **2**). After standardization, the α-diversity of the samples was analyzed. The measures of species richness and diversity, such as Chao1 and Shannon index, are shown in **Supplementary Table 1**. The findings revealed that the quantity and diversity of bacterial and fungal communities changed during the fermentation of flat peach wine. The Chao1 index, the observed species, and the Shannon and Simpson indices of the fungal communities showed a decreasing trend, indicating that the diversity and richness of fungi gradually decreased during fermentation. In contrast, bacterial communities showed the opposite trend (**Supplementary Figure 3**). The common and unique bacterial OTUs observed at different stages of fermentation were also characterized. There were 164, 127, 138, 115, 60, and 66 fungal OTUs on days 0, 3, 6, 9, 13, and 16, respectively. Of these, 18 OTUs were common to all six fermentation stages. For bacteria, 162, 126, 145, 118, 114, and 109 OTUs were detected at different stages, respectively, with 49 OTUs common to all stages (**Supplementary Figure 4**). Thus, the microbial community structure in flat peach wine showed differences across different fermentation stages.

Microbial Succession

HTS was used to fully characterize the bacterial and fungal communities present during the spontaneous fermentation of flat peach wine and reveal the diversity and succession of microbial communities. Eighteen wine samples were collected from six fermentation processes, and the number of fungal and bacterial taxa at each classification level was examined during the fermentation of flat peach wine using Illumina sequencing (**Supplementary Figure 5**). The numbers of taxa detected at the genus level for fungi and bacteria were 48 and 40 at day 0, respectively. However, at day 16, the number of detectable taxa at the genus level gradually decreased to 20 and 30, respectively.

In order to assess community succession during fermentation, sequencing data were classified at the phylum and genus levels. The results showed that in the fungal community, the species distribution of the Ascomycota phylum was denser than that of other phyla, accounting for 27.75% of the total microbiota (**Figure 3A**). Ascomycetes were the dominant fungi during the fermentation process. In contrast, Firmicutes, Cyanobacteria, and Proteobacteria were the dominant bacterial phyla, accounting for 24.93, 19.62, and 5.42% of the bacteria, respectively (**Figure 3C**). These results were consistent with those from a previous study (Zhu et al., 2021). In the early phases of fermentation, Cyanobacteria and Anaplasma were predominant. However, their abundance declined with the growth of Firmicutes, which substantially increased in proportion after day 2.

At the genus level, the fungi *Aspergillus* (19.67%), *Alternaria* (19.06%), *Filobasidium* (16.97%), *Aureobasidium* (13.05%), *Naganishia* (11.53%), and *Mycosphaerella* (8.53%) had the highest relative abundance at stage A (**Figure 3B**). These findings differed from previous findings, likely owing to the cultivar of the flat peaches used and their origin. Notably, *Kazachstania* and *Pichia* gradually became dominant during the middle and late stages of fermentation. *Kazachstania*, a common yeast found in kimchi (Suzuki et al., 2018), sourdough (Minervini et al., 2015; Decimo et al., 2017), and feed (Santos et al., 2017), is strongly linked with the formation of flavor substances such as acids and alcohols in fermented products. *Pichia*, a fungal genus commonly found in fermented foods, can secrete esterases to promote the biocatalytic synthesis of ethyl ester compounds, which are important flavor substances in strong spiced white wine (van Rijswijck et al., 2019; Vicente et al., 2021). The relative abundance of *Aspergillus* showed significant fluctuations during fermentation, which may account for the increased alcohol concentration. Moreover, it has been reported that *Aspergillus* are the main microorganisms responsible for citric acid accumulation. This may be why flat peach wine has a higher citric acid content.

The bacterial diversity during flat peach wine fermentation was higher than the fungal diversity (**Figure 3D**). The main bacterial genera present at stage A of fermentation were *Tatumella* (20.57%), *Halomonas* (20.32%), and *Pantoea* (15.84%). The percentage of these three genera decreased as fermentation proceeded, probably due to the high enrichment of lactic acid bacteria in the later stages. *Pantoea* is an endophytic bacterium that is widely present on plant surfaces, grains, and fruits (Megías et al., 2016; Jung et al., 2018; Kour et al., 2021). The bacteria, detected at stage A, probably originated from the raw materials and environment. Subsequently, *Fructobacillus* maintained a relatively high abundance from stage B onward and was the dominant bacterial genus during flat peach wine fermentation. *Leuconostoc* and *Lactobacillu* showed a moderate relative abundance. These microorganisms typically grow better under low-oxygen and low-pH post-fermentation conditions as they are typically facultative anaerobes and acid-tolerant bacteria (McDonald et al., 1990). *Leuconostoc* can not only produce some flavor compounds, such as acetaldehyde and ethyl acetate, but can also secrete substances such as glucans (Yang X. et al., 2020). *Lactobacillus* is also one of the most significant genera involved in fruit wine production. It can create lactic acid and antimicrobial compounds such as bacteriocins, which limit the growth of pathogens and spoilage bacteria during the brewing process, increasing the flavor of fruit wine (Xu Z. et al., 2021). In addition to these bacteria, *Gluconobacter*, a functional bacterium, was also present in small amounts at stages A, B, and C. *Gluconobacter* is generally sensitive to alcohol, and its growth can be suppressed by high levels of alcohol (Habe et al., 2021). Hence, its abundance dropped significantly throughout the fermentation process in the present study. *Gluconobacter* is reported to be among the dominant flora in wine (Philippe et al., 2018) and white wine (Battling et al., 2020). Interestingly, pathogenic bacteria such as *Klebsiella* and *Rosenbergiella* were discovered during the fermentation process. However, as brewing progressed, their quantity reduced, possibly due to an increase in the abundance of lactic acid bacteria in the latter stages of fermentation.

Microbial diversity was assessed using principal component analysis (PCA) to determine the variations and similarity in microbial communities (**Supplementary Figure 6**). The PCA based β-diversity analysis of fungal and bacterial structures

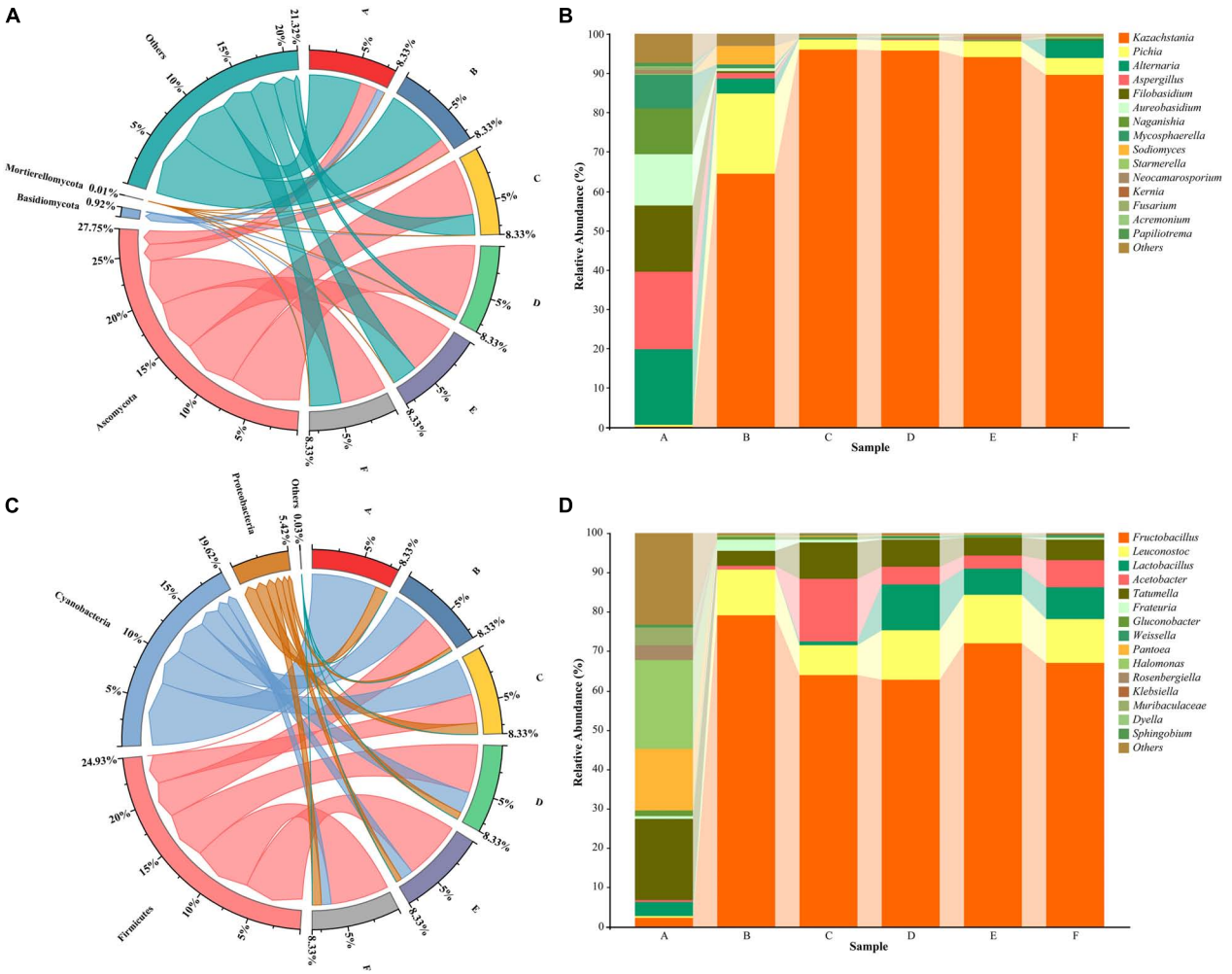

FIGURE 3 | Differences in fungal **(A)** and bacterial **(C)** communities after different fermentation periods at the phylum level. The relative abundance of the top 15 fungi **(B)** and bacteria **(D)** at the genus level. A, B, C, D, E, and F Represent samples collected on fermentation days 0, 3, 6, 9, 12, and 16, respectively.

during wine fermentation showed that the first principal component (PC1) explained 50.2% of the variation between samples. Moreover, the second principal component (PC2) explained 16.4% of the variation. The contribution of PC1 to the bacterial structure was 46.8%, while the contribution of PC2 was 18.4%. As fermentation progressed, the microbial composition of the samples changed. The microbiota at stage A was different from that at other stages. However, the microbiota was comparable between stages E and F, toward the end of fermentation, because the samples were similar. In conclusion, the findings suggested that the size of the microbial population varies depending on the stage of fermentation.

Microbial Interrelationships

Microbial interactions are considered to be important for supporting the microbial community structure (Tempère et al., 2018). Pearson rank coefficients reveal whether microorganisms have positive or antagonistic associations. In this study, correlation analysis of fungal genera showed that *Pichia* was weakly negatively correlated with almost all other fungal genera except *Sodiomyces*, *Starmerella*, and *Kernia*. Further, similar findings were observed for *Kazachstania*. In contrast, *Alternaria*, *Filobasidium*, *Aureobasidium*, *Naganishia*, and *Mycosphaerella* showed a co-occurrence pattern with *Neocamarosporium* and *Papiliotrema* (**Figure 4A**). Among the bacteria, *Papiliotrema* and *Leuconostoc* showed negative correlations with *Pantoea* and *Halomonas*. *Fructobacillus*, *Lactobacillus*, and textitFrateuria were positively correlated with *Leuconostoc*, *Enterococcus*, and *Dyella*, respectively (**Figure 4B**). In addition, a correlation analysis of bacteria and fungi showed that *Pantoea* and *Halomonas* were also positively correlated with *Alternaria*, *Aspergillus*, *Filobasidium*, *Aureobasidium*, *Naganishia*, *Mycosphaerella*, *Neocamarosporium*, *Fusarium*, and *Papiliotrema*. In contrast, *Fructobacillus*, *Leuconostoc*, *Tatumella*, *Gluconobacter*, and *Klebsiella* showed exclusion patterns with *Alternaria*, *Aspergillus*, *Filobasidium*, *Aureobasidium*, *Naganishia*, and *Mycosphaerella* (**Figure 4C**).

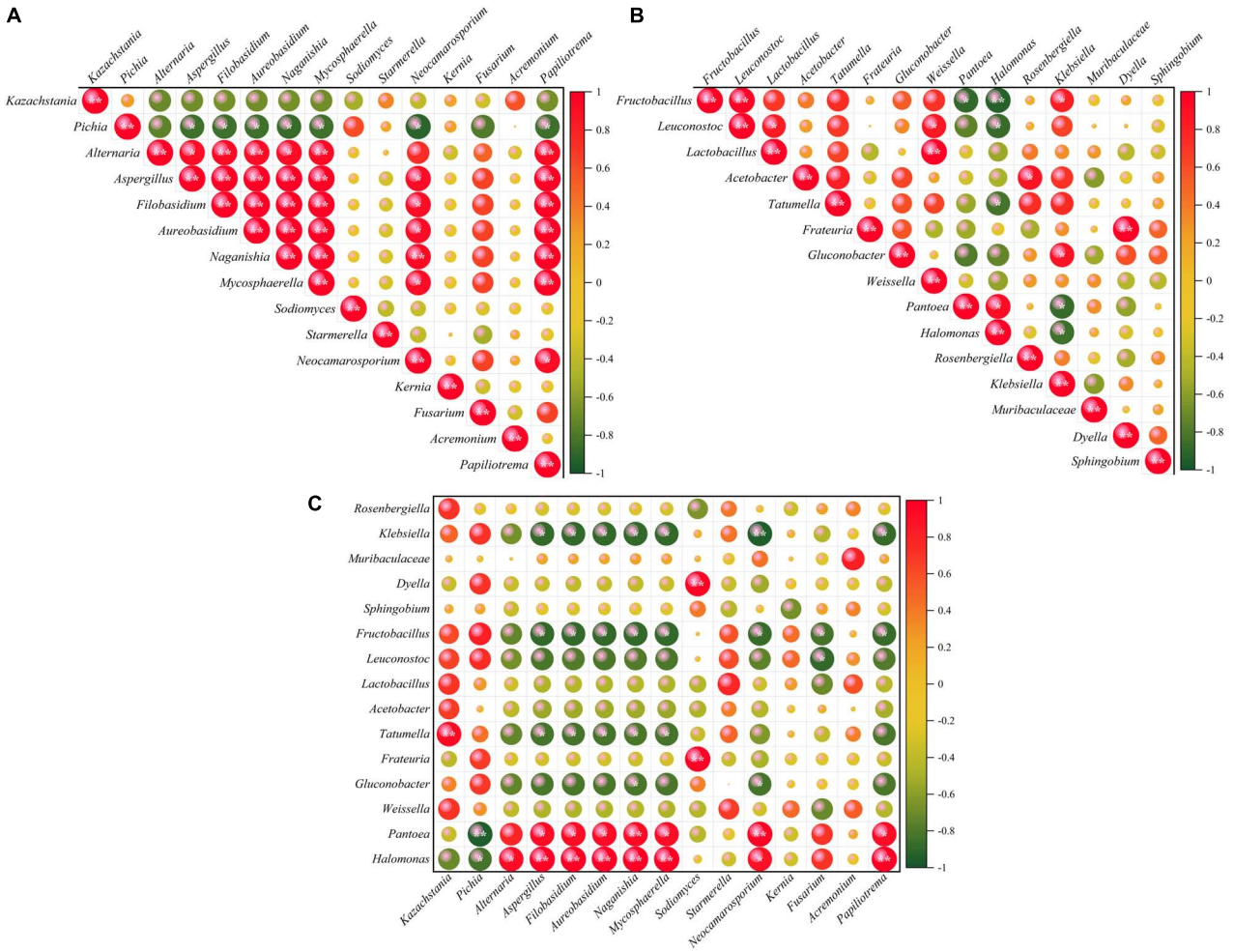

FIGURE 4 | Co-occurrence and co-exclusion relationships between different bacteria **(A)** and fungi **(B)** and between bacteria and fungi **(C)**. The Pearson rank correlation matrix showing the abundance of the top 30 fungi and bacterial genera is depicted. Strong correlations are indicated by large circles, whereas weak correlations are indicated by small circles. The color of the scale bar denotes the nature of the correlation, with 1 indicating a perfect positive correlation (red) and -1 indicating a perfect negative correlation (green). Significant correlations ($|r| > 0.7$, $P < 0.01$) and ($|r| > 0.9$, $P < 0.01$) are indicated by * and **, respectively.

The HTS results revealed that as the duration of fermentation and environment changed, the dominant bacterial genera in flat peach wine also changed. This implies that some microbial taxa, such as *Pantoea*, *Halomonas*, *Klebsiella*, *Aureobasidium*, and *Papiliotrema*, may be unable to adapt to the selective environment of accumulating ethanol levels and increasing acidity created by *Fructobacillus*, *Leuconostoc*, *Kazachstania*, and *Pichia*. In contrast to previous reports that *Lactobacillus* was the dominant flora in rice wine (Yang Y. et al., 2020) and koumiss (Meng et al., 2021), we found that *Fructobacillus* and *Leuconostoc* were the dominant lactic acid bacteria during the spontaneous fermentation flat peach wine and were also the probably main cause of pH fluctuations (Huang et al., 2018). During the brewing process, these bacteria can produce antimicrobial compounds such as bacteriocins that limit the growth of a vast number of microorganisms, including pathogens and spoilage germs (Collins et al., 2018). As dominant fungal genera, *Kazachstania* and *Pichia* exhibit efficient fermentation catabolism and tolerance to acid and ethanol and are highly competitive and dominant throughout the fermentation process. Some species of *Kazachstania*, a non-*Saccharomyces* yeast, have been shown to have a fermentation biology similar to that of brewer's yeast (Merico et al., 2007).

Changes in Volatile Compounds

Composition and Cluster Analysis of Volatile Compounds

The volatile compounds in flat peach wine were analyzed using HS-SPME-GC-MS. The changes in the composition and content of volatiles in flat peach wine during spontaneous fermentation are shown in **Figure 2B**. A total of 53 volatile compounds were detected at the six time-points (**Table 1**), including esters (23), alcohols (13), aldehydes (6), ketones (2), terpenes (3), phenol (1), and acids (5). The main constituents of flat peach are esters, aldehydes, and alcohols.

TABLE 1 | Dynamic changes in the content of flavor compounds during the fermentation process (μ g/L).

Compounds	RI	A	B	C	D	E	F	Odor threshold	OAV[1]
Esters									
Ethyl acetate	612	744.07 ± 0.58^{c}	3216.51 ± 152.25^{a}	1968.87 ± 117.83^{b}	1576.59 ± 124.87^{c}	1997.31 ± 191.85^{b}	3170.56 ± 324.2^{a}	7750	0.1–1
Isoamyl acetate	876	Nd	145.62 ± 3.83^{b}	296.36 ± 0.61^{a}	142.94 ± 9.15^{b}	158.39 ± 5.93^{b}	19.14 ± 2.20^{c}	30	0.1–1
Pentyl acetate	911	Nd	Nd	Nd	Nd	Nd	12.09 ± 0.77^{a}	43	0.1–1
Ethyl hexanoate	1,000	Nd	31.42 ± 0.83^{e}	133.51 ± 2.34^{ab}	114.04 ± 2.86^{bc}	160.72 ± 6.87^{a}	71.25 ± 0.88^{d}	5	> 1
Hexyl acetate	1,011	44.12 ± 0.63^{d}	995.05 ± 3.13^{a}	635.89 ± 25.22^{b}	318.01 ± 12.73^{c}	238.37 ± 5.92^{c}	60.26 ± 0.89^{d}	670	< 0.1
3-Hexen-1-yl acetate	1,005	132.04 ± 22.66^{a}	21.67 ± 0.72^{c}	10.14 ± 0.01^{c}	120.56 ± 6.05^{a}	96.22 ± 0.16^{b}	24.37 ± 0.26^{c}	13	> 1
Ethyl lactate	815	Nd	Nd	176.19 ± 0.13^{c}	256.21 ± 2.27^{b}	397.98 ± 4.23^{a}	262.76 ± 9.02^{b}	154,636	< 0.1
Isoamyl lactate	1,047	Nd	1.37 ± 0.04^{c}	12.17 ± 0.83^{b}	15.51 ± 0.2^{b}	24.68 ± 1.9^{a}	21.05 ± 1.45^{a}	/	
3-Hexenyl isobutyrate	1,145	13.69 ± 1.53^{a}	0 ± 0	Nd	Nd	Nd	Nd	/	
2-Hexen-1-ol acetate	1,006	105.4 ± 0.78^{a}	56.21 ± 4.23^{b}	26.86 ± 0.45^{c}	3.31 ± 0.22^{d}	Nd	Nd	/	
Ethyl caprylate	1,196	8.97 ± 0.26^{d}	24.86 ± 0.26^{c}	235.17 ± 3.66^{a}	33.3 ± 2.33^{c}	245.67 ± 4.01^{a}	190.71 ± 7.57^{b}	5	> 1
Ethyl non-anoate	1,296	3.41 ± 0.15^{d}	1.69 ± 0.31^{d}	40.99 ± 0.7^{b}	138.45 ± 2.44^{a}	29.94 ± 1.37^{c}	29.09 ± 2.89^{c}	1,300	< 0.1
Ethyl caprate	1,396	2.74 ± 0.01^{d}	53.55 ± 0^{c}	355.53 ± 10.98^{a}	10.02 ± 0.01^{d}	357.58 ± 5.36^{a}	225.95 ± 18.35^{b}	200	> 1
Ethyl benzoate	1,171	11.63 ± 0.47^{c}	23.99 ± 2.57^{b}	15.4 ± 0.28^{c}	15.07 ± 0.05^{c}	20.08 ± 0.76^{b}	934.12 ± 24.13^{a}	53	> 1
Ethyl phenylacetate	1,246	Nd	3.17 ± 0.05^{c}	2.67 ± 0.12^{c}	4.57 ± 0.4^{b}	6.97 ± 0.69^{a}	Nd	155.5	< 0.1
Ethyl laurate	1,595	Nd	Nd	15.1 ± 0.07^{c}	46.96 ± 4.92^{a}	49.88 ± 1.33^{a}	26.33 ± 0.94^{b}	500	< 0.1
Phenethyl acetate	1,258	329.44 ± 2.99^{d}	752.9 ± 2.33^{c}	3985.34 ± 272.48^{a}	3505.94 ± 4.2^{a}	3406.42 ± 66.17^{a}	2514.08 ± 9.96^{b}	1,800	> 1
Ethyl tetradecanoate	1,794	Nd	Nd	1.23 ± 0.01^{c}	2.77 ± 0.54^{b}	2.43 ± 0.02^{b}	7.44 ± 0.31^{a}	2,000	< 0.1
γ-Decalactone	1,470	434.39 ± 45.81^{a}	375.85 ± 30.84^{b}	152.88 ± 2.04^{c}	84.94 ± 3.49^{d}	154.7 ± 3.32^{b}	110.02 ± 7.09^{c}	1.1	> 1
Ethyl palmitate	1,993	Nd	Nd	2.71 ± 0.5^{c}	15.39 ± 2.4^{a}	8.05 ± 0.04^{b}	17.06 ± 0.75^{a}	1,000	< 0.1
Tetradecalactone	1,935	Nd	Nd	Nd	Nd	17.73 ± 0.23^{a}	13.28 ± 0.15^{b}	29	0.1–1
γ-Dodecalactone	1,678	10.09 ± 1.62^{a}	4.02 ± 0.85^{c}	4.45 ± 0.32^{c}	4.27 ± 0.19^{c}	9.17 ± 0.04^{a}	6.09 ± 0.06^{b}	0.43	> 1
Methyl benzoate	1,094	6.67 ± 0.08^{d}	40.12 ± 0.01^{c}	367.72 ± 5.46^{b}	502.98 ± 9.18^{b}	823.4 ± 16.55^{a}	20.58 ± 1.82^{c}	73	0.1–1
Alcohols									
Ethanol	324	Nd	986.83 ± 47.26^{c}	2398.01 ± 140.01^{a}	2196.84 ± 139.8^{a}	886.33 ± 61.04^{b}	233 ± 8.49^{d}	950	> 1
3-Methyl-1-butanol	736	Nd	126.23 ± 18.55^{d}	791.3 ± 7.99^{c}	1111.01 ± 78.5^{b}	1309.73 ± 77.59^{a}	874.02 ± 2.84^{c}	7,000	0.1–1
1-Hexanol	868	Nd	1221.71 ± 1.21^{a}	830.23 ± 14.3^{b}	731.61 ± 22.35^{c}	843.07 ± 4.9^{b}	533.48 ± 9.53^{d}	5,200	0.1–1
3-Hexen-1-ol	852	186.32 ± 21.46^{a}	162.09 ± 8.55^{a}	105.73 ± 4.76^{c}	85.51 ± 0.36^{d}	112.82 ± 1.99^{b}	96.68 ± 4.72^{d}	400	0.1–1
Cyclohexanol	880	576.53 ± 0.12^{a}	356.79 ± 26.01^{b}	Nd	Nd	Nd	Nd	300	
2-Octanol	998	Nd	Nd	Nd	5.93 ± 0.66^{a}	4.8 ± 0.57^{b}	Nd	120	
Cyclohexanemethanol	/	103.76 ± 2.48^{a}	Nd	Nd	Nd	Nd	Nd	/	
1-Octanol	1,071	Nd	18.98 ± 1.36^{a}	14.96 ± 2.13^{b}	4.26 ± 0.12^{c}	21.37 ± 2.87^{a}	Nd	800	
2,3-Butanediol	1,071	Nd	18.98 ± 2.81^{ab}	14.96 ± 0.47^{b}	4.26 ± 0.54^{c}	21.37 ± 2.38^{a}	Nd	800	
2-Non-anol	/	Nd	2.7 ± 0.49^{d}	8.9 ± 0.64^{c}	83.75 ± 2.65^{b}	15.79 ± 0.56^{c}	143.46 ± 9.52^{a}	20–50	> 1
Benzyl alcohol	1,173	Nd	68.24 ± 12.9^{a}	Nd	Nd	Nd	Nd	600	
Phenylethyl alcohol	1,036	12.29 ± 0.03^{d}	584.32 ± 59.62^{a}	422.52 ± 1.78^{b}	284.16 ± 17.08^{c}	506.31 ± 11.53^{a}	287.62 ± 5.39^{c}	2,0000	< 0.1
β-ionol	1,116	8.7 ± 0.3^{e}	170.91 ± 43.07^{d}	583.62 ± 2.56^{c}	492.85 ± 9.09^{c}	1061.17 ± 43.96^{a}	869 ± 48.79^{b}	10,000	< 0.1
Aldehydes									
Hexanal	800	221.18 ± 0.69^{a}	5.03 ± 1.44^{b}	Nd	Nd	Nd	Nd	5–15	
2-Hexenal	851	1070.62 ± 3.83^{a}	Nd	Nd	Nd	Nd	Nd	30	
2,4-Heptadienal	1,012	2.91 ± 0.29^{a}	Nd	Nd	Nd	Nd	Nd	15.4	
Benzaldehyde	962	4.23 ± 0.02^{d}	256.52 ± 18.75^{b}	384.66 ± 21.68^{a}	238.98 ± 6.35^{b}	164.84 ± 3.42^{c}	133.46 ± 2.45^{c}	2,000	< 0.1
2,5-Dimethylbenzaldehyde	1,208	56.73 ± 0.34^{d}	85.65 ± 4^{d}	135.94 ± 11.27^{c}	282.24 ± 15.73^{b}	245.35 ± 0.25^{b}	347.97 ± 5.64^{a}	200	> 1
4-Undecanolide	1,576	Nd	Nd	2.03 ± 0.02^{a}	1.98 ± 0.34^{b}	1.87 ± 0.01^{b}	Nd	2.1	0.1–1
Ketones									
3-Octanone	986	10.85 ± 0.48^{a}	10.87 ± 0.62^{a}	4.56 ± 0.4^{b}	1.79 ± 0.56^{c}	Nd	Nd	21.4	
Geranylacetone	1,453	Nd	Nd	Nd	Nd	8.4 ± 0^{b}	9.83 ± 0.59^{a}	60	0.1–1
Terpenes									
Linalool	1,099	22.68 ± 0.02^{d}	45.21 ± 0.15^{c}	72.71 ± 8.99^{b}	67.71 ± 1.92^{b}	113.95 ± 10.57^{a}	Nd	25	
β-Ionone	1,491	3.93 ± 0.9^{d}	18.62 ± 0.44^{c}	19.23 ± 0.16^{bc}	20.23 ± 1.58^{b}	23.54 ± 0.38^{ab}	25.28 ± 4.44^{a}	8.4	> 1

(Continued)

TABLE 1 | (Continued)

Compounds	RI	A	B	C	D	E	F	Odor threshold	OAV[1]
Geraniol	1,255	Nd	Nd	Nd	6.32 ± 0.23^{c}	16.28 ± 0.91^{a}	8.09 ± 0.06^{b}	0.99	> 1
Phenols									
Eugenol	1,357	0.28 ± 0.01^{d}	32.7 ± 1.91^{c}	152.03 ± 29.72^{a}	111.6 ± 1.13^{b}	125.2 ± 10.75^{ab}	136.87 ± 19^{a}	5	> 1
Acids									
1-Hexanoic acid	990	10.11 ± 0.79^{d}	463.64 ± 45^{a}	122.07 ± 14.9^{b}	55.1 ± 3.61^{c}	112.97 ± 9.17^{b}	66.41 ± 4.53^{c}	420	0.1–1
Octanoic acid	1,180	1.3 ± 0.05^{d}	62.56 ± 0.4^{b}	75.29 ± 1.92^{b}	43.78 ± 1.26^{c}	116.29 ± 4.45^{a}	41.37 ± 0.97^{c}	500	< 0.1
Non-anoic acid	1,273	Nd	Nd	5.09 ± 0.06^{b}	2.97 ± 0.69^{c}	12.89 ± 2.04^{a}	6.47 ± 0.05^{b}	500–800	< 0.1
Decanoic acid	1,373	Nd	13.36 ± 0.96^{c}	22.6 ± 1.84^{b}	23.42 ± 2.42^{b}	50.69 ± 7.56^{a}	15.52 ± 1.07^{c}	1,000	< 0.1
Benzoic acid	1,170	Nd	Nd	15.2 ± 0.14^{c}	304.25 ± 31.89^{b}	826.66 ± 54.21^{a}	Nd	1,000	

A, B, C, D, E, and F represent samples collected on fermentation days 0, 3, 6, 9, 12, and 16, respectively. Data are expressed as the means ± standard (n = 3). The different lowercase letters in each row indicate a significant difference between the samples (P < 0.05). Nd, not detected. RI, retention index; OAV, odor activity value.
[1]OAV was calculated by dividing concentration by the odor threshold value of the compound.

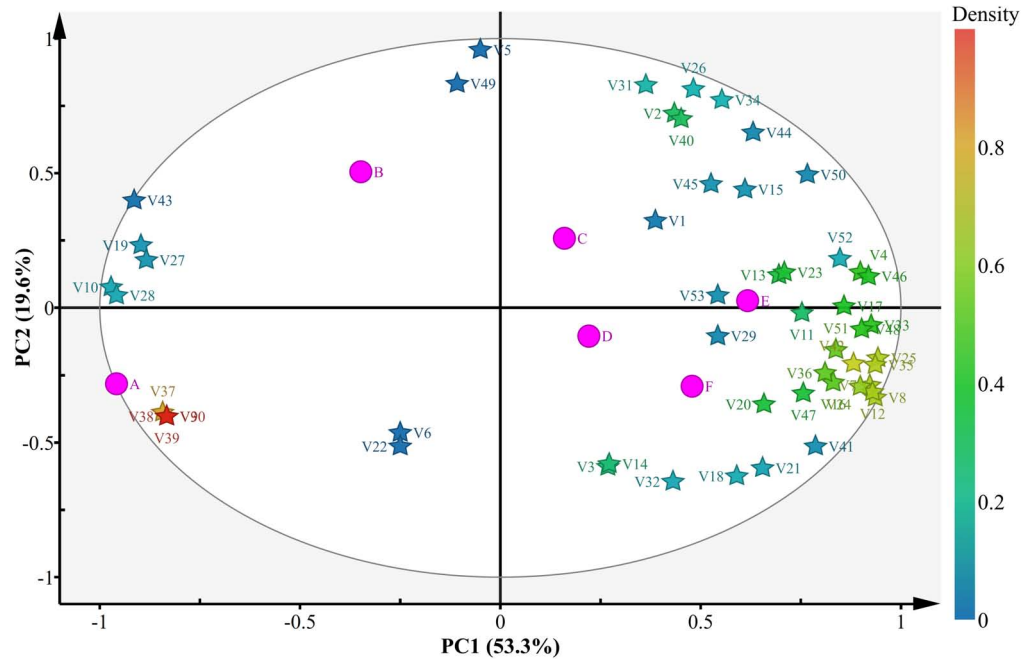

FIGURE 5 | Bioplot of the PCA for volatile compounds present in the samples. A, B, C, D, E, and F Represent samples collected on fermentation days 0, 3, 6, 9, 12, and 16, respectively. "V" represents volatile compounds.

The complexity of the volatiles increased with the duration of fermentation, especially for esters and alcohols. The esters that give flat peach wine its distinct flavor can be synthesized by esterifying alcohols with fatty acids. Moreover, microbial cells can generate these molecules using acetyl coenzyme A and higher alcohols as substrates during fermentation through alcohol acetyltransferases (Wang et al., 2014).

PCA was used to understand the relationships and differences between scent components in different wines (**Figure 5**). Among them, 53 different components explained 74.1% of the variance, with PC1 and PC2 explaining 53.3 and 19.6% of the variance, respectively. The volatile components at stage A were significantly different from those at stages B–F, indicating that the volatile components in flat peach wine were significantly different from those in the fermentation products generation during fermentation. Most volatile compounds were found at stages E and F, confirming the flat peach wine has a greater concentration of volatile components. The remaining samples contained only a few volatile compounds, consistent with the lower volatile compound concentrations observed in these samples throughout the experiment. These variations suggest that the aroma of the flat peach wine varied across different stages of fermentation. It is worth noting that at stage E, half of the volatile chemicals (alcohols and esters) were found in the lower right quadrant.

Characteristic Flavor Substances of Flat Peach Wine

The fragrance composition was studied during the spontaneous fermentation process, where the color intensity was related to

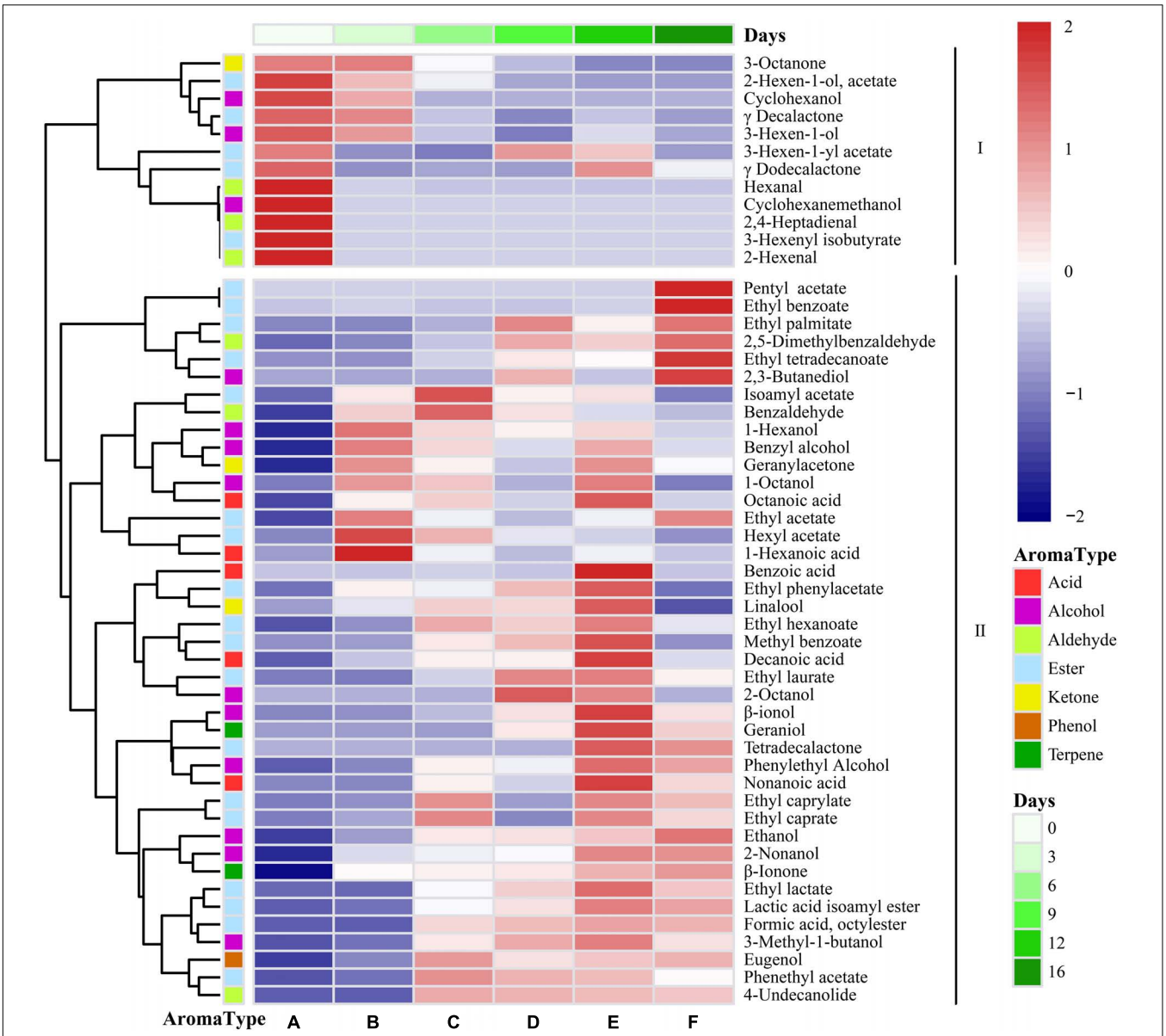

FIGURE 6 | Heatmap cluster analysis of the volatile components identified during fermentation. The colors correspond to normalized mean levels, from low (blue) to high (red); the scale is shown at the top. A, B, C, D, E, and F) Represent samples collected on fermentations days 0, 3, 6, 9, 12, and 16, respectively.

the relative quantity of volatile chemicals, to better understand the dynamics of these volatile compounds (**Figure 6**). The volatile components could be split into two groups based on their patterns during the fermentation process. There were 12 major volatile compounds present in flat peaches, including 3-hexen-1-yl acetate, 3-octanone, hexanal, 3-hexen-1-ol, 2-hexenal, γ-decalactone, and δ-decalactone. This was consistent with previous findings (Zhu and Xiao, 2019). Hexanal, 3-hexen-1-ol, and 2-hexenal are C_6 compounds that are generated as byproducts after the enzyme-catalyzed degradation of unsaturated fatty acids. Lactones, and particularly γ-decalactone and δ-decalactone, are the "character shock" components of flat peach flavor. There were 41 volatile compounds present in Class II, and these represented the main volatile substances produced during the late stage of spontaneous flat peach wine fermentation. Because these were present at greater quantities during the fermentation process, several of these volatile chemicals were intermediate products.

Esters are important flavor substances during the fermentation of flat peach wine because they confer fruit-like flavors (Tufariello et al., 2012). During the spontaneous fermentation of flat peach wine, the main esters were isoamyl acetate, pentyl acetate, ethyl laurate, ethyl caprate, ethyl acetate, hexyl acetate, phenethyl acetate, and ethyl caprylate. Due to the high concentration of alcohol and the corresponding presence of acetyl coenzyme A and acyltransferase, large amounts of acetate and ethyl esters were

produced (Mason and Dufour, 2000; van Rijswijck et al., 2019). The main esters with odor activity values (OAV) > 1 at the end of fermentation were ethyl hexanoate (pineapple and banana aroma), 3-hexen-1-yl acetate (banana aroma), ethyl caprylate (fruit and wax aroma), ethyl caprate (fruit aroma), ethyl benzoate (fruity and medicinal fragrance), phenethyl acetate (fruity and floral fragrance), γ-decalactone (peach fragrance), and γ-dodecalactone. This could be due to the high acyltransferase and alcohol acetyltransferase expression during spontaneous fermentation (Procopio et al., 2011). Ethyl lactate and isoamyl acetate were identified during the middle and late phases of fermentation, indicating that they were mostly generated by yeast metabolism and esterification processes. In addition, during the mid-late fermentation stage, the concentration of phenethyl acetate—which is produced by yeasts from higher alcohols during fermentation and boosts olfactory complexity by providing banana, pear, and apple scents—rose significantly.

Alcohols are an important source of alcoholic sweetness and act as aroma enhancers for wine. They are precursors to esters, which provide floral and fruity aroma (Gao et al., 2014). The flat peach wine produced after spontaneous fermentation contained high concentrations of ethanol, 3-methyl-1-butanol, 1-hexanol, and benzyl alcohol. However, due to their relatively high odor threshold, these alcohols (with the exception of ethanol) did not favorably enhance the flavor of the wine. The concentration of these compounds decreased during fermentation, likely because they were used in esterification for the synthesis of the corresponding esters (Abeijón Mukdsi et al., 2018). Aldehydes and ketones are also important components of the aroma of fruit wines (Tufariello et al., 2012). Decanal, which provides fatty aromas and fatty flavors, had an OAV > 1 in flat peach wine. The OAV of benzaldehyde, a versatile aromatic aldehyde, was < 0.1 at the end of fermentation. The release of acid and the breakdown of flavor substances result in the formation of ketones through β-oxidation (Montel et al., 2014). Geranylacetone was present in trace amounts at the end of fermentation.

Correlation Analysis Between Core Microbiota and Volatile Compounds

Screening of Core Microorganisms and Core Flavor Substances

Three criteria were used to identify the major functioning microorganisms during the fermentation process: (i) The abundance of the microorganisms and volatile compounds varied relatively steadily throughout the fermentation process; (ii) the significance of the predictive component (VIP) values for the microorganisms and volatiles was > 1.0; and (iii) the absolute value of the linear correlation coefficient between the distribution of volatile component concentrations and the distribution of relative microbe abundance was > 0.6 (Zheng et al., 2018).

Microorganisms (fungi and bacteria) with the 40 highest relative abundance levels during the spontaneous fermentation of flat peach wine were selected to identify the core microbiota.

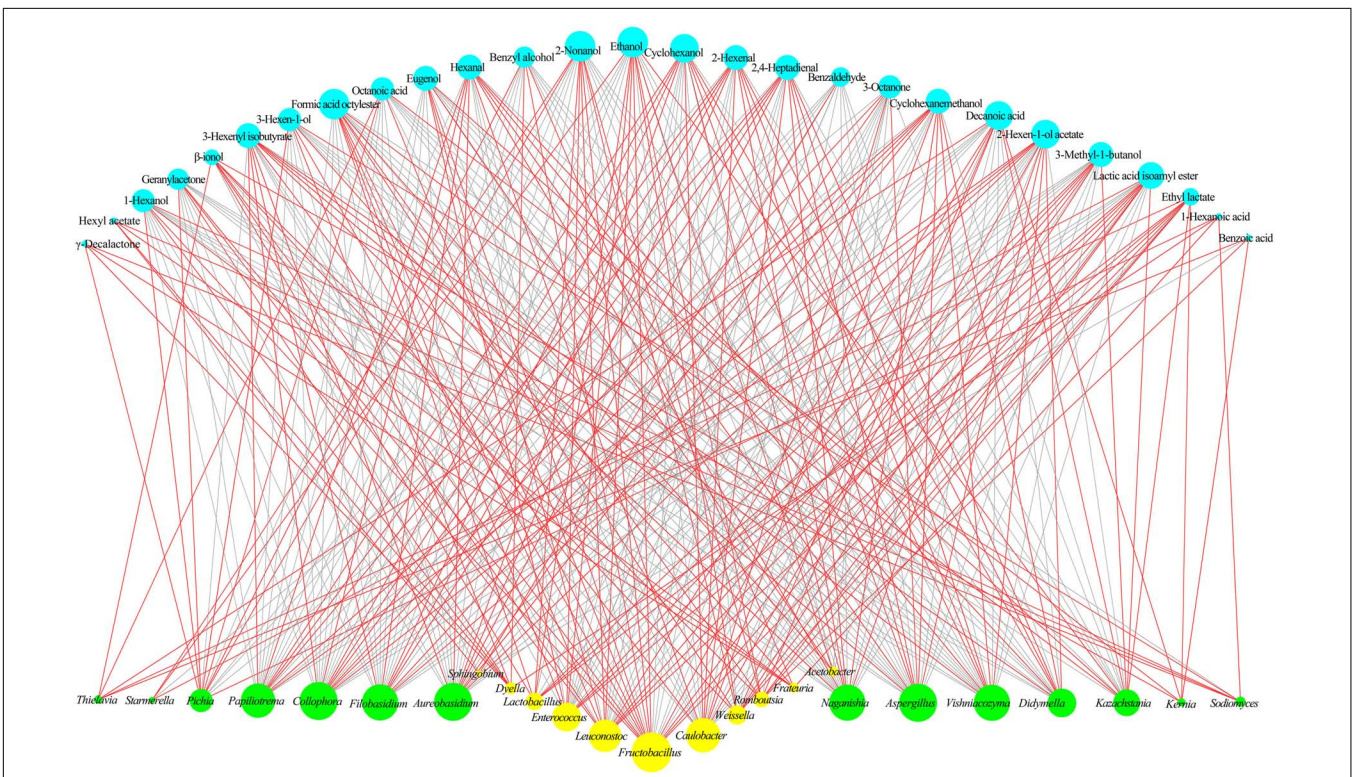

FIGURE 7 | Correlation analyses between the microbiota and volatile compounds during fermentation. The core fungal and bacterial genera are shown in yellow and green, respectively. The core volatile compounds are shown in blue. Red and gray lines indicate positive and negative correlations, respectively.

Variables (x) and attribute variables (y) were assigned to microorganisms and all volatile chemicals, respectively. VIP values were calculated for each fungal and bacterial group at the genus level with respect to the volatile compounds. VIP values > 1 for the fungal and bacterial groups are indicated in red and blue red, respectively, to indicate that the fungal and bacterial groups are important in the synthesis of volatile chemicals (**Supplementary Figure 7**). The VIP values of the analyzed microbes varied between 0.289 and 1.285; 25 microbial genera (VIP > 1.0), including 14 fungi and 11 bacteria, had a significant impact on volatile flavors. The principal contributors to the generation of volatile metabolites during the spontaneous fermentation of flat peach wine included *Lactobacillus*, *Caulobacter*, *Enterococcus*, *Fructobacillus*, *Acetobacter*, *Leuconostoc*, *Kazachstania*, *Pichia*, *Aspergillus*, *Vishniacozyma*, and *Naganishia*. Based on the three criteria listed previously, 27 core volatiles were chosen, including ethanol, benzyl alcohol, and eugenol (**Supplementary Figure 8**).

Microbe and Flavor Correlation Analysis

During the spontaneous fermentation of flat peach wine, the correlation between the core microbiota and the core volatile compounds was investigated (**Figure 7**). Some alcohols and esters are favorably associated with yeasts typically found in fruit wines, such as *Kazachstania* and *Pichia*. *Kazachstania* is a non-*Saccharomyces* yeast that can assimilate lactic acid and hydrolyze glucuronide to provide metabolic substrates for heterofermentative lactic acid bacteria, enabling them to produce acetic acid from fructose (Corsetti et al., 2001). *Kazachstania* has also been shown to exhibit some probiotic effects (Kim et al., 2019). *Pichia* is an important producer of several secondary metabolites (Vicente et al., 2021). In this study, *Aspergillus*, *Filobasidium*, *Aureobasidium*, *Naganishia*, *Papiliotrema*, *Didymella*, *Collophora*, and *Vishniacozyma* were found to be highly correlated with aldehydes, alcohols, and esters (e.g., hexanal, cyclohexanol, and 3-hexenyl isobutyrate). Among them, *Aspergillus* shows a high level of environmental flexibility and is acid- and ethanol-resistant. *Aspergillus* has been used as a fermenting agent in some fermented foods and shown good results. *Vishniacozyma* also deserves attention as the predominant dominant fungi found in the grapes of organic vineyards in Xinjiang (Zhu et al., 2021) and in the ice wine produced in Yili, Xinjiang, China (Chen et al., 2020). Although *Vishniacozyma* was not the predominant dominant flora during the fermentation of flat peach wine, its contribution to volatile compounds cannot be ignored. According to Gramisci et al. (2018), *Vishniacozyma* produces antimicrobial compounds and enzymes to preserve its ecological niche, which may be connected to the generation of aldehydes and acids during fermentation.

Among the bacteria, the lactic acid bacteria *Fructobacillus*, *Leuconostoc*, *Lactobacillus*, and *Weissella* were associated with the production of 2-nonanol, ethanol, 3-methyl-1-butanol, octyl formate, isoamyl lactate, and ethyl lactate. According to reports, these lactic acid bacteria play a crucial role in fermented foods by delivering pleasant sensory and nutritional advantages (Kavitake et al., 2018). During the fermentation of foods, *Weissella* produces esters, organic acids, and short-chain fatty acids (Kamboj et al., 2015). This indicates that during the spontaneous fermentation of flat peach wine, *Weissella* could increase the development of taste compounds. Sumby et al. (2019) noted that *Leuconostoc* was positively correlated with ester production, and *Acetobacter* was positively correlated with organic acids and esters. This may be due to the enzymatic activity of these microbes, since *Acetobacter* synthesizes ethanol dehydrogenase and oxygenase, which stimulate the synthesis of acetic acid and competitively inhibit the enzymes involved in acetic acid catabolism (Trèek et al., 2015). *Sphingobium* was only found to show a high correlation with benzoic acid and β-ionol. Early reports suggest that *Sphingobium* can assimilate a large amount of carbon sources, reducing the level of volatile compounds (Poroyko et al., 2011).

This study shows that native microorganisms present on peach skin reflect the health of the peach and play an important role in the flavor and quality of flat peach wine. To our knowledge, this study is the first to use the HTS approach to evaluate microbial succession during the spontaneous fermentation of flat peach wine. The results of our multivariate analysis revealed a substantial association between bacteria and volatile compounds. However, further investigation using a multi-omics approach will be required in order to verify the relationships between core microorganisms and specific flavors. Moreover, additional studies on the locally dominant flora detected in this study may help elucidate their contribution to the sensory quality of flat peach wine, as well as microbiological safety.

CONCLUSION

In this study, we monitored the dynamic changes in the physicochemical properties, volatile metabolite content, and microbial community succession during the spontaneous fermentation of flat peach wine. Spontaneous fermentation enhances the aromatic characteristics of flat peach wine. HTS revealed a significant decrease in fungal community diversity and a significant increase in bacterial community diversity with an increase in the duration of flat peach wine fermentation. An evaluation of the interactions between volatile components and the core functional microbiota at various fermentation stages revealed that microorganisms are important components of flat peach wine and are responsible for the generation of aromatic and volatile compounds (including many esters and alcohols) that are characteristic of flat peach wine. *Fructobacillus*, *Leuconostoc*, *Lactobacillus*, *Acetobacter*, *Kazachstania*, *Pichia*, and *Aspergillus* are the dominant microbes that contribute to microbial community succession and may also be related to the taste and flavor structure of flat peach wine. The study's findings contribute to an improved understanding of the mechanism underlying the spontaneous fermentation of flat peach wine and lay the foundation for improved quality control during fermentation.

DATA AVAILABILITY STATEMENT

The data presented in the study are deposited in the NCBI repository. Available at: https://www.ncbi.nlm.nih.gov/sra, accession number PRJNA849518 and https://www.ncbi.nlm.nih.gov/biosample, accession numbers, 29093450–29093467.

AUTHOR CONTRIBUTIONS

XX performed the experiments, collected the test data, and drafted the manuscript. YM processed the data. HW and TL provided data for the study. PY, CL, and RZ made the graphs and tables. XS and BW designed the study and revised the manuscript. All authors reviewed the manuscript.

FUNDING

This study was supported by the National Natural Science Foundation of China (No. 31960465), the key areas Programs for Science and Technology Development of Corps (No. 2020AB014), and the Youth Innovative Talents Program of Shihezi University (No. CXBJ202004).

SUPPLEMENTARY MATERIAL

The Supplementary Material for this article can be found online at: https://www.frontiersin.org/articles/10.3389/fmicb.2022.919047/full#supplementary-material

REFERENCES

Abeijón Mukdsi, M. C., Maillard, M. B., Medina, R. B., and Thierry, A. (2018). Ethyl butanoate is synthesised both by alcoholysis and esterification by dairy lactobacilli and propionibacteria. *LWT* 89, 38–43. doi: 10.1016/j.lwt.2017.10.012

Amoros, A., Serrano, M., Riquelme, F., and Romojaro, F. (1989). Levels of ACC and physical and chemical parameters in peach development. *J. Hortic. Sci.* 64, 673–677. doi: 10.1080/14620316.1989.11516007

Battling, S., Wohlers, K., Igwe, C., Kranz, A., Pesch, M., Wirtz, A., et al. (2020). Novel plasmid-free *Gluconobacter oxydans* strains for production of the natural sweetener 5-ketofructose. *Microb. Cell Fact.* 19:54. doi: 10.1186/s12934-020-01310-7

Belda, I., Ruiz, J., Alastruey-Izquierdo, A., Navascués, E., Marquina, D., and Santos, A. (2016). Unraveling the enzymatic basis of wine "Flavorome": a phylo-functional study of wine related yeast species. *Front. Microbiol.* 7:12. doi: 10.3389/fmicb.2016.00012

Bianchi, T., Weesepoel, Y., Koot, A., Iglesias, I., Eduardo, I., Gratacós-Cubarsí, M., et al. (2017). Investigation of the aroma of commercial peach (*Prunus persica* L. Batsch) types by Proton Transfer Reaction-Mass Spectrometry (PTR-MS) and sensory analysis. *Food Res. Int.* 99, 133–146. doi: 10.1016/j.foodres.2017.05.007

Bolyen, E., Rideout, J. R., Dillon, M. R., Bokulich, N. A., Abnet, C. C., Al-Ghalith, G. A., et al. (2019). Reproducible, interactive, scalable and extensible microbiome data science using QIIME 2. *Nat. Biotechnol.* 37, 852–857. doi: 10.1038/s41587-019-0209-9

Budak, N. H., Özdemir, N., and Gökırmaklı, Ç (2021). The changes of physicochemical properties, antioxidants, organic, and key volatile compounds associated with the flavor of peach (*Prunus cerasus* L. Batsch) vinegar during the fermentation process. *J. Food Biochem.* 2021:e13978. doi: 10.1111/jfbc.13978

Chanprasartsuk, O. O., Prakitchaiwattana, C., Sanguandeekul, R., and Fleet, G. H. (2010). Autochthonous yeasts associated with mature pineapple fruits, freshly crushed juice and their ferments; and the chemical changes during natural fermentation. *Bioresour. Technol.* 101, 7500–7509. doi: 10.1016/j.biortech.2010.04.047

Chen, Y., Zhang, W., Yi, H., Wang, B., Xiao, J., Zhou, X., et al. (2020). Microbial community composition and its role in volatile compound formation during the spontaneous fermentation of ice wine made from Vidal grapes. *Proc. Biochem.* 92, 365–377. doi: 10.1016/j.procbio.2020.01.027

Collins, F. W. J., Mesa-Pereira, B., OConnor, P. M., Rea, M. C., Hill, C., and Ross, R. P. (2018). Reincarnation of bacteriocins from the *Lactobacillus* Pangenomic Graveyard. *Front. Microbiol.* 9:1298. doi: 10.3389/fmicb.2018.01298

Corsetti, A., Lavermicocca, P., Morea, M., Baruzzi, F., Tosti, N., and Gobbetti, M. (2001). Phenotypic and molecular identification and clustering of lactic acid bacteria and yeasts from wheat (species *Triticum durum* and *Triticum aestivum*) sourdoughs of Southern Italy. *Int. J. Food Microbiol.* 64, 95–104. doi: 10.1016/S0168-1605(00)00447-5

Decimo, M., Quattrini, M., Ricci, G., Fortina, M. G., Brasca, M., Silvetti, T., et al. (2017). Evaluation of microbial consortia and chemical changes in spontaneous maize bran fermentation. *AMB Exp.* 7:205. doi: 10.1186/s13568-017-0506-y

Fan, Q., Tian, S. P., Xu, Y., Wang, Y., and Jiang, A. L. (2000). Biological control of postharvest brown rot in peach and nectarine fruits by *Bacillus subtilis* (B-912). *Acta Botanica Sinica* 42, 1137–1143.

Fernández-Trujilio, J. P., Martıinez, J. A., and Artes, F. (1998). Modified atmosphere packaging affects the incidence of cold storage disorders and keeps 'flat' peach quality. *Food Res. Int.* 31, 571–579. doi: 10.1016/S0963-9969(99)00030-7

Gao, W., Fan, W., and Xu, Y. (2014). Characterization of the key odorants in light aroma type chinese liquor by gas chromatography-olfactometry, quantitative measurements, aroma recombination, and omission studies. *J. Agric. Food Chem.* 62, 5796–5804. doi: 10.1021/jf501214c

Gramisci, B. R., Lutz, M. C., Lopes, C. A., and Sangorrín, M. P. (2018). Enhancing the efficacy of yeast biocontrol agents against postharvest pathogens through nutrient profiling and the use of other additives. *Biol. Cont.* 121, 151–158. doi: 10.1016/j.biocontrol.2018.03.001

Habe, H., Sato, Y., Tani, H., Matsutani, M., Tanioka, K., Theeragool, G., et al. (2021). Heterologous expression of membrane-bound alcohol dehydrogenase-encoding genes for glyceric acid production using Gluconobacter sp. CHM43 and its derivatives. *Appl. Microbiol. Biotechnol.* 105, 6749–6758. doi: 10.1007/s00253-021-11535-0

Hao, D. C., Song, S. M., Mu, J., Hu, W. L., and Xiao, P. G. (2016). Unearthing microbial diversity of Taxus rhizosphere via MiSeq high-throughput amplicon sequencing and isolate characterization. *Sci. Rep.* 6:22006. doi: 10.1038/srep22006

Hu, K., Jin, G. J., Xu, Y. H., and Tao, Y. S. (2018). Wine aroma response to different participation of selected *Hanseniaspora uvarum* in mixed fermentation with *Saccharomyces cerevisiae*. *Food Res. Int.* 108, 119–127. doi: 10.1016/j.foodres.2018.03.037

Huang, Z. R., Hong, J. L., Xu, J. X., Li, L., Guo, W. L., Pan, Y. Y., et al. (2018). Exploring core functional microbiota responsible for the production of volatile flavour during the traditional brewing of Wuyi Hong Qu glutinous rice wine. *Food Microbiol.* 76, 487–496. doi: 10.1016/j.fm.2018.07.014

Izquierdo-Llopart, A., Carretero, A., and Saurina, J. (2020). Organic acid profiling by liquid chromatography for the characterization of base vines and sparkling wines. *Food Anal. Methods* 13, 1852–1866. doi: 10.1007/s12161-020-01808-1

Jia, L., Huang, X., Zhao, W., Wang, H., and Jing, X. (2020). An effervescence tablet-assisted microextraction based on the solidification of deep eutectic solvents for the determination of strobilurin fungicides in water, juice, wine, and vinegar samples by HPLC. *Food Chem.* 317:126424. doi: 10.1016/j.foodchem.2020.126424

Joshi, V. K., Panesar, P. S., Rana, V. S., and Kaur, S. (2017). "Chapter 1 - Science and Technology of Fruit Wines: An Overview," in *Science and Technology of Fruit Wine Production*, eds M. R. Kosseva, V. K. Joshi, and P. S. Panesar (San Diego: Academic Press), 1–72.

Jung, M. Y., Kim, T. W., Lee, C., Kim, J. Y., Song, H. S., Kim, Y. B., et al. (2018). Role of jeotgal, a Korean traditional fermented fish sauce, in microbial dynamics and metabolite profiles during kimchi fermentation. *Food Chem.* 265, 135–143. doi: 10.1016/j.foodchem.2018.05.093

Kamboj, K., Vasquez, A., and Balada-Llasat, J. M. (2015). Identification and significance of *Weissella* species infections. *Front. Microbiol.* 6:204. doi: 10.3389/fmicb.2015.01204

Kavitake, D., Kandasamy, S., Devi, P. B., and Shetty, P. H. (2018). Recent developments on encapsulation of lactic acid bacteria as potential starter culture in fermented foods – A review. *Food Biosci.* 21, 34–44. doi: 10.1016/j.fbio.2017.11.003

Kim, J. H., Kim, K., Kanjanasuntree, R., and Kim, W. (2019). *Kazachstania turicensis* CAU Y1706 ameliorates atopic dermatitis by regulation of the gut–skin axis. *J. Dairy Sci.* 102, 2854–2862. doi: 10.3168/jds.2018-15849

Kour, D., Rana, K. L., Kaur, T., Yadav, N., Yadav, A. N., Kumar, M., et al. (2021). Biodiversity, current developments and potential biotechnological applications of phosphorus-solubilizing and mobilizing microbes: a review. *Pedosphere* 31, 43–75. doi: 10.1016/S1002-0160(20)60057-1

Li, Y., and Wang, L. (2020). Genetic resources, breeding programs in china, and gene mining of peach: a review. *Horticult. Plant J.* 6, 205–215. doi: 10.1016/j.hpj.2020.06.001

Liu, Y., Rousseaux, S., Tourdot-Maréchal, R., Sadoudi, M., Gougeon, R., Schmitt-Kopplin, P., et al. (2017). Wine microbiome: a dynamic world of microbial interactions. *Crit. Rev. Food Sci. Nutr.* 57, 856–873. doi: 10.1080/10408398.2014.983591

Lu, Y., Guan, X., Li, R., Wang, J., Liu, Y., Ma, Y., et al. (2021). Comparative study of microbial communities and volatile profiles during the inoculated and spontaneous fermentation of persimmon wine. *Proc. Biochem.* 100, 49–58. doi: 10.1016/j.procbio.2020.09.023

Ma, R., Yu, M., Du, P., Guo, H., and Song, H. (2002). *Evaluation of germplasm resources and breeding of flat peach*. Leuven: International Society for Horticultural Science (ISHS), 161–167.

Mason, A. B., and Dufour, J. P. (2000). Alcohol acetyltransferases and the significance of ester synthesis in yeast. *Yeast* 16, 1287–1298. doi: 10.1002/1097-0061(200010)16:14<1287::AID-YEA613>3.0.CO;2-I

Mato, I., Suárez-Luque, S., and Huidobro, J. F. (2005). A review of the analytical methods to determine organic acids in grape juices and wines. *Food Res. Int.* 38, 1175–1188. doi: 10.1016/j.foodres.2005.04.007

McDonald, L. C., Fleming, H. P., and Hassan, H. M. (1990). Acid tolerance of *Leuconostoc mesenteroides* and *Lactobacillus plantarum*. *Appl. Environ. Microbiol.* 56, 2120–2124. doi: 10.1128/aem.56.7.2120-2124.1990

Megías, E., Megías, M., OlleroFrancisco, J., and Hungria, M. (2016). Draft genome sequence of pantoea ananatis strain AMG521, a rice plant growth-promoting bacterial endophyte isolated from the guadalquivir marshes in southern spain. *Genome Announc.* 4, e01615–e01681. doi: 10.1128/genomeA.01681-15

Meng, Y., Chen, X., Sun, Z., Li, Y., Chen, D., Fang, S., et al. (2021). Exploring core microbiota responsible for the production of volatile flavor compounds during the traditional fermentation of Koumiss. *LWT* 135:110049. doi: 10.1016/j.lwt.2020.110049

Merico, A., Sulo, P., Piškur, J., and Compagno, C. (2007). Fermentative lifestyle in yeasts belonging to the Saccharomyces complex. *FEBS J.* 274, 976–989. doi: 10.1111/j.1742-4658.2007.05645.x

Miller, G. L. (1959). Use of dinitrosalicylic acid reagent for determination of reducing sugar. *Anal. Chem.* 31, 420–428. doi: 10.1021/ac60147a030/

Minervini, F., Lattanzi, A., De Angelis, M., Celano, G., and Gobbetti, M. (2015). House microbiotas as sources of lactic acid bacteria and yeasts in traditional Italian sourdoughs. *Food Microbiol.* 52, 66–76. doi: 10.1016/j.fm.2015.06.009

Montel, M. C., Buchin, S., Mallet, A., Delbes-Paus, C., Vuitton, D. A., Desmasures, N., et al. (2014). Traditional cheeses: rich and diverse microbiota with associated benefits. *Int. J. Food Microbiol.* 177, 136–154. doi: 10.1016/j.ijfoodmicro.2014.02.019

Perkins-Veazie, P., Roe, N., Lasswell, J., and McFarland, M. J. (1999). Temperature manipulation improves postharvest quality of a mid-season peach. *J. Food Qual.* 22, 75–84. doi: 10.1111/j.1745-4557.1999.tb00928.x

Philippe, C., Krupovic, M., Jaomanjaka, F., Claisse, O., Petrel, M., and Le Marrec, C. (2018). Bacteriophage GC1, a novel tectivirus infecting gluconobacter cerinus, an acetic acid bacterium associated with wine-making. *Viruses* 10:39. doi: 10.3390/v10010039

Poroyko, V., Morowitz, M., Bell, T., Ulanov, A., Wang, M., Donovan, S., et al. (2011). Diet creates metabolic niches in the" inmature gut" that shape microbial communities. *Nutr. Hosp.* 26, 1283–1295. doi: 10.1590/S0212-16112011000600015

Procopio, S., Qian, F., and Becker, T. (2011). Function and regulation of yeast genes involved in higher alcohol and ester metabolism during beverage fermentation. *Eur. Food Res. Technol.* 233:721. doi: 10.1007/s00217-011-1567-9

Raybaudi-Massilia, R. M., Mosqueda-Melgar, J., Soliva-Fortuny, R., and Martín-Belloso, O. (2009). Control of pathogenic and spoilage microorganisms in fresh-cut fruits and fruit juices by traditional and alternative natural antimicrobials. *Compr. Rev. Food Sci.* 8, 157–180. doi: 10.1111/j.1541-4337.2009.00076.x

Ross, B. D., Verster, A. J., Radey, M. C., Schmidtke, D. T., Pope, C. E., Hoffman, L. R., et al. (2019). Human gut bacteria contain acquired interbacterial defence systems. *Nature* 575, 224–228. doi: 10.1038/s41586-019-1708-z

Ryan, J., Hutchings, S. C., Fang, Z., Bandara, N., Gamlath, S., Ajlouni, S., et al. (2020). Microbial, physico-chemical and sensory characteristics of mango juice-enriched probiotic dairy drinks. *Int. J. Dairy Technol.* 73, 182–190. doi: 10.1111/1471-0307.12630

Sánchez, G., Venegas-Calerón, M., Salas, J. J., Monforte, A., Badenes, M. L., and Granell, A. (2013). An integrative "omics" approach identifies new candidate genes to impact aroma volatiles in peach fruit. *BMC Genom.* 14:343. doi: 10.1186/1471-2164-14-343

Santos, M. C., Golt, C., Joerger, R. D., Mechor, G. D., Mourão, G. B., and Kung, L. (2017). Identification of the major yeasts isolated from high moisture corn and corn silages in the United States using genetic and biochemical methods. *J. Dairy Sci.* 100, 1151–1160. doi: 10.3168/jds.2016-11450

Shi, W. K., Wang, J., Chen, F. S., and Zhang, X. Y. (2019). Effect of *Issatchenkia terricola* and *Pichia kudriavzevii* on wine flavor and quality through simultaneous and sequential co-fermentation with Saccharomyces cerevisiae. *LWT* 116:108477. doi: 10.1016/j.lwt.2019.108477

Sivilotti, P., Falchi, R., Herrera, J. C., Škvarè, B., Butinar, L., Sternad Lemut, M., et al. (2017). Combined effects of early season leaf removal and climatic conditions on aroma precursors in sauvignon blanc grapes. *J. Agric. Food Chem.* 65, 8426–8434. doi: 10.1021/acs.jafc.7b03508

Sumby, K. M., Bartle, L., Grbin, P. R., and Jiranek, V. (2019). Measures to improve wine malolactic fermentation. *Appl. Microbiol. Biotechnol.* 103, 2033–2051. doi: 10.1007/s00253-018-09608-8

Suzuki, A., Muraoka, N., Nakamura, M., Yanagisawa, Y., and Amachi, S. (2018). Identification of undesirable white-colony-forming yeasts appeared on the surface of Japanese kimchi. *Biosci. Biotechnol. Biochem.* 82, 334–342. doi: 10.1080/09168451.2017.1419853

Tan, F., Wang, P., Zhan, P., and Tian, H. (2022). Characterization of key aroma compounds in flat peach juice based on gas chromatography-mass spectrometry-olfactometry (GC-MS-O), odor activity value (OAV), aroma recombination, and omission experiments. *Food Chem.* 366:130604. doi: 10.1016/j.foodchem.2021.130604

Tempère, S., Marchal, A., Barbe, J. C., Bely, M., Masneuf-Pomarede, I., Marullo, P., et al. (2018). The complexity of wine: clarifying the role of microorganisms. *Appl. Microbiol. Biotechnol.* 102, 3995–4007. doi: 10.1007/s00253-018-8914-8

Trèek, J., Mira, N. P., and Jarboe, L. R. (2015). Adaptation and tolerance of bacteria against acetic acid. *Appl. Microbiol. Biotechnol.* 99, 6215–6229. doi: 10.1007/s00253-015-6762-3

Tufariello, M., Capone, S., and Siciliano, P. (2012). Volatile components of Negroamaro red wines produced in Apulian Salento area. *Food Chem.* 132, 2155–2164. doi: 10.1016/j.foodchem.2011.11.122

Tufariello, M., Pati, S., D'Amico, L., Bleve, G., Losito, I., and Grieco, F. (2019). Quantitative issues related to the headspace-SPME-GC/MS analysis of volatile compounds in wines: the case of Maresco sparkling wine. *LWT* 108, 268–276. doi: 10.1016/j.lwt.2019.03.063

van Rijswijck, I. M. H., Kruis, A. J., Wolkers-Rooijackers, J. C. M., Abee, T., and Smid, E. J. (2019). Acetate-ester hydrolase activity for screening of the variation in acetate ester yield of Cyberlindnera fabianii, Pichia kudriavzevii and Saccharomyces cerevisiae. *LWT* 104, 8–15. doi: 10.1016/j.lwt.2019.01.019

Vicente, J., Calderón, F., Santos, A., Marquina, D., and Benito, S. (2021). High potential of *pichia kluyveri* and other *pichia* species in wine technology. *Int. J. Mol. Sci.* 22:1196. doi: 10.3390/ijms22031196

Wang, L., Dou, G., Guo, H., Zhang, Q., Qin, X., Yu, W., et al. (2019). Volatile organic compounds of *Hanseniaspora uvarum* increase strawberry fruit flavor and defense during cold storage. *Food Sci. Nutr.* 7, 2625–2635. doi: 10.1002/fsn3.1116

Wang, P., Mao, J., Meng, X., Li, X., Liu, Y., and Feng, H. (2014). Changes in flavour characteristics and bacterial diversity during the traditional fermentation of Chinese rice wines from Shaoxing region. *Food Cont.* 2014, 58–63. doi: 10.1016/j.foodcont.2014.03.018

Wang, P., Tian, H., Tan, F., Liu, Y., Yu, B., and Zhan, P. (2020). Impact of commercial processing on volatile compounds and sensory profiles of flat peach juices by PLSR and BP network. *J. Food Proc. Preserv.* 44:e14575. doi: 10.1111/jfpp.14575

Wang, X., Du, H., Zhang, Y., Xu, Y., and Björkroth, J. (2018). Environmental microbiota drives microbial succession and metabolic profiles during chinese liquor fermentation. *Appl Environ. Microbiol.* 84, 2369–2317. doi: 10.1128/AEM.02369-17

Wang, Y., Yang, C., Li, S., Yang, L., Wang, Y., Zhao, J., et al. (2009). Volatile characteristics of 50 peaches and nectarines evaluated by HP-SPME with GC-MS. *Food Chem.* 116, 356–364. doi: 10.1016/j.foodchem.2009.02.004

Xu, X., Li, T., Ji, Y., Jiang, X., Shi, X., and Wang, B. (2021). Origin, succession, and control of biotoxin in wine. *Front Microbiol.* 12:3391. doi: 10.3389/fmicb.2021.703391

Xu, Z., Walker, M. E., Zhang, J., Gardner, J. M., Sumby, K. M., and Jiranek, V. (2021). Exploring the diversity of bacteriophage specific to *Oenococcus oeni* and *Lactobacillus spp* and their role in wine production. *Appl. Microbiol. Biotechnol.* 105, 8575–8592. doi: 10.1007/s00253-021-11509-2

Yang, X., Hu, W., Xiu, Z., Jiang, A., Yang, X., Sarengaowa, et al. (2020). Microbial dynamics and volatilome profiles during the fermentation of Chinese northeast sauerkraut by *Leuconostoc mesenteroides* ORC 2 and *Lactobacillus plantarum* HBUAS 51041 under different salt concentrations. *Food Res. Int.* 130:108926. doi: 10.1016/j.foodres.2019.108926

Yang, Y., Hu, W., Xia, Y., Mu, Z., Tao, L., Song, X., et al. (2020). Flavor formation in chinese rice wine (huangjiu): impacts of the flavor-active microorganisms, raw materials, and fermentation technology. *Front. Microbiol.* 11:247. doi: 10.3389/fmicb.2020.580247

Zhang, B., Shen, J. Y., Wei, W. W., Xi, W. P., Xu, C. J., Ferguson, I., et al. (2010). Expression of genes associated with aroma formation derived from the fatty acid pathway during peach fruit ripening. *J. Agric. Food Chem.* 58, 6157–6165. doi: 10.1021/jf100172e

Zheng, X., Liu, F., Shi, X., Wang, B., Li, K., Li, B., et al. (2018). Dynamic correlations between microbiota succession and flavor development involved in the ripening of Kazak artisanal cheese. *Food Res. Int.* 105, 733–742. doi: 10.1016/j.foodres.2017.12.007

Zhu, J., and Xiao, Z. (2019). Characterization of the key aroma compounds in peach by gas chromatography-olfactometry, quantitative measurements and sensory analysis. *Eur. Food Res. Technol.* 245, 129–141. doi: 10.1007/s00217-018-3145-x

Zhu, L., Li, T., Xu, X., Shi, X., and Wang, B. (2021). Succession of fungal communities at different developmental stages of cabernet sauvignon grapes from an organic vineyard in xinjiang. *Front. Microbiol.* 12:718261. doi: 10.3389/fmicb.2021.718261

Conflict of Interest: The authors declare that the research was conducted in the absence of any commercial or financial relationships that could be construed as a potential conflict of interest.

Publisher's Note: All claims expressed in this article are solely those of the authors and do not necessarily represent those of their affiliated organizations, or those of the publisher, the editors and the reviewers. Any product that may be evaluated in this article, or claim that may be made by its manufacturer, is not guaranteed or endorsed by the publisher.

frontiers | Frontiers in Microbiology

MINI REVIEW
published: 07 July 2022
doi: 10.3389/fmicb.2022.930658

Humanization of Yeasts for Glycan-Type End-Products

Xingjuan Li, Jianlie Shen, Xingqiang Chen, Lei Chen, Shulin Wan, Xingtao Qiu, Ke Chen, Chunmiao Chen and Haidong Tan**

Guangzhou Shenjingya Agricultural Technology Co., Ltd., Guangzhou, China

Yeasts are often considered microorganisms for producing human therapeutic glycosylated end-products at an industrial scale. However, the products with non-humanized glycans limited their usage. Therefore, various methods to develop humanized glycosylated end-products have been widely reported in yeasts. To make full use of these methods, it is necessary to summarize the present research to find effective approaches to producing humanized products. The present research focuses on yeast species selection, glycosyltransferase deletion, expression of endoglycosidase, and expression of proteins with galactosylated and or sialylated glycans. Nevertheless, the yeasts will have growth defects with low bioactivity when the key enzymes are deleted. It is necessary to express the corresponding repairing protein. Compared with N-glycosylation, the function of yeast protein O-glycosylation is not well-understood. Yeast proteins have a wide variety of O-glycans in different species, and it is difficult to predict glycosylation sites, which limits the humanization of O-glycosylated yeast proteins. The future challenges include the following points: there are still many important potential yeasts that have never been tried to produce glycosylated therapeutic products. Their glycosylation pathway and related mechanisms for producing humanized glycosylated proteins have rarely been reported. On the other hand, the amounts of key enzymes on glycan pathways in human beings are significantly more than those in yeasts. Therefore, there is still a challenge to produce a large body of humanized therapeutic end-products in suitable yeast species, especially the protein with complex glycans. CRISPR-Cas9 system may provide a potential approach to address the important issue.

Keywords: humanized glycosylation, yeasts, genetically engineering, end-products, galactosylated complex-type glycans

OPEN ACCESS

Edited by:
Wanping Chen,
University of Göttingen, Germany

Reviewed by:
Kentaro Inokuma,
Kobe University, Japan

****Correspondence:***
Jianlie Shen
sjlccm@126.com
Haidong Tan
1809050351@qq.com

Specialty section:
This article was submitted to Food Microbiology, a section of the journal Frontiers in Microbiology

Received: *28 April 2022*
Accepted: *31 May 2022*
Published: *07 July 2022*

Citation:
Li X, Shen J, Chen X, Chen L, Wan S, Qiu X, Chen K, Chen C and Tan H (2022) Humanization of Yeasts for Glycan-Type End-Products. Front. Microbiol. 13:930658. doi: 10.3389/fmicb.2022.930658

INTRODUCTION

Engineering Escherichia coli has been widely used for the production of human advanced biopharmaceutical products (Arico et al., 2013). However, the recombinant proteins in non-glycosylated forms often suffer from short-term half-life, low activity, rapid clearance, and side effects. Pharmacokinetic studies in Wistar rats revealed 1.3-fold increase in plasma half-life for glycosylated IFN α2b compared to standard IFN α2b produced by *E. coli* (Baghban et al., 2018). Therefore, it is necessary to develop humanized glycosylated therapeutic products (Cheon et al., 2012). Yeasts are often firstly considered microorganisms for producing human therapeutic glycosylated end-products at an industrial scale. Long historical usage, vast data, and rich experiences have paved the way for *Saccharomyces cerevisiae* as an important expression

platform and a microbial cell factory for producing human therapeutic products (Corbacho et al., 2005). In *S. cerevisiae*, the recombinant proteins are often typically hypermannosylated ($Man_{>50}GlcNAc_2$), which also affects the half-life, tissue distribution, and immunogenicity of the end-products. It is critical to developing the engineering of *S. cerevisiae* for producing the proteins with humanized glycosylation patterns by modulating mannosyltransferase and or other enzymes responsible for the chain biosynthesis of N-glycans (Crauwels et al., 2015).

Pichia pastoris expression system is one of the most popular tools for producing a recombinant protein with many advantages, including the low incidence of hyperglycosylated, appropriate folding in the endoplasmic reticulum (ER), and secretion expression with high purity (De Pourcq et al., 2012). Much effort has been paid to improving the N-glycosylation pathway of *P. pastoris* to mimic the human N-glycosylation pathway. Successful utilization of the CRISPR-Cas9 system has been used for the humanization of the glycosylation pathways in *P. pastoris* by disrupting och1 and alg3 (mannosyltransferase) genes (Dolashka-Angelova et al., 2010). *Kluyveromyces lactis* is a food-grade yeast commonly used for industrial applications. Gene modification has been applied to construct a humanized N-linked glycosylation pathway in *K. lactis*. Besides the above conventional yeast species, other established yeast expression systems include *Hansenula polymorpha* (Gündüz Ergün et al., 2019; Fukunaga et al., 2021a,b; Giorgetti et al., 2021; Gallo et al., 2022), *Yarrowia lipolytica* (Hamilton et al., 2013; Karbalaei et al., 2020; Jin et al., 2021), *Schizosaccharomyces pombe* (Kim et al., 2006; Katla et al., 2019; Lawton et al., 2021), *Kluyveromyces marxianus* (Lee et al., 2020), *Candida albicans* (Li et al., 2019), and *Zygosaccharomyces cidri* (Liu et al., 2009). The strategies to produce humanized glycosylated end-products were explored by using these yeast species.

N-GLYCOSYLATED FORMS OF PROTEINS IN YEASTS AND MAMMALIAN CELLS

The N-glycosylation has been widely studied in yeast species, indicating that the glycosylated signaling pathway is similar to that in mammalian cells. $Man_3GlcNAc_2$ is the common core of eukaryotic N-glycans, which further yields the $Man_8GlcNAc_2$ core *via* oligosaccharyltransferase. $Man_8GlcNAc_2$-Asn-protein is produced in the endoplasmic reticulum (ER) and conveyed to Golgi (**Figure 1A**). In Golgi, there is a significant difference in the glycosylation formation of proteins, $Man_8GlcNAc_2$ glycan is truncated into $Man_5GlcNAc_2$ *via* mannosidase in mammalian cells (**Figure 1B**) while $Man_8GlcNAc_2$ in yeasts is extended to form $Man_9GlcNAc_2$ and hypermannosylation *via* mannosyl transferase (**Figure 1A**), which will be cleared in human blood because of its non-human glycan (Ma et al., 2019). Genome-wide analysis for *S. cerevisiae* shows 19 different genes associated with mannoprotein-linked oligosaccharide generation, including CAX4 (dolichyl pyrophosphate (Dol-PP) phosphatase), OST4 (oligosaccharyltransferase), OCH1/LDB12 (Mannosyltransferase), MNN(Mannosyltransferase)2/LDB8, MNN4, MNN5, KTR6/MNN6, ANP1/MNN8, MNN9, MNN10, MNN11, GDA1 (Golgi GDPase), HOC1/LDB12 (glycosyltransferase), VAN1/LDB13 (glycosylation of secreted invertase), OST3, RHK1/ALG(mannosyltransferase)3, ALG5, ALG6, and ALG9, which mainly existed in nucleic ER and Golgi ER (**Figure 1A**; Narimatsu et al., 2019). Most yeast species produce the glycosylated protein with mannose units with long chains.

Comparatively, the transferases in mammalian cells are significantly more than those in *S. cerevisiae*. More than 170 human glycosyltransferases have been found in the glycosylation pathway (**Figure 1B**; Oh et al., 2008). Most mammals produce the glycosylated protein with the mannose, galactose, and sialic acid N-glycolylneuraminic acid (Neu5Gc) units in the short-chain (**Figure 1B**). Therefore, the glycosylated proteins in yeast species are significantly longer than those in mammalian cells while the ingredients in mammalian cells are more complex than those in yeast species.

O-GLYCOSYLATED FORMS OF PROTEINS IN YEASTS AND MAMMALIAN CELLS

Compared with N-glycosylation, the function of yeast protein O-glycosylation is poorly understood. Yeast proteins have a wide variety of O-glycans in different species, and it is difficult to predict glycosylation sites, which limits the humanization of O-glycosylated yeast proteins. The first mannose linked to yeast protein is provided by polyterpenoid phosphate mannose (Dol-P-Man). Dol-P-Man is synthesized from guanosine diphosphate-mannose (GDP-Man) and polyterpenoid phosphate mannose (Dol-P) under the catalysis of Dol-P-Man synthase, and then, enters the endoplasmic reticulum to initiate protein O-glycosylation (**Figure 1C**). In contrast, mucin-type O-glycan synthesis in human cells starts with an N-acetylgalactosamine (GalNAc) residue attached with specific Ser/Thr residues with eight-type cores. The initiating residues are further elongated with a variety of monosaccharides. In the Golgi apparatus, the elongation of oligosaccharides is catalyzed by GalNAc transferases using UDP-GalNAc as a donor (**Figure 1D**). However, manufacturing the O-glycosylation pathway is not as progressive as N-glycosylation. Humanized mucin-type O-glycans had been identified in *S. cerevisiae* to provide a biosynthetic pathway for UDP-GalNAc and UDP-Gal/GalNAc-4-epimerase production (Luu et al., 2019).

AN EXPLORATION OF STRATEGIES TO REGULATE GLYCOSYLATION OF END-PRODUCTS IN YEASTS

Although yeasts have the potential to produce various types of industrial proteins, their failures to produce humanized glycoproteins limit their usage. Therefore, it is necessary to explore the strategies to regulate glycan forms of end-products in yeasts.

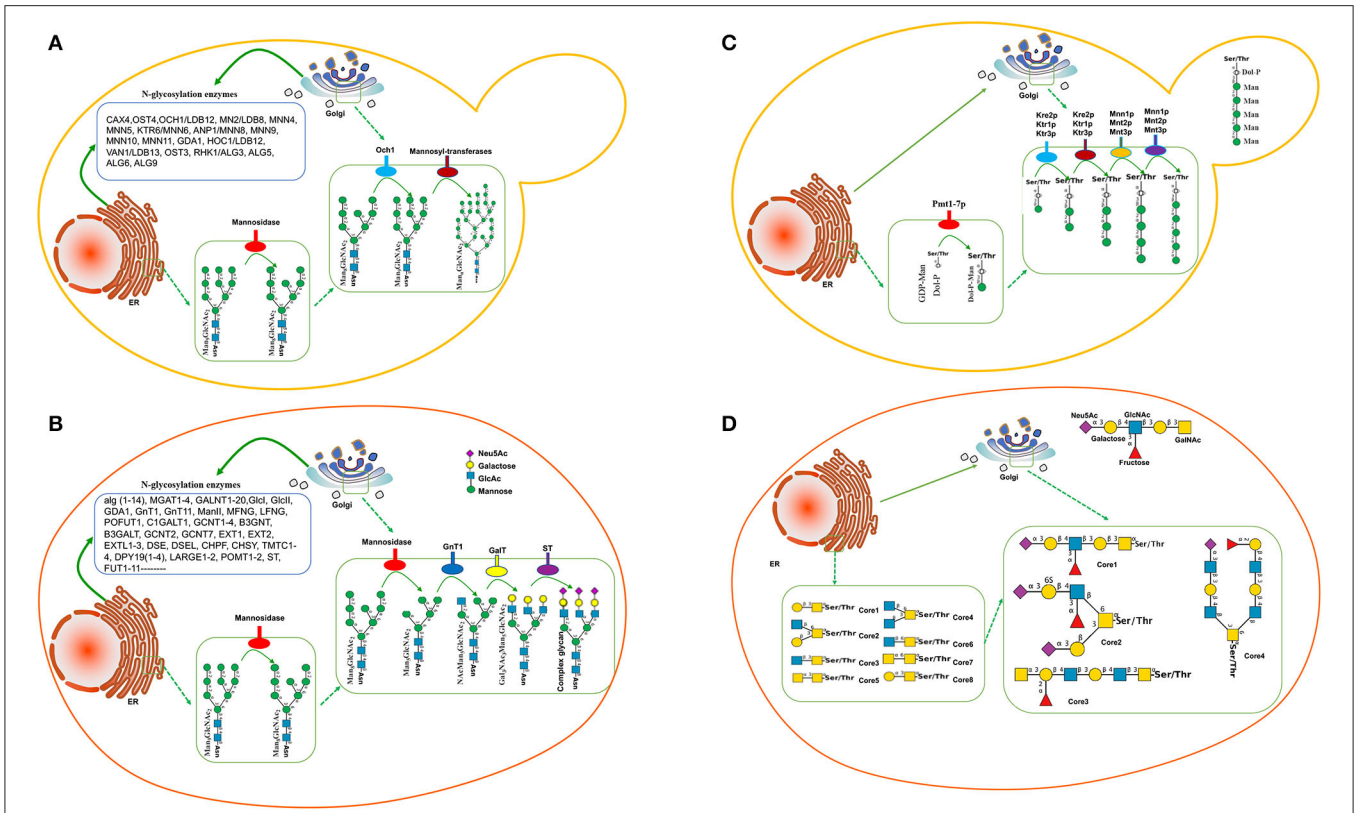

FIGURE 1 | Glycosylation pathway between yeasts and mammalian cells. **(A)** N-glycosylation pathway in yeasts. **(B)** N-glycosylation pathway in mammalian cells. **(C)** O-glycosylation pathway in *Saccharomyces cerevisiae*. In the ER, the first mannose residue is added *via* protein-O-mannosyltransferases (Pmt1-7p). O-glycosylation is further elongated in the Golgi *via* several mannosyltransferases. **(D)** Mucin-type O-glycan synthesis in human cells.

Deletion of Mannosyltransferase

The glycan chains in yeast species are often longer than those in human beings. To fix the flaw, the key enzyme mannosyltransferase, which existed in N-glycosylation pathways, is often considered to be blocked. Och1(α-1,6-mannosyltransferase) and MNN1 (α-1,3-mannosyltransferase) produce mostly high-mannose glycans of the Man8GlcNAc2 (**Figure 1A**). Inactivation of the OCH1 gene is often an effective approach to eliminate hypermannosylation in *H. polymorpha* (Fukunaga et al., 2021b; Gallo et al., 2022), *K. lactis* (Park et al., 2011), *P. pastoris* (Ma et al., 2019), *S. cerevisiae* (Piirainen et al., 2022), and *Y. lipolytica* (Karbalaei et al., 2020), which results in the expressed proteins with short-chain glycan from $Man_3GlcNAc_2$ to $Man_{14}GlcNAc_2$ (**Table 1**). Especially in *H. polymorpha*, the deletion of OCH1 and alg3, and/or alg3 and alg11 can produce the protein with $Man_3GlcNAc_2$ (Gündüz Ergün et al., 2019; Fukunaga et al., 2021b). The expression of alg6 in *S. pombe* also produces the short-chain glycoprotein (Hamilton et al., 2013).

Overexpression of Repairing Proteins

Protein glycosylation is often associated with cell wall integrity and its disruption may affect yeast bioactivity. The yeasts will have growth defects and low bioactivity when the key enzymes are deleted. Inactivation of the OCH1 gene will damage *S. cerevisiae* viability. The overexpression of glycosylphosphatidylinositol (GPI)-anchored protein can restore the bioactivity (**Table 1**; Prabhakar et al., 2019). Therefore, overexpression of repairing proteins may be an effective approach to improve the yields of humanized products.

Overexpression of Endoglycosidase

The overexpression of endoglycosidase α-1,2-mannosidase can prevent the glycan chain from further extending in *P. pastoris* (Ma et al., 2019). ENGase isoform possesses great hydrolytic activities toward high-mannose N-glycans and short-chain glycan was produced after the ENGase was expressed in *P. pastoris* (Prill et al., 2005). EndoS2, an IgG-specific endoglycosidase, also has a similar function to ENGase and was expressed in *S. cerevisiae* to produce a single N-acetylglucosamine residue (Ryckaert et al., 2005).

Production of Galactosylated Protein

In mammalian cells, GlcNAc sugars are attached to the paucimannose core with 2-4 GlcNac sugars, which can be further prolonged by adding galactose *via* GalTI (β-1,4-galactosyltransferase I). GalTI was expressed in *H. polymorpha* and increased the formation of galactosylated complex-type glycans (Giorgetti et al., 2021). A human galactosyltransferase

TABLE 1 | Humanized glycoprotein expression in genetically modifying yeasts or naturally yeasts.

Yeast species	Δ Glycosyltransferases (overexpression of enzyme)	End-products and manosylated types			References
		Expressed protein	Wild species	Mutant species	
Hansenula polymorpha	OCH1, alg3(GnT1)	α-1,2 mannosidase		$GlcNAc_1Man_5GlcNAc_2$ $GlcNAc_1Man_3GlcNAc_2$	Fukunaga et al., 2021a
	OCH1, alg3	α-1,2 mannosidase		$Man_3GlcNAc_2$	Fukunaga et al., 2021b
	OCH1, OCR1	α-1,2 mannosidase	$Man_8GlcNAc_2$	$Man_5GlcNAc_2$	Gallo et al., 2022
	alg3, alg11(GnTI, GnTII, GalTI)			$Gal_2GlcNAc_2Man_3GlcNAc_2$	Giorgetti et al., 2021
	alg3, alg11	Glucose oxidase		$Man_3GlcNAc_2$	Gündüz Ergün et al., 2019
Kluyveromyces cicerisporus		Exo-inulinase		$Man_{3-9}GlcNAc_2$	Vervecken et al., 2004
Kluyveromyces lactis	OCH1, MNN1	HAS, GM–CSF	$Man_{>30}GlcNAc_2$	$Man_{9-11}GlcNAc_2$, $Man_{13-14}GlcNAc_2$	Wang et al., 2013
	KlOCH1	HAS, GAA		Shorter β1,6-glucan and more branches	Park et al., 2011
	KlPMR1	HAS	HGS	NHGS	Wang et al., 2020
Kluyveromyces marxianus		Cu/Zn SOD	$Man_5GlcNAc_2$		Lee et al., 2020
Pichia pastoris	OCH1 (MS/AT/GT)		Up to $Man_{40}GlcNAc_2$	$Man_5GlcNAc_2$ $GlcNAcMan_5GlcNAc_2$	Ma et al., 2019
	(Endo-T)	IgG1-Fc	Up to $Man_{40}GlcNAc_2$	*N*-GlcNAc	Prill et al., 2005
	Glycoengineered strain	IFN α2b		SuperMan5	Baghban et al., 2018
	PMT1, PMT5	TG		$Man1_2GlcNAc_2$ ~ $Man16GlcNAc_2$	Watanasrisin et al., 2016
	alg3, alg11(GTFU)	CWP and SP		$Man_3GlcNAc_2$ GNG	Selas Castiñeiras et al., 2018
Saccharomyces cerevisiae	(AST)			SOG	Song et al., 2010
	(Endos2)	Fc γ receptors		SNR	Ryckaert et al., 2005
	OCH1, MNN1, alg3			$Man_5GlcNAc_2$ $Man_8GlcNAc_2$	Piirainen et al., 2022
	Pmd1 null mutant	P-glycoprotein		No glycosylation	Xu et al., 2017
Schizosaccharomyces pombe	OCH1 (ST)			Glycan with sialic acid	Shenoy et al., 2021
			3 Glc and 9 Man	5 Man	Katla et al., 2019
	Gmn2			DPGNO	Kim et al., 2006
	Gmh1p, Gmh2p Gmh3p, Gmh6p			Downregulated galactosylation	Lawton et al., 2021
Yarrowia lipolytica	(alg6)	α-1,2-mannosidase		$Man_3GlcNAc_2$	Hamilton et al., 2013
	MPO1	CWPs			Jin et al., 2021
	OCH1	Lipase	$Man_{12}GlcNAc_2$	$Man_8GlcNAc_2$	Karbalaei et al., 2020

alg, asparagine-linked glycosylation protein; Complex glycan, the glycan with galactose and sialic acid; AST, β-1,2-N-acetylglucosaminyltransferase 1; CWPs, crude cell wall mannoproteins; Cu/Zn SOD, Cu/Zn-superoxide dismutase; CWP and SP, cell wall proteins and secreted proteins; DPGNO, defects in protein glycosylation of N-linked oligosaccharides; EndoS2, An IgG-specific endoglycosidase; Endo-T, ENGase isoform which possesses powerful hydrolytic activities toward high-mannose type N-glycans; FTVI, α-1, 3-fucosyltransferase VI; GAA, glucoamylase; Gal10, UDP-glucose 4-epimerase; GalTI, β-1,4-galactosyltransferase I; GM–CSF, granulocyte–macrophage colony-stimulating factor fusion protein; Gmh1p, Gmh2p, Gmh3p, and Gmh6p, α1,2-galactosyltransferases and α1,3-galactosyltransferases; GNG, galactosylated N-glycans complex; GnTI, β-1,2-N-acetylglucosaminyltransferase I; GnTII, β-1,2-N-acetylglucosaminyltransferase II; GTFU, a human galactosyltransferase fused protein with a UDP-glucose 4-epimerase domain from Schizosaccharomyces pombe; HAS, human serum albumin; HGS, hyperglycosylated protein; KlOCH1, β1,6- mannosyltransferase; KlPMR1, a Ca2+-ATPase localized in the Golgi apparatus involved in the glycosylation and cell wall morphogenesis; MNT, a-1,2-Mannosyltransferase; MNN1, α1,3-mannosyltransferase; MPO1, MNN4 homolog; MS/AT/GT, α-1,2-mannosidase, N-acetylglucosaminyltransferase I and β-1,4-galactosyltransferase; OCH1, α1,6-mannosyltransferase; NHGS, non-hyperglycosylated protein; PMD1, leptomycin efflux transporter Pmd1; PMT1 and PMT5, O-mannosyltransferase; P-glycoprotein, the transporters determine the uptake and efflux of drugs; SOG, sialic acid-O-linked glycan; ST, sialyltransferase; SNR, a single N-acetylglucosamine residue; TG, therapeutic glycoproteins.

fused protein with a UDP-glucose 4-epimerase domain from *S. pombe* was expressed in *P. pastoris* and also produced galactosylated proteins (Selas Castiñeiras et al., 2018).

Production of Sialylated Glycoproteins

The lack of sialylation on glycoprotein will reduce its efficacy as a therapeutic agent because of the rapid clearance of the protein from the human bloodstream. Human glycans are often capped terminally with sialic acid *via* sialyltransferase (ST, localized in Golgi, **Figure 1B**). A more effective biocatalyst system for producing sialylated glycoproteins was established in *S. cerevisiae via* the deletion of OCH1 and expression of ST more than one decade ago (Shenoy et al., 2021). Sialylated O-linked glycans were produced in *P. pastoris via* the expression of β-1,2-N-acetylglucosaminyltransferase 1 (AST; Song et al., 2010).

Selection of Yeast Species

Among all the selected yeast species, *H. polymorpha*, *K. marxianus*, *S. pombe*, and *Y. lipolytic* tend to produce short-chain-glycan proteins than other yeast species (**Table 1**). Therefore, these yeast species may be more suitable to produce humanized end-products.

DISCUSSION

Over the past decades, engineering modification of N-glycosylation pathways in yeast species has developed significantly. Most yeast strains are suitable to produce the end-products with hybrid N-glycosylation, galactosylation, and sialyation complex glycans at high uniformity (**Table 1**). With the development of the yeast expression system, it is expected that yeast strains with the ability to generate fully humanized proteins or end-products will be attainable shortly. Nonetheless, there are still some challenges in exploring the yeast expressing system.

1) *Arxula adeninivorans* is an unconventional, non-pathogenic, and haploid yeast and maybe a new expression platform (Song et al., 2007). *Brettanomyces bruxellensis*, a wine yeast, mainly contributes to spontaneous beer fermentations associated with industrial fermentation ecosystems (Tanaka et al., 2021). *Brettanomyces claussenii*, a yeast often found on pineapple or other tropical fruits, expands the potential for the valorization of dairy by-products to functional beverages (Turakainen et al., 1994). *Candida utilis* is a commercial food additive and a potentially beneficial host for producing heterologous protein (Uccelletti et al., 2004). *Hanseniaspora uvarum* (anamorph *Kloeckera apiculata*) is an apiculate yeast species normally found on wine grapes and other fruits and has a strong influence on wine quality. *Zygosaccharomyces bailii* is a yeast species widely present in wine, tea, and vinegar fermentations (Uccelletti et al., 2006). However, these yeasts, and their N-glycosylation pathway and related mechanisms for producing humanized glycosylated proteins have rarely been reported.
2) There are more than 20 glycosyltransferases found in the glycosylation pathway in *S. cerevisiae* (**Figure 1A**; Narimatsu et al., 2019) and 170 human glycosyltransferases found in the glycosylation pathway (**Figure 1B**; Oh et al., 2008). Therefore, there is still a challenge to produce a large body of humanized therapeutic end-products with complex glycan in suitable yeasts. Making full use of the CRISPR-Cas9 technique may be a potential strategy to address the important issues (Ueda et al., 1993; Dolashka-Angelova et al., 2010).

AUTHOR CONTRIBUTIONS

XL, XC, LC, SW, and CC collected and analyzed all data. XQ, XL, XC, JS, KC, and HT contributed to the conception and designing the article and interpreted the relevant literature. XL and HT drafted and revised the article. The manuscript has been read and approved by all authors before submission.

FUNDING

The present work was supported by Guangzhou Zengcheng Qiaomengyuan Branch Project (Grant No. 20210300X).

REFERENCES

Arico, C., Bonnet, C., and Javaud, C. (2013). "N-glycosylation humanization for production of therapeutic recombinant glycoproteins in Saccharomyces cerevisiae," in *Glycosylation Engineering of Biopharmaceuticals*, ed A. Beck (Berlin: Springer), 45–57. doi: 10.1007/978-1-62703-327-5_4

Baghban, R., Farajnia, S., Ghasemi, Y., Mortazavi, M., Zarghami, N., and Samadi, N. (2018). New developments in *Pichia pastoris* expression system, review and update. *Curr. Pharmaceut. Biotechnol.* 19, 451–467. doi: 10.2174/1389201019666180718093037

Cheon, S. A., Kim, H., Oh, D.-B., Kwon, O., and Kang, H. A. (2012). Remodeling of the glycosylation pathway in the methylotrophic yeast *Hansenula polymorpha* to produce human hybrid-type N-glycans. *J. Microbiol.* 50, 341–348. doi: 10.1007/s12275-012-2097-2

Corbacho, I., Olivero, I., and Hernández, L. M. (2005). A genome-wide screen for *Saccharomyces cerevisiae* non-essential genes involved in mannosyl phosphate transfer to mannoprotein-linked oligosaccharides. *Fungal Genet. Biol.* 42, 773–790. doi: 10.1016/j.fgb.2005.05.002

Crauwels, S., Steensels, J., Aerts, G., Willems, K., Verstrepen, K., and Lievens, B. (2015). *Brettanomyces bruxellensis*, essential contributor in spontaneous beer fermentations providing novel opportunities for the brewing industry. *BrewingScience* 68, 110–121.

De Pourcq, K., Tiels, P., Van Hecke, A., Geysens, S., Vervecken, W., and Callewaert, N. (2012). Engineering *Yarrowia lipolytica* to produce glycoproteins homogeneously modified with the universal Man3GlcNAc2 N-glycan core. *PLoS ONE* 7:e39976. doi: 10.1371/journal.pone.0039976

Dolashka-Angelova, P., Moshtanska, V., Kujumdzieva, A., Atanasov, B., Petrova, V., Voelter, W., et al. (2010). Structure of glycosylated Cu/Zn-superoxide dismutase from Kluyveromyces yeast NBIMCC 1984. *J. Mol. Struct.* 980, 18–23. doi: 10.1016/j.molstruc.2010.06.031

Fukunaga, T., Sakurai, Y., Ohashi, T., Higuchi, Y., Maekawa, H., and Takegawa, K. (2021a). Overexpression of cell-wall GPI-anchored proteins restores cell growth of N-glycosylation-defective och1 mutants in *Schizosaccharomyces pombe*. *Appl. Microbiol. Biotechnol.* 105, 8771–8781. doi: 10.1007/s00253-021-11649-5

Fukunaga, T., Tanaka, N., Furumoto, T., Nakakita, S., Ohashi, T., Higuchi, Y., et al. (2021b). Substrate specificities of α1, 2-and α1, 3-galactosyltransferases and characterization of Gmh1p and Otg1p in *Schizosaccharomyces pombe*. *Glycobiology* 31, 1037–1045. doi: 10.1093/glycob/cwab028

Gallo, G. L., Valko, A., Herrera Aguilar, N., Weisz, A. D., and D'alessio, C. (2022). A novel fission yeast platform to model N-glycosylation and the bases of congenital disorders of glycosylation type I. *J. Cell Sci.* 135:jcs259167. doi: 10.1242/jcs.259167

Giorgetti, S. I., Etcheverrigaray, M., Terry, F., Martin, W., De Groot, A. S., Ceaglio, N., et al. (2021). Development of highly stable and de-immunized versions of recombinant alpha interferon: promising candidates for the treatment of chronic and emerging viral diseases. *Clin. Immunol.* 233:108888. doi: 10.1016/j.clim.2021.108888

Gündüz Ergün, B., and Hüccetogullari, D., Öztürk, S., Çelik, E., and Çalik, P. (2019). Established and upcoming yeast expression systems. *Recombinant Protein Production Yeast* 1, 1–74. doi: 10.1007/978-1-4939-9024-5_1

Hamilton, S. R., Cook, W. J., Gomathinayagam, S., Burnina, I., Bukowski, J., Hopkins, D., et al. (2013). Production of sialylated O-linked glycans in *Pichia pastoris*. *Glycobiology* 23, 1192–1203. doi: 10.1093/glycob/cwt056

Jin, Y., Yu, S., Liu, J.-J., Yun, E. J., Lee, J. W., Jin, Y.-S., et al. (2021). Production of neoagarooligosaccharides by probiotic yeast *Saccharomyces cerevisiae* var. boulardii engineered as a microbial cell factory. *Microbial Cell Factor.* 20, 1–10. doi: 10.1186/s12934-021-01644-w

Karbalaei, M., Rezaee, S. A., and Farsiani, H. (2020). *Pichia pastoris*: a highly successful expression system for optimal synthesis of heterologous proteins. *J. Cell. Physiol.* 235, 5867–5881. doi: 10.1002/jcp.29583

Katla, S., Yoganand, K., Hingane, S., Kumar, C. R., Anand, B., and Sivaprakasam, S. (2019). Novel glycosylated human interferon alpha 2b expressed in glycoengineered *Pichia pastoris* and its biological activity: N-linked glycoengineering approach. *Enzyme Microbial Technol.* 128, 49–58. doi: 10.1016/j.enzmictec.2019.05.007

Kim, M. W., Kim, E. J., Kim, J.-Y., Park, J.-S., Oh, D.-B., Shimma, Y.-I., et al. (2006). Functional characterization of the *Hansenula polymorpha* HOC1, OCH1, and OCR1 genes as members of the yeast OCH1 mannosyltransferase family involved in protein glycosylation. *J. Biol. Chem.* 281, 6261–6272. doi: 10.1074/jbc.M508507200

Lawton, M. R., Dana, L. D., and Alcaine, S. D. (2021). Lactose utilization by *Brettanomyces claussenii* expands potential for valorization of dairy by-products to functional beverages through fermentation. *Curr. Opin. Food Sci.* 42, 93–101. doi: 10.1016/j.cofs.2021.05.006

Lee, M.-H., Hsu, T.-L., Lin, J.-J., Lin, Y.-J., Kao, Y.-Y., Chang, J.-J., et al. (2020). Constructing a human complex type N-linked glycosylation pathway in *Kluyveromyces marxianus*. *PLoS ONE* 15:e0233492. doi: 10.1371/journal.pone.0233492

Li, S., Sun, P., Gong, X., Chang, S., Li, E., Xu, Y., et al. (2019). Engineering O-glycosylation in modified N-linked oligosaccharide ($Man1_2GlcNAc_2$ ~ $Man16GlcNAc_2$) *Pichia pastoris* strains. *RSC Adv.* 9, 8246–8252. doi: 10.1039/C8RA08121B

Liu, B., Gong, X., Chang, S., Yang, Y., Song, M., Duan, D., et al. (2009). Disruption of the OCH1 and MNN1 genes decrease N-glycosylation on glycoprotein expressed in *Kluyveromyces lactis*. *J. Biotechnol.* 143, 95–102. doi: 10.1016/j.jbiotec.2009.06.016

Luu, V.-T., Moon, H. Y., Yoo, S. J., Choo, J. H., Thak, E. J., and Kang, H. A. (2019). Development of conditional cell lysis mutants of *Saccharomyces cerevisiae* as production hosts by modulating OCH1 and CHS3 expression. *Appl. Microbiol. Biotechnol.* 103, 2277–2293. doi: 10.1007/s00253-019-09614-4

Ma, J., Li, Q., Tan, H., Jiang, H., Li, K., Zhang, L., et al. (2019). Unique N-glycosylation of a recombinant exo-inulinase from *Kluyveromyces cicerisporus* and its effect on enzymatic activity and thermostability. *J. Biol. Eng.* 13, 1–14. doi: 10.1186/s13036-019-0215-y

Narimatsu, Y., Joshi, H. J., Nason, R., Van Coillie, J., Karlsson, R., Sun, L., et al. (2019). An atlas of human glycosylation pathways enables display of the human glycome by gene engineered cells. *Mol. Cell* 75, 394–407.e395. doi: 10.1016/j.molcel.2019.05.017

Oh, D. B., Park, J. S., Kim, M. W., Cheon, S. A., Kim, E. J., Moon, H. Y., et al. (2008). Glycoengineering of the methylotrophic yeast *Hansenula polymorpha* for the production of glycoproteins with trimannosyl core N-glycan by blocking core oligosaccharide assembly. *Biotechnol. J.* 3, 659–668. doi: 10.1002/biot.200700252

Park, J.-N., Song, Y., Cheon, S. A., Kwon, O., Oh, D.-B., Jigami, Y., et al. (2011). Essential role of Yl MPO1, a novel *Yarrowia lipolytica* homologue of *Saccharomyces cerevisiae* MNN4, in mannosylphosphorylation of N-and O-linked glycans. *Appl. Environ. Microbiol.* 77, 1187–1195. doi: 10.1128/AEM.02323-10

Piirainen, M. A., Salminen, H., and Frey, A. D. (2022). Production of galactosylated complex-type N-glycans in glycoengineered *Saccharomyces cerevisiae*. *Appl. Microbiol. Biotechnol.* 106, 301–315. doi: 10.1007/s00253-021-11727-8

Prabhakar, A., Vadaie, N., Krzystek, T., and Cullen, P. J. (2019). Proteins that interact with the mucin-type Glycoprotein Msb2p include a regulator of the actin cytoskeleton. *Biochemistry* 58, 4842–4856. doi: 10.1021/acs.biochem.9b00725

Prill, S. K. H., Klinkert, B., Timpel, C., Gale, C. A., Schröppel, K., and Ernst, J. F. (2005). PMT family of *Candida albicans*: five protein mannosyltransferase isoforms affect growth, morphogenesis and antifungal resistance. *Mol. Microbiol.* 55, 546–560. doi: 10.1111/j.1365-2958.2004.04401.x

Ryckaert, S., Martens, V., De Vusser, K., and Contreras, R. (2005). Development of a *S. cerevisiae* whole cell biocatalyst for *in vitro* sialylation of oligosaccharides. *J. Biotechnol.* 119, 379–388. doi: 10.1016/j.jbiotec.2005.04.010

Selas Castiñeiras, T., Williams, S. G., Hitchcock, A. G., and Smith, D. C. (2018). *E. coli* strain engineering for the production of advanced biopharmaceutical products. *FEMS Microbiol. Lett.* 365:fny162. doi: 10.1093/femsle/fny162

Shenoy, A., Yalamanchili, S., Davis, A. R., and Barb, A. W. (2021). Expression and display of glycoengineered antibodies and antibody fragments with an engineered yeast strain. *Antibodies* 10:38. doi: 10.3390/antib10040038

Song, H., Qian, W., Wang, H., and Qiu, B. (2010). Identification and functional characterization of the HpALG11 and the HpRFT1 genes involved in N-linked glycosylation in the methylotrophic yeast *Hansenula polymorpha*. *Glycobiology* 20, 1665–1674. doi: 10.1093/glycob/cwq121

Song, Y., Choi, M. H., Park, J.-N., Kim, M. W., Kim, E. J., Kang, H. A., et al. (2007). Engineering of the yeast *Yarrowia lipolytica* for the production of glycoproteins lacking the outer-chain mannose residues of N-glycans. *Appl. Environ. Microbiol.* 73, 4446–4454. doi: 10.1128/AEM.02058-06

Tanaka, N., Kagami, A., Hirai, K., Suzuki, S., Matsuura, S., Fukunaga, T., et al. (2021). The fission yeast gmn2+ gene encodes an ERD1 homologue of *Saccharomyces cerevisiae* required for protein glycosylation and retention of luminal endoplasmic reticulum proteins. *J. General Appl. Microbiol.* 2020:2. doi: 10.2323/jgam.2020.07.002

Turakainen, H., Hankaanpää, M., Korhola, M., and Aho, S. (1994). Characterization of MEL genes in the genus Zygosaccharomyces. *Yeast* 10, 733–745. doi: 10.1002/yea.320100605

Uccelletti, D., Farina, F., Mancini, P., and Palleschi, C. (2004). KlPMR1 inactivation and calcium addition enhance secretion of non-hyperglycosylated heterologous proteins in *Kluyveromyces lactis*. *J. Biotechnol.* 109, 93–101. doi: 10.1016/j.jbiotec.2003.10.037

Uccelletti, D., Farina, F., Rufini, S., Magnelli, P., Abeijon, C., and Palleschi, C. (2006). The *Kluyveromyces lactis* α1, 6-mannosyltransferase KlOch1p is required for cell-wall organization and proper functioning of the secretory pathway. *FEMS Yeast Res.* 6, 449–457. doi: 10.1111/j.1567-1364.2006.00027.x

Ueda, K., Shimabuku, A. M., Konishi, H., Fujii, Y., Takebe, S., Nishi, K., et al. (1993). Functional expression of human P-glycoprotein in *Schizosaccharomyces pombe*. *FEBS Lett.* 330, 279–282. doi: 10.1016/0014-5793(93)80888-2

Vervecken, W., Kaigorodov, V., Callewaert, N., Geysens, S., De Vusser, K., and Contreras, R. (2004). *In vivo* synthesis of mammalian-like, hybrid-type N-glycans in *Pichia pastoris*. *Appl. Environ. Microbiol.* 70, 2639–2646. doi: 10.1128/AEM.70.5.2639-2646.2004

Wang, H., Song, H.-L., Wang, Q., and Qiu, B.-S. (2013). Expression of glycoproteins bearing complex human-like glycans with galactose terminal in *Hansenula polymorpha*. *World J. Microbiol. Biotechnol.* 29, 447–458. doi: 10.1007/s11274-012-1197-9

Wang, S., Rong, Y., Wang, Y., Kong, D., Wang, P. G., Chen, M., et al. (2020). Homogeneous production and characterization of recombinant N-GlcNAc-protein in *Pichia pastoris*. *Microbial Cell Factor.* 19, 1–11. doi: 10.1186/s12934-020-1280-0

Watanasrisin, W., Iwatani, S., Oura, T., Tomita, Y., Ikushima, S., Chindamporn, A., et al. (2016). Identification and characterization of *Candida utilis* multidrug efflux transporter CuCdr1p. *FEMS Yeast Res.* 16:fow042. doi: 10.1093/femsyr/fow042

Xu, Y., Zhi, Y., Wu, Q., Du, R., and Xu, Y. (2017). *Zygosaccharomyces bailii* is a potential producer of various flavor compounds in chinese maotai-flavor

liquor fermentation. *Front. Microbiol.* 8:2609. doi: 10.3389/fmicb.2017.02609

Conflict of Interest: XL, JS, XC, LC, SW, XQ, KC, CC, and HT were employed by Guangzhou Shenjingya Agricultural Technology Co., Ltd.

Publisher's Note: All claims expressed in this article are solely those of the authors and do not necessarily represent those of their affiliated organizations, or those of the publisher, the editors and the reviewers. Any product that may be evaluated in this article, or claim that may be made by its manufacturer, is not guaranteed or endorsed by the publisher.

frontiers | Frontiers in Microbiology

ORIGINAL RESEARCH
published: 15 July 2022
doi: 10.3389/fmicb.2022.951266

Diverse Effects of Amino Acids on *Monascus* Pigments Biosynthesis in *Monascus purpureus*

Sheng Yin[1,2,3]*, *Yiying Zhu*[3], *Bin Zhang*[3], *Baozhu Huang*[3] and *Ru Jia*[3]

[1] Beijing Advanced Innovation Center for Food Nutrition and Human Health, Beijing Technology and Business University, Beijing, China, [2] Beijing Engineering and Technology Research Center of Food Additives, Beijing Technology and Business University, Beijing, China, [3] School of Food and Health, Beijing Technology and Business University, Beijing, China

Amino acids could act as nitrogen sources, amido group donors, or bioactive molecules in fungi fermentation, and consequently, play important roles in *Monascus* pigments (MPs) biosynthesis. But the understanding of the effects of various amino acids on MPs biosynthesis is still incomprehensive. In this work, 20 free amino acids were added to the fermentation medium to evaluate their effects on MPs biosynthesis in *Monascus purpureus* RP2. Six amino acids, namely, histidine (HIS), lysine (LYS), tyrosine (TYR), phenylalanine (PHE), methionine (MET), and cysteine (CYS), were selected as the valuable ones as they exerted significant effects on the production yield and even on the biosynthesis metabolic curves of MPs. Moreover, the dose-dependent and synergistic effects of valuable amino acids on MPs biosynthesis were observed by tests of serial concentrations and different combinations. In addition, it revealed that HIS and MET were the prominent amino acids with dominant and universal influences on MPs biosynthesis. The analog compounds of HIS (amitrole) and MET [calcium 2-hydroxy-4-(methylthio)] were added to the fermentation medium, and the results further confirmed the extraordinary effects of HIS and MET and their analogs on MPs biosynthesis. Furthermore, the gene transcription profile indicated that a differential expression pattern was observed in the polyketide synthase (PKS) cluster responsible for MPs biosynthesis in response to HIS and MET, revealing that they could oppositely regulate MPs biosynthesis in different ways. These findings would benefit the understanding of MPs biosynthesis regulation mechanism in *M. purpureus* and contribute to the industrial production of MPs by fermentation.

Keywords: amino acids, *Monascus* pigments, biosynthesis, *Monascus purpureus*, PKS cluster

OPEN ACCESS

Edited by:
Xucong Lv,
Fuzhou University, China

Reviewed by:
Zhilong Wang,
Shanghai Jiao Tong University, China
Guozhong Zhao,
Tianjin University of Science and Technology, China

***Correspondence:**
Sheng Yin
yinsheng@btbu.edu.cn

Specialty section:
This article was submitted to Food Microbiology, a section of the journal Frontiers in Microbiology

Received: *23 May 2022*
Accepted: *21 June 2022*
Published: *15 July 2022*

Citation:
Yin S, Zhu Y, Zhang B, Huang B and Jia R (2022) Diverse Effects of Amino Acids on Monascus Pigments Biosynthesis in Monascus purpureus. Front. Microbiol. 13:951266. doi: 10.3389/fmicb.2022.951266

INTRODUCTION

Monascus pigments (MPs) are a large class of secondary polyketide metabolites with a common azaphilone skeleton produced by *Monascus* spp. (Chen et al., 2015; Chen W. et al., 2017). Because of their bright red, orange, and yellow colors, MPs have been used as traditional natural colorants in China for thousands of years. The traditional natural colorant compounds are still widely used in industries of food, pharmaceutical, cosmetic manufacture, and dyeing in modern society (Lin et al., 2008; Mapari et al., 2010; Feng et al., 2012; Patakova, 2013; Dufosse et al., 2014;

Mostafa and Abbady, 2014; Srianta et al., 2014; Chen et al., 2015). Consequently, continuous studies have been conducted on biosynthesis and the large-scale production of MPs.

Recent research advances reveal that MPs biosynthesis is controlled by the polyketide synthase (PKS) gene cluster. The PKS cluster is highly conserved in different *Monascus* species and is composed of a dozen of gene elements encoding various enzymes and transcription factors (Yang et al., 2014; Chen et al., 2015; Chen W. et al., 2017). However, due to the complex biosynthesis process involved with a dozen of biotransformation reactions, there are still controversies about the details on MPs formation pathway, especially regarding how the red, yellow, and orange pigments are dividedly synthesized. In addition, the expression and the regulation of the PKS gene cluster seem complicated and ambiguous.

It's generally recognized that secondary metabolites biosynthesis in fungi is regulated by various factors, including temperature, pH, light, and carbon or nitrogen sources (Calvo et al., 2002; Calvo and Cary, 2015; Liu et al., 2016; Lind et al., 2018). For MPs biosynthesis in *Monascus* by fermentation, nitrogen sources are not only essential nutrients to support mycelium growth but also bioactive compounds that may exert regulatory effects. Previous reports indicated that the addition of different nitrogen sources in fermentation resulted in significant impacts on the yield and composition of MPs (Chen and Johns, 1993; Jung et al., 2003, 2005; Hajjaj et al., 2012; Zhang et al., 2013; Said et al., 2014; Shi et al., 2015). Jung et al. (2003) investigated the color characteristics and structures of the MPs derivatives produced by *Monascus* fermentation with separate addition of 20 amino acids. It revealed that the amino acids serine, glutamine, glycine, alanine, and histidine were responsible for red MPs production, and the amino acids phenylalanine, valine, leucine, and isoleucine contributed to yellow and orange MPs production. Besides, it's confirmed that derivative MPs contained the moieties of some added amino acids, suggesting that some amino acids were incorporated into MPs. Hajjaj et al. (2012) investigated the effects of 13 free amino acids on red MPs production in *Monascus ruber* and found 5 amino acids (i.e., glycine, tyrosine, arginine, serine, and histidine) as sole nitrogen sources that favored red MPs production. Besides, *in vitro* chemical reactions demonstrated that some amino donors, such as arginine, lysine, γ-aminobutyric acid, and ammonia, directly get involved in the formation of red MPs molecules (Chen W. et al., 2017), suggesting that free amino acids could possibly be utilized as donors of amido group for MPs biosynthesis. Moreover, the specific bioactive amino acids, such as methionine and S-adenosylmethionine (SAM), play essential roles in multiple biological processes (Brosnan et al., 2007) and also get involved in MPs biosynthesis regulation (Yin et al., 2022).

Although some advances in the effects of amino acids on MPs biosynthesis have been achieved by previous studies, due to the complexity and diversity of the metabolism of different amino acids, systematic investigations are still indispensable to seek comprehensive insights into the roles of various amino acids in MPs biosynthesis and regulation. Therefore, this work investigated the effects of 20 free amino acids to select the valuable ones for MPs production in *Monascus purpureus* RP2, evaluated the dose-dependent and the synergistic effects of valuable amino acids, and conducted a comparative analysis of the different roles of histidine and methionine in PKS gene cluster expression and MPs biosynthesis. The findings in this study would benefit the understanding of MPs biosynthesis regulation in *M. purpureus* and contribute to the industrial production of MPs by fermentation.

MATERIALS AND METHODS

Strains and Culture Conditions

The wild strain *M. purpureus* RP2 (Laboratory collection) was cultured at 30°C in potato dextrose agar (PDA) medium. For MPs production by liquid-state fermentation, *M. purpureus* RP2 was cultured at 30°C in PDA medium for 10 days, and the spore suspension was prepared by washing the mycelium with sterile water and collected by filtration with sterile gauze. The spore suspension (10%) was inoculated into seed medium (40 g/L rice flour, 8 g/L peptone, 5 g/L soybean meal, 1 g/L $MgSO_4{\cdot}7H_2O$, 2 g/L KH_2PO_4, and 2 g/L $NaNO_3$) and cultured at 33°C with vigorous shaking at 200 rpm on a shaking incubator with a rotational radius of 10 cm for 48 h. The seed culture (10%) was then inoculated into a fermentation medium (20 g/L glucose, 5 g/L yeast nitrogen base w/o amino acids, 5 g/L $K_2HPO_4{\cdot}3H_2O$, 0.5 g/L $MgSO_4{\cdot}7H_2O$, 5 g/L KH_2PO_4, 0.1 g/L $CaCl_2$, 0.03 g/L $MnSO_4{\cdot}H_2O$, 0.01 g/L $FeSO_4{\cdot}7H_2O$, and 0.01 g/L $ZnSO_4{\cdot}7H_2O$) and cultured at 33°C with vigorous shaking at 200 rpm on a shaking incubator with a rotational radius of 10 cm for 14 days. For colony morphology observation, *M. purpureus* was cultured at 30°C in a fermentation medium containing agar (20 g/L) for 9 days.

Effects of Addition of Amino Acids in Fermentation on *Monascus* Pigments Biosynthesis

A total of 20 amino acids (5 g/L) were added to the fermentation medium containing yeast nitrogen base without free amino acids, respectively, and liquid fermentation with *M. purpureus* RP2 was conducted for 14 days. The yield of red, yellow, and orange MPs was determined every 2 days during fermentation to investigate the influences of different amino acids on MPs biosynthesis in *M. purpureus* RP2.

The amino acids that exerted obvious effects on MPs biosynthesis were selected for further analysis of dose-dependent effect on MPs biosynthesis. Serial gradient concentrations (1∼9 g/L) of amino acids were added to the fermentation medium, and fermentation with *M. purpureus* RP2 and MPs production determination were performed as described earlier.

The synergistic effect of different amino acids on MPs biosynthesis was investigated by the combined addition of multiple amino acids that exhibited similar effects in the fermentation medium. Fermentation and MPs production determination were performed as described earlier.

To figure out the mode of action of specific amino acids, the selected amino acid was partially or completely replaced with

its structural analog compound and added to the fermentation medium for fermentation and MPs production determination.

Measurement of *Monascus* Pigments Production

For the measurement of MPs production, the fermentation broth was centrifuged at 8,000 × *g* for 10 min to collect mycelia and supernatant. The mycelia or broth supernatant samples were soaked in 50 ml of 70% (v/v) ethanol and incubated in the water bath (60°C) for 1 h to extract MPs. The mixture was centrifuged at 8,000 × *g* for 10 min to collect supernatant, which was used to measure MPs concentration by spectrophotometer (OD 410 nm for yellow MPs, OD 470 nm for orange MPs, and OD 505 nm for red MPs) (Yin et al., 2022).

DNA Manipulation Techniques

Standard DNA manipulation techniques were performed as described by Green and Sambrook (2012). Total RNA from *M. purpureus* was prepared using the RNAprep Pure Plant Kit (TIANGEN, Beijing, China) following the manufacturer's instructions. RNA was subjected to reverse transcription to generate cDNA using Quantscript RT Kit (TIANGEN, Beijing, China) following the manufacturer's protocol. Quantitative Real-Time PCR (q RT-PCR) was performed using the SuperReal PreMix Plus (SYBR Green) Kit (TIANGEN, Beijing, China) in CFX96 Touch Real-Time PCR System (Bio-Rad, Hercules, CA, United States) with the following cycling conditions: 95°C for 2 min, followed by 40 cycles of 94°C for 20 s, 63°C for 45 s, and 60°C for 5 min. The *GAPDH* gene was used for transcript normalization. All reactions were performed in triplicate. Data were analyzed using the $2^{-\Delta\Delta Ct}$ method corrected for primer efficiencies using the untreated group mean as the reference condition (Schmittgen and Livak, 2008). Primers used for gene transcription level assay by q RT-PCR were listed in **Supplementary Table 1**.

Comparative Analysis of *Monascus* Pigments Biosynthesis Polyketide Synthase Gene Cluster From *Monascus purpureus* Strains

The PKS gene cluster responsible for MPs biosynthesis in *M. purpureus* RP2 was analyzed by genome sequencing, assembly, and comparative analysis. The genome of *M. purpureus* RP2 was sequenced by single-molecule, real-time (SMRT) sequencing technology. Sequencing was performed at the Beijing Novogene Bioinformatics Technology Co., Ltd. The Augustus 2.7 program was used to retrieve the related coding gene. Databases used to predict gene functions included GO, KEGG, COG, NR, TCDB, Swiss-Prot, and TrEMBL. The secondary metabolite biosynthesis gene clusters were predicted with antiSMASH. A whole-genome Blast search was performed against the above databases. Genomic alignment between the sample genome and reference genome was performed using the MUMmer and LASTZ tools.

RESULTS AND DISCUSSION

Effects of Different Amino Acids on *Monascus* Pigments Biosynthesis

The effects of amino acids on MPs biosynthesis in *M. purpureus* RP2 were systematically investigated by fermentation with the addition of 20 free amino acids using the fermentation medium containing YNB without free amino acids as the nitrogen source. Fermentation results showed that various patterns of changes in MPs biosynthesis were observed in response to the addition of different amino acids (**Figure 1**). Compared with the fermentation without free amino acids, most amino acids added to the fermentation medium exhibited inhibiting effects to different degrees on MPs production, while histidine (HIS), lysine (LYS), tryptophan (TRY), tyrosine (TYR), and phenylalanine (PHE) gave rise to increased MPs production (**Figure 1**). HIS was the only amino acid that led to the most significant increase in all three kinds of MPs biosynthesis; the peak yields of red, yellow, and orange MPs were raised by 49, 27, and 31%, respectively. The addition of LYS only exerted a positive effect on yellow MPs biosynthesis, whose peak yield was increased by 22%. Besides, it's noteworthy that TRY, TYR, and PHE not only promoted MPs production but also obviously changed the metabolic curve of MPs biosynthesis; the fermentation time when the peak yield of MPs appeared was postponed from 6 to 10 days and 12 days, which consequently facilitated more MPs generation. However, TYR and PHE only acted on yellow and orange MPs biosynthesis in the special pattern, and they reduced the production of red MPs and hardly affected the normal metabolic curve. With regard to the amino acids with negative influences on MPs biosynthesis, methionine (MET) and cysteine (CYS) were the most outstanding ones and contributed to the approximate 50% decrease in yields of red, yellow, and orange MPs.

Dose-Dependent Effects of Different Amino Acids on *Monascus* Pigments Biosynthesis

To investigate the effect of different concentrations of amino acids on MPs biosynthesis, serial gradient concentrations (1–9 g/L) of selected amino acids (HIS, LYS, TYR, PHE, MET, and CYS) were added to the fermentation medium, respectively. The results indicated that the positive or negative impact on MPs biosynthesis exerted by specific amino acids generally depended on the added dose. As shown in **Figure 2**, the production of red, yellow, and orange MPs synchronously increased as the concentration of HIS rose from 3 to 7 g/L, while 1 g/L of HIS decreased the MPs production and the yield of MPs generated by 9 g/L of HIS was lower than that of 7 g/L. The addition of LYS only enhanced yellow MPs biosynthesis at the concentration of 3 and 5 g/L, and 9 g/L of LYS extremely reduced all three kinds of MPs production by about 50∼60% (**Supplementary Figure 1**). TYR enhanced yellow and orange MPs biosynthesis at each concentration, and 3 g/L was detected as the optimal dose (**Supplementary Figure 1**). PHE led to a continuous sharp rise in yellow and orange MPs biosynthesis during 14 days of fermentation at a concentration of higher than 1 g/L, and a

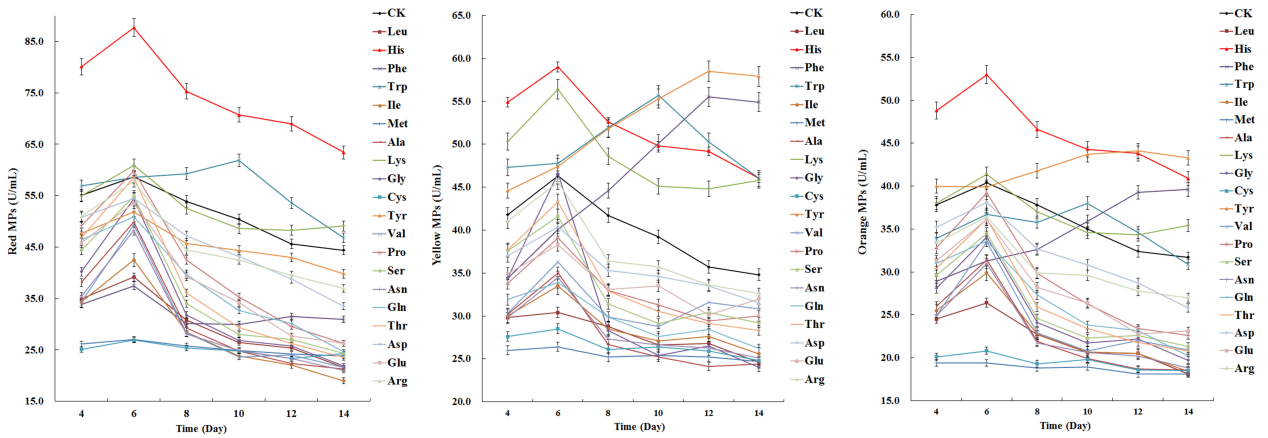

FIGURE 1 | Effects of 20 amino acids on *Monascus* pigments (MPs) production in *Monascus purpureus* RP2 fermentation. CK, *M. purpureus* RP2 fermentation without the addition of amino acid; Leu, *M. purpureus* RP2 fermentation with the addition of leucine (LEU); His, *M. purpureus* RP2 fermentation with the addition of histidine (HIS); Phe, *M. purpureus* RP2 fermentation with the addition of phenylalanine (PHE); Trp, *M. purpureus* RP2 fermentation with the addition of tryptophan (TRP); Ile, *M. purpureus* RP2 fermentation with the addition of isoleucine (ILE); Met, *M. purpureus* RP2 fermentation with the addition of methionine (MET); Ala, *M. purpureus* RP2 fermentation with the addition of alanine (ALA); Lys, *M. purpureus* RP2 fermentation with the addition of lysine (LYS); Gly, *M. purpureus* RP2 fermentation with the addition of glycine (GLY); Cys, *M. purpureus* RP2 fermentation with the addition of cysteine (CYS); Tyr, *M. purpureus* RP2 fermentation with the addition of tyrosine (TYR); Val, *M. purpureus* RP2 fermentation with the addition of valine (VAL); Pro, *M. purpureus* RP2 fermentation with the addition of proline (PRO); Ser, *M. purpureus* RP2 fermentation with the addition of serine (SER); Asn, *M. purpureus* RP2 fermentation with the addition of asparagine (ASN); Gln, *M. purpureus* RP2 fermentation with the addition of glutamine (GLN); Thr, *M. purpureus* RP2 fermentation with the addition of threonine (THR); Asp, *M. purpureus* RP2 fermentation with the addition of aspartic acid (ASP); Glu, *M. purpureus* RP2 fermentation with the addition of glutamic acid (GLU); Arg, *M. purpureus* RP2 fermentation with the addition of arginine (ARG).

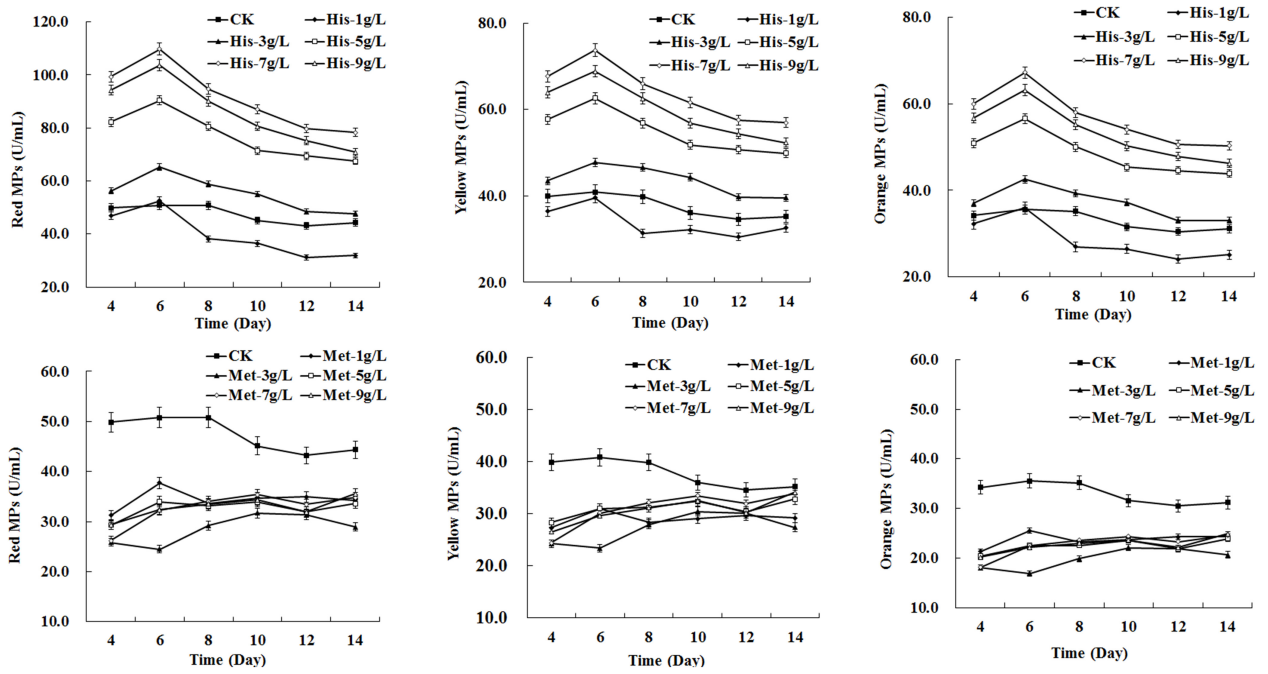

FIGURE 2 | Effects of amino acids at different concentrations on *Monascus* pigments (MPs) production in *Monascus purpureus* RP2 fermentation. CK, *M. purpureus* RP2 fermentation without the addition of amino acid; His, *M. purpureus* RP2 fermentation with the addition of HIS; Met, *M. purpureus* RP2 fermentation with the addition of MET.

positive correlation was observed between MPs yield and PHE dose ranging from 3 to 7 g/L (**Supplementary Figure 1**). With respect to MET and CYS, each concentration from 1 to 9 g/L displayed an inhibiting effect on three kinds of MPs production, and the dose with significant effect was observed to be 3 g/L for MET and 5 g/L for CYS (**Figure 2** and **Supplementary Figure 1**).

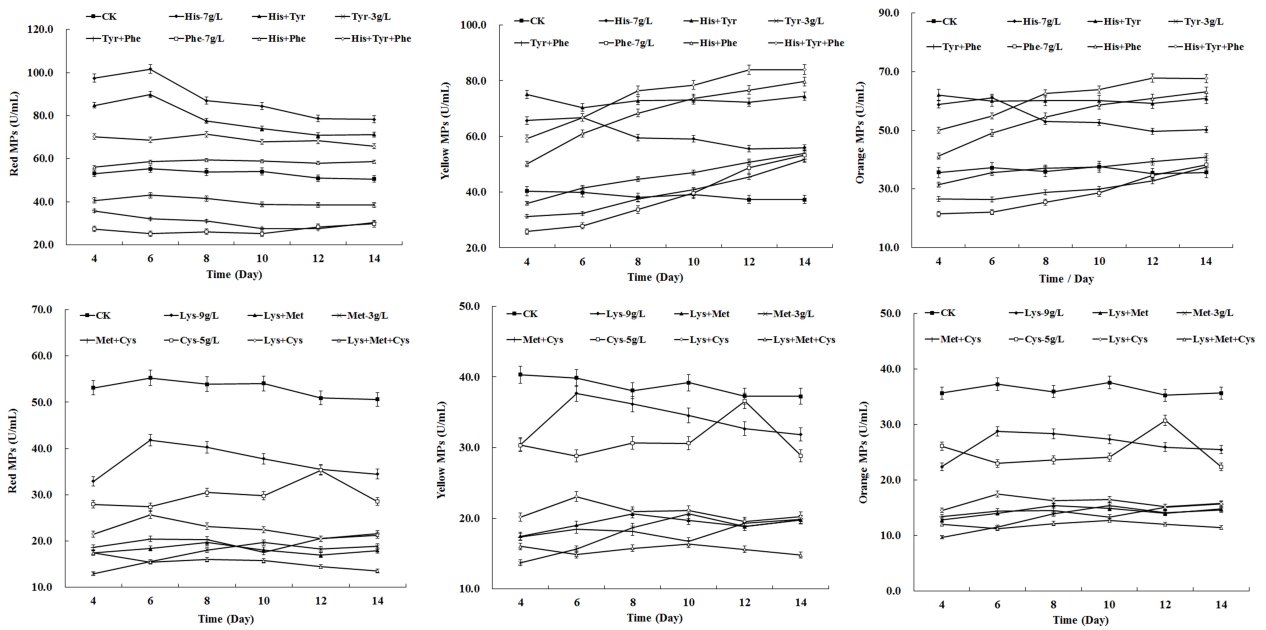

FIGURE 3 | Effects of combination of amino acids on *Monascus* pigments (MPs) production in *Monascus purpureus* RP2 fermentation. CK, *M. purpureus* RP2 fermentation without the addition of amino acid; His, *M. purpureus* RP2 fermentation with the addition of HIS; Tyr, *M. purpureus* RP2 fermentation with the addition of TYR; Phe, *M. purpureus* RP2 fermentation with the addition of PHE; Met, *M. purpureus* RP2 fermentation with the addition of MET; Lys, *M. purpureus* RP2 fermentation with the addition of LYS; Cys, *M. purpureus* RP2 fermentation with the addition of CYS.

Synergistic Effects of Different Amino Acids on *Monascus* Pigments Biosynthesis

To investigate the synergistic effect of amino acids on MPs biosynthesis, the amino acids that displayed positive effects (7 g/L of HIS, 3 g/L of TYR, 7 g/L of PHE) and negative effects (3 g/L of MET, 5 g/L of CYS, 9 g/L of LYS) on MP production were mixed and added to the fermentation medium of *M. purpureus* RP2. As shown in **Figure 3**, HIS exerted a dominant role in enhancing the yields of red, yellow, and orange MPs. When mixed with TYR and PHE, HIS obviously reversed the negative effect of TYR and PHE on red MPs production and further promoted the positive effect of TYR and PHE on yellow and orange MPs production (**Figure 3**). TYR and PHE exhibited a dominant role in altering the typical biosynthesis metabolic curves of yellow and orange MPs, but they hardly gave a remarkable contribution to the yield (**Figure 3**). It revealed that HIS, TYR, and PHE displayed a synergistic enhancement effect on the biosynthesis of yellow and orange MPs. The synergistic effect was also observed among MET, CYS, and LYS, and their combination led to a maximum decrease in the yield of all three kinds of MPs in comparison with the addition of any one or two amino acids (**Figure 3**). But it's indicated that MET was the one with the dominant influence on inhibiting MPs biosynthesis. Although different amino acids mentioned above expressed the synergistic promoting or inhibiting effect on MPs production, it's noteworthy that HIS and MET were the dominant ones that exerted universal effects on MPs biosynthesis.

Effects of Analogs of Histidine and Methionine on *Monascus* Pigments Biosynthesis

To investigate the mode of action of HIS and MET on MPs biosynthesis, the HIS analog amitrole (3-amino-1, 2, 4-triazole) and the MET analog calcium 2-hydroxy-4-(methylthio) butyrate (CHMTB) were used to completely or partially substitute for the two amino acids in the fermentation of *M. purpureus* RP2. As shown in **Figure 4**, CHMTB represented almost the same effect as MET on both MPs production and the biomass of *M. purpureus* RP2, revealing that it followed the metabolism mode similar to MET. With respect to amitrole, significant differences were detected in MPs biosynthesis and growth of *M. purpureus* RP2 between HIS and its analog. The mixture of amitrole and HIS at the total concentration of 7 g/L led to the increased yields of MPs, and the yields went higher as the proportion of amitrole rose in comparison with 7 g/L of HIS, but amitrole did not change the metabolic curve of MPs biosynthesis in the presence of HIS. However, in the absence of HIS, amitrole at 7 g/L totally changed the metabolic curve of MPs biosynthesis, which went straight up during fermentation, and more MPs were generated than that of HIS or the mixture after 9 days of fermentation. But 7 g/L of amitrole indeed inhibited the growth of *M. purpureus* RP2 since the biomass was quite lower than that of HIS or the mixture. The results suggested that the HIS analog amitrole probably was not incorporated into the HIS metabolism network in *M. purpureus* RP2, and consequently, it could continuously promote MPs biosynthesis and accumulation. With respect to the

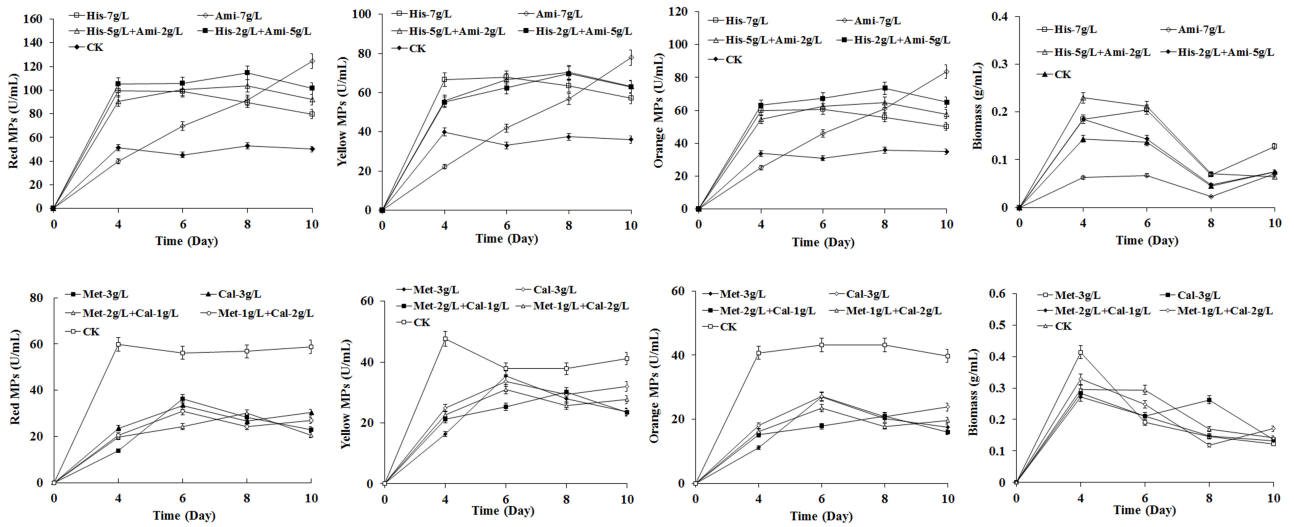

FIGURE 4 | Effects of analogs of HIS and MET on *Monascus* pigments (MPs) production in *Monascus purpureus* RP2 fermentation. CK, *M. purpureus* RP2 fermentation without the addition of amino acid; His, *M. purpureus* RP2 fermentation with the addition of HIS; Ami, *M. purpureus* RP2 fermentation with the addition of amitrole; Met, *M. purpureus* RP2 fermentation with the addition of MET; Cal, *M. purpureus* RP2 fermentation with the addition of calcium 2-hydroxy-4-(methylthio) butyrate.

structural similarity with HIS, amitrole is the derivative of 1H-1, 2, 4-triazole substituted by an amino group (**Supplementary Figure 2**). It has toxicity in humans and is widely used as an herbicide. Heim and Larrinua (1989) revealed that amitrole toxicity in *Arabidopsis thaliana* was not caused by histidine starvation nor by the accumulation of a toxic intermediate of the histidine pathway, suggesting that this compound did not interfere with histidine metabolism. Hence, it is possible that amitrole could continuously contribute to MPs production due to its characteristics of structural similarity with HIS and no limitations from HIS metabolism regulation. When it comes to CHMTB, the analog shares a high structural similarity with MET except the amino group substituted by hydroxyl (**Supplementary Figure 2**). It is commonly used as an effective feed nutrient supplement of dietary MET for livestock (Lobley et al., 2006). This compound has the same biological potency as MET, and it proved that CHMTB could be converted to MET within body tissues (Lobley et al., 2006). Therefore, it is supposed that CHMTB added to the fermentation medium could be utilized *via* the MET metabolic pathway in *M. purpureus* RP2, which probably accounts for the same effects of MET and CHMTB on MPs biosynthesis.

Histidine and Methionine Regulated *Monascus* Pigments Biosynthesis Genes Expressions in Different Ways

Secondary metabolites biosynthesis is coupled with asexual and sexual development in *Aspergillus* fungi (Lind et al., 2018). Hence, 7 g/L of HIS and 3 g/L of MET were added to the fermentation agar plates for the cultivation of *M. purpureus* RP2. Colony morphology observation indicated that significant differences were detected between colonies of *M. purpureus* RP2 cultured in plates with HIS and MET (**Figure 5**). The addition of MET contributed to the early colony development and consequent MPs production of *M. purpureus* RP2 after 2–3 days of cultivation, while the colony formation in the plate with HIS laid behind and the colony size was quite smaller than that of MET. Besides, the colony morphology in the plate with MET was quite different from that in the plate with HIS or without amino acid, indicating that the addition of MET changed the mycelial development of *M. purpureus* RP2. With respect to MPs yield, the addition of HIS generated much more MPs as the bright colors of red, orange, and yellow MPs became much more intensive within and around the colony during the later period of cultivation (**Figure 5**).

The classical PKS gene cluster is responsible for MPs biosynthesis in *Monascus*. To investigate the influences of HIS and MET on MPs biosynthesis genes expression, the PKS gene cluster was searched in *M. purpureus* RP2 and analyzed by genome sequencing. Analysis results showed that a conserved PKS cluster was found, and it consisted of 15 functional enzymes encoding genes and two regulatory elements (**Figure 6**). The PKS cluster shared high homologies in sequences of most genes and a high similarity in structure composition with that of *M. purpureus* YY-1 (Yang et al., 2014). Two unrelated or unknown genes (C5.126.1 and C5.13) present in the PKS cluster of *M. purpureus* YY-1 were found to be vanished from that of *M. purpureus* RP2 (**Figure 6**), suggesting that those genes were redundant for MPs biosynthesis and probably were abandoned during evolution. *M. purpureus* RP2 also harbored a redundant gene (*Mon2A4593*) encoding a hypothetical protein with unknown function, which was inserted between the fatty acid synthase α and β subunits genes (*Mon2A4592* and *Mon2A4594*) and fortunately did not lead to disruption of the fatty acid synthase.

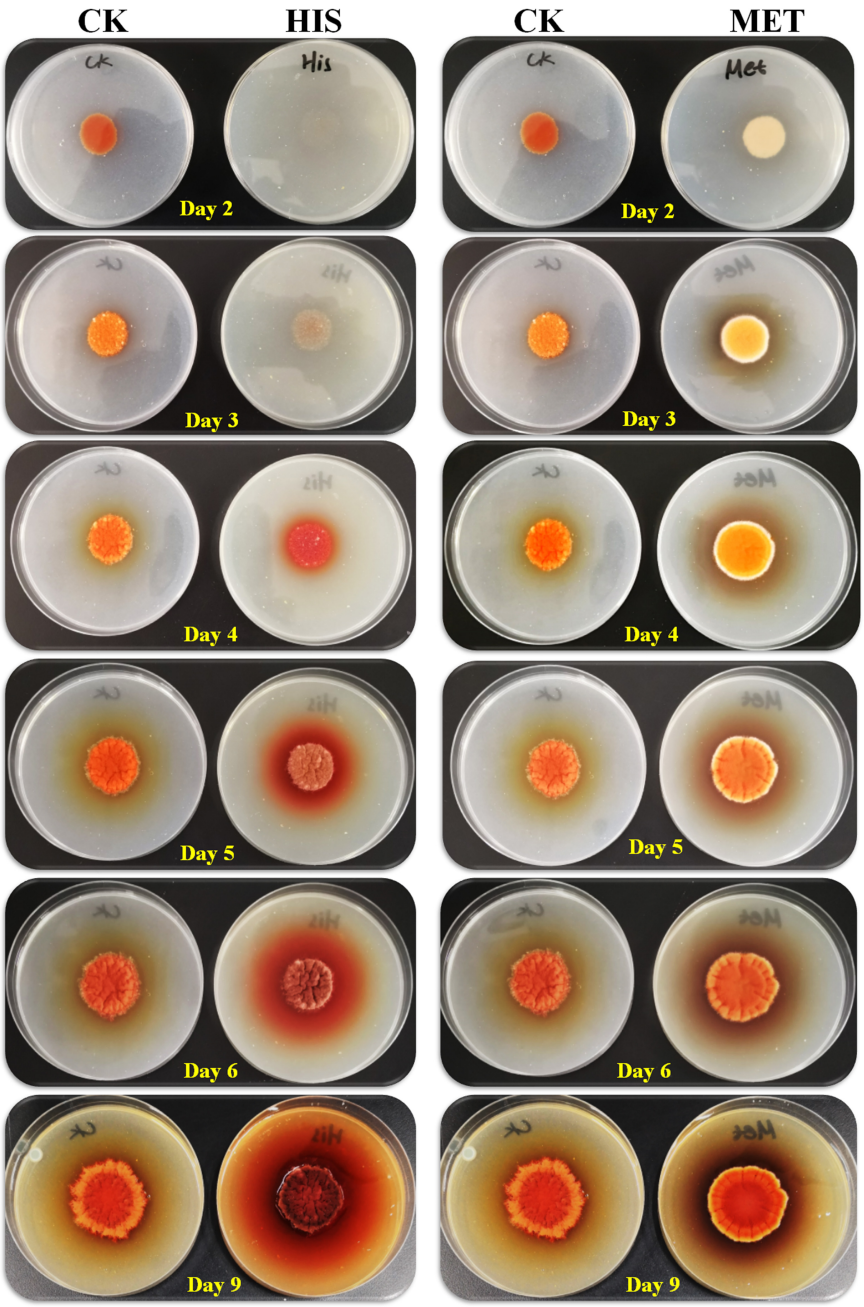

FIGURE 5 | Growth of *Monascus purpureus* RP2 in fermentation plates with the addition of HIS and MET. CK, growth of *M. purpureus* RP2 in the fermentation plate without the addition of amino acid; HIS, growth of *M. purpureus* RP2 in the fermentation plate with the addition of HIS; MET, growth of *M. purpureus* RP2 in the fermentation plate with the addition of MET.

The transcriptional levels of the PKS cluster genes were further profiled in *M. purpureus* RP2 fermentation with HIS and MET. Differential expressions of the PKS genes were observed in response to HIS and MET (**Figure 7**). Generally, in comparison with fermentation without amino acid addition, HIS enhanced transcriptions of most of the PKS cluster genes, while MET generated the reversed results. According to previous reports on the MPs biosynthesis pathway (Chen W. et al., 2017; Liang et al., 2018), 12 key enzymes encoded by the PKS cluster probably got involved in MPs biosynthesis in *M. purpureus* RP2 (**Figure 8**). The expression levels of 6 key enzymes (PKS Mon2A4603, short-chain alcohol dehydrogenase Mon2A4601, 3-*O*-acetyltransferase Mon2A4600, oxidoreductase Mon2A4599, FAD-dependent dehydrogenase Mon2A4598, and serine hydrolase Mon2A4597) encoding genes were significantly increased as MPs biosynthesis enhanced in fermentation with

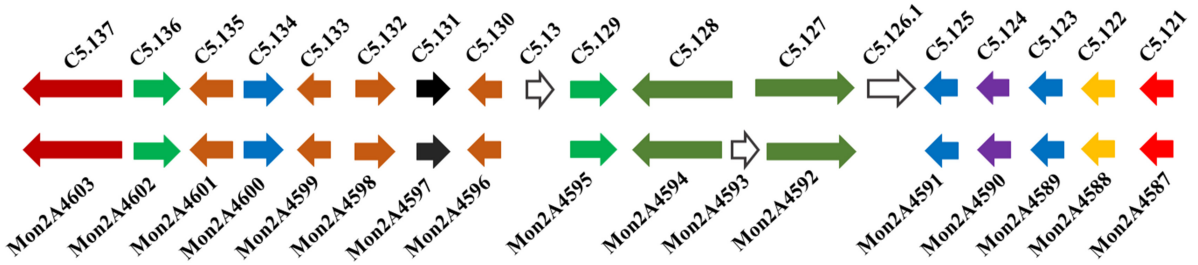

FIGURE 6 | Polyketide synthase (PKS) gene clusters from *Monascus purpureus* YY-1 (C5.121-5.137) and *M. purpureus* RP2 (Mon2A 4587-4603). C5.121 and Mon2A4587 (100 and 98% identity with GenBank No. ANS12245.1): MFS multidrug transporter. C5.122 and Mon2A4588 (100% identity with GenBank No. ANS12244.1): decarboxylase. C5.123 and Mon2A4589 (100% identity with GenBank No. QGA67179.1): deacetylase. C5.124 and Mon2A4590 (100% identity with GenBank No. QGA67182.1): monooxygenase. C5.125 and Mon2A4591 (100% identity with GenBank No. QGA67225.1): acyltransferase. C5.126.1 (100% identity with GenBank No. QGA67184.1): ankyrin repeat protein. C5.127 and Mon2A4592 (100% identity with GenBank No. QGA67211.1): fatty acid synthase β subunit. Mon2A4593 (100% identity with GenBank No. TQB69636.1): hypothetical protein. C5.128 and Mon2A4594 (100% identity with GenBank No. QGA67228.1): fatty acid synthase α subunit. C5.129 and Mon2A4595 (100% and 95% identity with GenBank No. QGA67229.1): transcription factor. C5.13 (100% identity with GenBank No. TQB67922.1): hypothetical protein. C5.130 and Mon2A4596 (100% identity with GenBank No. APZ73943.1): reductase like-protein. C5.131 and Mon2A4597 (100% identity with GenBank No. APZ73942.1): serine hydrolase. C5.132 and Mon2A4598 (100% identity with GenBank No. APZ73941.1): FAD dependent dehydrogenase. C5.133 and Mon2A4599 (100% identity with GenBank No. AHA93896.1): oxidoreductase. C5.134 and Mon2A4600 (100% identity with GenBank No. AGI63864.1): 3-*O*-acetyltransferase. C5.135 and Mon2A4601 (98 and 100% identity with GenBank No. AGI63865.1): short-chain alcohol dehydrogenase. C5.136 and Mon2A4602 (100 and 99% identity with GenBank No. QGA67219.1): transcription factor. C5.137 and Mon2A4603 (100 and 99% identity with GenBank No. QGA67237.1): polyketide synthase.

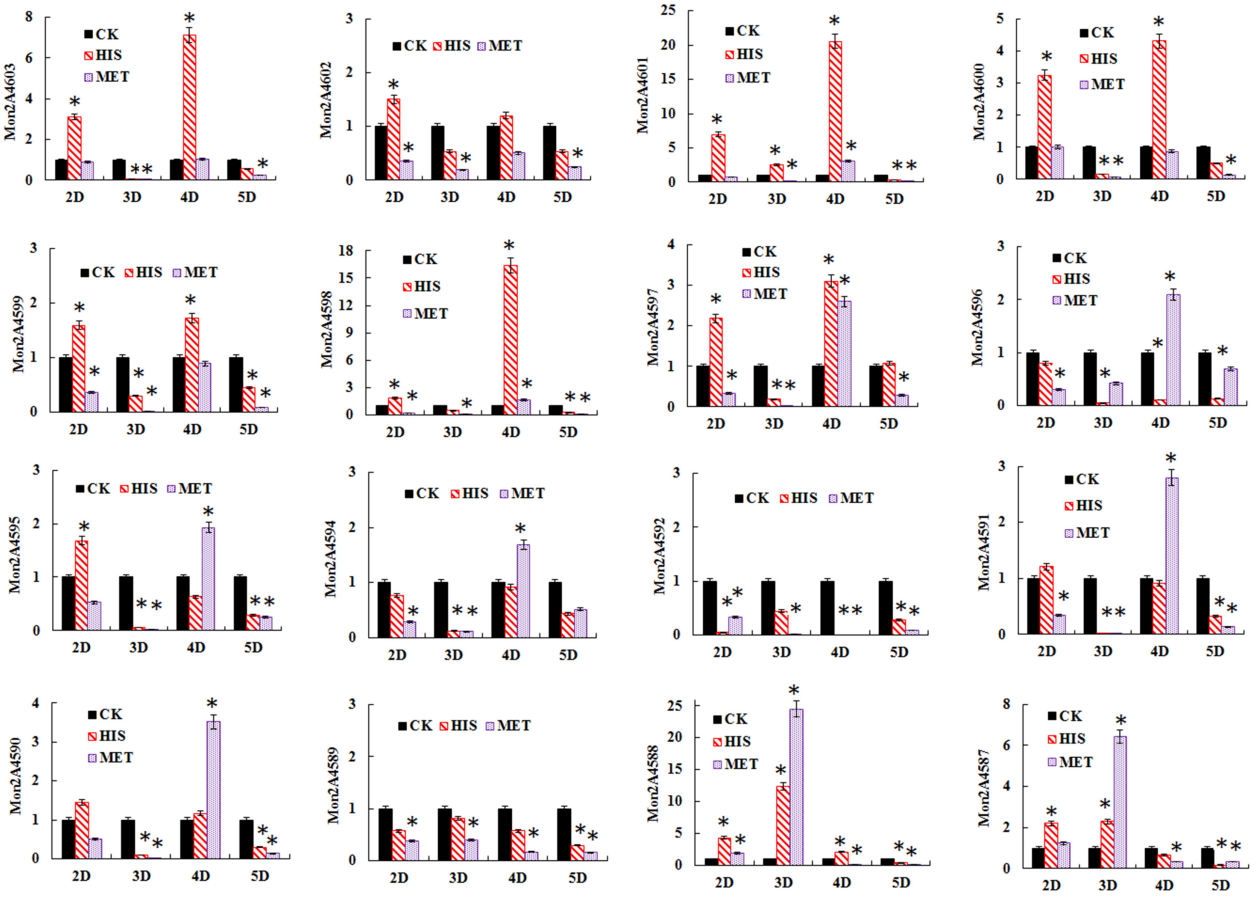

FIGURE 7 | Gene transcription profile of the polyketide synthase (PKS) cluster in *Monascus purpureus* RP2 fermentation with HIS and MET. CK, *M. purpureus* RP2 fermentation without the addition of amino acid; HIS, *M. purpureus* RP2 fermentation with the addition of HIS; MET, *M. purpureus* RP2 fermentation with the addition of MET; D, fermentation time (Day). Bars with asterisks (*) are significantly different ($P < 0.05$).

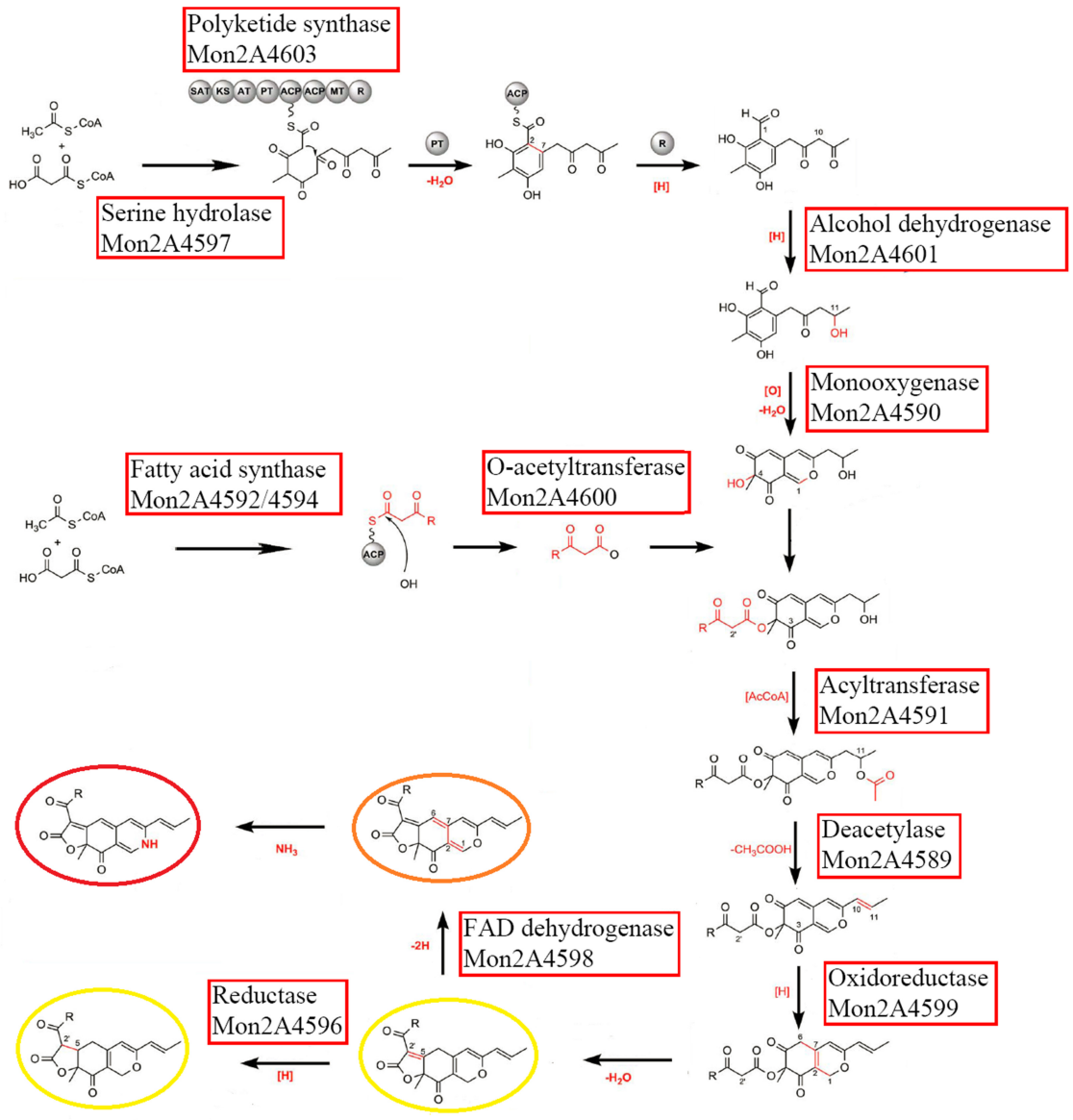

FIGURE 8 | Putative *Monascus* pigments (MPs) biosynthesis pathway involved with the polyketide synthase (PKS) enzymes in *Monascus purpureus* RP2. The figure was modified with reference to Scheme 2 by Chen W. et al. (2017).

HIS. Liang et al. (2018) reported that PKS (C5.137), short-chain alcohol dehydrogenase (C5.135), 3-*O*-acetyltransferase (C5.134), reductase like-protein (C5.130), and fatty acid synthase (C5.127 and C5.128) exhibited high expression levels when pigment production rapidly increased in *M. purpureus* YY-1 after 8 days of cultivation. Although the results shared a basic consistency, expressions of reductase-like protein (Mon2A4596), fatty acid synthase (Mon2A4594 and Mon2A4592), and deacetylase (Mon2A4589) were downregulated by the addition of HIS and MET in *M. purpureus* RP2. With respect to the two regulatory elements in the PKS cluster, it's reported that they were expressed at higher levels under high pigment production conditions in *M. purpureus* YY-1 (Yang et al., 2014) and *M. purpureus* M9 (Chen D. et al., 2017). In *M. purpureus* RP2, expressions of Mon2A4602 and Mon2A4595 were both upregulated by HIS and downregulated by MET, which probably accounted for differential expressions of most PKS enzymes encoding genes and different MPs production yield in response to HIS and MET.

Even though the PKS cluster responsible for MPs biosynthesis is confirmed to be highly conserved in different *Monascus* strains, the temporal and spatial expression pattern of the PKS genes is still indistinct. Nevertheless, in the conditions of this work, most functional genes of the PKS cluster displayed an opposite expression pattern in response to the addition of HIS and MET, revealing that the two amino acids with universal and dominant influences could regulate MPs biosynthesis by

controlling the PKS cluster expression. It is noteworthy that the addition of MET also led to a remarkable change in the colony morphology, while HIS hardly exerted the same effect. Since there is a close correlation between mycelial development and secondary metabolites biosynthesis in fungi (Lind et al., 2018), it is reasonable to speculate that MET could also regulate MPs biosynthesis by controlling the mycelial development. Regarding the molecular mechanism of MPs biosynthesis regulation by amino acids, it is believed that there are diverse pathways according to various metabolic networks of different amino acids. In our previous study (Yin et al., 2022), it was evident that MET inhibited MPs biosynthesis by inducing the expression of SAM synthetase; however, other regulation pathways possibly exist because a seemingly contradictory result was observed that the addition of SAM indeed promoted MPs biosynthesis. The gene expressions of several important enzymes (histidine decarboxylase, histidine methyltransferase, and aminotransferase) involved in HIS metabolism were also assayed, but no significant changes were found in response to the addition of HIS in the fermentation of *M. purpureus* RP2 (data not shown). Previous studies reported that histidine degradation and utilization played crucial roles in metal homeostasis management, nutritional flexibility, and virulence in fungi (Brunke et al., 2014; Dietl et al., 2016). In addition, histidine phosphorylation involved with histidine phosphotransferase and histidine kinase was proved to regulate cell growth, sporulation, secondary metabolism, morphological differentiation, biofilm formation, and virulence in fungi (Li et al., 2010; Fuhs and Hunter, 2017; Mohanan et al., 2017). These research progresses indicated that histidine could participate in metabolic regulation in different ways. As for the regulatory role of HIS in MPs biosynthesis, it's indispensable to dig out more detail information on the molecule components and their interactions involved in the regulation network.

Secondary metabolites biosynthesis in fungi is regulated by various factors, including temperature, pH, light, and carbon or nitrogen sources (Calvo et al., 2002; Calvo and Cary, 2015; Liu et al., 2016; Lind et al., 2018). In this work, we systematically investigated the effects of the addition of different amino acids in the fermentation on MPs biosynthesis in *M. purpureus* RP2. It revealed that specific amino acids played a role of regulatory factor rather than nitrogen molecule in MPs biosynthesis, which not only affected MPs production yield but also altered MPs biosynthesis metabolic curves. Although the molecular mechanism of MPs biosynthesis regulation by amino acids is unclear and needs necessary in-depth studies, the findings in this work would benefit the understanding of MPs biosynthesis regulation mechanism in *M. purpureus* and contribute to the industrial production of MPs by fermentation.

DATA AVAILABILITY STATEMENT

The datasets presented in this study can be found in online repositories. The names of the repository/repositories and accession number(s) can be found below: NCBI BioProject - PRJNA842148, SAMN28647902, JAMLEA000000000.

AUTHOR CONTRIBUTIONS

SY conceived and designed the experiments, wrote the manuscript, and contributed to manuscript revision, financial support, and supervision. YZ, BZ, BH, and RJ performed the experimental work and data analysis. All authors contributed to the article and approved the submitted version.

FUNDING

This study was supported by the National Natural Science Foundation of China (31401669), the Joint Program of Beijing Natural Science Foundation and Beijing Municipal Education Commission (KZ201910011014), the Support Project of High-Level Teachers in Beijing Municipal Universities (IDHT20180506), and the Talent Training Quality Construction-First Class Professional Construction (PXM2019-014213-000010).

SUPPLEMENTARY MATERIAL

The Supplementary Material for this article can be found online at: https://www.frontiersin.org/articles/10.3389/fmicb.2022.951266/full#supplementary-material

REFERENCES

Brosnan, J. T., Brosnan, M. E., Bertolo, R., and Brunton, J. A. (2007). Methionine: a metabolically unique amino acid. *Livest. Sci.* 112, 2–7. doi: 10.1016/j.livsci.2007.07.005

Brunke, S., Seider, K., Richter, M. E., Bremer-Streck, S., Ramachandra, S., Kiehntopf, M., et al. (2014). Histidine degradation *via* an aminotransferase increases the nutritional flexibility of *Candida glabrata*. *Eukaryot. Cell* 13, 758–765. doi: 10.1128/EC.00072-14

Calvo, A. M., and Cary, J. W. (2015). Association of fungal secondary metabolism and sclerotial biology. *Front. Microbiol.* 6:62. doi: 10.3389/fmicb.2015.00062

Calvo, A. M., Wilson, R. A., Bok, J. W., and Keller, N. P. (2002). Relationship between secondary metabolism and fungal development. *Microbiol. Mol. Biol. Rev.* 66, 447–459. doi: 10.1128/MMBR.66.3.447-459.2002

Chen, D., Chen, M., Wu, S., Li, Z., Yang, H., and Wang, C. (2017). The molecular mechanisms of *Monascus purpureus* M9 responses to blue light based on the transcriptome analysis. *Sci. Rep.* 7:5537. doi: 10.1038/s41598-017-05990-x

Chen, M. H., and Johns, M. R. (1993). Effect of pH and nitrogen source on pigment production by *Monascus purpureus*. *Appl. Microbiol. Biot.* 40, 132–138. doi: 10.1007/BF00170441

Chen, W., Chen, R., Liu, Q., He, Y., He, K., Ding, X., et al. (2017). Orange, red, yellow: biosynthesis of azaphilone pigments in *Monascus* fungi. *Chem. Sci.* 8, 4917–4925. doi: 10.1039/c7sc00475c

Chen, W., He, Y., Zhou, Y., Shao, Y., and Chen, F. (2015). Edible filamentous fungi from the species *Monascus*: early traditional fermentations, modern molecular biology, and future genomics. *Compr. Rev. Food Sci. F.* 14, 555–567. doi: 10.1111/1541-4337.12145

Dietl, A. M., Amich, J., Leal, S., Beckmann, N., Binder, U., Beilhack, A., et al. (2016). Histidine biosynthesis plays a crucial role in metal homeostasis and virulence of *Aspergillus fumigatus*. *Virulence* 7, 465–476. doi: 10.1080/21505594.2016.1146848

Dufosse, L., Fouillaud, M., Caro, Y., Mapari, S. A., and Sutthiwong, N. (2014). Filamentous fungi are large-scale producers of pigments and colorants for the food industry. *Curr. Opin. Biotech.* 26, 56–61. doi: 10.1016/j.copbio.2013.09.007

Feng, Y., Shao, Y., and Chen, F. (2012). *Monascus* pigments. *Appl. Microbiol. Biot.* 96, 1421–1440. doi: 10.1007/s00253-012-4504-3

Fuhs, S. R., and Hunter, T. (2017). pHisphorylation: the emergence of histidine phosphorylation as a reversible regulatory modification. *Curr. Opin. Cell Biol.* 45, 8–16. doi: 10.1016/j.ceb.2016.12.010

Green, M., and Sambrook, J. (2012). *Molecular Cloning: A Laboratory Manual, edition no.4*. New York, NY: Cold Spring Harbor Laboratory Press.

Hajjaj, H., François, J. M., Goma, G., and Blanc, P. J. (2012). Effect of amino acids on red pigments and citrinin production in *Monascus ruber*. *J. Food Sci.* 77, M156–M159. doi: 10.1111/j.1750-3841.2011.02579.x

Heim, D. R., and Larrinua, I. M. (1989). Primary site of action of amitrole in *Arabidopsis thaliana* involves inhibition of root elongation but not of histidine or pigment biosynthesis. *Plant Physiol.* 91, 1226–1231. doi: 10.1104/pp.91.3.1226

Jung, H., Kim, C., and Shin, C. S. (2005). Enhanced photostability of *Monascus* pigments derived with various amino acids *via* fermentation. *J. Agric. Food Chem.* 53, 7108–7114. doi: 10.1021/jf0510283

Jung, H., Kim, C., Kim, K., and Shin, C. S. (2003). Color characteristics of *Monascus* pigments derived by fermentation with various amino acids. *J. Agric. Food Chem.* 51, 1302–1306. doi: 10.1021/jf0209387

Li, D., Agrellos, O. A., and Calderone, R. (2010). Histidine kinases keep fungi safe and vigorous. *Curr. Opin. Microbiol.* 13, 424–430. doi: 10.1016/j.mib.2010.04.007

Liang, B., Du, X. J., Li, P., Sun, C. C., and Wang, S. (2018). Investigation of citrinin and pigment biosynthesis mechanisms in *Monascus purpureus* by transcriptomic analysis. *Front. Microbiol.* 9:1374. doi: 10.3389/fmicb.2018.01374

Lin, Y. L., Wang, T. H., Lee, M. H., and Su, N. W. (2008). Biologically active components and nutraceuticals in the *Monascus*-fermented rice: a review. *Appl. Microbiol. Biot.* 77, 965–973. doi: 10.1007/s00253-007-1256-6

Lind, A. L., Lim, F. Y., Soukup, A. A., Keller, N. P., and Rokas, A. (2018). An LaeA- and BrlA-dependent cellular network governs tissue-specific secondary metabolism in the human pathogen *Aspergillus fumigatus*. *mSphere* 3, e50–e18. doi: 10.1128/mSphere.00050-18

Liu, Q., Cai, L., Shao, Y., Zhou, Y., Li, M., Wang, X., et al. (2016). Inactivation of the global regulator LaeA in *Monascus ruber* results in a species-dependent response in sporulation and secondary metabolism. *Fungal Biol.* 120, 297–305. doi: 10.1016/j.funbio.2015.10.008

Lobley, G. E., Wester, T. J., Calder, A. G., Parker, D. S., Dibner, J. J., and Vázquez-Añón, M. (2006). Absorption of 2-hydroxy-4-methylthiobutyrate and conversion to methionine in lambs. *J. Dairy Sci.* 89, 1072–1080. doi: 10.3168/jds.S0022-0302(06)72175-0

Mapari, S. A., Thrane, U., and Meyer, A. S. (2010). Fungal polyketide azaphilone pigments as future natural food colorants? *Trends Biotechnol.* 28, 300–307. doi: 10.1016/j.tibtech.2010.03.004

Mohanan, V. C., Chandarana, P. M., Chattoo, B. B., Patkar, R. N., and Manjrekar, J. (2017). Fungal histidine phosphotransferase plays a crucial role in photomorphogenesis and pathogenesis in *Magnaporthe oryzae*. *Front. Chem.* 5:31. doi: 10.3389/fchem.2017.00031

Mostafa, M. E., and Abbady, M. S. (2014). Secondary metabolites and bioactivity of the *Monascus* pigments review article. *Glob. Biotech. Biochem.* 9, 1–13. doi: 10.5829/idosi.gjbb.2014.9.1.8268

Patakova, P. (2013). *Monascus* secondary metabolites: production and biological activity. *J. Ind. Microbiol. Biot.* 40, 169–181. doi: 10.1007/s10295-012-1216-8

Said, F. M., Brooks, J., and Chisti, Y. (2014). Optimal C:N ratio for the production of red pigments by *Monascus ruber*. *World J. Microbiol. Biotechnol.* 30, 2471–2479. doi: 10.1007/s11274-014-1672-6

Schmittgen, T. D., and Livak, K. J. (2008). Analyzing real-time PCR data by the comparative C_T method. *Nat. Protoc.* 3, 1101–1108. doi: 10.1038/nprot.2008.73

Shi, K., Song, D., Chen, G., Pistolozzi, M., Wu, Z., and Quan, L. (2015). Controlling composition and color characteristics of *Monascus* pigments by pH and nitrogen sources in submerged fermentation. *J. Biosci. Bioeng.* 120, 145–154. doi: 10.1016/j.jbiosc.2015.01.001

Srianta, I., Ristiarini, S., Nugerahani, I., Sen, S. K., Zhang, B. B., Xu, G. R., et al. (2014). Recent research and development of *Monascus* fermentation products. *Int. Food Res. J.* 21, 1–12.

Yang, Y., Liu, B., Du, X., Li, P., Liang, B., Cheng, X., et al. (2014). Complete genome sequence and transcriptomics analyses reveal pigment biosynthesis and regulatory mechanisms in an industrial strain, *Monascus purpureus* YY-1. *Sci. Rep.* 5, 8331–8331. doi: 10.1038/srep08331

Yin, S., Yang, D., Zhu, Y., and Huang, B. (2022). Methionine and S-adenosylmethionine regulate *Monascus* pigments biosynthesis in *Monascus purpureus*. *Front. Microbiol.* 2022:921540. doi: 10.3389/fmicb.2022.921540

Zhang, X., Wang, J., Chen, M., and Wang, C. (2013). Effect of nitrogen sources on production and photostability of *Monascus* pigments in liquid fermentation. *IERI Procedia* 5, 344–350. doi: 10.1016/j.ieri.2013.11.114

Conflict of Interest: The authors declare that the research was conducted in the absence of any commercial or financial relationships that could be construed as a potential conflict of interest.

Publisher's Note: All claims expressed in this article are solely those of the authors and do not necessarily represent those of their affiliated organizations, or those of the publisher, the editors and the reviewers. Any product that may be evaluated in this article, or claim that may be made by its manufacturer, is not guaranteed or endorsed by the publisher.

frontiers | Frontiers in Microbiology

ORIGINAL RESEARCH
published: 28 July 2022
doi: 10.3389/fmicb.2022.915721

The ABCT31 Transporter Regulates the Export System of Phenylacetic Acid as a Side-Chain Precursor of Penicillin G in *Monascus ruber* M7

Rabia Ramzan[1,2,3], *Muhammad Safiullah Virk*[1,2] *and Fusheng Chen*[1,2*]

[1] *Hubei International Scientific and Technological Cooperation Base of Traditional Fermented Foods, Huazhong Agricultural University, Wuhan, China,* [2] *College of Food Science and Technology, Huazhong Agricultural University, Wuhan, China,* [3] *Department of Food Science and Technology, Government College Women University, Faisalabad, Pakistan*

OPEN ACCESS

Edited by:
Xucong Lv,
Fuzhou University, China

Reviewed by:
Chan Zhang,
Beijing Technology and Business University, China
Hafiz A. R. Suleria,
The University of Melbourne, Australia
Muhammad Sohaib,
University of Veterinary and Animal Sciences, Pakistan

****Correspondence:***
Fusheng Chen
chenfs@mail.hzau.edu.cn

Specialty section:
This article was submitted to Food Microbiology, a section of the journal Frontiers in Microbiology

Received: *08 April 2022*
Accepted: *16 May 2022*
Published: *28 July 2022*

Citation:
Ramzan R, Virk MS and Chen F (2022) The ABCT31 Transporter Regulates the Export System of Phenylacetic Acid as a Side-Chain Precursor of Penicillin G in Monascus ruber M7. Front. Microbiol. 13:915721. doi: 10.3389/fmicb.2022.915721

The biosynthesis of penicillin G (PG) is compartmentalized, and the transportation of the end and intermediate products, and substrates (precursors) such as L-cysteine (L-Cys), L-valine (L-Val) and phenylacetic acid (PAA) requires traversing membrane barriers. However, the transportation system of PAA as a side chain of PG are unclear yet. To discover ABC transporters (ABCTs) involved in the transportation of PAA, the expression levels of 38 ABCT genes in the genome of *Monascus ruber* M7, culturing with and without PAA, were examined, and found that one *abct* gene, namely *abct*31, was considerably up-regulated with PAA, indicating that *abct*31 may be relative with PAA transportation. Furthermore the disruption of *abct*31 was carried out, and the effects of two PG substrate's amino acids (L-Cys and L-Val), PAA and some other weak acids on the morphologies and production of secondary metabolites (SMs) of Δ*abct*31 and *M. ruber* M7, were performed through feeding experiments. The results revealed that L-Cys, L-Val and PAA substantially impacted the morphologies and SMs production of Δ*abct*31 and *M. ruber* M7. The UPLC-MS/MS analysis findings demonstrated that Δ*abct*31 did not interrupt the synthesis of PG in *M. ruber* M7. According to the results, it suggests that *abct*31 is involved in the resistance and detoxification of the weak acids, including the PAA in *M. ruber* M7.

Keywords: ABC transporter, secondary metabolites, phenylacetic acid, amino acid, weak acid

INTRODUCTION

In view of the present antibiotic resistance crises and the slowing rate of antibiotic discovery, there has been a worldwide push to look into the large quantity of unexplored natural product sources for novel antibiotics or their precursors (Seiple et al., 2016). Even though β-lactam antibiotics have been present since the 1920s, they remained the most commonly utilized antibiotic class.

Meanwhile, new routes for biosynthesis of β-lactam are continually being found (Gaudelli et al., 2015). In China and some other Asian regions, *Monascus* spp. are popular as conventional edible fungi. Their fermented products, namely red yeast rice, red mold rice (RMR), Anka, or Hongqu, have been widely utilized in China as folk cures and culinary colorants for 2,000 years (Lee et al., 2010; Lee and Pan, 2012; Guo et al., 2019). Researchers have publicized that *Monascus* spp. can create both useful and harmful secondary metabolites (SMs), such as *Monascus* pigments, aminobutyric acid, dimurumic acid, and monacolin K, and a typical type of mycotoxin, which is known as citrinin (Ozcengiz and Demain, 2013; Yuliana et al., 2017; Chen and Pan, 2019). Recently, Chen (2015) found a probable gene cluster having liability for β-lactam synthesis in the genome of *M. ruber* M7, and one β-lactam biosynthesis gene was identified in the gene cluster (Ramzan et al., 2019). *M. purpureus* was also proved to produce γ-lactam according to Wei et al. (2017).

Many microorganisms, including filamentous fungi, actinomycetes, and Gram-negative bacteria, may synthesize several types of β-lactam antibiotics (Lobanovska and Pilla, 2017). During the biosynthetic pathway of the β-lactam antibiotics, the non-ribosomal peptide synthetase initially condenses the three precursor amino acids, L-α-aminoadipic acid, L-cysteine and L-valine, to form the basic nucleus of β-lactam antibiotic, isopenicillin N (IPN) with hydrophilic feature (Fernández-Aguado et al., 2014). The IPN fabrication is taken place in the cytoplasm of β-lactam producers (Barreiro and García-Estrada, 2019). Then, the conversion of IPN is taken place into penicillin G (PG) in the peroxisomal matrix of β-lactam producers (Van Den Berg et al., 2008; Ávalos et al., 2014). During this process, an hydrophilic α-aminoadipyl side chain, phenylacetic acid (PAA), is catalyzed into a hydrophobic phenyl acetyl CoA of IPN by the IPN acyl transferase (García-Estrada et al., 2008). The entry of the side chain of PG, PAA, into the cells takes place via passive diffusion. And acidification of cytosol is caused by the influx of PAA. After entering the cells, PAA is dissociated and releases protons. Due to the acidification of cytoplasm, enzymatic activities are inhibited, which causes the ultimate death of the cell (Weber et al., 2012). Nevertheless, cytoplasmic acidification is unlikely to be the only cause of mild acid toxicity. The more hydrophobic sorbic acid, for example, may impair the organization of the membrane, leading to oxidative stress due to a lesser functioning of the respiratory chain, and so toxicity could be a multidimensional phenomenon. So, during the biosynthesis of penicillin, the shipping of intermediates and their precursors across the cellular membranes is an important matter (Martín et al., 2005). Several transporters are not fully explored (Fernández-Aguado et al., 2013, 2014). According to their abilities to transport diverse organic composites, the transporters are classified into the extrusion of multidrug and toxic compounds, small multidrug resistance, ATP-binding cassette (ABC) superfamily, major facilitator superfamily, and so on (Martín et al., 2005).

Binding and hydrolyzing ATP to transport the substrates across the lipid bilayer is the characteristic ability of the ABC transporter family (Wilkens, 2015). The well-studied ABC exporters in prokaryotes and eukaryotes play a central role in

TABLE 1 | Primers for all ABC transporter genes in *M. ruber* M7 and used in the construction of deletion cassettes for the gene *abct*31.

Name	Sequence 5' 3'	Product length
AbctF1	ACAAAAGCCAAAGGATGACGA	193
AbctR1	CGTCTGTTACTGCTGAACGCTA	
AbctF2	TCCTCGGGTTCATTTTCGTC	175
AbctR2	TTCACCCCAGCTGTACCAA	
AbctF3	ACGCTCACGAATCATAAGTGGA	193
AbctR3	CTGCCATGACCTCTCCGTTC	
AbctF4	ACTAACAGGAGCTAAGCCCAA	183
AbctR4	GCTGCACATGTATTATCTTGACC	
AbctF5	GCATATACCTACGCAGTGTCC	191
AbctR5	GCCAATACCTCGACCGCTA	
AbctF6	CCTCTGAATTTGCAATGCCTT	151
AbctR6	ACCCCATCTCTTCAAAATATGCT	
AbctF7	CTCAAGATAAAGCAGCAATCCAC	155
AbctR7	ATCGGTTTGAGGAGGGTTCTA	
AbctF8	AGATCAGCATTAAGCGCCACA	168
AbctR8	CATGTCCTTAATTATCGCCAGT	
AbctF9	TCCTGCTTTGTACATCGTCCA	175
AbctR9	TATACTGTAACCGCGCTAGCC	
AbctF10	GGCGTACTTCAAACAGACCGAT	176
AbctR10	TCGTCTTCTCCTCGGGCTCT	
AbctF11	ATGATCCCTGTCAGTGCTCCC	158
AbctR11	TCGTCCTTTTCCTCCGCACAC	
AbctF12	CCCAATGACCATATACACGAA	173
AbctR12	TAGACGACAAGACGCTCCA	
AbctF13	ACATGACAATGCCTGAAAGGTT	188
AbctR13	CCAACGGCCAGCATACCTC	
AbctF14	CAAAAGTACCCTGCTAGACCA	200
AbctR14	GGTTTGATTTGCAAGCTCCT	
AbctF15	GAGTCTGCACCAACATGATCG	176
AbctR15	ATATGTACCAGCAGACGCAAT	
AbctF16	AGACAGCCAGTTCTACGCATC	191
AbctR16	TTGAGATAGAGCCCGCCAT	
AbctF17	ATGCCGTCAATAGCTCGACA	152
AbctR17	ATTCAGGACCTATGGCCTT	
AbctF18	CACCAACTCTCCGCTCAGT	198
AbctR18	CTGTTTTGCCTCCCGTCT	
AbctF19	TTATTGTGCTCGCCTTCGTTG	174
AbctR19	TTCTTCAGCCCGACCGTTG	
AbctF20	GTTTCTCTAATTCTGGGACCG	93
AbctR20	ATATATGCTGGAAGTTGGCTC	
AbctF21	CACTTTTGCACACCAATCCAG	173
AbctR21	AAAGAATAACCAGACCGCACT	
AbctF22	ACGTCGAAGAGCAGAGGGATG	85
AbctR22	AGCATCTGGAGCCGTCACT	
AbctF23	CCAAACACACTAAGCCCGAAC	194
AbctR23	ATAAGCATCACCACGTAGCAAG	
AbctF24	TTCAGCAGCAAGATCTACACT	143
AbctR24	CTCCATGTCAAGAACCTCGAT	
AbctF25	CCCGTATGTCATAGTAGGCTT	177
AbctR25	CATGGCCTTCAGACTAGCAG	

(Continued)

TABLE 1 | Continued

Name	Sequence 5' 3'	Product length
AbctF26	AACGCCATAACCTCCATTGCT	151
AbctR26	CCATCAACCGCACAACTCCC	
AbctF27	AATCGCATCAATTAGTCTGGG	146
AbctR27	CATTCGTCCAGGTATGCAAC	
AbctF28	TCAATTTCTGGACGCCGTGA	190
AbctR28	AGGCTCAAAACTTCAACGTCT	
AbctF29	TGAAATCCAGGTCTCACGGAA	162
AbctR29	TGTTGTACACGGGCAATCCTC	
AbctF30	GCCAGCGTCCATCACAAAA	160
AbctR30	ACTCCATTACAAACTGGCCGACT	
AbctF31	TCCCAGCCAAATTTTCCGTTC	119
AbctR31	CAAGATTGCAAAAGCTCGAGT	
AbctF32	ACTACACGATTTCTGAAGCCTA	141
AbctR32	AGAACAGTCACAATACGTCCA	
AbctF33	TTGCCATGTCTGTGAATACCG	164
AbctR33	TCTTGGAAGCCTTAGTCCGTA	
AbctF34	CAGTACAAAGCACGCCACA	176
AbctR34	AGCAGCTACACAATACTGGTC	
AbctF35	GAAGCCTACCAAGTCCCCT	177
AbctR35	ATACAGAACCCGATGTCCAC	
AbctF36	ACTATAATGACGAGCGCCACT	153
AbctR36	CTTGAACAAATTCTTCGCACAGG	
AbctF37	GGCATCTATCCTGGCAACCC	170
AbctR37	TGACAACTTTATTCCCTGCGGTA	
AbctF38	TCGATGTCAATAAAGCGCAGT	127
AbctR38	AGGCGATTATTCTCTTTGTCGT	
γ-actin F	CTGGCGGTATCCACGTCACC	
γ-actin R	AGGCCAGAATGGATCCACCG	
*abct*31-5F *abct*31-5R	CCCAAGCTTCAAGGGCTGTGCT CGGTA CAATATCATCTTCTGTCGACTGA AAACAGCGGCAATGG	For the amplification of the 770 bp of the 5' flanking region of the *abct*31 gene
*abct*31-3F *abct*31-3R	GAGGTAATCCTTCTTTCTAGGTCA TCCTCGGCTTTTGC CGGGGTACCTGTGCGGT GAATAGGTGC	For the amplification of the 434 bp of the 3' flanking region of the *abct*31 gene
hphF hphR	GTCGACAGAAGATGATATTG CTAGAAAGAAGGATTACCTC	For the amplification of the 2,317 bp of the hph cassette from the plasmid pSKH
*abct*31F *abct*31R	CGCAATGGAGAAGACGGT CGGTGCGATTGAGTTCCA	For the amplification of the 750 bp of the partial *abct*31 gene

life activities. There have been expansive investigations of their association with many human diseases (Fletcher and Mullins, 2010; Tang et al., 2021) and resistance to multiple drugs (Al Shawi et al., 2011). Weber et al. (2012) found that PAA in higher concentrations could be toxic to the cells, and the proliferation of the common ancestor of the recent penicillin-producing strains, *P. chrysogenum* Wisconsin 54-1255, is not possible at a high concentration (18 mM) of PAA. The high penicillin-producing strain *P. chrysogenum* DS17690, on the other hand, is generally insensitive to such PAA doses, showing that DS17690 cells have established PAA resistance mechanisms. Likewise, a weak acid extrusion system has been identified in *Saccharomyces cerevisiae*. PDR12 is an ABC transporter from *S. cerevisiae* that prevents cytoplasmic acidification and transports metabolites of yeast metabolism out of the cells (Hazelwood et al., 2006; Zhang et al., 2021).

Though several features of the traffic systems of β-lactam antibiotics need to be investigated further, it has been thought that the involvement of the transmembrane transporter proteins plays a role in their synthesis. As a result, more researches about the involvement of transporters in the β-lactam antibiotic gene cluster are required. Moreover, it has been strongly predicted that the ABC transporters encoding genes are present in the gene clusters. In the present study, the expression and identification of all ABC transporters present in the genome of *M. ruber* M7 for the biosynthesis of the β-lactam antibiotics have been investigated after being grown in the presence and absence of PAA. In the presence of PAA, the results revealed one ABC transporter (ABCT31), whose role in β-lactam antibiotic production was explored via *abct31*-deletion. Furthermore, compared to *M. ruber* M7, the resistance of the mutant to the weak acid toxicity was assessed at various concentrations with the presence and absence of PAA.

MATERIALS AND METHODS

Materials

The Δ*abct*31 mutant was created using the *M. ruber* M7 strain (CCAM 070120, Culture Collection of State Key Laboratory of Agricultural Microbiology, <city>Wuhan</city>, China), which can produce *Monascus* pigments and citrinin but not monacolin K. (Chen and Hu, 2005). Czapek yeast extract agar (CYA), potato dextrose agar (PDA), glycerol nitrate agar (G25N 25%), and malt extract agar (MA) media were used for the phenotypic analyses (He et al., 2013). On PDA, resistance markers hygromycin B (30 μg/mL) and neomycin (15 μg/mL) were used for transformants screening. PDA slants of strains were prepared and kept at 28°C.

Extraction of the DNA

The strains were cultured on the PDA plates with cellophane covers. Extraction of the genomic DNA of the grown strains from their mycelia was done using the cetyltrimethylammonium bromide method by Shao et al. (2009).

Quantitative Real-Time PCR (qRT-PCR) Analysis

The method described by Liu et al. (2014) was followed to conduct the qRT-PCR using the SLAN Fluorescence Quantitative Detection System from Wuhan Good Biotechnology Co., Ltd., (Wuhan, Hubei, China).

Computational Structural Analysis of *abct*31

Table 1 lists the primer pairs utilized in the current investigation. The *abct*31gene was amplified by PCR using *M. ruber* M7

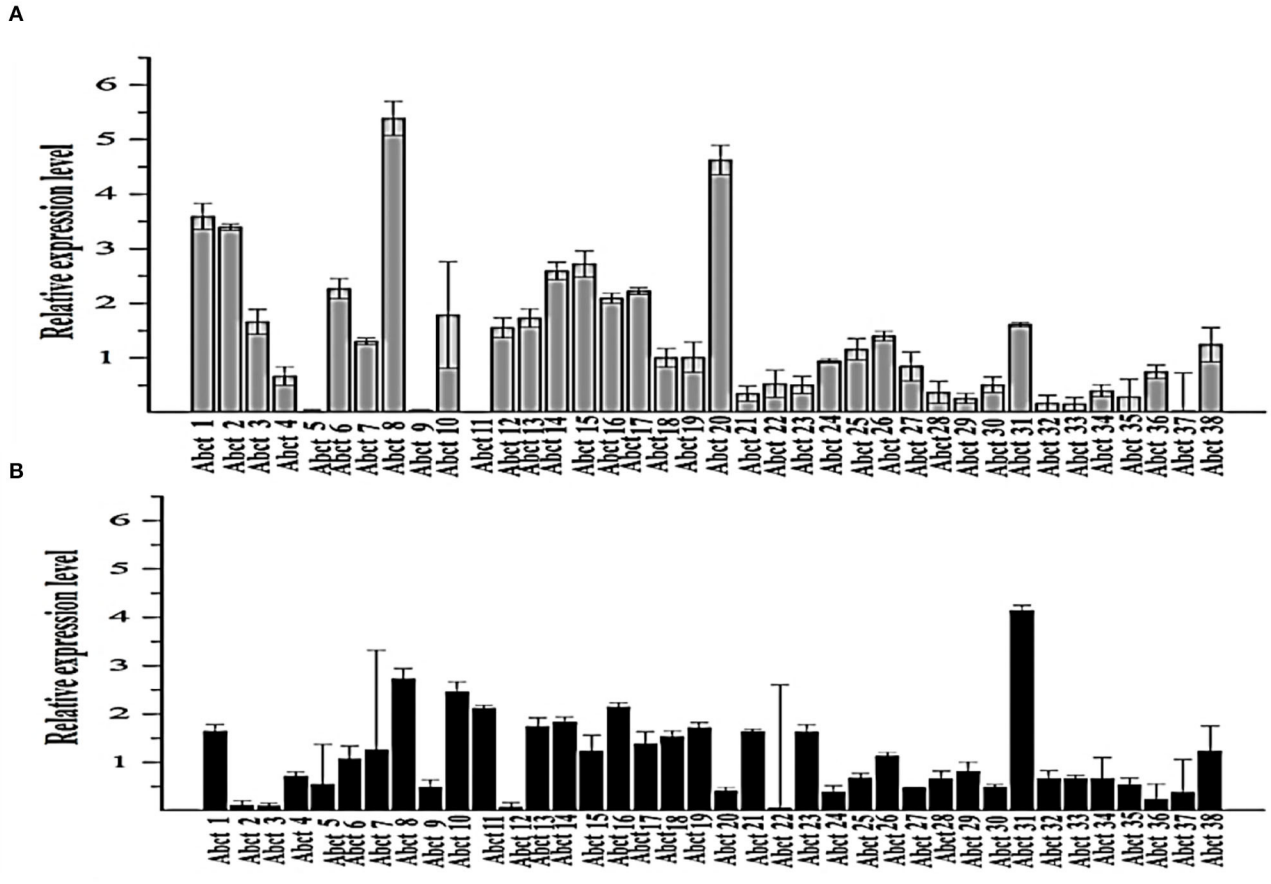

FIGURE 1 | Quantitative real-time PCR analysis of the expression of all ABC transporter genes in the *M. ruber* M7 toward PAA. **(A)** The comparative expression of all ABC transporter genes in *M. ruber* M7 without PAA; **(B)** A comparative expression of all ABC transporter genes in *M. ruber* M7 with PAA. *M. ruber* M7 was cultivated and incubated at 28°C for 7 d in the presence (black bar) and absence (gray bar) of PAA at 10 mM. The values were represented as average values ± sd.

genomic DNA under the subsequent conditions. The first denaturation step was performed for 5 min at 94°C, preceded by 35 amplification cycles at 94°C for 30 s, at 58°C for 30 s, and for 1 min at 72°C. However, the T100 Thermal Cycler was used at the end during the extension phase at 72°C for 10 min (Bio-Rad, Hercules, CA, USA) (Chen et al., 2012a,b). SoftBerry's FGENESH software (https://linuxl.softberry.com/berry.phtml) was used to anticipate the ABCT31 amino acid sequences. The Pfam 27.0 program (http://pfam.xfam.org/) was used to examine the ABCT31 functional regions. While the BLASTP program (https://blast.ncbi.nlm.nih.gov/Blast.cgi) was utilized to interpret the homology of the presumed amino acid sequences of ABCT31. Moreover, the PSIPREDv3.2 server (http://bioi nf.cs.ucl.ac.uk/psip red/) (Buchan et al., 2013; Waterhouse et al., 2018) and RaptorX server (http://rapt orx.uchi cago.edu/) (Wang et al., 2016b) were employed, respectively, to explain the predictions of genes for secondary structural elements. Similarly, from the PSIPRED server, HMMTOP, MEMSAT3, and MEMSAT-SVM programs were used to describe membrane helix and topology predictions (Pandey et al., 2018). The Deep Loc-1.0 server (https://services.healthtech.dtu.dk/service.php?DeepLoc-1.0) was used to determine the likely subcellular protein localization (Emanuelsson et al., 2000). Predictions of all genes ontology domains for the probable gene term annotations were done using the FFPred 3 program (http://bioi nf.cs.ucl.ac.uk/psip red/) (Pandey et al., 2018).

Construction of the *abct*31 Gene Deletion

The approach of Shao et al. (2009) was used to delete the targeted gene *abct*31. The construction of the cassette for gene disruption (5'UTR-*hph*-3'UTR) was carried out with a double-joint PCR procedure. The primer pairs are listed in **Table 1**, whereas **Figure 1A** demonstrates the schematic illustration (Wang et al., 2011). For the development of the deletion strain (Δ*abct*31), construction of the *Agrobacterium tumefaciens* cells expressing the disruption vector (pC- *abct*31) of *abct*31 was done, and its co-cultivation was carried out with *M. ruber* M7.

Southern Hybridization Analysis

The *abct*31 gene deletion strain was further confirmed utilizing the DIG-High Prime DNA Labeling & Detection Starter kit's method by applying PCR and Southern blot method (Roche,

Mannheim, Germany). The restriction enzyme XbaI was used to digest the DNA of the putative Δ*abct*31 strain and *M. ruber* M7, respectively. As shown in **Table 1**, the respective primer pairs hphF/hphR and *abct*31F/*abct*31R were used to amplify the *hph* gene (probe 2) and *abct*31 gene (probe 1) by the PCR. Finally, probes 1 and 2 confirmed the Δ*abct*31 strain.

Phenotypic Characterization

In order to study the phenotypic characteristics, colonial and microbiological features of parental (*M. ruber* M7) and Δ*abct*31strains were inoculated on PDA, G25N, MA, and CYA media plates and incubated at 28°C for 15 days (Chen et al., 2017a).

Estimation of the Biomass

Estimation of the biomasses of *M. ruber* M7 and Δ*abct*31 was accomplished by the gravimetric method. The collection of mycelia on PDA plates was done following the drying at 60°C until the constant weights were obtained. Three replicates were used to compute the mean biomasses (Wang et al., 2016a).

PG Contents' Extraction and Measurement

PG Extraction

The PG was extracted from the respective *M. ruber* M7 (wild-type) and Δ*abct*31 by the previously defined method (Ramzan et al., 2019).

HPLC Detection of the PG

The previously reported method (Ullán et al., 2008; Ramzan et al., 2019) was used for the analysis of intra- and extracellular PG contents.

Verification of PG and IPN by UPLC-MS/MS

The mass profile of the extract was produced using electrospray ionization (ESI) coupled Acquity TQD tandem quadruple mass spectrometer (Waters, Manchester, UK). The conditions for the ESI-MS to detect MS were set according to Ramzan et al. (2019). The presence of PG metabolites in the extract was confirmed using a PG standard with a purity of more than 98.0 percent (Sigma-Aldrich) (Lopes et al., 2013).

Effects of Precursor Amino Acids Feeding on PG Production

The feeding of amino acids was used to investigate the transportation role of the *abct*31 gene (Yang et al., 2012). For this purpose, Δ*abct*31 and *M. ruber* M7 were separately grown on PDA with 2 mM concentrations of PG pathway amino acids such as D-Val, L-Cys and PAA, respectively. Then, phenotypic characteristics, biomasses, and PG synthesis were analyzed.

Weak Acids Sensitivity Experiments

The feeding of mutants and *M. ruber* M7 on PDA with the addition of some weak acids including PAA, acetic acid, adipic acid and sorbic acid was used to examine the transportation mechanism of the *abct*31 gene (Weber et al., 2012). This procedure was carried out according to the method described by Weber et al. (2012) with slight modification such as PAA (mM): 50, 62.5, 75, 100, and 125; acetic acid (mM): 5, 10, 15, 20, and 25; adipic acid (mM): 12.5, 25, 37.5, and 50; and sorbic acid (mM): 2, 2.75, 3.5, and 4.25 concentration. The phenotypical features and relative expression of *abct*31 gene in *M. ruber* M7 were analyzed.

TABLE 2 | Putative functions of ABCT31 analyzed by Pblast and CDD program.

Name	Accession	Description	Interval
MRP-assoc-pro	TIGR00957	Mutltidrug resistance protein	29–1017
PLN03130	PLN03130	ABC transporter C family member	29–1027
ABC_tran	pfam00005	ABC transporter family responsible for translocation	722–955

Statistical Analyses

All of the experiments were carried out in triplicate. The statistical studies were performed using the Statistics 8.1 program (Analytical Software, USA). After performing the Tukey test, a $P < 0.05$ was taken as statistically significant, and a $P < 0.01$ was considered highly significant.

RESULTS AND DISCUSSION

Evaluation of ABCT31 Sensitivity Toward PAA

To understand the proper mechanism of the *abct*31 gene as a transporter in the translocation of intermediates metabolites of the PG pathway, *M. ruber* M7 was cultivated for 7 days at 10 mM in the +PAA (presence) or –PAA (absence). The determination of the transcript levels of all ABC transporter genes in the genome of *M. ruber* M7 was done while the γ-actin gene used as a reference gene (**Figure 1**).

The ABC transporter expression levels have been noted in *M. ruber* M7 with or without PAA. The experiment results revealed a notable upsurge in the expression of *abct*31 (**Figure 1B**) in the presence of PAA in *M. ruber* M7, whereas without the PAA (**Figure 1A**), the expression of *abct*31 was considerably lower. In the +PAA/–PAA, all other ABC transporter genes displayed no expression or did not show a distinct variation in their transcript levels in *M. ruber* M7 (**Figures 1A,B**).

Identification of Putative Function of *abct*31

The ABCT31 protein sequence from *M. ruber* M7 was analyzed using NCBI's blast tool (https://blast.ncbi.nlm.nih.gov/Blast.cgi) and homologous aligning of the *abct*31 with 27 distinct ABC transporters from other genomes as well as identification of different conserved domains were discovered (**Table 2**). Softberry's FGENESH software was also used to predict the 1,257 amino acid sequence. *abct*31 corresponds to the ABC transporter family, according to a database search using the Pfam 27.0 tool (http://pfam.xfam.org/). The expression of an ABC-membrane family C domain (PLN03130, pfam00005) represents hydrophobic transmembrane helices, (Schulz and Kolukisaoglu,

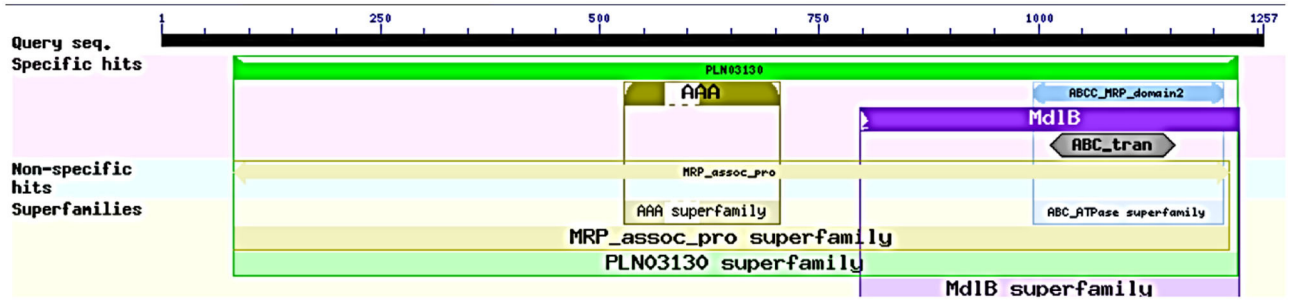

FIGURE 2 | Domain analysis of *abct*31 analyzed by CDD program.

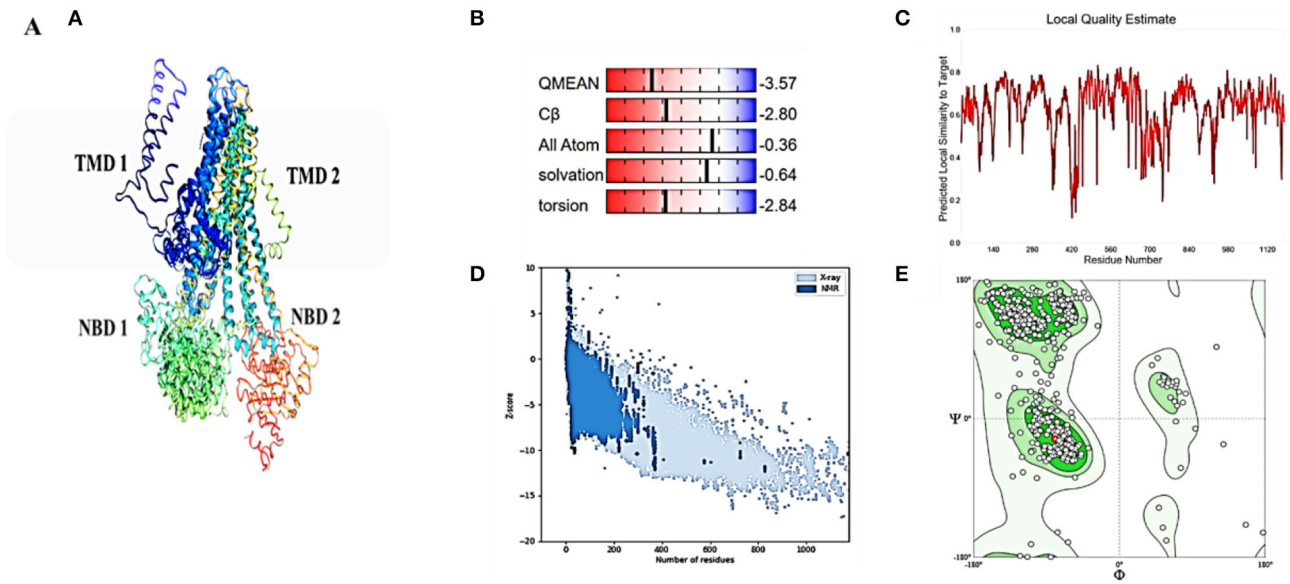

FIGURE 3 | Homology model and checking results for ABCT31 protein. Verification of homology modeling **(A)** Homology model of ABCT31 protein TMD, Transmembrane domain; NBD, Nucleotide-binding domains; **(B)** Plot displaying the model's normalized Q mean score; **(C)** Plot displaying the model's local quality; **(D)** Z score value of the model developed; **(E)** Ramachandran plot validating the energy-minimized model's backbone dihedral angles.

2006), and a key component of ABC transport proteins and its recognition is conserved by the low E values (**Figure 2**).

Model Validation and Homology Modeling

Although atomic resolution crystal structures of various soluble proteins have been discovered, equivalent advancement has not been reported for transporter proteins. The key challenge is the severe exertion in crystallizing them due to flexibility in their conformation. As a result, developing a homology-based protein model is a viable option (Gao et al., 2021). The ABCT31's final 3D structure (**Figure 3A**), which was created using the SWISS-MODEL software and a template-based homology model, was visualized using Procheck. The basic layout of all ABC transporters is the same, with two transmembrane domains (TMDs) and two nucleotide-binding domains (NBDs). The structural analysis has revealed that ABCT31 protein performed as an importer and possessed two TMDs marked as TMD1 and TMD2, similarly to NBDs grouped into NBD1 and NBD2 in the three-dimensional structure presented in **Figure 3A**. In ABCT31, protein is fused between TMDs and NBDs. The ABC transporter's fundamental unit comprises all of these domains. The ABC signature motifs, Walker A (P-loop) and Walker B, which are prevalent but not limited to ABC transporters, are used to classify the NBD.

The assemblage, dynamics, surface characteristics, and thermodynamics of inorganic, polymeric, and biological systems have been studied using molecular modeling approaches. The target protein 3D framework has been developed using the SWISS-MODEL software and template-based homology modeling. The findings suggest that the ABCT31 protein seems to have a homological similarity with the 6pza 1 (ATP-binding cassette, sub-family C member 8). The highest template for homology-based modeling for ABCT31 was reported as having a sequence identical score of 33.17 percent.

TABLE 3 | PROCHECK projected statistics of the proposed three-dimensional model.

Parameter	Score
Dihedrals	−0.26
Covalent	−0.04
Overall	−0.15

The QMEAN-Z score was found to be 3.57 in the context of the global score by QMEAN, indicating the relatively strong quality of the model (<4) (**Figure 3B**). The model quality determinant is the Z score value representing the structure's total energy. The observed Z score value of ABCT31 was noted as −10.34, as shown in **Figure 3D**, which falls in the range normally found in comparable protein chains in the PDB, demonstrating the structure's dependability. The energy plot presented in **Figure 3E** depicts the quality of the local model by graphing energies as a function of the position of amino acids in sequence, with +ve values corresponding to problematic or incorrect regions of a model in general. The residues further validated the projected model's consistency with negative energy (Kulkarni and Devarumath, 2014).

WHAT IF was used to assess the packing environment for residues of the modeled ABCT31 to the experimental structures. An equal or <-5.0 score indicates poor structural packing (Singh et al., 2016; Stitou et al., 2021). Compared with the template X-ray structure (**Figure 3C**), the produced structure has similar packing scores, with only a few residues having poor packing, as their score values have been shown (−1.074) lesser than −5.0. The ABCT31's stereochemical and energetic features were evaluated using a Ramachandran plot, which revealed that 1.3 percent of residues (15) in the disallowed/outlier region, 5.6 percent of residues (66) in the allowed region, and 93.1 percent of residues (1094) in the most favored zones, of the RAMPAGE server (**Figure 3E**). The statistics in the preferred and allowed regions and the low proportion in the outlier show the acceptability of the *abct*31's Ramachandran plot. The PROCHECK goodness factor (G-factor) revealed important information about the distances of covalent and overall bond angles. However, after the analysis of the G-factor for the modeled ABCT31 was > 0.502, indicating that the quality of the projected model was extremely high. The G-factor and the overall Ramachandran plot properties ensured the ABCT31structure's quality (**Table 3**). The overall quality factor of ABCT31 was 88.1651, according to an ERRAT analysis. The quality of the 3D protein model generated in this work is confirmed by the findings acquired from multiple quality evaluation servers.

Identification of Structural Features of ABCT31

As described in section Model Validation and Homology Modeling, the NBDs possess some conserved motifs, which play an important role in the hydrolysis and binding of ATP in the opening and closing mechanism of the TMDs'. NBDs dominate the subunits of ABC, and these might be divided into two constituent domains: the conserved Walker A motif or P-loop (GXXGXGK(S/T), which is contained in the catalytic core domain, Walker B motif (ϕϕϕϕD, ϕ represents the hydrophobic residue), switch region (also known as Q-loop and H-motif) together with an α-helical domain that is more diverse on a structural basis, and it contains the signature motif of ABC (LSXGQXXXXX). The nucleotide state affects the comparative alignment of the catalytic domains and helix. The ABC subunits were packed together in a "head-to-tail" configuration in an intact transporter so that one subunit's P loop is positioned toward the other subunit's signature. In the present ABC protein, the sequence of Walker A (GPIGSGKTS), Walker B (IVLLDD) ABC transporter signature (LSRGQKQRIA), and the three-loop structures Q (FCDQ), D (SGLD), and H (VLVTHAN) was also identified and located, respectively, as shown in **Figure 4A**.

Low E values (**Figure 1**) determined by the CDD software indicated that most amino acids in the ABC-MRP domains (accession: cd03250 and cd03244) are substantially retained in all homologs. The extremely preserved amino acid motifs are contained in the NBD of the ABC-MRP domain and play a role in generating the required energy, which is ultimately used for powering the transport mechanism (Ghilarov et al., 2021). The Walker A [GXXGXGK(S/T)] and Walker B (hhhhDE, where h represents the hydrophobic amino acid) motifs were discovered to be ATP-binding motifs inside the NBD (**Figure 4A**). The establishment of formally extensive connections with an ATP molecule's phosphate group is done by the Walker A motif. Similarly, the coordination of water and Mg^{2+} at the catalytic site is done by the Asp of the Walker B motif.

In contrast, the catalytic glutamate is essential for the hydrolysis of ATP (Zaitseva et al., 2005). Likewise, a conserved Gln plays an important function in coordinating the ATP molecule. This is located between the Walker sequences in the Q-loop. The identification of the conserved D-loop and switch or H-loop as additional motifs was done downstream of the Walker B motif and, respectively, termed as Asp and His. These coordinate the γ-phosphate through the collaboration of either D-loop (water molecule) or H-loop (direct hydrogen binding) (George and Jones, 2012). The Walker sequences of each NBD bearing the conserved amino acid sequence LSGGQ were also identified. This discovered subdomain is also implicated in ATP binding and is termed a helical subdomain or an ABC signature motif (Zaitseva et al., 2005; Chen et al., 2017b).

Hydropathy Profile of ABCT31 Protein

MEMSAT SVM is a support vector machine (SVM) oriented predictor, which is very dependable software that can also predict pore-lining residues. MEMSAT 3, HMMTOP, and MEMSAT SVM are transmembrane protein topological predicting tools. With a total entropy of 18.8083, these programs indicated 11 transmembrane helices (**Figure 4B**). The illustrated transmembrane helices have a high number of hydrophobic amino acids, and the MEMSAT SVM software was used to represent the final interpreted topology of this transmembrane protein, as shown in **Figure 4B**. It also discovered four pore-lining helices with a pore stoichiometry of 1, containing residues from 222 to 239, 366 to 396, 804 to 819, and 884 to 903. It

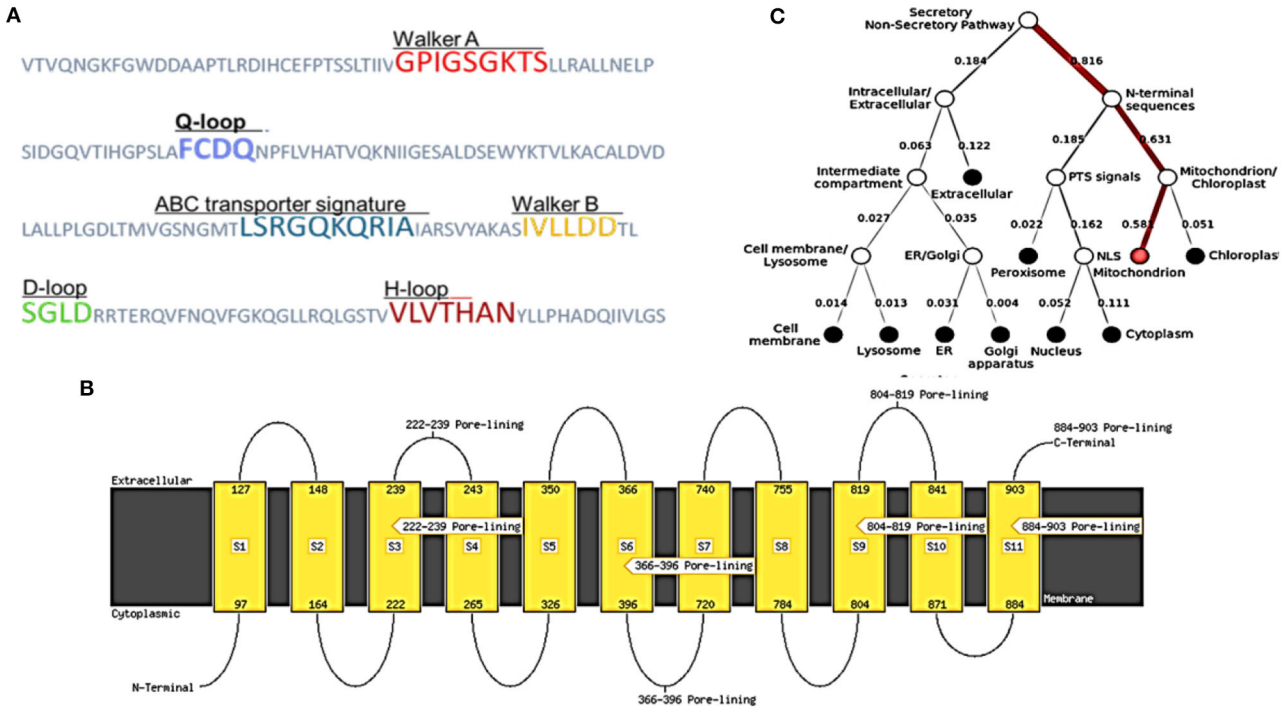

FIGURE 4 | Structural features and location analysis of the ABCT31 protein. **(A)** Features loop and walker of the *abct*31 protein; **(B)** Topology analysis of the ABCT31 protein; **(C)** Location of *abct*31 gene in *M. ruber* M7.

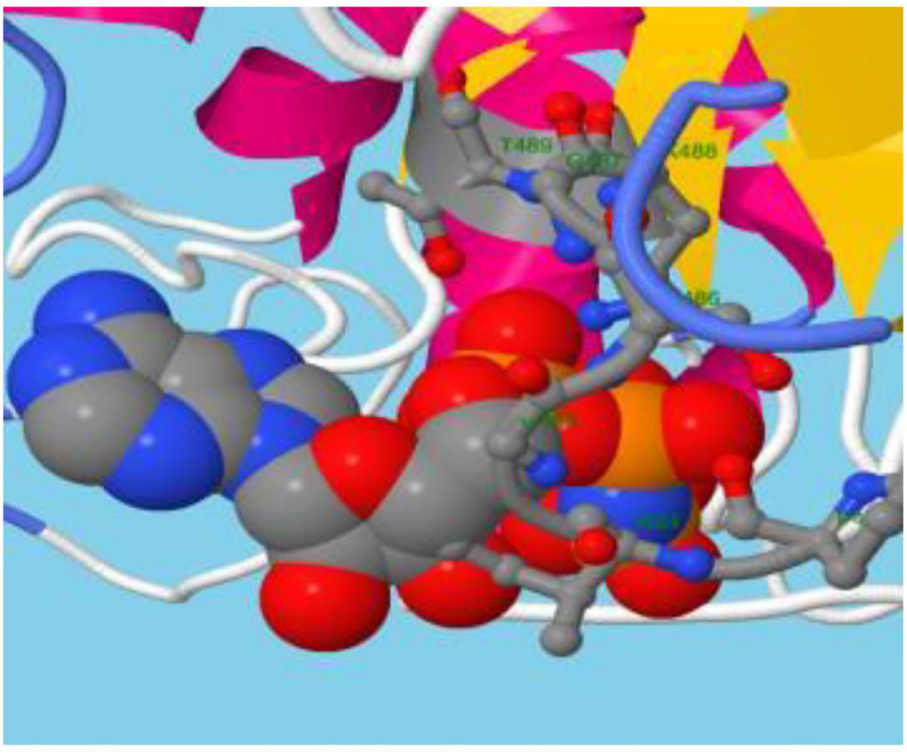

FIGURE 5 | ABC transporter carries the substrate.

has been observed that the transmembrane domain area of transporter proteins forming transport channels is mostly made up of membrane-spanning alpha-helices with bends and kinks, giving significant structural variation that is necessary for the channel's activity (Moussatova et al., 2008; Nugent and Jones, 2012). The occurrence of transmembrane with hydrophobic regions revealed its membrane-embedded architecture and participation in transmembrane transportation, which can be confirmed further through functional and structural analysis.

Subcellular Localization of *abct*31 Gene in *M. ruber* M7

FFPred predicted the biological function as transmembrane transport with 0.907 probability based on gene ontology. Molecular function analysis predicted transmembrane transporter activity as 0.963 and substrate-specific activity of transmembrane transporter as 0.769. However, the cellular component prediction was predicted as an intrinsic or integral part of the membrane with a probability of 1.0. Deeploc server identified that *abct*31 protein is a membrane type with 0.9973 scores while the soluble scoring is 0.0027. It also predicted that it is located in the cell membrane with a score of 0.378 (**Figure 4C**).

Substrate Binding Properties of ABCT31 Protein

Structural information, outcomes of GO prediction, and domain analysis altogether recommend the localization and function of ABCT31 protein membrane in the transportation of substrates through transmembrane, especially the transportation of phenylacetic acid is needed to be studied further through the 3D structure analysis. However, another trusted online method known as the RaptorX-binding site prediction tool identified PA as the potential ligand and discovered two binding sites regulated by residues G487 P483, I484, G485, S486, K488, and T489 (**Figure 5**).

Genetic Deletion of *abct*31 Gene for the Construction of Δ*abct*31

To examine the role of *abct*31 *in vivo*, the development of the *abct*31 gene disruption strain (Δ*abct*31) was done by using a method (Shao et al., 2009; Liu et al., 2014, 2019). The amplification of the upstream 5' flanking region and downstream 3' flanking region (**Figure 6B**) was done from the genomic DNA of *M. ruber* M7 (schematic presentation in **Figure 6A**). At the same time, the pKSH vector was used to amplify the *hph* gene fragment (**Figure 6C**). All amplified fragments were purified by gel electrophoresis and a gel purification kit (**Figure 6D**). During the next step, the disruption cassette was ligated with the linearized pCAMBIA3300 vector by T4 ligase to make the knock-out vector (pC- *abct*31) of *abct*31. The successful ligation was further confirmed by double digestion of pC-*abct*31 (Lane 1-2); two bands, 8.0 kb by pCAMBIA3300 and 3.3 kb of disruption cassette, are presented in **Figure 6E**.

The six putative deleted (Δ*abct*31) strains obtained by *Agrobacterium*-mediated T-DNA transformation to *M. ruber* M7 as a recipient were also identified and authenticated by PCR analyses. One of the mutants was subjected to further PCR verification, and the results are as shown in **Figure 6F**. The 3 pairs of primers Abct31-5F/Abct31-3R, Abct31F/Abct31R, and hphF/hphR (**Table 1**) used for the validation of the homologous recombination event. Lane 2 for the M7 genomic DNA and Lane 1 for the Δ*abct*31 strain, the primer pair Abct5F/Abct3R 3.3 kb and 6.0 kb band, were amplified, respectively. In the case of ORF prime pair Abct31F/Abct31R, nothing was amplified from the Δ*abct*31 strain while the 800 bp band amplified M7 genomic DNA. Controversially, the hphF/hphR primer pair 2.1 kb band appeared in Lane 1 (Δ*abct*31 strain), and nothing was seen in Lane 2. The above PCR results are demonstrated in **Figure 6F**, the main differences in genomic DNA of Δ*abct*31 strain and *Monascus ruber* (wild type) strain.

Furthermore, performing the transformant Southern hybridization verification, the results are shown in **Figure 6G**; with Probe 2 (**Table 1**) as a probe, a single hybridization band appeared in the transformant Δ*abct*31 and nothing appeared in M7 DNA. However, ORF (**Table 1**) was used as a Probe 1; no hybridization band appeared for Δ*abct*31 strain. Hybridization bands indicate that the *abct*31 gene in the mutant has been successfully replaced by the single copy of the *hph* resistance gene.

Many genes involved in the manufacture of pigments, antibiotics, herbicides, and other secondary metabolites have been cloned in the previous decade. The biosynthetic genes for cephalosporin, penicillin, cephamycins, and penicillin are grouped in clusters, as are the biosynthetic genes for other secondary metabolites and antibiotics (Ullán et al., 2002). Homologous recombination (HR) is the core tool in DNA repair that is efficiently used for gene knockout from any part of DNA (Aguilera and Gómez-González, 2008). This study shows that HR is an extremely useful tool for gene removal in filamentous fungi. The *abct*31 encodes the ABC transporter in the β-Lactam gene cluster of M7. The Δ*abct*31 (deletion mutant) of this gene is created by using the gene disruption cassette (5'UTR-*hph*-3'UTR). In this cassette, the *hph* is used as a resistant gene for the screening of the mutant. The cassette's 5'UTR (770 bp) and 3'UTR (434 bp) fragments are amplified from the upstream and downstream regions of the gene, respectively. Further verification of the gene's role in *abct*31 β-lactam gene cluster of M7 has been conducted by evaluating the relative expression level toward weak organic acid.

Phenotypic Characterization of Δ*abct*31

The phenotypical structures were observed to explore the morphological development differences between the Δ*abct31* strain as related to *M. ruber* M7. Both deletion and wild-type strains were inoculated on four different media, including PDA, G25N, CYA, and MA, and cultivated at 28°C for 15

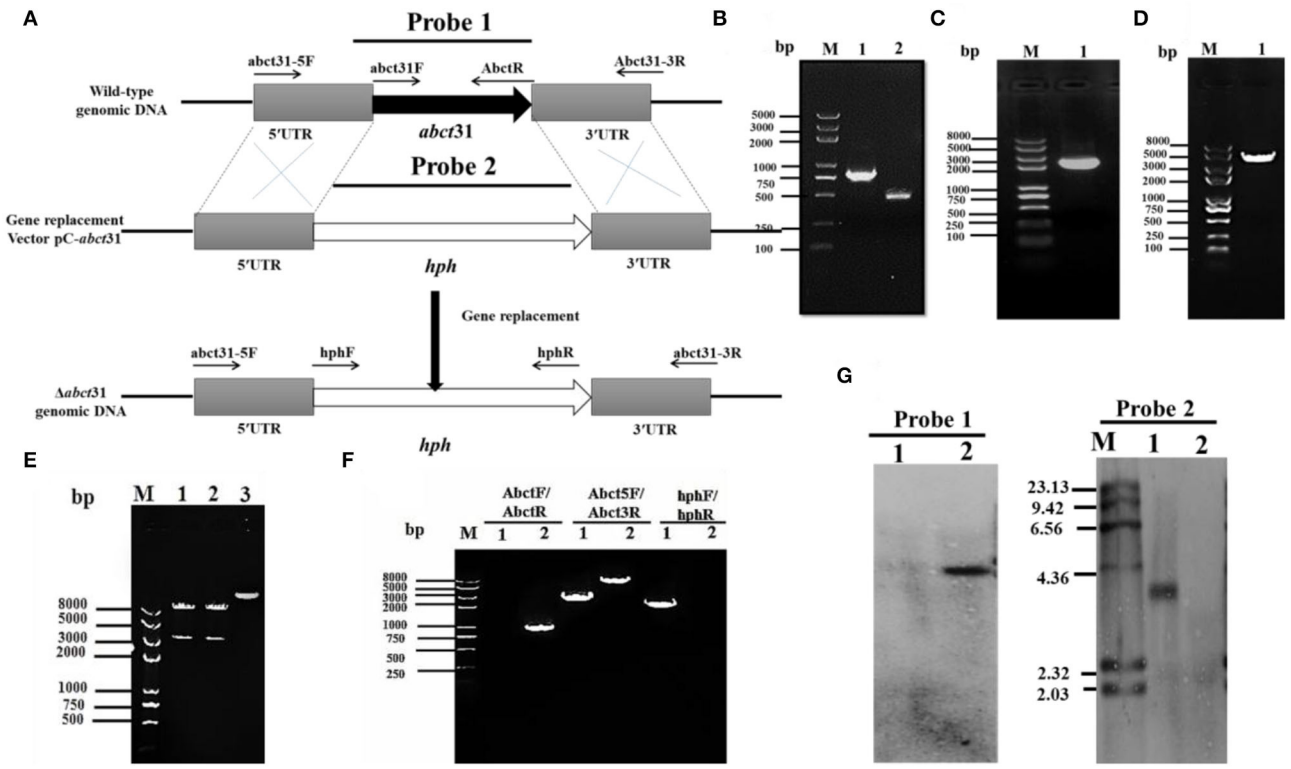

FIGURE 6 | Construction and verification of Δ*abct*31 strain. **(A)** Pictorial presentation for the homologous recombination approach to create *abct*31 disruption strains. **(B)** M: Trans 2k II Marker; Lane1: PCR product of 5' franking region (770 bp); Lane 2: PCR product of 3' franking (434 bp). **(C)** M: Trans 2k plus II Marker; Lane 1: *hph* (2,137 bp). **(D)** M: Trans 2k plus II Marker; Lane 1: PCR product of recombinant fragment of 5'UTR, *hph* and 3'UTR (3341 bp). **(E)** M: Trans 2k plus II Marker; Lane1: Restriction enzyme digestion analysis of vector pC-*abct*31 (*KpnI*/*HindIII*). **(F)** Validation of *abct*31 homologous recombination events. M: Trans 2k plus II Marker; Lane 1, the *abct*31 strain; Lane 2, the wild-type strain (M7). Different distinct bands were obtained by PCR amplification for selected pair of primer. **(G)** Southern hybridization analysis. Lane 1, Xba1 digested genomic DNA of Δ*abct*31; lane 2, Xba1 digested genomic DNA of M7 respectively; M: λDNA/*HindIII* marker; Probe 1: *abct*31 gene; Probe 2: *hph* gene.

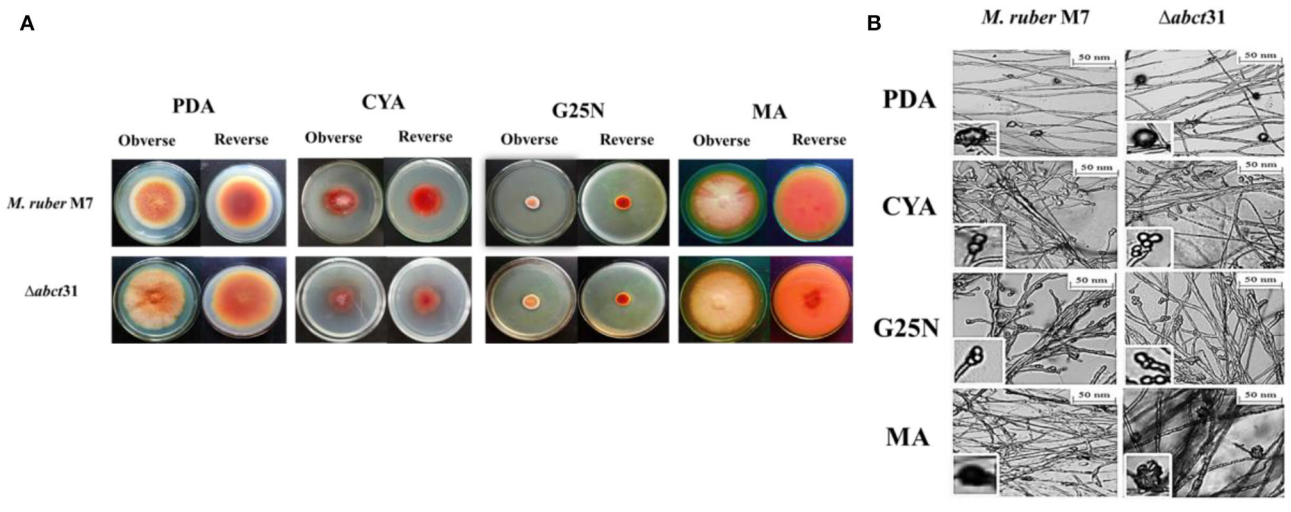

FIGURE 7 | Morphological comparison of *M. ruber* M7and Δ*abct*31. **(A)** Colony morphology of *M. ruber* M7 and Δ*abct*31 on PDA, CYA, G25N, MA plates, and cultured at 28°C for 15 days; **(B)** Cleistothecia and conidia development in *M. ruber* M7and Δ*abct*31 inoculated on PDA, CYA, G25N, MA plates, and cultured at 28°C for 8 days.

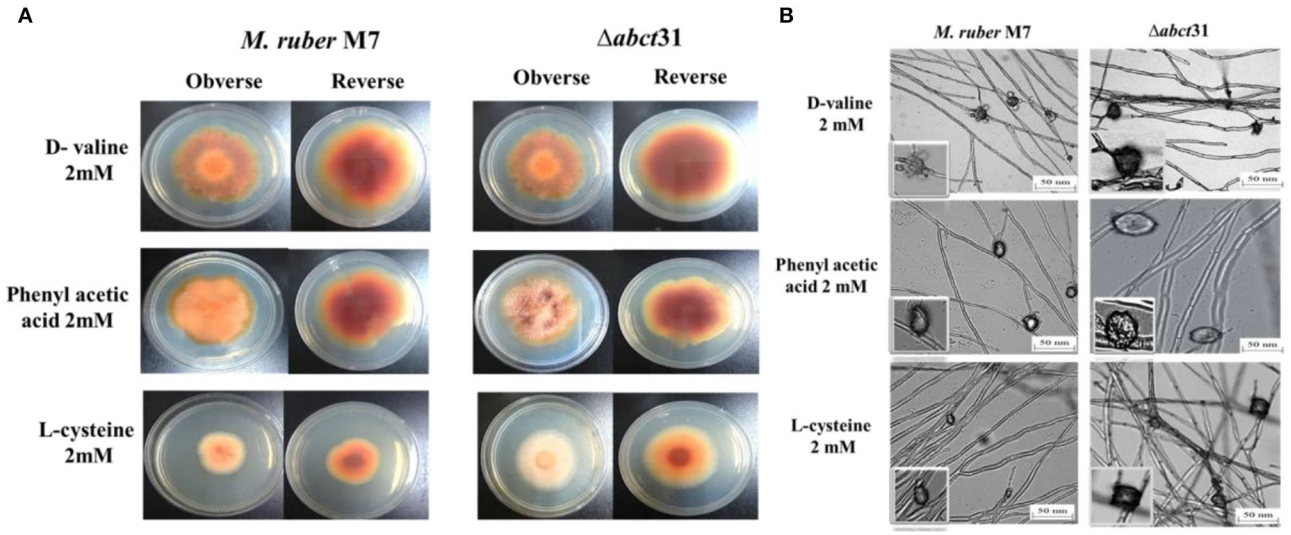

FIGURE 8 | Morphological comparison of *M. ruber* M7and Δ*abct*31 to evaluate the sensitivity toward pathway amino acid supplementation. **(A)** Colony morphology of *M. ruber* M7 and Δ*abct*31 inoculated on PDA plates supplemented with D-valine, phenylacetic acid, and L-cysteine at 2 mM concentrations for each cultured at 28°C for 15 days. **(B)** Cleistothecia and conidia development in *M. ruber* M7 and Δ*abct*31 cultured on PDA plates which supplemented with D-valine, phenylacetic acid, and L-cysteine at 2 mM concentrations for each and cultured at 28°C for 10 days.

days. The colony size, color, and other morphological properties observed (**Figure 7A**) are commonly applied to investigate the morphological characteristics of *Monascus* strains (Li et al., 2010, 2014).

While seeing the results of *M. ruber* M7 and *abct*31 deletion strain (Δ*abct*31), it was observed that the colonies of Δ*abct*31 normally grew when these were compared with colonies of wild-type *M. ruber* M7 for all media (**Figure 7A**). However, there was a substantial difference between the strains on PDA and MA medium plates in terms of phenotypic analyses, such as colony appearance, colony edges, the size of PDA, colony diameter, and growth rate (**Figure 7A**). But when it comes to CYA, Δ*abct*31's colony color was darker than *M. ruber* M7's. There were slight changes in the colony color and size of Δ*abct*31 when compared with *M. ruber* M7 in G25N.

From **Figure 7B**, it can be seen that the Δ*abct*31 mutant can produce a cleistothecium compared with *M. ruber* M7 on PDA and MA. There was no change observed in the cleistothecia growth pattern and size. However, the conidia structure can be observed in CYA and G25N. In both media, the conidia were observed in normal shape and size. It was clearly noted that no difference was found in the quality and quantity of cleistothecium and conidium (**Figure 7B**). As a result, there were no differences in cleistothecia and conidia's overall development and phenotypic characteristics between the Δ*abct*31 (mutant strain) and *M. ruber* M7 (wild strain).

As well as considering the growth and structure of the hyphae in mutant Δ*abct*31 strain remained unchanged compared with the control of *M. ruber* M7. There were no structural abnormalities found in mycelia regarding the diameter and shape. Moreover, the branching pattern and growth of the mycelia also typically look normal in spreading form, as shown in **Figure 7B**.

Phenotypic Characterization of Δ*abct*31 for Feeding Precursor Amino Acids

Initially, the morphological changes in the development of the colony and pigments of the *M. ruber* M7 and Δ*abct*31 strains were explored against PAA, L-cysteine, and D-valine at 2 mM concentration (**Figure 8A**). The effect on the development of conidia and cleistothecia was also perceived (**Figure 8B**).

Whereas seeing the outcomes of *M. ruber* M7 and Δ*abct*31, a substantial difference was detected related to the phenotypic characteristics, such as the size and appearance of the colony and the colony growth rate and diameter. Considering the Δ*abct*31 on PDA supplemented with PAA, the colony size exhibits resistance to growth, the colony color is clearly reddish, and colony edges are dissimilar from the *M. ruber* M7 on the PDA-PAA plate. Similarly, from colony diameter, the Δ*abct*31 displayed less sensitivity toward L-Cys supplementation. Moreover, colony color is a pale orange on the PDA-L-Cys feed plate for Δ*abct*31 when compared with wild-type *M. ruber* M7 and colony diameter is higher than wild type (**Figure 8A**). On the PDA-D-Val plate, the Δ*abct*31 mutant colony color and appearance look similar to *M. ruber* M7 (**Figure 8A**). Hence, Δ*abct*31 has a strong sensitivity toward PAA feeding.

From the results shown in **Figure 8B**, it can be seen that the Δ*abct*31 can produce a cleistothecium compared with *M. ruber* M7 on PDA for the supplementation of all pathway precursors. It was clearly noted that there is no difference in the quantity of cleistothecium for all precursors. Furthermore,

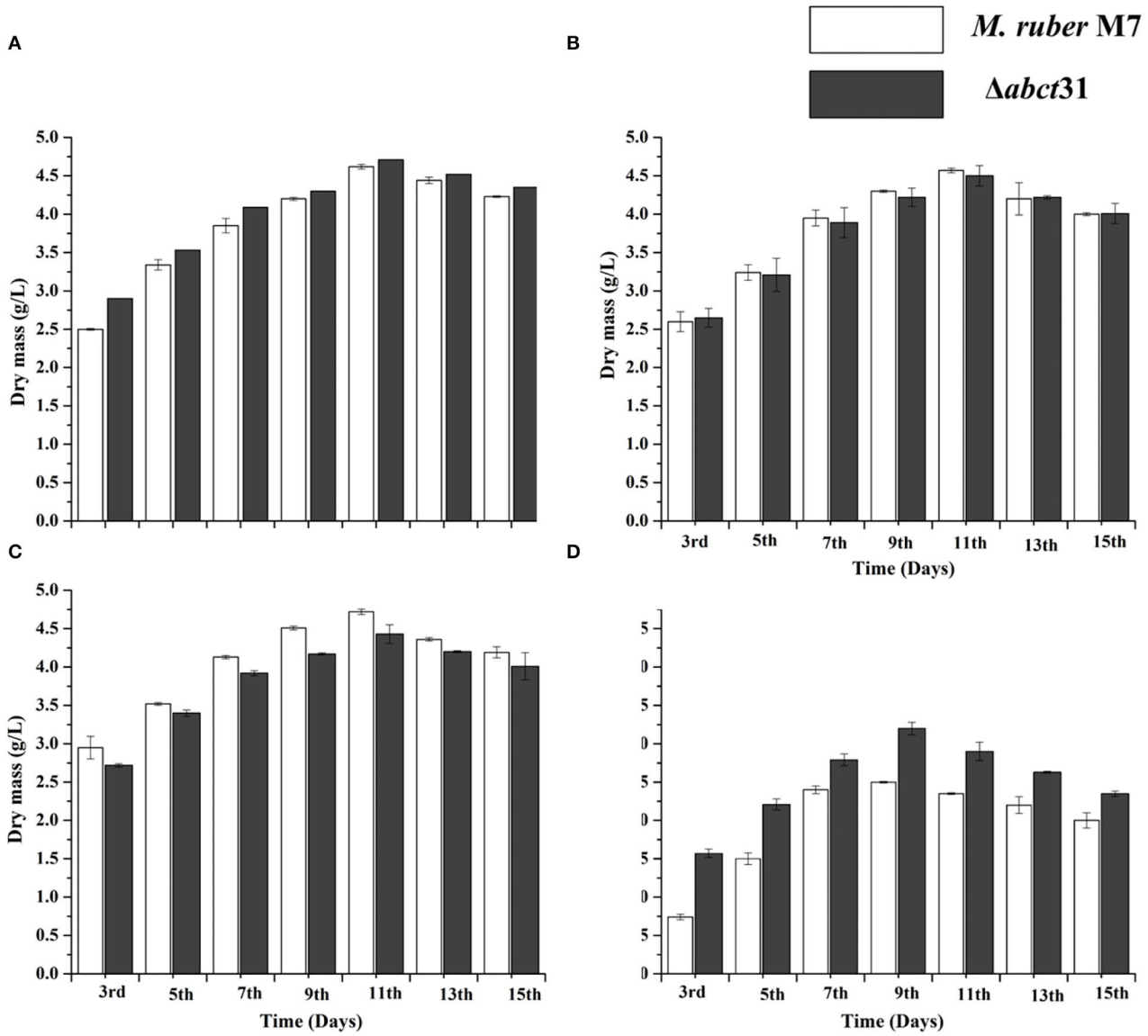

FIGURE 9 | Comparison of biomass (dry cell weight) of the *M. ruber* M7 and Δ*abct*31 against pathway amino acid. **(A)** PDB medium without amino acid (control); **(B)** PDB medium with D-valine; **(C)** PDB medium with phenylacetic acid; **(D)** PDB medium with L-cysteine, at 2 mM concentrations and incubated at 28°C without agitation. The bar representing the mean of triplicate values and error bars show standard deviation.

when comparing the mutant strains to the wild strain for D-Val and L-Cys, there were no differences in general development and phenotypic of cleistothecia. However, in the case of PAA feeding, the cleistothecia size increased compared to the wild type. Besides, considering the growth and structure of the hyphae in mutants Δ*abct*31 strains looks normal and parallel to the control of *M. ruber* M7 for all precursors. No structural defects such as weakening or inflammation were found in the hyphae of the mycelium by supplementation of precursors.

Moreover, the branching pattern and growth of the mycelia were also typically scattered, as presented in **Figure 8B**. Hence, the feeding of pathway precursors such as D-Val, and L-Cys at 2 mM has no effect on the Δ*abct*31 regarding microscopic structures. In contrast, Δ*abct*31 exhibits a sensitivity toward PAA feeding regarding cleistothecia size.

Effect of *abct*31 Gene Deletion on Biomass Production Without and With the Feeding of Precursor Amino Acids

The biomasses (dry mycelium) of the *M. ruber* M7 and Δ*abct*31 were appraised employing the gravimetric process. All strains were uniformly spread on PDA plates covered with cellophane-sheet without and with supplementation of the phenylacetic acid, L-cysteine, and D-valine at 2 mM concentration, cultivated at

TABLE 4 | Comparison of pigments production of *M. ruber* M7 and Δ*abct*31 feeding D-Val, PAA, L-Cys.

Days	*M. ruber* M7	Δ*abct*31
3rd	42.79 ± 0.27^{g}	41.92 ± 0.18^{g}
5th	70.59 ± 0.13^{f}	72.83 ± 0.15^{f}
7th	86.36 ± 0.15^{e}	89.87 ± 0.08^{e}
9th	94.58 ± 0.14^{d}	98.63 ± 0.11^{d}
11th	103.32 ± 0.22^{c}	106.24 ± 0.05^{c}
13th	110.31 ± 0.17^{b}	114.33 ± 0.13^{b}
15th	117.04 ± 0.20^{a}	120.27 ± 0.17^{a}
3rd	42.79 ± 0.27^{g}	41.92 ± 0.18^{g}
D-Val		
3rd	22.63 ± 0.45^{g}	26.33 ± 0.20^{g}
5th	40.74 ± 0.11^{f}	42.02 ± 0.10^{f}
7^{t}h	56.36 ± 0.32^{e}	58.44 ± 0.08^{e}
9th	64.58 ± 0.29^{d}	66.86 ± 0.12^{d}
11th	78.32 ± 0.36^{c}	80.12 ± 0.09^{c}
13th	84.31 ± 0.31^{b}	87.86 ± 0.08^{b}
15th	95.04 ± 0.32^{a}	98.94 ± 0.28^{a}
PAA		
3rd	52.80 ± 0.05^{g}	52.23 ± 0.03^{g}
5th	87.11 ± 0.06^{f}	92.54 ± 0.10^{f}
7th	106.56 ± 0.07^{e}	110.95 ± 0.04^{e}
9th	116.71 ± 0.10^{d}	119.46 ± 0.09^{d}
11th	121.32 ± 0.23^{c}	125.67 ± 0.06^{c}
13th	138.72 ± 0.04^{b}	139.93 ± 0.03^{b}
15^{th}	144.43 ± 0.03^{a}	146.90 ± 0.08^{a}
L-Cys		
3rd	14.75 ± 0.22^{g}	19.93 ± 0.14^{g}
5th	17.15 ± 0.05^{f}	21.06 ± 0.11^{f}
7th	23.45 ± 0.20^{e}	28.12 ± 0.03^{e}
9th	28.44 ± 0.14^{d}	32.84 ± 0.02^{d}
11th	34.49 ± 0.27^{c}	39.97 ± 0.11^{c}
13th	39.86 ± 0.20^{b}	43.09 ± 0.09^{b}
15^{th}	42.81 ± 0.27^{a}	47.13 ± 0.05^{a}

Analysis for comparing the pigment production in M. ruber M7 and Δabct31 mutant cultivated on PDA without and with supplementation of the phenylacetic acid, D-valine, and L-cysteine at 2 mM concentration, incubated at 28°C up to 15 d, mycelia and medium were collected from 3rd to 15th d with an alternate day interval. The values are represented as the mean of extracellular and intracellular values ± sd.

28°C. The mycelia were collected at a specific time interval and then dried in an oven at 60°C until constant weights were obtained. The average weight of biomass was calculated and presented in **Figure 9**.

The samples of biomass of *M. ruber* M7 and Δ*abct*31 cultured on PDA and incubated at 28°C for 15 days were collected on alternate days for the 3rd−15th day for biomass comparison. The mean of the triplicate data is represented by the bar, while the error bars illustrate the standard deviation. By weighing the weight of the dried mycelia, the biomass (dry mass) of *M. ruber* M7 (control) to Δ*abct*31 strain was determined. The data shown in **Figure 9A** revealed a substantial ($p < 0.05$) increase in biomass values for both strains up to the 15th day without supplementation. However, the highest dry cell weight was found on the 11th day, and onwards, the inclination in biomass was observed.

The biomass results presented in **Figures 9B–D** reveal that among the precursors such as D-Val, PAA, and L-Cys feeding fermentation, a variation in biomass production was observed for mutant Δ*abct*31 when compared with the wild type (*M. ruber* M7). However, mycelium production starts to increase after the 3rd day of fermentation. The results are presented in **Figure 9B**; for the D-Val, feeding fermentation showed a non-significant reduction in the biomass for Δ*abct*31 when compared with the *M. ruber* M7, up to 11th d; for PAA feeding (**Figure 9C**), the biomass for Δ*abct*31 was significantly lower when compared with the *M. ruber* M7 until the 15th d, and significantly ($p < 0.01$) higher biomass was observed in the L-Cys feeding case for Δ*abct*31 when compared with *M. ruber* M7 (**Figures 5–9D**). However, the results presented in **Figures 9B,C** exhibited a significant ($p < 0.05$) increase in the biomass quantity for Δ*abct*31 and *M. ruber* M7 up to 11th d for D-Val and PAA, at 9th d of L-Cys supplementation, shown in **Figure 9D**, and a clear reduction in the biomass value was shown in L-Cys<PAA<D-Val precursors. Overall, in the L-Cys feeding experiment, biomass production value was the lowest compared to other precursors.

Effect of *abct*31 Gene Deletion on the Production of Pigments Without and With the Feeding of Precursor Amino Acids

Monascus spp. can yield numerous secondary metabolites (Chen et al., 2017b), especially *Monascus* pigments (MPs) such as red (Monascorubramine and Rubropunctamine), orange (Monascorubrin and Rubropunctatin), and yellow (Ankaflavin and Monascin). To check the effect of Δ*abct*31 gene deletion on MPs, the MPs profile was detected without and with supplementation of the phenylacetic acid, L-cysteine, and D-valine, at 2 mM. **Table 4** presents the MPs' average results. The production of the overall pigment rose significantly ($p < 0.01$) from days 3 to 15 for all strains.

When any strain is grown in a liquid media, it produces metabolites and transports them to growth media via a well-defined transport system. After the fermentation of Δ *abct*31 and wild-type strains in PDB, both extracellular and intracellular contents of pigments were observed. The overall means of extracellular and intracellular MPs were calculated. The results (**Table 4**) showed that MPs slightly increased in Δ*abct*31 for control and D-Val, PAA, and L-Cys precursor feeding, during PDB fermentation duration from 3rd to 15th d. The slight increase of MPs of Δ*abct*31 might be due to their role in transporting intermediates. This may be due to the side chain amino acid level increased in the medium; more substrates are available for the pigment production.

Detection of PG by HPLC

The HPLC was used to study the involvement of the *abct*31 gene for penicillin production in *M. ruber* M7 and deletion (Δ*abct*31). Furthermore, the role of the feeding of precursors, i.e., D-Val, PAA, and L-Cys at 2 mM on PG production in both strains was

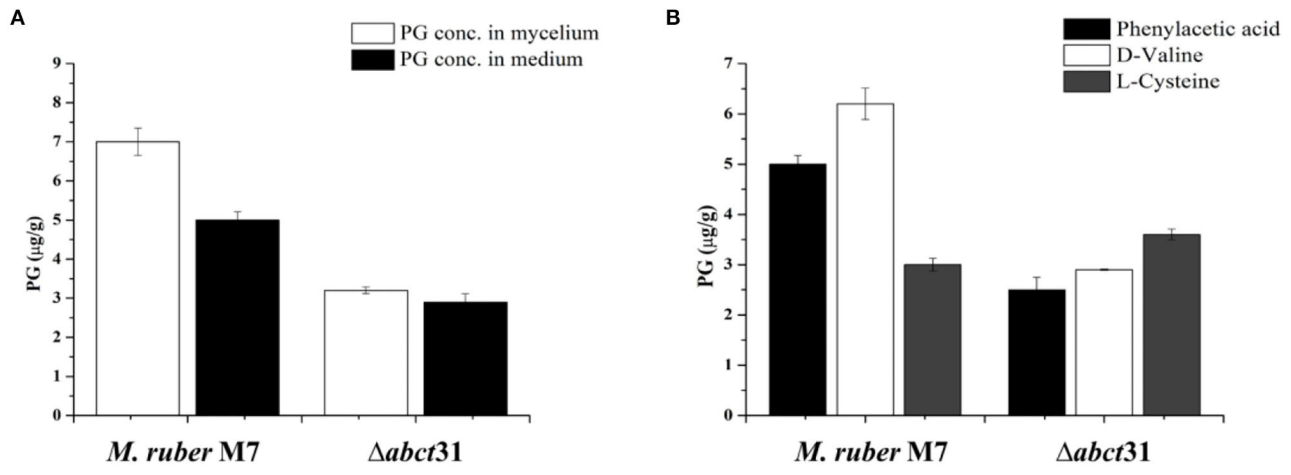

FIGURE 10 | Comparison of PG concentration of the wild-type strain and the Δ*abct*31 transformants on the 7th day. **(A)** PG concentration in mycelium and medium; **(B)** Comparison of PG concentration affected by supplementation of D-valine, phenylacetic acid, and L-cysteine at 2 mM on 7th day. The bar representing the mean of triplicate values and error bars show standard deviation.

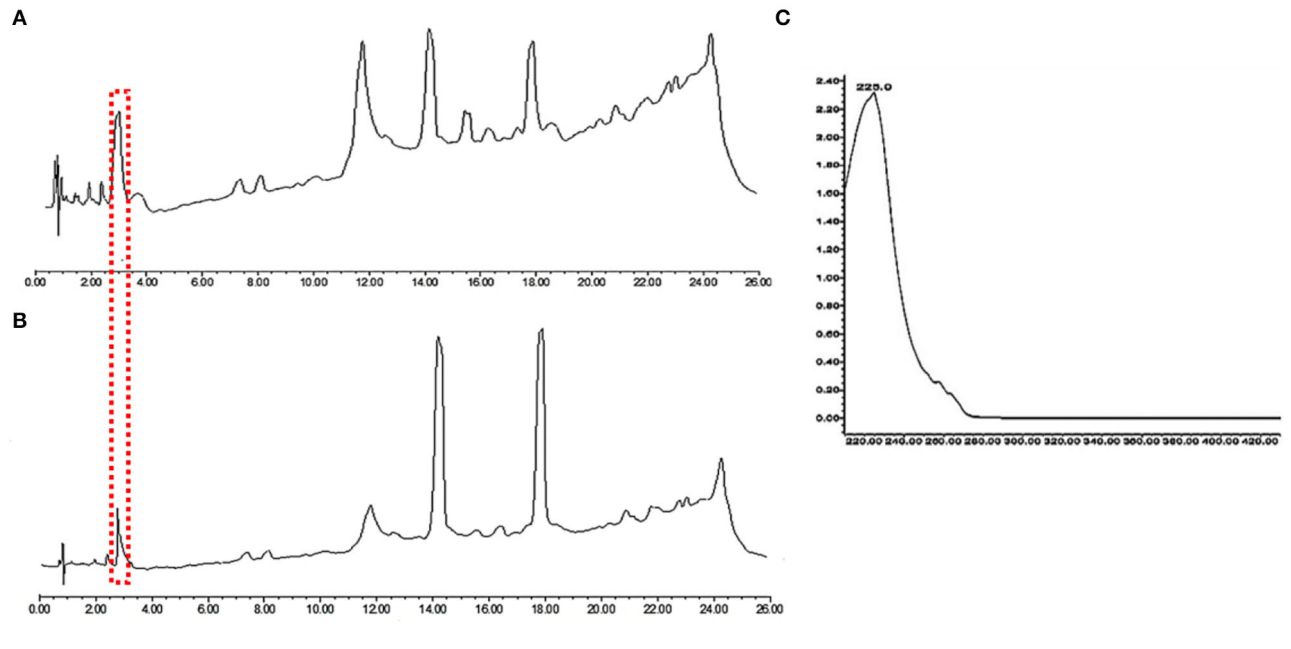

FIGURE 11 | Comparison of eluted products of *M. ruber* M7 and Δ*abct*31 transformant for solid-state fermentation on rice. **(A)** Metabolic profile of *M. ruber* M7 at 250 nm; **(B)** Metabolic profile of Δ*abct*31 at 250 nm; **(C)** UV-Vis spectrum of benzyl penicillin (PG) which is shown by the arrows in metabolic profiles.

also observed. The samples collected on the 7th day, in addition to the treated samples, were analyzed by HPLC for PG estimation.

In the Δ*abct*31 strains, the PG level was observed in intracellular and extracellular. However, the HPLC results showed that these strains could produce the PG at the intracellular level and in the extracellular medium for the 7th day (**Figure 10**). But the concentration of PG is significantly decreased in the extra- and intracellular part of the mutant when compared with *M. ruber* M7. The average yield of PG in transformants' (Δ*abct*31) intracellular portion is calculated as 3.2 ± 0.08 μg/g, when compared with the parental strain's yield (**Figure 10A**). However, the extracellular results showed a similar pattern for PG production Δ*abct*31, yielding the PG, 2.9 ± 0.21 μg/g when compared with the parental strain (**Figure 10A**).

From **Figure 10B**, it has been observed that the individual feeding of D-Val, PAA, and L-Cys at 2 mM concentration has a substantial impact on the *M. ruber* M7. The highest PG concentration was 6.20 ± 0.17 μg/g observed for the D-Val feeding, in contrast to the L-Cys the lowest PG

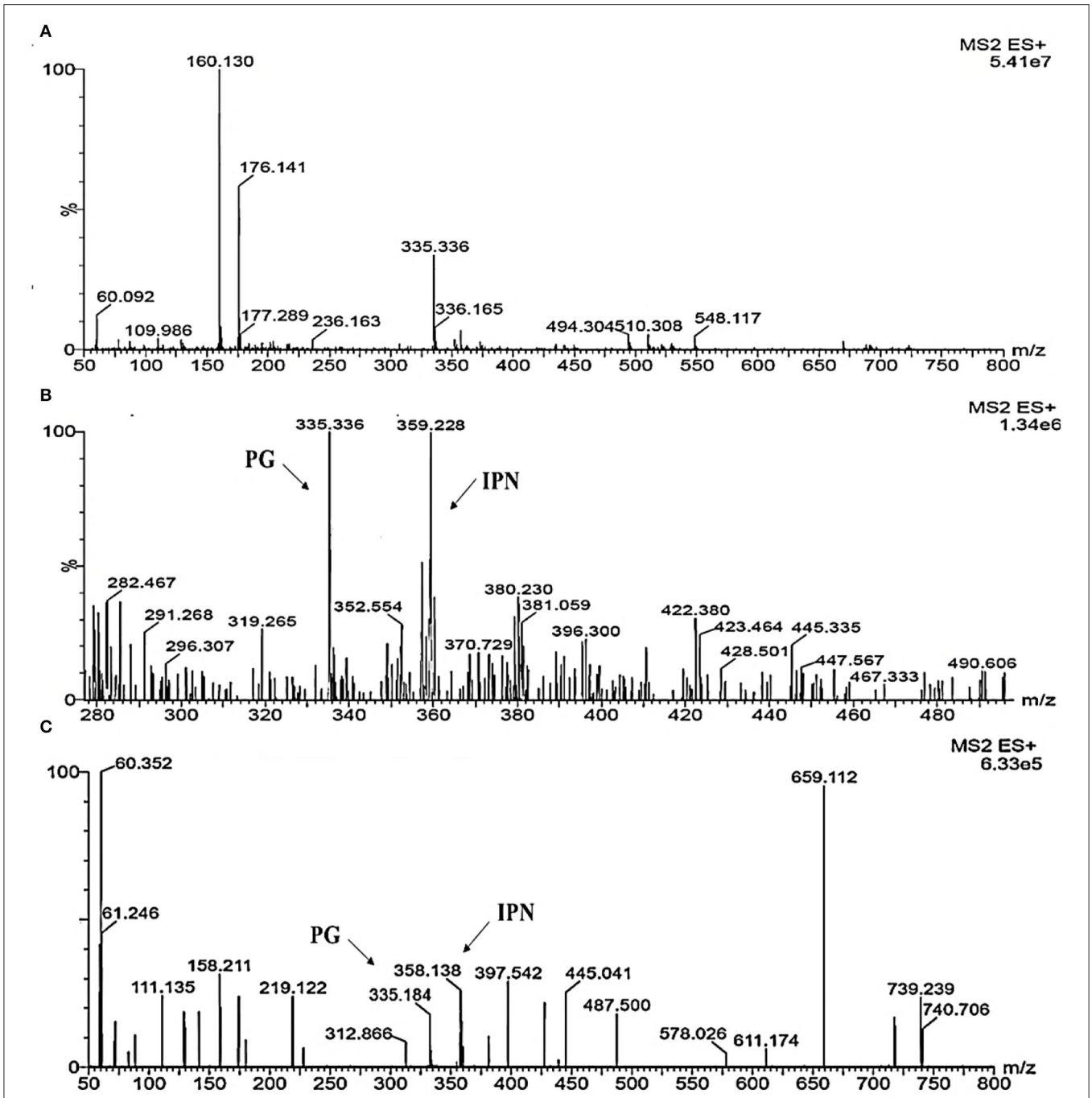

FIGURE 12 | Detection of β-metabolites detected *M. ruber* M7 and Δ*abct*31 transformants by UPLC-MS/MS. UPLC-MS/MS spectrogram of the *M. ruber* M7 and Δ*abct*31 for solid-state fermented on rice displays that the atomic mass of ion (m/z 335.336) matched well with the standard penicillin, the molecular weight for isopenicillin N is 359.3 g/mol, in spectrogram ion m/z 359.00 representing the isopenicillin N peak. **(A)** Spectra in A penicillin G (PG) standard with the mass 335.336; **(B)** A pattern of fragmentation of *M. ruber* M7; **(C)** A pattern of fragmentation of Δ*abct*31.

level (3.23 ± 0.12 μg/g). However, for Δ*abct*31 mutants, the lowest PG production of 2.50 ± 0.24 μg/g in Δ*abct*31 mutants has been detected for PAA feeding. While among these precursors feeding in Δ*abct*31, the highest PG level was observed for L-Cys 3.64 ± 0.10 μg/g, presented in **Figure 10B**. From all results of feeding experiments, it has been concluded that Δ*abct*31 has the highest sensitivity toward PAA precursor.

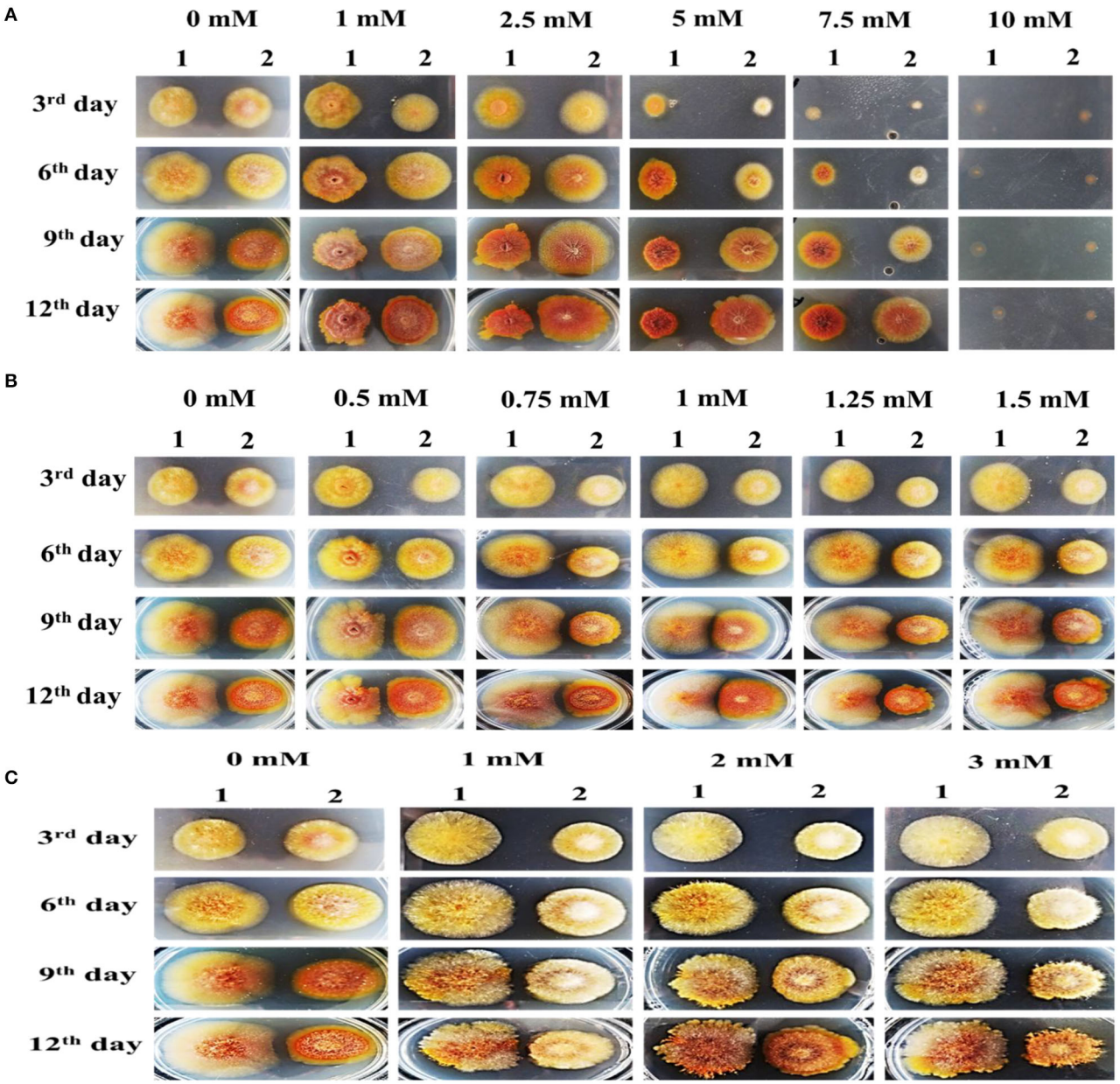

FIGURE 13 | Colony morphology of *M. ruber* M7 and Δ*abct*31 for the feeding of weak acids. The morphologies of *M. ruber* M7 (1st vertical row) and Δ*abct*31 (2nd vertical row) colonies on PDA plates supplemented with weak acid at 28°C for 12d. **(A)** Colony morphology of *M. ruber* M7 and Δ*abct*31 for the feeding of sorbic acids at 0, 1, 2.5, 5, 7.5, and 10 mM concentration, respectively; **(B)** Colony morphology of *M. ruber* M7 and Δ*abct*31 for the feeding of acetic acids at 0, 0.5, 0.75, 1, 1.25, 1.5 mM concentration, respectively; **(C)** Colony morphology of *M. ruber* M7 and Δ*abct*31 for the feeding of adipic acids at 0, 1, 2, and 3 mM concentration, respectively.

Metabolic Profile by Ultra-Performance Liquid Chromatography (UPLC)

In order to investigate further the difference in the metabolic profile between *M. ruber* M7 and mutant (Δ*abct*31), ultra-performance liquid chromatography (UPLC) was used for more elaboration of the HPLC results. The results are shown in **Figure 11**. The penicillin G spectrum is shown in **Figure 11C**. As shown in **Figures 11A,B**, the peak appearance for penicillin G took place at around 3.8 min for sample filtrates of *M. ruber* M7 and Δ*abct*31, respectively. The UV-Vis spectra confirm the presence of PG in both strains; however, the overall peak area was reduced. Hence, *abct31* might be involved in the transportation of intermediate (IPN and PAA) compounds to produce PG in *M. ruber* M7. For additional validation about the function of

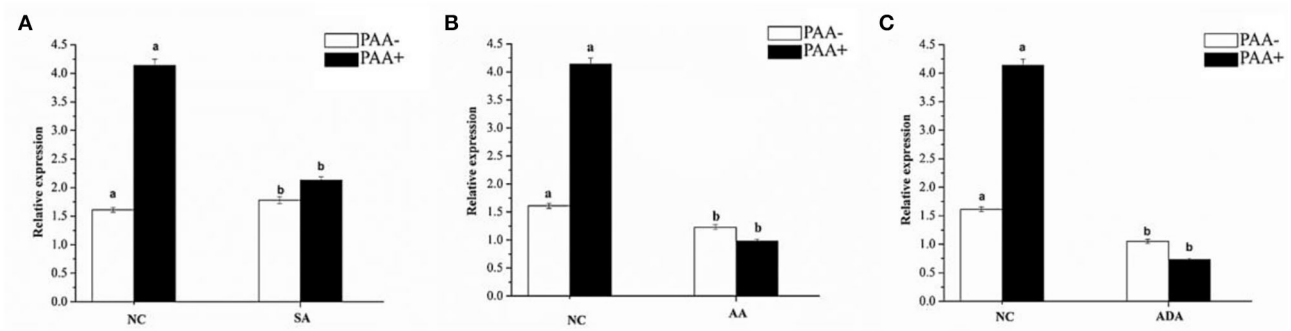

FIGURE 14 | Expression of *abct*31 in *M. ruber* M7 to weak acid supplementation with or without PAA. NC was presented in the control group in which *M. ruber* M7 was cultivated on PDA without sorbic acid. SA presented the sorbic acid group in which *M. ruber* M7 was cultivated on a PDA with **(A)** Sorbic acid at 7.5 Mm; **(B)** Acetic acid at 1.5 Mm; **(C)** Adipic acid at 3 mM. Both groups were incubated at 28°C for 7d in the presence (black vertical bar) and absence (empty vertical bar) of PAA at 10 mM.

the *abct*31 gene regarding the PG production, UPLC-MS/MS has been performed.

Detection of β-Lactam Metabolites in Metabolic Profile Using UPLC-MS/MS

To investigate the metabolites, a mass profile of *M. ruber* and Δ*abct*31 was developed using the rice (solid-state fermentation) filtrate. Because the filtrate revealed a wider range of biological compounds, **Figure 12** shows the findings of the footprinting of the numerous metabolites found in *M. ruber* M7.

According to **Figure 12**, molecular masses associated with β-Lactam such as PG and their intermediates IPN were discovered in the culture filtrate. As a result, PG and IPN in the extract *M. ruber* M7 were also observed in the UPLC-MS/MS study. The existence of the 335.336 m/z peaks for PG and 395 m/z for isopenicillin N in the crude extract of M7 (**Figure 12B**) and alike fragmentation design present in the penicillin G standard (**Figure 12A**) has confirmed the identity of this metabolite. Moreover, as **Figure 12C** shows that the PG and IPN peaks were also detected in Δ*abct*31.

From the above results, the presence of the IPN peak in **Figure 12C** demonstrated that *abct*31 might be responsible for the transportation of intermediate, phenylacetic acid. For further clarification, the sensitivity toward weak acids has also been evaluated.

Weak Acid Sensitivity

The toxicity of PAA with weak acids was tested for Δ*abct*31 and in the *M. ruber* M7 since the Δ*abct*31 gene was substantially expressed when the parental strain was cultured in the presence of PAA. Herein, the spores of *M. ruber* M7 and Δ*abct*31 were plated on PDA with the supplementation of increased concentrations of sorbic acid, acetic acid, and adipic acid at pH 6.2. Further analyses were done for the colony morphologies and relative expression.

Colonial Sensitivity of *abct*31 Toward Weak Acids

To evaluate the difference in the colonies between Δ*abct*31 and *M. ruber* M7, both of them were inoculated on individual PDA plates supplemented with sorbic acid at different concentrations (0, 1, 2.5, 5, 7.5, 10 mM) with acetic acid (0, 0.5, 0.75, 1, 1.25, 1.5 mM) concentrations and also with adipic acid at different concentration levels (0, 1, 2, 3 mM) and then incubated for 12 d at 28°C; the colony sizes, color, and other morphological properties were observed (**Figure 13**).

The results in **Figure 13A** have shown that Δ*abct*31 colonial sizes were bigger than those of M7 for all tested concentrations of sorbic acid, and Δ*abct*31 colonial colors were a little bit light when compared with *M. ruber* M7 when the concentrations of sorbic acid were (1, 2.5, 5, 7.5 mM). Although the colonial sizes of *M. ruber* M7 were reduced as the concentrations of sorbic acid were increased, the colonial colors seemed reddish. The colonial edges were dissimilar from the controlled growth of *M. ruber* M7. Similarly, from colonial diameters, it was observed that Δ*abct*31 displayed less sensitivity for sorbic acid supplementation. At the highest concentration of sorbic acid 10 mM, both strains did not show any growth up to 12d (**Figure 13A**).

The observation in **Figure 13B** shows that when compared with wild-type *M. ruber* M7, the colonial sizes of Δ*abct*31 on PDA supplemented with acetic acid were smaller for higher concentrations, such as 0.75, 1, 1.25, and 1.5 mM, and the colonial color was darker than *M. ruber* M7. In the M7 strain, colonial size exhibited resistance to growth, and the colonial color was clearly lighter on the PDA-acetic acid plate at higher concentrations of 1–1.5 mM. In comparison, at a lower concentration of acetic acid (0.5 mM), the colonial size looked similar in contrast to higher concentrations. Hence, the Δ*abct*31 strain exhibited acetic acid supplementation sensitivity at higher concentrations than *M. ruber* M7 (**Figure 13B**).

The results shown in **Figure 13C** illustrate that Δ*abct*31 colonial sizes were smaller than those of *M. ruber* M7 for

all tested concentrations of adipic acid. The Δ*abct*31 colonial colors remained pale yellow up to the 9th day when compared with M. ruber M7 when the tested concentration of adipic acid was 1–3 mM used. The colonial color of *M. ruber* M7 strain also considerably changed to control the colonial growth of *M. ruber* M7. On the 12th day, the colonial color's profile of Δ*abct*31 strain changed for 2 and 3 mM concentration and the colonial colors turned to orange. As well as considering the colonial edges looked more irregular, the compacted growth of mycelium in the colonies could be observed when compared with the *M. ruber* M7, which were typically spread (**Figure 13C**).

So, in the following experiments, 7.5 mM sorbic acid, 1.5 mM acetic acid, and 3 mM adipic acid were used to check the *abct*31 gene response.

Expression Sensitivity of *abct*31 in *M. ruber* M7 Toward Weak Acids

The effect of sorbic acid, adipic acid, and acetic acid at 7.5, 1.5, and 3 mM, respectively, on the expression level of the *abct*31 gene in *M. ruber* M7 with and without PAA at 10 mM has been investigated. The results are revealed in **Figure 14**.

From **Figure 14**, it has been observed that *abct*31 in *M. ruber* M7 exhibited a high transcription level with PAA when compared with the absence of PAA for all weak acids. Although the sorbic acid at 7.5 mM, acetic acid at 1.5 mM, and adipic acid at 3 mM significantly decreased the transcriptional level of *abct*31 in the absence of PAA, all the weak acids toxicity caused a highly significant ($p < 0.01$) decrease in the expression level of *abct*31 in the presence of PAA. Overall, sorbic acid at 7.5 mM causes the *abct*31 expression level more in the presence of PAA, whereas acetic acid at 1.5 mM and adipic acid at 3 mM cause more expression levels in the absence of PAA.

The findings of this work demonstrate that knocking out the ABC transporter *abct*31 in *M. ruber* M7 does not stop the formation of β-lactams, indicating that *abct*31 does not appear to play a direct part in this process. Nevertheless, when cells develop in +PAA, *abct*31 expression increases dramatically, indicating more functioning *abct*31 transport proteins in the cell. To see the effect on gene expression, we needed a high concentration of PAA in our PAA challenge assessments. Furthermore, when compared with its other β-lactam generating strains *P. chrysogenum*, the *abct*31 gene expression was higher in *M. ruber* M7 strains carrying only one copy of the penicillin biosynthetic gene cluster. Altogether, our findings indicate that *abct31* expression is influenced by the quantity of its inducer, PAA. When the *abct*31 gene was expressed, cells became more sensitive to PAA and sorbic acid, accompanied by a drop in *abct*31 transcript levels when the cells were subjected to these substances.

The side-chain precursor PAA, which is transferred from the cytosol to the peroxisomal matrix and is encoded by the *paaT* gene in *P. chrysogenum*, has recently been examined. It encodes a drug/H + antiporter with 12 TMSs, one of which is found in the membrane of peroxisomes as discovered using fluoresce targeted microscopy (Fernández-Aguado et al., 2013, 2014; Martín et al., 2013).

Many other weak acids, such as acetic and adipic acids, were shown to have no effect on the expression of *abct*31. As a result, they act as inducers through an as-yet-unidentified mechanism. It is possible that *abct*31 is not the only transporter engaged in exporting PAA. Expressions of the all-other residual ABC transporters were unaffected in the Δ*abct*31 strain cultured in the presence of PAA (unpublished data), indicating that no additional candidates for PAA export were discovered. Transporters from the major facilitator superfamily (MFS) may play a role in the residual low acid resistance potential. As a result of these findings, *abct*31 appears to play the same role as an ATP-dependent extrusion system for the weak acids to protect cells against these substances. These findings are backed by the theory that an ATP-dependent exporter is involved in the active secretion of the PAA (Xu et al., 2017).

According to our findings, it can be concluded that *M. ruber* M7 depends on at least two separate detoxifying mechanisms to deal with the PAA during fermentation. These mechanisms might be the conversion of PAA enzymatically into the PG and the active extrusion of PAA from the cell. However, the *abct*31 transporter is expressed in strains (deletion) with low penicillin G production rates, allowing a detoxifying process that also relies on the ATP-dependent extrusion of PAA.

CONCLUSION

The outcomes of our study suggest that ABCT31 is the prime ABC transporter, primarily involved in this process of β-lactam synthesis. Additionally, based on these findings, it might be concluded that *M. ruber* depends upon two separate detoxifying mechanisms to deal with the higher PPA concentrations in the fermentation broth. These mechanisms could be the extrusion of PAA from the cell and then converting PAA into penicillin G by using enzymatic activity. Because of the residuals of PAA, the ABCT31 transporter is expressed and permits a detoxifying pathway. The detoxification mechanism also relies on the extrusion of PAA, which is ATP-dependent extrusion. Understanding the mechanisms governing the intake of these side-chain precursors aid in the clarification of the penicillin biosynthetic pathway. Still, it will also be beneficial economically for the β-lactams producers.

DATA AVAILABILITY STATEMENT

The data presented in the study are deposited in MetaboLights repository, accession number MTBLS4681.

AUTHOR CONTRIBUTIONS

RR has designed and carried out the present research work, conducted experiments, analyzed the data, and

written the present manuscript. MV helped in doing the experiments and gave technical guidance. FC provided a place in the laboratory and gave access to the lab facilities for experimentation and funds for the present work. All authors contributed to the article and approved the submitted version.

FUNDING

This work was supported by the Major Program of the National Natural Science Foundation of China (Nos. 31730068 and 31330059 to FC) and the National Key Research and Development Program of China (No. 2018YFD0400404 to FC).

REFERENCES

Aguilera, A., and Gómez-González, B. (2008). Genome instability: a mechanistic view of its causes and consequences. *Nat. Rev. Genet.* 9, 204–217. doi: 10.1038/nrg2268

Al Shawi, A., Rasul, A., Khan, M., Iqbal, F., and Tonghui, M. (2011). Eupatilin: a flavonoid compound isolated from the artemisia plant, induces apoptosis and G2/M phase cell cycle arrest in human melanoma A375 cells. *African J. Pharm. Pharmacol.* 5, 582–588. doi: 10.5897/AJPP 11.079

Ávalos, J., Díaz-Sánchez, V., García-Martínez, Jorge Castrillo, M., Ruger-Herreros, M., and Limón, M. C. (2014). Biosynthesis and molecular genetics of fungal secondary metabolites. *Fungal Biol.* 2, 67–79. doi: 10.1007/978-1-4939-1191-2

Barreiro, C., and García-Estrada, C. (2019). Proteomics and *Penicillium chrysogenum*: unveiling the secrets behind penicillin production. *J. Proteomics*. 198, 119–131. doi: 10.1016/j.jprot.2018.11.006

Buchan, D. W. A., Minneci, F., Nugent, T. C. O., Bryson, K., and Jones, D. T. (2013). Scalable web services for the PSIPRED protein analysis workbench. *Nucleic Acids Res.* 41, 349–357. doi: 10.1093/nar/gkt381

Chen, C.-L., and Pan, T.-M. (2019). Beneficial effects of Monascus purpureus NTU 568-fermented products on cholesterol in vivo and clinical trial: a review. *Integr. Clin. Med.* 3, 1–3. doi: 10.15761/ICM.1000161

Chen, F., and Hu, X. (2005). Study on red fermented rice with high concentration of monacolin K and low concentration of citrinin. *Int. J. Food Microbiol.* 103, 331–337. doi: 10.1016/j.ijfoodmicro.2005.03.002

Chen, G., Bei, Q., Huang, T., and Wu, Z. (2017a). Tracking of pigment accumulation and secretion in extractive fermentation of Monascus anka GIM 3.592. *Microb. Cell Fact.* 16, 1–13. doi: 10.1186/s12934-017-0786-6

Chen, W. (2015). *Insights Into Biological Characteristics Of Monascus Ruber M7 by Genomics Approaches*. (Doctor thesis), Huazhong Agricultural University, Wuhan, Hubei, China.

Chen, W., Chen, R., Liu, Q., He, Y., He, K., Ding, X., et al. (2017b). Orange, red, yellow: biosynthesis of azaphilone pigments in monascus fungi. *Chem. Sci.* 8, 4917–4925. doi: 10.1039/C7SC00475C

Chen, W., Xie, T., Shao, Y., and Chen, F. (2012a). Genomic characteristics comparisons of 12 food-related filamentous fungi in tRNA gene set, codon usage and amino acid composition. *Gene.* 497, 116–124. doi: 10.1016/j.gene.2012.01.016

Chen, W., Xie, T., Shao, Y., and Chen, F. (2012b). Phylogenomic relationships between amylolytic enzymes from 85 strains of fungi. *PLoS ONE* 7, e49679. doi: 10.1371/journal.pone.0049679

Emanuelsson, O., Nielsen, H., Brunak, S., and Von Heijne, G. (2000). Predicting subcellular localization of proteins based on their N-terminal amino acid sequence. *J. Mol. Biol.* 300, 1005–1016. doi: 10.1006/jmbi.2000.3903

Fernández-Aguado, M., Martín, J. F., Rodríguez-Castro, R., García-Estrada, C., Albillos, S. M., Teijeira, F., et al. (2014). New insights into the isopenicillin N transport in *Penicillium chrysogenum*. *Metab. Eng.* 22, 89–103. doi: 10.1016/j.ymben.2014.01.004

Fernández-Aguado, M., Ullán, R. V., Teijeira, F., Rodríguez-Castro, R., and Martín, J. F. (2013). The transport of phenylacetic acid across the peroxisomal membrane is mediated by the PaaT protein in *Penicillium chrysogenum*. *Appl. Microbiol. Biotechnol.* 97, 3073–3084. doi: 10.1007/s00253-012-4425-1

Fletcher, D. A., and Mullins, R. D. (2010). Cell mechanics and the cytoskeleton. *Nature* 463, 485–492. doi: 10.1038/nature08908

Gao, S., Yu, S., and Yao, S. (2021). An efficient protein homology detection approach based on seq2seq model and ranking. *Biotechnol. Biotechnol. Equip.* 35, 633–640. doi: 10.1080/13102818.2021.1892522

García-Estrada, C., Vaca, I., Fierro, F., Sjollema, K., Veenhuis, M., and Martín, J. F. (2008). The unprocessed preprotein form IATC103S of the isopenicillin N acyltransferase is transported inside peroxisomes and regulates its self-processing. *Fungal Genet. Biol.* 45, 1043–1055. doi: 10.1016/j.fgb.2008.03.005

Gaudelli, N. M., Long, D. H., and Townsend, C. A. (2015). β-Lactam formation by a non-ribosomal peptide synthetase during antibiotic biosynthesis. *Nature* 520, 383–387. doi: 10.1038/nature14100

George, A. M., and Jones, P. M. (2012). Perspectives on the structure-function of ABC transporters: the Switch and Constant Contact Models. *Prog. Biophys. Mol. Biol.* 109, 95–107. doi: 10.1016/j.pbiomolbio.2012.06.003

Ghilarov, D., Inaba-Inoue, S., Stepien, P., Qu, F., Michalczyk, E., Pakosz, Z., et al. (2021). Molecular mechanism of SbmA, a promiscuous transporter exploited by antimicrobial peptides. *Sci. Adv.* 7, eabj5363. doi: 10.1126/sciadv.abj5363

Guo, X., Li, Y., Zhang, R., Yu, J., Ma, X., Chen, M., et al. (2019). Transcriptional regulation contributes more to Monascus pigments diversity in different strains than to DNA sequence variation. *World J. Microbiol. Biotechnol.* 35, 1–13. doi: 10.1007/s11274-018-2566-9

Hazelwood, L. A., Tai, S. L., Boer, V. M., De Winde, J. H., Pronk, J. T., and Daran, J. M. (2006). A new physiological role for Pdr12p in Saccharomyces cerevisiae: export of aromatic and branched-chain organic acids produced in amino acid catabolism. *FEMS Yeast Res.* 6, 937–945. doi: 10.1111/j.1567-1364.2006.00094.x

He, Y., Liu, Q., Shao, Y., and Chen, F. (2013). *ku70* and *ku80* null mutants improve the gene targeting frequency in *Monascus ruber* M7. *Appl. Microbiol. Biotechnol.* 97, 4965–4976. doi: 10.1007/s00253-013-4851-8

Kulkarni, P. A., and Devarumath, R. M. (2014). *In silico* 3D-structure prediction of SsMYB2R: a novel MYB transcription factor from *Saccharum spontaneum*. *Indian J. Biotechnol.* 13, 437–447.

Lee, B. H., and Pan, T. M. (2012). Benefit of monascus-fermented products for hypertension prevention: a review. *Appl. Microbiol. Biotechnol.* 94, 1151–1161. doi: 10.1007/s00253-012-4076-2

Lee, Y. M., Li, H., Hong, J., Cho, H. Y., Bae, K. S., Kim, M. A., et al. (2010). Bioactive metabolites from the sponge-derived fungus *Aspergillus versicolor*. *Arch. Pharm. Res.* 33, 231–235. doi: 10.1007/s12272-010-0207-4

Li, L., He, L., Lai, Y., Shao, Y., and Chen, F. (2014). Cloning and functional analysis of the Gβ gene Mgb1 and the Gγ gene Mgg1 in Monascus ruber. *J. Microbiol.* 52, 35–43. doi: 10.1007/s12275-014-3072-x

Li, L., Shao, Y., Li, Q., Yang, S., and Chen, F. (2010). Identification of Mga1, a G-protein α-subunit gene involved in regulating citrinin and pigment production in Monascus ruber M7. *FEMS Microbiol. Lett.* 308, 108–114. doi: 10.1111/j.1574-6968.2010.01992.x

Liu, J., Lei, M., Zhou, Y., and Chen, F. (2019). A comprehensive analysis of the small GTPases Ypt7 involved in the regulation of fungal development and secondary metabolism in monascus ruber M7. *Front. Microbiol.* 10, 452. doi: 10.3389/fmicb.2019.00452

Liu, Q., Xie, N., He, Y., Wang, L., Shao, Y., Zhao, H., et al. (2014). MpigE, a gene involved in pigment biosynthesis in Monascus ruber M7. *Appl. Microbiol. Biotechnol.* 98, 285–296. doi: 10.1007/s00253-013-5289-8

Lobanovska, M., and Pilla, G. (2017). Penicillin's discovery and antibiotic resistance: lessons for the future? *Yale J. Biol. Med.* 90, 135–145.

Lopes, F. C., Tichota, D. M., Sauter, I. P., Meira, S. M. M., Segalin, J., Rott, M. B., et al. (2013). Active metabolites produced by *Penicillium chrysogenum* IFL1 growing on agro-industrial residues. *Ann. Microbiol.* 63, 771–778. doi: 10.1007/s13213-012-0532-6

Martín, J. F., Casqueiro, J., and Liras, P. (2005). Secretion systems for secondary metabolites: how producer cells send out messages of intercellular communication. *Curr. Opin. Microbiol.* 8, 282–293. doi: 10.1016/j.mib.2005.04.009

Martín, J. F., García-Estrada, C., and Ullán, R. V. (2013). Transport of substrates into peroxisomes: the paradigm of β-lactam biosynthetic intermediates. *Biomol. Concepts* 4, 197–211. doi: 10.1515/bmc-2012-0048

Moussatova, A., Kandt, C., O'Mara, M. L., and Tieleman, D. P. (2008). ATP-binding cassette transporters in *Escherichia coli*. *Biochim. Biophys. Acta - Biomembr.* 1778, 1757–1771. doi: 10.1016/j.bbamem.2008.06.009

Nugent, T., and Jones, D. T. (2012). Membrane protein structural bioinformatics. *J. Struct. Biol.* 179, 327–337. doi: 10.1016/j.jsb.2011.10.008

Ozcengiz, G., and Demain, A. L. (2013). Recent advances in the biosynthesis of penicillins, cephalosporins and clavams and its regulation. *Biotechnol. Adv.* 31, 287–311. doi: 10.1016/j.biotechadv.2012.12.001

Pandey, V., Krishnan, V., Basak, N., Marathe, A., Thimmegowda, V., Dahuja, A., et al. (2018). Molecular modeling and in silico characterization of GmABCC5: a phytate transporter and potential target for low-phytate crops. *3 Biotech.* 8, 1–16. doi: 10.1007/s13205-017-1053-6

Ramzan, R., Safiullah Virk, M., Muhammad, Z., Ahmed, A. M. M., Yuan, X., and Chen, F. (2019). Genetic modification of mfsT gene stimulating the putative penicillin production in Monascus ruber M7 and exhibiting the sensitivity towards precursor amino acids of penicillin pathway. *Microorganisms* 7, 1–22. doi: 10.3390/microorganisms7100390

Schulz, B., and Kolukisaoglu, H. Ü. (2006). Genomics of plant ABC transporters: The alphabet of photosynthetic life forms or just holes in membranes? *FEBS Lett.* 580, 1010–1016. doi: 10.1016/j.febslet.2006.01.002

Seiple, I. B., Zhang, Z., Jakubec, P., Langlois-Mercier, A., Wright, P. M., Hog, D. T., et al. (2016). A platform for the discovery of new macrolide antibiotics. *Nature* 533, 338–345. doi: 10.1038/nature17967

Shao, Y., Ding, Y., Zhao, Y., Yang, S., Xie, B., and Chen, F. (2009). Characteristic analysis of transformants in T-DNA mutation library of Monascus ruber. *World J. Microbiol. Biotechnol.* 25, 989–995. doi: 10.1007/s11274-009-9977-6

Singh, R., Singh, S., and Pandey, P. N. (2016). *In-silico* analysis of Sirt2 from *Schistosoma mansoni*: Structures, conformations, and interactions with inhibitors. *J. Biomol. Struct. Dyn.* 34, 1042–1051. doi: 10.1080/07391102.2015.1065205

Stitou, M., Toufik, H., Bouachrine, M., and Lamchouri, F. (2021). Quantitative structure–activity relationships analysis, homology modeling, docking and molecular dynamics studies of triterpenoid saponins as Kirsten rat sarcoma inhibitors. *J. Biomol. Struct. Dyn.* 39, 152–170. doi: 10.1080/07391102.2019.1707122

Tang, K., Xin, Y., Li, K., Chen, X., and Tan, Y. (2021). Cell cytoskeleton and stiffness are mechanical indicators of organotropism in breast cancer. *Biology* 10, 1–14. doi: 10.3390/biology10040259

Ullán, R., Liu, G., Casqueiro, J., Gutiérrez, S., Bañuelos, O., and Martín, J. (2002). The cefT gene of *Acremonium chrysogenum* C10 encodes a putative multidrug efflux pump protein that significantly increases cephalosporin C production. *Mol. Genet. Genomics.* 267, 673–683. doi: 10.1007/s00438-002-0702-5

Ullán, R. V., Teijeira, F., and Martín, J. F. (2008). Expression of the *Acremonium chrysogenum* cefT gene in *Penicillum chrysogenum* indicates that it encodes an hydrophilic β-lactam transporter. *Curr. Genet.* 54, 153–161. doi: 10.1007/s00294-008-0207-9

Van Den Berg, M. A., Albang, R., Albermann, K., Badger, J. H., Daran, J. M., M., et al. (2008). Genome sequencing and analysis of the filamentous fungus *Penicillium chrysogenum*. *Nat. Biotechnol.* 26, 1161–1168. doi: 10.1038/nbt.1498

Wang, L., Dai, Y., Chen, W., Shao, Y., and Chen, F. (2016a). Effects of light intensity and color on the biomass, extracellular red pigment, and citrinin production of monascus ruber. *J. Agric. Food Chem.* 50, 9506–9514. doi: 10.1021/acs.jafc.6b04056

Wang, L., Wang, W., and Xu, G. (2011). Promotion of monacolin K production by *Agrobacterium tumefaciens*-mediated transformation in *Monascus albidus* 9901. *Curr. Microbiol.* 62, 501–507. doi: 10.1007/s00284-010-9735-x

Wang, S., Li, W., Liu, S., and Xu, J. (2016b). RaptorX-Property: a web server for protein structure property prediction. *Nucleic Acids Res.* 44, 430–435. doi: 10.1093/nar/gkw306

Waterhouse, A., Bertoni, M., Bienert, S., Studer, G., Tauriello, G., Gumienny, R., et al. (2018). SWISS-MODEL: homology modelling of protein structures and complexes. *Nucleic Acids Res.* 46, 296–303. doi: 10.1093/nar/gky427

Weber, S. S., Kovalchuk, A., Bovenberg, R. A. L., and Driessen, A. J. M. (2012). The ABC transporter ABC40 encodes a phenylacetic acid export system in *Penicillium chrysogenum*. *Fungal Genet. Biol.* 49, 915–921. doi: 10.1016/j.fgb.2012.09.003

Wei, W., Lin, S., Chen, M., Liu, T., Wang, A., Li, J., et al. (2017). Monascustin, an unusual γ-lactam from red yeast rice. *J. Nat. Prod.* 80, 201–204. doi: 10.1021/acs.jnatprod.6b00493

Wilkens, S. (2015). Structure and mechanism of ABC transporters. *F1000Prime Rep.* 7, 14. doi: 10.12703/P7-14

Xu, Y., Seelig, A., and Bernèche, S. (2017). Unidirectional transport mechanism in an ATP dependent exporter. *ACS Cent. Sci.* 3, 250–258. doi: 10.1021/acscentsci.7b00068

Yang, J., Xu, X., and Liu, G. (2012). Amplification of an MFS transporter encoding gene penT significantly stimulates penicillin production and enhances the sensitivity of *Penicillium chrysogenum* to phenylacetic acid. *J. Genet. Genomics*. 39, 593–602. doi: 10.1016/j.jgg.2012.08.004

Yuliana, A., Singgih, M., Julianti, E., and Blanc, P. J. (2017). Derivates of azaphilone *Monascus pigments*. *Biocatal. Agric. Biotechnol.* 9, 183–194. doi: 10.1016/j.bcab.2016.12.014

Zaitseva, J., Jenewein, S., Jumpertz, T., Holland, I. B., and Schmitt, L. (2005). H662 is the linchpin of ATP hydrolysis in the nucleotide-binding domain of the ABC transporter HlyB. *EMBO J.* 24, 1901–1910. doi: 10.1038/sj.emboj.7600657

Zhang, B., Chen, L., Jin, J. Y., Zhong, N., Cai, X., Zou, S. P., et al. (2021). Strengthening the (R)-pantoate pathway to produce D-pantothenic acid based on systematic metabolic analysis. *Food Biosci.* 43, 101283. doi: 10.1016/j.fbio.2021.101283

Conflict of Interest: The authors declare that the research was conducted in the absence of any commercial or financial relationships that could be construed as a potential conflict of interest.

Publisher's Note: All claims expressed in this article are solely those of the authors and do not necessarily represent those of their affiliated organizations, or those of the publisher, the editors and the reviewers. Any product that may be evaluated in this article, or claim that may be made by its manufacturer, is not guaranteed or endorsed by the publisher.

frontiers | Frontiers in Microbiology

TYPE Methods
PUBLISHED 01 August 2022
DOI 10.3389/fmicb.2022.952323

OPEN ACCESS

EDITED BY
Xucong Lv,
Fuzhou University, China

REVIEWED BY
Zhilong Wang,
Shanghai Jiao Tong University, China
Zhenqiang Wu,
South China University of Technology, China

*CORRESPONDENCE
Fusheng Chen
chenfs@mail.hzau.edu.cn

†These authors have contributed equally to this work and share first authorship

SPECIALTY SECTION
This article was submitted to Food Microbiology, a section of the journal Frontiers in Microbiology

RECEIVED 25 May 2022
ACCEPTED 27 June 2022
PUBLISHED 01 August 2022

CITATION
Xu N, Li L and Chen F (2022) Construction of gene modification system with highly efficient and markerless for *Monascus ruber* M7. *Front. Microbiol.* 13:952323. doi: 10.3389/fmicb.2022.952323

Construction of gene modification system with highly efficient and markerless for *Monascus ruber* M7

Na Xu[1,2†], Li Li[1,2,3,4†] and Fusheng Chen[1,2*]

[1]Hubei International Scientific and Technological Cooperation Base of Traditional Fermented Foods, Huazhong Agricultural University, Wuhan, China, [2]College of Food Science and Technology, Huazhong Agricultural University, Wuhan, China, [3]Hubei Key Laboratory of Quality Control of Characteristic Fruits and Vegetables, Hubei Engineering University, Xiaogan, China, [4]College of Life Science and Technology, Hubei Engineering University, Xiaogan, China

Monascus spp. are traditional medicinal and edible filamentous fungi in China, and can produce various secondary metabolites, such as *Monascus* pigments (MPs) and citrinin (CIT). Genetic modification methods, such as gene knock-out, complementation, and overexpression, have been used extensively to investigate the function of related genes in *Monascus* spp.. However, the resistance selection genes that can have been used for genetic modification in *Monascus* spp. are limited, and the gene replacement frequency (GRF) is usually <5%. Therefore, we are committed to construct a highly efficient gene editing system without resistance selection marker gene. In this study, using *M. ruber* M7 as the starting strain, we successfully constructed a so-called markerlessly and highly genetic modification system including the mutants Δ*mrpyrG*Δ*mrlig4* and Δ*mrpyrG*Δ*mrlig4*::*mrpyrG*, in which we used the endogenous gene *mrpyrG* from *M. ruber* M7 instead of the resistance marker gene as the screening marker, and simultaneously deleted *mrlig4* related to non-homologous end joining in *M. ruber* M7. Then, the morphology, the growth rate, the production of MPs and CIT of the mutants were analyzed. And the results show that the mutant strains have normal mycelia, cleistothecia and conidia on PDA+Uridine(U) plate, the biomass of each mutant is also no different from *M. ruber* M7. However, the U addition also has a certain effect on the orange and red pigments yield of *M. ruber* M7, which needs our further study. Finally, we applied the system to delete multiple genes from *M. ruber* M7 separately or continuously without any resistance marker gene, and found that the average GRF of Δ*mrpyrG*Δ*mrlig4* was about 18 times of that of *M. ruber* M7. The markerlessly and highly genetic modification system constructed in current study not only will be used for multi-gene simultaneous modification in *Monascus* spp., and also lays a foundation for investigating the effects of multi-genes modification on *Monascus* spp..

KEYWORDS

Monascus ruber* M7, genetic modification system, resistance selection marker, *mrlig4*, *mrpyrG

Introduction

Monascus spp., a group of traditional medicine and edible filamentous fungi in China, can produce abundant benefit secondary metabolites (SMs) such as *Monascus* pigments (MPs), γ-aminobutyric acid, monacolin K, and ergosterol (Endo, 1979; Feng et al., 2012; Patakova, 2013; Wu et al., 2013). But some *Monascus* strains may also yield a kind of mycotoxin, citrinin (CIT) (Blanc et al., 1995; Lin et al., 2008). So, there are a lot of studies on how to improve benefit SMs amount and to decrease and even eliminate CIT content in *Monascus*-related products (de Carvalho et al., 2006; Hajjaj et al., 2012; Feng et al., 2014). Among them, the genetic modification method such as gene knock-out, complementation, and overexpression is considered as one of the most significant approaches to control benefit SMs and CIT production (Liu et al., 2014, 2016, 2021; Zhang et al., 2019).

However, as we know, up to now, there are limited antibiotic selection marker genes available for the genetic modification of *Monascus* spp., such as the genes of hygromycin (*hph*), neomycin (*neo*) (Li, 2011), pyrithiamine (*pyr*) (Cui and Li, 2012), and aureobasidin A (*aba*) (Shimizu et al., 2006). Therefore, it is very difficult to simultaneously modify multiple genes in the same *Monascus* strain. Moreover, the antibiotic resistance marker genes remaining in the *Monascus* mutants may affect their growth and metabolism, and when the mutants are used in the production of foods and food additives, there also exist potential food safety hazards (Tuteja et al., 2012; Yang et al., 2015). So, the development of the genetic modification method without antibiotic screening marker gene residues is requisite for *Monascus* gene modification.

The uridine (U) auxotroph has been exploited widely in the genetic transformation system for many filamentous fungi (Wang et al., 2010; Arentshorst et al., 2015; Huang et al., 2016; Nguyen et al., 2016; Zhang et al., 2020). In fungi, orotidine 5′-phosphate decarboxylase (OMP decarboxylase) encoded by *pyrG* gene is a key enzyme involved in the pyrimidine biosynthesis, which can catalyze the decarboxylation of OMP to form uridine monophosphate (UMP) (Caroline and Davis, 1969; Garavaglia et al., 2012). OMP decarboxylase can also transform the pyrimidine analog 5-fluoroorotic acid (5-FOA) to the toxic compound to fungi, 5′-fluoro-UMP, to kill the fungal cells with *pyrG* (Ying et al., 2013; Zhang et al., 2020). Therefore, U combined with 5-FOA can be used to screen a markerless knockout strain, Δ*pyrG,* which does not contain the foreign gene including any antibiotic selection marker gene. The strains containing *pyrG* can synthesize U by themselves and can grow on the media without U, so they are called as U prototrophic or U independent strains, while the strains without *pyrG* such as Δ*pyrG* cannot synthesize U by themselves and also cannot grow on the media without U, so they are known as U auxotrophic or U-dependent strains. Therefore, taking Δ*pyrG* as the starting strain, replacing the target gene with *pyrG*, and combining U with 5-FOA, the markerless modifier of the target gene can be achieved. Wang et al. (2010) obtained a *pyrG* gene point mutant strain of *M. aurantiacus* by ultraviolet mutagenesis, and successfully transferred *pyrG* back to the *pyrG* mutant strain. However, there is no report about their subsequent application research of this system.

Several studies have showed that the gene homologous recombination efficiency (GRF) of fungal gene modification is relatively low due to the existence of the non-homologous end-joining (NHEJ) pathway in fungal cells (Ishibashi et al., 2006; Shrivastav et al., 2008; Liu et al., 2018; Pannunzio et al., 2018). And usually, the GRF of *Monascus* genetic modification is <5% (Li and Chen, 2020). He et al. (2013, 2014) knocked out the relative genes with NHEJ pathway, including the genes of DNA-dependent protein kinase catalytic subunits of Ku70 and Ku80, and ligase 4 (Symington and Gautier, 2011), leading that GRF of *Monascus* was increased by 2–4 times. However, the obtained high-efficiency strains cannot continue to be used for multi-gene modification of *M. ruber* M7 due to the limitation of resistance screening genes.

In current research, we have developed a marker recycling and highly genetic modification system, including the mutants Δ*mrpyrG*Δ*mrlig4*::*mrpyrG* (Δ*pyrG*+*lig4*::*pyrG*) and Δ*mrpyrG*Δ*mrlig4* (Δ*pyrG*+*lig4*) for *M. ruber* M7, in which we used the endogenous gene *mrpyrG* (the homologous gene of OMP decarboxylase gene) in *M. ruber* M7 instead of the resistance marker gene as the screening marker, and simultaneously deleted *mrlig4* related to the NHEJ. Then, the morphologies, growth rates, the production of MPs and CIT of the mutants were determined. Finally, we applied the system to delete multiple genes including *mrpigG*, *mrpigH*, and *mrpigI* relative to MPs biosynthesis in *M. ruber* M7 (Chen et al., 2017) separately or continuously without any resistance marker gene, and found that the average GRF of Δ*pyrG*+*lig4* was about 18 times of that of *M. ruber* M7, which shows that the system is suitable for multiple genes modification of *Monascus* spp..

Materials and methods

Fungal strains, culture media and growth conditions

M. ruber M7 [CCAM 070120, Culture Collection of State Key Laboratory of Agricultural Microbiology, which is part of China Center for Type Culture Collection (CCTCC), Wuhan, China] (Chen and Hu, 2005), the model microorganism in our lab, was used as a DNA donor and for transformation (Shao et al., 2009). All the strains used in this study are described in Table 1. All the strains are maintained on PDA slants with/without 10 mmol/ml uridine and 0.75 mg/ml 5-FOA at 28°C (Thai et al., 2021).

TABLE 1 *Monascus ruber* strains used and constructed in this study.

Strains	Parents	Sources
M. ruber M7	–	Laboratory preservation
Δ*mrpyrG*	*M. ruber* M7	This study
Δ*mrlig4*Δ*mrpyrG* (Δ*pyrG*+*lig4*)::*mrpyrG*	Δ*mrpyrG*	This study
Δ*pyrG*+*lig4*	Δ*pyrG*+*lig4*::*pyrG*	This study
Δ*pyrG*+*lig4*+*pigG*	Δ*pyrG*+*lig4*	This study
Δ*pyrG*+*lig4*+*pigI*	Δ*pyrG*+*lig4*	This study
Δ*pyrG*+*lig4*+*pigG*+*pigH*	Δ*pyrG*+*lig4*+*pigG*	This study
Δ*pyrG*+ *lig4*+*pigG*+*pigH*+*pigI*	Δ*pyrG*+*lig4*+*pigG*+*pigH*	This study

Cloning and analysis of the *pyrG* gene

Amino acid sequences encoded by *mrpyrG* were predicted using SoftBerry's FGENESH program (http://www.softberry.com), and the *mrpyrG* functional regions were analyzed using the Pfam 33.1 program (http://pfam.xfam.org/). Homology of the deduced amino acid sequence was analyzed using the BlastP program on the NCBI website (http://blast.ncbi.nlm.nih.gov/Blast.cgi).

Deletion of the *mrpyrG* and *mrlig4* genes

To construct a markerlessly and highly efficient genetic modification system, the genes of *mrpyrG* and *mrlig4* were deleted according to the homologous recombination strategy as described previously (Liu et al., 2014). Genomic DNA of *M. ruber* M7 was extracted according to previous description (Shao et al., 2009) for amplification of the entire *mrpyrG* and *mrlig4* gene sequences and their 5′- and 3′-flanking regions. Using these amplified DNA sequences, the *mrpyrG* deletion cassette was constructed by double-joint PCR (Yu et al., 2004), and the *mrlig4* cassette was constructed using the Seamless Cloning and assembly kit (Li et al., 2021). Then, these two cassettes were digested separately by *Kpn* I/*Xba* I, *Hind* III/*Kpn* I, and then ligated with pCAMBIA3300 vector digested with the same restricted enzymes to form recombinant vectors respectively, which were transformed into *Agrobacterium tumefaciens* EHA105 cells that were used to introduce the constructed cassettes region into the hosts (Shao et al., 2009). The construction procedure is showed in Figure 1 (Li et al., 2021). The relative primer pairs are shown in Table 2.

Excision of the *mrpyrG* marker by using 5-FOA

Since the U auxotrophs were resistant to 5-FOA in *M. ruber* M7, positive selection for Δ*mrpyrG* strains was carried out using 5-FOA. It was expected that the *pyrG* inserted at the *lig4* locus would be excised out by homologous recombination with the direct repeats, in which the flanking regions of the *lig4* were directly connected without leaving any ectopic/foreign DNA fragments (Figure 1B). Conidia of the Δ*pyrG*+*lig4*::*pyrG* strains(10^5 cfu/ml) were spread onto the agar medium containing 5-FOA and U after 5–8 day cultivation and the resulting 5-FOA resistant strains exhibited U auxotrophy.

Analysis of phenotypic characterization and biomass

M. ruber M7, Δ*mrpyrG*, Δ*pyrG*+*lig4*::*pyrG*, Δ*pyrG*+*lig4*, were, respectively, inoculated on PDA, PDA+U, PDA+U+5-FOA plates for 5 days at 28°C to observe the colonial and microscopic morphologies (Huang et al., 2016).

Biomass was determined according to the published paper (Lai et al., 2011) with minor modification. One milliliter freshly harvested spore (10^5 cfu/ml) of each strain was inoculated on PDA and PDA+U plates covered with cellophane membranes, and incubated at 28°C for 11 days, the samples were taken every 2 days from the 3rd day to the 11th day of culture. Then, these samples were vacuum freeze-dried and weighed.

Detection of citrinin and *Monascus* pigments

In total, 1 ml freshly harvested spore (10^5 cfu/ml) of aforementioned strains was inoculated on PDA and PDA+U plates covered with cellophane membranes, and incubated at 28°C for 11 days, respectively, to detect the intracellular MPs and extracellular CIT.40 mg freeze-dried media powder was extracted by 1 mL 80% (v/v) methanol, and subjected to 30 min ultrasonication treatment to detect the citrinin content by UPLC (Waters, America) with previous method (Liu et al., 2019), and injection volume was 2 μL. And 20 mg freeze-dried mycelia was extracted by 1 mL 80%(v/v) methanol, and subjected to

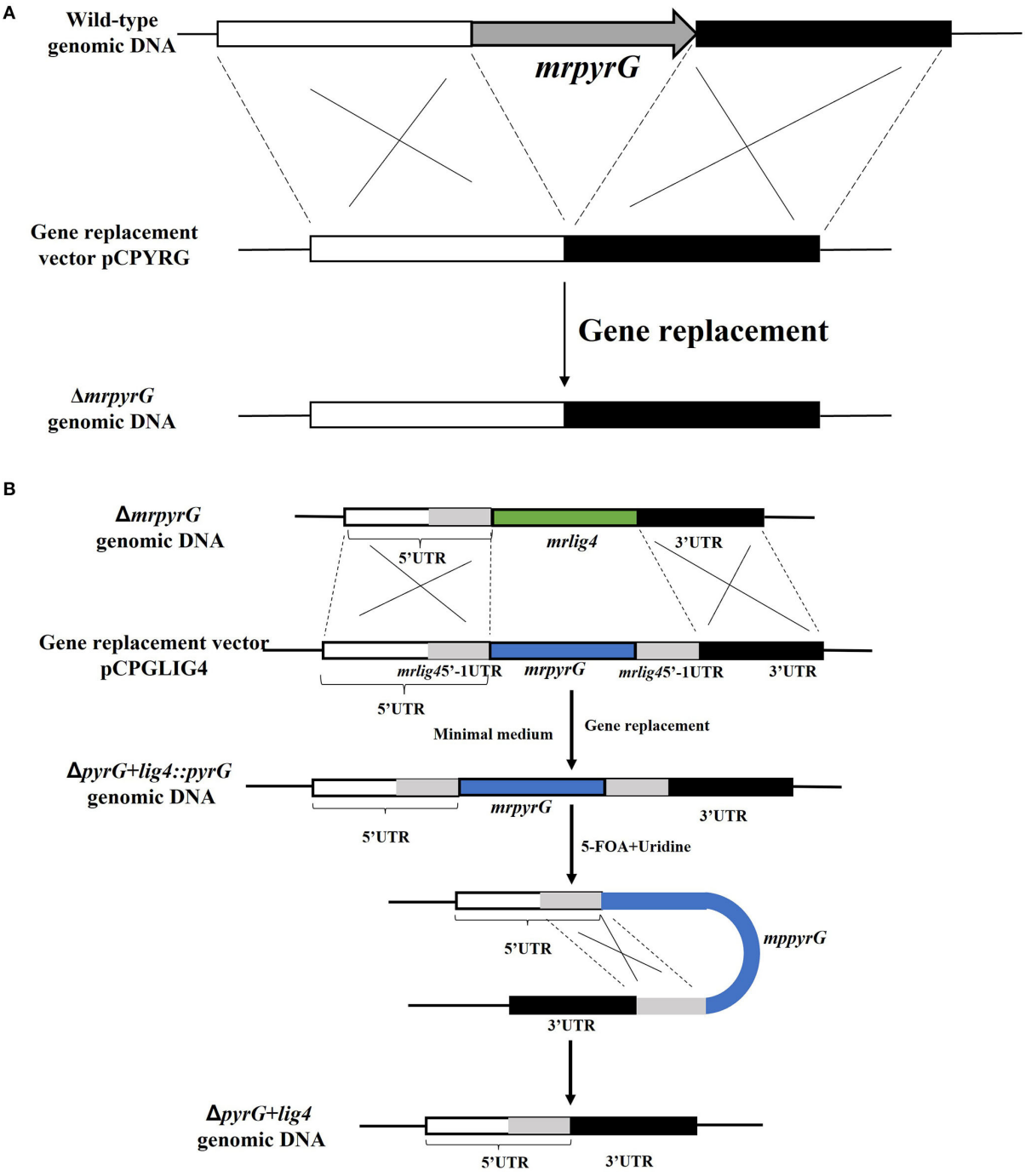

FIGURE 1
Deletion of *mrpyrG* and *mrlig4* in *M. ruber* M7. **(A)** Strategy to construct *mrpyrG* markerless deletion strain. **(B)** Strategy to construct *mrlig4* markerless deletion strain.

30 min ultrasonication treatment. Dilute the methanol extract to an appropriate amount, use 80% (v/v) methanol as the control (CK), and measure the absorbance at 380 nm, 470 nm, and 520 nm by the ultraviolet-visible spectrophotometry. The absorbance value multiplied by the dilution factor is the color value of yellow, orange, and red MPs, respectively. The final contents of Monascus pigments and citrinin were expressed as U/mg and μg/mg, respectively.

TABLE 2 Primers used in this study.

Names	Sequences (5'→ 3')	Descriptions
pyrG-5F	GGGGCTGCTCCACATGAATC	For amplification of 896 bp of 5' flanking regions of *pyrG*
pyrG-5R	CAAGGATTTCGTGCTGGGGT	
pyrG-3F	ACCCCAGCACGAAATCCTTGGGCAAGCGGGTTCGGATGGT	For amplification of 829 bp of 3' flanking regions of *pyrG*
pyrG-3R	ACGCTAGACTCGTCCTCGGA	
pyrG-F2	GTGCATACTCTACAGAT	For amplification of 498 bp of a part of *pyrG*
pyrG-R2	CCAAGAAGACGAATGTGA	
lig4pyrG-5F	GATATCGAATTCCCAATACTCTACCTTTGAATACTTAACA	For amplification of 1,041 bp of 5' flanking regions of *lig4*
lig4pyrG-5R	AGTTTCTCAGCGTCTTGTCT	
lig4pyrG-pyrGeF	[A]AGACAAGACGCTGAGAAACTATTATCGTATAGAGCAATA	For amplification of the whole *pyrG* gene (1,276 bp)
lig4pyrG-pyrGeR	TCACTGGTTCTTACAGCCGT	
lig4pyrG 5-1F	ACGGCTGTAAGAACCAGTGAGGAAGGGTCCTACTTGCCAT	For amplification of 470 bp of 5'-1 flanking regions of *lig4*
lig4pyrG 5-1R	AGTTTCTCAGCGTCTTGTCT	
lig4pyrG-3F	[a]AGACAAGACGCTGAGAAACTGACATTCTTCTTCCTTACGA	For amplification of 1,009 bp of 3' flanking regions of *pyrG*
lig4pyrG-3R	CTGCAGGAATTCCCAATACTAACTAATACTTCGTGTAACT	
lig4-F	GAGATGGCGAAAGGATGTAG	For amplification of a part of *lig4* (2,174 bp)
lig4-R	CACCTTCACCGTCCCTGTAG	
pigGpyrG-5F	GATATCGAATTCCCAATACTCGTCCCCCTTCTGCCCAAGA	For amplification of 873 bp of 5' flanking regions of *pigG*
pigGpyrG-5R	CCGAACTCCTTGTAGACCGA	
PigGpyrG-pyrGeF	[B]TCGGTCTACAAGGAGTTCGG GATTATCGTATAGAGCAATA	For amplification of the whole *pyrG* gene (1,276 bp)
PigGpyrG-pyrGeR	TCACTGGTTCTTACAGCCGT	
pigGpyrG 5-1F	ACGGCTGTAAGAACCAGTGAGCAGTCCGCAGTTCCTGGCT	For amplification of 539 bp of 5'-1 flanking regions of *pigG*
pigGpyrG 5-1R	GAGATGGAGCGTGCTGTCGT	
PigGpyrG-3F	[b]ACGACAGCACGCTCCATCTCGTGCCGATCAAGACGAAGGA	For amplification of 867 bp of 3' flanking regions of *pigG*
PigGpyrG-3R	CTGCAGGAATTCCCAATACTCTCTTCCAGCAGGACCAACT	
pigG-F	GCGCTGGCTGCGCTCAT	For amplification of a part of *pigG* (503 bp)
pigG-R	CCTCCCACTCCATAACCC	
pigHpyrG 5F	GATATCGAATTCCCAATACTCGTTACCCCGTCCAAGATGG	For amplification of 955 bp of 5' flanking regions of *pigH*
pigHpyrG 5R	CGGTGGCAGTCGAAGGGGCA	
pigHpyrG pyrGeF	[C]TGCCCCTTCGACTGCCACCGGATTATCGTATAGAGCAATA	For amplification of the whole *pyrG* gene (1,276 bp)
pigHpyrG pyrGeR	TCACTGGTTCTTACAGCCGT	
pigHpyrG 5-1F	ACGGCTGTAAGAACCAGTGA CGCACACACGTTTCGCACGG	For amplification of 531 bp of 5'-1 flanking regions of *pigH*
pigHpyrG 5-1R	CGGTGGCAGTCGAAGGGGCA	
pigHpyrG 3F	[c]TGCCCCTTCGACTGCCACCG GGCTGGATGCTGCATGTTTT	For amplification of 775 bp of 3' flanking regions of *pigH*
pigHpyrG 3R	CTGCAGGAATTCCCAATACTCGCCGAAGCCCCCTTCCTCT	
pigH F	GTGCTGGTGCCCGACCTGAC	For amplification of a part of *pigH* (583 bp)
pigH R	CGAAGATGAAATTCGACTTGA	
pigIpyrG 5F	GATATCGAATTCCCAATACTGCTGTCAAAGAAATAGAGAA	For amplification of 993 bp of 5' flanking regions of *pigI*
pigIpyrG 5R	GCTGCCGACCGCATTCTGCT	
pigIpyrG pyrGeF	[D]AGCAGAATGCGGTCGGCAGCGATTATCGTATAGAGCAATA	For amplification of the whole *pyrG* gene (1,276 bp)
pigIpyrG pyrGeR	TCACTGGTTCTTACAGCCGT	
pigIpyrG 5-1F	ACGGCTGTAAGAACCAGTGAGATGCCCCGTCTCACTGACC	For amplification of 483 bp of 5'-1 flanking regions of *pigI*
pigIpyrG 5-1R	GTCCAAGATGGCGGTCCAGT	
pigIpyrG 3F	[d]ACTGGACCGCCATCTTGGACGAAACCCTCCATGACACCTA	For amplification of 1,019 bp of 3' flanking regions of *pigI*
pigIpyrG 3R	CTGCAGGAATTCCCAATACTCGTCTACAATTTGATTCATT	
pigI F	GATCCTGTCGGCGATGCTCC	For amplification of a part of *pigI* (767 bp)
pigI R	TCTGGACGGTGCTGGGCTGC	

Labeled with double wavy line letters are nucleotide sequences of pBLUE-T; Labeled with single underline letters are nucleotide sequences of 5'UTR of *mrpyrG*; Labeled with double underline letters are nucleotide sequences of *mrpyrG*; [A,B,C,D]Labeled with wavy line letters are nucleotide sequences of 5′ flanking regions of *mrlig4*, *mrpigG*, *mrpigH*, and *pigI*, respectively; [a,b,c,d]Labeled with dotted lines letters are nucleotide sequences of 5′-1 flanking regions of *mrlig4*, *mrpigG*, *mrpigH*, and *mrpigI*, respectively.

Results

Construction of genetic modification system with markerless and highly efficient system

Sequence analysis of *mrpyrG* in *M. ruber* M7

Sequence prediction of *mrpyrG* by SoftBerry's FGENESH program has revealed that the putative *mrpyrG* gene consists only of an 828 bp open reading frame (ORF) which consists of 2 exon and encodes 275 amino acids. A database search with NCBI-Blastp has demonstrated that the deduced 275-amino acid sequence encoded by *mryrG* shares 100% similarity with the amino orotidine-5′-phosphate decarboxylase of *M. aurantiacus* (GenBank: ADE43948.1), 81.39% similarity with PyrG of *Penicillium chrysogenum* (GenBank: XP-002 558877.1). Besides, prediction of Pfam has indicated that *MrpyrG* belongs to the DRE–TIM metallolyase superfamily.

Verification of the Δ*mrpyrG*, Δ*pyrG+lig4::pyrG*, Δ*pyrG+lig4* strains

Through genetic transformation mediated by *Agrobacterium tumefaciens*, 2 putative *mrpyrG* mutants (Δ*mrpyrG*), 2 putative mutants (Δ*pyrG+lig4*::*pyrG*), and 1 Δ*pyrG+lig4* mutant were obtained, respectively. The PCR verification results of these mutants are shown in Figure 2.

The results from Figure 2A reveal that no DNA band was amplified when the genome of the putative Δ*mrpyrG* strain was used as template with the primer pair pyrG-F2/pyrG-R2 (Table 2). Meanwhile, amplicons of *M. ruber* M7 (1.73 kb) and Δ*mrpyrG* (2.3 kb) different in sizes were observed when primers pyrG5F/pyrG3R (Table 2) were used. The results from Figure 2B show that no DNA band was amplified when the genome of the putative Δ*pyrG+lig4*::*pyrG* strain was used as template with the primer pair lig4F/lig4R (Table 2), while a 2.2 kb product appeared using the genome of the Δ*mrpyrG* strain. Meanwhile, amplicons of Δ*pyrG+lig4*::*pyrG* (3.8 kb) and Δ*mrpyrG* (4.37 kb) different in sizes were observed when primers lig4pyrG5F/lig4pyrG5R (Table 2) were used. The 2.1 kb band in Lane 1 of Figure 2B generated by the primer lig4pyrG5F/lig4pyrG5R may be the homogenous sequence of 5′UTR and 5′-1UTR of the *mrlig4* knockout cassette. The results from Figure 2C displays that no DNA band was amplified when the genome of the putative Δ*pyrG+lig4* strain was used as DNA template with the primer pair lig4F/lig4R and pyrGF2/pyrGR2, while a 2.2 kb product and a 0.5 kb product appeared, respectively, using the genome of the Δ*pyrG+lig4*::*pyrG* strain. Meanwhile, amplicons of *M. ruber* M7 (4.37kb) and Δ*pyrG+lig4* (2.1 kb) different in sizes were observed when primers lig4pyrG5F/lig4pyrG3R (Table 2) were used. Besides, amplicons of *M. ruber* M7 (1.73 kb) and Δ*pyrG+lig4* (2.3 kb) different in sizes were observed when primers pyrG5F/pyrG3R were used. These PCR results demonstrate that all the mutants are successfully constructed.

Characteristics of *M. ruber* M7, Δ*mrpyrG*, Δ*pyrG+lig4*::*pyrG* and Δ*pyrG+lig4*

Morphologies and biomasses of *M. ruber* M7, Δ*mrpyrG*, Δ*pyrG+lig4::pyrG* and Δ*pyrG+lig4*

M. ruber M7, Δ*mrpyrG*, Δ*pyrG+lig4*::*pyrG* and Δ*pyrG+lig4* strains were cultured for 5d at 28°C to observe colonial morphologies on PDA, PDA+U, and PDA+U+ 5-FOA plates. At the same time, these strains were cultured for 7 d at 28°C to observe microscopic morphologies on PDA and PDA+U plates.

It can be seen from Figure 3I that *M. ruber* M7 with *mrpyrG* can synthesize U and transform 5-FOA into the toxic compound 5-fluorouracil, so it can grow on PDA plate but not on PDA+5-FOA plate. U auxotrophic strains (Δ*mrpyrG* and Δ*pyrG+lig4*) cannot synthesize U and cannot transform 5-FOA into 5-fluorouracil, and cannot grow on PDA plate, but can grow on PDA+U and PDA+U+5-FOA plates. The colonial morphologies of U prototrophic strain (Δ*pyrG+lig4*::*pyrG*) on PDA, PDA+U, and PDA+U+5-FOA plates is consistent with *M. ruber* M7. These results once again show that the construction of each mutant is right. Meanwhile, the microscopic results in Figure 3II shows that *mrpyrG*-deficient strains (Δ*pyrG* and Δ*pyrG+lig4*) have normal mycelia, cleistothecia, and conidia on PDA+U plate, which are no different from *M. ruber* M7. At the same time, the U prototrophic strain (Δ*pyrG+lig4*::*pyrG*) also normal mycelia, cleistothecia and conidia on PDA and PDA+U plates, which is also no difference from *M. ruber* M7. Moreover, the biomass of each mutant on PDA and/or PDA+U plate is not obviously different from that of *M. ruber* M7 (Figure 3III).

MPs and CIT production analysis of Δ*mrpyrG*, Δ*pyrG+lig4::pyrG*, Δ*pyrG+lig4* and *M. ruber* M7

Previous studies (Chen et al., 2017) have demonstrated that *M. ruber* M7 can produce MPs and CIT, but no MK, so the yields of MPs and CIT produced by *M. ruber* M7 and its mutants, were analyzed to uncover the effect of *mrpyrG* on them (Figure 4).

Compared with *M. ruber* M7, the yellow pigment production of all the mutant strains changed to some extent, but it showed an irregular trend (Figure 4I). And for the U auxotrophic strains Δ*mrpyrG* and Δ*pyrG+lig4*, the addition of U affected the production of orange and red pigments to a certain extent (Figures 4II,III). In addition, it can be found that the U addition also has a certain effect on the orange and red pigments yield of *M. ruber* M7.

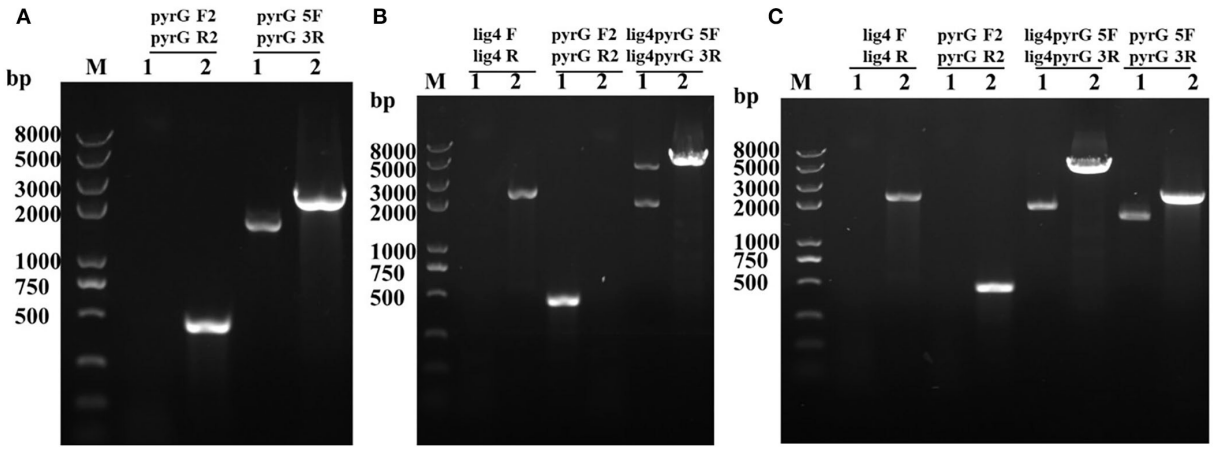

FIGURE 2
PCR analysis of Δ*mrpyrG*, Δ*pyrG+lig4::pyrG*, and Δ*pyrG+lig4*. **(A)** Confirmation of *mrpyrG* deletion. Lane 1: Δ*mrpyrG*; Lane 2: M7; M: Trans 2K plus II marker; **(B)** Confirmation of *mrlig4* markerless deletion in Δ*mrpyrG* strain. Lane 1: Δ*pyrG+lig4::pyrG*; Lane 2: Δ*mrpyrG*; **(C)** Confirmation of *mrpyrG* homologous recombination events in Δ*pyrG+lig4::pyrG* strain. Lane 1: Δ*pyrG+lig4*; Lane 2: M7; M: Trans 2K plus II marker.

With regard to CIT, the results (Figure 4IV) show that CIT produced by Δ*mrpyrG*, Δ*pyrG+lig4::pyrG* and Δ*pyrG+lig4* was not apparently different from those of *M. ruber* M7 on different media, which indicates that *mrpyrG* and *mrlig4* have no effect on the CIT production.

Application of gene markerless and highly efficient modification system

Taking *M. ruber* M7 and Δ*pyrG+lig4* as the starting strains to knock out *mrpigG* and *mrpigI* in the MPs gene cluster of *M. ruber* M7 (Chen et al., 2017), respectively, and calculate the number of transformants and the number of disruptants (knockouts) via PCR verification with related primers shown in Table 2 from both starting strains. And the GRFs, referred as the number of disruptants divided by the number of transformants, are shown in Table 3. Furthermore, taking Δ*pyrG+lig4+pigG* as a starting strain, *mrpigH* and *mrpigI* genes were continuously deleted, and successfully got the multi-gene mutants Δ*pyrG+lig4+pigG +pigH+pigI*, and Δ*pyrG+lig4+pigG+pigH+ pigI::pyrG*. As shown in Table 3, when *mrpigG* was knocked out using the Δ*pyrG+lig4* strain as the starting strain, the GRF reached to 46.7% (21/45), while using *M. ruber* M7 as the starting strain, the GRF of *pigG* was only 2.6% (3/115). Meanwhile, when *mrpigI* was knocked out, the GRF was 44.4% (4/9) in the Δ*pyrG+lig4* strain and 2.4% (2/85) in *M. ruber* M7. In general, the average GRFs for *mrpigG* and *mrpigI* in Δ*pyrG+lig4* was about 18 times of that of *M. ruber* M7.

Discussion

In 2008, Maruyama and Kitamoto first described that the multiple gene disruptions with marker recycling were done in the highly efficient gene-targeting background in filamentous fungi (Maruyama and Kitamoto, 2008). They generated a *ligD*(*lig4*)-disruptant for highly efficient gene-disruption frequency in *A. oryzae*., then two proteinase genes(*tppA* and *pepE*) were disrupted continuously at very high frequency (~90%) in Δ*ligD* strain with *pyrG* as the screening marker. After that, *pyrG* has been successfully applied to *Aspergillus terreus* (Huang et al., 2016) and *Aspergillus niger* (Arentshorst et al., 2015) as a selection marker. But, there are no related reports in *Monascus* spp.. In recent years, genes involved in the biosynthesis of citrinin, monacolin K (MK), and pigments, and G protein signaling pathway (Sakai et al., 2009; Li, 2011; Shao et al., 2014; Chen et al., 2017, 2019) have been cloned and analyzed, which made an important step forward in understanding the secondary metabolism in *Monascus* spp.. However, because of the limitation of resistance selection marker genes, multiple-gene editing cannot be performed in the same strain. In this study, based on the issues that there are limited antibiotic screening marker genes available for *Monascus* gene modification and the low GRF (He et al., 2014), *mrpyrG* and *mrlig4* genes from *M. ruber* M7 were knocked out in sequence, leading that a so-called markerlessly and highly efficient gene modification system was successfully constructed without any antibiotic screening marker gene, in which GRF is about 18 times higher than that of *M. ruber* M7. And single or multiple gene(s) related with MPs of *M. ruber* M7 was (were) deleted by this gene modification system.

10.3389/fmicb.2022.952323

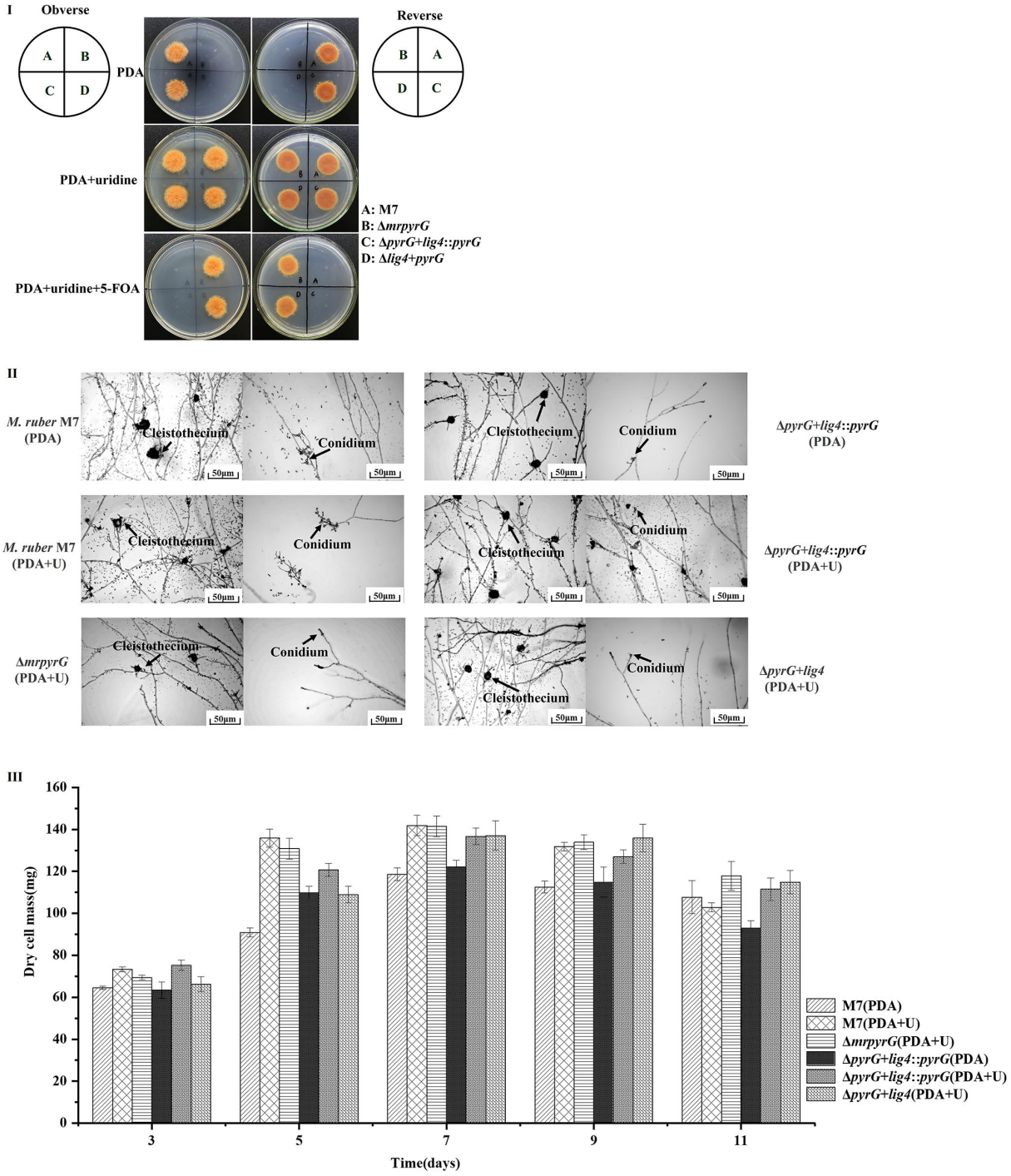

FIGURE 3
Morphologies and biomasses of *M. ruber* M7 and derivative markerless deletion strains. **(I)** Colonial morphologies on PDA, PDA+U and PDA+U+5-FOA plates. **(II)** Cleistothecia and conidia formation on PDA and PDA+U plates. **(III)** Biomass (dry cell weight).

Although the colonial and microscopic morphologies, biomasses (Figures 3I,III) and CIT production (Figure 4IV) of auxotrophic strains (Δ*mrpyrG* and Δ*pyrG*+*lig4*) and U prototrophic strain (Δ*pyrG*+*lig4*::*pyrG*) on PDA, PDA+U, and PDA+U+5-FOA plates were consistent with those of *M. ruber* M7, U addition could obviously affected the production of orange and red pigments of the U prototrophy strains and some U auxotrophy strains (Δ*mrpyrG*) (Figures 4I,III). Therefore,

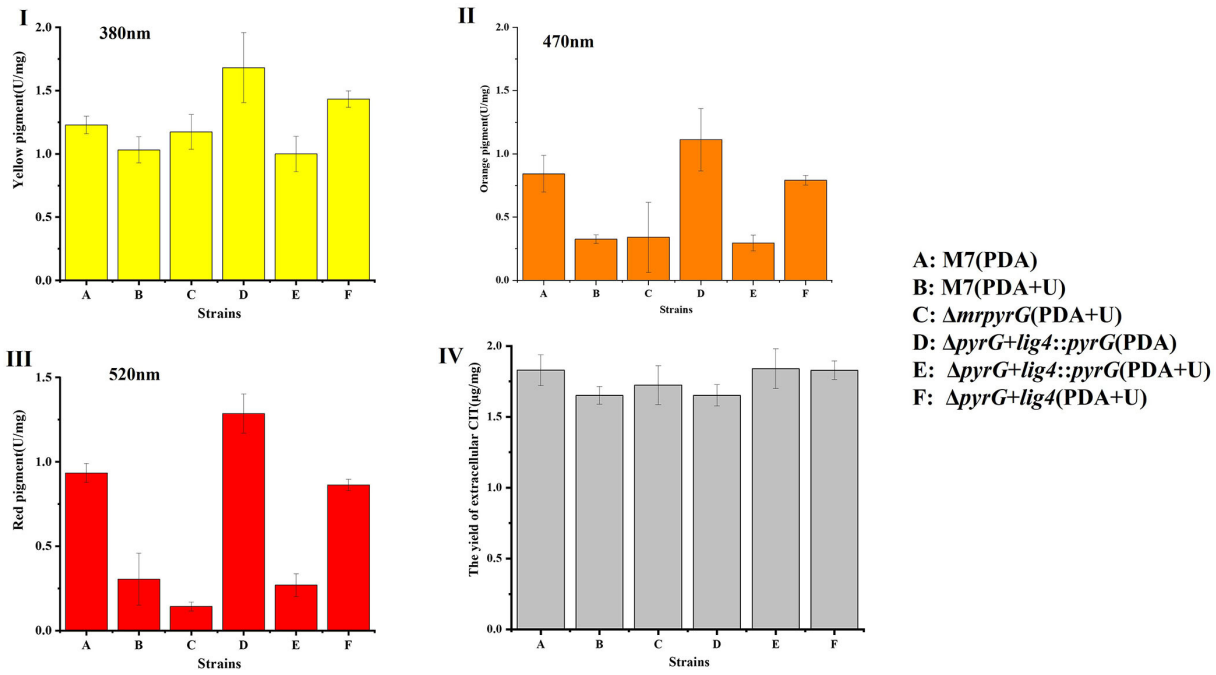

FIGURE 4
Production of intracellular MPs and extracellular CIT by *M. ruber* M7 and derivative markerless deletion strains on the PDA supplied with/without uridine. **(I)** The yield of yellow pigments; **(II)** The yield of orange pigments; **(III)** The yield of red pigments; and **(IV)** The yield of CIT.

TABLE 3 GRF in the wild-type (M7) and Δ*pyrG*+*lig4* strains.

Target genes	GRF of Δ*mrpyrG*+*lig4* (Disruptants[a] /Transformants[b])	GRF of M7 (Disruptants[a] /Transformants[b])
mrpigG	46.7% (21/45)	2.6% (3/115)
mrpigI	44.4% (4/9)	2.4% (2/85)

[a]The number of disruptants verified by PCR analyzed; [b]The number of transformants.

when the gene markerless modification system constructed in this study is used to investigate the gene(s) function(s) from *Monascus* spp., especially the function(s) of related gene(s) in the MPs gene cluster, it is necessary to re-introduce *pyrG* into the mutants without *pyrG* to avoid the extra addition of U. And why U addition has an effect on the production of the orange and red pigments needs to further be explored.

When the Δ*pyrG*+*lig4* strain from *M. ruber* M7 was taken as the starting strain, its GRFs for *mrpigG* and *mrpigI* reached 46.7 and 44.4%, respectively, due to *mrlig4* loss, which is much (18 times) higher than those of *M. ruber* M7 used as the starting strain (Table 3). However, the positive effect of the *mrlig4* mutant of *M. ruber* M7 on the GRF did not reach the level observed in some other fungi, which GRFs of almost 100% were obtained (Ishibashi et al., 2006; Bugeja et al., 2012). There are also studies that showed inactivation of the *ku70* or *ku80* genes involved in the NHEJ DNA repair pathway can greatly increase GRFs of filamentous fungi (Zhang et al., 2011; He et al., 2013). Therefore, in the future the GRFs may be further improved if the relative genes, such as *mrku70* or/and *mrku80,* with NHEJ pathway, is/are knocked out. Moreover, the characteristics of the multi-gene mutants Δ*pyrG*+*lig4*+*pigG*+*pigH*+*pigI* and Δ*pyrG*+*lig4*+*pigG*+*pigH*+*pigI*::*pyrG* should be investigated, too.

In this study, we construct a markerlessly and highly efficient gene modification system successfully to knock out endogenous *mrpyrG* and *mrlig4* gene without introducing any antibiotic screening marker gene, in which GRF is about 18 times higher than that of *M. ruber* M7. Besides, we have successfully applied this system to multiple-gene knock out in *Monascus* spp.. However, in our study, we also found that the U addition can make an effect on the yield of MPs, and the mechanism is not clear, which requires our further study.

Data availability statement

The original contributions presented in the study are included in the article/supplementary materials, further inquiries can be directed to the corresponding author/s.

Author contributions

NX and LL conceived, designed, and did research. NX wrote the manuscript, too. FC revised the manuscript. All authors read and approved the manuscript.

Funding

This work was supported by the National Natural Science Foundation of China (Nos. 31730068 and 31330059).

Acknowledgments

Funding from the National Natural Science Foundation of China (Nos. 31730068 and 31330059) is gratefully acknowledged.

Conflict of interest

The authors declare that the research was conducted in the absence of any commercial or financial relationships that could be construed as a potential conflict of interest.

Publisher's note

All claims expressed in this article are solely those of the authors and do not necessarily represent those of their affiliated organizations, or those of the publisher, the editors and the reviewers. Any product that may be evaluated in this article, or claim that may be made by its manufacturer, is not guaranteed or endorsed by the publisher.

References

Arentshorst, M., Lagendijk, E. L., and Ram, A. F. (2015). A new vector for efficient gene targeting to the *pyrG* locus in *Aspergillus. niger*. *Fungal. Biol.. Biotechnol.* 2, 2. doi: 10.1186/s40694-015-0012-4

Blanc, P. J., Laussac, J. P., Le Bars, J., Le Bars, P., Loret, M. O., Pareilleux, A., et al. (1995). Characterization of monascidin A from *Monascus* as citrinin. *Int. J. Food. Microbiol* 27, 201–213. doi: 10.1016/0168-1605(94)00167-5

Bugeja, H. E., Boyce, K. J., Weerasinghe, H., Beard, S., Jeziorowski, A., Pasricha, S., et al. (2012). Tools for high efficiency genetic manipulation of the human pathogen *Penicillium marneffei Fungal. Genet. Biol.* 49, 772–778. doi: 10.1016/j.fgb.2012.08.003

Caroline, D. F., and Davis, R. H. (1969). Pyrimidine synthesis in *Neurospora. crassa*: Regulation of enzyme activities. *J. Bacteriol.* 100, 1378–1384. doi: 10.1128/jb.100.3.1378-1384.1969

Chen, F., and Hu, X. (2005). Study on red fermented rice with high concentration of monacolin K and low concentration of citrinin. *Int. J. Food. Microbiol.* 103, 331–337. doi: 10.1016/j.ijfoodmicro.2005.03.002

Chen, W., Chen, R., Liu, Q., He, Y., He, K., Ding, X., et al. (2017). Orange, red, yellow: Biosynthesis of azaphilone pigments in *Monascus* fungi. *Chem. Sci.* 8, 4917–4925. doi: 10.1039/C7SC00475C

Chen, W., Feng, Y., Molnar, I., and Chen, F. (2019). Nature and nurture: confluence of pathway determinism with metabolic and chemical serendipity diversifies *Monascus* azaphilone pigments. *Nat. Prod. Rep.* 36, 561–572. doi: 10.1039/C8NP00060C

Cui, H., and Li, Y. (2012). Transformation of *Monascus* protoplasts using pyridine thiamin resistance gene as selective marker. *J. Anhui. Agri.* 40, 11591–11593.

de Carvalho, J. C., Pandey, A., Oishi, B. O., Brand, D., Rodriguez-Léon, J. A., Soccol, C. R., et al. (2006). Relation between growth, respirometric analysis and biopigments production from *Monascus* by solid-state fermentation. *Biochem. Eng. J.* 29, 262–269. doi: 10.1016/j.bej.2006.01.008

Endo, A. (1979). Monacolin K, a new hypocholesterolemic agent produced by a *Monascus* species. *J. Antibiot.* 32, 852–854. doi: 10.7164/antibiotics.32.852

Feng, Y., Shao, Y., and Chen, F. (2012). *Monascus* pigments. *Appl. Microbiol. Biotechnol.* 96, 1421–1440. doi: 10.1007/s00253-012-4504-3

Feng, Y., Shao, Y., Zhou, Y., and Chen, F. (2014). Production and optimization of monacolin K by citrinin-free *Monascus pilosus* MS-1 in solid-state fermentation using non-glutinous rice and soybean flours as substrate. *Eur. Food. Res. Technol.* 239, 629–636. doi: 10.1007/s00217-014-2259-z

Garavaglia, M., Rossi, E., and Landini, P. (2012). The pyrimidine nucleotide biosynthetic pathway modulates production of biofilm determinants in *Escherichia. coli*. *PLoS ONE* 7, e31252. doi: 10.1371/journal.pone.0031252

Hajjaj, H., Francois, J. M., Goma, G., and Blanc, P. J. (2012). Effect of amino acids on red pigments and citrinin production in *Monascus ruber*. *J. Food Sci.* 77, M156–9. doi: 10.1111/j.1750-3841.2011.02579.x

He, Y., Liu, Q., Shao, Y., and Chen, F. (2013). *Ku70* and *ku80* null mutants improve the gene targeting frequency in *Monascus ruber* M7. *Appl. Microbiol. Biotechnol.* 97, 4965–76. doi: 10.1007/s00253-013-4851-8

He, Y., Shao, Y., and Chen, F. (2014). Efficient gene targeting in *ligase. IV*-deficient *Monascus ruber* M7 by perturbing the non-homologous end joining pathway. *Fungal. Biol.* 118, 846–854. doi: 10.1016/j.funbio.2014.07.003

Huang, X., Chen, M., Li, J., and Lu, X. (2016). Establishing an efficient gene-targeting system in an itaconic-acid producing *Aspergillus terreus* strain. *Biotechnol. Lett.* 38, 1603–1610. doi: 10.1007/s10529-016-2143-y

Ishibashi, K., Suzuki, K., Ando, Y., Takakura, C., and Inoue, H. (2006). Nonhomologous chromosomal integration of foreign DNA is completely dependent on MUS-53 (human Lig4 homolog) in *Neurospora*. *Proc. Natl. Acad. Sci. U.S.A.* 103, 14871–14876. doi: 10.1073/pnas.0604477103

Lai, Y., Wang, L., Qing, L., and Chen, F. (2011). Effects of cyclic AMP on development and secondary metabolites of. *Monascus ruber* M7. *Lett. Appl. Microbiol.* 52, 420–426. doi: 10.1111/j.1472-765X.2011.03022.x

Li, L. (2011). *Cloning and functional analysis of genes of G-protein signaling pathways in Monascus ruber* (Dissertation). Huazhong Agricultural University, Wuhan, China.

Li, L., and Chen, F. (2020). Effects of *mrpigG* on development and secondary metabolism of *Monascus ruber* M7. *J. Fungi (Basel).* 6, 156. doi: 10.3390/jof6030156

Li, L., Xu, N., and Chen, F. (2021). Inactivation of *mrpigH* gene in *Monascus ruber* M7 results in increased *Monascus* pigments and decreased citrinin with *mrpyrG* selection marker. *J. Fungi.* 7, 1094. doi: 10.3390/jof7121094

Lin, Y. L., Wang, T. H., Lee, M. H., and Su, N. W. (2008). Biologically active components and nutraceuticals in the *Monascus*-fermented rice: a review. *Appl. Microbiol. Biotechnol.* 77, 965–973. doi: 10.1007/s00253-007-1256-6

Liu, J., Lei, M., Zhou, Y., and Chen, F. (2019). A comprehensive analysis of the small GTPases Ypt7 involved in the regulation of fungal development and secondary metabolism in *Monascus ruber* M7. *Front. Microbiol.* 10, 452. doi: 10.3389/fmicb.2019.00452

Liu, J., Wu, J., Cai, X., Zhang, S., Liang, Y., Lin, Q., et al. (2021). Regulation of secondary metabolite biosynthesis in *Monascus purpureus* via cofactor metabolic engineering strategies. *Food. Microbiol.* 95, 103689. doi: 10.1016/j.fm.2020.103689

Liu, M., Rehman, S., Tang, X., Gu, K., Fan, Q., Chen, D., et al. (2018). Methodologies for Improving HDR Efficiency. *Front. Genet* 9, 691. doi: 10.3389/fgene.2018.00691

Liu, Q., Cai, L., Shao, Y., Zhou, Y., Li, M., Wang, X., et al. (2016). Inactivation of the global regulator LaeA in *Monascus ruber* results in a species-dependent response in sporulation and secondary metabolism. *Fungal. Bio*. 120, 297–305. doi: 10.1016/j.funbio.2015.10.008

Liu, Q., Xie, N., He, Y., Wang, L., Shao, Y., Zhao, H., et al. (2014). *MpigE*, a gene involved in pigment biosynthesis in *Monascus ruber* M7. *Appl. Microbiol. Biotechnol*. 98, 285–296. doi: 10.1007/s00253-013-5289-8

Maruyama, J., and Kitamoto, K. (2008). Multiple gene disruptions by marker recycling with highly efficient gene-targeting background (Δ*ligD*) in *Aspergillus oryzae*. *Biotechnol. Lett*. 30, 1811–1817. doi: 10.1007/s10529-008-9763-9

Nguyen, K. T., Ho, Q. N., Pham, T. H., Phan, T. N., and Tran, V. T. (2016). The construction and use of versatile binary vectors carrying. *pyrG* auxotrophic marker and fluorescent reporter genes for *Agrobacterium*-mediated transformation of. *Aspergillus. oryzae. World. J. Microbiol. Biotechnol*. 32, 204. doi: 10.1007/s11274-016-2168-3

Pannunzio, N. R., Watanabe, G., and Lieber, M. R. (2018). Nonhomologous DNA end-joining for repair of DNA double-strand breaks. *J. Biol. Chem*. 293, 10512–10523. doi: 10.1074/jbc.TM117.000374

Patakova, P. (2013). *Monascus* secondary metabolites: Production and biological activity. *J. Ind. Microbiol. Biotechnol.* 40, 169–181. doi: 10.1007/s10295-012-1216-8

Sakai, K., Kinoshita, H., and Nihira, T. (2009). Identification of *mokB* involved in monacolin K biosynthesis in *Monascus pilosus*. *Biotechnol. Lett*. 31, 1911–1916. doi: 10.1007/s10529-009-0093-3

Shao, Y., Ding, Y., Zhao, Y., Yang, S., Xie, B., Chen, F., et al. (2009). Characteristic analysis of transformants in T-DNA mutation library of. *Monascus ruber*. *World. J. Microbiol. Biotechnol.* 25, 989–995. doi: 10.1007/s11274-009-9977-6

Shao, Y., Lei, M., Mao, Z., Zhou, Y., and Chen, F. (2014). Insights into *Monascus* biology at the genetic level. *Appl Microbiol. Biotechnol.* 98, 3911–3922. doi: 10.1007/s00253-014-5608-8

Shimizu, T., Kinoshita, H., and Nihira, T. (2006). Development of transformation system in *Monascus purpureus* using an autonomous replication vector with aureobasidin A resistance gene. *Biotechnol. Lett* 28, 115–120. doi: 10.1007/s10529-005-4956-y

Shrivastav, M., De Haro, L. P., and Nickoloff, J. A. (2008). Regulation of DNA double-strand break repair pathway choice. *Cell. Res.* 18, 134–147. doi: 10.1038/cr.2007.111

Symington, L. S., and Gautier, J. (2011). Double-strand break end resection and repair pathway choice. *Annu. Rev. Genet*. 45, 247–271. doi: 10.1146/annurev-genet-110410-132435

Thai, H. D., Nguyen, B. T., Nguyen, V. M., Nguyen, Q. H., and Tran, V. T. (2021). Development of a new *Agrobacterium*-mediated transformation system based on a dual auxotrophic approach in the filamentous fungus *Aspergillus oryzae*. *World. J. Microbiol. Biotechnol.* 37, 92. doi: 10.1007/s11274-021-03060-z

Tuteja, N., Verma, S., Sahoo, R. K., Raveendar, S., and Reddy, I. N. (2012). Recent advances in development of marker-free transgenic plants: regulate and biosafety concern. *J. Biosci*. 37, 167–197. doi: 10.1007/s12038-012-9187-5

Wang, B. H., Xu, Y., and Li, Y. P. (2010). Use of the *pyrG* gene as a food-grade selection marker in *Monascus. Biotechnol. Lett*. 32, 1631–1635. doi: 10.1007/s10529-010-0336-3

Wu, M. D., Cheng, M. J., Yech, Y. J., Chen, Y. L., Chen, K. P., Yang, P. H., et al. (2013). Monascusazaphilones A-C, three new azaphilone analogues isolated from the fungus *Monascus purpureus* BCRC 38108. *Nat. Prod. Res*. 27, 1145–1152. doi: 10.1080/14786419.2012.715289

Yang, F., Njire, M. M., Liu, J., Wu, T., Wang, B., Liu, T., et al. (2015). Engineering more stable, selectable marker-free autoluminescent mycobacteria by one step. *PLoS ONE*. 10, e0119341. doi: 10.1371/journal.pone.0119341

Ying, S. H., Feng, M. G., and Keyhani, N. O. (2013). Use of uridine auxotrophy (*ura3*) for markerless transformation of the mycoinsecticide *Beauveria bassiana*. *Appl Microbiol. Biotechnol*. 97, 3017–3025. doi: 10.1007/s00253-012-4426-0

Yu, J. H., Hamari, Z., Han, K. H., Seo, J. A., Reyes-Dominguez, Y., Scazzocchio, C., et al. (2004). Double-joint PCR: A PCR-based molecular tool for gene manipulations in filamentous fungi. *Fungal. Genet. Biol*. 41, 973–981. doi: 10.1016/j.fgb.2004.08.001

Zhang, C., Liang, J., Zhang, A., Hao, S., Zhang, H., Zhu, Q., et al. (2019). Overexpression of monacolin K biosynthesis genes in the. *Monascus purpureus* azaphilone polyketide pathway. *J. Agric. Food. Chem*. 67, 2563–2569. doi: 10.1021/acs.jafc.8b05524

Zhang, J., Mao, Z., Xue, W., Li, Y., Tang, G., Wang, A., et al. (2011). *Ku80* gene is related to non-homologous end-joining and genome stability in *Aspergillus niger*. *Curr Microbiol*. 62, 1342–1346. doi: 10.1007/s00284-010-9853-5

Zhang, L., Zheng, X., Cairns, T. C., Zhang, Z., Wang, D., Zheng, P., et al. (2020). Disruption or reduced expression of the orotidine-5'-decarboxylase gene *pyrG* increases citric acid production: A new discovery during recyclable genome editing in *Aspergillus niger*. *Microb. Cell. Fac*. 19, 76. doi: 10.1186/s12934-020-01334-z

Advantages of publishing in Frontiers

OPEN ACCESS
Articles are free to read for greatest visibility and readership

FAST PUBLICATION
Around 90 days from submission to decision

HIGH QUALITY PEER-REVIEW
Rigorous, collaborative, and constructive peer-review

TRANSPARENT PEER-REVIEW
Editors and reviewers acknowledged by name on published articles

Frontiers
Avenue du Tribunal-Fédéral 34
1005 Lausanne | Switzerland

Visit us: www.frontiersin.org
Contact us: frontiersin.org/about/contact

REPRODUCIBILITY OF RESEARCH
Support open data and methods to enhance research reproducibility

DIGITAL PUBLISHING
Articles designed for optimal readership across devices

FOLLOW US
@frontiersin

IMPACT METRICS
Advanced article metrics track visibility across digital media

EXTENSIVE PROMOTION
Marketing and promotion of impactful research

LOOP RESEARCH NETWORK
Our network increases your article's readership